EMPIRICAL DYNAMICS OF A SMALL SCALE COASTAL UPWELLING REGION

CAIRNS A R BAIN

Ph D Thesis
Physical Oceanography
University of Cape Town

November 1991

Supervisor: Professor G B Brundrit

Can anyone measure the ocean by handfuls ...
Can anyone tell the LORD what to do?
Isaiah 40 vs 12

for Carol-Anne
who waited so patiently

A B S T R A C T

The study investigates the dynamics of a small space scale (less than 10 km) coastal upwelling region at the temporal scales spanning hours to years. Three to four year time series data sets of, sea temperatures at different depths (2 m, 5 m and 8,5 m) one kilometer offshore, of wind and of waves, obtained from Eskom for the Koeberg nuclear power station site study near Melkbosstrand (33° 41'S, 18° 26'E) were digitized on an hourly basis. An emphasis is placed on the study of the wind and sea temperature data, the latter being an unique data set in the South African context. The data were filtered into different frequency bands (<12,0 <0,5 <0,025 cpd). Simple statistics, linear correlation and spectral analysis were used to characterize these bands. Dominant temporal scales were identified as the seasonal, event (synoptic) and diurnal time scales. The characterization of the latter two time scales were supplemented with field work which inter alia measured: sea temperature profiles and transects; sea surface temperature distribution with the airborne radiation thermometry technique and Lagrangian currents.

At all the frequencies studied, the local wind was found to be the chief forcing mechanism for coastal variability, the sea temperature responding to an upwelling/downwelling dynamic process. At the seasonal and event time scale the alongshore winds have most significant correlation with the temperature but at the diurnal time scale the across shore winds also have a very prominent role. The long time series data enabled a coastal climatology in part to be established for the region. The seasonal data gives a bimodal sea temperature signal with warm winters. Spectral analysis shows a broad energy maximum between 8 and 15 days corresponding to synoptic events of passing depressions and coastal lows. In contrast, for the mesoscale phenomena range, very prominent peaking occurs at the diurnal frequency. Direct insolation is found to have a limited contribution to the temperature response with the chief forcing ascribed to modulation of the primary upwelling response by the diurnal land/sea breeze.

The study reveals in spring, a definite rapid transition between seasonal temperature regimes due to a single offshore cumulative Ekman transport event of magnitude 3×10^9 $g.cm^{-1}$ and duration of 5 days. This transition indicates a possible dynamic counterpart at the larger scale.

Discoveries at the small space scale include a distinctive "focus" of upwelling, with dimensions one kilometer or larger, associated with a coastal offset; (this is wind forced at the event time scale) and an insolation forced diurnally modulated thermal band (width of order of 0,5 km) adjacent to the coast line.

The offshore displacement of the intersection of the thermocline with the surface is successfully predicted under certain circumstances using a simple inertial two layer upwelling model using as input an alongshore wind impulse. The study hints at a possible coastal boundary layer structure.

The findings have relevance to fisheries and nearshore biology and to studies of the discharge of thermal and other effluents in the coastal zone.

A C K N O W L E D G E M E N T S

The Atomic Energy Corporation of South Africa is gratefully acknowledged for providing staff and financial support for the field work reported here. Drs J K Basson and D van As are thanked for their long-term moral support. Eskom willingly granted permission to use and publish their data collected for site investigations at the Koeberg nuclear power station. Their staff members Charles Maxwell and Dennis Rattey are particularly thanked for their generous help. C Bates and J Hanekom are thanked for their able assistance as is A Britten-Jones who knew just how to coax the twin outboards in a force six wind. Various pilots of the UCT flying club assisted with aerial work. John Newmarch and all the staff of the UCT Computer Centre are especially thanked for their competent help in taming the main-frame. Roy McMurray and staff of the then Southern Universities Nuclear Institute, Faure (now the Van de Graaff Group of the National Accelerator Centre) are thanked for their support.

The early ideas and work for this thesis were stimulated by Dr T W F (Sandy) Harris and brought to fruition by the sincerely acknowledged supervision and guidance of Prof G B Brundrit of the Department of Physical Oceanography. Many useful discussions were had with Drs F A Shillington and D van Foreest.

A special thanks to Dr Brian Hambleton-Jones for his motivation and encouragement and a final thank you to Susan Human for word processing of the text.

REPRESENTATION OF EARLY STAGE OF UPWELLING GROWTH CENTRE

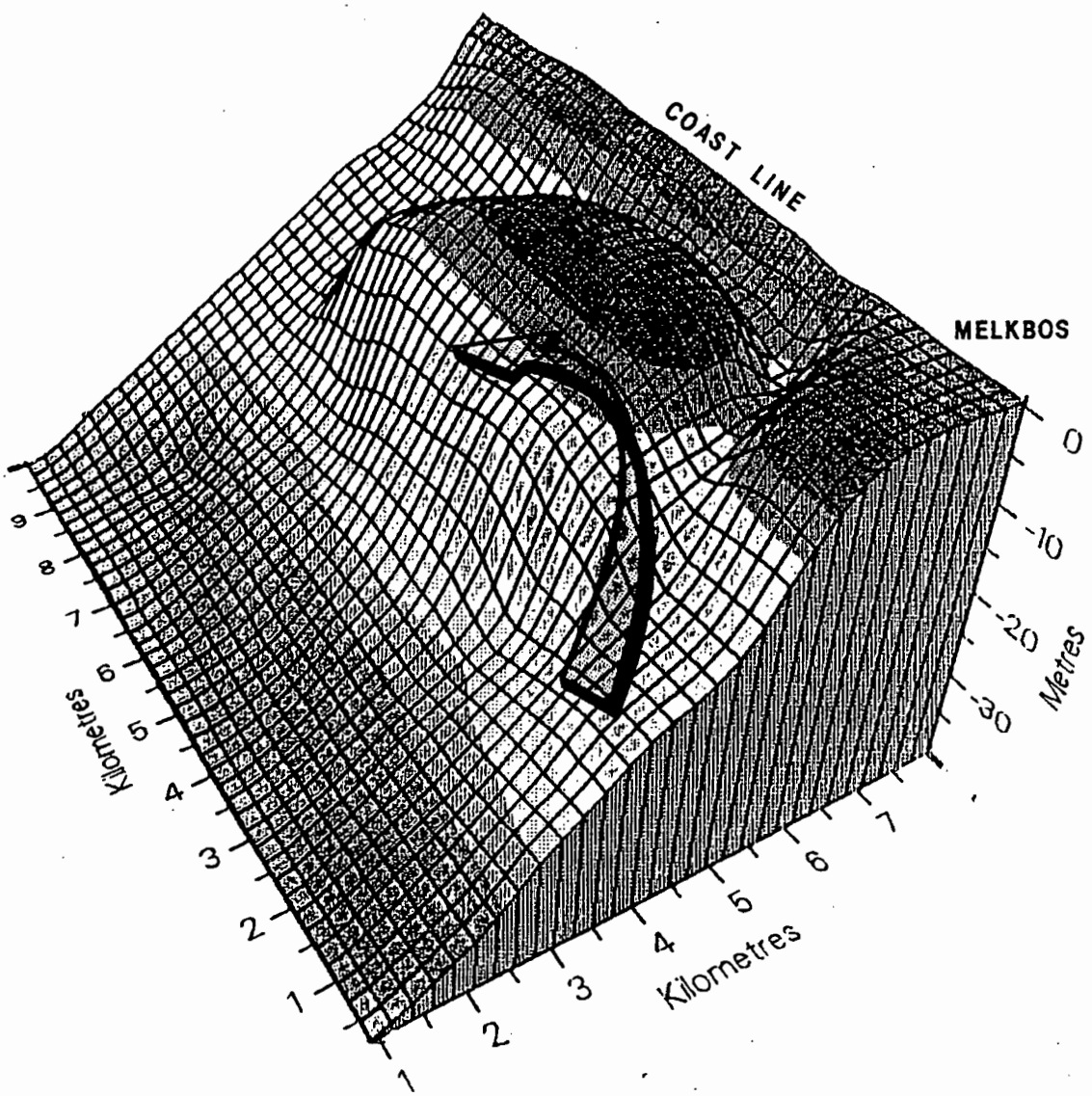

C O N T E N T S

LIST OF FIGURES

CHAPTER ONE

CHAPTER TWO

CHAPTER FOUR

Page

CHAPTER FIVE

FIG. 5.12 MULTIPLE DAY HOURLY MEAN FOR THE DIURNAL CYCLE OF HIGH FREQUENCY FILTERED (ZERO MEAN) 2 M and 8 M DEPTH TEMPERATURES. STANDARD DEVIATIONS FOR SELECTED DATA POINTS ARE DISPLAYED. A VISUALLY FITTED CURVE IS PROVIDED FOR 8 M DATA IN CASE a AND b 5.34

a) MEAN FOR 14-17 APRIL 1977
b) MEAN FOR 25-30 APRIL 1977
c) MEAN FOR 21-25 JULY 1977
d) MEAN FOR 4-7 AUGUST 1977

LIST OF TABLES

CHAPTER 1:

INTRODUCTION AND RESEARCH METHODOLOGY

C O N T E N T S

CHAPTER ONE

INTRODUCTION AND RESEARCH METHODOLOGY

1.1 INTRODUCTION

Historically the southwestern tip of the African continent has carried at various times the names of Cape of Storms and Cape of Good Hope. More recently the appellation "Cape of Upwelling" could be applied with some justification in the light of its growing recognition as a distinctive site amongst the four major upwelling systems of the world's oceans. The others are off California, Peru and North-West Africa as cited by Cushing (1969). The South Atlantic gyre has on its eastern boundary the north flowing Benguela current system. The upwelling region extending from Cape Point (34 °S) in the south up the west coast to Cape Frio (18 °S) in the north, is by association termed the Benguela Upwelling area, which has recently been highlighted in several review articles viz, Andrews and Hutchings (1980), Nelson and Hutchings (1983), and Shannon (1985a). The authors stress the uniqueness in the Southern Benguela area of the Cape Peninsula as a site with intense orographically controlled SE winds that result in a number of upwelling centres that merge to form a prominent baroclinic jet. The study reported here deals with the characterisation of a small localized centre of upwelling with a scale of less than the Rossby baroclinic radius of deformation ($\sim$10 km) near Melkbosstrand, several kilometres north of the Cape Peninsula.

Traditionally the science of oceanography concerned itself with gross or macroscale features of the oceans and matters that affected shipping such as tides and winds. In recent decades as the economic importance of upwelling areas for world fisheries was realized, a major increase in coastal upwelling studies occurred (O'Brien, 1983). However, the scale of investigations was still relatively large, of the order of 100 km. At the opposite scale of coastal oceanography the surface wave dominated shore line area with its complexities of shoaling waves, rip currents, littoral currents and sediment transport dynamics also received attention as man's impact on the coastal environment increased. Marine biologists and coastal engineers are particularly active in studies at this scale. The neglected area appears to include both a space and time scale. The space scale is that of the region between the wave dominated shoreline and the offshore coastal current area of width about 10 km (Murray, 1975). The time domain of continuous Eulerian records of temperature, currents, sea level etc. for duration of months or years

has only relatively recently been entered at selected sites with the advent of recording meters and subsequent computer processing of the data (Monin, 1977). Few nearshore data exist for quantifying the phase relationship between inner and midshelf currents (Schwing, Oey and Blanton, 1985). It is in the domain of this small space scale and continuous multi-year data base that the present study makes a contribution.

1.2 LITERATURE REVIEW

Although this study concerns itself with the characterisation of the empirical dynamics of a small scale shallow coastal upwelling region the literature review will, due to the scarcity of small scale studies also cover some larger scale work. At a later stage the relevance to the smaller scale and shallower waters will be judged. The emphasis will fall on: coastal upwelling processes; coastal or shallow water wind forced dynamics; time and space scales of the various processes. The literature review will be rounded off with a survey of Southern Africa studies.

1.2.1 Upwelling and Coastal Processes

The classical definition of upwelling is a motion resulting from "... a wind in the Southern Hemisphere which blows parallel to the coast, with the coast on the right hand side. In this case the light (warm) surface water will be transported away from the coast and must, owing to the continuity of the system, be replaced near the coast by heavier (colder) subsurface water" (Sverdrup, Johnson and Fleming, 1942). The displacement of the surface layer is referred to as Ekman transport after Valfried Ekman (1905) who attributed the deflection of surface waters away from the wind direction to the combined effects of the earth's rotation (Coriolis force) and the frictional forces.

Ekman (1905) showed that for a homogeneous deep sea with a constant kinematic eddy viscosity A that the pure drift current generated by the wind had a spiral depth dependence given by the two velocity components

$$u = V_o\, e^{-(\pi/D)z}\, \mathrm{Cos}\left(45^\circ - \frac{\pi}{D} z\right)$$

$$v = V_o\, e^{-(\pi/D)z}\, \mathrm{Sin}\left(45^\circ - \frac{\pi}{D} z\right)$$

where V_o is the surface velocity (a function of wind stress, the coriolis parameter and A)

z is vertical depth from surface and

D is the Ekman depth (of frictional influence)

$$D = \pi(2A.f^{-1})^{1/2}$$

where f is the coriolis parameter.

The equations show that the surface current vector is 45° to the right of the wind stress (for the Northern Hemisphere) and that the Ekman depth D occurs after a rotation of the velocity vector of π radians and a decrease in amplitude of $e^{-\pi}$. A useful derived depth is the e-folding scale depth $D_e = D/\pi$ which occurs after a rotation of the current vector of 1 radian and a decay in amplitude by a factor e. A typical value of D is 60 m.

Important recent experimental confirmation of firstly, Ekman spiral behaviour for wind driven currents with periods of 5 to 10 days is given by Stacey Pond and Le Blond (1986) for depths down to 160 m and secondly, of Ekman transport is given by Price Weller and Schudlich (1987) for a strongly surface (25 m) trapped summer case which also displays a "stratified" Ekman spiral.

Although upwelling can occur on any coastline where a favourable wind blows for sufficient duration, we have mentioned four major upwelling sites. Considerable research activity has occurred since the 1970's at these sites and great progress had been made in understanding coastal upwelling (O'Brien, 1983).

Common features of various phenomena that occur in the near surface waters during coastal upwelling are summarized by Brink (1983). His first comment that Ekman Layer theory is successful is almost trivial. There are however departures from the theory for the higher frequencies above the inertial frequency, and the vertical structure of the cross-shelf circulation is not completely understood. Secondly the surface offshore density gradient or front associated with the cross-shelf transport of upwelled water is related with a geostrophically balanced alongshore flow. The upwelled front lends order to the sea surface temperature and can be particularly intense off the Cape Peninsula (Bang, 1973) where temperatures are observed to change by several degrees within as many hundreds of meters offshore. The complex dynamics associated with this front is discussed theoretically by Brundrit (1981). The order in temperature structure tends to disorder or patchiness for weak winds or reversal of wind direction. This is observed in Benguela waters by Bang (1973) and on a smaller scale by Boyce (1977) in the Great lakes where 1 to 10 km meanders and eddies occur. This patchiness or

patterning of flow is now recognized to be of importance to plankton distribution and subsequent fisheries biology (Owen, 1980 and Hutchings, 1981).

Brink's third comment is the need to recognize that in the prototype situation a three dimensional process always exists that is often imposed by varied coastal topography. Upwelling is often observed at Capes or near heads of undersea canyons (Mittelstaedt, 1983) or at other changes in bathymetry. In the Coastal Ocean Dynamics Experiment off California the study of the relaxation phase of coastal upwelling highlights three dimensional effects and the asymmetry between up- and downwelling (Send, Beardsley and Winant, 1987). Meteorological forcing can besides the standard uplift of the isopycnals also cause coastally trapped waves that have remote forcing responses (Gill and Schumann, 1974); (Clarke, 1977); (Mitchum and Clarke, 1986b). Such responses are often dominated by topographic irregularities in the longshore direction on the scale of the Rossby baroclinic radius of deformation (Killworth, 1978). The subject of centres of upwelling will be further pursued later under the heading spatial scales, (1.2.2).

The Rossby baroclinic radius of deformation L, is an important parameter in the dynamics of upwelling and other boundary effects and is defined as

$$L = (g \frac{\Delta\rho}{\rho} h)^{1/2} . f^{-1}$$

where g is the acceleration of gravity
ρ is reference density
$\Delta\rho$ is the density difference between layers
h is the typical thickness of the layer
f is the Coriolis parameter

L has a typical value of 10 km at the coast and relates to the relative offshore scale of the upward tilt of the pycnocline but does not seem to directly determine the offshore distance to which the surface front can move. A description of the Rossby baroclinic radius of deformation is given by Gill (1982) as being that horizontal length scale at which rotation effects become as important as buoyancy effects, or as put by Pedlosky (1978b) the width of the upwelling zone is the Rossy deformation radius. This scale can under certain conditions be expressed as L = N/f where N is the Brunt-Vaisala buoyancy frequency given in the following equation:

$$N = (-\frac{g}{\rho}\frac{\partial \rho}{\partial z})^{1/2}$$

$\frac{\partial \rho}{\partial z}$ is the vertical density gradient.

N is a measure of the stability of the water column. The value is relatively large in surface waters but decreases with depth; typical values being 0,02 rad.s^{-1} to 0,002 rad.s^{-1}. Values of N and L relevant to the study site are given in 1.4.3.

Once the larger scale seasonal front is formed the inshore part of the pycnocline can flop about during subsequent wind event cycles in a barotropic type response which is linked to the baroclinicity of the main front (Brundrit, 1981). The inshore behaviour is relevant to the present study. In a simple upwelling model Csanady (1977a) maintains that initially in a wind event the energy is shared between establishing the alongshore jet and lifting the pycnocline but once the pycnocline outcrops on the surface, most of the energy is used to displace it further offshore and not to intensify the coastal jet. This model involves the alongshore propagation of the upwelled front as an internal Kelvin wave mode for which there is observational evidence from Lake Ontario (Csanady, 1977a). In an extention of a model by Clarke (1977), Hua and Tomasset (1983) include mixed layer dynamics and obtain an upwelled front not scaled to the Rossby baroclinic radius. In a continuously stratified sea, Pedlosky (1978b) develops a two dimensional non linear model for onset of coastal upwelling. The model stretches apart the density surfaces near the coast thus reducing the local value of N the Brunt-Vaisala frequency and in turn decreases the local Rossby baroclinic radius L. The consequence is accelerated upwelling and the formation of a frontal discontinuity, the gradient of which has a scale less than the initial Rossby radius. Such intense fronts are observed (Bang 1973, Curtin 1979).

Besides wind induced upwelling the wind plays a dominant role in the dynamics of most coastal seas. Some sites have tidal dominance but even there under storm conditions wind forcing is important (Grant and Madsen, 1986). The response to wind and tides varies from site to site as various factors of climate, geomorphology and stratification dominate (Winant, 1980). Here emphasis is placed either directly or indirectly on wind forced processes. Over and above studies in upwelling regimes many studies on local wind forcing occur. In judging what is relevant to this study the paradox arises

that dynamics and currents are central to most reports whereas here there is a lack of good quality current data particularly in the form of time series data. Dynamic concepts can thus be assessed for this site usually only indirectly. With this in mind some shelf models are considered but concentration will be on a few small scale or shallow sites that have similarities with respect to this site of bathymetry and depth of instrumentation.

The understanding of the wind forced dynamics of the coastal area and shelf waters is extended by several theoretical approaches and models. Various linear and non-linear analytical models exist that employ consideration of coastal-trapped waves, bottom friction, horizontal friction, alongshore variations in bottom topography and stratification. These are reviewed by Allen (1980) as are 2 and 3 dimensional numerical models. This review by Allen largely ignores the shallow near-shore region and most models assume the surface and bottom boundary layer are small in relation to the water depth.

A widely employed theory for the behaviour of currents on the continental shelf is that of wind forced, frictional, long coastal-trapped waves or long-wave theory, (Chapman 1987). A significant early contribution to a forced wave theory is that of Gill and Schumann (1974) who considered the frictionless barotropic response. This was extended by Gill and Clarke (1974) to include stratification and then by Clarke (1977) to include shelf topography where the wave models are hybrids between shelf waves and Kelvin waves. Recently realistic bottom frictional response has been considered by Brink (1982) , Clarke and Brink (1985), Mitchum and Clarke (1986a and 1986b) and Chapman (1987). These long-wave theories are particularly suitable for forcing by synoptically fluctuating wind stress and for predicting a time series response, as compared with the frictionally dominated arrested topographic wave theory of Csanady (1978) that neglects time dependence. Another approach to model wind driven currents on the shelf is statistical in nature in that theoretical transfer functions between wind stress and observable parameters in the frequency and alongshore wave number domain are used to estimate observable statistics in the frequency domain. This stochastic model of Brink Chapman and Halliwell (1987) shows that free coastal-trapped wave physics operates mainly between period limits of 9h and 20 days. Outside these limits at the shorter time (and space) scales there is a lack of "resonant" wind stress energy and at the longer periods frictional damping predominates.

Most of the models mentioned above ignore the shallow nearshore zone in that a shore side vertical boundary condition is specified that is

often equated to a minimum water depth of $3.D_e$ where D_e is the Ekman e-folding scale depth (defined earlier in this section). In practice this mimimum depth is about 60 m for the west coast of the USA where these models are often evaluated. This value near the present study site is of the same order as above whereas the study's data base is for depths less than 40 m and mostly at 11 m. The direct relevance of these models to this study is therefore limited and the models are consequently treated superficially.

In general the findings of the several long-wave theory models mentioned above tend to agree with observations of alongshelf velocity and bottom pressure. Good matching with time variability of currents (Chapman 1987) and with coastal sea levels (Mitchum and Clarke 1986b) are achieved. Poor agreement with cross-shelf currents are obtained in general. They also have poor correlation with vertical midshelf current behaviour (Chapman 1987) and with amplitude of windstress - current gain (Brink, Chapman and Halliwell, 1987). Long-wave theory is useful for separating local and remote forcing effects on shelf dynamics (Chapman, 1987 and Mitchum & Clarke, 1987b) where in the latter case most of the wind induced energy on the West Florida shelf is due to a local forced wave and the remainder comes from a free wave generated remotely. The contributions of local and remote forcing is modelled numerically for the California Current system by Pares-Sierra and O'Brien (1989) for the seasonal and interannual response. They show that most of the interannual variability in coastal sea level is due to trapped kelvin waves that propagate from the equatorial region.

The shallow nearshore region has complicated dynamics that are not well understood nor widely studied (Mitchum and Clarke 1986a and Csanady 1976b) and few data exist of nearshore currents and their phase relationship with further offshore currents (Schwing, Oey and Blanton 1985). This nearshore region could be defined by the common boundary condition of various longwave models (Clarke and Brink, 1985; Mitchum and Clarke, 1986b; Chapman, 1987) that exclude the region shallower than three times the Ekman e-folding scale depth. At greater depths the Ekman surface and bottom layers can be formulated separately but inshore the layers interact, there is a frictional response and blocking of the surface Ekman flux occurs (Mitchum and Clarke, 1986a). The mean circulation of a mid-shelf region of the Mid-Atlantic Bight away from the "chaotic" nearshore region is successfully modelled with Ekman dynamics by Csanady (1976b).

The nearshore region is modelled by Mitchum and Clarke (1986a) with a linear barotropic model (the nearshore region is assumed well mixed by turbulence) having a synoptic wind event time scale and alongshore length scale large compared to the nearshore frictional region. The model confirms the dominance of alongshore synoptic wind stress in forcing the nearshore current. As the depth decreases more of the surface stress is transferred directly to bottom stress. This forcing occurs over a narrow shelf region where the ratio of water depth to Ekman layer e-folding scale varies from 0,2 to 2,5. The model is evaluated by Mitchum and Clarke (1986a) on the shallow West Florida Shelf, where with the e-folding scale equal to 8,5 m the larger ratio is equivalent to a water depth of 21 m which occurs at a relatively far offshore distance of $\sim$100 km due to the gentle slope. For a 25 day time series of alongshore currents they obtain quite a good fit between the data and model predictions. Local dynamics control the frictional nearshore currents while further offshore non-local effects of forced coastal-trapped wave dynamics have influence and as such the model of Mitchum and Clarke (1986a) complements those models that ignore the nearshore region.

The shallow shelf off New Jersey is numerically modelled by Bennett and Magnell (1979) with a two dimensional non-linear barotropic model over a 12 km offshore scale and compared to data from a site 4 km offshore at a 13 m depth. Turbulent friction is parameterized with a non-linear vertical eddy viscosity. With a constant alongshore pressure gradient and input of observed winds and sea level the model-generated currents have some correspondence to measured values. Because of the shallowness of the water the model shows for steady flows that the offshore wind component is more effective in forcing transverse circulation. The Ekman depth is then greater than the water depth. The model fails to reproduce the observed 4 hour dominant response time and its barotropic nature is a significant limitation.

On the relatively small space scales, coastal research has taken place in the Great Lakes of North America and off Long Island on the north east coast of the USA. At both areas transect lines generally extended less than 16 km offshore and were intended to encompass the "Coastal Boundary Layer" (CBL) a term first used by Csanady in 1972 (Csanady, 1972a). When the coastal boundary layer transect (COBALT) experiment was started in 1975 off Long Island very little was known observationally or conceptually about the CBL. The concept of a CBL has since been expanded by Scott and Csanady (1976), Csanady (1982a), Boyce (1977), Murthy and Dunbar (1981) and Schwing, Oey and Blanton (1985).

Observationally there is now a distinct difference between some "nearshore" region and the adjoining shallow sea. Pulsing wind events force transient currents that are trapped close to the coast. Repeated wind impulses result in a coastal current climatology that is markedly different from mid shelf currents. Near the shore the currents are essentially linear in nature whereas further offshore they have a much greater rotary component close to the inertial frequency. The boundary for the nearshore region is set differently depending on the perspective of the relevant study. For long-wave theory modelling of the shelf, it can be set at a depth of 3 times the Ekman scale depth (Mitchum and Clarke 1986a). Empirically it can be set on some kinetic energy criteria (Murthy and Dunbar 1981) or on a phase relationship between currents and coastal sea level (Schwing et al., 1985).

Murthy and Dunbar (1981) quantify and subdivide the CBL. They propose (for Lake Huron) a CBL made up of an inner boundary layer within 2 km (30 m depth) of the coast where bottom friction gradually brings the flow to zero at the shore. This is termed the frictional boundary layer (FBL). Beyond the 2 km mark an outer boundary flow develops as a consequence of the adjustment of inertial oscillations to the shore-parallel flow and is termed the inertial boundary layer (IBL). The boundary between the two (at about 2 km) or 30 m depth is chosen at the distance offshore where the total kinetic energy of the currents is a maximum. The outer boundary of the CBL is arbitrarily set at where the inertial fraction of the kinetic energy equals 50 % or more of the total energy as estimated from a spectral analysis of the currents. In the Great Lakes this is typically at about 10 km (70 to 100 m depth) and at the Long Island site is inshore of the 12 km point at 30 m (Csanady, 1980). Agreement with frictionless inertial response theory is found by Csanady (1982) to be limited to depths exceeding 30 m. Fig. 1.1 adapted from Blanton (1974) shows the distribution across the CBL of current kinetic energy for both long period and inertial currents.

A boundary between nearshore waters and midshelf water for a shallow continental shelf subject to synoptic wind forcing has been proposed by Schwing Oey and Blanton (1985) from results of a linear frictional barotropic model. The boundary, at the point where alongshelf current is in phase with the coastal sea level, has on the nearshore side a frictional dominated flow with the inertial terms being more important further offshore. For the South Atlantic Bight (SAB) off the eastern shore of the USA this boundary occurs 30 to 50 km offshore at the 30 m depth contour. The SAB observations of currents at 10 m, 30 m and 40 m contours and coastal sea level and their

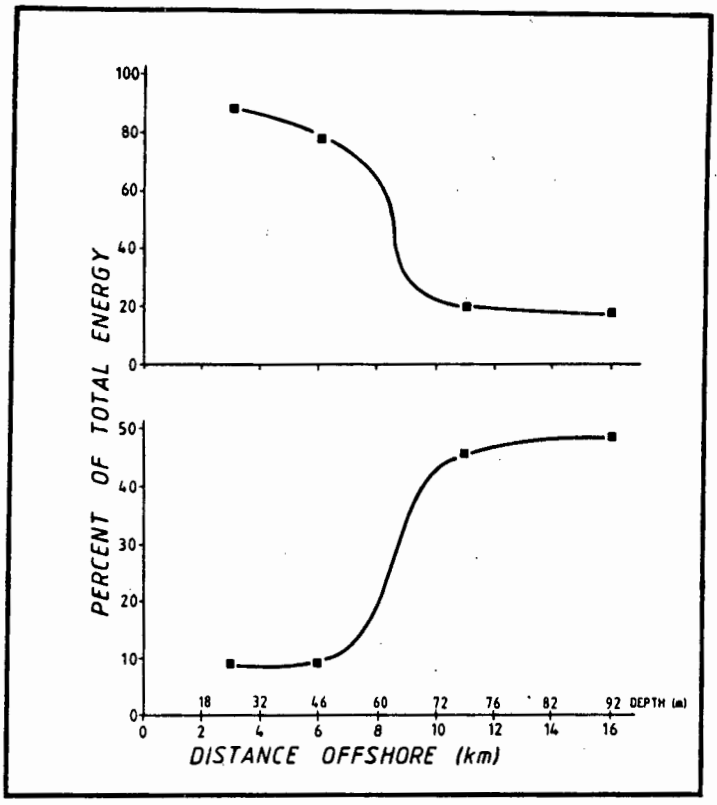

FIG. 1.1. PERCENTAGE DISTRIBUTION OF CURRENT KINETIC ENERGY ACROSS THE COASTAL BOUNDARY LAYER IN LAKE ONTARIO FOR LONG PERIOD CURRENTS (TOP) AND INERTIAL OSCILLATIONS (BOTTOM) AFTER BLANTON (1974)

phases in relation to synoptic wind forcing (sub-inertial frequencies) are well explained by the model (Schwing Oey and Blanton 1985). The barotropic assumption of the model is well met by their study site which is unstratified even in summer with minimal density effects. The other assumption of the model is local wind dominance which implies non applicability for shelf regions where forced or freely travelling continental shelfwaves are predominant. In a subsequent paper Schwing, Oey and Blanton (1988) show that for the SAB, remote forcing plays a role during transition in wind regimes when decoupling of the sea level and currents from the local winds occurs.

It is not possible to do a direct comparison of the different criteria of Murthy and Dunbar (1981) and Schwing et al., (1985) for setting the CBL boundary since the data provided are incompatible. Qualitatively the data of Schwing et al., (1985) show the currents at the 10 m and 30 m contours are more rectilinear than at 40 m. However, it is the phase response between alongshore currents and the coastal sea level which are very different between the 10 m and 30 m currents that indicates a boundary between these depth contours. For comparable data the criteria of Schwing et al., (1985) for setting a boundary is preferable since it is based on a clearer distinction between the variables. It would be instructive to see the data for phase differences extended to include the inertial frequencies.

It is worth noting that for all the different criteria there is a common boundary depth of order 30 m despite the large range in offshore scales: 2 to 12 km for Murthy and Dunbar (1981) and Csanady (1980), 30 to 50 km for Schwing et al., (1985) and 100 km for $3.D_e$ of 27 m for Mitchum and Clarke (1986a). Such a diversity in space scales will bring complexity to the identity of the nearshore zones from the effects of three dimensionality, wind homogeneity and remote forcing. In this study, future reference to the CBL will assume a nominal offshore boundary depth of 30 m.

The essentially linear alongshore flow of currents close to the coast between 300 m (5 m depth) and 800 m (15 m depth) offshore even under near normal to the shore winds is also demonstrated by Lagrangian float track experiments off West Florida by Murray (1975). He also observes subtle on and offshore flows which are important for shallow water upwelling dynamics.

Boyce (1977) has introduced the concept and need for a coastal climatology. Because the CBL is dynamically and spatially so complex with eddies and meanders of scale 1 to 10 km and dependent on coastal topography, the chances of setting up a deterministic model of the coastal flow is slight. There is therefore a need to identify dynamically homogeneous zones along the coast and then within each zone to undertake field observations of reasonable length time series of winds, currents, sea levels and temperatures to build up a regional coastal climatology. Coastal science first needs a good description of the dynamics before they can be modelled.

The initial motivation for the CBL studies and coastal climatological approach reported above was linked to environmental impact of effluent outfalls and coastal nuclear power station thermal releases, the flows of which are typically orders of magnitude greater than other effluent flows. There was therefore a great need to predict the fate of pollutants in the coastal zone.

The literature shows little work has been done within the coastal boundary layer particularly in the way of modelling the processes occurring there. The question is posed if the findings of the shelf dynamics can be extended into the CBL region. One of the recent advances in shelf oceanography is the recognition that many shelf processes are driven by barotropic dynamics. One of the physical parameters that apparently helps control the response is the shelf slope, which is related to frictional response, Schwing et al., (1985) and to a barotropic response, Clarke and Brink (1985).

If the slope is gentle enough then even with a stratified water column the wind driven response can be barotropic if the condition

$$N^2.\alpha^2.f^{-2} << 1, \text{ specified by}$$

Clarke and Brink (1985), is met. N^2 is the shelf-averaged Brunt-Vaisala frequency squared, α is the average bottom slope, f is the coriolis parameter. This criteria is applied to the Middle Atlantic Bight and has a value of $8,7 \times 10^{-3}$ which confirms its barotropic nature (Clarke and Brink, 1985). Local application of this criteria is given in Section 1.4.3.

Bottom friction is of importance for the dynamics of both the whole shelf and the nearshore region. Bottom braking is considered as important as surface stress (Csanady 1982). The shelf response is dominated by bottom friction for gentle shelf slopes less than a value given by Schwing et al., (1985) which is a function of latitude, the frequency of the motion and a friction coefficient which can be related to tidal current strength. For the South Carolina shelf area assuming a friction coefficient of 2×10^{-4} $m.s^{-1}$ this slope value is $2,4 \times 10^{-4}$ for a frequency of 0,2 cpd and Schwing et al., (1985) show that the shelf is in fact frictionally dominated.

There are various approaches to parameterization of bottom stresses. In water depths comparable to the Ekman depth, Scott and Csanady (1976) assume a linear form is more appropriate than a quadratic form for wind driven currents when these are less energetic than the tidal currents and of a lower frequency. Tidal currents tend to linearize the relationship between time averaged wind stress and bottom velocities, Bennett and Magnell (1979). The quadratic drag law parameterization and the linear relationship are compared by Winant and Beardsley (1979) for four shallow (30 m) sites; a factor four variability between the computed coefficients does not point to one parameterization being more accurate than the other. The variability indicates that even in shallow water sites the surface and bottom stress need balancing with alongshore pressure gradient and Coriolis forces, (Winant et al., 1979). More recently in a long-wave theory model for stratified frictional flow on the shelf Clarke and Brink (1985) show that the response with synoptic wind forcing is critically dependent on the type of bottom stress parameterization. They indicate that the effects noted by Grant and Madsen (1979) of surface gravity waves of period 5 - 20 s on enhancing low-frequency bottom stresses are applicable. Although the parameterization of Grant and Madsen (1979) is basically quadratic a linearization scheme is used by Clarke and Brink (1985) in applying it to their model. In

a review of the continental shelf bottom boundary layer (BBL) Grant and Madsen (1986) state that the size of bottom friction terms is still poorly known and that no complete data set for the stably stratified shelf BBL has been published. Surface gravity waves travelling above a rough bottom result in a significant increase in bottom friction. The mean friction may be increased by more than a factor 2 as a result of bioturbation altering the microtopography of the bottom surface. Because of increased friction the thickness of the BBL is larger than earlier suspected and goes counter to the assumption of small boundary layers made by many shelf models (Grant and Madsen 1986).

The Ekman depth is an important parameter in many models; it's value may be deduced indirectly from the bottom drag coefficient, the bottom friction velocity linked to the vertical eddy viscosity and surface stress as shown by Marmorino (1983).

Common to the dynamics of the coastal waters of the Great Lakes, the NE American seaboard and the US west coast, is the rapid response to alongshore wind impulses. Correlation between the wind and the current is good (Huyer et al., 1979; Chapman, 1987). However there are important differences. The dynamics in the Great Lakes with no tides and off the US west coast with weak tides can be grouped together. Although bottom friction cannot be ignored on the US west coast (Brink and Chapman, 1987) the coastal waters there and in the Great Lakes respond to wind forcing primarily in the inertial mode whereas on the NE seaboard (Long Island site) the response is dominated by bottom friction because of the strong tides of the area (Csanady, 1982a). Non-local effects due to fluctuations in the Gulf Stream play a part in the shelf dynamics of the Long Island site but off Oregon remote influences are not as important as the local wind forcing. The relatively simple dynamic response off Oregon and in the Great Lakes aids in the study of wind forcing episodes there.

The Melkbosstrand site has very low tidal currents and it will be instructive in this study to compare its dynamics to those quoted above.

Besides the wind event scale implied in the previous discussion higher frequency processes are also of importance in the coastal zone. The variability of currents on the California shelf at different frequencies is described by Winant and Bratkovich (1981). It is particularly at those frequencies greater than 1 cpd that Winant and Olson (1976) report that the understanding of current systems, in shallow coastal waters, has not kept pace with theoretical and experimental advances in coastal and nearshore

processes. One study of theirs was sited off the Californian coast on an instrumented tower situated 1.6 km offshore in a mean depth of 18 m. This is very similar to the position of the ESCOM sea tower set at 1 km offshore in 11 meters of water reported in this study. Winant and Olson (1976) elucidate aspects of the vertical structure of shallow coastal currents. For the summer season at these higher frequencies the onshore and longshore currents are found to be essentially uncoupled through the water column; longshore currents are tidally forced but longshore winds also induce strong alongshore currents; the onshore currents are more energetic than the alongshore currents; the baroclinic onshore flow is associated with energy at frequencies of both internal semidiurnal tides and internal waves. The maximum tidal range is about 2 m. In an earlier study at the same site Cairns and Nelson (1970) studied temperature structure in the water column and observed large 5 °C to 8 °C semidiurnal oscillations at mid depth throughout the summer season. Winant (1974) who also measured temperature responses of 5 °C in one second in only 5 m depths off the Scripps pier in La Jolla California, proposes such responses are due to internal surges, the possible generation mechanism being the coupling of long surface waves (tides) and internal wave modes at the shelf break and the resultant propagation of internal waves to the coast. At that site the initial shelf break occurs about 15 km offshore compared to 60 km off Melkbosstrand. Hayes and Halpern (1976) report that the steepness of the continental slope is critical for the propagation of internal semidiurnal energies to the coast. The coastward propagation of interfacial tides is related to the slope of the continental shelf and continental slope in a simple two layer theory of Largier (1987) which is applied to the Agulhas Bank area (Largier and Swart, 1987).

There are a number of references in the literature to diurnal heating effects for the near surface layers of oceanic waters, but a limited number referring specifically to shallow nearshore water (<20 m depth, <10 km offshore). Insolation together with the other components of the radiation budget viz, back radiation, reflected radiation, sensible heat exchange between air and water, and latent heat of evaporation or condensation can have significant diurnal effects on the temperature of the water column (Roll, 1965). Estimates by Deschamps and Frouin (1984) show that 1 000 $w.m^{-2}$ absorbed in the top 10 m will give a heating rate of 0,1 $°C.h^{-1}$ and a daily variation of less than 0,5 °C. Under summer conditions with zero winds thermal trapping is limited to about a 1m surface layer with a diurnal amplitude of 2 to 3 °C (Halpern and Reed, 1976).

Many of the oceanic studies of insolation effects are linked to the role of wind forcing in investigations of the mixed layer. The competing effects of a stabilizing surface heat flux and a destabilizing surface wind stress in studied by Price Weller and Pinkel (1986) to determine the trapping depth for a diurnal cycle. They observe a near surface diurnal jet that accelerates downwind during the morning and midday and turns into the wind by early evening due to the Coriolis force. The velocity and temperature profiles are roughly matched by their numerical model (Price et al., 1986). The response of the upper ocean to solar heating is modelled in two linked papers. Firstly, Woods and Barkmann (1986) predict the diurnal mixed layer depth over an annual cycle with seasonal winds and find nocturnal convection plays a dominant role. They prefer to define the mixed layer not in terms of the density or temperature profile but in terms of turbulence; the bottom boundary of the mixed layer is the turbocline below which turbulence is intermittent and weaker than above. Below the turbocline is the diurnal pycnocline followed by the seasonal pycnocline. Secondly, Woods and Strass (1986) consider the diurnal behaviour of the current profile for a steady wind stress. Momentum diffuses deeply at night and is left to rotate inertially in the diurnal pycnocline or thermocline during the day when the mixed layer is shallow. The inertial current is termed the diurnal jet and has important consequences for generating shear turbulence and affects the deepening of the mixed layer (Woods and Strass, 1986). The deepening of the mixed layer for time scales of the diurnal period and shorter is modelled by Spigel, Imberger and Rayner (1986) who consider effects of mixing due to both Kelvin-Helmholtz billowing and thermocline erosion. They get good agreement with observation over a diurnal cycle including calm and strong wind forcing.

Associated with wind forcing is the theoretical Ekman transport of the surface waters. Experimental observations by Price, Weller and Schudlich (1987) confirm the Ekman transport to within about 10 % for a strongly surface trapped flow. The surface trapping (25 m) is produced by the diurnal heating cycle. Discussion on other papers on diurnal and inertial period wind forcing such as by Pollard (1970), Boyd (1981), O'Brien (1977) and Rosenfeld (1988) is given in chapter 5, where the few papers on shallow water insolation effects such as by Smith (1977a), Morita (1978), Jacobs (1978) are also discussed.

Non local effects that can impinge on coastal dynamics include various shelf waves and topographic Kelvin waves that are forced by remote synoptic windfields. In the Great Lakes, Kelvin waves are seen to reverse the coastal current flow (Csanady, 1976a and Clarke, 1977). Forced barotropic shelfwaves along the South African coast

are discussed by Jury MacArthur and Shillington (1989). Variability on the California shelf due to both local and remote forcing including a suggested barotropic Kelvin wave is presented by Davis and Bogden (1989). Off Peru longshore current fluctuations are related to a poleward propagating baroclinic shelf wave (Smith, 1978). Topographically trapped waves are reviewed by Mysak (1980). Wind forced long coastal-trapped waves are shown to play a role in the dynamics of various coastlines, Chapman (1987), Mitchum and Clarke (1986b), Strub (1987a).

1.2.2 Spatial Scales and Upwelling Centres

At the major upwelling regions the spatial distribution of wind and sea temperature has been studied e.g. Stuart (1981), Mittelstaedt (1983), Huyer (1983) and Jury (1984 and 1987). Other noteworthy studies have occurred in the Great Lakes e.g. Scarpace and Green (1979); Blanton (1975) and in the Mediterranean-Gulf of Lions, Millot (1979). In many cases centres and filaments of upwelling that have a constant geographic base have been observed. The spatial scale of such features varies from a few kilometers to several tens of kilometers or longer. At each site different factors seem to control the location of the upwelling feature. Brink (1983) points out that the physics of these features is largely unknown and although there are theories that try to predict the origin of the structures, no theories exist that deal with the actual near-surface dynamics. More recently Brink (1986) reviews physical aspects of upwelling filaments and their biological implications. A long curved cool sea surface temperature pattern with a radius of curvature of 420 km extending from the coast into the Gulf of Tehuantepec (Mexico) is linked by Clarke (1988) to a strong orographic channelling of an inertial wind jet over the Gulf. The cold surface water is due to wind mixing of the shallow thermocline but a SST gradient to the right of the wind suggests surface Ekman flow effects, Clarke (1988). The response of the coastal ocean to this strong offshore wind is modelled by McCreary et al (1989).

The upwelling centre near Cabo Nazca, Peru with a base of 10 to 20 km is located on a relatively straight segment of coast. Its size and shape is controlled by variable winds and its position is thought to be mainly controlled by bottom topography (Brink, 1983). Off NW Africa Mittelstaedt (1983) observed enhanced upwelling on the lee of Capes where local bathymetry generates flow divergence. He also finds fixed small scale upwellings at the head of submarine canyons. For reasons similar to Mittelstaedt, Schumann, Perrins and Hunter (1982) using satellite infra-red imagery of the South African South coast observes 10 to 40 km scale centres of upwelling on the lee of Cape Recife, Cape St Francis and Cape Seal. Off Vancouver Island

Ikeda and Emery (1984) also using satellite imagery have correlated a meandered form of an upwelling boundary with submarine ridges and coastline irregularities on a scale of 25 km. Jury (1988) illustrates spatial distribution of upwelling between 29 - 34° S on the African West Coast with links to orography and local topography.

In the Gulf of Lions, Millot (1979) considers that coastline shape and orientation are the main cause and not bottom topography for centering upwelling features (10 to 20 km base) on straight segments of coast. There, strong winds often blow nearly perpendicularly offshore and no preferential upwelling occurs at capes. On a scale of a few kilometers at Lake Ontario Blanton (1975) reports zones of upwelling associated with the interaction of the coastal boundary layer flow with small cuspate features of the shoreline.

Various theoretical models attempt to explain the observations. The models are generally of the mesoscale and include those of Yoshida and Mao (1957) and Hurlburt (1974), that indicate enhanced upwellings at capes. The theoretical three dimensional model of Peffley and O'Brien (1976) supports the findings such as at Cabo Nazca, Peru, that bottom relief is more important than coastline curvature in localizing upwelling centres. In contrast, the numerical model of Hua and Tomasset (1983) using a flat bottom successfully reproduces the Gulf of Lions upwelling centres as a function of coastline geometry only. In the latter model the shape of the upwelling centres is better mimiced by the inclusion of mixed layer dynamics. The model implicates forced Kelvin wave fronts generated by coastline variability in determining the position of the upwelling centres; the mixing dynamics slow down the Kelvin wave fronts allowing the upwelling features to spread out.

No detailed studies on upwelling centres of scale less than 10 km have been found in the literature and the relevance of the above reported cases will be assessed in this study.

Just as the centres of upwelling have different space scales other features of the upwelling and coastal processes have varied scales. The coastal boundary layer (CBL) in the Great Lakes and off Long Island typically hugs the coast in a 10 km wide band within which Boyce (1977) observes meanders and eddies from 1 to 10 km in size. Internal wave dynamics can result in even smaller scales (Winant and Olson, 1976). Upwelling fronts are a rich source of varied space scales as shown by vortex dipoles on the Benguela front (Stockton and Lutjeharms, 1986b). The dynamics of the different scale processes are important for mixing and dispersion characteristics which are of interest to biologists and environmentalists. Owen (1980) discusses for anchovy fisheries in upwelling areas the relevance of and

characteristics of processes from the mesoscale down to the microscale as small as the sub-metre scale. While Wolanski and Hamner (1988) indicate the biological importance of topographically controlled fronts in coastal waters.

Space scales serve to show how complex an environment we are dealing with. A set of Eulerian data from a single fixed point in the coastal zone can be misleading about other not too distant parts of the system (Blanton, 1975). Multiple arrays of meters are costly and Lagrangian tracking of flows has some advantages. For sea surface temperature surveys airborne radiation thermometry (ART) is an excellent way to observe a large area in a near synchronous manner, Andrews and Cram (1969), Saunders (1973), Jury (1980) (see Section 1.5.4.3).

1.2.3 Time scales

For the open ocean Monin (1977) has classified the non stationary processes into seven different time scales that vary from seconds to centuries. Coastal processes too have greatly varying time scales that are best explored through the analysis of long duration time series data. The analysis can include simple averaging or filtering of the data to remove certain frequencies or can employ spectral analysis techniques For instance through spectral analysis Winant (1983) proposes for the Southern Californian shelf that there are three frequency bands of importance: the highest energy is for a low frequency band with periods longer than a day with currents directed mainly alongshore; an intermediate frequency band with periods from one day to two hours in which the direction of currents is ill defined; and a high frequency band for motions such as are induced by internal waves and which are directed across the shelf. The energy of this band is several orders of magnitude lower than the previous band, but the high frequency band processes are still important for dispersion and mixing. The direction sences quoted are obtained through rotary spectral analysis (Gonnella, 1972 and Section 1.5.3). In a review paper on coastal circulation Winant (1980) compares the current spectra from the NE coast of the USA and the Oregon shelf on the west coast. The comparison shows several fundamental features of the variability of coastal currents, notably the greater inertial response (relative to the diurnal response) for the Oregon waters.

In a study of the high frequency (greater than 1 cpd) structure during a coastal upwelling wind event off Oregon, Hayes and Halpern (1976) use a multiple shot time series spectral analysis approach that yield a wealth of information of interrelations of different processes during the upwelling. Included is the observation that the

inertial frequencies are strongly excited at the start of the upwelling and the semidiurnal ones are suppressed as the upwelling developes. The generation of inertial oscillations in the first stage of coastal upwelling is a common feature and has been observed on the smaller scale in the Great Lakes (Blanton, 1975) and in the Mediterranean-Gulf of Lions (Millot and Crepon, 1981). In the Gulf of Lions the surface layer currents are strongly correlated to the local wind and have a spectral peak exactly at the inertial frequency; the depth averaged temperature response has a broader peak of frequency slightly greater than the inertial frequency which is due to a long internal wave of frequency greater than the inertial frequency generated at the shore which drives the baroclinic wave.

In another approach to the use of time series data Csanady (1976b) takes the simple average over about one month to obtain the 'mean' or 'first order' flow patterns of currents in shallow seas. The averaging period is long enough to smooth out tidal and wind driven transients but not so long as to suppress the seasonal variability. This enables the seasonal flow pattern to be discerned which is a lot less random than the often chaotic short term wind driven flow. This mean flow can be used both to predict the movement of nutrients or pollutants or to quantify dynamical balances which can be tested with simple linear flow models, (Csanady, 1976b and Csanady and Scott, 1980). Through such an analysis Csanady and Scott (1980) show that in the mean summer circulation, momentum advection is important within a 10 km width coastal band subject to intermittent full upwelling.

Huyer, Sobey and Smith (1979) use different sets of filters on long time series of currents, winds and sea levels off Oregon to study both seasonal trends and more transient wind episodes. A distinct difference between winter and spring oceanographic regimes is noted. The spring transition for the Northern California shelf is described by Lentz (1987). Huyer (1983) stresses understanding is lacking on the interaction of processes with different time scales in the upwelling regime. A 19 year set of wind stress data is used in a numerical model by Pares-Sierra and O'Brien (1989) to study the seasonal and interannual variability of the California Current system.

The different time scales are associated with varying forcing processes, e.g. wind forced processes respond, at a seasonal time scale as macroscale pressure systems are modified, at a synoptic time scale for long coastal-trapped waves and at a diurnal time scale for land-sea breeze events.

1.2.4 Southern Africa Studies

If one separates the Benguela and other shelf studies from the smaller scale coastal boundary layer (CBL) region then very little reported work has occurred at the latter scale for the Southern Africa coastline. At an even smaller scale coastal engineers studying sites for effluent outfalls or harbour development usually limit their investigations to a few surf widths. In isolated cases the study extends a few kilometers offshore (Pearce, 1973 and Russell Pers Com). The data so collected are usually analysed in a conventional statistical sense and not linked to larger dynamic processes. The concept of a coastal boundary layer has not in any significant sense been applied to local studies (Schumann Pers Com and Russell Pers Com). For reference purposes a map of southern Africa is given in Fig. 1.2a.

The most important area for upwelling studies in the Southern African context is the Benguela area but since coastal upwelling can occur on any coastline with favourable winds of sufficient duration other upwelling sites have been identified. Such non-Benguela sites have not been studied to any great detail. Upwelling effects are masked by the strong Agulhas current dynamics on the east coast (Pearce, 1977). Pople (1979) and Schumann (1979) report upwelling off Natal and East London respectively. Satellite imagery has revealed a number of upwelling centres with a shore attachment length of greater than 20 km on the leeward side of prominent capes of the Cape South coast (Schumann, Perrin and Hunter, 1982), which is collaborated with a study of daily sea temperatures at Cape Recife by Beckley (1983). The latter study is extended to Humewood and Sundays River Beach in Algoa Bay where the observed cold water is thought to come from upwelling further east at Cape Padrone (Beckley 1988). The penetration of upwelled water from Cape Padrone into Algoa Bay is discussed by Schumann, Ross and Goschen (1988). Agulhas current induced upwelling in Algoa Bay is reported by Goschen and Schumann (1988) and topographically induced upwelling is observed in the Natal Bight by Lutjeharms et al. (1989). At the Kariega estuary, localized upwelling is linked to the flux of organic carbon into the salt marshes (Taylor and Allanson, 1987).

Although the Benguela upwelling area has been actively researched in recent years, Nelson and Hutchings (1983) in their review state "The Benguela system remains relatively unexplored from the purely physical point of view ... studies are merely in support of fisheries science. Only recently have current meters etc been used so that very little is known of the shelf zone circulation, shelf waves or the response of the system to atmospheric forcing." A review of the literature shows that for the southern Benguela region there is a

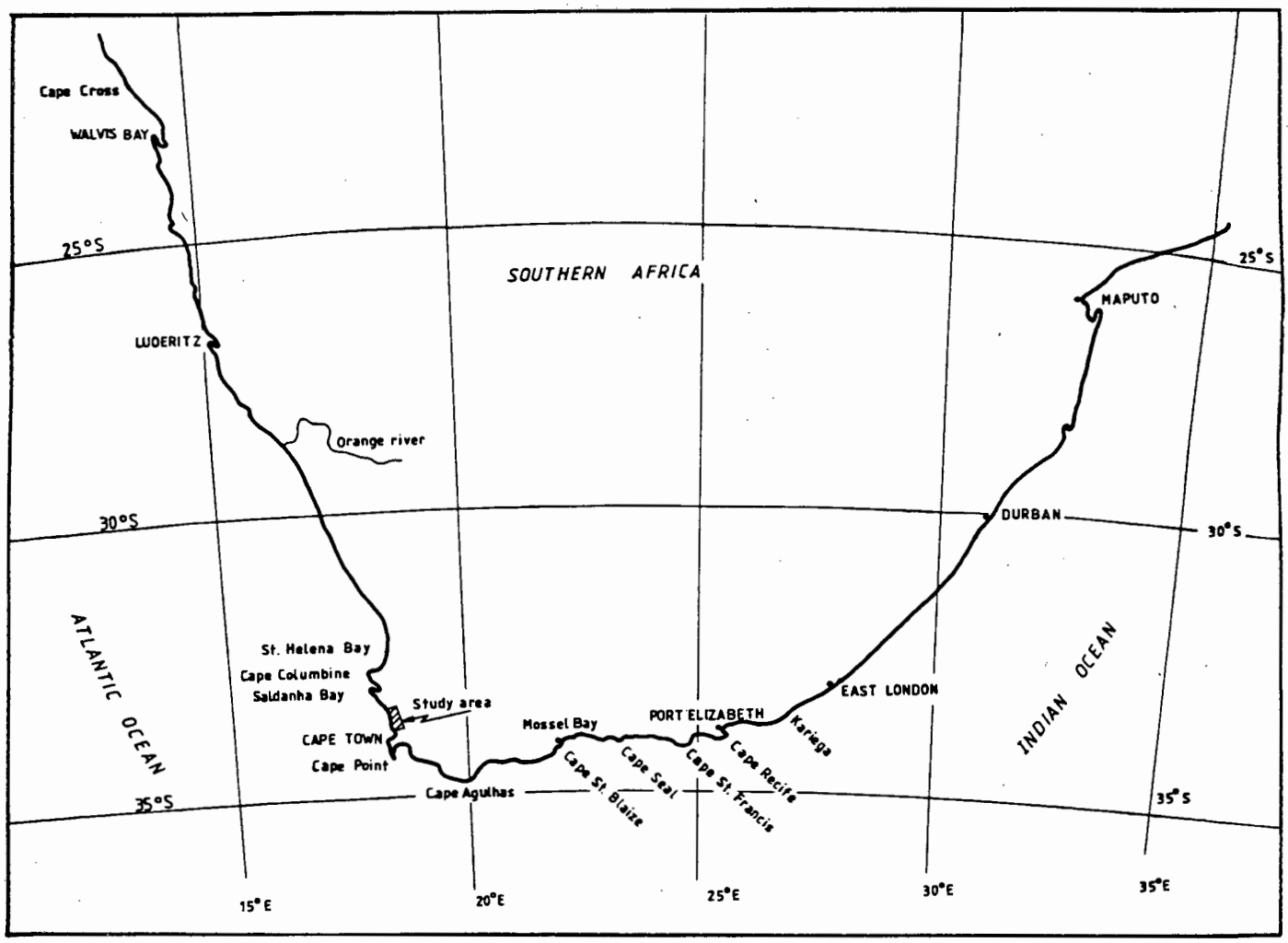

FIG. 1.2a LOCATION MAP FOR SOUTHERN AFRICA STUDIES

lack of reliable values and in some cases even estimates of some important oceanographic parameters such as bottom roughness, friction velocity, vertical eddy viscosity, Ekman scale depth and the Brunt-Vaisala frequency. Values for the latter parameter are mentioned in a paper by Nelson (1985). See section 1.4.3 for further details.

Recently, time series current meter data have been published for the area (Nelson and Polito, 1987; Holden, 1987) but these records do not fully meet the climatological requirements formulated by Boyce (1977, Section 1.2.3) and positionally tend to be more than 10 km offshore at depths exceeding 20 m. Except for waves and tides in general and the hourly sea temperature data reported in this study, there are no other published hourly-sampled long time-series data exceeding one year in duration from a single site for any coastal

parameter in South African waters. The main features of the new current data (Nelson and Polito, 1987) are: the poleward deep flow - the wave-like coastal currents with net poleward flow over periods of weeks - and the near surface jet which rounds Cape Point and moves northward. Holden (1987) observes alongshore current variations linked to barotropic coastal-trapped waves forced by synoptic scale winds. However, in general, synoptic time scale data are meagre and even for one of the major programmes to cover this gap, CUEX-1, it is admitted that the cruises did not fully realize that objective, (Shannon, Nelson and Jury, 1981).

Only one long term study on both the synoptic time scale and small spatial scale of less than 10 km has been reported (Gunn, 1977a and 1977b). Gunn characterized the circulation in two embayments, Matroosbaai and Buffelsbaai 16 km and 19 km respectively north of Melkbosstrand. The predominant forcing agents were found to be the wind and waves with a virtual lack of tidal currents and no evidence for any prevailing coastal current. In the smaller bay, Matroosbaai (1,5 x 0,5 km) the wave forces were dominant. In Buffelsbaai (4,5 x 1,5 km) the circulation had contributions from both wind and wave forces. Strong winds dominated the wave forces there. Some evidence for active upwelling in Matroosbaai was observed but stronger upwelling occurred in Buffelsbaai, but was less than that occurring at Melkbosstrand. Temperatures were found to dominate density changes and the salinities during upwelling were similar to that found at a depth of 400 to 600 m in the South Atlantic Ocean, deeper than that normally quoted of 300 m (Shannon, 1970). At a distance of 1 km offshore of the headland between the bays, currents were found to correlate well with local wind events and there was no indication of a net southward current as had been proposed by Duncan and Nell (1969) and more recently by Nelson and Hutchings (1983) and Nelson (1985) for further offshore. Current meter data west of Bok Point has a net southward trend but shows wavelike current reversals that seem to be moderated at the synoptic scale (Nelson, 1985, and Nelson and Polito, 1987). Similarly inspection of the UCT/ESCOM current data to a distance of about 10 km offshore does not show a net southward current. Further north however between St Helena Bay and Saldanha Bay, Lamberth and Nelson (1986) present some evidence of southward moving inshore surface currents.

The most pertinent study in the area of course is that conducted by the University of Cape Town Oceanography Dept in collaboration with the Electricity Supply Commission (ESCOM) for the evaluation of site characteristics north of Melkbosstrand for the release of thermal waters from the Koeberg nuclear power station. The earlier study of van Ieperen (1971) covering Table Bay up to Melkbosstrand was extended by the ESCOM programme to cover additional transect lines

slightly further north. ESCOM also set up two instrumentation towers; one in the sea a kilometer offshore included sea temperature probes and the other on land at Ou Skip had an anemometer and radar-set for wave direction studies. From the programmes inception in 1969 until April 1977 the UCT/ESCOM oceanographic investigations were presented in a series of 16 reports (Malory and Maxwell, 1969-1977). After April 1977 the routine running of the project was taken over by ESCOM who continued to issue quarterly data reports (Maxwell and Rattey, 1977 ff). Aspects of data collection are also given by Loewy et al. (1976). Since the objective of the Escom study was for thermal water dispersion problems and for design of the civil engineering works for the nuclear power station cooling water system, the data therefore tended to be presented in a statistical way such as monthly wind and current roses. However, valuable raw time series plots of wind/wave and wind/sea temperatures correlations were made. Very definite coastal upwelling effects were noticed with the strong southerly wind events. An important part of the work reported here makes use of the different UCT/ESCOM data sets.

Another study that has covered the region of interest but on a larger scale is that of Jury (1980 and 1984), who in aerial surveys mapped the wind field and sea surface temperature of the Cape Peninsula area as far north as Cape Columbine. His findings under southerly wind conditions of an intense wind (Cape Flats Jet) funnelled over the study area and a lee effect behind Table Mountain that extended northwards past Robben Island are of importance to this study and are discussed in the relevant sections. The role of coastal lows in forcing a coastal response is discussed by Jury MacArthur and Shillington (1989)

The surface wind data on Robben Island and in the hinterland surrounding the nuclear power station are reported by Norden et al. (1982) and Redding et al. (1982) and are of relevance in the determination of spatial aspects of the wind field over the adjacent coastal zone.

At the synoptic time scale for a duration of 24 days and at the micro spatial scale, Field et al. (1981) investigated the wind induced water movements in a kelp bed at Oudekraal on the Cape Peninsula coast. Grid stations covered only a 0,25 km^2 area with the maximum distance offshore being about 500 m in a depth of 22 m. Intense winds are orographically channelled over the site. The measurements of temperatures and Lagrangian currents at various depths at each of the grid positions occurred twice per day. Ekman transport correlated with the wind and in one case a decrease in current speed with depth apparently displayed an Ekman spiral. No correlation between currents and tide was noted. Unfortunately the structure of

the thermocline was not studied and although the winds were strong no major upwelling event occurred during the investigation. At the same site but further offshore in 35 m depth Boyd (1979) reports inertial current motion under calm conditions.

A relatively long sea temperature record from 1974 to 1986 is also available for the Oudekraal site. Although the instrument used records continuously (Fricke and Thum, 1975) only daily minimum and maximum values have been tabulated (Jarman, Per Com). Data sections appear in Walker et al. (1984) and Anderson and Hay (1986) but no significant sections have been correlated with local wind forcing.

A study by Boyd (1981) in the northern Benguela area near Cape Cross although only two weeks in duration and more than 7 km offshore is interesting because it is one of the very few that have studied the diurnal and multiday time scale processes in the region. An approximately rectangular grid of stations (with a main station in the centre) extending from 7 to 26 km offshore in depths between 25 m and 90 m was used in obtaining wind data, temperature profiles and currents at different depths using radar tracked drogues. Diurnal current structures were observed and the relationship between inertial currents and land sea breeze system noted. Useful comparisons with the theory of O'Brien (1977) for movement of a surface layer subject to sea breeze forcing were made.

In the study of currents in St Helena Bay using radio-tracked drifters on a scale of 10 to 30 km, Holden (1985) reports on diurnal aspects and the possibility of inertial currents. In a subsequent paper, Holden (1987) gives spectra of current meter data from the same area and correlates it to diurnal and synoptic wind forcing. In further offshore west coast waters, Schumann and Perrins (1982) give spectral evidence for tidal and inertial currents.

Other studies in the southern Benguela area that characterize the larger scale are discussed in Section 1.4 which outlines the attributes of the study area.

An overview of the literature review reveals that internationally there is a scarcity of studies in the coastal zone for small space scales of the order of less than the Rossby internal radius of deformation ($\sim$10 km) and for data on diurnal effects in shallow water less than 20 m in depth. Even for deeper waters on the shelf the scarcity of studies on diurnal effects is highlighted by the recent comment of Rosenfeld (1988) that his paper represents the first integrated analysis of diurnal period wind stress and currents. In addition to these shortcomings the southern African literature uncovers a lack of oceanographic studies at the synoptic time scale

and a general lack of hourly-sampled long time-series data (exceeding 1 year in duration) for any coastal variable except waves and tides. A detailed climatological and statistical assessment of coastal dynamics in Southern Africa does not exist and no coastal boundary layer has been identified.

1.3 THE STUDY OBJECTIVES AND MOTIVATION

At the site chosen near Melkbosstrand, multi-year time-series records of wind, sea temperature and waves are available. These data together with that obtained through additional synoptic time scale field work, form the data base of this study which has the overall aim of characterizing the dynamics of a small scale upwelling region (of order 10 km) over varying time scales. The importance of forcing by the local wind will be explored but effects on the dynamics of waves, tides, diurnal insolation and remote forcing, will also be considered.

This study will aim to:

- Characterize the dynamics of a small scale upwelling region
- Analyse statistically and spectrally the unique long time-series of coastal variables
- Establish the dominant time scales within the one hour to few year time scale and to establish the processes operating in these time scales and their causal relationships
- Identify any seasonal regimes, their characteristics and possible rapid transition between them
- Explore the effect of synoptic wind events on sea temperature response, thermocline structure and, to a limited extent, on currents
- Identify the effects of diurnal insolation and land/sea breeze cycles on the temperature response and dynamics
- Identify the spatial characteristics of the upwelling and the associated forcing factors including the role of coastline orientation
- Predict the upwelling response of the thermocline with a simple model
- Provide evidence for a coastal boundary layer
- Link shelf scale dynamics to processes within the coastal boundary layer.

The study will reveal the role of sea temperature in characterizing the physical oceanography of the area and will aim to complement the knowledge of the larger scale Benguela upwelling region and shelf dynamics and the smaller scale investigations of Gunn (1977). Man's

impact on the coastal environment continues to escalate and more needs to be known of small scale coastal dynamics in South African waters in order to assess the potential stress to this environment (Cloete, 1979).

The study site is already receiving the thermal releases from South Africa's first commercial nuclear power station; because additional power reactors will be erected on other coastal sites, the need for further impact assessment still remains for which this study may in part be useful. Knowledge of coastal zone processes can also aid fisheries studies and coastal marine biological studies in general (Owen, 1980).

In general the evaluation and application of models for shelfwater dynamics to the study area under consideration was not considered feasible, as the models are for a relatively large space scale (hundreds of kilometers) and for depths exceeding three times the Ekman scale depth. The model by Mitchum and Clarke (1986a) for the shallow nearshore region assumes a well mixed barotropic water column, as does the model of Bennett and Magnell (1979). Frequent stratification at the study site reduces the relevance of such models. Furthermore the testing of the above models requires detailed reliable current data which are lacking at the present site. However, a simpler model for the upwelling aspects by Csanady (1977a) is chosen for later assessment with the limited data base.

Although some of the diurnal data available could be used for a limited mixed layer study this was not attempted for various reasons given below. Even for oceanic sites advection of different water masses severely contaminates the diurnal temperature signal (Price et al., 1986). At a shallow nearshore coastal site vertical motions and advection due to alongshore currents, upwelling and rip currents should place even more severe restrictions on mixed layer studies. For meaningful mixed layer observations McCormick and Meadows (1988) exclude the nearshore zone and choose a site beyond the coastal boundary layer. Further the lack of suitable current data again precludes a viable study been made of either mixed layer dynamics or of friction parameters which are important in shallow water dynamics. In fact, Chapman (1987) states that it is not at all clear how the bottom friction coefficient should be estimated in regions where little or no current data exist.

In the following section the attributes of the site that will aid in achieving the aims of the study are discussed.

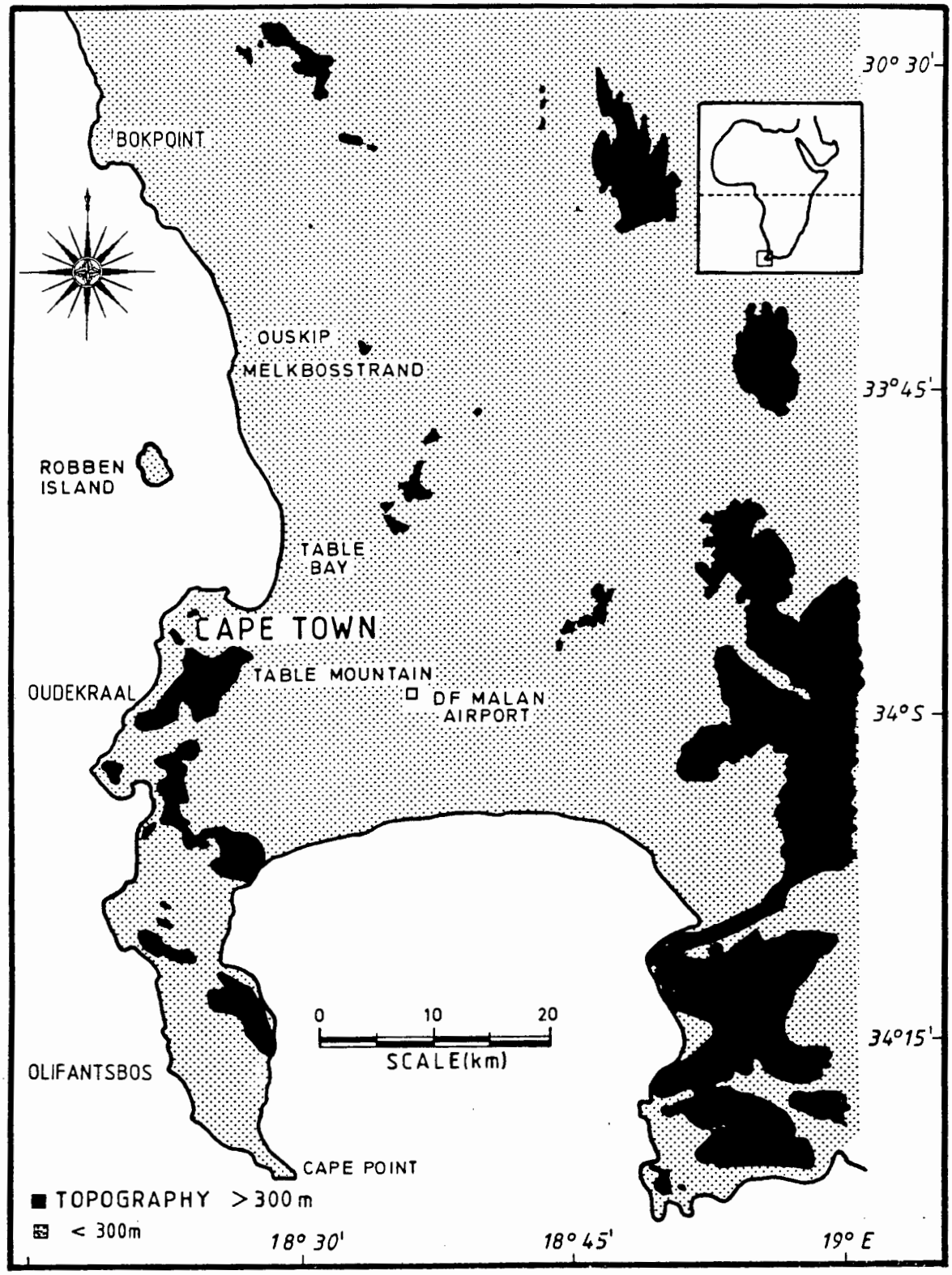

FIG. 1.2B THE STUDY AREA IN REGIONAL CONTEXT AND TOPOGRAPHIC FEATURES ABOVE 300 m

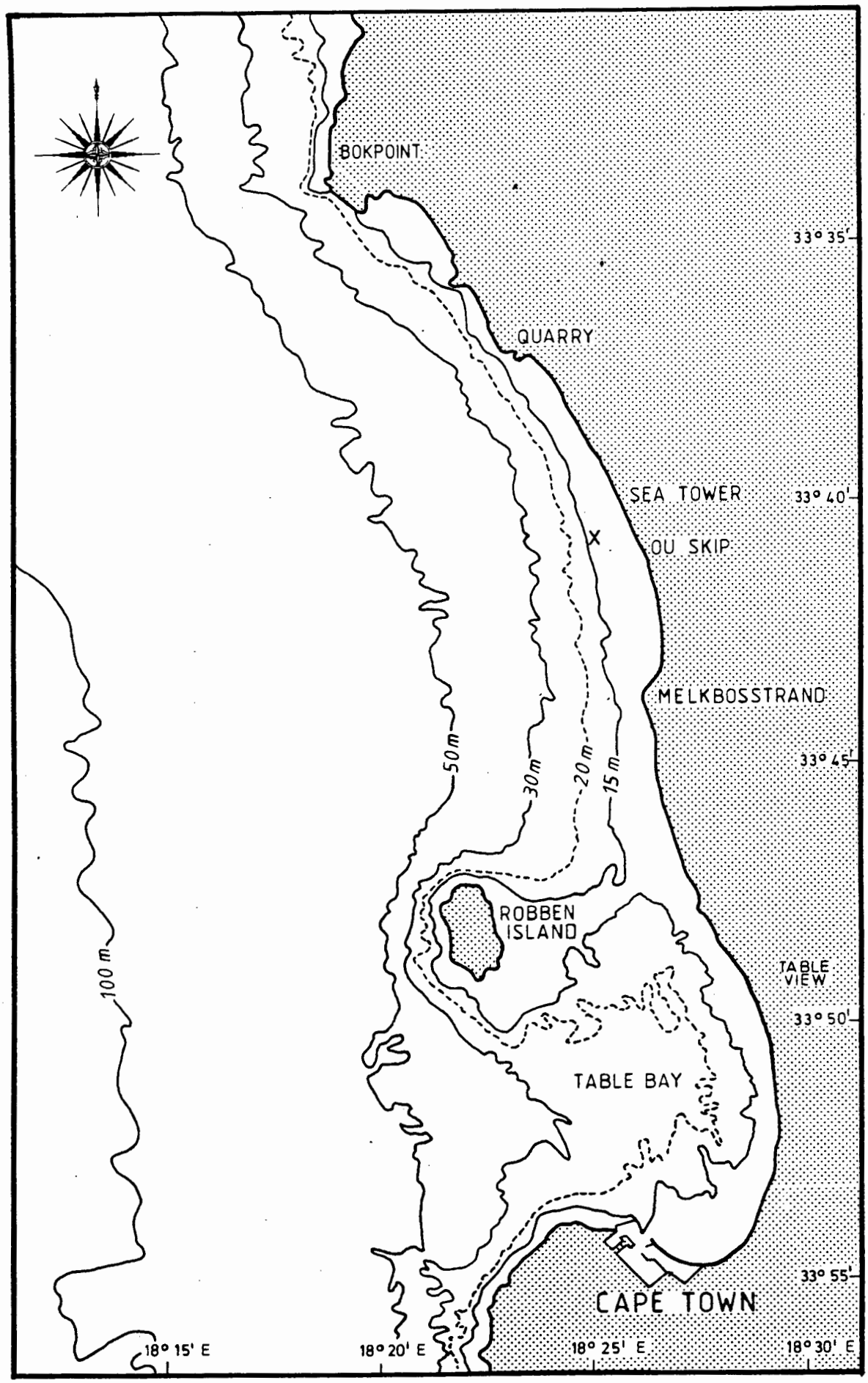

FIG. 1.3 THE BATHYMETRY OF THE STUDY AREA

1.4 THE STUDY SITE

1.4.1 Physical Character

The study site lies near the south west tip of South Africa and is centred some 25 km north of Cape Town close to Melkbosstrand, 33° 44' S, 18°26' E (Fig. 1.2b). Investigations cover a coastal length of 40 km from Table Bay in the south to Bok Point in the north. Intensive studies extend from the Melkbosstrand headland 7 km alongshore in a northerly direction to the sea tower and 6 km offshore. The bathymetry (Fig. 1.3) is fairly uniform directly offshore from the Melkbosstrand area with the depth contours lying essentially parallel to the coastline. The average bottom slope to the 100 m depth is 1:200, and to the 40 m depth (6 km offshore) is 1:150. The adjacent shelf has a width of order 60 km and an average slope of 1:250, while the continental slope is 1:23. The only noteworthy bathymetric feature in the local area is the shallower water between the mainland and Robben Island, lying some 10 km south west from Melkbosstrand. The coastline consists mainly of long sandy beaches with a few small rocky promontories. The largest change in coastline orientation occurs at Melkbosstrand headland. The sea floor is also mainly sandy in nature.

On the larger scale at distances greater than 30 km from Melkbosstrand the orography rises to over 1000 m (Fig. 1.2b) and is of considerable significance in affecting the gross wind field (Jury, 1984). However nearer to Melkbosstrand the orography is insignificant with the highest hill some several kilometers SE of the site being less than 200 m above sea level.

1.4.2 The Meteorology of the Site

A Mediterranean type climate prevails at this south west tip of Africa. Dry summers and wet winters are characteristic of the area. The causative conditions are the seasonal variation of the latitudinal position of the South Atlantic high pressure system. In summer the South Atlantic anticyclonic cell with a latitudinal axis at about 30 °S ridges in south of the continent and causes strong south and south-east winds which are enhanced by the continental and escarpment influence. These winds are upwell favouring from Cape Point northwards up the west coast. The mean isobars for mid summer (January) are shown in Fig. 1.4a which is adapted from Fig. 4.1 in Taljaard, Van Loon and Newton (1972). By mid winter (July, Fig. 1.4b) the anticyclone has migrated NW to be centred at about 26 °S. This equatorward shift allows the cyclonic depressions that advect eastwards to intercept the southern part of the west coast and results in NW to SW winds often accompanied by rain.

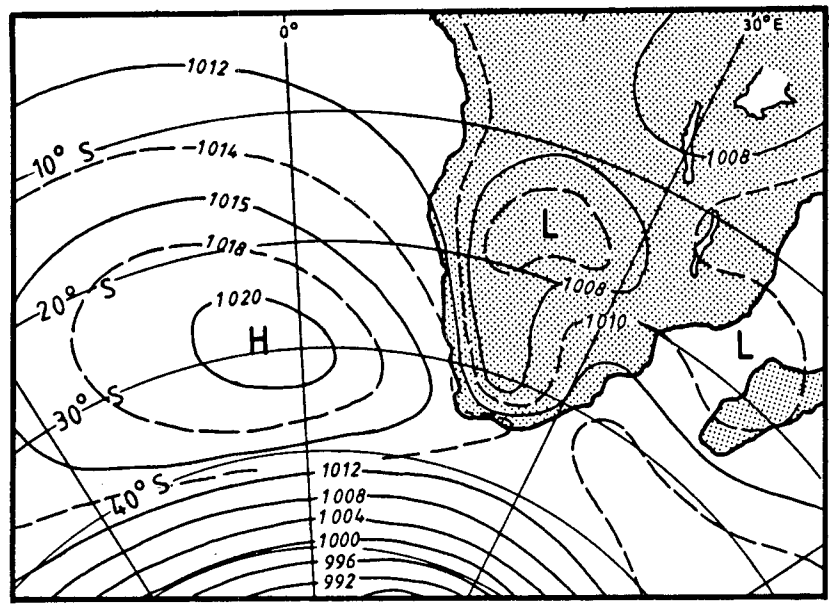

(a) JANUARY

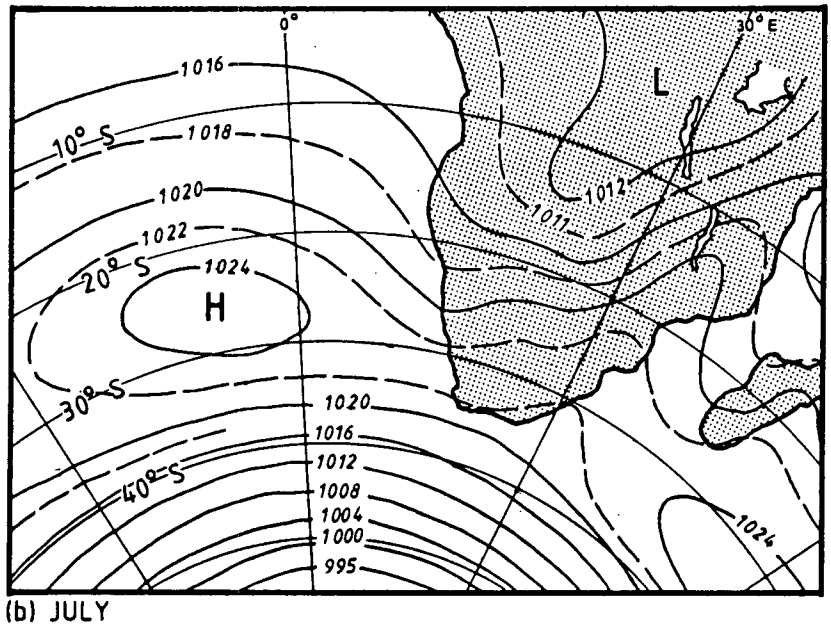

(b) JULY

FIG. 1.4a,b. THE MEAN SEA LEVEL ISOBARS OVER THE SOUTHERN AFRICA REGION FOR a) JANUARY AND b) JULY AFTER FIG. 4.1 OF TALJAARD ET AL. (1972)

The predominant winds of the southwestern Cape viz, southerly, northerly and variable can be attributed to three broad categories of synoptic conditions (Keen, 1979). These are a) a South Atlantic anticyclone off the west coast ridging into the south of the country that produces stable southerly winds b) cold, frontal systems that pass over or just south of the Cape, that result in northerly winds and c) a South Atlantic anticyclone that lodges over the Cape interior, and has associated light and variable winds. The northerly winds associated with the (winter) cold fronts are unstable (Keen, 1979) and the direction of northerly "events" are more variable than

the southerly "events" in summer. Other workers (Redding, et al. 1982; Jury, 1980) expand and subdivide these broad categories. The main addition is the ubiquitous presence of coastal lows that play a crucial role in the local wind event cycles (Hunter, 1987) and in the decay phase of coastal upwelling (Jury, 1986). Coastal lows, the passage of which are characterized by sharp changes in the wind direction from southerly to northerly in the study area, are generated by two general types of synoptic situations (De Wet, 1984). The first is when a high pressure system ridges in south of the land causing interior easterly flow with descending air along the west coast. Due to vortex stretching as the winds descend over the coastal escarpment a cyclonic lee effect then produces the coastal low. Secondly when a trough of low pressure moves across the southern parts of the country to the east, a "leader cell" of low pressure forms along the south and southeast coast. In both cases the systems are very shallow. The independent propagation of the coastal low southwards along the coast has been equated to a coastally trapped Kelvin wave, with non-linear effects giving more prominence to the low than to the high pressure systems, Gill (1977). The generation of such trapped coastal lows for South African conditions has been modelled by Ahn and Gill (1981). The link between these trapped atmospheric waves and associated trapped barotropic shelfwaves is discussed in detail for the South African coast by Jury, MacArthur and Shillington (1989). In a study of data covering winter and spring, Schumann (1989) finds a significant difference between the propagation of air pressure systems and wind systems along the South African coast and suggests that the west coast low and south coast lows are generally separate systems. Some case studies for coastal lows presented by Hunter (1987) for the Cape south coast favours, in contrast to the Gill concept, a continual generation process (de Wet, 1984).

Four summer wind regimes are identified by Jury (1980) over the Cape Peninsula. These are further discussed and itemized by Jury (1987) as:

a) A post cold front SSW wind
b) A ridging anticyclone with deep SE wind
c) A pre-coastal low condition with shallow ESE winds and
d) a wave cyclone with WNW winds.

It must be pointed out that these wind directions used by Jury to name the regimes are for a larger scale and because of the steep orography and varied topography the actual wind direction can be quite different from place to place. In the study area, lying north of the main Peninsula mountain chain, the Cape Flats Jet (Jury, 1980) is steered more SSW to SSE and no strong ESE winds are experienced

there. Such spatial effects of the wind field are discussed more fully in Section 4.4. The offshore directed winds at the site from the NNE to E sectors are associated with the occurrence of "berg winds" another large scale meteorological feature of the region. Berg winds, more common in autumn and winter are linked to high pressure systems that cause offshore flow from the plateau of dry adiabatically heated air and are often precursors to coastal lows, (Shannon 1985).

Another feature of the study site is the diurnal modulation of the alongshore winds by a relatively regular and strong sea breeze system in summer. With little cloud cover in summer the high insolation strenghtens the thermal contrast between the land and the cold coastal waters and enhances the sea breeze system (Jury, Kamstra and Taunton-Clark, 1985).

In comparison, on the Cape south coast the land breeze is relatively stronger (Hunter 1987). Coriolis deflection of the sea breeze is additive to the gradient southerly winds in the evening; at mid morning opposition to the gradient winds is observed (Jury 1980). The prominent orography of the Cape Peninsula produces, for southerly winds, variable wind wakes that can influence the study area and with the gradient winds being diminished in the leeward areas the land/sea breeze system can play a more dominant role, (Jury, 1987).

The percentage occurrence throughout the year for different synoptic categories is according to Redding, et al. (1982) as follows:

a) for the anticyclone ridging in south of the country - 43 %
b) for cold frontal system passing over the Cape - 32 %
c) for anticyclone lodged over the Cape giving light variable winds - 3 %
d) for coastal lows moving around the Cape - 22 %.

Keen (1980) estimates that about 40 % of all southerly wind conditions are the shallow southeaster type, and that sea breeze conditions occur on 20 % of summer days.

The statistics for the passage of coastal lows is not well established being based on analysis of approximately one year long data sets of Walker (1984) for the west coast in 1981 and Hunter (1987) for the Cape south coast in 82/83. During February and October, Walker (1984) observes the passage of coastal lows to occur once every 6 days on average and for the whole year about 1 in 10 days. Hunter (1987) observes a more frequent passage of 10 per month. Although more coastal lows can be expected on the Cape south coast where "new" coastal lows can be generated, the data base used

unfortunately includes the anomalous summer of 82/83 when a series of weak cold fronts passed the area (Brundrit, Diab and Jury 1984). However, the main point to be stressed on this aspect of coastal lows is that they are relatively frequent and at the site often delineate a coastal wind event cycle. A typical cycle follows in sequence, the four summer wind regimes categorized by Jury above. Between his regime c) and d) a coastal low can intervene.

Additional aspects of the local meteorology will be discussed in subsequent chapters.

These varying wind conditions lend a distinctive seasonal, synoptic and mesoscale character to the area. Further, the steep orography of the Cape Peninsula and the eastern hinterland, coupled to the varying inversion heights radically alters the wind fields (Jury, 1984 and 1985) with pronounced effects on coastal upwelling. This leads on to a discussion of oceanographic features.

1.4.3 Oceanographic Features

The chief comment is that the study site is embedded in the larger scale southern Benguela upwelling region. Although the northflowing Benguela "current" forms a portion of the South Atlantic anticyclonic gyre it is not well defined as an oceanic current and is more fittingly described as the Benguela system (Shannon, 1985a). It lies tens of kilometers offshore in the south and tends to move offshore further north as revealed by satellite tracked drogues (Harris and Shannon, 1979 and Nelson and Hutchings, 1983). Its flow is augmented by the shelf edge jets off Cape Columbine and the Cape Peninsula (Bang, 1973). These jets which are the most prominent feature of the seasonal upwelling system are the result of strong SE winds that are intensified through interaction with the steep orography of the South West Cape (Jury, 1984; Jury, 1987). The CUEX-1 programme studied the "plume" dynamics off the Cape Peninsula and showed that the current field was remarkably barotropic away from the coast and that the closer currents were weaker but strongly baroclinic (Shannon, Nelson and Jury, 1981). More recent current time series data however show for nearshore sites the dominance of barotropic motions at the synoptic time scale (Nelson and Polito, 1987 and Holden, 1987). Shannon et al. (1981) also measured strong channeling of flow up the Cape Point Canyon which could be important for the overall upwelling response of the area. Aspects of currents off the study area are given in Section 1.2.4.

For the southern Benguela region there is a lack of published values for some important oceanographic parameters - bottom roughness, friction velocity, vertical eddy viscosity, Ekman depth etc. Values

for some parameters are estimated here.

The classical Ekman depth is based on a constant (kinematic) eddy viscosity A. (see section 1.2.1). If the latter is assumed to be 200 x 10^{-4} $m^2.s^{-1}$ then at the site 34 °S where the Coriolis parameter f = 0,82 x $10^{-4}.s^{-1}$ the Ekman depth will be D = 69 m. The value of A however is not reliably known (Price, Weller and Schudlich, 1987) and can vary widely. As bounds to the value of A we can take a low value of 60 x 10^{-4} $m^2.s^{-1}$ and a high value of 540 x 10^{-4} $m^2.s^{-1}$ as found by Price, Weller and Schudlich (1987) for a diurnally stratified site at 34 °N. If these values are used in the classical Ekman equation then D is 38 m and 114 m respectively. The indirect method of Marmorino (1983) for determining the Ekman depth from various parameters, including the friction velocity, is subject to too much uncertainty for local waters because of the lack of reliable parameter values. However, use of generic parameter values suggest that the local Ekman depth is closer to the shallower value given above. Clearly the scale depth of the wind generated mean current depth varies greatly and affects the local scale dynamics. (This will be addressed in Chapter 5).

With regard to stability of the water column, values of the Brunt-Vaisala frequency and its variation are sparsely reported for the region. It is expected to have a high variability as shown by standard deviations of the frequency profiles off California (Chapman, 1987). Largier and Swart (1987) use a Brunt-Vaisala frequency, N = 0,013 $rad.s^{-1}$ in the Agulhas Bank region while Nelson (1985) reports that for the off-shelf region west of the Cape Peninsula N varies from 0,03 $rad.s^{-1}$ near the surface to <0,008 $rad.s^{-1}$ below 50 m. On the shelf off Bok Point the shelf-averaged Brunt-Vaisala frequency squared is calculated from sigma-t section data in fig. 10 of Nelson (1985). The shelf-averaged N^2 value is estimated from the mean of four vertical profiles spaced across the shelf (10, 30, 50 and 70 km) where at each position the vertically averaged N^2 value is determined with 10 m vertical steps. For the case chosen this yields a value of $N^2 = 3,06 \times 10^{-4} rad.s^{-1}$. The associated Rossby baroclinic radius of deformation is estimated to be about 10 km. (See 1.2.1).

The Brunt-Vaisala parameter together with the shelf slope can be used in the criteria of Clarke and Brink (1985), $N^2\alpha^2f^{-2}<<1$, to do a rapid check on the likelihood of a barotropic shelf water response to synoptic wind forcing - see Section 1.2.1, p 1.11 for details. For the shelf off Bok Point the mean slope from the four positions mentioned in the previous paragraph is $3,6 \times 10^{-3}$; $f = 0,82 \times 10^{-4}$ and N^2, calculated above, is $3,06 \times 10^{-4}$ $rad.s^{-1}$. Substituting these values into the criteria gives a value of 0,59. Choosing a less

stratified case e.g. Fig 8 of Nelson, 1985, and doing similar calculations to the above gives a criteria value only slightly smaller. Such values are interpreted by Clarke and Brink (1985) as suggesting that the shelf can have either a baroclinic or barotropic response. This ambivalence is supported by the previously cited findings of baroclinic and barotropic activities on the local shelf.

Density of the water mass is mainly temperature controlled (Shannon, 1985a and Gunn, 1977). There is no significant fresh water flow into the area. The Little Salt River (Fig. 1.7) is virtually dry in summer and has episodic flows in winter that average less than 1 $m^3.s^{-1}$. The isopycnals are perenially upward tilting below 50 m with the westerly downwelling winds affecting mainly the top 50 m region. At times an intense front develops on the upwelling plume and can be reduced to patchiness with relaxing winds (Bang, 1973).

Non local effects are as yet not well defined for the area, although van Foreest (1981) and van Foreest et al. (1984) have linked some mesoscale features further north to barotropic shelf waves; Shannon (1985a) discusses the possibility of the spring priming of the southern Benguela region being mediated from equatorially generated coastal Kelvin waves and Holden (1987) presents evidence for poleward propagating continental shelf waves on the west coast. The latter are associated with synoptic weather systems such as coastal lows and link in with associated sea level fluctuations over a large space scale, reported by Brundrit (1984) and De Cuevas, Brundit and Shipley (1986). Case studies for the coastal low forcing a barotropic shelfwave are discussed by Jury MacArthur and Shillington (1989).

For distances up to 100 km offshore Christensen (1980) has prepared monthly ten year average sea temperature charts for the South African coast. Also from shipping data Boyd (1983) gives seasonal average sea temperatures along the west coast for sea areas 30 to 250 km offshore. Similarly, Kamstra (1985) uses 50 year ships data to give quarterly sea surface temperature maps for the south east Atlantic between the Orange River and Cape Agulhas. These data tend to mask upwelling effects but show the gross feature that in summer about 100 km offshore of the site the temperature is 20 °C and in winter is 16 °C. This is of course a mean picture and at times such temperatures can be quite close inshore as revealed by satellite imagery that also shows Agulhas water rounding Cape Point (Lutjeharms, 1981 and 1988). In fact the influence of the Agulhas Current System is considered important in the dynamics of the southern Benguela upwelling region (Shannon, 1985a) with the occurrence of energetic Agulhas rings in the SE Atlantic contributing to the complexity of the system (Lutjeharms and Gordon 1987). Even subantartic water can episodically enter the Benguela region in the

form of cold filaments that can act as perturbations of two month duration (Shannon et al., 1989).

Van Ieperen (1971) did a study of currents, temperatures and salinities in Table Bay. The currents, mainly measured using drogues and floats were found to be almost exclusively wind driven and predominantly to the north (81 % in summer and 69 % in winter). A small east-west tidal current south of Robben Island was estimated to be less than 7 cm/s and negligible elsewhere. Although temperature data were collected they were not interpreted in terms of upwelling dynamics. Inspection of Van Ieperen's (1971) tabulated monthly temperature data for the deepest stations (50 m) shows that the 10 °C isotherm is generally at a depth exceeding 50 m for May to September and often shallower than 25 m for summer. Shannon (1985a) quoting from Duncan (1964) gives for the offshore area at 33 °S a thermocline depth of 39 m in winter and 17 m in summer.

Other more local oceanographic features include the following: The tidal range at spring tide at Table Bay is 1.4 m and that at neap tide is 0,5 m. Tidal currents are negligible in the region and even at the mouth of Saldanha Bay moored current meters do not show strong tidal influences (CSIR, 1976). The study area is exposed to the prevailing SW swells and lies on a section of the South African coastline that experiences the greatest wave energy (Russouw, 1982 and Retief, 1982). Maximum wave heights of over 10 m have been observed near Melkbosstrand (Jury et.al. 1986).

In summary the following attributes of the Melkbosstrand site make it interesting for a small scale upwelling study. It is on the inshore edge of a major upwelling site and as such can complement the larger scale studies. There are no obvious prevailing oceanic or coastal currents closer than several kilometers from the site. Tidal currents are negligible. The bottom topography is uniform and gently sloping. The coastline too is uniform except for the offset at Melkbosstrand. The immediate orography can be neglected as an influence on the wind. These attributes lead to the proposition that the prevailing winds are by far the major forcing factor in the local oceanographic environment. As such the site can serve as a relatively uncomplicated prototype in the same sense as proposed by Csanady (1982a) for the study site in the Great Lakes and off Oregon. However the unique features of the larger scale and possible remote effects will be borne in mind.

1.5 RESEARCH METHODOLOGY

1.5.1 Introduction

The basic approach adopted is empirical in nature. The research methodology has two main facets; that of the analysis of local site specific time series data and the collection and analysis of additional field data for both the small scale spatial characteristics and for the synoptic or shorter time scale.

The literature review has shown that time series data provides a valuable framework for characterizing different processes. An emphasis is placed on time series data of wind and sea temperature. The behaviour of the latter parameter can indirectly give a reasonable idea of dynamic processes taking place, since locally, temperature controls the water density (Shannon, 1985a) and temperature spectra are shown (Fofonoff, 1969 and Winant, 1983) to correlate with kinetic energy spectra. Lagrangian tracking of flow has some advantages in supplementing Eulerian point source data sets and is used in this study. In general because of rapid changes within the study area the choice of supplementary field techniques has aimed to gain simultaneous data coverage over the spatial scale studied. The time series data base is now discussed followed by the different stages of time series analysis.

1.5.2 Time Series Data Base

Over a number of years ESCOM collected continuous time series data that included wind, sea temperature and waves at a site north of Melkbosstrand where South Africa's first nuclear power station now operates, Fig. 1.3. As outlined in the section on motivation for the study, wind and sea temperature are considered important parameters in the area and in particular these are chosen for detailed analysis.

The wind data are derived from a Lambrecht anemometer set at a height of 14 m above ground level some 10 m from the high water mark at Ou Skip (Fig. 1.3). The hourly tabulations of direction and speed produced by ESCOM are used as input to the data base for computer manipulation. Winds less than 7 $km.h^{-1}$ are classified as calm or light airs. The Lambrecht is considered a standard type of anemomenter and the data quality is good. The continuity of the data is better than 98,8 % over the four year period 1975 to 1978 chosen. It is shown later in Chapter 3 that wind data from DF Malan airport situated 35 km SSE from the site correlates reasonably with Ou Skip data and any gaps in the latter are interpolated with DF Malan data.

The instrumentation on the ESCOM sea tower at a distance of 1 km

offshore in a depth of 11 m (Fig. 1.3) included three temperature probes at 2 m, 5 m and 8,5 m below mean sea level. [For the sake of brevity, future reference to the 8,5 m level will quote 8 m.] The output of these probes (Model 1331 Rustrak thermistors) were recorded continuously on a multichannel chart recorder (Diel) that operated at a chart speed of about 5 cm/hour. Although the time response of the temperature probes in their protective housing was less than a few minutes and theoretically allowed digitization to occur at 5 min intervals, ESCOM had only extracted the temperature data from the chart record at a six (6) hour or occasionally at a three (3) hour time step which was considered too long for this study. A sample interval of 1 hour which corresponded to the interval of the available wind data was chosen for digitization.

The digitization, editing and quality control of the temperature data proved to be a major undertaking. Because of the accessibility problem the sea tower was usually serviced once a week which, with breaks in the data, and occasional calibration drifts, led to possible ambiguous time references and temperature level problems which had to be resolved. All digitized data were plotted on a large scale and checked visually for errors. Although the temperature record is available from 1974 to June 1978 the time consuming nature of manual digitizing and verification of the data limited the analysis of hourly data to the period November 1975 to July 1978 for the three probe depths. A 12 hourly data set for the 5 m depth probe covers the period, August 1974 to May 1978.

The stability of the temperature probes was 0,1 °C. The absolute accuracy was limited to 0,5 °C which sometimes resulted in a probe at a lower depth apparently measuring warmer temperatures than that above it. Temperature overturning due to evaporation effects has been reported by Pople (1971) for tropical waters. Such effects were checked for in other sources of temperature data for the area e.g. Bathythermograph traces, van Ieperens (1971) Table Bay and Melkbosstrand studies and CSIR cruise report (NRIO rept 8121). On only two occasions in these data sets were slight temperature inversions anomalies noted that were not compensated by salinity differences. Adjacent stations did not show such anomalies and it is concluded that such data represent statistical outliers and not an overturning event.

Because of the generally good correlation between temperatures at different depths any breaks in the temperature record at one depth could usually be interpolated with available data from another depth. (Where appropriate, allowance was made for a temperature gradient.) A back-up chart recorder (RUSTRACK 2133) on the sea tower provided some redundancy in the temperature data and this was also

used at times to interpolate any gaps in the primary record. The continuity of the temperature record using the interpolation procedures mentioned was 95 % for the three years covered. The remaining gaps were interpolated linearly to provide continuity for time series analysis. Aliasing effects due to the digitizing interval chosen was not considered a problem; occasional higher frequency fluctuations were observed in the raw temperature data but these were of amplitude less than 0,2 °C and would represent very low energy in the frequency spectrum.

1.5.3 Analysis of the Time Series Data

The analysis of time series data has many facets. An overview of the different stages of analysis is given in a flow diagramme representation in Fig. 1.5. Spectral analysis is seen to be a subset of time series analysis. The different stages are now discussed and are partly based on techniques given by Jenkins and Watts (1968) and by Bendat and Piersol (1971).

After the first stage of formation of the time series through the digitization procedures, subsamples comprising years, seasons or events are selected and further processed. Vector data are first decomposed into orthogonal components. Following the methodology of Huyer, Sobey and Smith (1979) the vectors are rotated to lie 20° west of north such that the one component lies alongshore (approximately north/south) and the other lies across-shore (approximately east/west). For the wind vector this alignment is similar to the principal ellipse axis given by the rotary spectral analysis (Table 5.4) and is supported by the wind rose data given in Table 3.1.

The next stage is filtering of the digitized data. This is done to suppress certain frequencies with either a high pass, low pass or band pass type filter. This has the effect of partitioning the data into different frequency bands and if residuals are used then a detrended data set is obtained. Physical oceanographic data are commonly divided into a high frequency region (with frequencies in the inertial range or greater), an intermediate frequency region (frequency less than the diurnal frequency but greater than the synoptic frequency range) and a low frequency or very low frequency range that reveals seasonal trends (Huyer, et al., 1979). The choice of subdivision frequencies can be based on minima in the spectral energy which often indicate a transition from one dominant process to another (Lee and Mayer, 1977).

In this study a running mean type filter applied twice as discussed by Chelton and Davis (1982) was initially used but the filter frequency response function has unsatisfactory cut-off characteristics and

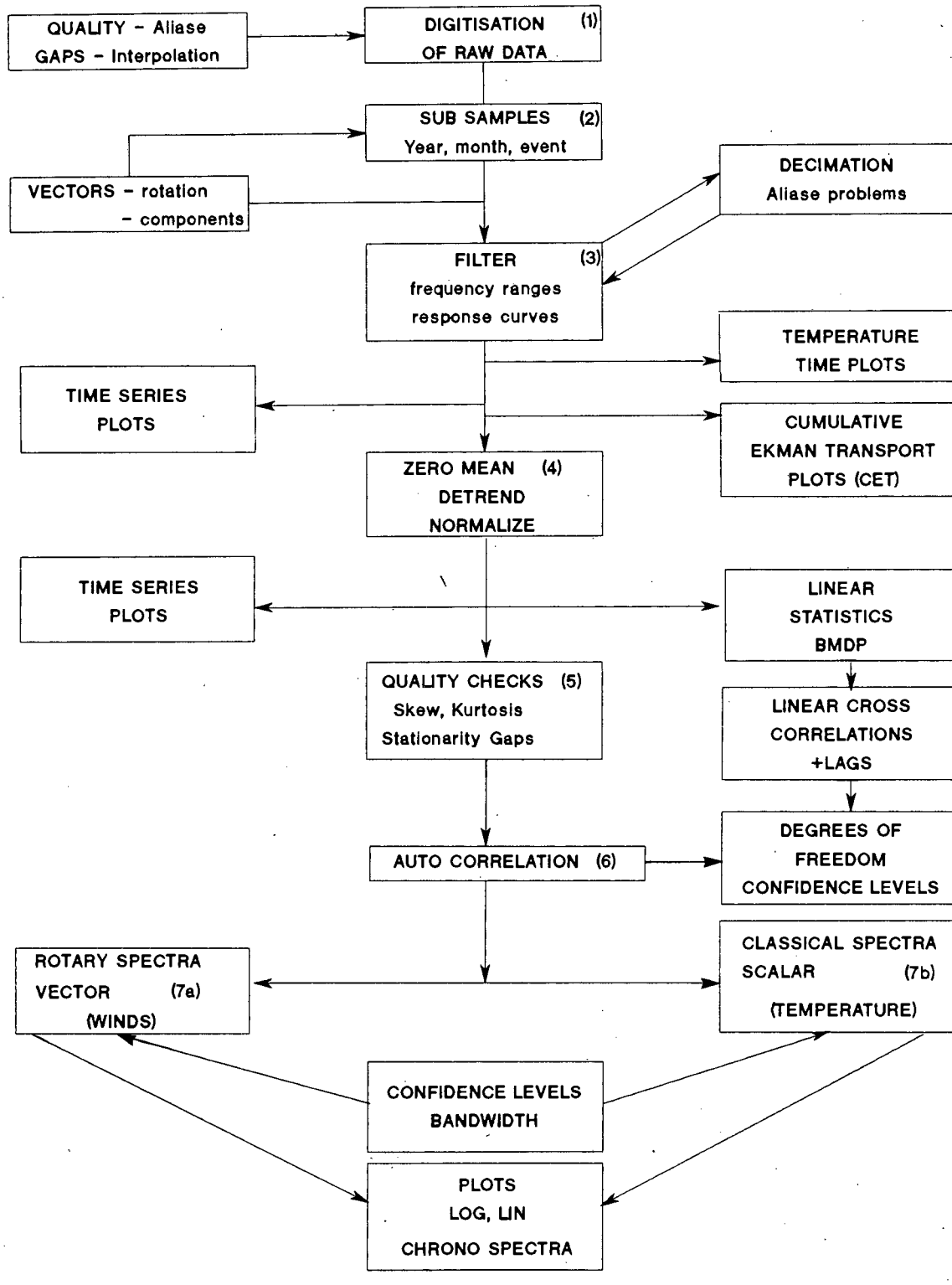

FIG. 1.5. FLOW DIAGRAM REPRESENTATION OF STAGES IN TIME SERIES ANALYSIS.

the Lanczos-cosine filter was subsequently used for all the filtering (Mooers, 1968). In the latter filter the position in the frequency domain where cut off is required is specified by the user selected quarter power point and the steepness of the cut off can be enhanced by increasing the number of weights used. The computer code version of Schumann and Swart (Pers Com) is adapted for use in this study. The frequency response curve for the low frequency range with a quarter power point at 1/36 cph and using 97 weights is given in Fig. 1.6. The low frequency (LF) data for frequencies less than 0,5 cpd are obtained by applying the above described filter. The high frequency (HF) data for frequencies greater than 0,5 cpd are obtained as the hourly residual of the original data minus the LF data. The very low frequency (VLF) data for frequencies less than 0,025 cpd are obtained by decimating the LF data to each 12th point and applying the Lanczos-cosine filter now with a quarter power point of 1/40 cpd having 49 weights. The intermediate low frequency (ILF) data for frequencies between 0,025 and 0,5 cpd are obtained as the daily residual of the LF data minus the VLF data.

The highest possible frequency for the hourly digitized data is 0,5 cph - the Nyquist frequency f_c. For a frequency f less than f_c the higher frequencies that are aliased with f include $2f_c \pm f$. The original character of the wind and temperature data is such that aliasing effects can be neglected in that frequency range. However care must be exercised at the decimation step in forming the VLF data. A decimation of every 24th point results in some aliasing problems whereas the 12th point decimation used is satisfactory.

After filtering, the data can be represented in various graphical plots for visual inspection. The HF data are plotted with an hourly interval and the LF and VLF data are plotted with a daily increment. The LP filtered wind data are used to calculate the wind stress using a constant value of $1{,}58 \times 10^{-6}$ g.cm^{-3} for the combined air density and drag coefficient factors after Jury (1984). Although the drag formulation of Large and Pond (1981) which varies with wind speed above 11 m.s^{-1} is generally preferred for (over-the-water) wind stress calculations the constant value used here is adequate because, 1) in comparison, the subsequent cumulative Ekman transport (CET) calculation has larger uncertainties due to shallow water restrictions and 2) the stress is not used in any shelf model evaluations. The cumulative Ekman transport is calculated according to the method of Huyer et al. (1979) where a time integral over the standard Ekman transport is taken beginning when the alongshore wind stress component, τ changes sign at t_o and terminating when it changes sign again.

$$\text{i.e. } CET(t) = \int_{t_o}^{t} f^{-1}.\tau(t)\, dt$$

At any point in time the value is proportional to the Ekman transport since the beginning of the wind event. Although for shallow water this calculated CET is an oversimplification it does provide a useful measure of upwelling (and downwelling) events particularly when presented graphically (Csanady, 1982a).

The fourth stage of the analysis is to create a version of the filtered time series with a zero mean. (The HF data set being a residual already has a zero mean.) Each individual subset (year, month, etc) is detrended by establishing a straight line fit to the data using a least squares procedure and subtracting it from the data. Finally each data set is normalized by its variance. This allows a meaningful comparison to be made between different variables and is essential if cross correlation analysis is undertaken (Düing et al., 1977). A standard software package for statistical analysis (Biomedical Data Processing, BMDP) on a Sperry mainframe computer is used to extract linear statistical information from the time series and is also used together with a suitable algorithm to lag one variable against another to evaluate linear cross correlation coefficients for variable lags.

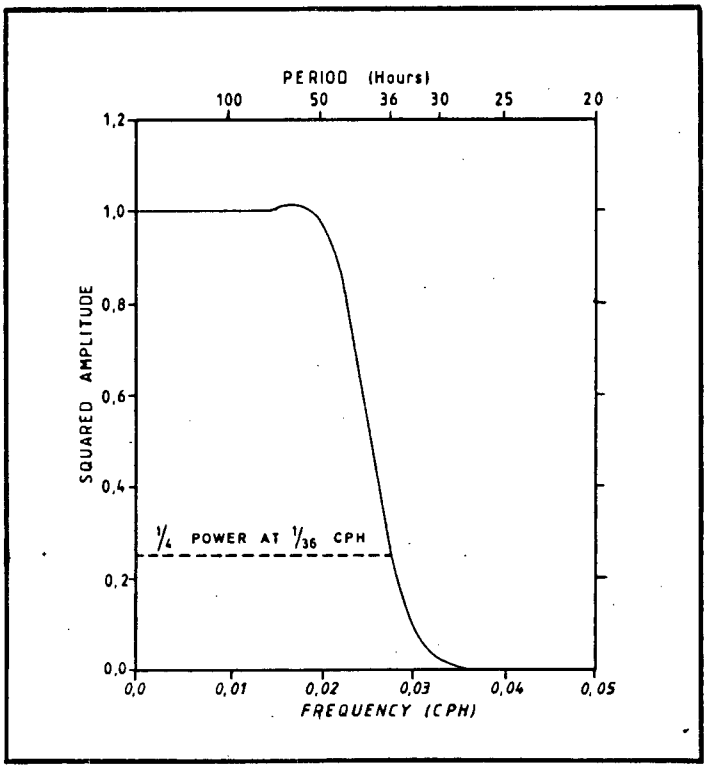

FIG. 1.6. FREQUENCY RESPONSE CURVE FOR THE LOW FREQUENCY LANCZOS-COSINE FILTER USING A QUARTER POWER POINT OF 1/36 cph AND 97 WEIGHTS

The fifth stage is to perform data quality checks on the detrended normalized data. For statistical reasons spectral analysis assumes that the time series data are stochastic, stationary and that the probability distribution associated with the observations are Gaussian (Jenkins and Watts, 1968). In order to check how closely the data meet these requirements various checks are done on the data; skewness and kurtosis statistical calculations are done to establish the Gaussian character; the stationarity is checked by observing the distribution about the mean of the segmented data set (Bendat and Piersol, 1971). Statistical theory assumes that an adequate description of a stochastic stationary process is given by the lower moments of its probability distributions which include the mean, variance, autocovariance and the power spectrum (Jenkins and Watts, 1968). This understanding leads to the following analysis stage which is the formation of the sample autocovariance function.

The autocovariance function is a measure of the correlation between neighbouring points in the time series and when it is normalized by the covariance at zero lag the autocorrelation function results. The main use of the autocorrelation function in this analysis is as input for the formation of the power spectrum but two other aspects are first discussed.

1) The plot of the autocorrelation function gives a measure of the decay scale of the attenuation of the correlation with lag time. The time of the first zero crossing of the function can be identified with one quarter of the dominant period in the time series (Le Blond and Mysak, 1978).

2) It can be used in estimating the confidence levels of linear crosscorrelation coefficients (Davis, 1976).

Further comments on the latter use are merited. When time series data are filtered to produce a low frequency data set, the effective number of degrees of freedom decreases because adjacent data points become linked. The decrease is variable depending on the filter used and the time scales operating in each individual time series analysed. Knowledge of the number of degrees of freedom is crucial in determining the critical correlation coefficients corresponding to say the, 95 % and 99 % confidence levels of the crosscorrelation coefficients. The method of Davis (1976) is used to determine the degree of freedom, which is proportional to the summation of the product of the two autocorrelation functions that are being cross-correlated. A problem arises when filters are used where the length of the time series is short relative to the quarter power period of the filter because the number of degrees of freedom can drop below 10, as is the case here with the 1/40 cpd quarter power point filter

applied to annual data. The rate of change of the critical correlation coefficient is rapid with change in degrees of freedom when the latter has a small value and one degree of freedom more or less can change the significance status of the correlation coefficient. Sciremammano (1979) warns that for data with degrees of freedom less than 10 the robustness of the crosscorrelation distribution to non normality breaks down and no satisfactory general method is available for setting significance levels. Strongly periodic time series data with an ill damped autocorrelation function can also introduce uncertainties in the determination of the number of degrees of freedom.

The seventh stage is to form the power spectrum through the Fourier transform relation with the autocorrelation coefficient. This is the spectral analysis method of Blackman and Tukey (1958) and is detailed in Jenkins and Watts (1968). The spectrum is a measure of the distribution in frequency space of the variance of a stochastic process. Inspection of the spectrum reveals any dominant frequencies which in turn can be linked to the geophysical forcing processes that caused the variability in the time series data.

Spectral analysis can be extended to vector series where due to the rotation of the earth, asymmetry is expected in the Fourier components. Gonella (1972) and Mooers (1973) have formulated rotary spectrum methods where correlations and spectral relations for vector components are invariant under component axis rotation. Middleton (1982) points out some inconsistencies in the paper by Mooers (1973). These methods are in wide use for both meteorological and oceanographic data (e.g. Gonella, 1972; Halpern, 1974; Livingstone et al., 1980; Winant, 1980). The method yields clockwise and anticlockwise spectra that give the sense of rotation of the wind or current vector. Inertial processes that have a definite sense of rotation (anticlockwise in the Southern hemisphere) can be easily identified. When the clockwise and anticlockwise spectral estimates are equal (at a given frequency) the motion is linear; unequal estimates give a measure of ellipticity of the motion. The orientation of the major axis of the ellipse, if it is statistically significant or stable gives an indication at that frequency of the dominant direction of motion. The ellipse stability or average coherence is tested for the 95 % confidence level according to the method of Jenkins and Watts (1968, p 380).

When different variables are available in time series data sets then it can be useful to form cross correlation functions, cross spectra and the associated coherence and phase spectra. The coherence or coherence squared spectra and phase spectra are particularly useful in that they provide a non-dimensional measure of correlation between

two time series as a function of frequency. In oceanographic applications the phase relationships of different vector quantities as a function of frequency can be explored as reported by Bennett and Magnell (1979) and Lee and Mayer (1977) for shelf currents. Scalar variables such as temperature and pressure can be included in the analysis (Schumann (1989), Duing et al (1977) and Wolanski (1986)). Coherence and phase spectra can be applied to determine if bands of frequencies are significantly correlated and if common phase behaviour exists in such bands.

For both the rotary spectra and the standard spectra the following statistical parameters are evaluated: Bandwidths, based on the Hanning window used in the analysis and the number of degrees of freedom are calculated according to Bendat and Piersol (1971, p 278 and 192). The 95 % confidence limits are estimated from the method of Jenkins and Watts (1968, p 255). If the spectral energy is plotted on a logarithmic scale then the confidence interval is simply represented by a constant interval about the spectral estimate. Other attributes of the spectra such as power law regions will be discussed in appropriate sections later. For the annual spectra using hourly HF data the maximum lag number choice of 720 is based on the Jenkins and Watts (1968) criteria to keep the maximum lag less than 10 % of the number of data points. For the 1/12 decimated hourly ILF data 60 lags are used in the annual spectral analysis although only 30 are plotted.

The techniques for forming coherence squared spectra and phase spectra are given in Jenkins and Watts (1968). Plotting of such spectra follows the suggestion of Jenkins and Watts (1968, p 379) to transform the Y axis as the arctanh (coherence) where coherence is the square root of the coherence squared. The significance levels for coherence are evaluated according to the method of Thompson (1979) and Julian (1975).

The final stage is to plot the spectral functions. The clockwise and anticlockwise spectra can be plotted on a negative and positive frequency axis respectively but in this study are both displayed on the positive frequency axis together with the total spectrum. A plot of the log of the spectral power versus log of the frequency is useful to obtain an overall picture of the data and reveals any power law trends. A linear axis for frequency is useful to view finer structure of selected frequency bands. In order to distinguish between the rotary spectra and the standard power spectra in this work, the latter is termed the autospectra and applies to spectra of either individual vector components or to scalar quantities. The software used in the spectral analysis is based on a programme

developed by Perrins (1980) and V Swart (per com).

Note on spectral breakthrough

The wind and sea temperature time series that are analysed reveal a very high spectral power at the diurnal frequency. Under certain circumstances spectral breakthrough can occur at harmonics of the primary peak frequency and lead to erroneous interpretations. Smith (1977a) points out that asymmetrical cyclical data that depart from circular or elliptical rotation characteristics can introduce harmonic breakthrough in the spectrum. This fact seems to be neglected in the general literature. Close inspection of published current spectra with one dominant peak indicate the presence of subsidiary peaks at the harmonics (e.g. Webster, 1969; Fofonoff, 1969; Hayes and Halpern, 1976). The spectral analysis software used in this study was tested with synthetic data with different characteristics viz 1) circularly polarized vector data 2) elliptically polarized data and 3) non sinusoidal data, all with a primary periodicity of 24 hours and a few months duration. In the case of 1) and 2) only a strong peak at 24 h is observed whereas in the case of 3) additional prominent peaks at the 12 h and 8 h harmonic are observed. Both the wind and sea temperature data have asymmetric diurnal periodicities (Fig. 5.5 and Fig. 5.16) and any peaks in the spectrum at the harmonics are probably largely due to an artefact of the data analysis and not due to a physical process.

1.5.4 Field Work Techniques

In order to supplement the time series data and provide data in the synoptic wind event time scale various field techniques were employed. These techniques were generally chosen to provide near simultaneous cover of the quickly changing parameters over the time and space scales studied. A small 5 m ski boat (Surf Rider) with twin 25 HP outboard motors provided good mobility in the transect surveys and drogue deployment operations. A light single engine aircraft (overwing Cessna equipped with a removable panel in the floor for aerial photography and dye bombing) allowed rapid coverage of the extended study area. Despite the additional field work a limiting factor in this study is a lack of a good time series of current data. A brief description of the different techniques employed is now given (see also Bain and Harris, 1975ff).

1.5.4.1 Sea transect measurements

Transects to obtain sea temperature profile and current data were done with the aid of the ski boat covering three lines perpendicular to the coast. The southernmost was opposite the

Melkbosch headland and the northernmost opposite Ou Skip (see Fig. 1.7). The lines extended 6 km offshore. These lines straddled the "focus" of upwelling that had been revealed by aerial sea surface temperature surveys. Measurement stations were at half kilometer intervals up to 3 km then at the kilometer marks. Navigation to these positions was accomplished with the aid of compass fixes on predetermined land marks. At each station a surface bucket temperature was recorded and temperature profiles were determined with the standard bathythermograph technique (Neumann and Pierson, 1966). At the inner and outer stations usually two current drogues were released from the anchored boat and tracked for a measured time with the aid of a sighting compass (Suunto) and a navigational range finder (Barr and Stroud). The wind speed was determined with a hand held anemometer. The two current drogues, of the tin float type described by Gunn (1977) were respectively set at the 1 meter depth and at a depth below the thermocline as revealed by the bathythermograph trace.

A set of transects was done on each of several successive days in order to intercept a wind cycle event. Occasionally transects were repeated the same day.

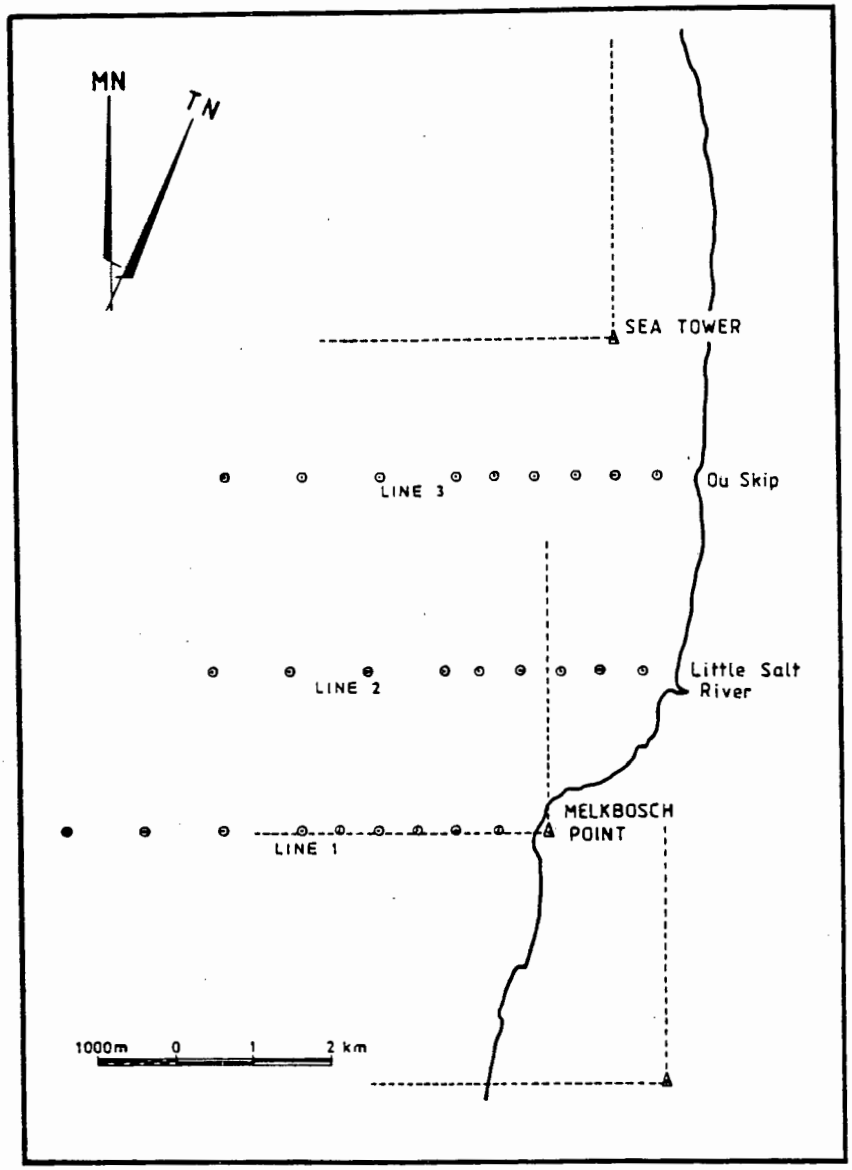

FIG. 1.7. MAP SHOWING TRANSECT LINES FOR FIELD MEASUREMENTS

1.5.4.2 Lagrangian current tracking

Besides the Lagrangian current tracks determined during the transect measurements the following current measurements were also undertaken:

a) Dye bomb current drogues. These drogues for surface currents were based on a design by Welsh (1967) and consisted of a float and dye bag (fluorescein) attached to a 40x40 cm drogue which all fitted inside a 1 kg jam tin for deployment from the light aircraft. Up to twenty were deployed in a grid pattern over the study area at any one time. Their progress was followed with the aid of sequential time lapse aerial photography using a 35 mm camera fitted with a 28 mm wide angle lens. A number of 2x2 m orange coloured raft floats had been moored at different positions along the coast to allow for easier alignment of the photographs. This technique gave a good relative idea of surface current patterns at a "snap shot" in time and semiquantitative data

on current speeds in the study area. The technique was particularly useful under strong wind conditions when other methods were impracticable.

b) Radar tracked current drogues. Because ESCOM operated a radar tower at Ou Skip for wave direction studies the opportunity was taken to develop radar reflective current drogues which could be tracked with the help of automatic time lapse photography of the Plan Position Indicator (PPI) screen of the radar set (Decca RM919). The development of the method is reported by Bain and Harris (1975ff) and the drogue is described by Boyd (1981). Because of windage effects on the drogue and associated excessive wave clutter echos on the PPI under moderate or stronger winds this technique was only used to check on residual currents under calm conditions. Up to ten radar floats with drogues set at different depths were deployed at a time from the ski boat and tracked simultaneously with the camera system. The advantages of the method included a) tracking in the dark or in misty conditions and b) the unattended mode of camera operation (exposures every 20 min) that allowed over-night tracking and in one extended calm period allowed tracking for a continuous period of three days. The useful range of the radar for this purpose was 5 km.

c) Moored buoy current system. A system similar to that used by van Ieperen (1971) and ESCOM and described by Harris (1964) was used for semiquantitative near surface current data. Observations were only made once or twice a day and basically gave an indication of whether currents were up or down the coast, or on or offshore.

1.5.4.3 Sea surface temperature measurements

The technique of airborne radiation thermometry (ART) is widely used for determining sea surface temperatures; locally it has been used by Andrews and Cram (1969), Cram (1970) and Jury (1981), and internationally by Chermack (1970), Thomson (1972), Saunders (1973). The sea surface has a thin viscous boundary layer of thickness less than 1 mm; this layer under a range of wind conditions is cooler by about 0,2 °C than the well mixed layer which starts at a depth of a few millimeters (Grassl, 1976). The technique only measures the temperature of the submillimeter thick surface skin but since the accuracy is of the order of 0,5 °C the instrument (Barnes, PRT5) effectively records the well mixed sea surface temperature. However under very calm conditions with "glassy" seas the radiometer measurements in

daytime were found to give unreliable fluctuating values up to several °C above the bulk temperature.

The technique was developed here for operation from a light aircraft traversing a relatively small grid with an offshore scale of less than 10 km (Bain and Harris, 1975ff). Basically two grids were flown; a) from Table Bay in the south to Bok Point in the north and b) a few kilometers south of Melkbosstrand to 10 or 15 km further north. Flights at an altitude of 300 m were done on successive days to intercept wind event cycles. At times two ART flights were done per day - one at dawn and the other in the afternoon to check on diurnal insolation effects. This effect was also checked by a series of hourly manual thermometer readings at a one meter depth in the surf zone starting at dawn and ending at sunset. Before and after each flight the radiometer was calibrated to an accuracy of 0,1 °C. Surface truth comparisons showed that the ART values were mostly within the 0,5 °C error range. Because the emphasis was on a relative picture of the sea surface temperature distribution other corrections for humidity etc were not made. However data collected under cloudy conditions or glassy seas were rejected.

The output data of the radiometer were recorded on a chart which was subsequently digitized and computer plotted on a grid of the flight path. The data were then hand contoured. Colour aerial photographs were taken to correlate the sea colour changes with the temperature structure. Overall the ART technique was most useful in revealing the intricate and dynamic nature of the sea surface temperature structure.

1.5.4.4 Quality of field data

In all cases the quality of the field data was checked using relevant calibration procedures. The bathythermograph was temperature checked and calibrated at various depths and found to be within specifications. A calibration curve was produced for the range finder and readings corrected accordingly. As has been mentioned previously the radiometer for the ART surveys was calibrated before and after each flight. Both the radar tracked and range finder tracked current drogues were tested in the CSIR wind/wave tunnel at Stellenbosch for wind drag effects. Similar results were found for windage correction factors as described in detail by Gunn (1977) and Boyd (1981).

In general the field techniques did not require an absolute accuracy but just a relative one in order to compare spatial or temporal differences. The positional accuracy of the ski boat

and the ART survey aeroplane although only a few hundred meters is considered adequate for this study. The range finder tracked drogues give inadequate accuracy under strong wind conditions. This Lagrangian method is not suited to obtaining a profile of current velocities with depth but is probably adequate for comparing currents above and below the thermocline.

1.6 OVERVIEW OF THE THESIS

In this first chapter the general and South African literature on coastal and upwelling processes have been reviewed with an emphasis on wind forcing. The spatial scales and centering of upwelling on particular coastlines are discussed as are the time scales of various processes. The review identifies a scarcity of studies on small scale upwelling and on processes within the coastal boundary layer and on shallow water diurnal effects. In the South African context shortcomings exist in synoptic time-scale coastal process studies and in analysis of time series data exceeding one year in duration. This research addresses these shortcomings and besides finding relevance for physical oceanography it relates to the assessment of both the impact of thermal discharges from coastal nuclear power stations and other effluent outfalls and it complements studies on the larger scale of the economically important Benguela region.

The study site at Melkbosstrand is described in terms of physical meteorological and oceanographic attributes. The research methodology is outlined. It is empirical in nature and embraces both time series analysis of multiyear wind and sea temperature hourly data and the conduction of field work to delineate small space scale and synoptic and shorter time scale processes.

In Chapter 2 the time series wind and sea temperature data are filtered into high, low and very low frequency ranges. Spectral analysis is used to help identify the dominant temporal scales of processes occurring in the study region. Possible causal relationships between wind and temperatures are identified. The subsequent chapters each in turn consider the character of the site in the context of the three main time scales identified and in particular the role of the alongshore and across shore wind components is stressed. Chapter 3 considers the seasonal character of the site by using the very low frequency filtered time series data of wind, temperatures, and waves. Simple statistics and linear correlations between wind and temperature and between wind and waves indicate causal relationships. Three seasonal regimes are distinguished. The barometric forcing factors are identified and the links between the study site and the larger space scale of both wind fields and oceanographic features are discussed. The

representativeness of the time series data sets is assessed in relation to inter-annual variability.

The event time scale character is covered in Chapter 4 by using the low and intermediate low frequency filtered time series data. Simple statistics, linear correlations and spectral analysis are employed to characterize the site. Typical barometric event cycles are identified. The alongshore wind forcing necessary to displace the thermocline is quantified in a simple two layer upwelling model and compared with case studies. The spatial variability of the wind and sea temperature is investigated and reveals a distinct localized "focus" of upwelling. Aspects of the coastal boundary layer are addressed. The transition between seasons is discussed.

The high frequency wind and temperature data are used to characterize mesoscale phenomena in Chapter 5. Spectral analysis shows the dominance of diurnal processes. The temperature response to both diurnal wind and insolation forcing is considered in detail. Dynamic processes are deduced from the temperature response at two depths. Spatial aspects at the diurnal time scale are identified.

Whereas in the foregoing chapters the meteorological and oceanographic characteristics of the site were separated into different time scales the final chapter seeks to link the processes together. The findings are also summarized and put into perspective by considering the relevance to other investigations in coastal regions.

PRINCIPAL CONCLUSIONS

This study has contributed, sometimes significantly, to the objective of characterizing a small scale upwelling region of (order 10 km) over varying time scales. It is found that at this site the dominant forcing mechanism at all time scales from seasonal down to diurnal is the wind.

With a paucity of current data, sea temperature fluctuations are used effectively to characterize the site. These fluctuations of 2 °C to 8 °C in summer are largely due to upwelling and downwelling dynamics forced by a synoptic barometric sequence as follows - postcold front SSW wind - ridging anticyclone with deep SE winds - precoastal low - coastal low passage - wave cyclone with westerly winds. This characterization of synoptic events over several days has filled a gap in South African studies.

The synoptic data base confirmed that the distance offshore at which the upwelling thermocline outcrops at the surface can be predicted with a simple wind impulse model, Csanady (1977a).

Two aspects relate to the fine scale of the investigations

a) A noteworthy discovery in this small scale coastal study is the existence of a well localized "focus" of upwelling just north of Melkbosstrand Point. Because of the lack of bathymetric or orographic effects it is concluded that the coastal offset provides the localization of the growth centre for upwelling. Airborne radiation thermometry clearly shows a small 1 km diameter cold patch that progressively elongates as the upwelling event continues. This is represented in a three dimensional artists impression of the upwell growth centre illustrated in the frontispiece.

b) Also of note is the observation of a narrow, 0,5 km wide band of warm water against the coastline due to insolation effects on the shallow water over the gently sloping beach. Closer study of such features can provide thermal diffusion coefficients and residence times which are of importance in assessing impacts of thermal effluents from nuclear power stations.

The last point highlights diurnal effects which was a study objective. The site has other strong diurnal signals, as seen in both the wind and sea temperature spectra. Although insolation plays a role the temperature signal as recorded at the sea tower is largely controlled by the wind forcing of the thermocline structure. This is also reinforced by strong coherence between wind and temperature at the diurnal frequency. An important finding is that at the lower frequencies associated with synoptic processes the alongshore winds force the upwelling response when the 8 m depth temperature correlate better with the alongshore wind. While at the higher diurnal frequencies the across shore land-sea breeze winds excite the higher frequency upwelling signal when the 2 m depth temperature is better correlated. The diurnal processes effectively modulate the primary synoptic forcing. The study finds support for the concept of a Coastal boundary layer (CBL) in the area with an offshore boundary depth of about 30 m. Such a CBL has a dynamic identity different to further offshore waters.

This small space scale study did provide links to the larger scale of the Benguela System. The bimodal seasonal temperature structure has a counterpart in offshore data. Although no seasonal transition dynamics are available for the Benguela System this study indicates on the local scale that a cumulative Ekman transport exceeding 3×10^9 g.cm^{-1} with a duration 5 days, or longer is required to cause the spring transition in temperature character.

Many of the above findings are based on a detailed time series analysis of a multi-year hourly time series data base which is unique for a South African coastal site.

The study met its aims of characterizing a small scale, order of Rossby radius of deformation, coastal site especially at the synoptic and diurnal time scales. The findings are relevant to fisheries biology and siting of thermal outfalls and bridges the gap between traditional coastal engineering studies and shelf oceanography.

CHAPTER TWO

THE DOMINANT TEMPORAL SCALES

C O N T E N T S

CHAPTER TWO

THE DOMINANT TEMPORAL SCALES

2.1 INTRODUCTION

This chapter seeks to establish the dominant time scales of the physical processes operating in the study area. Instabilities in the ocean lead to a cascade of turbulent energy transfer. Monin (1977) shows that distinct frequency ranges are associated with differing processes eg quasistationary oceanic circulation and non-stationary currents occur in the synoptic range; internal waves, inertial fluctuations and tidal processes occur in the inertial frequency range; while wind wave processes are associated with a time scale of seconds. A space-time spectrum of sea temperature variations is used by Stommel (1963) to illustrate that in oceanographic processes a wide range of space and time scales are encountered that vary from seconds and centimeters to decades and thousands of kilometers. One can therefore highlight particular processes through their characteristic time scales which are suitably revealed by analysis of time series type data. Monin (1977) stresses that the action of the atmosphere accounts for most non-stationary processes in the sea. The momentum transfer to the sea from the atmosphere controls many types of wave motion although due to the seas inertia it often has a lagged response. The analysis of a wind data set can therefore give insight to attendant oceanographic processes.

At the study site a good time series set of hourly wind data and sea temperature data at three depths is available and is described in Chapter 1. At this site the sea temperature fluctuations follow closely the density fluctuations since salinity changes are small in comparison (Bang, 1973 and Gunn, 1977a). The temporal picture of the sea temperatures measured at the three depths will thus be linked to changes in the water mass. Although a good time series of current data and salinity data would have been invaluable for this study the wind and temperature data available have been adequate to gain valuable insight into the processes occurring at the site and are used in this chapter to establish the dominant temporal scales in the region. Subsequently cross-correlation analysis is used in an attempt to suggest causal relationships at the various time scales.

2.2 FREQUENCY RANGES FOR ANALYSIS

Time series data can be analysed in a number of different ways. In this study the data are filtered to form different frequency ranges. Time series data in these frequency ranges are plotted later. The autocorrelation function is used to do spectral analysis on the filtered data. This form of analysis is adequate for our purpose although it makes the assumption that the physical processes are linear in nature which is not generally true in the mixed layer. Non-linear energy transfer processes are studied by Yoa et al. (1975, 1977) using the higher order bi-spectrum analysis procedure.

Since the aim of the initial analysis is to uncover the dominant temporal scales, the time series data are broken up into year long hourly sets and analysed separately. The separation into years also helps in the subsequent investigation of inter-annual variability. At a later stage a 3 year set is analysed.

2.2.1 Coherence and Phase Spectra

Information from coherence and phase spectra can assist in the choice of time scales or frequency bands for further investigation. From the unfiltered, detrended 1977 data sets, the coherence and phase spectra are formed between the 8 m temperature data and the two wind components as per Jenkins and Watts (1968) discussed in 1.5.3. The auto spectra for the 8 m temperture and north/south wind component and the corresponding coherence and phase spectra are plotted for the frequency range 0.00 to 0.10 cycles per hour in Fig 2a.

For these spectra an expanded plot over the frequency range 0.00 to 0.02 cycles per hour is given in Fig. 2b. The 95 % significance level as per section 1.5.3 (Thompson, 1979) is indicated on the coherence spectra. The equivalent spectra for the 8 m temperature and east/west wind component data are plotted in Fig 2c and 2d.

In Fig 2a for the 8 m temperature versus the North/South wind component the main feature of the phase spectrum is its obvious division into two frequency regions. Firstly for frequencies greater than 0,03 cph where the phase is very variable and oscillates $\pm 180°$ and secondly for lower frequencies less than 0,03 cph where the phase is relatively more stable with fluctuations of about 50°.

The corresponding coherence spectrum in a similar low frequency region has an appreciable section above the 95 % significance level (see Fig 2b). At higher frequencies there is a prominent significant peak at the diurnal frequency with a lesser significant peak at the harmonic frequency of 0,083 cph (12 h period). Generally however the

coherence is noisy and variable and on average low for frequencies greater than about 0,03 cph with few other peaks lying above the 95 % significance level.

Considering the phase spectrum the size of the fluctuations can be expected from the calculated degrees of freedom (15) and the corresponding confidence band which can be well over 50° for associated low coherence, Jenkins and Watts, 1968 p 381. The expanded plot of the lower frequencies (Fig 2b and 2d) shows clearly the more stable phase behaviour for high coherence regions. Furthermore, phase spectra oscillating over ±180° are commonly seen in oceanographic data with low coherence; Winant and Olson (1976), Duing et al (1977), Wunsch and Wimbush (1977). Even for high coherence the phase can oscilate wildly, Winant, Beardsley and Davis (1987). The essential feature in the phase spectrum illustrated here is the obvious change in phase behaviour at 0,03 cph (period of 33 h) and one is probably justified in identifying two broad frequency bands on each side of this point over which to average.

Later, detailed discussions will be given of the auto spectra and rotary spectra. At this stage it can be stated that the coherence spectrum reveals essentially the same features with possibly more structure in the low frequency region (Fig 2b). However, this spectrum has a relatively broad band of frequencies 0,009 cph (4.6 d) to 0,0013 (32 d) that has a consistently high coherence with no low minima in this region. The dominance of this region should allow averaging over a somewhat broader frequency band extended to a shorter period of about two days without compromising further conclusions when standard cross correlation analysis is applied.

In the case of the 8 m temperature versus the across shore or east/west wind component the spectra (Fig 2c and 2d) show similar features to those with the north/south wind component. The phase is again very variable with an obvious short stable low frequency region correlating with the significant coherence region between 0,001 and 0,007 cph (Fig 2d). In general the coherence is less than with the north/south winds. The coherence at the diurnal frequency (and semi diurnal frequency) is again strongly significant, with no other significant peaks in the high frequency region . A similar case to that of the alongshore wind can be made to subdivide the frequency into two regions.

In both cases there is also support for a third very low frequency region. For the North/South wind case Fig 2b the coherence has a minima at 0,00126 cph or 33 d which then rises steeply to lower frequencies. The corresponding phase shows a distinct step. For the

East/West wind the coherence falls sharply from 0,001 cph (38 d) to lower frequencies with an accompanying marked phase change. This indicates a seasonal frequency band.

The coherence and phase spectra anlaysis is also applied to the 2 m depth temperature data with essentially the same results (not illustrated).

In summary the coherence and phase spectra analysis is applied to the data sets and allows certain insights to be gained. The characteristics of the spectra lend support to subdivide the data into three frquency bands and subsequently to average over these bands. The choice of these frequency ranges are dictated by the hourly nature of the digitized data, the phase coherence findings and accepted subdivision criteria for such physical oceanographic data e.g. Huyer et al (1979), Monin (1977) and Section 1.5.

2.2.2 Frequency Ranges

Common to the analysis of both the wind and temperature records is the subdivision into the following frequency bands by applying appropriate filters.

HIGH FREQUENCY RANGE (HF) for frequencies greater than 0.25 or 0.5 cpd (depending on filter used) and less than 12.0 cpd; i.e. for periods shorter than 4 or 2 days but longer than 2 hours.

LOW FREQUENCY RANGE (LF) for frequencies less than 0.5 cpd; i.e. for periods greater than 2 days.

INTERMEDIATE LOW FREQUENCY RANGE (ILF) with the same upper limit as the LF range but with a lower limit greater than 0.025 cpd; i.e. for periods shorter than 40 days but longer than 2 days.

VERY LOW FREQUENCY RANGE (VLF) for frequencies less than 0.025 cpd; i.e. periods greater than 40 days.

The details of the Lanczos-cosine filter and its application to the data are given in the Research Methodology section (1.5). In summary the LF data are obtained by applying to the hourly data a low pass filter with a quarter power point of 1/36 cph; the VLF data are obtained by decimating the LF data to each 12th point and applying a further filter with a quarter power point of 1/40 cpd. The ILF data are obtained as the daily residual of LF data minus the VLF data. The HF data are the hourly residual of the original data minus the LF data obtained with either a 1/36 or 1/96 cph quarter power point filter.

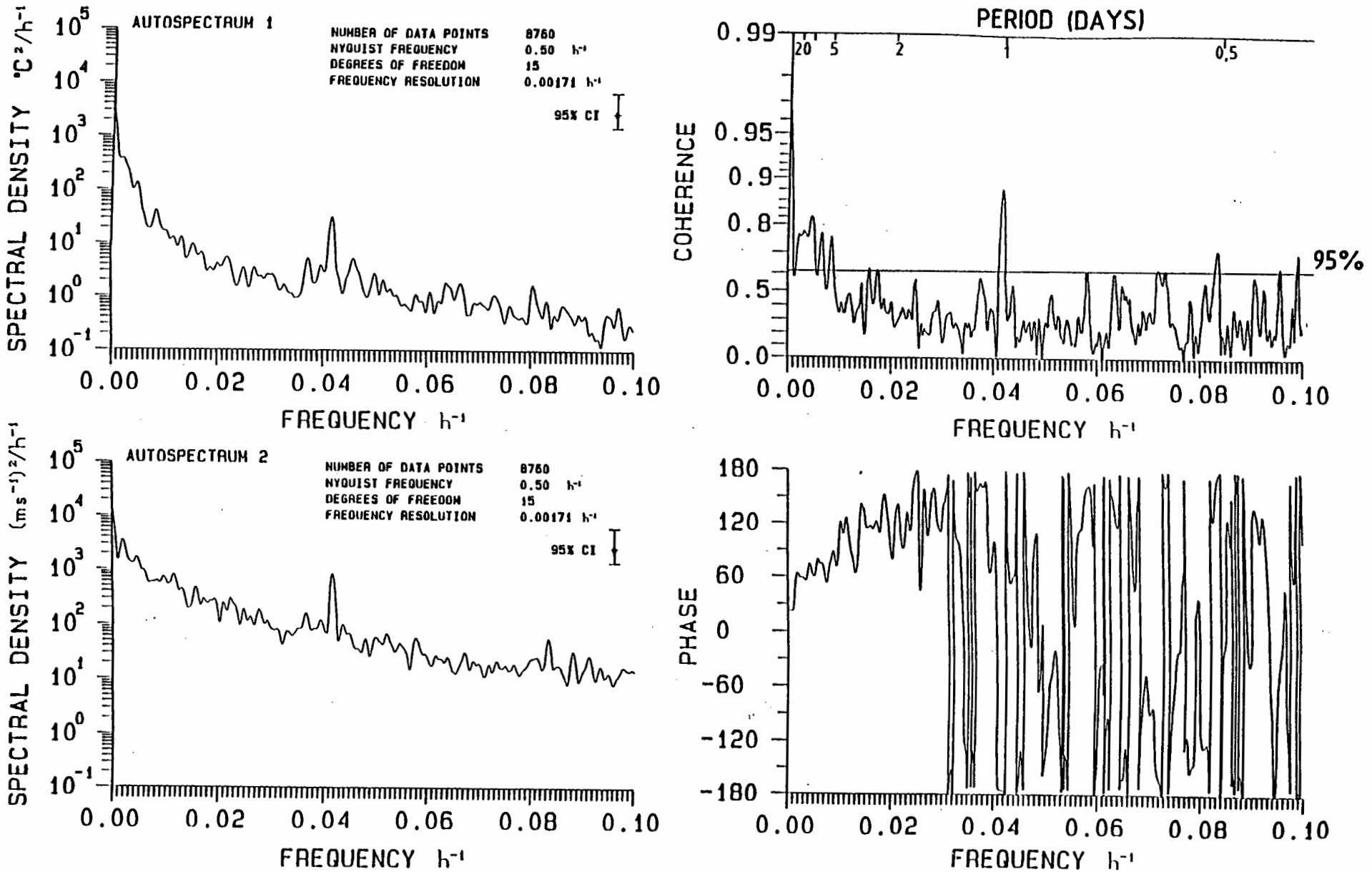

OUSKIP - UPWELLING 1977

FIGURE 2a temperature at 8 metres vs North-South wind

2.2c

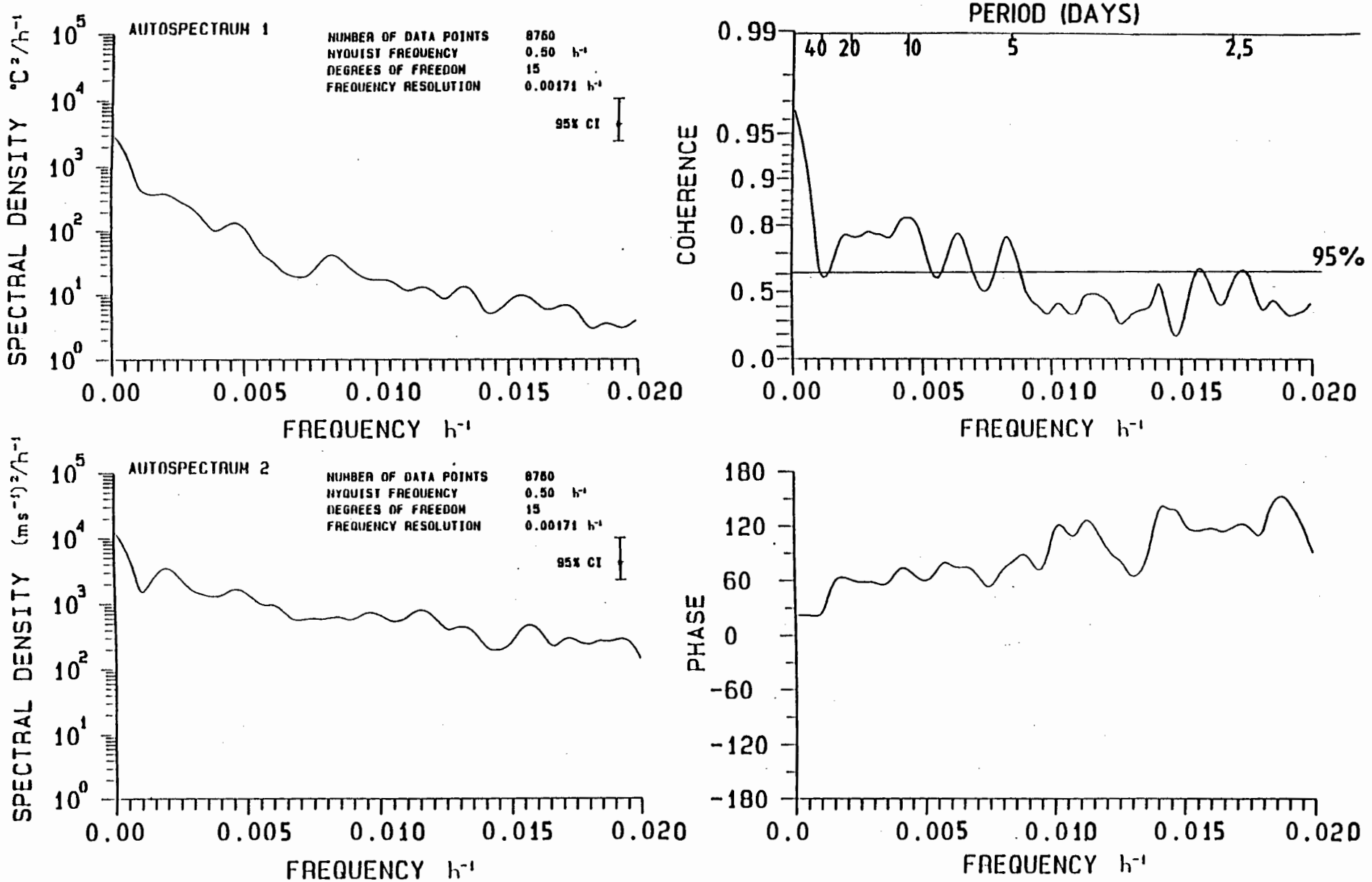

OUSKIP - UPWELLING 1977

FIGURE 2b temperature at 8 metres vs North-South wind

2.2d

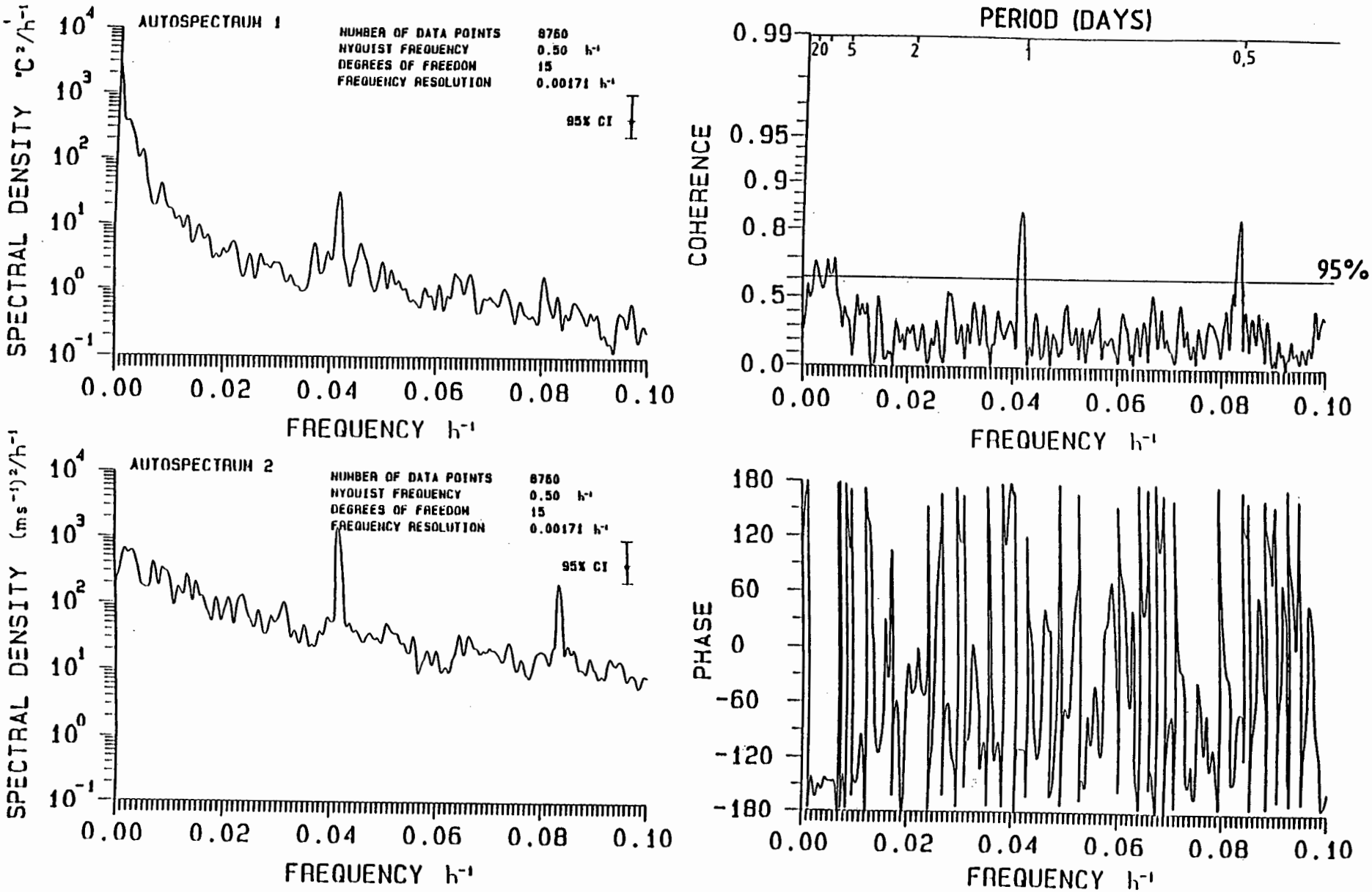

OUSKIP - UPWELLING 1977

FIGURE 2c temperature at 8 metres vs East-West wind

2.2e

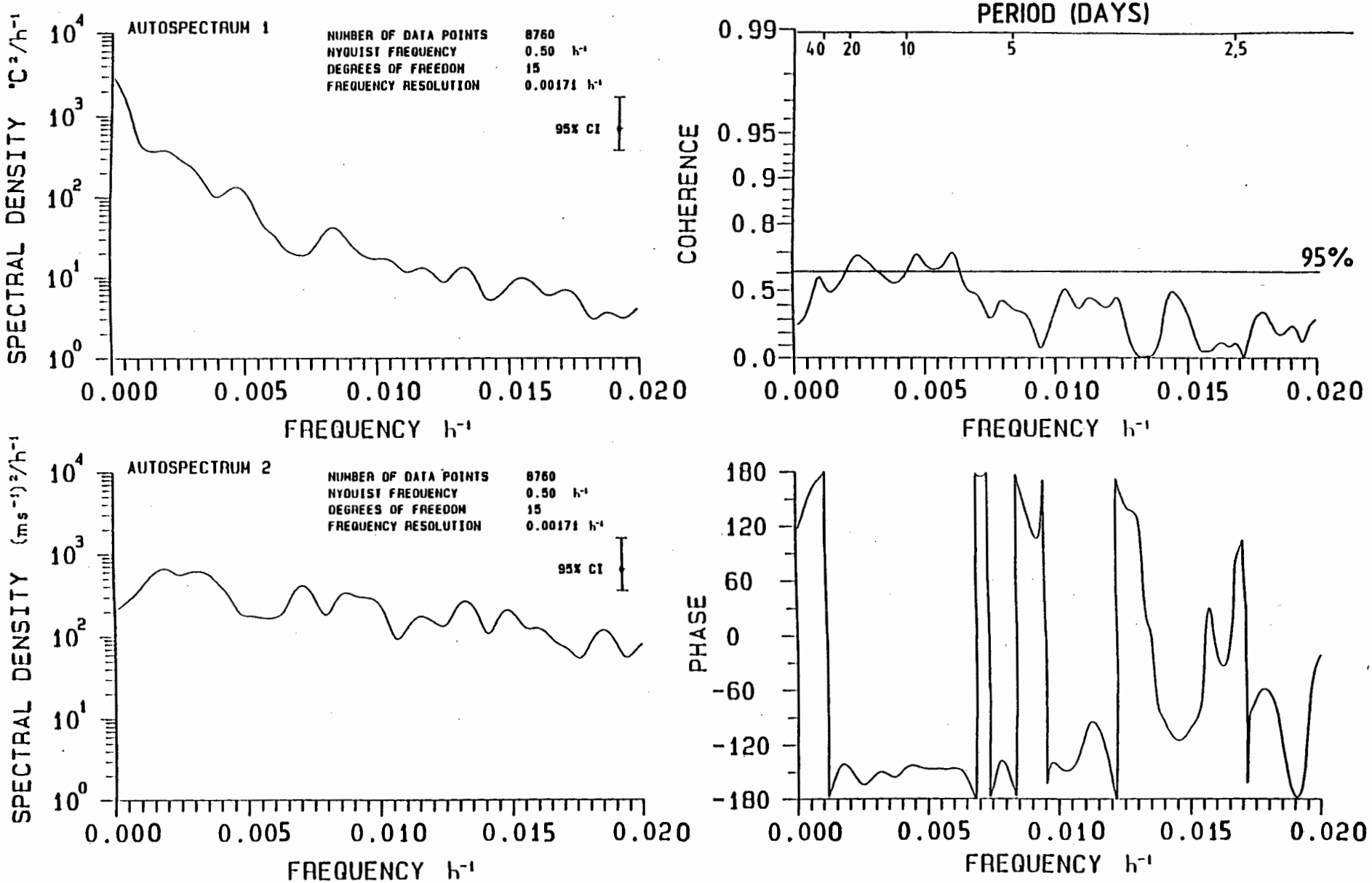

OUSKIP - UPWELLING 1977

temperature at 8 metres vs East-West wind

FIGURE 2d

2.2f

The Nyquist frequency limits the upper frequency of the data to 0.5 cph. A quarter power point near a period of 40 hours lies between the important diurnal and tidal frequencies and those of synoptic processes with lower frequencies (Monin, 1977). The choice of quarter power point at 96 hours allows a check of filter cutoff effects of the low pass filter, and extends the HF spectral data into the start of the synoptic region. The VLF choice allows seasonal effects to be studied, while the ILF data are effectively a band passed filtered set that removes the seasonal trend from the LF data. Thus the LF and the ILF data will be discussed together either with or without the long term trend respectively.

The Ou Skip wind data are rotated 20° to the west of north to align with the average coastline orientation of the site which is similar to the principal wind axis and decomposed into alongshore (north) and across-shore (east) components before analysis (see 1.5.3). Both the wind and temperature data in the HF, LF and ILF ranges are subjected to various statistical data quality checks (Section 2.5) prior to spectral analysis. The time series data in the VLF range are plotted and visually inspected but not spectrally analysed, although the autocorrelation function is determined. The results of these analyses for the different frequency ranges, firstly for the wind data and then the temperature data are now presented.

2.3 WIND SPECTRA

The wind vector data are analysed by the rotary spectral analysis method (Gonella, 1972) which decomposes the velocity variance of the data into clockwise and anti-clockwise rotating components of various frequencies. The sum of clockwise and anti-clockwise spectra yield the classical total energy spectrum. Details of the analyses and the various parameters e.g. ellipse orientation, stability, rotary coherence, are discussed in Chapter 1.5.3.

The temporal features revealed in each of the three frequency bands follows.

2.3.1 High Frequency Range

The rotary spectrum obtained in this frequency range for the wind data of 1977 is shown in Fig. 2.1. It is a log/log plot of the spectral power for the total, clockwise and anti-clockwise

contributions versus frequency in cycles per hour. The analysis is done with the 8760 hourly values for the year and maximum lag number of 720. The maximum lag number choice is based on standard spectral analysis procedure to keep it less than 10 % of the number of data points (Jenkins & Watts, 1968). The symbols on the plot are for each 10th lag number. The 95 % confidence levels and the band width are displayed on the plot. They are evaluated according to the method of Jenkins and Watts (1968) described in Section 1.5.3. In a log/log plot the band width displayed is for that specific frequency where the error bars are placed. The band width at other frequencies can be estimated as 0.266 of the interval between each 10th lag number.

The main features of the total spectrum (Fig. 2.1) are a very prominent peak at the diurnal frequency with a spectral power of 58 $(km/h)^2/cph$ and a significant semi-diurnal peak with a spectral power of 7 $(km/h)^2/cph$. Both these peaks are spectrally significant since they exceed the 95 % confidence levels and the band width criteria.

The latter peak caused considerable confusion but is most probably merely a harmonic of the strong diurnal peak. Smith (1977a) has remarked on such breakthrough peaks in data that contain a strong non-sinusiodal periodicity. Tests for confirmation of breakthrough with synthetic data are reported in Section 1.5.3. In Fig. 2.1 another less prominent harmonic peak occurs at a period of 8 hours or 0.125 cph.

There is some structure at the lower frequencies corresponding to periods between 1 and 3 days which is better seen in the log/linear plot (Fig. 2.2) which covers only a portion of the frequency range shown in the log/log spectral plot (Fig. 2.1). The lower frequencies are cut off by the filter used which has a quarter power point at 0,0104 cph (96 hours) and a 3 % dropoff at 0,0139 cph (3 days). See also the frequency response function, Fig. 1.6. In general the anti-clockwise component dominates the clockwise component particularly at the lower frequencies. This indicates the largely rotary nature of the wind vector variations due to atmospheric forcing processes. In this section the other parameters of the rotary spectral analysis will not be discussed except to say that the major peaks have significantly stable ellipse orientations.

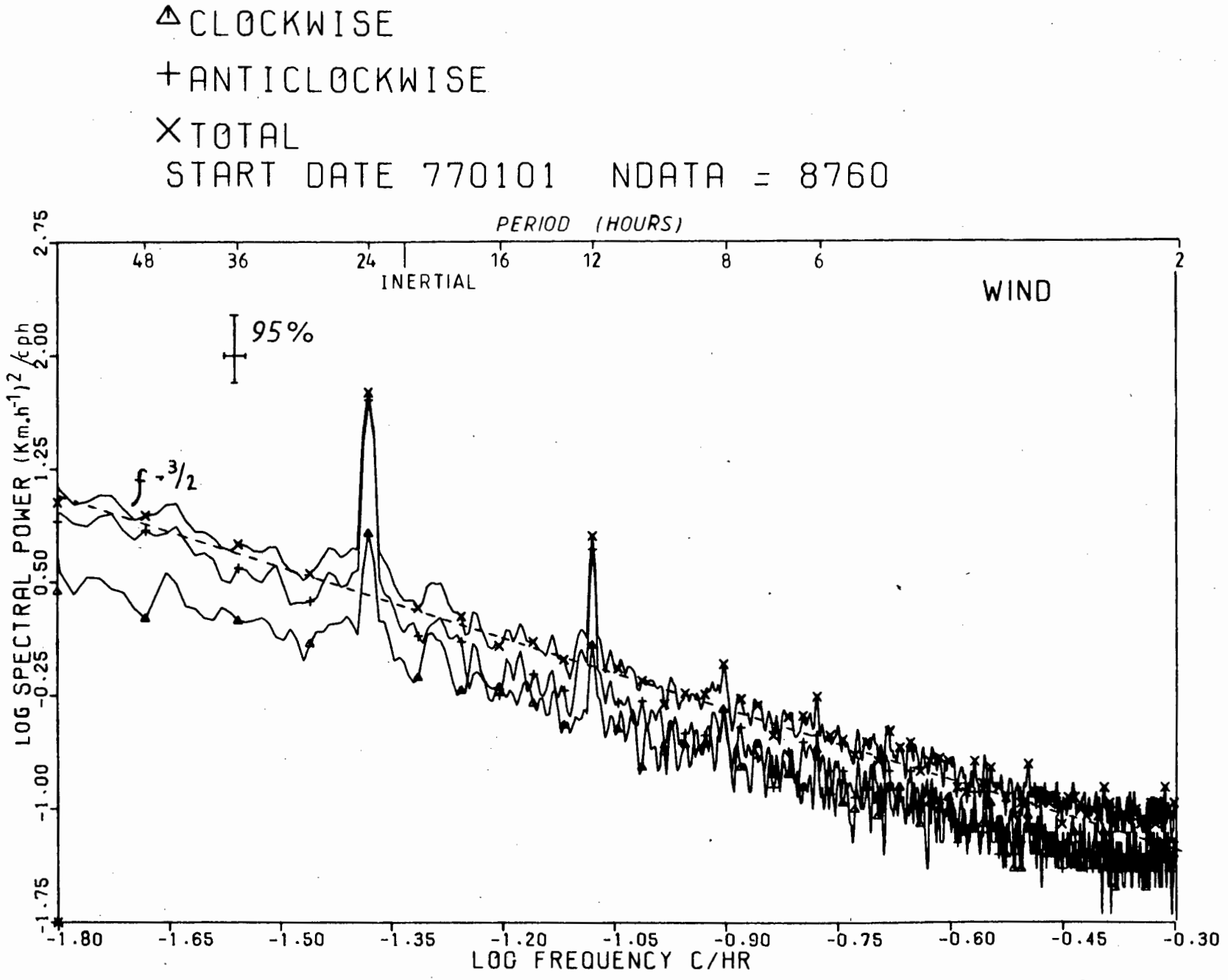

FIG. 2.1 , LOG/LOG PLOT OF ROTARY SPECTRA FOR HIGH FREQUENCY FILTERED OU SKIP WIND DATA FOR 1977. MAXIMUM LAG NUMBER, 720. PLOTTED SYMBOLS INDICATE EACH 10TH LAG NUMBER

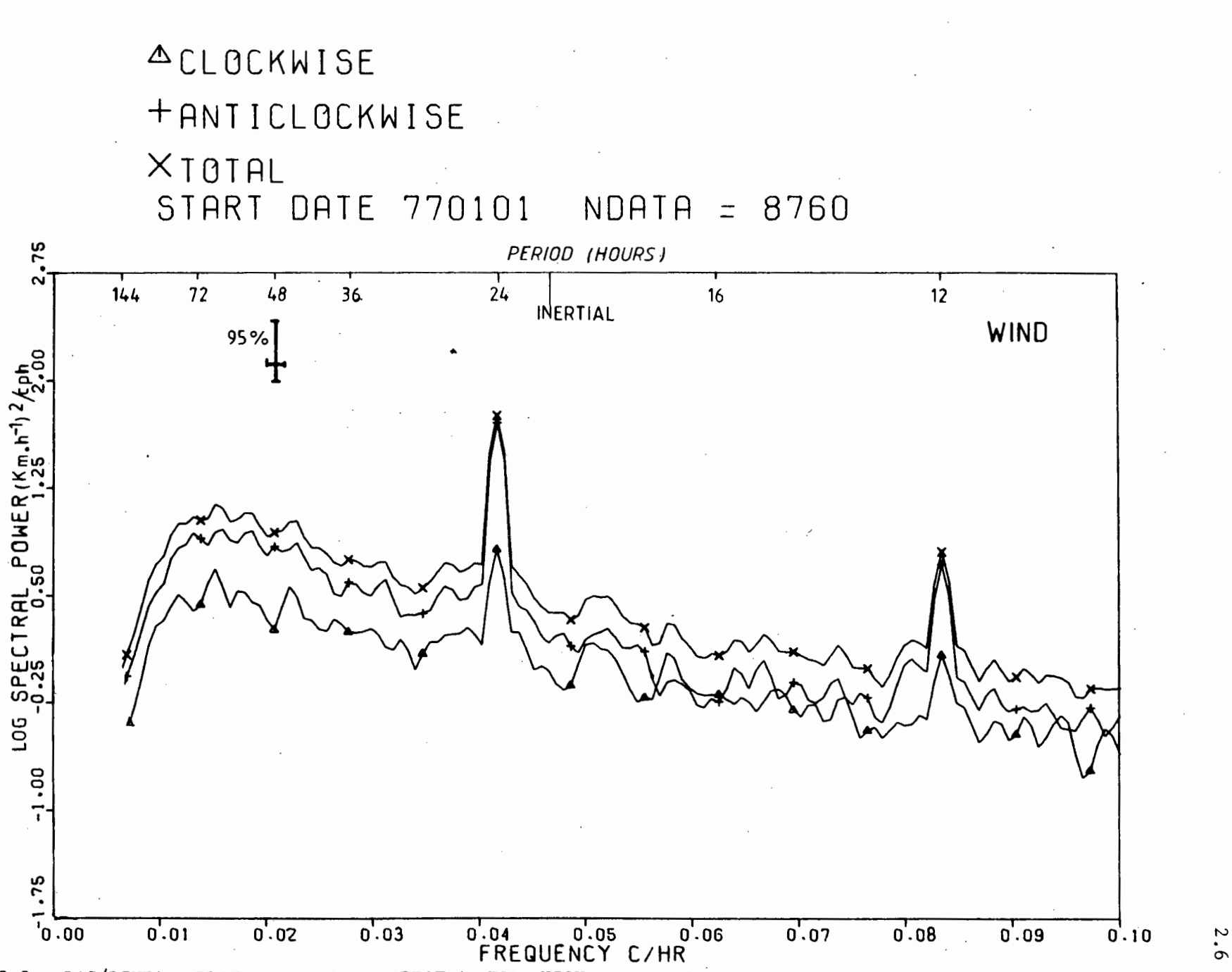

FIG. 2.2 LOG/LINEAR PLOT OF ROTARY SPECTRA FOR HIGH FREQUENCY FILTERED OU SKIP WIND DATA FOR 1977, COVERING THE LOWER FREQUENCY PORTION OF FIG. 2.1

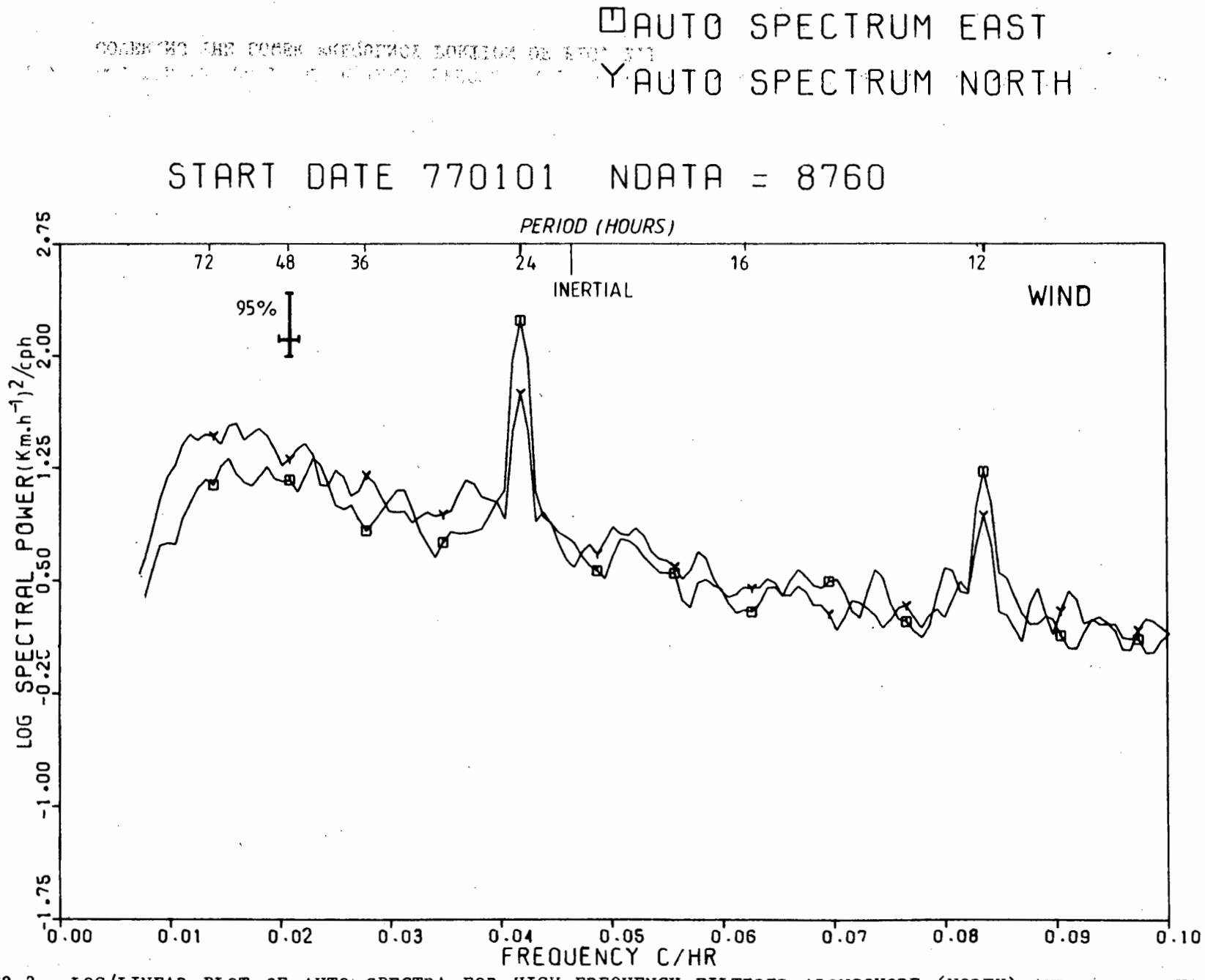

FIG. 2.3 LOG/LINEAR PLOT OF AUTO SPECTRA FOR HIGH FREQUENCY FILTERED ALONGSHORE (NORTH) AND ACROSS-SHORE (EAST) OU SKIP WINDS FOR 1977

The log/log plot of the rotary spectrum (Fig. 2.1) also reveals a fall off in power with increasing frequency that follows approximately a $f^{-3/2}$ power law. The slope may be slightly different across the diurnal frequency portion.

The autospectra of the across-shore (easterly) and alongshore (northerly) wind components for the same 1977 data set are shown plotted on log/linear axes in Fig. 2.3. The features in the spectra are of course similar to the rotary spectra but reveal differences between the two components. The across-shore component spectrum has a much stronger diurnal peak than the alongshore component spectrum i.e. 174 versus 57 $(km/h)^2/cph$. This is probably due to the land seabreeze process that tends to align across-shore. In autospectra for other years there is some evidence for a small peak at the inertial frequency (0.0462 cph) in the case of the alongshore component but not the across-shore component. The inertial nature is supported by an anti-clockwise dominance at that frequency in the corresponding rotary spectrum. The across-shore autospectrum generally has a flatter response and less energy than the alongshore spectrum for frequencies less than the diurnal frequency. Because of the suspected breakthrough nature of the semidiurnal peak no comparisons are made at that frequency.

2.3.2 The Low Frequency Range

In this range we include that of the ILF range. For the latter the rotary spectrum obtained for wind data of 1977 is shown in Fig. 2.4 as a log/log plot. Although there is some structure in the spectrum there are no peaks that exceed the 95 % confidence levels. The bandwidth is fairly wide because of the relatively few number of lags possible in this frequency range for a one year long data set. There is a general decrease in spectral power with increasing frequency which follows approximately a f^{-1} power law. A maximum occurs at a period of 15 to 20 days. The response function of the filter predicts a 0.2 % fall-off at 20 days and 12 % at 30 days. The observed fall-off for periods longer than 20 days is faster than this, indicating that some peaking occurs about that region. The anti-clockwise component consistently has more energy than the clockwise between 15 and 20 days. The autospectra of the two components (Fig. 2.5) are similar to the rotary spectrum.

The across-shore component has a less steep rise in spectral energy with decreasing frequency than the alongshore component (Fig. 2.5). The former has less energy than the latter for periods greater than 6 days and the reverse is true for shorter periods. The alongshore component has a maximum at 20 days while the other has an earlier

maximum at 15 days.

The high and low frequency wind spectra display **power law trends** of $f^{-3/2}$ and f^{-1} respectively. There are no obvious theoretical explanations for the numerical values of these power laws whereas for the sea temperature spectra with a f^{-2} trend there are supportive explanations (see 2.4.1). Wind spectra with higher frequencies (greater than 1.0 cph) than are considered here extend into the atmospheric turbulence region for which there are well defined power laws (Kaimal et.al. 1972). Inspection of various published wind spectra for the frequency band of interest here do however indicate certain consistencies in power law regions. Generally the slopes are relatively steep around the diurnal frequencies then flatten out over the synoptic range as observed here and again steepen for periods exceeding 20 days. Spectra are reported to show variation with latitude, topography and continental influences (Wunsch 1980). Wind spectra for the CODE exercise off California show gentler falloff with frequency ($f^{-3/2}$) at the coast than offshore (f^{-2}), (Winant, Beardsley and Davis, 1987). Spectral attributes will be discussed in Chapter 4 and Chapter 5.

2.3.3 The Very Low Frequency Range

The VLF range is not analysed spectrally but the autocorrelation function (acf) is evaluated. The first zero crossing of the acf at a lag of 63 days multiplied by 4 indicates a dominant period in the time series of the order of 252 days (Le Blond and Mysak, 1978). The repeat zero crossing interval estimate, indicates some process occurring at a period greater than 80 days. The VLF time series data for both wind components are shown in Fig. 2.6 in the form of daily wind sticks. A seasonal time scale cycle is evident in the data, particularly for the alongshore (north) component, where a broad maximum northerly wind is present during the winter months and southerly wind maxima occur in spring and late summer. Shorter periodicities are also revealed.

2.4 TEMPERATURE SPECTRA

Since temperature is a scalar variable the autospectrum of a set of time series temperature data was formed by the standard classical spectral analysis method via the autocorrelation function. The temporal features revealed in each of the frequency ranges is now presented.

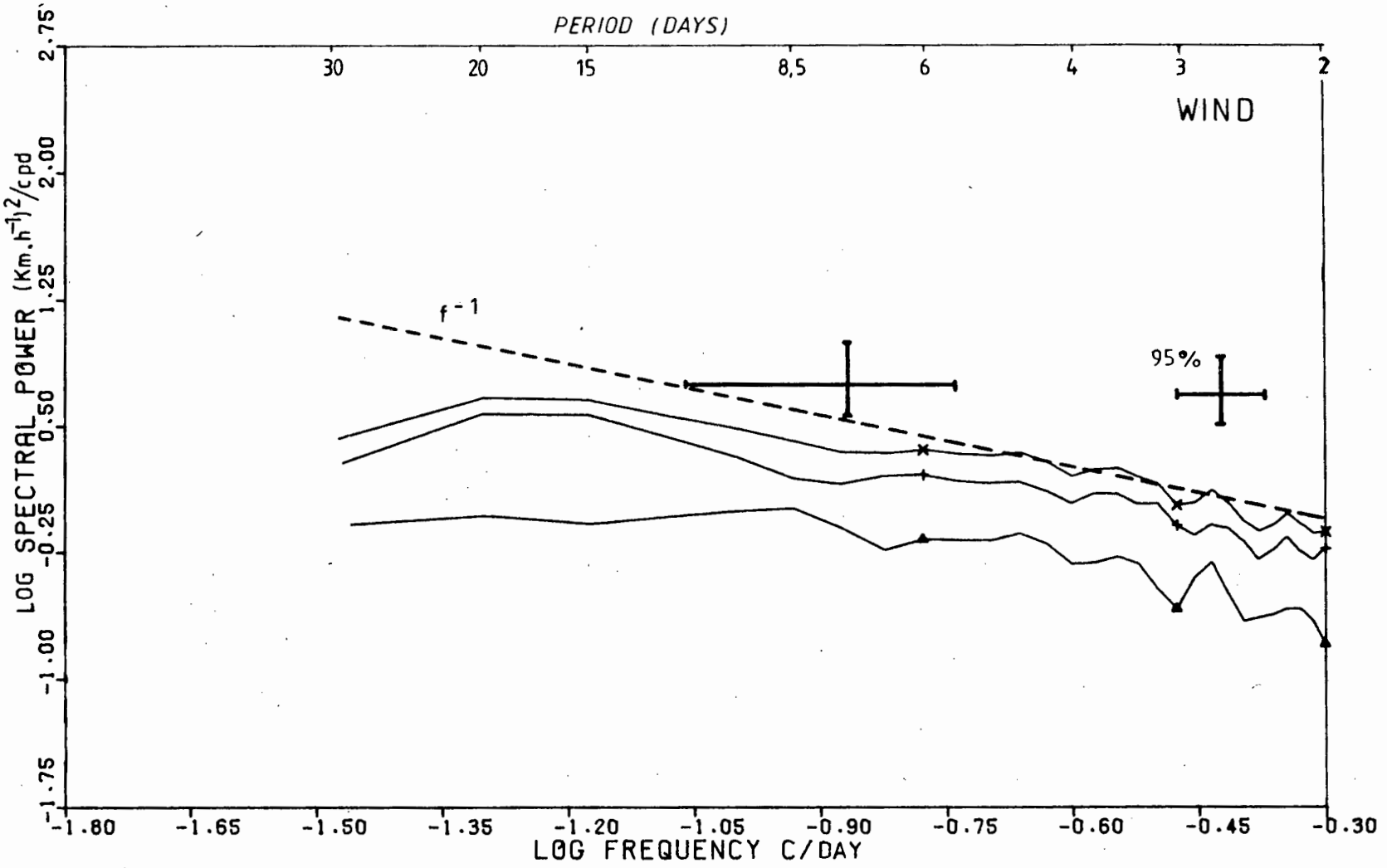

FIG. 2.4 LOG/LOG PLOT OF ROTARY SPECTRA FOR INTERMEDIATE LOW FREQUENCY FILTERED OU SKIP WIND DATA FOR 1977. MAXIMUM LAG NUMBER 60 BUT ONLY PORTION CORRESPONDING TO LOWER FREQUENCIES IS SHOWN. PLOTTED SYMBOLS INDICATE EACH 10TH LAG NUMBER

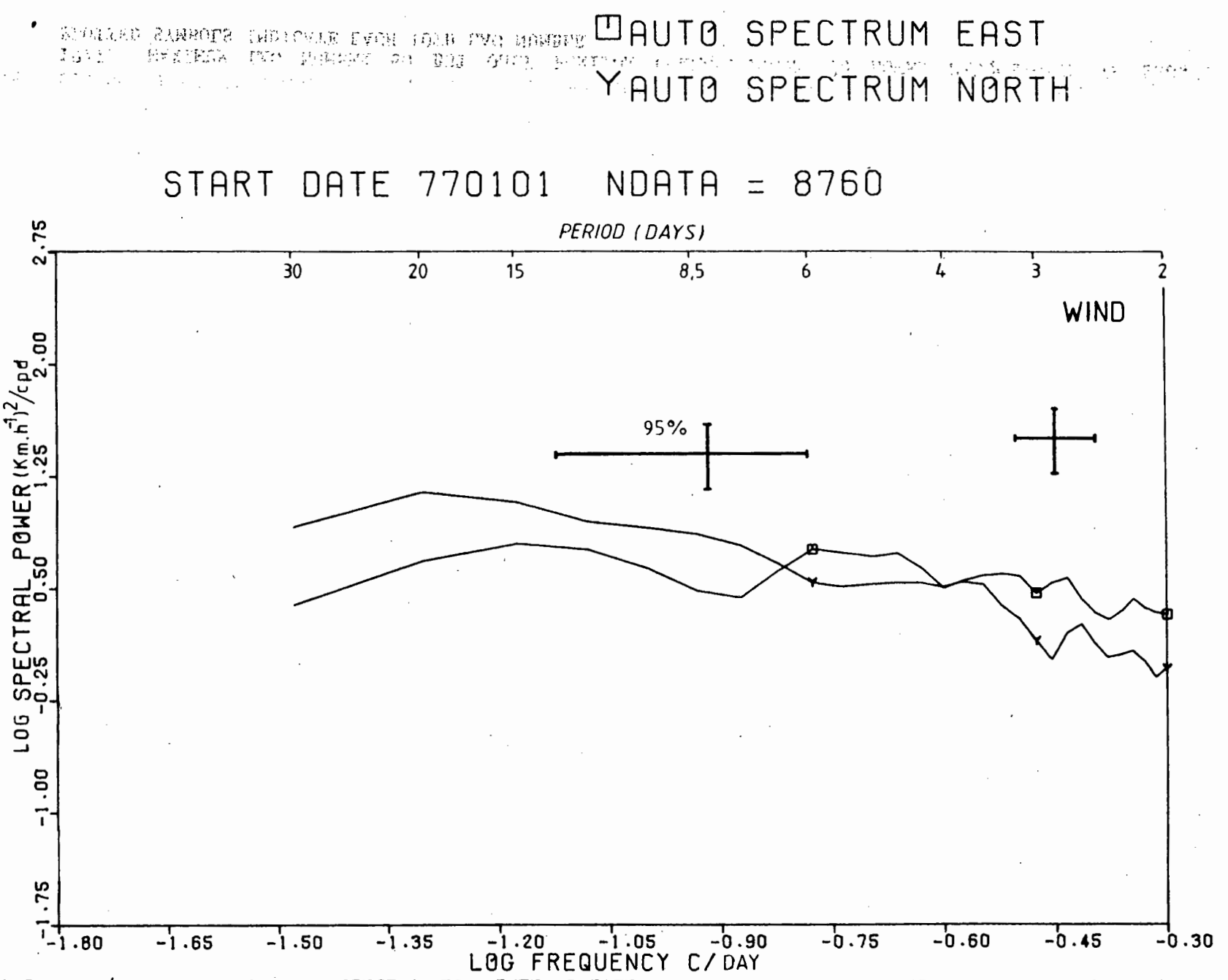

FIG. 2.5 LOG/LOG PLOT OF AUTO SPECTRA FOR INTERMEDIATE LOW FREQUENCY FILTERED ALONGSHORE (NORTH) AND ACROSS-SHORE (EAST) OU SKIP WINDS FOR 1977

2.4.1 The High Frequency Range

The spectra obtained in this HF range for the 1977 temperature data at the 2 m depth are shown in Fig. 2.7 as a log/log plot of spectral power versus frequency in cycles per hour. The number of data points, the lags used and the 95 % confidence levels are as described for the wind spectra in Section 2.3.1.

The main features of the 2 m depth temperature spectra (Fig. 2.7) are a) a very prominent peak at the diurnal frequency, 1/24 cph, with a spectral power of 118$(C°)^2$/cph; b) a smaller peak with a spectral power of 14.1 $(C°)^2$/cph at a frequency of 1/21.8 cph which is close to the inertial frequency of 1/21.64 cph for the site; c) a pair of peaks (which statistically fall just below the 95 % confidence level) near the semidiurnal frequency; one of which is at an exact frequency of 1/12.0 cph and probably has contributions from the main semidiurnal solar tide S2 and the harmonic breakthrough of the 24 hour peak as discussed in Section 2.3.1. The other is at a frequency of 1/12.4 cph which coincides with the main semidiurnal lunar tidal frequency (M2) of 1/12.42 cph.

These features are resolved better in the linear plot of part of the spectrum in Fig. 2.8. This figure shows up spectral structure at frequencies less than the diurnal frequency i.e. structure is seen up to a period of 3 days. The longer periods are cutoff by the filter used which has a quarter power point at 96 hours and a 3 % dropoff at 3 days. The log/log plot (Fig. 2.7) illustrates well the general decrease in spectral power with increasing frequency which follows approximately a f^{-2} power law. A f^{-2} power law region can be explained by either of two processes:

a) When the temperature is a passive component in the water column then a turbulent cascade of kinetic energy of temperature fluctuations gives a f^{-2} dependence in the spectra when plotted against a frequency axis as in Fig. 2.7. This can be compared directly with a 5/3 power law for turbulent cascade in a spectra with a wave number (space scale) axis. Brundrit (Pers com)

b) When the temperature structure in the water column occurs in a series of layers with sharp steps, Phillips (1971 and 1975) has shown that if the medium undulates then the measured temperature spectrum has a f^{-2} behaviour.

For the CODE data set off California, Winant et al., (1987) observes, over the subdiurnal band in the temperature spectra, a power law trend exceeding f^{-2}; the 10 m depth data however have a less steep

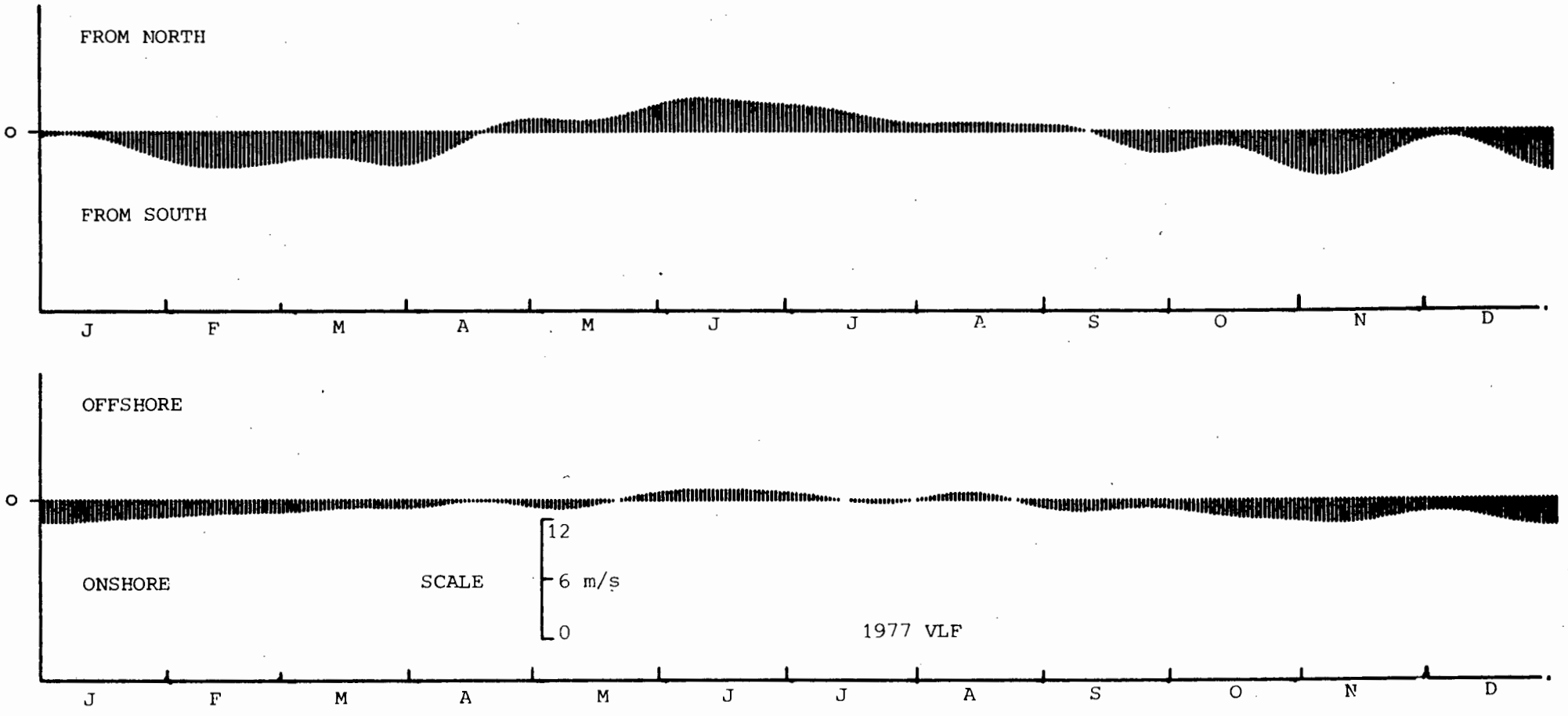

FIG. 2.6 TIME SERIES STICK DIAGRAMME OF DAILY VALUES OF VERY LOW FREQUENCY FILTERED OU SKIP WIND COMPONENTS FOR 1977. TOP - ALONGSHORE (NORTH), BOTTOM - ACROSS-SHORE (EAST)

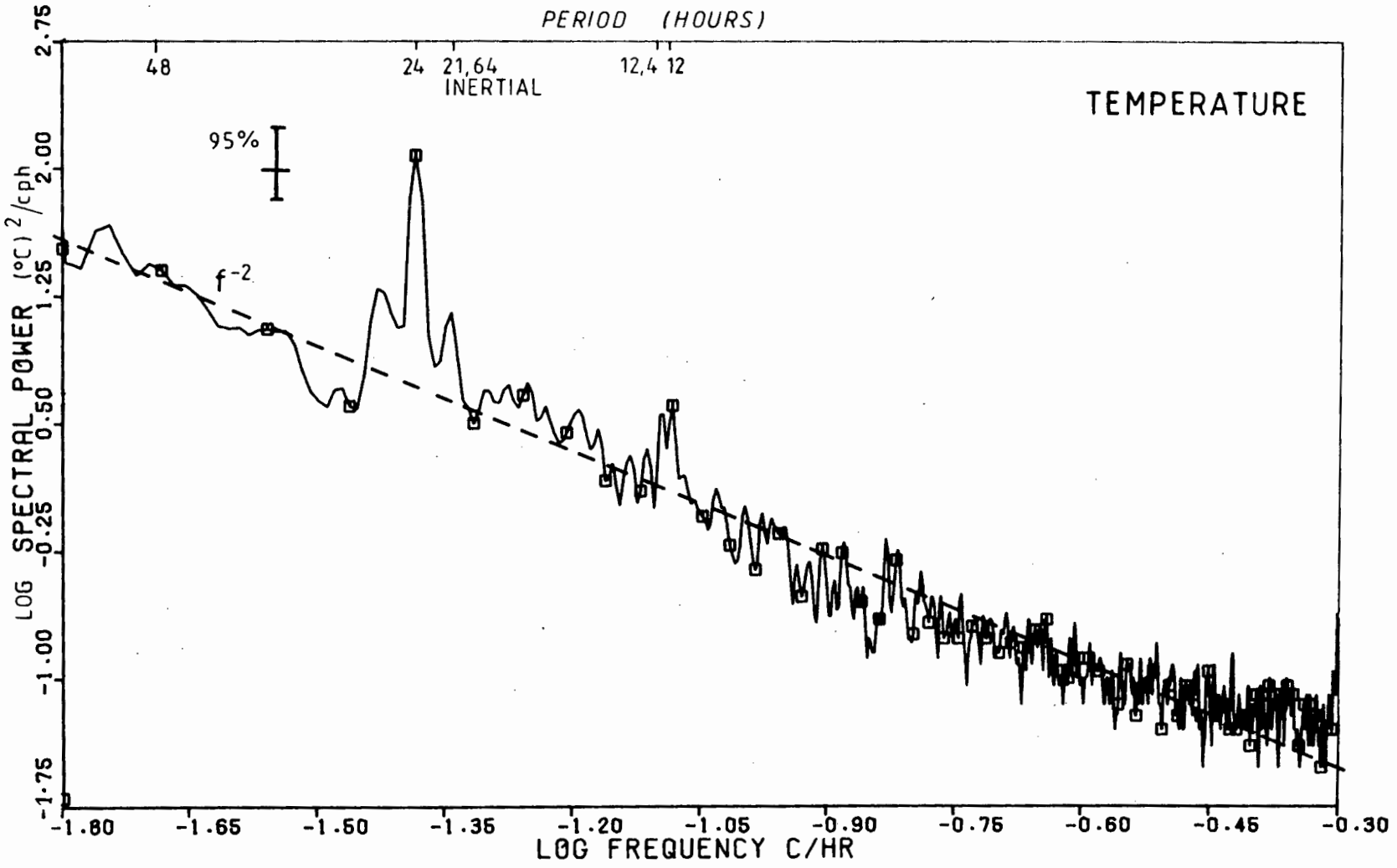

FIG. 2.7 LOG/LOG PLOT OF AUTO SPECTRUM FOR THE HIGH FREQUENCY FILTERED 2 M DEPTH SEA TEMPERATURE DATA FOR 1977. MAXIMUM LAG NUMBER, 720. PLOTTED SYMBOLS INDICATE EACH 10TH LAG NUMBER

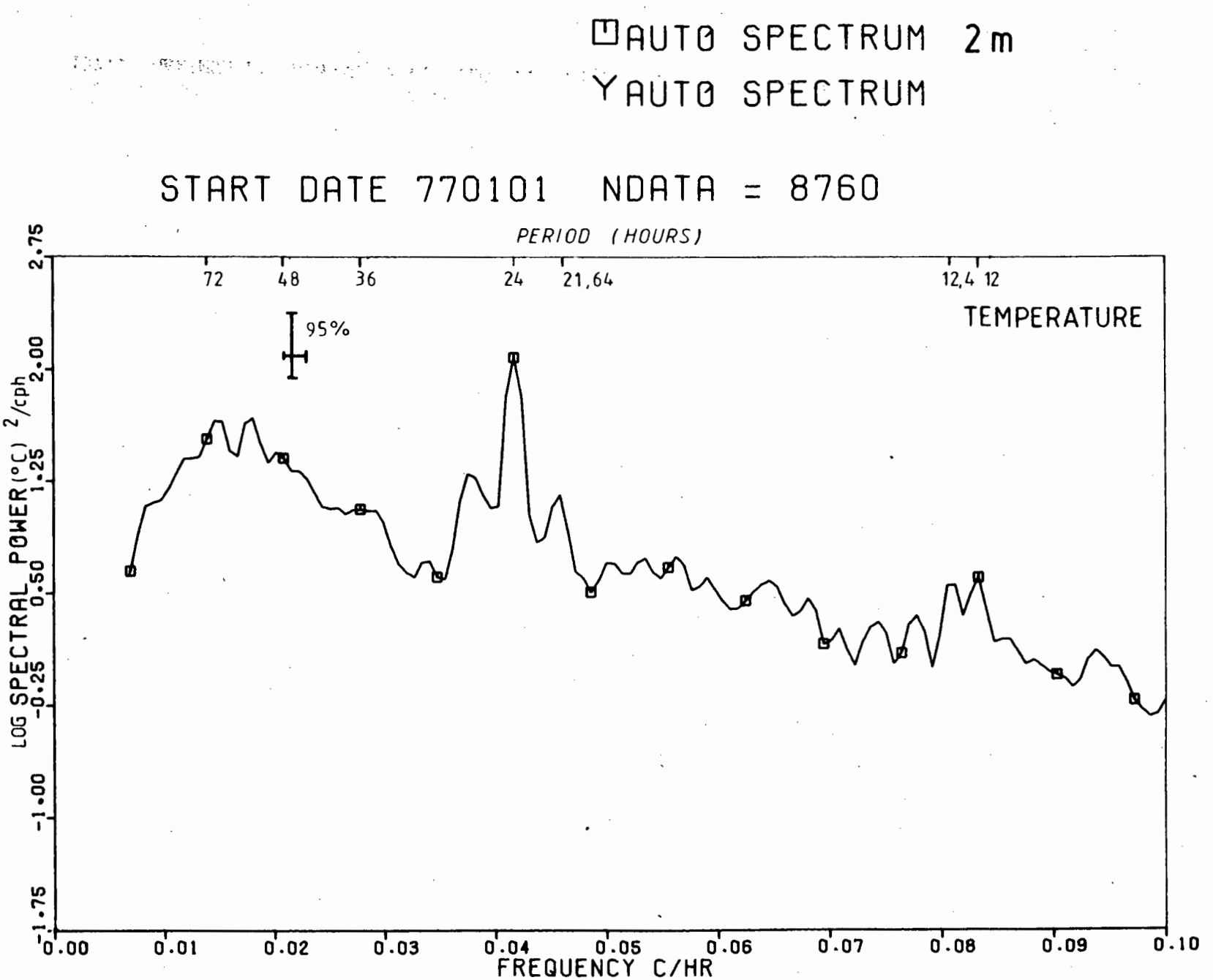

FIG. 2.8 LOG/LINEAR PLOT OF AUTO SPECTRUM FOR THE HIGH FREQUENCY FILTERED 2 M DEPTH SEA TEMPERATURE DATA FOR 1977, COVERING THE LOWER FREQUENCY PORTION OF FIG. 2.7

spectral decay than the 70 m data. Aspects of a) and b) will be discussed further in Chapter 5.

2.4.2 The Low Frequency Range

As with the wind data here we include the intermediate low frequency, ILF data. The log/log autospectral plot for the latter is shown in Fig. 2.9 also for the 2 m depth 1977 set. There is no prominent structure in the spectrum. A maximum is reached for a period of 20 days and a subsidiary maximum at 5 days. For frequencies less than 1/20 cpd this log/log plot, similar to the HF range, also shows a f^{-2} power law behaviour. Lee and Mayer (1977) in discussing current spectra in this frequency range comment that distinct energy peaks became lost in spectra of about year-long records due to the event nature of fluctuations which occur with many different time scales and tend to produce a red spectrum when analysed together. The generally featureless spectra seen here tend to fit this pattern although other aspects are discussed in Chapter 4 where an even longer record is analysed to help improve the resolution.

2.4.3 The Very Low Frequency Range

The VLF range is not analysed spectrally. The autocorrelation function (acf) indicates from the first zero crossing value that a dominant period of about 200 days exist. The repeat interval for zero crossing is estimated to be between 60 and 80 days which indicates a periodicity of between 120 to 160 days. The VLF time series data for the 2 m depth temperature data for 1977 are shown in Fig. 2.10 where they are plotted in the same format of daily values as the wind data (Fig. 2.6) to allow for direct comparison. (The fluctuations are better seen in Fig. 2.11.)

The seasonal time scale is evident in the figure as are some shorter period cycles. The annual cycle has a broad high average temperature in winter with minima in spring and late summer. This seemingly unusual behavior of temperature correlations with the seasons is directly attributed to the generally downwelling winds in winter and the upwelling southerly winds of spring and summer that bring cool deep water up to the surface in the coastal region.

Note: The relatively high temperatures evidenced near the start of the 1977 VLF data set (Fig. 2.10) is partly due to the anomalous failure of the sourtherly winds at the end of the previous year extending into the new year. This is discussed in detail in Chapter 3.

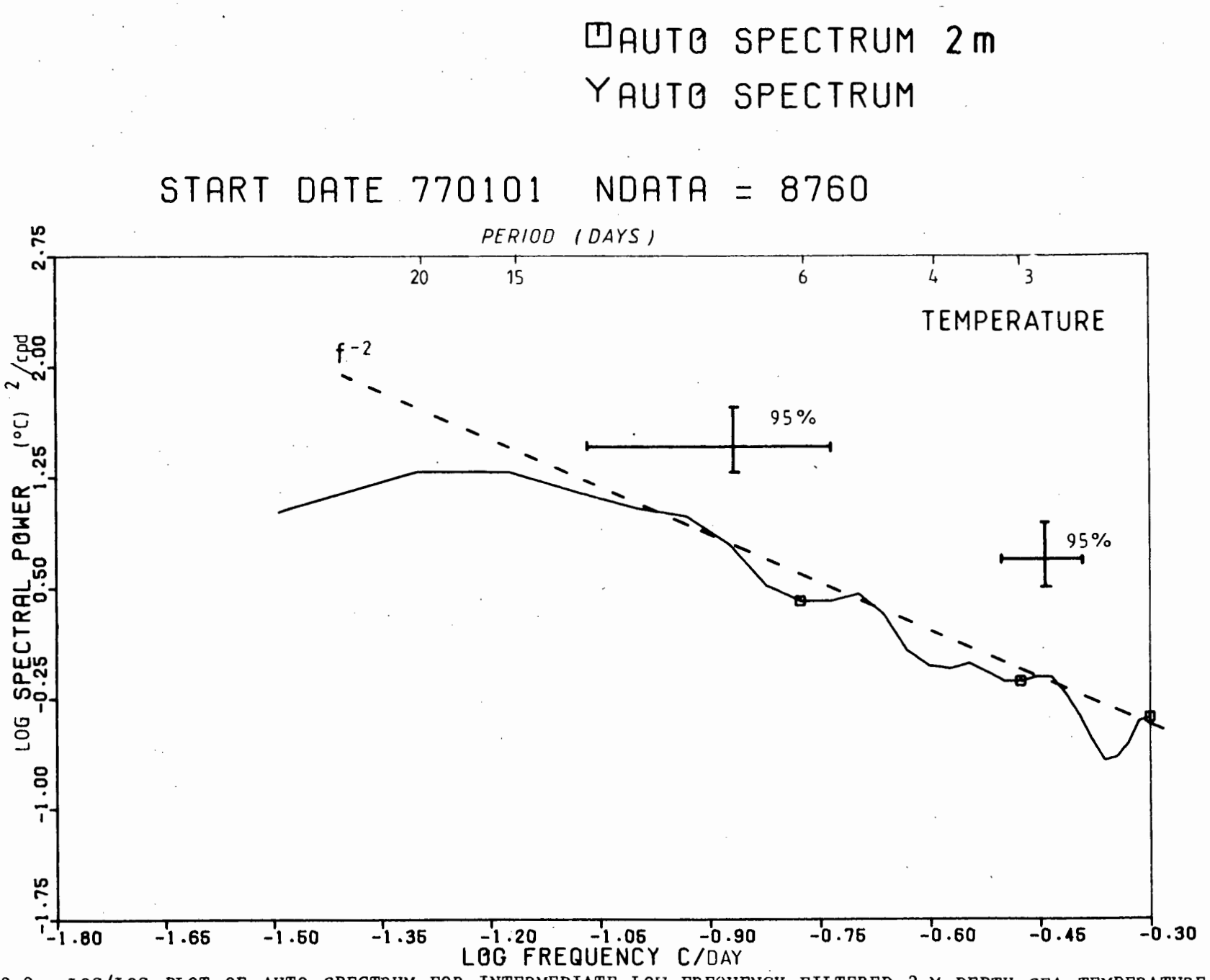

FIG. 2.9 LOG/LOG PLOT OF AUTO SPECTRUM FOR INTERMEDIATE LOW FREQUENCY FILTERED 2 M DEPTH SEA TEMPERATURE DATA FOR 1977

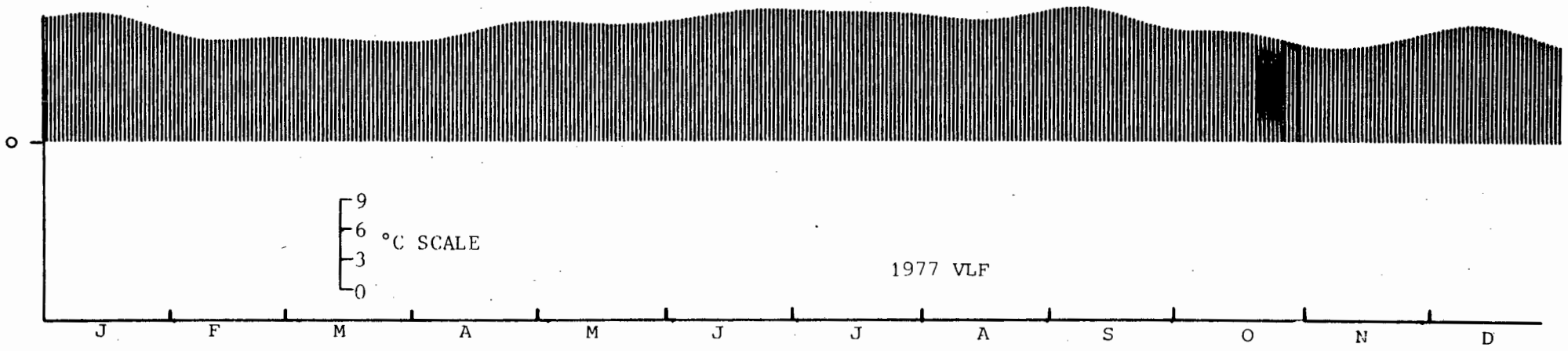

FIG. 2.10 TIME SERIES STICK DIAGRAMME OF DAILY VALUES FOR VERY LOW FREQUENCY FILTERED 2 M DEPTH SEA TEMPERATURES FOR 1977

2.5 RESULTS OF DATA QUALITY TESTS

The various data quality tests are mentioned in the Research Methodology section (1.5). Prior to filtering some data fail the stationarity test but all data after filtering and taking residuals pass the stationarity test at a 95 % confidence level. Even after preprocessing not all the data meet the requirements of the kurtosis and skewness tests. In the case of the wind data the high frequency set tends to be negatively skewed and light tailed. The temperature data quality also varies. Table 2.1 details the results.

Although the data partially fail the strict statistical tests the subsequent spectral analysis yields significant quantitative information on the dominant frequencies and hence indicates the possible processes occurring at the site. The quality of the data is therefore deemed to be of a sufficient standard for time series analysis.

2.6 DISCUSSION OF TIME SCALES

The frequency ranges for analysis have followed fairly standard oceanographic norms (Huyer, et al., 1979). The actual choice of time scales for further characterization depend on the analysis revealing features of interest. Such features are supported by coherence and phase spectra analysis (Section 2.2.1). This is particularly true for the high frequency data where a prominent diurnal peak occurs in both the wind and temperature spectra. The ILF spectra have limited structure but show a broad peaking at the 15 to 20 day periods. Their spectral power is greater than the HF spectra - the temperature spectrum continues the f^{-2} power law trend - the wind spectrum has a somewhat reduced trend of f^{-1} compared to the $f^{-3/2}$ power law in the HF spectrum. This change in slope together with the slight spectral minima at a frequency just below the diurnal frequency indicates a possible 'boundary' between time scales (Lee and Mayer, 1977). A division of time scales can therefore be proposed for periods of 24 hours and shorter and for periods from about 2 days to a few weeks. The VLF filtered time series data reveal definite cycles spaning the seasons for both winds and temperatures. Thus the seasonal time scale can be selected for investigation.

Three dominant time scales can therefore be defined viz. a) seasonal, being for a few weeks to many months b) event scale of several days and c) mesoscale phenomena of 24 hours or less. Monin (1977) for the deep ocean classifies seven non-stationary processes varying from time scales of a fraction of a second to centuries. The three classifications used here fall within his classifications of a) seasonal variations, b) synoptic variability and c) mesoscale

phenomena respectively. The three categories are now discussed.

2.6.1 The Seasonal Time Scale

This time scale covers periods from several weeks to about one year. Both the wind and temperature data reveal seasonal variations (Figs. 2.6 and 2.10). How "typical" the following descriptions of seasonality are will depend on analysis of longer time series given in Chapter 3. The alongshore or north component of the wind shows a clear seasonal cycle with southerly winds in summer and northerly winds in winter. The winter regime lasts about 130 days. The southerly wind strength fluctuates, with periods of 40 to 80 days being apparent.

The across-shore or east component of the wind tends to be much smaller than the north component. With the 20°-adjustment to the component axes, allowing alignment with the average coastline orientation, a seasonal cycle is more readily evident than without the adjustment. Thus we see offshore winds in mid-winter and onshore winds at other seasons for this component (Fig. 2.6).

The sea temperature has a clear seasonal cycle with a generally warm trend during the mid-winter and cooler waters during spring and late summer. The warmer sea temperatures in winter indicate that the temperature cycles at this time scale are not strongly influenced by a solar effect but are related to some other effect which we show is related to wind stress.

2.6.2 The Event Time Scale

This covers periods greater than the diurnal period and less than about three weeks. The HF and ILF spectra for both wind (Figs. 2.1 and 2.4) and temperature (Figs. 2.7 and 2.9) show an increase in energy for periods greater than 1.5 days and have a broad maximum around 15 to 20 days. In the case of the wind data the average slope in the ILF spectra is less steep than the $f^{-3/2}$ slope in the HF spectra. The temperature spectra continues to obey a f^{-2} power law at these lower frequencies. The power laws are discussed in 2.3.2 and 2.4.1.

The ILF spectra show some limited structure for periods between 2 and 10 days. The periods in the wind spectra are most probably due to modulation effects of the passage of different atmospheric events or synoptic systems past the region of the site. Hence the classification of this being the event time scale. Although a more definite structure is expected with the analysis of a longer than 1 year time series data base (see Chapter 4), it has already been noted

in 2.4.2 that Lee and Mayer (1977) observe that distinct energy peaks become lost in extended time series spectra at the event time scale.

2.6.3 Mesoscale Phenomena

This classification is for processes with periods between a few hours and one day. For frequencies greater or equal to that of the diurnal frequencies, it is the diurnal peak that greatly dominates the spectra of both wind and sea temperature. Clearly some solar process is strongly influencing the data set either directly or indirectly.

Inspection of spectra for other years show that a small peak occurs for both the wind and temperature data near the inertial frequency of 1.109 cpd for the site. The rotary spectra for the wind data confirm the anti-clockwise sense of rotation for this southern hemisphere data at the inertial frequency. (Wind data for one individual year, 1977, used in this chapter does not show the inertial peak in its spectra although it is present in the corresponding temperature data.) Although inertial effects are common in the sea (Gonella, 1971) the atmospheric contribution is unexpected especially at such low altitudes, the wind meter being at 14 m height, and is discussed in Chapter 5.

In the temperature data one other peak of interest lies at 12.4 hours corresponding to the main semi-diurnal lunar tide M2 of 12.42 hours. The peak at 12 hours is puzzling and as discussed in Section 2.3.1 is probably in the case of the wind due to a harmonic breakthrough of the strong 24 hour peak. But why is it less strong in the temperature spectrum? This question is addressed in Chapter 5.

2.7 CAUSAL RELATIONSHIPS BETWEEN WIND AND TEMPERATURE

Inspection of spectra and filtered time series of wind and temperature data show similarities that indicate clear links between the data sets. Both data sets exhibit seasonal trends, spectral structure in the 2 to 10 day range with broad maxima between 15 to 20 days, dominant diurnal peaks and spectral structures in the mesoscale range. An example of similarities in the time series data is given in Fig. 2.11 where the VLF data for the alongshore wind and the 2 m depth temperature for 1977 are plotted together. In seeking to establish what degree of correlation exists between wind and temperatures and what are the casual relationship we first undertake simple linear correlation analysis between the time series data in the different frequency bands.

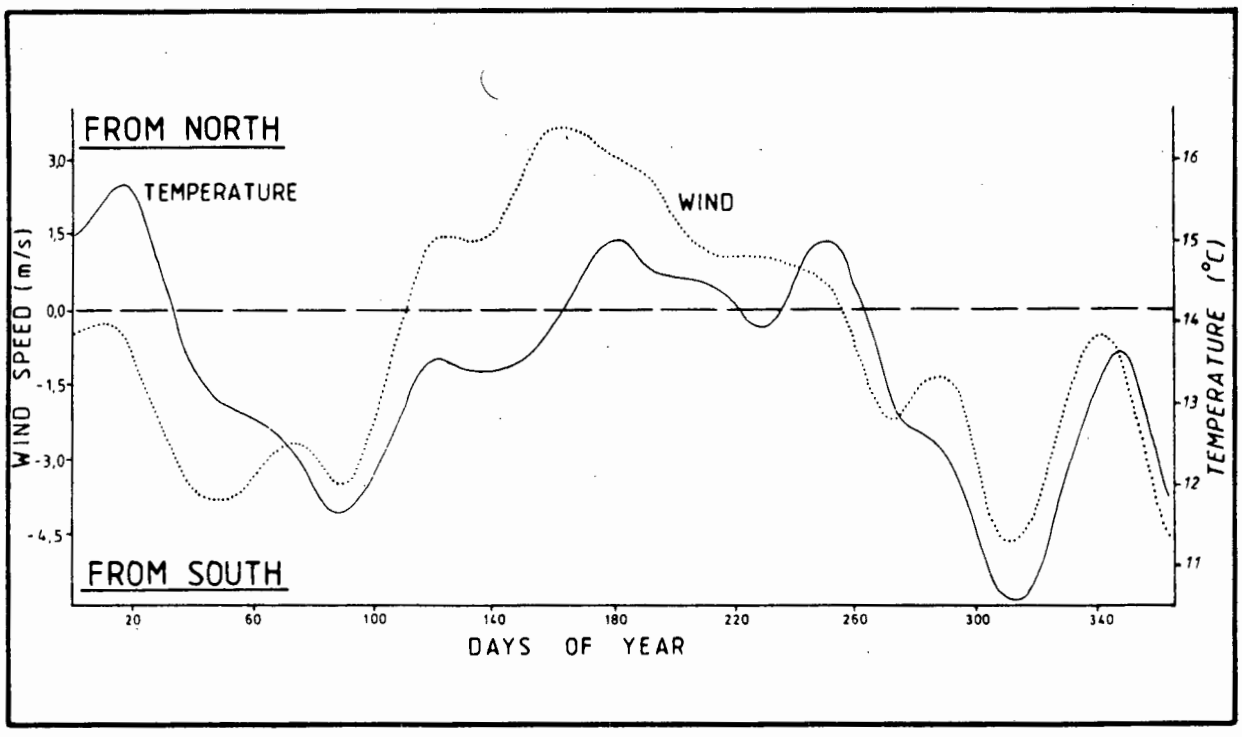

FIG. 2.11 COMBINED TIME SERIES PLOT OF VLF ALONGSHORE WIND AND VLF 2 M DEPTH TEMPERATURE FOR 1977

Prior to correlation analysis the filtered data are preprocessed by firstly detrending and reducing to zero mean and then normalizing by the variance. This enables more meaningful comparison to be made between the variables (Düing, et al., 1977). Details of this and estimation of the degrees of freedom and confidence levels of the correlation coefficient are given in the section on Research Methodology (1.5.3).

The linear correlation coefficients between a given wind component and the 2 m depth temperature for the years 1976 and 1977 are given in Table 2.2 for the different frequency ranges. In this table daily values for the full year are used for the VLF and ILF ranges. In the case of the HF data a selected 3 week long hourly record is used to illustrate correlation characteristics. The record lengths quoted in the table are less than the time-series length used because an order 26 lagging procedure is used. An estimate of the number of degrees of freedom and corresponding critical correlation coefficients is made in most cases. Reference should be made to Section 3.2.3 and Section 1.5.3 about correlation analysis.

For the VLF and ILF data at zero lag the alongshore component correlates very well with the temperature data, usually better than the 99 % confidence level. It is even better correlated when the temperature lags the wind. The across-shore component in

the VLF and ILF ranges is poorly or significantly negatively correlated with the temperature at zero lag; with some positive lag it is generally not correlated at the 95 % confidence level. The correlation characteristics in the HF range are different. Although the record length is short in terms of days it is adequate statistically for the hourly data and illustrates a fundamental change in correlation at this frequency range. At zero lag both the along and across-shore components have negative non-significant correlation with the sea temperature. The lagged correlation coefficients (Table 2.2) shows that only the across-shore component exceeds the 95 % confidence level with a negative correlation. The alongshore component correlation does increase but just fails to meet the 95 % limit.

These examples have shown therefore that there is good statistical evidence of linear correlations between wind and sea temperature. This indicates some causal relationships between these parameters which also have a varied lagged response in the different frequency ranges. In the HF range further information on causal relationships is gleaned from the rotary spectral analysis of the winds which indicates preferred angles of orientation of the major ellipse axis for different frequencies. At the diurnal frequencies these orientations can be broadly classified as lying parallel to the coast or orthogonal to it.

The causal connections between wind and sea temperature will be discussed in detail in following chapters. In summary however, the main causal link is due to an upwelling process next to the coast. A favourable equatorward wind will cause an Ekman divergence at this coast and cause cooler deeper water to upwell to compensate for the surface waters that have moved off-shore. Subsequent onshore or poleward winds will cause warmer surface waters to move onshore and downwelling occurs.

In the different frequency bands the wind is driven by a variety of processes. On a seasonal time scale the South Atlantic high pressure region moves southwards in summer causing south and southeast winds to ridge in at this southwest tip of Africa (Taljaard, et al., 1972). Cold fronts and coastal lows pass to the east on a time scale of one or several days. At the diurnal time scale insolation causes both some direct sea temperature effects and the land-sea breeze effect (Jury, 1980), which modulates the gradient wind. At each time scale the wind or pressure field has some different impact on oceanographic parameters which in turn affects the upwelling processes that are reflected in changes in sea temperature.

Other causal relationships are expected between the wind and waves and between the wind and coastal currents. These links are considered in later chapters.

2.8 SUMMARY OF THE CHAPTER

In this chapter, for wind and sea temperature data we have shown the existence of certain features in different frequency bands covering the range from 12 cpd to less than 0.0025 cpd. Dominant time scales have therefore been delineated as the seasonal, event (synoptic) and mesoscale time scales. This was done by using spectral analysis techniques on time series type data using different frequency response filters. The data quality is considered to be suitable for this study. Simple linear correlations between wind and temperature time series establishes that for certain cases very good (95 %) correlations do exist. This led to the proposal of some causal connections between wind and sea temperature. These proposals will be further illustrated as each time scale is explored in separate chapters.

TABLE 2.1

STATISTICAL DATA QUALITY FOR WIND AND TEMPERATURE

YEAR	VARIABLE	FREQ RANGE	SKEWNESS	KURTOSIS	STATIONARITY
1976	Wind - Across	HF	-0,45 (Neg)	0,37 (LT)	>95 %
1976	Wind - Along	HF	-0,14 (Neg)	0,93 (LT)	>95 %
1976	Wind - Across	VLF	-0,22 (Neg)	0,25 (Sym)	>95 %
1976	Wind - Along	VLF	0,04 (Sym)	-0,18 (Sym)	>95 %
1977	Wind - Across	HF	-0,46 (Neg)	0,40 (LT)	>95 %
1977	Wind - Along	HF	-0,01 (Sym)	0,46 (LT)	>95 %
1977	Wind - Across	VLF	-0,20 (Neg)	1,09 (LT)	>95 %
1977	Wind - Along	VLF	0,12 (Sym)	-0,10 (Sym)	>95 %
1976	Temperature 2 m	HF	0,08 (Pos)	2,69 (LT)	>95 %
1976	Temperature 8 m	HF	0,24 (Pos)	3,25 (LT)	>95 %
1976	Temperature 2 m	VLF	0,26 (Pos)	0,37 (Sym)	>95 %
1976	Temperature 8 m	VLF	0,34 (Pos)	0,35 (Sym)	>95 %
1977	Temperature 2 m	HF	-0,09 (Neg)	4,2 (LT)	>95 %
1977	Temperature 8 m	HF	0,16 (Pos)	4,0 (LT)	>95 %
1977	Temperature 2 m	VLF	-0,40 (Neg)	0,79 (LT)	>95 %
1977	Temperature 8 m	VLF	-0,38 (Neg)	1,07 (LT)	>95 %

Neg = Negative
Pos = Positive
Sym = Symmetrical
LT = Light Tailed

TABLE 2.2

LINEAR CORRELATION COEFFICIENTS BETWEEN LINEARLY DETRENDED WIND COMPONENTS AND 2 m DEPTH TEMPERATURE

DATE	RECORD LENGTH DAYS	WIND COMPONENT*	DEGREES OF FREEDOM	OBSERVED CORRELATIONS		LAG m DAYS	CRITICAL CORRELATION COEFFICIENT		
				C_o+	C_m+		95 %	99 %	99,9 %
A. VLF DATA (Daily)									
1976	340	N/S	10	0,63	0,73	8	,50	,66	,79
1976	340	E/W	9	0,04	0,11	26	,52	,68	,82
1977	340	N/S	7	0,78	0,84	10	,58	,75	,87
1977	340	E/W	9	0,59	0,72	14	,52	,68	,82
B. ILF DATA (Daily)									
1976	340	N/S	95	0,28	0,55	1	,17	,24	,31
1976	340	E/W	134	-0,25	0,09	9	,14	,20	,26
1977	340	N/S	83	0,31	0,55	1	,18	,25	,33
1977	340	E/W	-	-0,18	0,12	6	-	-	-
C. HF DATA (Hourly)						Hours			
1977 14 Oct to 7 Nov	600	N/S	42	-,11	+,23	6-8	,25	,35	,43
	600	E/W	29	-,21	-,35	3-4	,30	,42	,53

* Wind has been rotated 20° to align with coastline orientation
N/S = Alongshore component E/W = Across-shore component

+ C_o = Correlation coefficient at zero lag

+ C_m = Maximum correlation coefficient for Lag m

CHAPTER THREE

SEASONAL CHARACTER

C O N T E N T S

CHAPTER THREE

SEASONAL CHARACTER

3.1 INTRODUCTION

In the previous chapter we established a number of dominant time scales within which different processes could be proposed to explain the oceanographic regime. In this chapter we take a detailed look at the time scale that encompasses the very low frequency (VLF) data. This includes processes with periods longer than about 40 days, seasonal effects and also inter-annual trends. Broadly speaking the annual variations of insolation and of the atmospheric states account for the seasonal variability of oceanographic parameters (Monin, 1977). For this site the mean or seasonal character and its associated forcing processes will be established. Within the coastal boundary layer the flow is often chaotic, variable in time and spatially complex, but establishment of the mean conditions for periods greater than the tidal and weather events (Csanady, 1976b) can have practical benefits - both for identifying the key signature of processes and for predicting the fate of the transport of fish eggs or pollutants. The inter-annual mean will also be explored and the representativeness of the local data set checked. The links to the larger scale meteorological and oceanographic features of the area will be identified. The concept of "transition" between seasons will be investigated.

3.2 WIND AND TEMPERATURE CHARACTER

Since the best data set from a continuous time series point of view comprises wind and sea temperature records these are analysed in detail here. In later sections aspects of currents and wave data are given.

3.2.1 Filtered Time Series Data (VLF)

In this section we display and discuss graphical data of a multi-year set of very low frequency filtered Ou Skip winds and sea tower temperatures. The coordinate system for the wind vectors is rotated counter-clockwise by 20° to align the components alongshore (approximately north-south) and across-shore (approximately east-west). Because the process of filtering the data causes truncation, an extra 52 days unfiltered time series data were included at each end of an annual data set to achieve a filtered data set of exactly one calender year. The extra data were real data from

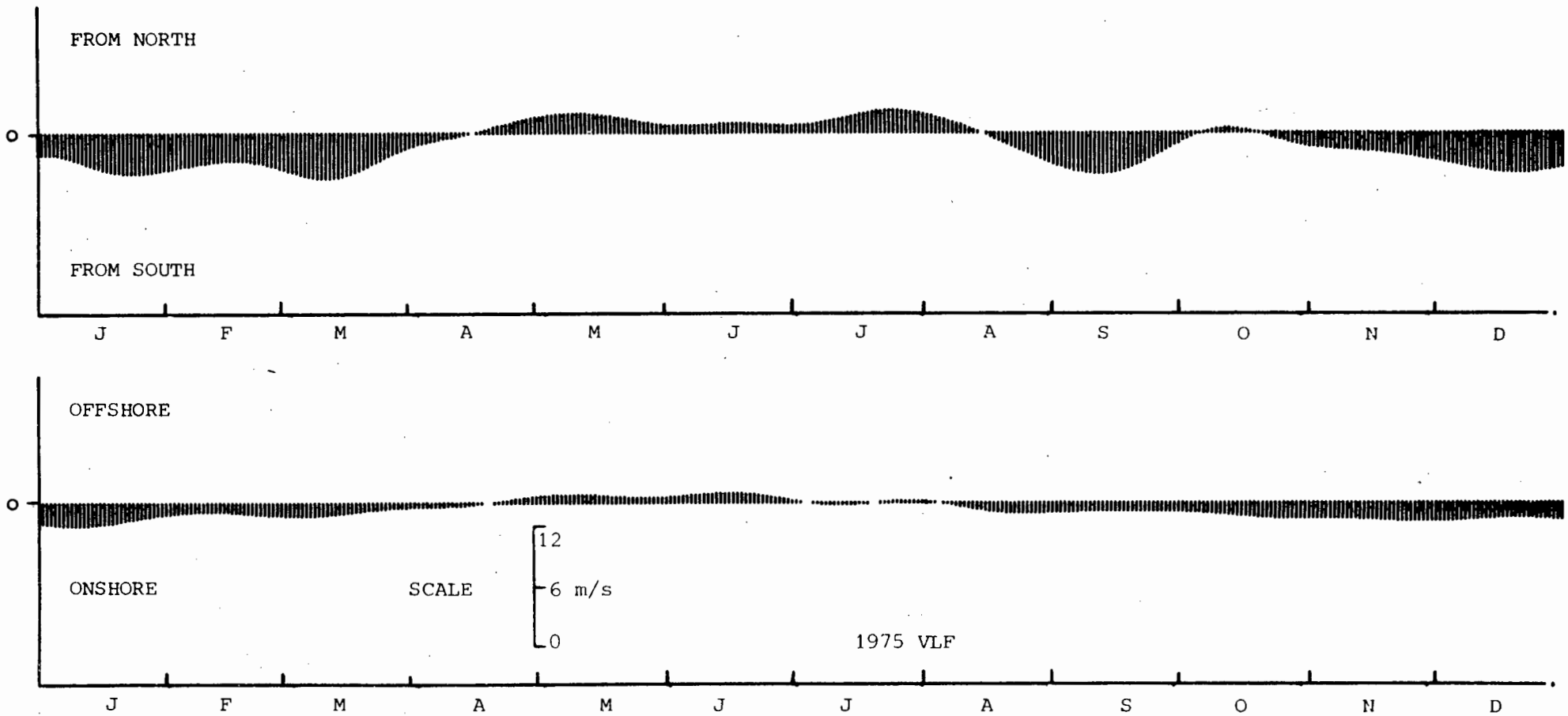

FIG. 3.1a 1975
TIME SERIES DIAGRAMME OF DAILY VALUES OF VLF FILTERED OU SKIP WIND COMPONENTS - ANNUAL SETS. TOP - ALONGSHORE (NORTH), BOTTOM - ACROSS-SHORE (EAST). COMPONENTS AXIS IS ROTATED 20° WEST OF NORTH

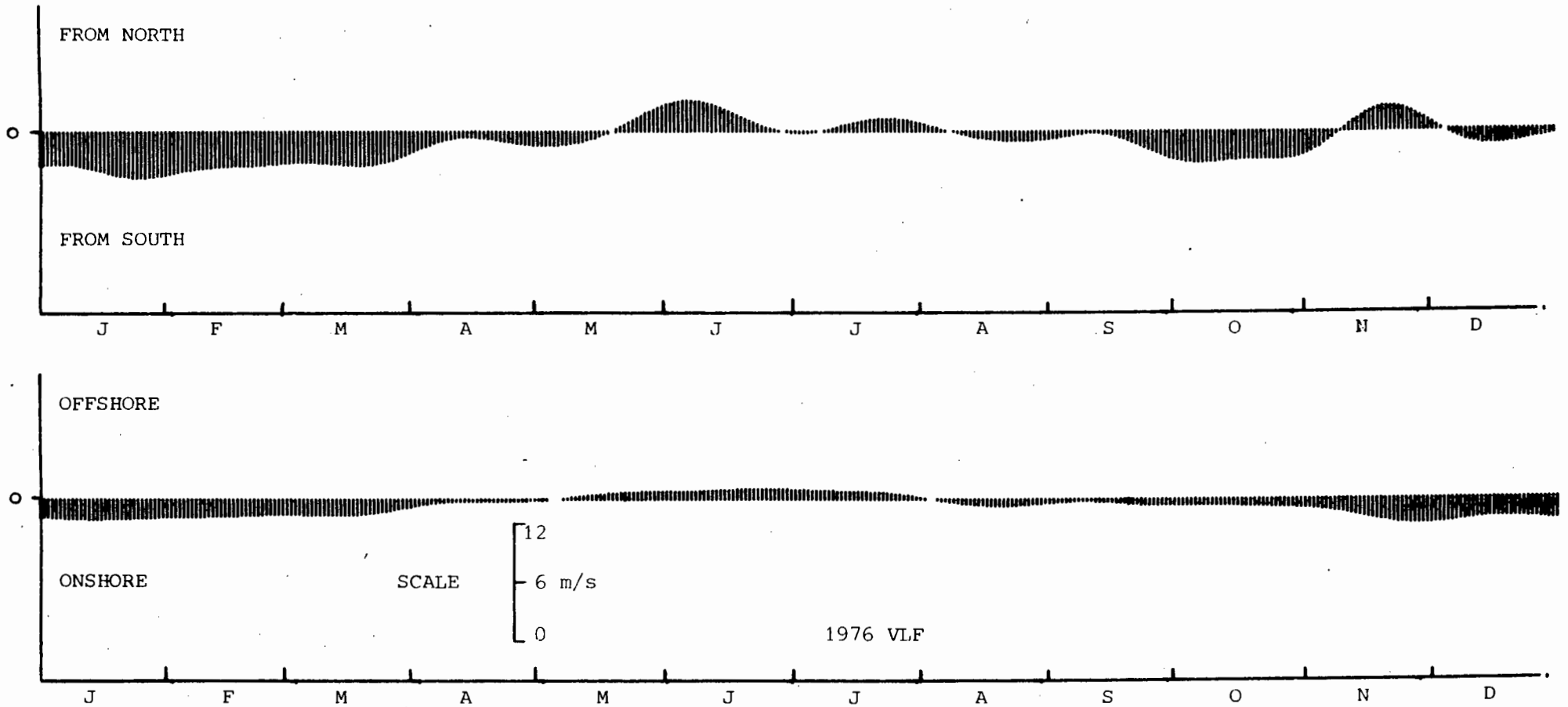

FIG. 3.1b 1976
TIME SERIES DIAGRAMME OF DAILY VALUES OF VLF FILTERED OU SKIP WIND COMPONENTS - ANNUAL SETS. TOP - ALONGSHORE (NORTH), BOTTOM - ACROSS-SHORE (EAST). COMPONENTS AXIS IS ROTATED 20° WEST OF NORTH

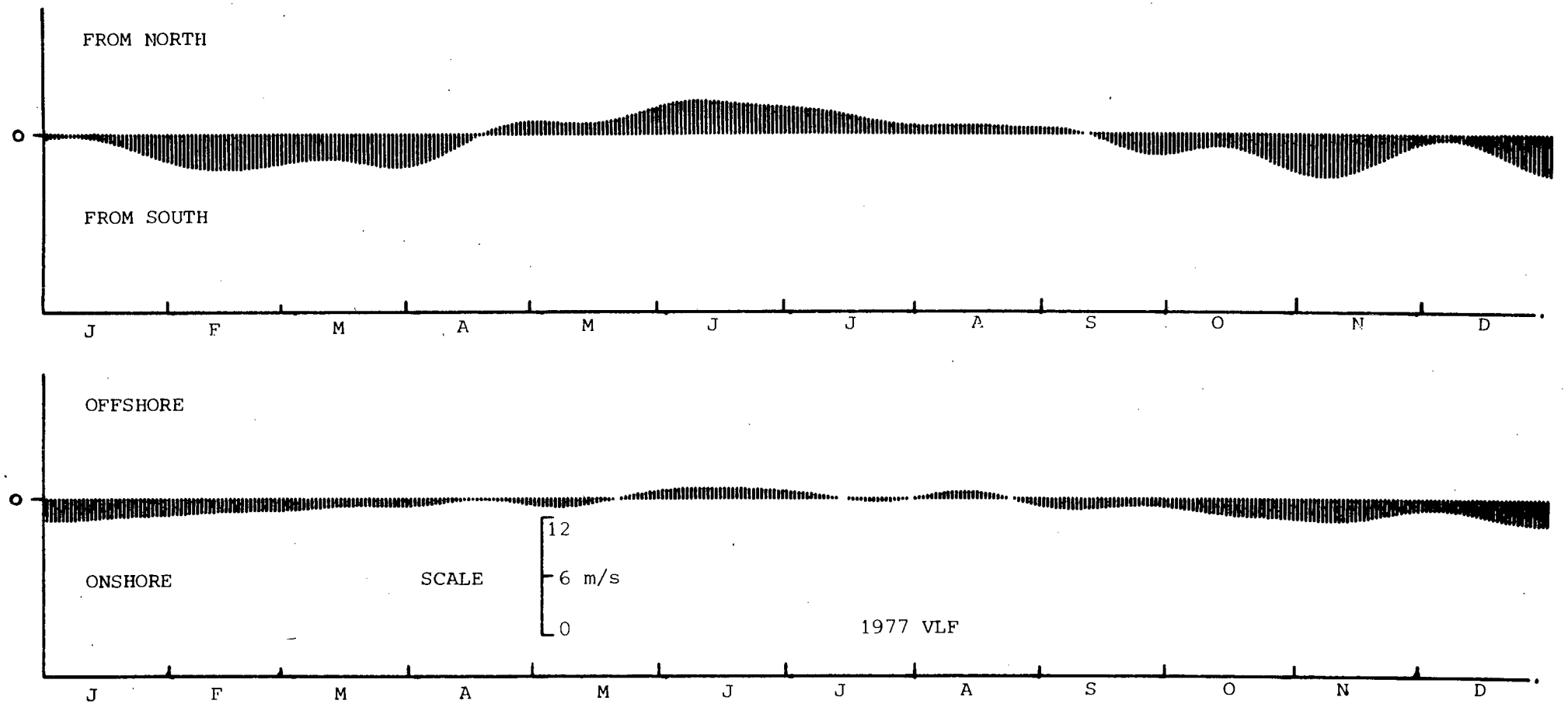

FIG. 3.1c 1977
TIME SERIES DIAGRAMME OF DAILY VALUES OF VLF FILTERED OU SKIP WIND COMPONENTS - ANNUAL SETS. TOP - ALONGSHORE (NORTH), BOTTOM - ACROSS-SHORE (EAST). COMPONENTS AXIS IS ROTATED 20° WEST OF NORTH

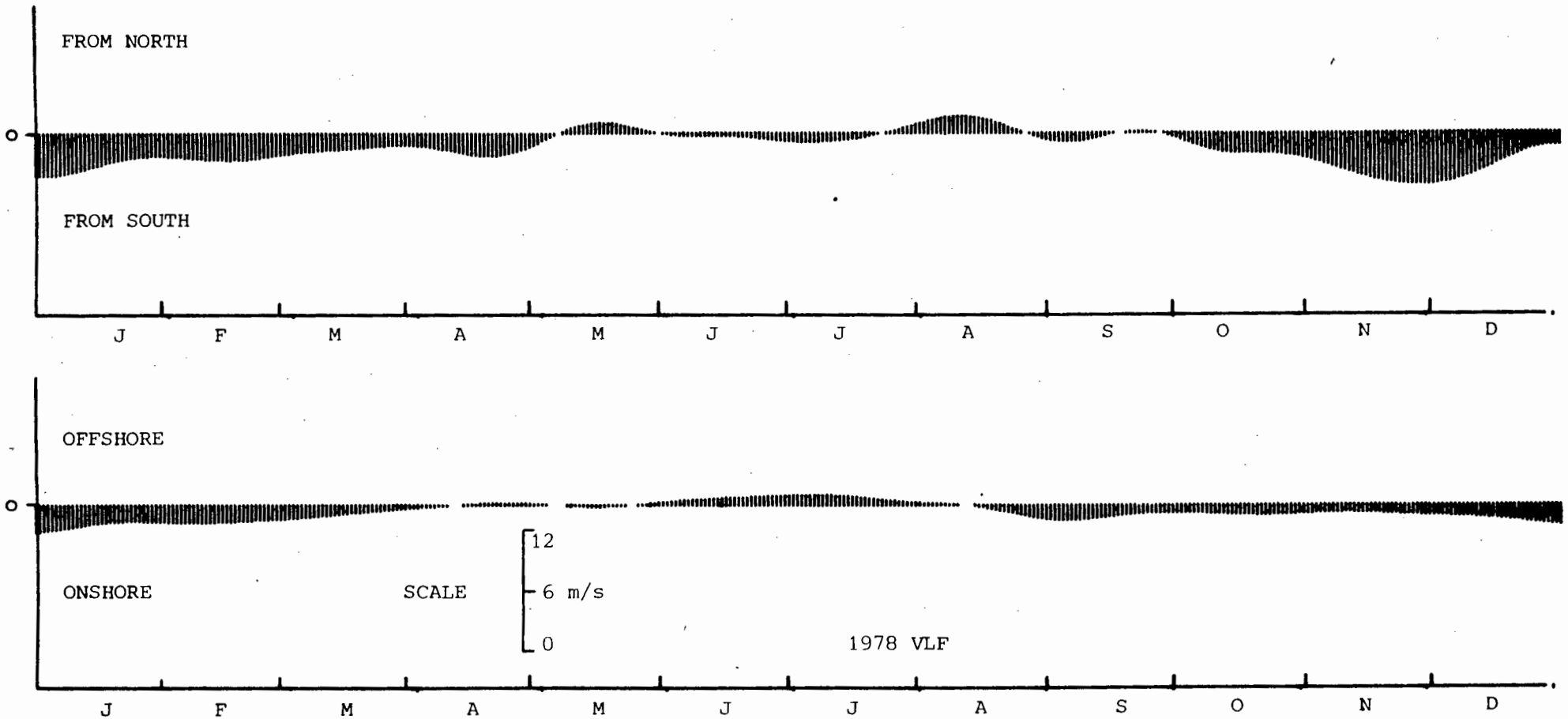

FIG. 3.1d 1978
TIME SERIES DIAGRAMME OF DAILY VALUES OF VLF FILTERED OU SKIP WIND COMPONENTS - ANNUAL SETS. TOP - ALONGSHORE (NORTH), BOTTOM - ACROSS-SHORE (EAST). COMPONENTS AXIS IS ROTATED 20° WEST OF NORTH

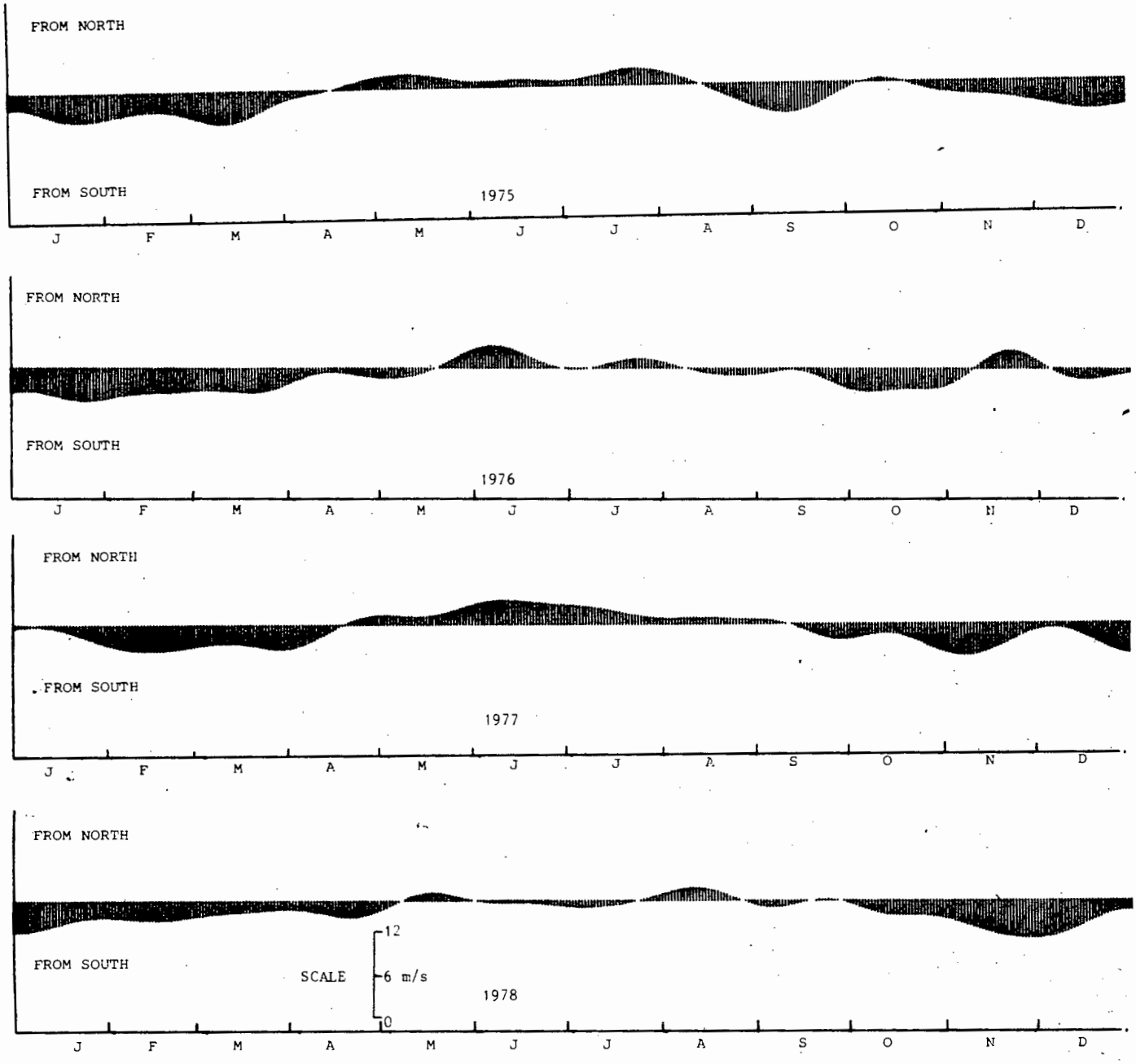

FIG. 3.2 AS FIG. 3.1 BUT A COMPOSITE OF THE FOUR ANNUAL CASES FOR ALONGSHORE (NORTH) COMPONENTS STARTING WITH 1975 AT THE TOP

the preceeding and following year. The VLF data are shown graphically for daily values of both components of the Ou Skip winds for 1975 to 1978 inclusive (Fig. 3.1a-d). For ease of comparison the alongshore component for each year are plotted together in Fig. 3.2. Similarly the daily values of the VLF 2 m depth temperatures (based on hourly data) for 1976 and 1977 inclusive are given in Fig. 3.3. In addition a 5 m depth 12 hourly temperature record covering a longer period from August 1974 till May 1978 is used. The 12 hour time step is adequate for this seasonal time scale analysis. In this case 48 days are truncated off each end of the total multi year record in the VLF filtering process yielding a record from 74-09-18 till 78-04-24. Results are plotted in Fig. 3.4 as annual segments of the record.

If we first consider the winds and look at their winter character between about May and August we see for the alongshore winds a definite northerly component. For this frequency range and for the years depicted no other significant northerly winds (except for November 1976) are experienced at other times of the year. The duration and intensity of this northerly winter regime does vary considerably from year to year. It commences between mid April and mid May and ends between early August and about mid September. The duration varies between 2,5 and 4,5 months. In the VLF data set the wind strength fluctuations during this time have a period of 30 to 40 days. Periods up to several months are classified in the synoptic variability range by Monin (1977). In contrast the east-west or across-shore component shows a much weaker characteristic during winter, when there is a trend for weak offshore winds and even weaker onshore winds of shorter duration. This offshore flow may seem surprising at first because the so-called northwester of the winter period will give an onshore component. However, inspection of the 4 year (1972-1975) mean monthly wind rose data for Ou Skip from UCT/ESCOM report No. 15 (Mallory and Maxwell, 1969 ff) and given here in Table 3.1 shows that the most common winter wind is from due north. In fact N, NNE and the easterly winds peak prominently in winter whereas the NW wind is more evenly distributed throughout the year with a slight peak in spring. This character of the northerly winds is also shown by data from DF Malan Airport and is discussed in Section 4.3.1. Bearing in mind the 20° west of north orientation of the coast, the wind rose data confirms the offshore tendency for the low frequency across-shore winds in winter. This tendency is also influenced by the enhancement of landbreezes during the cold winter months and by sustained "berg wind" conditions when an interior high-pressure area causes offshore flow. The duration of this weak offshore winter character is shorter, generally by several weeks from the stronger northerly alongshore character.

Outside this winter regime the winds are generally strong southerly (alongshore) with a weak onshore tendency for the across-shore component. During most of the years shown, there is a tendency for the southerly wind strength to decrease in December/January. This feature is more marked for data by Andrews and Hutchings (1980) for Cape Point winds, over a 16 year record. The 22 year wind record for D F Malan (Fig. 3.9a) however indicates a wind maximum in January to early February. The southerly wind is still relatively strong in March and then decreases in April as the transition to the winter regime commences. There appears to be a quicker transition from the southerly to the northerly regime than there is for the converse, i.e. the autumn change is more definite than the spring change. This is further discussed in Section 3.8.

In the four years of data depicted, (Fig. 3.2) the initial strong southerly blow in spring for the new season is followed by a marked reduction in wind strength and even a reversal of wind direction in the case of November 1976. The latter was an anomalous event (report no 5, Bain and Harris, 1975ff, Hutchings et al., 1984 and Trenberth, 1979) and is discussed in Section 3.4. At this time scale these initial southerly blows have broad maxima that peak as early as mid September (1975) and as late as the end of November (1978). A consistent weak onshore wind for the across-shore component occurs during the approximately 8 months total southerly regime. Reference to the mean wind rose data for Ou Skip (Table 3.1) shows that the strongest southerly winds are from SSE and S which will give a net onshore component for the 20° orientation of the coast. The enhancement of the seabreeze effects in the warm summer months (Jury, 1980 and Norden, et al., 1982, Jury and Spencer-Smith, in press) will also contribute to the weak onshore characteristics. Of course because of the much stronger southerly alongshore winds, Ekman transport effects gives a net offshore displacement of surface waters during this period.

We thus have two major wind regimes during the year; the northerly winds with onshore Ekman transport during the winter months of May to August and the southerly winds for the other months. Andrews and Hutchings (1980) and Nelson and Hutchings (1983) also note two wind regimes for the Cape Point data, and designate October to March as the summer period. In modelling the ecological effects of upwelling and downwelling water transport in a kelp bed off the Cape Peninsula Wulff and Field (1983) choose May to August for winter conditions and September to April for "summer" conditions.

The southerly wind regime can be divided into two further sub regimes, which we designate here as the spring (early summer) regime September to December and the (mid to late) summer regime January to April. The actual point of division is somewhat arbitary and is done partly as an aid to subsequent analysis. There is some justification for this subdivision into two regimes. If one compares the plots of alongshore winds (1975 to 1978, Fig. 3.2) for the periods September - December and January - April it is apparent that the former period is characterized with greater fluctuations in wind strength and even reversals of wind direction relative to the latter period, which tends to be more consistent in strength with a greater mean value. The spring regime period can be considered as a transition between the chiefly northerly flow of winter and the dominant southerly flow of the summer regime. This is borne out statistically for the years 1975 to 1978 where Table 3.2 shows for adjoining spring summer periods that a) the standard deviation in southerly wind strength of the spring period is generally greater than that for the summer period and b) the mean wind in spring is generally less than for the summer period. At the event time scale presented in the following chapter the cumulative Ekman transport (CET) plots Fig. 4.6 illustrate that more onshore events occur during the spring period than in the summer period. Over a much longer time base this tendency is confirmed for a) wind data of Andrews and Hutchings (1980) for Cape Point from 1963 to 1978 where more variability is shown in spring but also a more definite lull in southerly wind strength over December and January, and b) wind data for D F Malan Airport (Section 3.4) for the years 1957 to 1978 when the multi-year mean shows (Fig. 3.9a) a definite lull in wind strength during early spring and a less definite relaxation over December January.

Together with the winter regime the year is therefore divided into three approximately equal duration wind regimes, winter (May-August), spring (September-December), summer (January-April). In later discussions the spring and summer regimes are often combined to form the southerly regime.

The sea temperature data are represented by a little more than a three year record (Fig. 3.4), and are only analysed in detail for 1976 and 1977. Characteristics cannot therefore be as well defined as the wind, particularly when it is reiterated that the summer of 1976/1977 was anomalous. Nevertheless some obvious features are present.

The mid-year winter period does have sea temperatures warmer than the mean temperature for each year. The period September to April

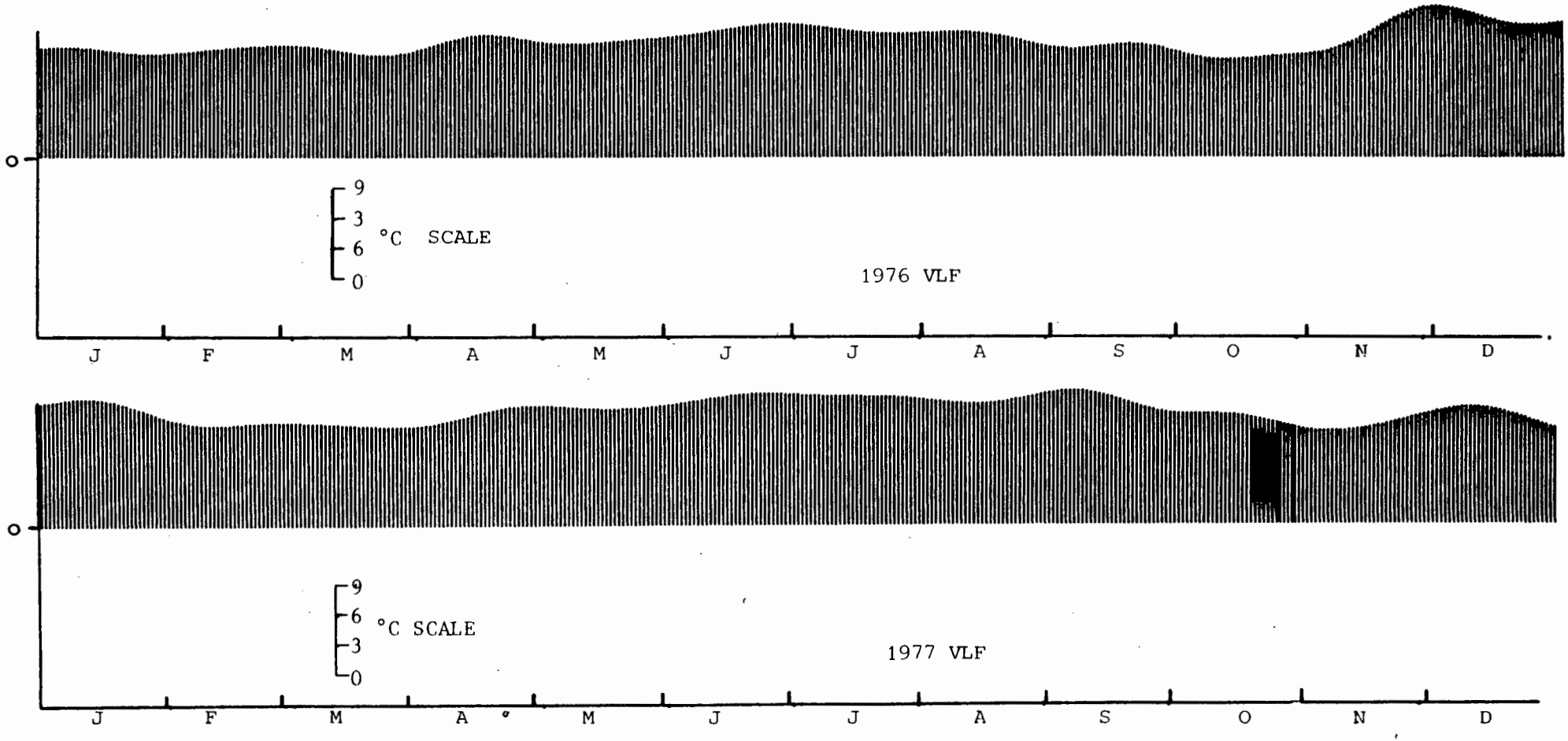

FIG. 3.3 TIME SERIES DIAGRAMME OF DAILY VALUES OF VLF FILTERED 2 M DEPTH TEMPERATURES - ANNUAL SETS. TOP - 1976, BOTTOM - 1977

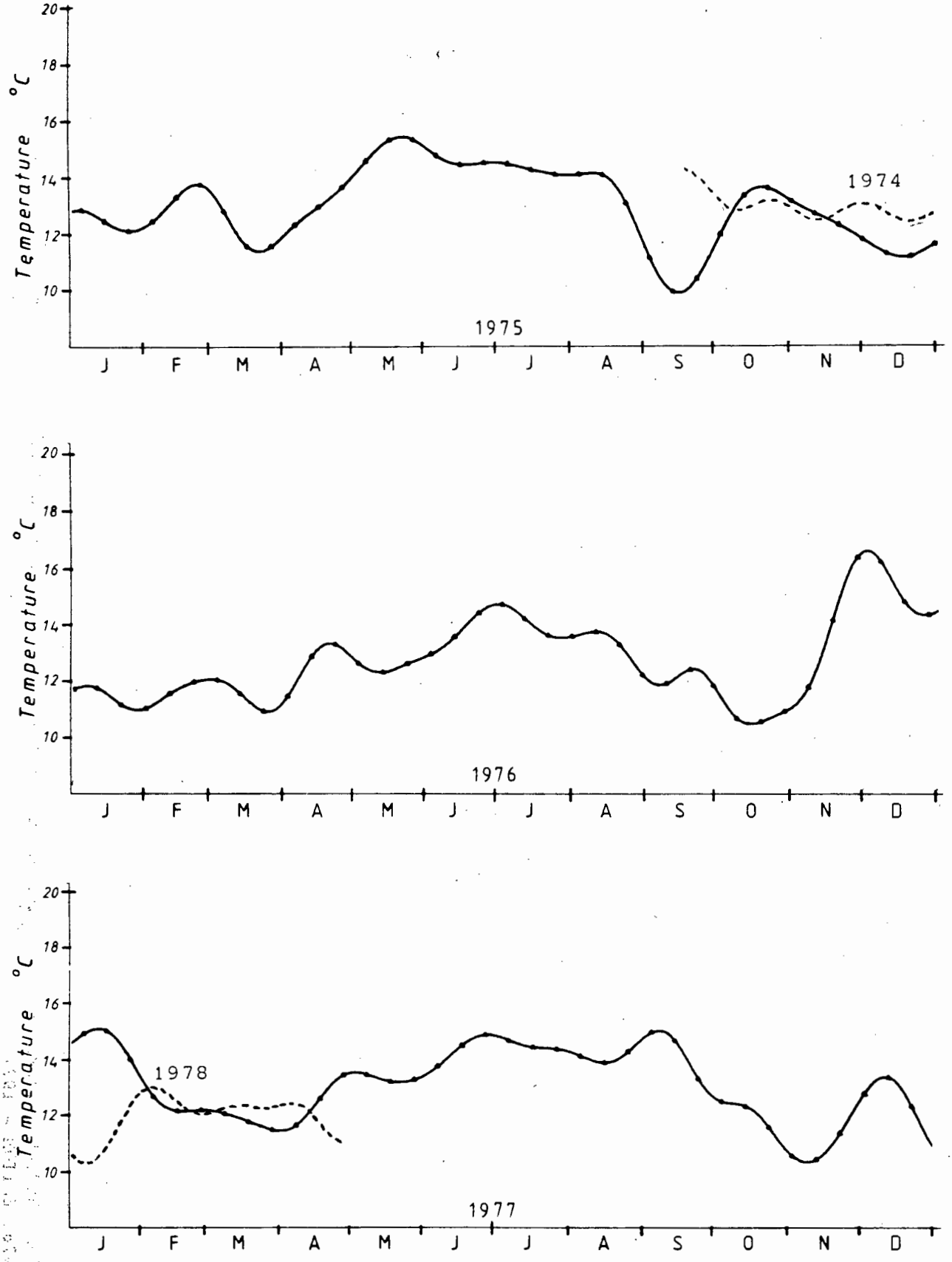

FIG. 3.4 MULTI-YEAR TIME SERIES OF VLF FILTERED 5 M DEPTH TEMPERATURE FORMED FROM 12 HOURLY DATA. THE FILTERED RECORD EXTENDS FROM 79-09-18 TO 78-04-24. THE INCOMPLETE YEAR PORTIONS ARE SUPERIMPOSED ON THE FIRST AND LAST COMPLETE YEARS DATA. THE TICK MARKS ON THE CURVE INDICATE EACH TENTH DAY OF DATA

corresponding to the southerly wind regime, generally has temperatures below the mean annual value. The temperature response is chiefly the result of upwelling dynamics generated by the southerly wind stress. Temperature minima occur in both the spring and summer wind regimes. The spring minimum is generally the colder of the two but it is also the shorter lived being followed by a significant rise in temperature (in 1975, 1976 and 1977) associated with a relaxation in southerly wind strength. The end of 1974 had more uniform winds and no sharp rise in temperature. The colder spring minima can be partly explained by the larger scale oceanographic feature observed by Andrews and Hutchings (1980) when a core of very cold water (8 °C) first comes onto the shelf generally in September-October but tends to decay and deepen and be displaced from the shelf by February-March. Their near surface data does however exhibit a bimodal temperature structure with a cooler period in February compared with March for the data presented here in Fig. 3.4 (In a subsequent paper Hutchings et al. (1984) questions the seasonal significance of the temperature section data quoted in Andrews and Hutchings (1980) but Hutchings (personal communication) does maintain that the spring occurrence of cold water on the shelf is generally colder than the later summer occurrence.)

The proposal for two major wind regimes with a subdivision of the southerly regime is reflected in the sea temperature data. The northerly downwelling winds of winter give warmer than the mean temperatures. The variability of the spring regime winds give a bigger standard deviation in the temperatures than in the summer regime with its more constant winds (Table 3.2). Although the summer regime has a higher southerly wind strength than the spring, the mean sea temperature is not generally colder. This is probably due to both the fact mentioned earlier that the cold core on the shelf dissipates by the summer period and the natural warming process of summer when the warmer oceanic surface waters are closer inshore (Christensen, 1980 and Boyd, 1983).

3.2.2 Simple Statistics

Simple statistics of the very low frequency (VLF) data are given in Table 3.2. Means and standard deviations are given for complete years of data and for the three regimes proposed in the previous section. The mean annual alongshore wind direction for all the years analysed is from the south. The across-shore component has an annual mean onshore flow that is the same order of magnitude as the mean alongshore component. The standard deviations for the alongshore winds are however a factor 2 greater than the standard deviation for the across-shore winds. The standard deviation for

the alongshore winds are much greater than their mean values; a factor 2x in 1976 and a factor 3x in 1977. This indicates that at this time scale the alongshore variations are the most important.

In general, inter-annual comparison (Table 3.2) shows that when the mean annual wind is stronger from the south i.e. more favourable to upwelling, the mean annual temperature is colder than for weaker annual winds. On a seasonal basis the standard deviation for both temperature and alongshore winds tended to be lower during the winter regime. (This is always the case with event time scale data (Table 4.1).) For successive spring-summer regimes the standard deviation for both temperature and alongshore winds is greater in spring.

The winter regime with the lowest positive mean alongshore wind (1976) also has the lowest mean temperature. Conversely stronger northerly winds result in warmer water in winter. This trend and that of colder means when southerly winds were stronger are confirmed over a longer period by comparison with DF Malan winds and Salt River power station inlet temperatures in Table Bay Harbour (Section 3.4). The winter warming effect can be attributed to two effects; the lack of southerly winds i.e. the reduction of cooling due to a decrease in the volume of cool upwelled water and secondly the wind assisted onshore advection of warmer surface water from the offshore region. Christensen (1980) and Kamstra (1985) show (Section 3.7.2) that throughout the year warmer water lies offshore in this region. This can be advected with favourable onshore winds. This is further illustrated with event time scale processes in Section 4.3.

The monthly mean and seasonal mean temperatures for different depths are given in Table 3.3(a) and 3.3(b) respectively. The coldest month for each year occurs during the spring regime i.e. in September 1975, October 1976 and November 1977. There is an obvious temperature gradient with depth. The annual mean temperature gradient over the two depth ranges, 2 m to 5 m and 5 m to 8.5 m are fairly uniform being about 0.3 °C/3 m for both years (1976 and 1977). The winter regime has generally the best mixed conditions, i.e. small temperature gradients of between 0,1 and 0,2 °C/3 m. Although the summer regime has the highest total gradient over the two depth ranges, the limited record over two years (including the anomaly) presented here does not allow a generalisation for other summer periods to be made. The shallowness of the site, 11 m total depth, precludes major seasonal stratification.

3.2.3 Simple Linear Correlations

This section quantifies the relationship between wind stress and sea temperature which is apparent from the simple statistics. Highly significant correlation coefficients generally indicate some causal relationships.

Linear correlation coefficients for linearly detrended wind and sea temperature data with zero means and normalized by their variances are given in Table 3.4. This table also includes some estimates of the critical correlation coefficients at the 95 %, 99 % and 99,9 % confidence levels. The confidence levels require comment. The method of Davis (1976) is used to estimate for some representative cases the number of degrees of freedom of the filtered time series data and hence the confidence levels. See section on Research Methodology 1.5.3. Sciremammano (1979) in discussing intercomparison of correlation coefficients points out that for data with the degrees of freedom less than 10 the statistical robustness is questionable and no satisfactory general method is available for setting significance levels. In Table 3.4 all the evaluated degrees of freedom are ≤ 10 and any intercomparison of correlation coefficients should be interpreted with caution.

For a full year's data the alongshore wind is positively correlated with the sea temperature at greater than the 95 % confidence level. The maximum correlation occurs for temperature lags of 8 and 10 days for 1976 and 1977 respectively. The across-shore winds for the 1976 annual case are not correlated significantly with temperature for any lag; however in the case of 1977, significant correlation occurs but it is positive. For an upwelling process a negative correlation is expected from the relative signs of the across-shore winds i.e. an offshore positive wind should cause a negative temperature change. Although the number of degrees of freedom for the regime data sets are even lower than for the annual sets, indications are that the alongshore wind correlates best in the summer and spring regime with a reduced initial correlation in winter. Lagging the temperature causes an increase in correlation coefficient particularly in winter, when the lags are also the longest i.e. 16 and 9 days for 1976 and 1977 respectively. The shorter lags in spring and summer indicate the quicker temperature response to changes in the wind in those seasons. Although the absolute number of days lag should be viewed with caution, the qualitatively longer lags in winter indicate a possible different mechanism may operate then - besides the increased lag required to upwell the deeper and further offshore thermocline, the delays in long range advection of warmer offshore surface waters with

northerly conditions may be a factor.

The correlation coefficients are very variable and both positive and negative for the across-shore winds for the different regimes (Table 3.4). In two cases there are apparently significant positive correlation coefficients at zero lag. In one case, Sep - Dec 1976 there is a significant negative correlation. A negative correlation can occur when a westerly (negative) wind is associated with a temperature increase. This period is in fact associated with the Nov - Dec anomaly of persistent westerly winds and warmer temperatures. The generally variable and non-significant correlation of the across-shore winds with temperature indicates that at this time scale it is not the primary forcing mechanism but is linked to its associated alongshore component. Thus because of the coastline orientation, due north winds in winter will give an easterly component and due south winds will give a westerly component both with a positive correlation coefficient.

The correlation between temperatures at different depths is not tabulated but for all seasonal regimes is maximum at zero lag with significance levels exceeding 99,9 %. This is expected at this time scale for such shallow water.

3.3 BAROMETRIC FORCING FACTORS

A clear seasonal wind pattern together with a correlated sea temperature response has been described using the time series data.

The barometric factors forcing the seasonal winds are largely due to the seasonal migration of the South Atlantic anticyclone further north in winter and the converse in summer. The mean surface pressure distribution over the South Atlantic for mid summer and mid winter have already been shown in Fig. 1.4 in Chapter I. From the individual years of data available a few selected mean monthly surface isobar maps are now discussed to illustrate the role of the barometric forcing factors in the observed VLF wind patterns.

The winds of November 1977 are seen in Fig 3.2 to have a relatively strong southerly component. The corresponding monthly mean surface isobar map is shown in Fig. 3.5. The South Atlantic high is centred at 30 °S and 0° Longitude with a ridge extending to the south east to below the continent. The isobars are compressed by the continental influence and strong southerly winds result at the south western tip of the continent. At the study site, the wind/sea interaction in this case being upwell favouring results in a marked drop in sea temperature as evidenced in the November portion of the

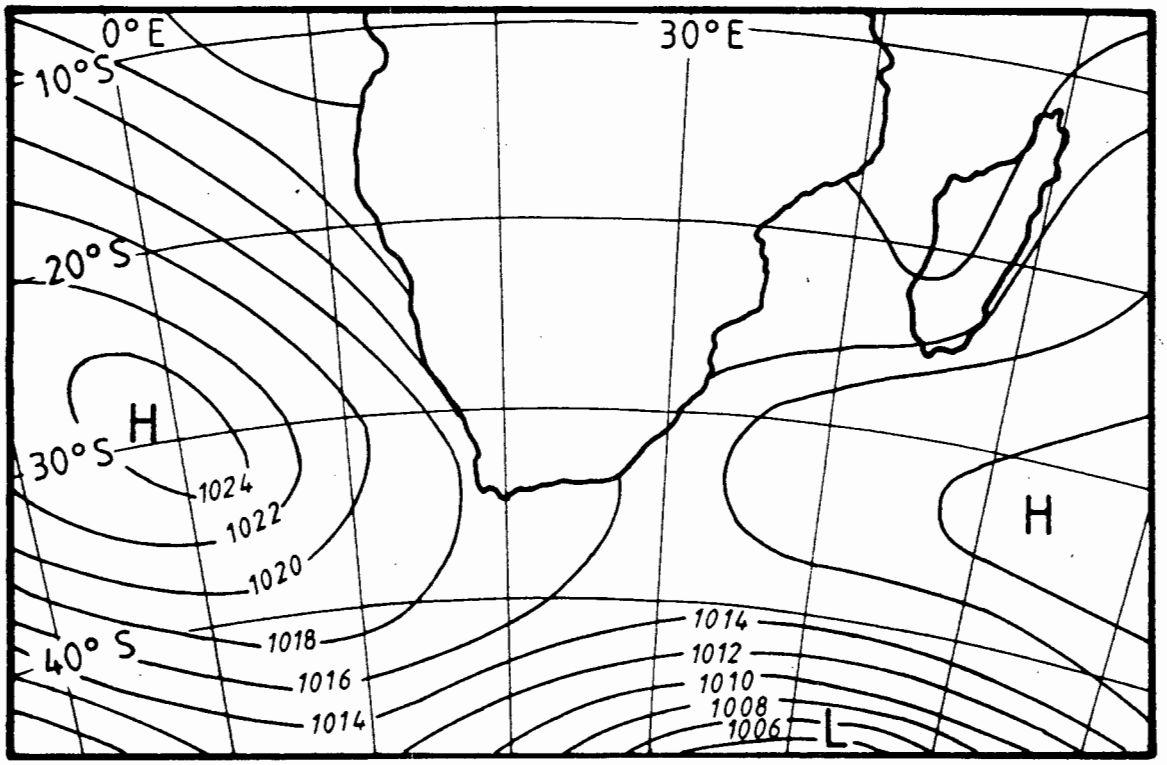

FIG. 3.5 MEAN MONTHLY SURFACE ISOBARS FOR NOVEMBER 1977 (CREDIT: SA WEATHER BUREAU)

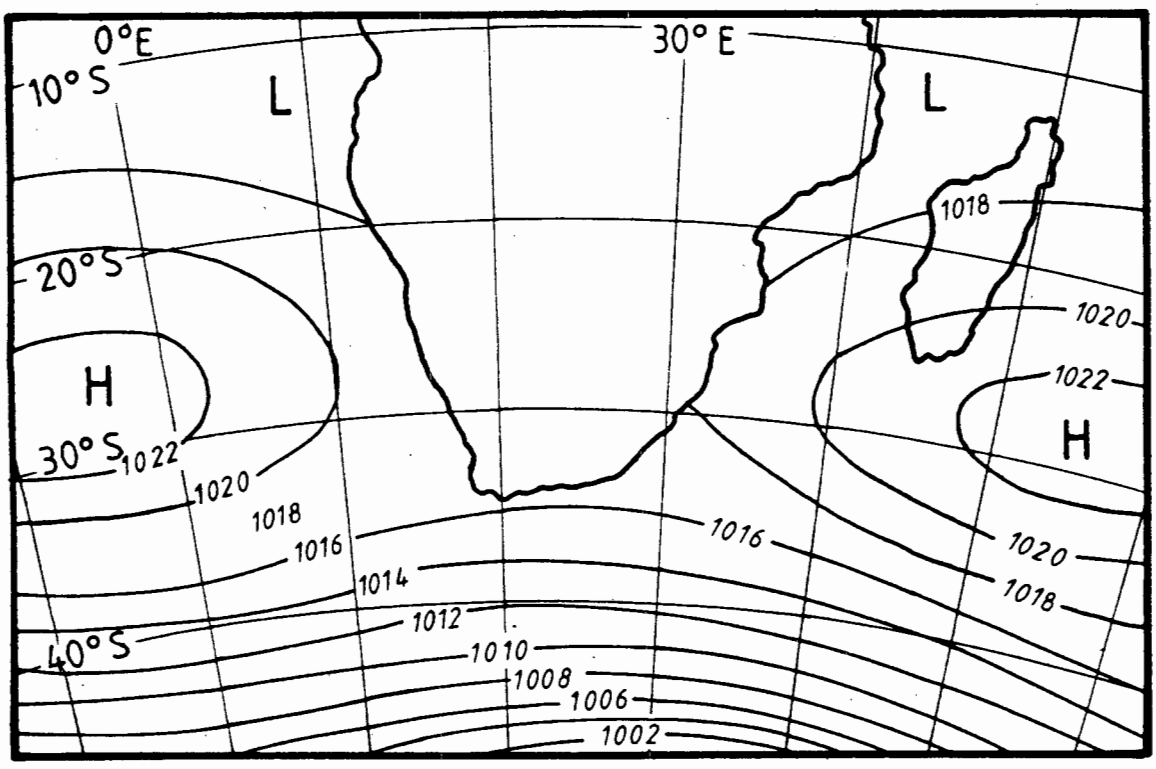

FIG. 3.6 MEAN MONTHLY SURFACE ISOBARS FOR JUNE 1977 (CREDIT: SA WEATHER BUREAU)

1977 annual temperature trace given in Fig. 3.4.

For an example of the winter regime the winds of June 1977 show a typical strong northerly alongshore component in Fig. 3.2. In Fig. 3.6 the June 1977 isobar map shows that relative to the November case the centre of the high pressure area has shifted further north west to 27°S and 5°W and that the isobars indicate a zonal onshore flow for the west coast. In practice, near the site itself the winds are often from the north or northwest because of the passage of easterly moving cyclones past the continent. The sea temperature for June 1977 responds with a gentle warming trend as seen in Fig. 3.4.

Although the coastal air pressure gradient is chiefly affected by the strength of the South Atlantic anticyclone other barometric influences on the wind may include the persistance of the Botswana thermal low over the interior of Southern Africa (Jury, 1981). A remote forcing process conjectured by Nelson (1985) is that major storms southwest of the continent may cause low frequency disturbances of the south Atlantic gyral motion which in turn may impact on the Southern Benguela region. At this main seasonal time scale the barometric forcing factors linked to the migration of the South Atlantic high do however clearly correlate with a sea temperature response at the study site. Imbedded within the overall seasonal variations are shorter 30 to 90 day variations - which may link with the 30, 50 and 60 day periodicities of circulation cells observed over the tropical Atlantic (50 day period is dominant over the tropical Pacific) which are conjectured by Madden and Julian (1972a) to interact with higher latitudes.

3.4 REPRESENTATIVENESS OF WIND AND TEMPERATURE DATA SETS

In attempting to characterize the meteorological and oceanographic systems the question is posed, how representative are the data sets of typical years? In the past decade the concept of a typical year itself has changed in that climatologists no longer consider climate a constant but that it is modified by complex changing influences (Tyson, 1986). El Niño like events bring about big departures from the annual mean values (Philander, 1983, Shannon, et al., 1984). Nevertheless there is merit in checking the data base to ascertain how it fits in a longer term trend i.e. are the usual or unusual attributes of the system being characterized?

In order to answer this question resource is therefore made of other much longer time series data sets from the local area. An hourly wind data set for the years 1957 to 1978 was obtained from the South

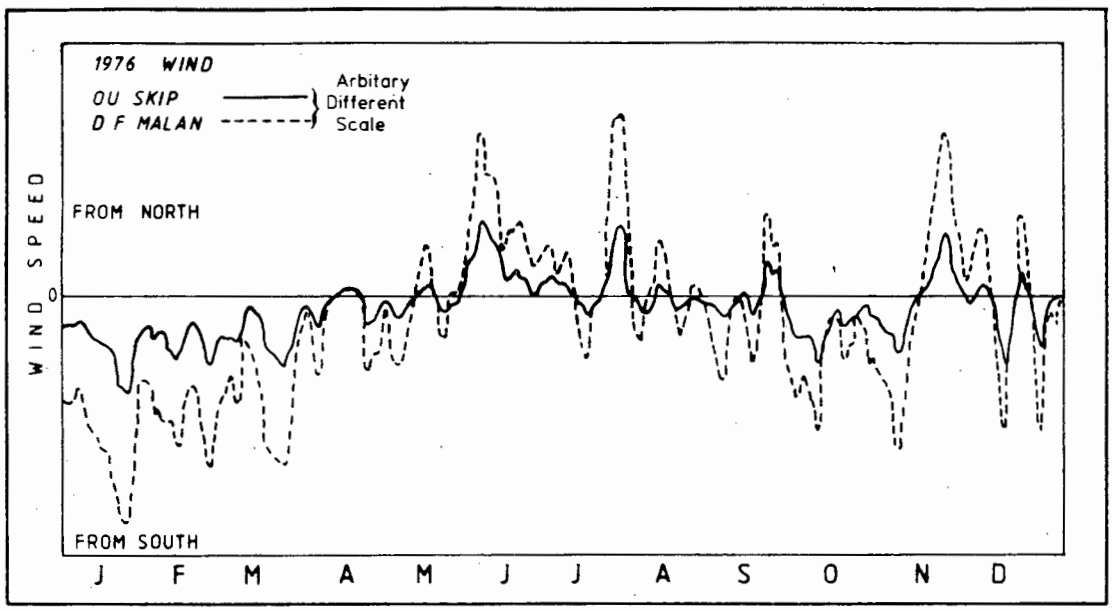

FIG. 3.7 TIME SERIES COMPARISON OF NORTH-SOUTH WIND COMPONENTS AT DF MALAN AND OU SKIP FOR 1976. A SEVEN DAY RUNNING MEAN OF HOURLY DATA IS USED. THE CURVES ARE PLOTTED ON DIFFERENT ARBITRARY VELOCITY SCALES

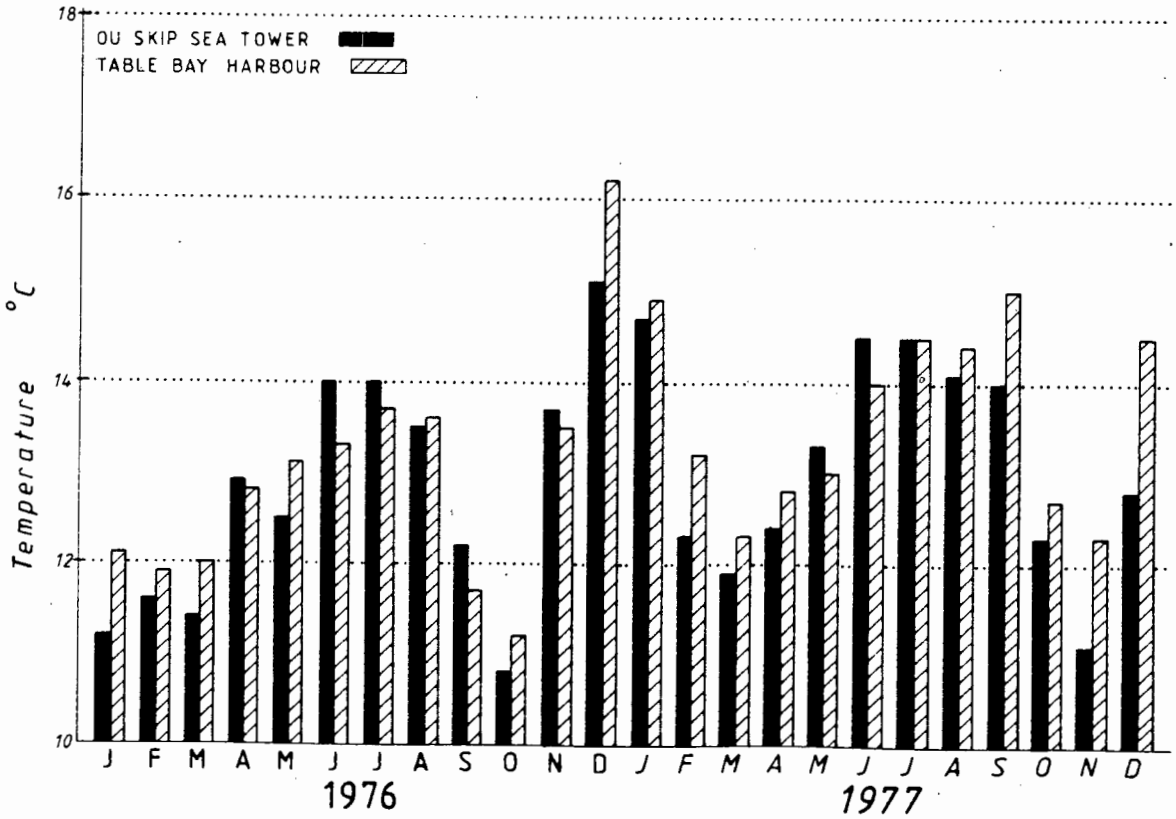

FIG. 3.8 COMPARISON OF MONTHLY MEAN SEA TEMERATURES AT TABLE BAY HARBOUR AND OU SKIP SEA TOWER FOR THE PERIOD JANUARY 1976 TO DECEMBER 1977

African Weather Bureau for the local airport, DF Malan, situated 35 km SSE of the Ou Skip site. A sea temperature data set for the years 1956 to 1980 was obtained from the ESCOM Salt River power station at the south end of Table Bay harbour.

Firstly the suitability of using these sites for long term comparison with Melkbosstrand data is assessed.

Since our primary concern is the wind in relation to sea temperature response, only the north-south component of the wind is compared here between the Ou Skip and DF Malan sites. In this case short term fluctuations are ignored and for each site the 1976 hourly vectors are resolved into north-south components, a daily mean evaluated and then a seven day running mean calculated. The resultant data are plotted on the same axes for both sites in Fig. 3.7. (The two curves are plotted at different scales and the relative magnitudes should be ignored here, although the DF Malan winds are generally stronger than at Ou Skip). At this time scale the visual correlation between the two data sets are good. This can be explained by the relative positions of the two sites and that the process of taking components tends to suppress directional differences. The sites are both subject to the Cape Flats Jet southerly winds (Jury, 1980 and Section 1.4.2). The northerly winds reach Ou Skip unhindered by orographic effects and proceed to DF Malan without much change. Although not shown here the east-west component winds do have differences between the sites but these are mainly attributed to land/sea breeze effects the time scale of which is not relevant here. The DF Malan wind data can therefore be used with a measure of confidence in checking the representativeness of the Ou Skip data set.

The Table Bay harbour temperature data exist in the form of monthly means based on two hourly readings taken throughout each 24 hour period of the cooling water inlet temperatures. Prior to 1974 the inlet position was inside the eastern side of Duncan dock; thereafter it was moved to inside the new extensions. The temperatures are therefore of protected waters but should show the mean trend of upwelling (and downwelling) events that have been observed to occur in the southern part of Table Bay (see Chapter 4, Fig. 4.18). The monthly mean temperatures for 1976 and 1977 are plotted for both the Table Bay harbour and the Melkbosstrand Ou Skip site on the same axes in Fig. 3.8. The Ou Skip data are the monthly means of the temperatures at the three depths (at the Sea Tower) extracted from the LF filtered daily values. In general the harbour site has warmer maxima and minima than the Melkbos site most probably due to the formers more protected environment. Overall the visual comparison of the plotted data from the two sites is good. The

linear correlation coefficients between the monthly data values at the two sites for 1976 and 1977 are 0,91 and 0,85 respectively which both indicate a coefficient differing from zero with a significance exceeding 0,995. The Table Bay harbour temperature data can therefore be used as a reliable indicator of temperatures at Melkbosstrand at this time scale.

The representativeness of the shorter record of Melkbosstrand data is now checked in relationship with the more long term data. The 22 year DF Malan wind record from 1957 to 1978 is used to form, for the north-south component a longterm mean daily value for each day of the year. This is smoothed with a seven day running mean. The resulting mean annual data are given in Fig. 3.9a. Similarly the 25 year sea temperature record (1956 to 1980) is used to calculate a mean for each calender month. This is plotted as a histogram about the 25 year mean annual temperature of 13,4 °C in Fig. 3.9b. The standard deviation on the mean monthly values are large; about $\pm$1,0 °C in summer and about $\pm$ 0,85 °C in winter (Table 3.7b). The features and comparison between Fig. 3.9a and b will be discussed later save for the comment now that there is reasonable correlation with the premise that southerly wind stress drops the sea temperature and northerly increases the temperature.

If individual years of Ou Skip VLF wind data (Fig. 3.2) are compared with the long term mean wind in Fig. 3.9a, two of the years, 1975 and 1977 compare well. Although the overall pattern is followed, the years 1976 and 1978 have a poorer match with the mean, in that 1976 has a short northerly winter regime and an anomolous November followed by weak southerly winds in December and the following January; 1978 has a very weak northerly regime in winter.

When individual years of Melkbosstrand sea temperature data (Fig. 3.4) are compared to the long term mean (Fig. 3.9b) the overall trend of warmer winters and cooler temperatures for the rest of the year is followed with the chief exception for the very warm November/December 1976 period. The times of occurrence of minima or maxima during the year differ from the long term case as can be expected from the large standard deviation in the latter data.

The overall assessment of the short data sets of wind and sea temperature available at Melkbos are that they are representative of longer term trends. The November/December 1976 observations are however outliers of the general trend (see next section). Further analysis of individual years of the long term data shows that some years can have considerable variability particularly in sea temperature but that this variability can be largely explained by

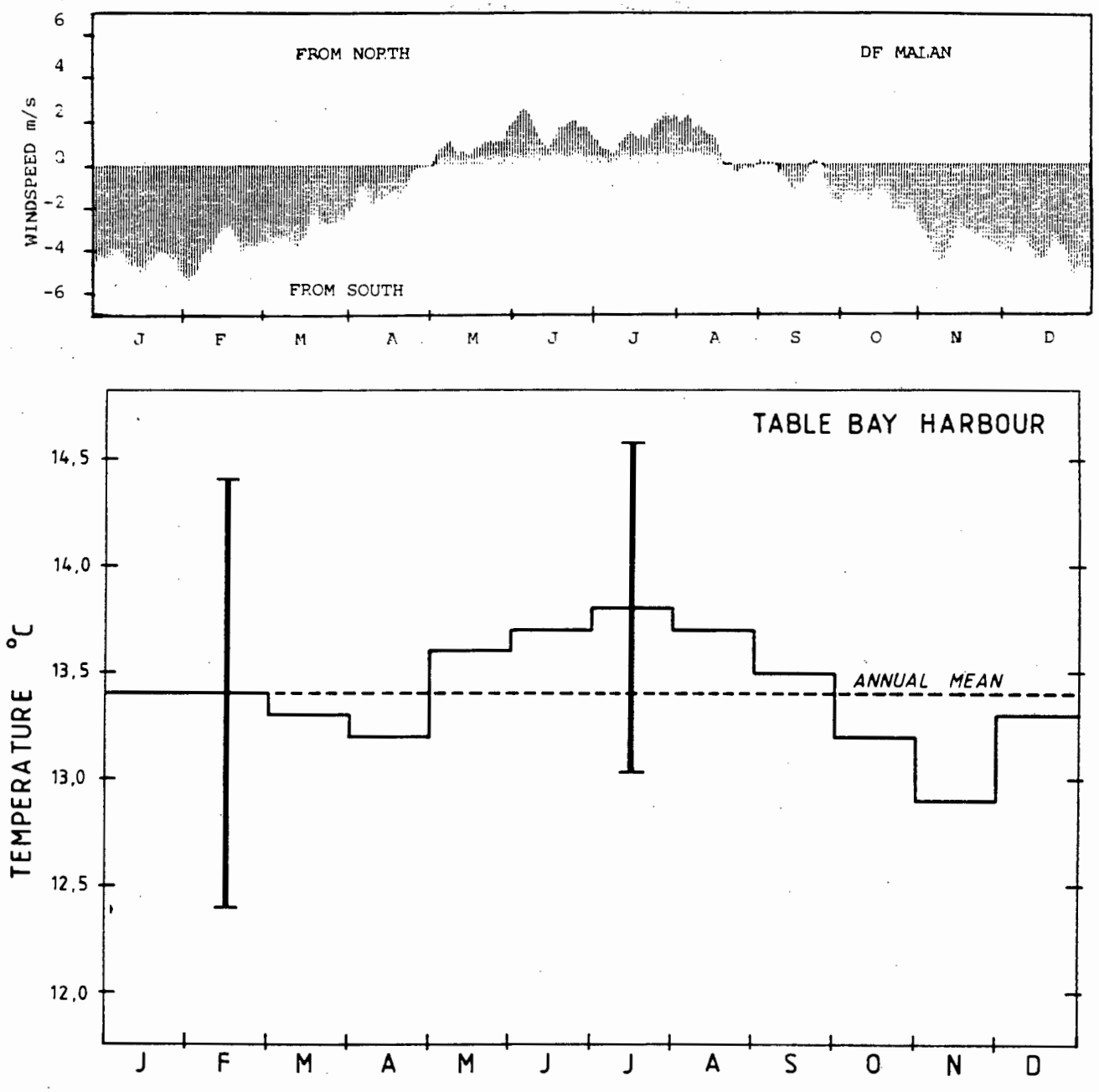

FIG. 3.9 LONG TERM MEAN DATA

a) TIME SERIES DIAGRAMME OF MEAN DAILY VALUES OF DF MALAN NORTH-SOUTH WIND COMPONENT OVER 22 YEARS (1957 TO 1978), SMOOTHED WITH A 7 DAY RUNNING MEAN

b) HISTOGRAM OF MONTHLY MEAN TABLE BAY HARBOUR TEMPERATURES OVER 25 YEARS (1956 TO 1980). STANDARD DEVIATIONS FOR A SUMMER AND WINTER MONTH ARE INDICATED

the different prevailing wind conditions (see Section 3.8). On an even longer time scale the sea temperature anomalies along the west coast region plotted for 1906 to 1985 (Taunton-Clark and Shannon, 1988) show that the period 1956 to 1980 had above average temperatures but that there were no major anomalies then. The detailed analysis of the relatively short record of Melkbosstrand data can therefore proceed with the assurance of being reasonably representative of longer term conditions, with due regard for some of the differences mentioned.

Note on the November/December 1976 anomaly. The anomaly of November/December 1976 has often been mentioned thus far. The elevated sea temperatures that exceeded 18 °C during that period have been reported by Bain and Harris (1975ff report no 5) who showed it was due largely to the failure of the southerly winds and their replacement with persistant northerly or onshore winds accompanied with much rain and that a similar event had not occurred in the previous 20 years. This time scale corresponds with Tyson's (1986, p. 71) classification of the west coast having a rainfall oscillation exceeding 20 years. Other investigators have also remarked on the anomaly at that time. Overall 1976 has been listed as a strong El Niño year (Shannon, et al., 1984). Inspection of data by van Loon and Rogers (1984) for the Southern Hemisphere inter-annual variations in pressure gradients and zonal wind at sea level show an anomaly in 1976. Trenberth (1979) also reports a very anomalous 500 mb zonal mean flow in December 1976 for the Southern Hemisphere when persistant atmospheric blocking occurred resulting in some extreme conditions at sea level. Inspection of progressive wind vector diagrammes of Cape Point wind data for the months October to March from 1957 to 1986 given by Hutchings (1986) show that the largest eastward displacement during this period occurred for the summer of 76/77. Another unusual aspect of the 1976 mean monthly temperature data set for Table Bay harbour is that the set holds the record during the period 1957 to 1980 for a) the greatest annual temperature range (5 °C) and b) both the coldest January (12,1 °C) and the coldest October (11,2 °C). The anomaly observed here at the end of 1976 certainly is noteworthy but it did not seem to last long enough to significantly affect the west coast fisheries (Hutchings et al., 1984).

3.5 VLF CURRENT CHARACTER

A definite relationship between the seasonal winds and sea temperature has been established. Other oceanographic variables at the site are also expected to show correlation with the wind forcing. One of these variables is currents. Unfortunately there is a lack of good time series current data of adequate duration at the site. Results of moored buoy current system measurements are presented in UCT/ESCOM Oceanographic Investigation reports (Mallory and Maxwell, 1969ff) in the form of current roses. Often only one observation per day was made on the buoy system and no attempt is made here to extract time series data from such records. The data does show that the currents are largely wind driven. A 16 month unbroken record of twice daily (nominally 8h00 and 18h00) surface current observations exists for a site further south at Table View in Table Bay (Fig. 1.3) where a moored buoy current system with a drogue set at 1,8 m depth was positioned 600 m offshore (van Ieperen, 1971). Although not considered as an optimum data set, it is thought worthwhile to analyse these data in order to reveal gross seasonal patterns.

The data are decomposed into alongshore (20° west of north) and across-shore (approximately east-west) components and subjected to the same filtering process as the wind and temperature data, to produce a very low frequency data set. This is presented in Fig. 3.10a and b for the alongshore and across-shore components respectively and cover the period October 1968 to November 1969, having made allowance for filter truncation. For this record the mean alongshore current is 9,7 $cm.s^{-1}$ to the north and the mean across-shore current is 5,6 $cm.s^{-1}$ offshore. The corresponding winds were not analysed but from the tabulations in van Ieperen (1971) it appears the winds generally followed the normal seasonal pattern. A weak El Niño is reported for 1969 but no untoward anomalies, for the observation period, are noted for either meridional winds or Table Bay temperatures in the time series of progressive monthly anomalies given by Taunton-Clark and Kamstra (1988). Only a few strong NW storms occurred in June, July and August and the southerly regime was marked with calms and northerlies in October 1968 and weaker winds in December 1968 and January 1969. The alongshore currents in Fig. 3.10a show the expected trend of going to the south during the short winter period June, July and August and moving up the coast for the remainder of the period. The north-going current strength decreased over December 1968/January 1969 when the southerly winds slackened. The across-shore current (Fig. 3.10b) indicates an offshore trend most of the year with a very limited onshore character in mid winter. Van Ieperen (1971) observes that there is a general anti-clockwise

circulation in Table Bay. This could tend to counteract to some extent the effects of northerly wind episodes - thus possibly further accounting for the low strength and short duration of mean south going and onshore currents.

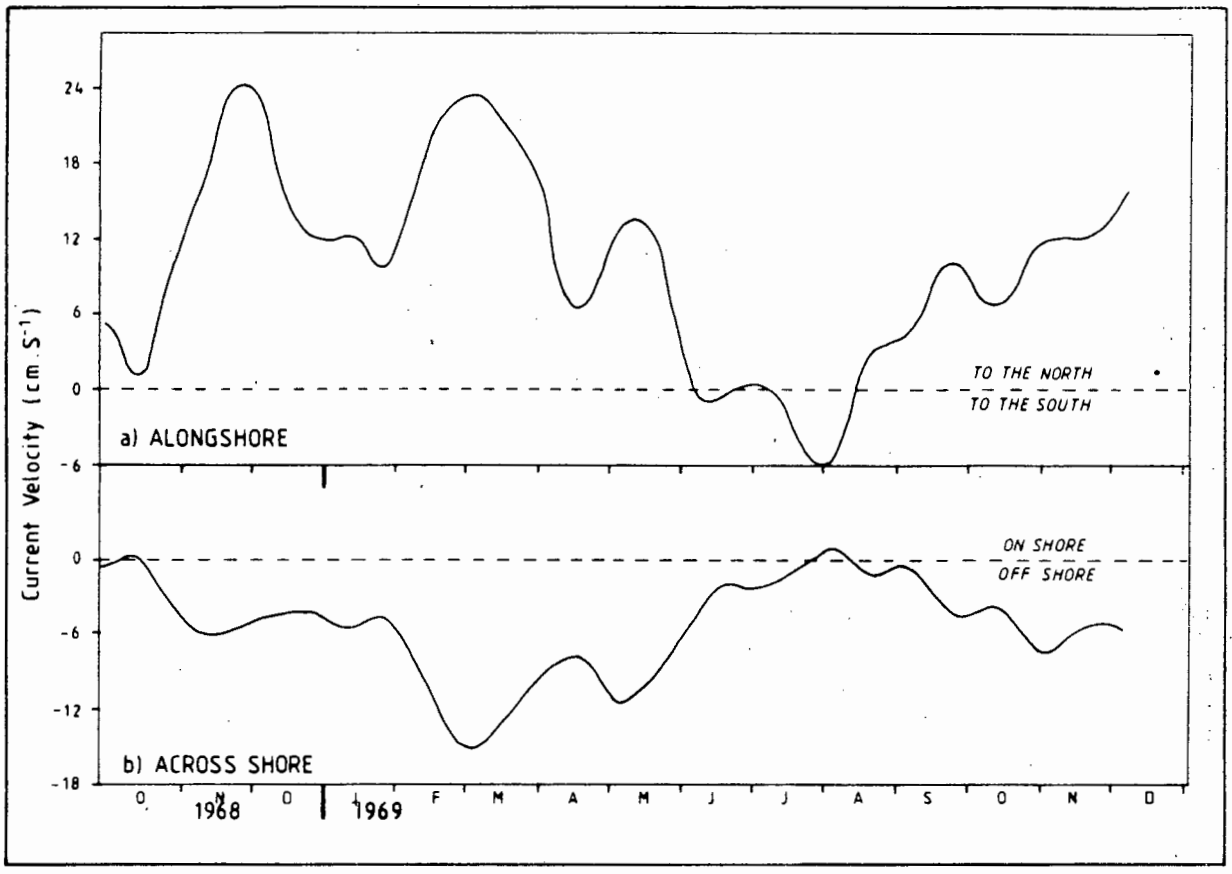

FIG. 3.10 VLF CURRENTS OFF TABLE VIEW FOR THE PERIOD OCTOBER 1968 TO DECEMBER 1969. CURRENT COMPONENTS HAVE BEEN ROTATED 20° WEST OF NORTH. a) ALONGSHORE CURRENT b) ACROSS-SHORE CURRENT BASED ON CURRENT BUOY DATA OF VAN IEPEREN (1971)

The moored buoy current measuring system has the disadvantages of only revealing gross changes in current direction and is subject to windage. However, the overall analysis confirms that the VLF surface current strength and direction is largely forced by the prevailing seasonal winds. A similar surface current character is expected for the Melkbosstrand site. From an extended time series point of view no adequate data exist for this study for currents within 10 km of the shore. Recently, on the larger scale, Nelson and Polito (1987) have reported some time series current data for adjacent waters beyond the 10 km zone. The spatial behaviour and character of the currents at higher frequencies will be discussed in subsequent chapters.

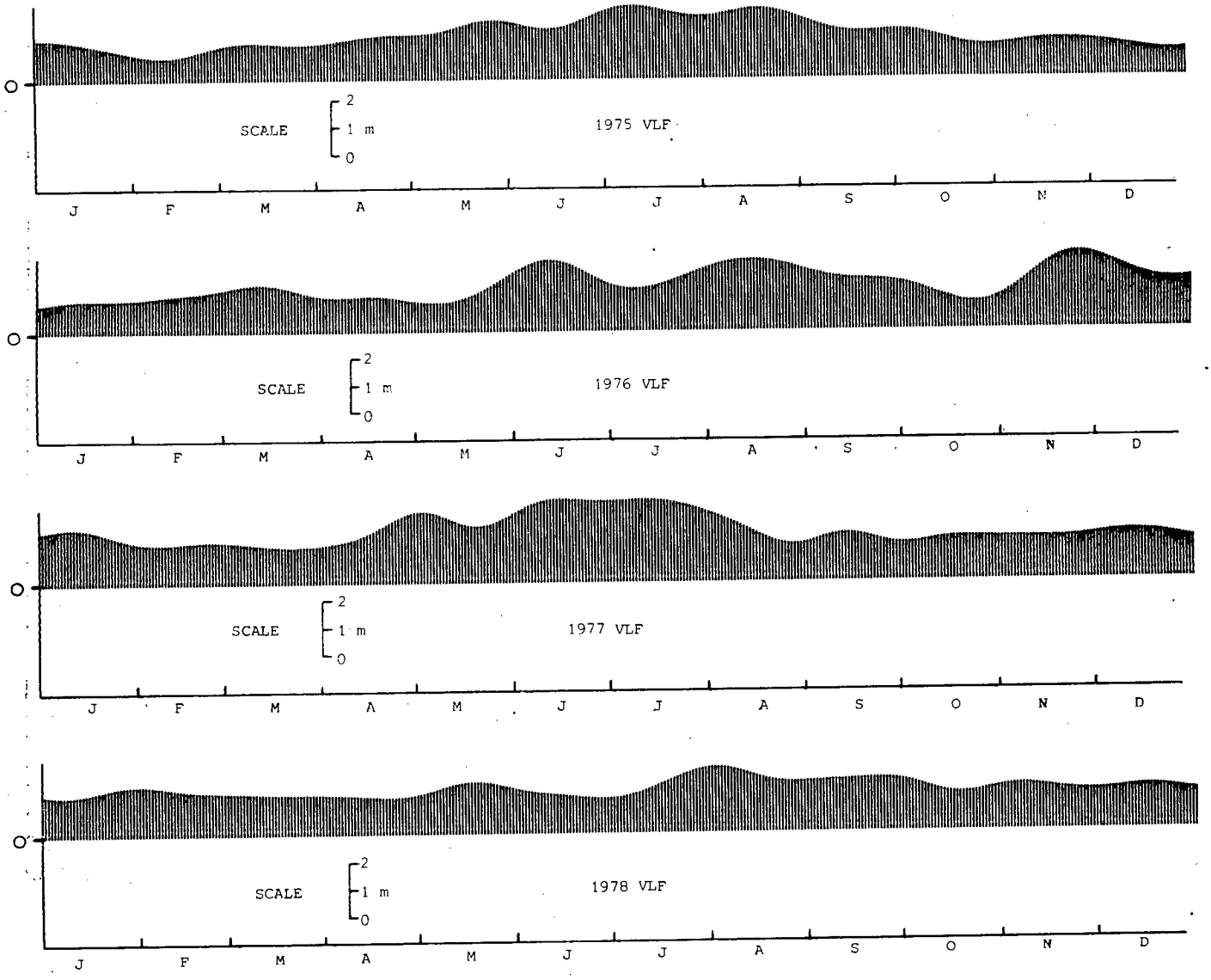

FIG. 3.11 TIME SERIES DIAGRAMME OF DAILY VALUES OF VLF FILTERED WAVE HEIGHTS; FOUR ANNUAL SETS 1975 TO 1978

3.6 VERY LOW FREQUENCY WAVE HEIGHT CHARACTER

A parameter for which good time series data exist at the site is wave data. The wave data used are the six hourly tabulations by ESCOM of data from a Wave Rider buoy situated in about 20 m of water 1,5 km offshore from Ou Skip (Malory and Maxwell, 1971 ff). The significant wave height Hs is used. The daily mean values of the wave data are filtered similarly to the wind and temperature data to yield a very low frequency data set. These filtered wave data are plotted in Fig. 3.11a-d for the years 1975 to 1978. The main feature is that maximum wave height generally occurs during the winter regime, while during the other periods the waves are smaller and more uniform in height. The exception is once again 1976 when although winter has high waves the maximum waves occur during November/December, correlating with the anomalous persistent north westerly winds.

Note: The 1977 wave data are, for the period of equipment failure between 15 July and 26 October based on daily visual estimates of wave height.

Table 3.5 gives the mean wave height and their standard deviations. The mean winter wave height is much larger than for the other periods. Linear correlation coefficients between wind and wave height are given in Table 3.6 as per procedures given in Section 3.2.3. The alongshore wind is correlated with wave height to a significance of better than 99 % for 1975 and 1976. The across-shore wind is not significantly correlated with wave height. Although one may expect a positive wind/wave correlation for onshore winds from the west, the coastal nature of the site will probably result in a negative correlation for offshore winds which then result in an overall non-correlation for across-shore winds.

The alongshore winds reflect the wind components from the northerlies in winter and the southerlies in summer. During winter with the South Atlantic anticyclone displaced further north conditions are more favourable for long wind fetches from both W and SW directions that are directed towards the South Western Cape coast (Shillington and Harris, 1978) which results in larger waves for this period. During spring and summer the 'south easter' which is a poor wave generating wind is often preceeded by a depression passing to the south of the land mass. This, for a brief period compared to winter conditions, presents a favourable SW fetch for wave generation. Hence the southerly winds with some lag will correlate with the waves. This is better illustrated with the event time

scale winds in Chapter 4.

The year with the greatest mean northerly wind for the winter period is 1977 (Table 3.2). This correlates in Table 3.5 with the greatest mean annual wave height of 1,94 m also in 1977. In Table 3.5 the standard deviation for annual wave heights is fairly uniform with a value of $\pm$0,5 m except for 1978 when it is $\pm$0,26 m. This corresponds with the very reduced northerly wind component (0,19 m/s) for winter of that year.

Implications of higher on average waves in winter are the enhancement of various wave generated processes. These include ripcurrent cells, longshore currents, sediment transport and deeper mixing of surface waters. The latter will tend to break down stratification in the shallow nearshore waters.

3.7 LINKS TO THE LARGER SPACE SCALE

Up until now the localized data have been discussed. The question arises, what larger scale processes affect the local site on a seasonal time scale? The windfield and oceanographic parameters are considered.

3.7.1 Spatial Variability of the Wind Field

It is proposed that at the seasonal time scale the spatial variation of the wind field across the immediate study site is of a minor nature and hence of little influence on the sea temperature character there. On a larger scale however the steep orography of the region starts to dominate the wind patterns. This is admirably shown to be important at the event time scale by Jury (1980) and is discussed in Section 4.4.1. For certain combinations of southerly winds and inversion conditions, the effect of Table Mountain can enhance wind speeds immediately to the east of it (the Cape Flats Jet) and can create a wind shadow extending to the north past Robben Island. On a seasonal basis such influences on the variation of the wind field are shown on the wind roses of wind stations selected from Reddings, et al. (1982) data. The wind roses in Figs. 3.12a and b are shown for the period bracketing October to March (summer) and the period April to September (winter) respectively, for five wind stations extending from the south end of Table Bay to about 15 km NE of Melkbos. The roses do not represent a true seasonal average as they are based on an incomplete data set but they are indicative of trends in the spatial distribution of the wind.

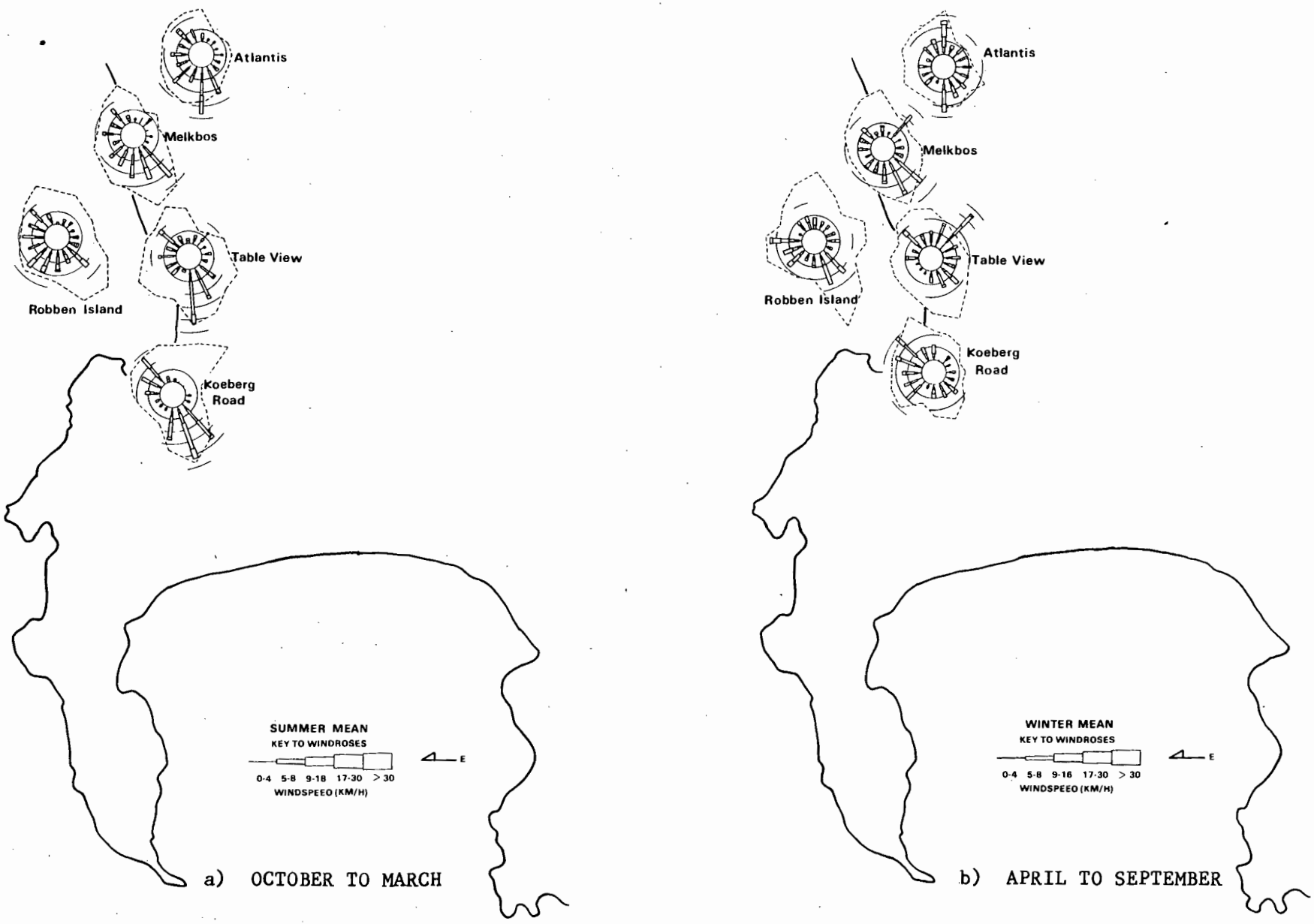

FIG. 3.12 PSEUDO SEASONAL WIND ROSES FOR SELECTED COASTAL STATIONS IN THE REGION OF THE STUDY SITE AFTER REDDING (1982)

Inspection of the wind roses (Fig. 3.12) reveals that for the summer period at the northern positions the southerly and northerly winds are more variable in direction and weaker than the southern-most station. Robben Island has the least south and south east winds. Compared to the southern station, the northern stations and Robben Island have more westerlies and south westerlies, partly because of the sea breeze effect. The lower wind speeds in the north and the greater proportion of onshore winds may imply less upwelling there and consequently relatively warmer sea temperatures on average. The stronger northerly winds in the south could accelerate the downwelling process in the south. However any spatially induced variability in the sea temperatures would probably be smoothed out by advected affects over the long temporal scale. This is certainly true for longshore effects but across-shore the frequent occurrence of the wind shadow cast by Table Mountain may result in on average warmer surface waters in the vicinity of Robben Island as the ingress of upwelled colder water is limited.

In winter when the sea temperatures are much more uniform the winds spatial variability (Fig. 3.12b) is of little importance at this time scale.

On the larger scale for atmospheric systems in the area there may be other direct or indirect seasonal effects on the local area. These are considered in the next section and in Section 3.8.

3.7.2 Larger Scale Oceanographic Influences

On the oceanic scale west of the site the ill-defined Benguela Current system flows northwards and is fed by a similarly directed baroclinic jet on the shelf edge (Bang and Andrews, 1974). Coastwards of this jet Nelson (1983 and 1985), Nelson and Hutchings (1983) and Nelson and Polito (1987) report variable north and south flowing currents which tend to a net southward flow closer to the coast. In this study and that of van Ieperen (1971) up to a distance of 8 km offshore no firm evidence is found of a net southward current or any obvious seasonal current trend (other than that directly related to the local wind forcing). As discussed under the winds spatial variability a wind shadow behind Table Mountain extends northwards of Robben Island. This region could support a southgoing counter current (Jury, 1981) but it probably does not extend closer than about 10 km to the study site. However, the very presence of a current from the north would enhance the return of warm water inshore to the study area with the advent of a failure of southerly winds. A reservoir of warm water is seasonally available as evidenced by the work of Boyd (1983) and Christensen (1980) who show that the 12 year mean offshore temperatures in winter are about 15 ° and in summer

about 19 °C. The source of warm water is supplemented by the advection of Agulhas water round the Cape and propagation of Agulhas rings into the region, as observed by satellite imagery (Lutjeharms, 1981 and Lutjeharms and Van Ballegooyen, 1988). In fact the influence of the Agulhas Current system on the dynamics of the Southern Benguela region is considered of some importance and has effects varying from the scale of days to months (Shannon, 1985a). The 1982/83 Benguela warm event is reported by Walker, Taunton-Clark and Pugh (1984) to be due to a failure of local southerly winds in summer and not due to an El Niño like advection of warm water for a great distance down the west coast. Similarly the warm anomaly of 1976 discussed in Section 3.4 is largely due to a failure of local upwelling winds, with slight remote influences. Cold water too, in the form of Subantartic water filaments, can be episodically advected into the Benguela region, Shannon et al. (1989).

In Section 1.4.3 an analysis of van Ieperen's (1971) data shows that the 10 °C isotherm is generally at a depth exceeding 50 m in winter and often at less than 25 m in summer. Shannon, Nelson and Jury (1981) conclude that on the larger scale the upward tilting of the isopycnals is perennial below 50 m. The coldest bottom water on the shelf tends to occur in spring (Andrews and Hutchings, (1980) and Hutchings, Pers Com.). Their data also shows a bimodal surface temperature with warmer waters in winter and, slight warming in December-January when Cape Point winds have a lull in southerly wind strength. These features in turn have an influence on the seasonal trends at the study site. Figs. 3.3 and 3.4 and Table 3.3a) show, the coldest temperatures occur in spring. Similarly the long term mean temperature at Table Bay harbour (Fig. 3.9b) has a minimum in spring and also indicates a bimodal distribution. The sea level at the site and along the west coast fluctuates seasonally by about 20 cm in association with the large scale seasonal effect of the wind (Brundrit, 1984).

In summary the seasonal effects are referred to Winant's (1980) identification on the larger scale of three classes of seasonal currents dependent on forcing mechanisms. a) Direct meteorological forcing. This is probably the chief cause here for seasonal differences. Both the wind and sea temperature data show within the main seasonal trends, 30 to 60 day or longer periodicities for which there are no definite explanations. There could be links to similar periodicities in the tropics (Madden and Julian, 1972a and Gray, 1988). The periodicities could be associated with changes in wave number dominance in the circumpolar jet stream or atmospheric blocking episodes as occurred during the late 1976 anomaly (Trenberth, 1979). For the Southern Hemisphere circulation Kidson (1988) reports that the dominant variance of the 500 hPa geopotential

anomalies is due to periodicities exceeding 50 days. Although such anomalies may persist for up to 4 months, the anomaly patterns show great variety and no "climatology" can be established (Kidson, 1988). For the open sea Monin (1977) reports temperature fluctuations with periods of 40 to 200 days and reports a dominant scale for upper thermocline variability of about 30 days. In the analysis of local winds and sea surface temperatures Kamstra and Taunton-Clark (1986) report, besides the seasonal dominance of fluctuations of these parameters, the presence of perturbations of some months duration. b) Forcing from adjoining deep ocean systems. The Agulhas Current System is considered important in affecting the dynamics of the southern Benguela region, probably on the scale of days to months (Shannon, 1985a). Taunton-Clark and Shannon (1988) present evidence that some process affects both the Agulhas Bank and the West Coast. Lutjeharms (1977) finds no seasonality in the spatial energy spectrum of the adjacent ocean circulation. The funneling of water up the Cape Point Canyon may significantly affect the Cape Peninsula upwelling system (Shannon, Nelson and Jury (1981)) but its seasonality is unknown except for the probable link to meteorological factors. c) Forcing from runoff of large rivers. This is not of relevance to this study site.

Although not a steady feature eddies and topographic Rossby waves can in principle encroach onto the shelf but due to friction will have greatly reduced energy in depths of 25 m (Winant, 1980). Intrusions of outer shelf water to within the nearshore zone to depths less than 25 m have been observed by Churchill (1985) for the northeast United States coast where the continental shelf is about 100 km wide. The main forcing mechanisms for such intrusions was wind stress. Local 100 km diameter eddies and vortex dipoles are observed on the Benguela upwelling front (Lutjeharms, 1981) and Stockton and Lutjeharms, 1988). Possible barotropic shelf waves are discussed by van Foreest (1981) and van Foreest, et al. (1984). The actual effect of such features in the study area is largely undocumented, although Holden (1987) at the synoptic time scale gives current meter evidence of continental shelfwave activity along the west coast. Mention should also be made of the possibility given by Shannon (1985a) that an equatorially generated coastally propagating Kelvin wave may initiate the seasonal ingress of cold bottom water locally in spring.

3.8 DISCUSSION

The seasonal character of the wind has been established together with the well known barometric forcing factors of the South Atlantic anticyclone. The seasonal attributes of the oceanographic parameters of sea temperature, waves and to a certain extent currents have also

been described. These parameters are seen to be largely forced by the wind. The winter sea temperatures are generally warmer than the annual mean and are fairly uniform. With strong southerly alongshore winds in spring the Ekman offshore transport at the surface results in cold upwelled water at the coast. Linked to the larger scale occurrence of the coldest shelf water for the year occurring in spring the seasonally coldest water at the study site is also observed then. The remaining summer wind period maintains cooler than average temperatures. The wave heights have also been seen to peak in the winter period with subdued energy in the remainder of the year. The limited current record also indicates a strong sympathy with the seasonal winds.

The anomaly of November/December 1976 in fact reinforces the importance of the local wind as the main forcing process at the local shallow coastal site.

The wind and temperature data set used was shown to be reasonably representative of long term mean conditions in the area. A closer look now at the long term mean winds at DF Malan (Fig. 3.9a) and the long term temperatures from Table Bay harbour (Fig. 3.9b) reveal additional information. (The implications of the large standard deviations on the mean temperatures are discussed a little later.)

These long term records tend to confirm the regime choices of May to August (winter), September to December (spring) and January to April (summer). The long term northerly period starts at the beginning of May and covers 3,5 months with corresponding elevated and uniform temperatures with a mean of 13,7$\pm$0,1 °C. The spring period shows initial reversals of wind and a more gradual build-up to a maximum in early November. The spring temperatures show (Fig. 3.9b) a marked decrease in each of the first three months of the period with a minimum in November. This is followed by a sharp rise in temperature which is not reflected by a significant relaxation in wind strength. The mean spring temperature is 13,2$\pm$0,25 °C with a relatively high standard deviation more than twice that of the other two periods.

The long term summer southerly winds are more consistent but decrease in strength to the northerly transition at the beginning of May. The associated temperatures are more uniform than spring but still cooler than winter; the mean being 13,3$\pm$0,1 °C. The long term annual mean is 13,4$\pm$0,3 °C.

The bimodal temperature distribution is a feature. The minimum in spring supports the association with the large scale effect of cold (oxygenated) water appearing on the shelf then and confirms that this limited observation of Andrews and Hutchings (1980) is a feature of

the inshore Benquela system. The rise over December January could be due to a combination of a) the usual seasonal increase in insolation, b) lull in southerly wind strength. This is more apparent in the Cape Point wind data reported by Andrews and Hutchings (1980) and indicates that larger scale winds may have an indirect influence at the local scale. c) The winds in December and January tend to have a greater onshore component (see wind frequency data Table 3.1) that can contribute to shoreward advection of warmer offshore waters.

The long term temperature dip in April is puzzling without an associated long term southerly wind maximum but could be due to a decrease in insolation or some larger scale effect. The minimum in April is confirmed on the slightly larger scale, of up to 25 km offshore and north of Cape Town, by mean ships-data over the period 1965 to 1980 (Taunton-Clark and Kamstra, 1988). Analysis of satellite imagery shows maximum wind related upwelling off the Cape Peninsula occurs in spring and autumn (Meeuwis and Lutjeharms, (1986). The even longer quarterly averaged data record (50 years) of large scale sea surface temperatures for the Southern Benguela region by Kamstra (1985), although it does not resolve monthly changes does show for the period February, March, April that the coldest water in the region (13 to 14 °C) lies in the small area of Table Bay to Bok Point. These months correlate with the temperatures in the Table Bay long term mean data being average or below average (Fig. 3.9b). Careful inspection of the multi-year monthly mean offshore isotherms of Christensen (1980) shows that along a transect perpendicular to the coast at Melkbosstrand, although the warmer water isotherms have a maximum displacement offshore in August there is a subsidiary maximum displacement in April. This then indicates besides the seasonal cooling for the austral winter there is some other perturbation in the larger scale on average in April that may be reflected in the long term inshore temperature data. Such a perturbation could be directly wind forced on the larger scale (e.g. Cape Point data have a wind maximum in March) or related to some periodic South Atlantic gyral input to the shelf (Nelson, 1985) or a seasonal fluctuation of Agulhas water input. Then again the equatorially produced poleward propagating coastal Kelvin wave proposed by Shannon (1985a) to initiate the ingress of cold bottom water onto the shelf in October may have a weaker equivalent in April.

What is interesting in Fig. 3.9b is that the two largest monthly changes in temperature (0,4 °C) are both positive changes. The first being the increase from April to May coinciding with the southerly to northerly transition and the second being the rise from November to December. The magnitude of this second feature is surprising and is

probably explained by the factors itemized a) to c) above. The large standard deviations on the mean temperature data should however lend caution to any categorical explanations.

INTER-ANNUAL TRENDS

In fact the large standard deviation on the temperature data (Fig. 3.9b) leads to an investigation as to why there is this variability. Three factors, separately or jointly could account for the variability.

1) Fluctuations about the mean annual temperature due to inter-annual changes
2) No inter-annual change but strong and weak seasonal variations
3) Phase shifts in the seasonal patterns.

Statistics of Table Bay harbour temperature data are given for individual years and for monthly means in Table 3.7a and b respectively.

There are inter-annual trends in the long term mean temperature data i.e. groups of successive annual means are above or below the long term mean. Statistical analysis shows (Table 3.7a) that the variation about the long term mean of 13,4 °C is 0,6 °C which is lower than the spread on individual years which have a mean standard deviation of 0,8 °C. This indicates that the seasonality has a slightly higher effect on the variability than the inter-annual trend. The seasonal variation again is smaller than the mean standard deviation of the monthly means of 1,0 °C. This indicates that seasonal phase shifts are more important in causing fluctuations than the seasonality itself. Inspections of individual years between 1957 and 1980 show that annual maxima or minima temperatures can occur in virtually any month. The mean annual range is 2,6 °$\pm$0,8 °C (the long term mean range is 0,9 °C) with only 20 % occurrence having a strong seasonal range greater than or equal to 3 °C. In turn the mean range for the monthly records is greater, being 3,6$\pm$0,5 °C.

It seems therefore that each of the three factors does play a role with each manifesting some outliers in character but probably the seasonal phase shift has a slightly more prominent contribution to the long term monthly mean variability. Highly variable seasonal phase and amplitude shifts are noted by Taunton-Clark and Shannon (1988) for the long term 1906 to 1985 data set and similar deductions from spectral evidence are made by Taunton-Clarke and Kamstra (1988). Correlation of the wind and temperature data for individual years of the long term data will not be made in this study but some comments on inter-annual trends follow.

A study of Fig. 2 of Walker et al. (1984) which shows the temperature anomalies for the Table Bay harbour data, and a comparison of Tables 3.3a and 3.7a reveals that the annual means for the period 1975-76-77 were close to the 26 year mean and that other groups of years had positive or negative anomalies. Although the few years of Melkbosstrand data are shown to be reasonably representative of the long term mean, the progressive monthly anomalies of atmospheric pressure, meridional wind and sea surface temperature given by Taunton-Clarke and Kamstra (1988) for the Cape Town area show the influence of the 1976 anomaly. The anomalies correlate in general with different prevailing winds and in the case of positive anomalies correlate with El Niño years (Walker, et al. 1984 and Kamstra and Taunton-Clark (1986) and Tauton-Clarke and Kamstra, 1988). This indicates some intermittant large scale effects on the region such as the observation of Gillooly and Walker (1984) that a northerly position of the Subtropical Convergence Zone (which is linked to the position of the South Atlantic anticyclone) is correlated with warmer temperatures in Table Bay as in 76/77 and 82/83. A more southerly position gives colder temperatures. The El Niño southern oscillation is very aperiodic with time between events covering 2 to 10 years (Philander, 1983). The longterm data of Taunton-Clarke and Shannon (1988) suggest a weak 10 year mean cycle for Benguela Niños. From a rainfall perspective the west coast area is subject to an oscillation exceeding 20 years (Tyson, 1986).

Using a 60 year long sea temperature record off Japan (34°N) Miita and Tawara (1984) report a 6 to 8 year periodicity. They also list other reported periodicities between 5 and 7 years for the Pacific region and link it to mid latitudinal influences of the nutational forces from free oscillation of the earth's rotational axis. There is some evidence for a 6 to 7 year cycle in local waters. Inspection of data for sea level (Brundrit, 1984), sea temperature (Walker, et al., 1984) and shift of the subtropical convergence zone Gillooly, et al. (1984) show peaks for either one of or combinations of these parameters for the years 62/3, 68/9, 76/7 and 82/3. Similarly, Buys (1959) for Cape waters and Stander (1963) for Namibian waters, report seven year cycles. The more quantitative analysis of Taunton-Clarke and Shannon (1988) however do not reveal a seven year period but show a non-significant 5-6 year peak in wind stress and sea temperatures. All these various oscillations highlight the complexity of delineating inter-annual trends.

REGIME TRANSITIONS

Two major regimes have been identified in the local area. Firstly a regime in winter, with northerly winds and relatively warmer waters and secondly for the rest of the year a regime with southerly winds

with cooler mean sea temperatures having a relatively high standard deviation. However, considering the observed departures from the mean conditions it is not possible to unambiguously identify the regimes from monthly means of the available parameters (wind, sea temperatures and wave height). Even with additional time series data of currents it may only be possible to give a more definite answer if the measurements are extended to the larger scale (10-20 km offshore). In identifying the oceanographic regimes off Oregon and California, Huyer, Smith and Sobey (1978) and Strub, Allen, Huyer and Smith (1987b) make use of an extensive current data set covering the continental shelf. Here we are limited to wind and sea temperature data gathered within 10 km of the coast and lack current data.

Although at this stage the oceanographic regimes cannot be fully characterized the existence of regimes have been identified. What is the nature of transitions between these regimes? Huyer et al. (1979) have admirably shown the rapid nature of the spring transition off Oregon for latitude 45°N. The more recent paper of Strub et.al (1987 a & b) considers the transition for a range of latitudes between 35°N and 48°N. In order to fully explore the transition Huyer had to investigate the event time scale. This will also be done in the next chapter but initially the seasonal time scale of transitions will be discussed here.

Because of the important role of wind forcing one can consider both an atmospheric transition and an oceanographic transition. Huyer et al. (1979) observe that the low frequency winds off Oregon do not show a rapid seasonal change. This agrees with later findings of Strub et.al (1987a) for the latitude of Oregon and further south. Similarly the low frequency spring transition in winds observed here (Fig. 3.2) is not rapid except perhaps for the 1975 case.

At the event time scale Huyer et al. (1979) and Strub et.al (1987b) report a more definite spring transition. Lentz (1987) links the spring transition off Oregon and California to a sudden shift and splitting of the Aleutian low pressure area which correlates with an increase in the interger value of the planetary wave number. However, Lentz reports that there is no detailed explanation for the suddenness of the atmospheric transition. In the southern hemisphere, wave number 1 and to a lesser extent number 3 dominate all year (Tyson, 1986, p. 106). Although there is a measure of variableness in this dominance there is apparently no seasonal link to any changes (Schulze per com). In fact there is a general lack of knowledge about Southern Hemisphere planetary waves and many features with their initiating physical mechanisms are obscure, Hansen and Sutera (1988). A feature of the US west coast case is the 1500 km scale for the coherence of the wind field (Strub et.al 1987b) which

is larger than here. Although the alongshore coherency for winds such as the offshore "berg winds" may reach 1 500 km (as evidenced by satellite imagery of wind blown sand - Shannon, 1985a) the important role in the upwelling dynamics of coastal lows of scale 150 km effectively lessens the coherency scale. Taunton-Clark and Shannon (1988) report that there is an environmental discontinuity in wind stress between the Namibian and South African west coast areas (25-30°S). Similarly although sea surface temperature trends are coherent over a large scale from 14° to 30°S those in the southern Benguela region near 34°S are out of phase with the more northern trend, (Walker, 1987). The strength and persistence of the transition along the US west coast varies with latitude, shelf width and wind strength (Strub et.al 1987b). Between 38°N and 42°N the shelf is narrow, there are strong equatorward winds but currents are less persistent equatorwards; further north the winds are weaker but currents stay equatorward after the transition; south of 37°N winds are stronger but sometimes no transition event is seen. With the above features the nature of the transitions between the regimes locally is therefore likely to be different from the US west coast case.

Inspection of the local wind data (Fig. 3.2) and the long term mean wind (Fig. 3.9a) shows there tends to be a more definite change over from southerly to northerly in autumn than vice versa in spring. There is collaborating evidence for a quicker atmospheric transition in autumn from the work of van Loon and Rogers (1984), Trenberth (1979) and Tyson (1986). The former authors show that for the half yearly cycle of sea level pressure gradients in the southern hemisphere, the differences in mean pressures between the different solstice and equinox months give the steepest pressure gradient off the SW Cape for the June minus March case and the weakest gradient for the September minus June case. Similarly Trenberth (1979) shows that at 35°S the change in wind strength is greater in autumn than in spring and that the latitudinal shift in maximum zonal wind has the most abrupt shift (to 32°S) in May. Tyson (1986) reports maximum latitudinal change for the South Atlantic cyclone occurs between April to May.

Locally the long term oceanographic parameter of temperature (Fig. 3.9b) shows an abrupt change from April to May. The individual VLF temperature data (Fig. 3.4) show however marginally more prominent changes at the end of winter than in autumn. So, although the atmosphere may have a more rapid seasonal transition in autumn a more definite statement about the oceanographic regime transition cannot be made until the event time scale is explored. On the larger scale locally, recent papers on the annual and interannual variability in the South-East Atlantic (Taunton-Clarke and Shannon, 1988) and near

Cape Town (Taunton-Clarke and Kamstra, 1988) do not mention a transition in seasonal regions; definite seasonal cycles in atmospheric pressure, wind stress and sea surface temperature are noted; sea level has a weak annual signal.

In this chapter the mean and seasonal oceanographic attributes of the site have been characterized together with the causative barometric forcing factors. The mean conditions show a preferential response for alongshore forcing as opposed to across-shore wind stress. Such mean attributes can be used as suggested by Csanady (1976b) for elucidating pollutant transport or biological processes. The data base has been shown to be representative of a longer term mean but inter-annual variability has also been highlighted and together with larger scale effects has an influence on the study site. Despite the lack of adequate current data aspects of the seasonal regime transitions have been described but need further definition with event time scale data which are analysed in the following chapter.

TABLE 3.1

FOUR YEAR MEAN (1972-1975) MONTHLY OU SKIP WIND FREQUENCIES FOR DIFFERENT WIND DIRECTIONS+

Monthly percentages

JAN	FEB	MAR	APR	MAY	JUN	JUL	AUG	SEP	OCT	NOV	DEC	4 YR MEAN	FORCE DIRECTION
1,54	1,21	1,01	0,31	0,40	-	0,37	0,94	0,31	-	1,98	1,50	0,80	7
5,25	6,65	4,23	2,19	1,01	1,43	1,71	2,69	2,52	2,86	7,60	5,19	3,62	6
10,76	11,73	10,28	6,98	3,82	6,66	9,14	8,80	10,22	8,52	11,36	12,86	9,26	5
21,09	26,03	22,18	16,25	16,63	16,68	18,28	18,56	22,04	23,62	25,52	24,51	20,94	4
21,11	18,14	21,47	19,48	20,06	20,86	20,61	24,26	26,87	22,70	10,69	21,97	21,44	3
21,79	21,06	19,86	24,79	31,55	29,43	30,12	28,37	22,89	25,56	18,44	19,03	24,41	2
18,46	15,18	20,97	30,00	26,53	24,94	19,77	16,38	15,15	16,65	15,41	14,94	19,53	Calm*
4,56	1,78	2,93	1,88	1,82	1,74	2,62	3,49	2,88	5,32	2,19	4,36	2,96	WNW
6,75	6,76	5,64	5,52	5,04	5,05	4,56	6,92	5,08	7,81	7,29	6,53	6,08	NW
4,02	4,00	3,22	2,19	4,53	5,21	4,96	4,29	4,57	5,31	3,54	4,22	4,17	NNW
2,08	3,67	3,83	4,58	11,68	16,93	15,37	10,72	9,06	4,09	3,95	3,50	7,46	N
0,50	0,56	1,11	1,46	5,04	6,44	4,62	2,94	3,19	1,23	0,84	0,65	2,38	NNE
1,04	0,66	0,70	1,77	4,28	6,40	3,06	3,59	1,50	2,03	0,62	0,73	2,20	NE
0,53	0,56	0,91	2,60	7,16	7,35	6,13	7,61	4,53	2,13	0,22	0,43	3,35	ENE
0,20	1,11	1,31	2,29	3,62	4,88	5,40	3,25	3,45	1,63	0,21	0,22	2,30	E
0,84	0,88	2,12	3,33	3,62	2,30	2,73	3,87	1,89	3,06	1,77	1,33	2,31	ESE
4,60	9,07	8,37	12,50	6,25	3,01	6,93	6,01	6,91	7,24	6,87	5,38	6,93	SE
14,88	21,70	22,08	14,49	6,65	3,73	6,16	7,53	12,03	10,69	18,54	19,80	13,19	SSE
12,90	12,40	10,78	4,79	3,22	4,43	3,17	6,93	12,23	7,41	15,93	10,34	8,71	S
9,62	11,60	7,46	6,14	3,32	1,70	2,29	4,18	5,27	6,61	9,60	11,15	6,58	SSW
11,39	6,74	5,14	3,33	4,43	2,48	5,67	5,64	6,17	8,96	9,06	10,46	6,62	SW
5,20	1,77	2,22	2,29	2,21	2,04	3,69	3,79	3,83	6,27	1,98	3,92	3,27	WSW
2,43	1,56	1,21	0,84	0,60	1,37	2,87	2,86	2,26	3,56	1,98	2,04	1,96	W
213	226	248	240	248	199	206	248	215	245	240	237	No of observations	

+ Data from UCT/ESCOM Progress Report no 15

* Calm: <7 $km.h^{-1}$

TABLE 3.2

SIMPLE STATISTICS OF VERY LOW FREQUENCY DATA FOR WINDS AND TEMPERATURES

Date	Period	TEMPERATURE Variable*	Mean °C	Std Dev	WIND Variable*	Mean $m.s^{-1}$	Std Dev
1976	Year	8 m	12,5	1,5	E/W	-0,76	1,11
1976	Year	2 m	13,0	1,4	N/S	-1,24	2,16
1976	JAN-APR	2 m	12,1	0,6	N/S	-3,23	1,33
1976	MAY-AUG	2 m	13,6	0,7	N/S	0,57	1,40
1976	SEP-DEC	2 m	13,1	2,0	N/S	-1,07	1,80
1977	Year	8 m	12,8	1,3	E/W	-0,87	1,06
1977	Year	2 m	13,5	1,2	N/S	-0,79	2,39
1977	JAN-APR	2 m	13,4	1,2	N/S	-2,15	1,58
1977	MAY-AUG	2 m	14,3	0,5	N/S	1,96	1,02
1977	SEP-DEC	2 m	12,9	1,3	N/S	-2,03	1,53
1977	JAN-APR	8 m	12,3	1,1			
1977	MAY-AUG	8 m	13,9	0,5			
1977	SEP-DEC	8 m	12,3	1,3			

Winds have been rotated 20° to align with coast line

* 2 m = 2 meter depth

N/S = Alongshore Component. From North > 0. From South < 0

E/W = Across shore Component. From East > 0. From West < 0

TABLE 3.3(a): MONTHLY AVERAGE TEMPERATURES FOR VERY LOW FREQUENCY DATA

Month	1975 5 m		1976 2 m		1977 2 m		1978 5 m	
	°C Mean	SD	°C Mean	SD	°C Mean	SD	°C Mean	SD
JAN	12,5	0,3	11,8	0,3	15,2	0,4	11,4	0,9
FEB	13,2	0,5	11,9	0,3	13,3	0,4	12,6	0,4
MAR	12,1	0,7	11,7	0,4	12,3	0,4	12,4	0,1
APR	12,9	0,6	12,9	0,6	12,7	0,7	11,9	0,5
MAY	15,0	0,4	12,7	0,2	13,6	0,1	12,6	0,3
JUN	14,6	0,2	14,2	0,5	14,6	0,4	11,6	0,3
JUL	14,3	0,2	14,1	0,4	14,6	0,2		
AUG	13,6	0,8	13,4	0,6	14,3	0,3		
SEP	10,5	0,5	12,2	0,2	14,3	0,8		
OCT	13,1	0,6	11,1	0,2	12,3	0,6		
NOV	12,6	0,4	14,1	1,9	11,4	0,7		
DEC	11,4	0,2	15,2	0,9	13,1	0,6		
ANNUAL MEAN	13,0	1,3	13,0	1,4	13,5	1,2		

TABLE 3.3(b): SEASONAL MEAN TEMPERATURES AT DIFFERENT DEPTHS

Year	Period	Depth 2 m °C	5 m °C	8,5 m °C	Temperature Differences 2 m - 5 m °C	5 m-8,5 m °C
1976	Year	13,0	12,8	12,5	,2	,3
1976	JAN-APR	12,1	11,9	11.4	,2	,5
1976	MAY-AUG	13,6	13,4	13,4	,2	,1
1976	SEP-DEC	13,2	13,0	12,7	,2	,2
1977	Year	13,5	13,2	12,8	,3	,3
1977	JAN-APR	13,4	12,9	12,3	,6	,6
1977	MAY-AUG	14,3	14,1	13,9	,2	,2
1977	SEP-DEC	12,8	12,5	12,3	,4	,2

NOTE: All calculations for means and differences were done to two decimal places then rounded for presentation here.

TABLE 3.4: LINEAR CORRELATION COEFFICIENTS BETWEEN LINEARLY DETRENDED VARIABLES VERY LOW FREQUENCY

					Correlation between Wind and Sea Temperature 2 m					
Date	Period	Wind Comp	Record Length Days	Deg of# Freedom	Observed Correla= tions** Co	Cm	Lag m Days	Critical Correlation@ Coefficients 95 %	99 %	99,9%
1976	Year	N/S	340	10	.63	.73	8	.497	.658	.795
1976	Year	E/W	340	9	.04	.11	26*	.521	.685	.820
1976	JAN-APR	N/S	94	4	.78	.93	5	.729	.882	.963
	MAY-AUG	N/S	94	-	.15	.70	16			
	SEP-DEC	N/S	94	-	.73	.99	8			
1976	JAN-APR	E/W	94	-	.59	.88	8			
	MAY-AUG	E/W	94	-	.81	-	-			
	SEP-DEC	E/W	94	-	-.89	-.94	3			
1977	Year	N/S	340	7	.78	.84	10	.582	.750	.875
1977	Year	E/W	340	9	.59	.72	14	.521	.685	.820
1977	JAN-APR	N/S	94	5	.97	.98	1	.669	.833	.935
	MAY-AUG	N/S	94	6	.76	.96	9	.622	.789	.905
	SEP-DEC	N/S	94	4	.90	.94	3	.729	.882	.963
1977	JAN-APR	E/W	94		-.32	.36	8			
	MAY-AUG	E/W	94		.37	.89	16			
	SEP-DEC	E/W	94		.75	.86	6			

Wind component N/S = alongshore, E/W = across shore
* 26 was maximum lag used
** Co is correlation at zero lag, Cm is maximum correlation at lag m
@ From Underhill (1981) Table 5
# See cautionary note in Section 3.2.3

TABLE 3.5

SIMPLE STATISTICS OF VERY LOW FREQUENCY WAVE DATA

Date	Period	Mean m	Std Dev m
1975	Year	1,64	0,51
1975	JAN-APR	1,26	0,24
1975	MAY-AUG	2,22	0,31
1975	SEP-DEC	1,60	0,11
1976	Year	1,74	0,53
1977	Year	1,94	0,55
1978	Year	1,64	0,26

TABLE 3.6

LINEAR CORRELATION COEFFICIENTS BETWEEN LINEARLY DETRENDED VARIABLES FOR VERY LOW FREQUENCY DATA

			Correlation Between Wind and Wave Height				
Date	Wind component	Record length Days	Degrees of freedom	Observed correlations C_o	Critical Correlation coefficients 95 %	99 %	99,9 %
1976	Alongshore	340	14	0,61	.426	.574	.711
1976	Across-shore	340	14	0,04	.426	.574	.711
1975	Alongshore	340	8	0,66	.549	.716	.847

TABLE 3.7

TABLE BAY HARBOUR SEA TEMPERATURE, MEANS, STANDARD DEVIATIONS AND RANGES FOR A) ANNUAL CASES AND B) MONTHS FOR THE PERIOD 1956 TO 1980

A) ANNUAL MEANS

YEAR	MEAN °C	STD DEV	RANGE
1956	12,9	0,7	2,2
1957	14,1	0,8	2,2
1958	13,4	1,0	3,3
1959	13,7	0,6	1,6
1960	13,8	0,7	2,2
1961	14,2	0,9	2,8
1962	13,8	0,9	2,8
1963	14,2	0,9	2,8
1964	13,7	0,6	2,2
1965	-	-	-
1966	14,1	0,9	2,2
1967	12,5	0,9	2,2
1968	13,1	0,7	1,7
1969	-	-	
1970	12,9	1,0	2,7
1971	12,3	0,8	2,7
1972	13,9	0,9	3,0
1973	13,7	0,6	1,7
1974	13,8	1,2	2,9
1975	13,4	1,0	3,6
1976	12,9	1,3	5,0
1977	13,6	1,0	2,7
1978	12,8	0,4	1,2
1979	12,8	0,6	1,9
1980	13,2	1,2	3,9
Mean	13,4	0,8	2,6
Std Dev	0,6	0,2	0,8

B) MONTHLY MEANS 1956-1980

MONTH	MEAN °C	STD DEV	RANGE
JAN	13,4	0,9	2,9
FEB	13,4	1,1	3,3
MAR	13,3	1,0	3,9
APR	13,2	1,2	4,0
MAY	13,6	0,8	3,3
JUN	13,7	0,9	3,5
JUL	13,8	0,8	2,9
AUG	13,7	0,7	3,3
SEP	13,5	1,2	4,4
OCT	13,2	1,0	3,8
NOV	12,9	0,9	3,9
DEC	13,3	1,1	4,5
Mean	13,4	1,0	3,6
Std Dev	0,3	0,2	0,5

CHAPTER FOUR

EVENT TIME SCALE CHARACTER

C O N T E N T S

CHAPTER FOUR

EVENT TIME SCALE CHARACTER

4.1 INTRODUCTION

In Chapter 2 the dominant time scales of processes that occur in the study area are identified. Each of these is considered in separate chapters. The first time scale discussed is that of the seasonal range in Chapter 3. The variability within the seasonal data and the transition between seasonal oceanographic regimes points to links at a shorter time scale, probably that of synoptic events. The synoptic weather mode, falling between the seasonal and diurnal time scales is considered by Jury (1980) to be the dominant locally occurring mode. By association the oceanographic response at this time scale is important. In fact Monin (1977), reports that for the ocean as a whole the synoptic variations of ocean-current velocities are the strongest of all oceanic variations. His synoptic classification includes periods between a few days and several months. In this chapter more emphasis is placed on the portion of this classification up to several weeks and is termed the event time scale. The aim is to characterize the event time scale using time series analysis, spectral analysis and other statistics; to consider the wind forcing of possible regime transitions. The evolution of a wind event and its effects on the thermocline structure will be explored together with a theoretical upwelling model predicting thermocline displacement. Lastly the spatial variability will be delineated using data of sea surface temperature and currents. Mechanisms for the findings will be proposed.

The intermediate low frequency (ILF) data and the low-passed frequency (LF) data are investigated here. The former covers frequencies between about 0,05 cpd and 0,5 cpd, where the data have effectively been band-passed to remove the higher frequencies related to diurnal, inertial and the main tidal processes and also to remove the lower frequencies for trends greater than about 20 days. The ILF data set, being composed of residuals gives a relative picture of the data tendencies. The low frequency (LF) data set, since it preserves the absolute trends in the time series data by including the very low frequencies, is also used to characterize the event time scale.

4.2 WIND AND TMEPERATURE DATA

4.2.1 Filtered Time Series Data

In this section a qualitative description of the graphical time series wind and sea temperature data is presented together with that of the cumulative Ekman transport (CET) plots. As in the case of the very low frequency data the wind vectors are rotated 20° (see Section 3.2.1). To allow for filter truncation effects an extra four days' real data are included at each end of the year-long data sets. The wind data for the years 1976 to 1978 were low-pass filtered as were the temperature data for the years 1975 to 1977 with just 5 months of 1978. Since the features revealed in the filtered data are similar for the different years just 1977 and 1978 are displayed. The latter year is included since it is later used to illustrate a case study, while 1977 is subsequently also illustrated for the high frequency range in Chapter 5. The data are shown graphically in stick diagrams for daily values of wind vectors, both wind components and for sea temperatures. The temperatures are given in 'stick' form to allow direct visual comparison with the winds. The low-pass filtered (LF) wind data for the years 1977 and 1978 are shown in Fig. 4.1a&b respectively. The equivalent temperature data for the year 1977 and five months of 1978 are shown in Fig. 4.2a&b. The intermediate low frequency (ILF) wind data for the years 1977 and 1978 are shown in Fig. 4.3a&b. The ILF temperature data for the years 1976 and 1977 are shown in Fig. 4.4a&b. The LF data contain the seasonal trend whereas the ILF data are detrended with zero mean and in essence show the fluctuations about the seasonal trend.

Because the primary temperature data set (hourly) only covers about two years an additional set of temperature data comprised of 12 hourly decimated values (at 5 m depth) from August 1974 to May 1978 was used. This was not low-pass filtered; the very low frequency filter was applied to a simple daily mean of the 12 hourly data. The residuals (intermediate frequency) between the mean daily and very low frequency temperature data for part of this extended period are shown in Fig. 4.5 (1975 to 1977 inclusive). Although temperature data are generally available at three depths, only data at one depth are plotted because at this time scale they are very similar.

The main feature of both wind and temperature stick diagram data is that the daily sticks occur in multiday groups or events. This is particularly obvious with the ILF data (which has the seasonal trend removed) of the temperature (Fig. 4.4a&b) and of the alongshore wind component (Fig. 4.3a&b), where groups of 2 to 10 days occur. In the case of the LF data (Fig. 4.1) where the trend is not removed, some events continue for up to twenty days. The other important feature

is the fairly uniform temperature response during winter (Fig. 4.2).

Firstly we consider aspects of the wind data. The LF wind data which include the seasonal trend show (Fig. 4.1) the southerly dominance of such events in spring and summer and the northerly trend in winter. Study of the vector representation reveals that the events often have a cyclic nature, the wind turning from SE through W to N or backing from the NW to S. These events are closely associated with the synoptic scale weather systems that pass the southern point of the continent Keen (1979). The ridging of the South Atlantic anticyclone south of the country, the cold fronts of winter, and the ubiquitous coastal lows all have their characteristic signatures; these are discussed in Section 4.3.1 and 1.4.2.

Inter-annual differences are more clearly seen when the alongshore wind data are used to calculate across-shore cumulative Ekman transport (CET) of surface waters for each event. The method of Huyer, et al. (1979), described in Section 1.5.3, is used to calculate CET values. Plots of the CET for Ou Skip winds for 1975 to 1978 are shown in Fig. 4.6. The individual events are clearly seen, where the height of each peak gives the total Ekman transport resulting from that event; positive values for onshore transport and negative for offshore transport that induce upwelling. In such shallow water as at the study site, Ekman veering is limited and the classical Ekman transport value is subject to error. It is however used in the form of CET plots to give a good visual indication of potential upwelling events locally and is assumed to relate to larger scale effects of the wind field.

Inter-annual and Seasonal aspects of the event data

The inter-annual variability of the CET events for the four years depicted in Fig. 4.6 are quite marked for the winter period, viz 1977 winter has numerous medium sized and a few large sized onshore events whereas 1978 winter has only a few small events.

The qualitative differences between the spring regime (September-December) and the summer wind regime (January-April) discussed in the previous chapter (3.2.1) are well illustrated by the CET plots (Fig. 4.6). If one looks at the persistance of very small or calm events and the number of reversals then the spring period is more varied than the summer period which has more consistent offshore flux with limited number of calms. This is illustrated quantitatively when for 1975 to 1978 the mean number of onshore events that exceed a CET of about $+0.5 \times 10^{9}$ $g.cm^{-1}$ in spring is 9.0 ± 1.1 compared with a mean number of 3.3 ± 1.5 for summer. The corresponding temperatures show a

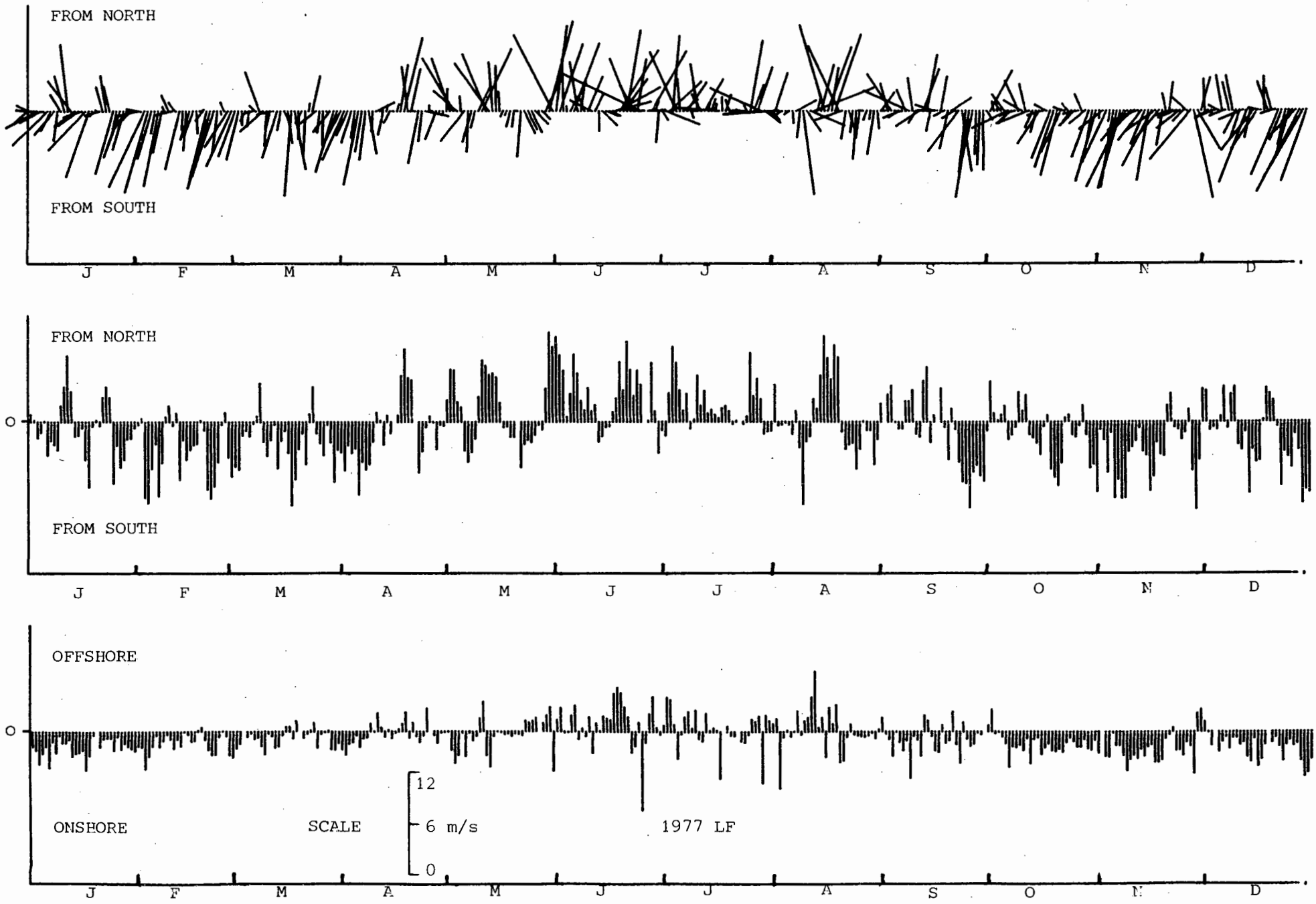

FIG. 4.1a. LF 1977 TIME SERIES DIAGRAMME OF DAILY VALUES OF LOW FREQUENCY (LF) FILTERED OU SKIP WINDS - ANNUAL SETS. TOP - WIND VECTORS, MIDDLE - ALONGSHORE (NORTH), BOTTOM - ACROSS-SHORE (EAST). COMPONENT AXIS IS ROTATED 20° WEST OF NORTH

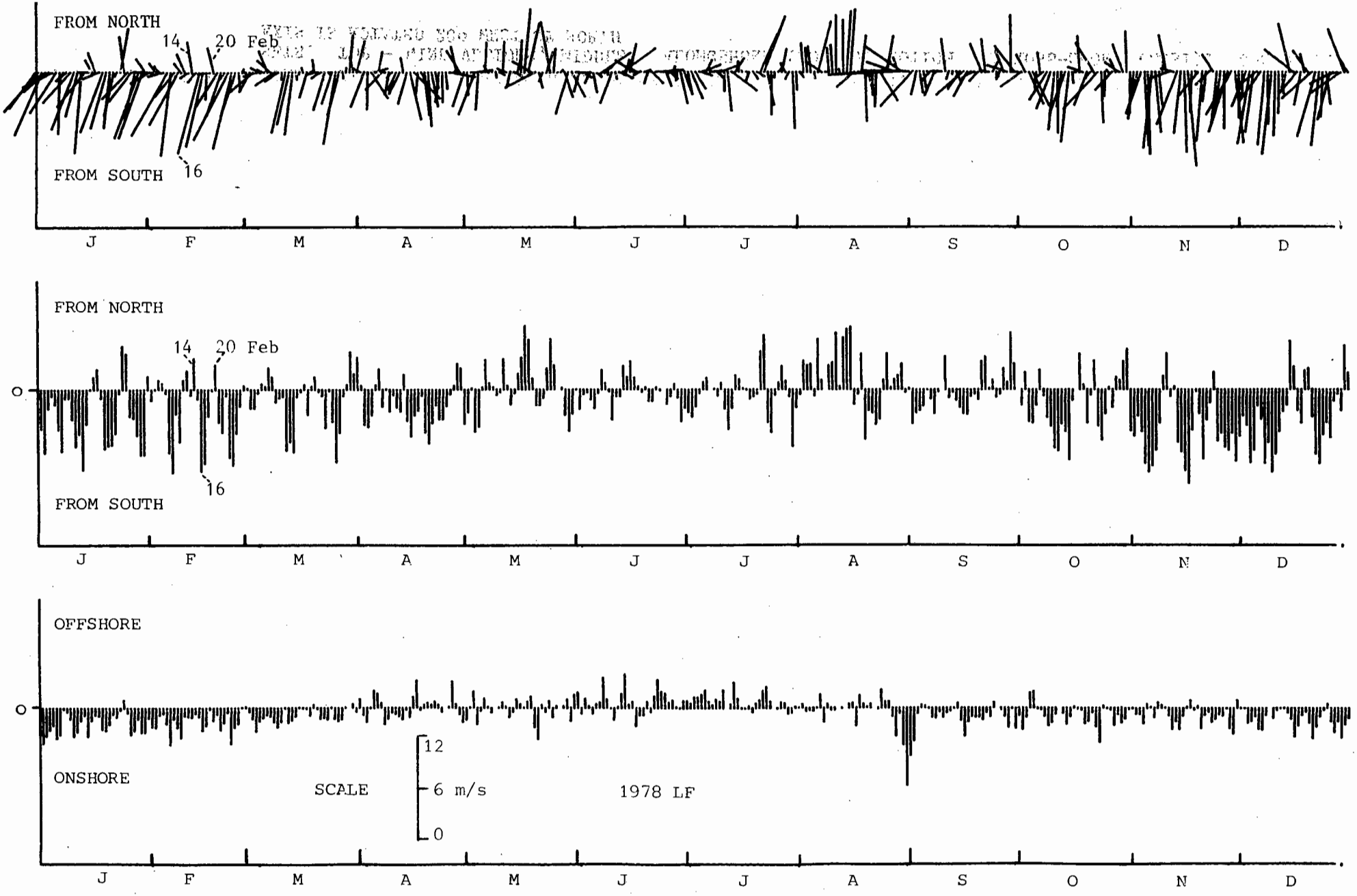

FIG. 4.1b LF 1978. FEBRUARY DATES REFER TO CASE STUDY IN 4.3.1
TIME SERIES DIAGRAMME OF DAILY VALUES OF LOW FREQUENCY (LF) FILTERED OU SKIP WINDS - ANNUAL SETS. TOP - WIND VECTORS, MIDDLE - ALONGSHORE (NORTH), BOTTOM - ACROSS-SHORE (EAST). COMPONENT AXIS IS ROTATED 20° WEST OF NORTH

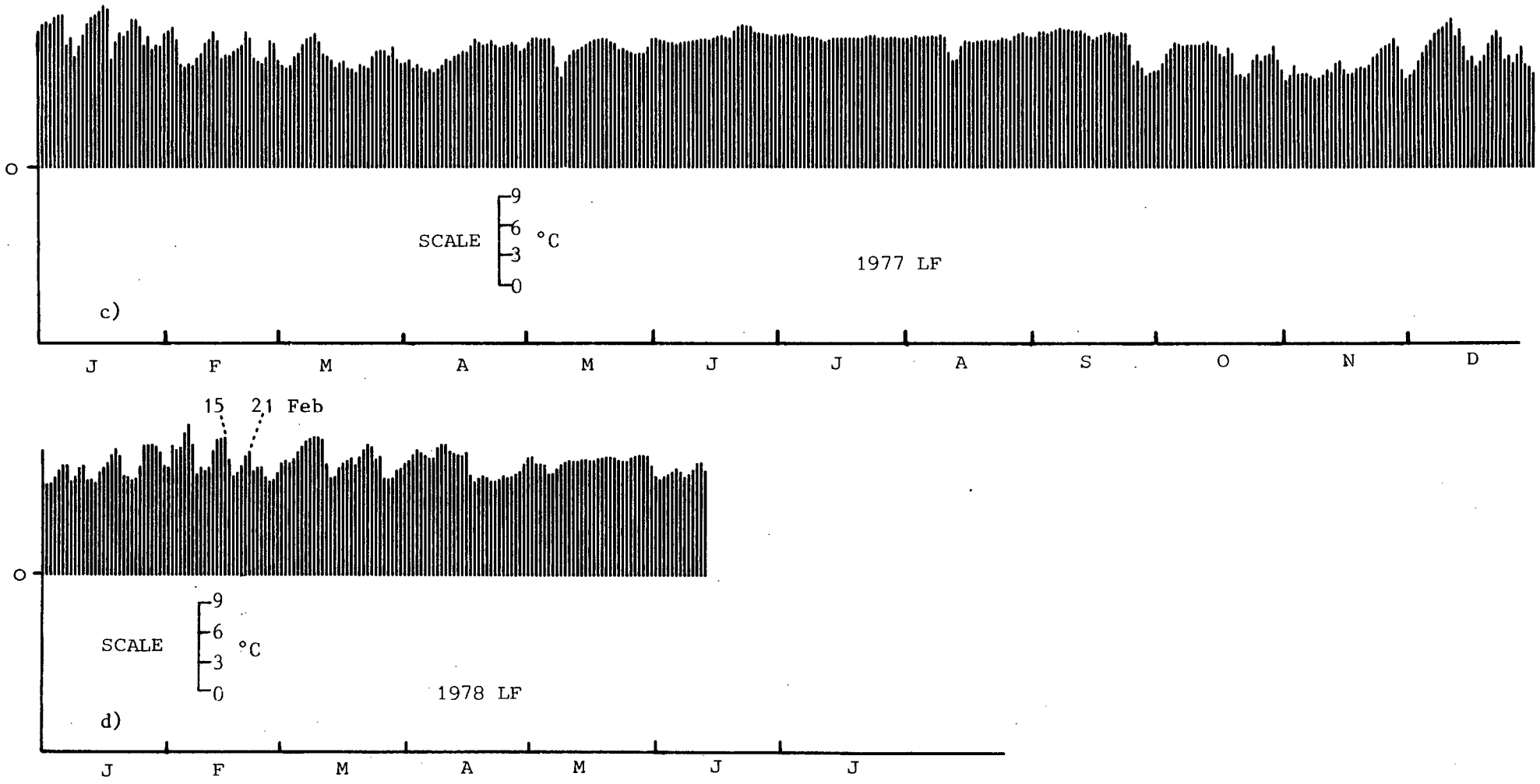

FIG. 4.2 TIME SERIES DIAGRAMME OF DAILY VALUES OF LOW FREQUENCY FILTERED SEA TEMPERATURE. ALL SETS FORMED FROM HOURLY 2 M DEPTH DATA EXCEPT FOR 1975 WHICH IS FORMED FROM 12 HOURLY 5 M DEPTH DATA
a) 1977 b) 1978 ~5 MONTHS. FEBRUARY DATES REFER TO CASE STUDY IN 4.3.1

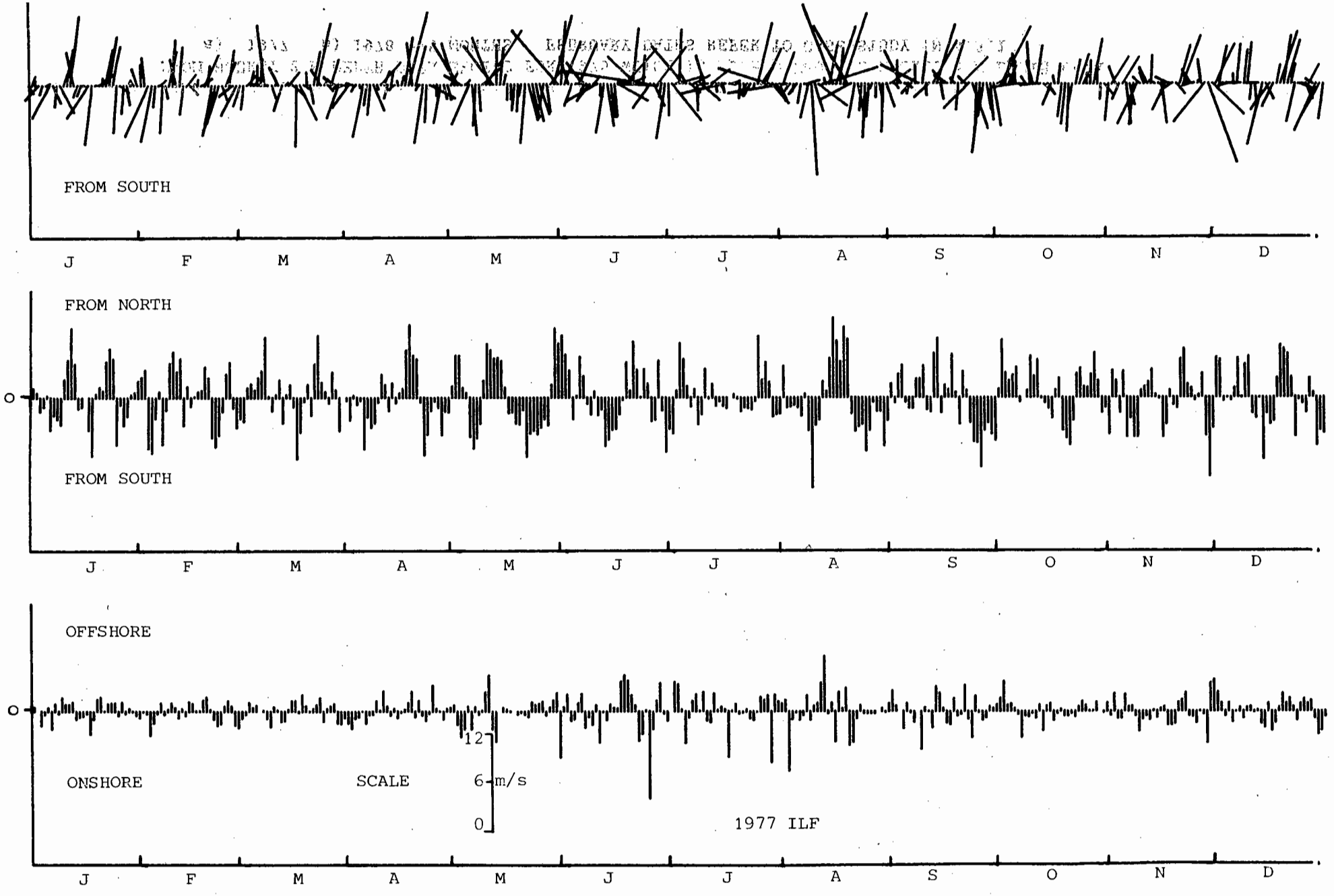

FIG. 4.3a ILF 1977 INTERMEDIATE LOW FREQUENCY (ILF) WIND DATA, OTHERWISE AS FIG. 4.1. THE WIND SENSE IS NOT ABSOLUTE

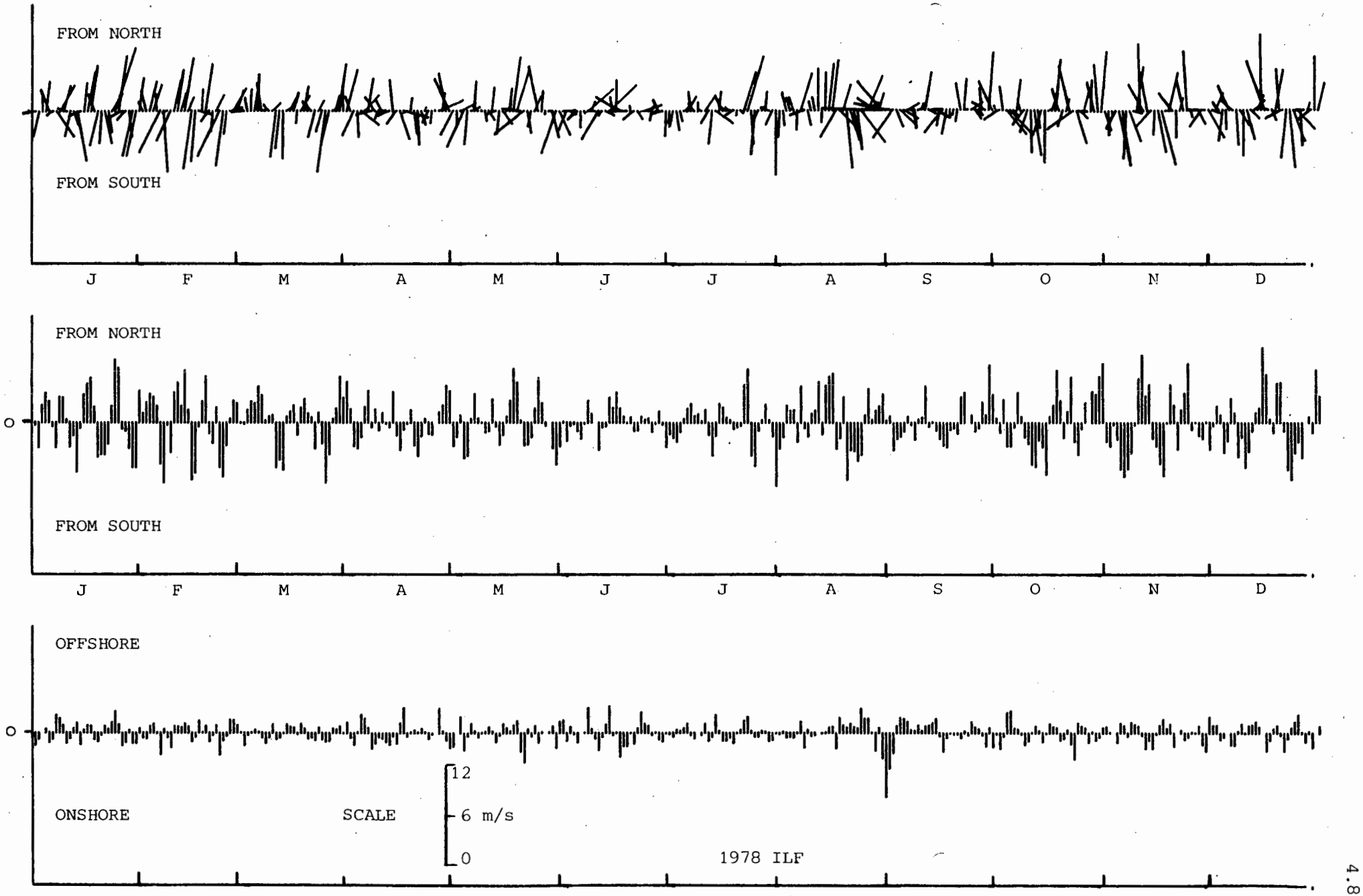

FIG. 4.3b ILF 1978 INTERMEDIATE LOW FREQUENCY (ILF) WIND DATA, OTHERWISE AS FIG. 4.1. THE WIND SENSE IS NOT ABSOLUTE

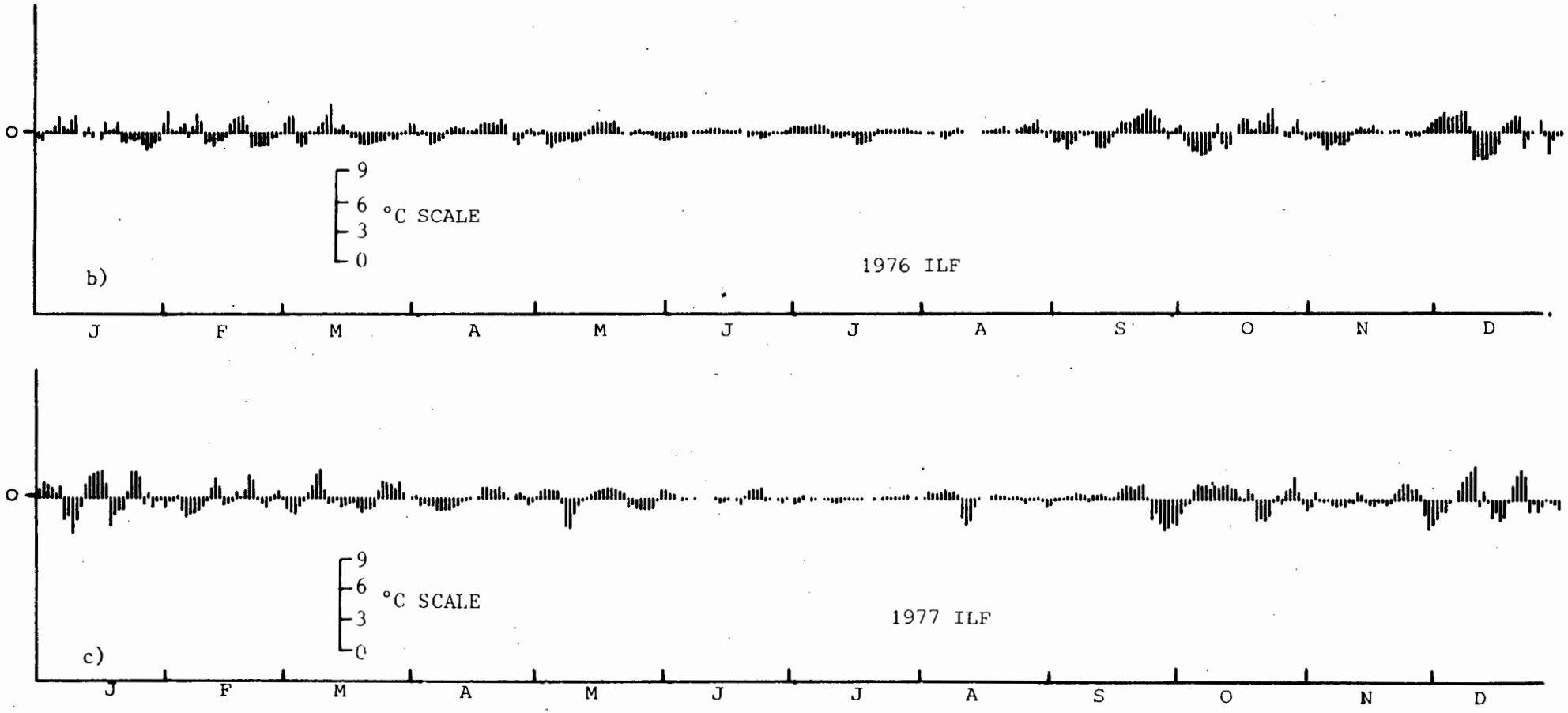

FIG. 4.4 INTERMEDIATE LOW FREQUENCY TEMPERATURE DATA (ZERO MEAN) OTHERWISE AS FIG. 4.2
a) ILF 1976, b) ILF 1977

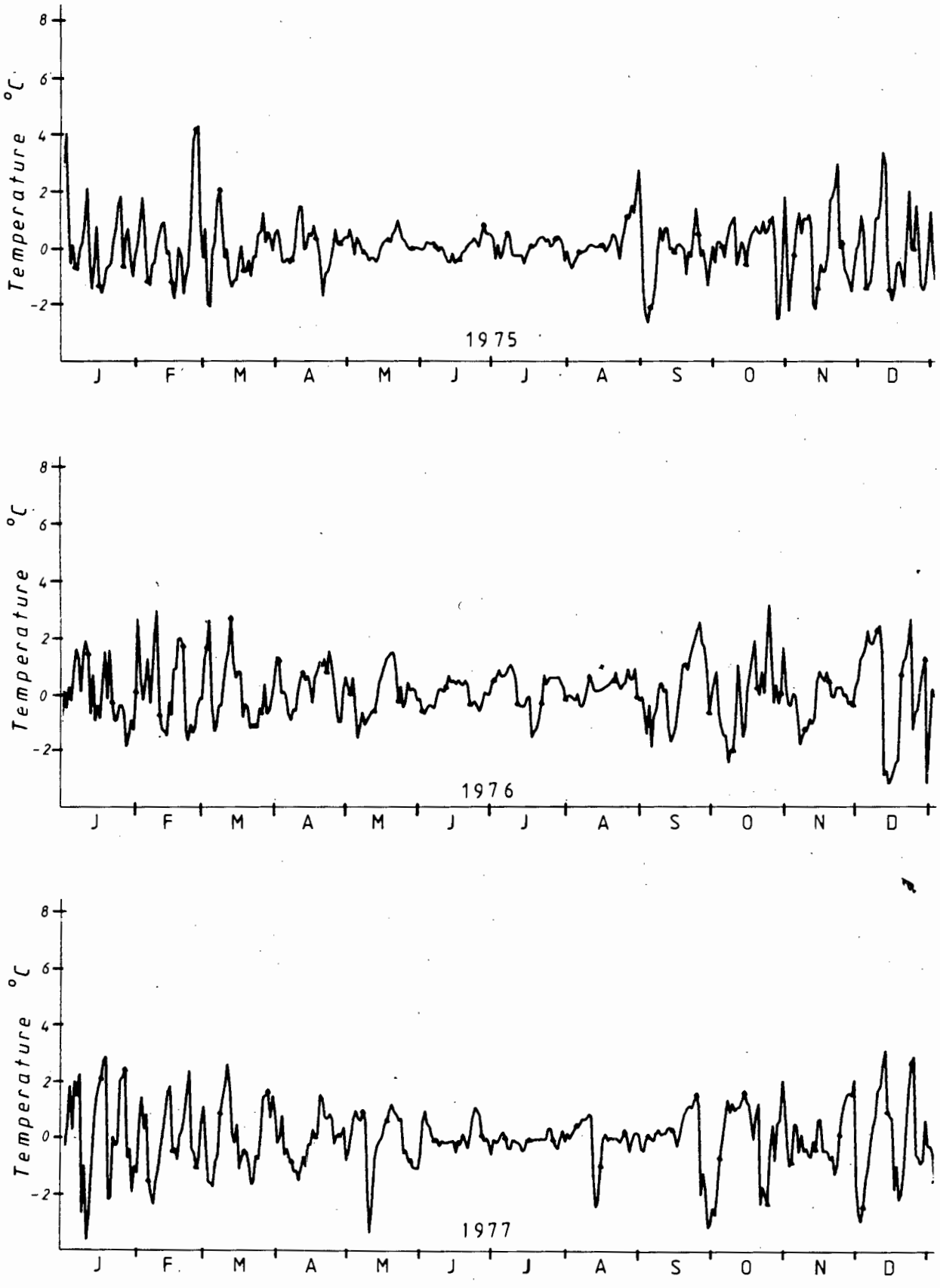

FIG. 4.5 MULTI-YEAR TIME SERIES OF INTERMEDIATE LOW FREQUENCY FILTERED 5 M DEPTH TEMPERATURES (ZERO MEAN) FORMED FROM 12 HOURLY DATA. THE PORTION JANUARY 1975 TO DECEMBER 1977 IS PLOTTED

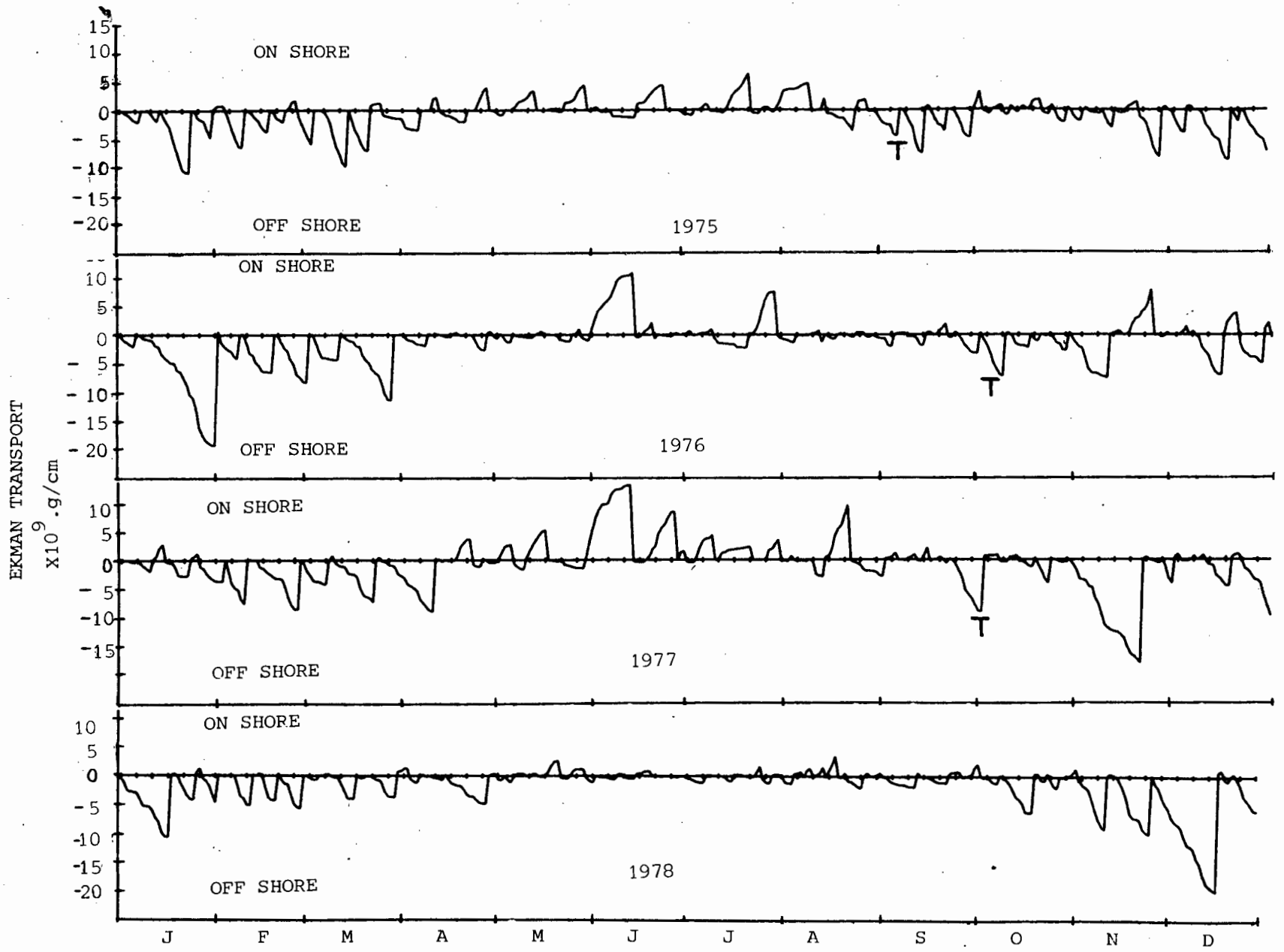

FIG. 4.6 CUMULATIVE EKMAN TRANSPORT (CET) DIAGRAMS FORMED FROM LF ALONGSHORE OU SKIP WIND STRESS WITH COMPONENT AXIS ROTATED 20° WEST OF NORTH FOR THE YEARS 1975 (TOP) TO 1978 (BOTTOM). TICK MARKS INDICATE EACH 5TH DAY. T = SPRING TRANSITION EVENT

similar varied response (e.g. Fig. 4.2a&b and Fig. 4.5). The overall temperature response has a very clear character difference between winter and the combined southerly regimes. During the latter period with offshore CET events the temperature has large oscillations of between ± 1 °C to ± 4 °C (Fig. 4.5) whereas in winter the temperatures are fairly uniform with about ± 1 °C fluctuations (Figs. 4.5 and 4.2a&b).

Some generalizations between CET events and their temperature response can be made. The greater the event the greater is the temperature change. Decreases in temperature lag the wind by 1 or 2 days. However, different sequence of events and seasonal differences bring exceptions to the rule. During the southerly regime medium offshore events bring cold water to the surface but very large events e.g. during January 1976 and November 1977 soon reach a limit to the coldness of the water upwelled and then tend to maintain the depressed temperature. Occasionally quite small offshore events can reduce the temperature appreciably e.g. the small event after the very large event in November 1977 (Fig. 4.6) gives as cold temperatures as the large event (Fig. 4.2a). The small events of May 1976, 1977 and 1978 all produce marked temperature drops.

Temperature increases invariably follow on after offshore events during the southerly regime even if there is merely a relaxation in wind strength and no actual reversal in wind direction (see 4.3.1.2). This has also been observed by Taunton-Clark (1983) off the Cape Peninsula. Such temperature response can be considerable but maximum increases are associated with an accompanying onshore event e.g. end of February 1975 (Fig. 4.5) and of course the anomaly of December 1976 (Bain and Harris, 1975ff; Trenberth, 1979) when record high temperatures were experienced corresponding with consistent onshore winds (Fig. 4.5).

In contrast the temperature response to individual onshore events is weak during winter, when temperatures are much more uniform. The mean winter temperatures do however respond to the inter-annual variability of mean winter conditions as discussed for the seasonal time scale (Section 3.2.2) e.g. the greater number of onshore events in winter 1977 give warmer mean temperatures and the 1976 winter with least onshore transport has the coldest mean temperature for a winter regime (Table 3.2). Careful observations of the event time scale temperature data reveal that the warmest winter events occur in the earlier part (May-June) of the period and also in Sept 1977 when there was a late start to the upwelling season; whereas July-August tend to be slightly cooler. This latter period coincides with the coldest air temperatures and when, on the larger scale, warm surface waters are furthest offshore (Kamstra, 1985 and Christensen, 1980,

Section 3.7.2). Besides the winter warm trend, maxima for individual onshore events generally occur in December, January and February, when the warm surface waters are closest inshore (Christensen, 1980) and when insolation is high.

Turning to minimum temperatures, inspection of Fig. 4.2a&b show that amongst the many temperature dips there are two periods of generally cooler water. The coldest events occur in the spring regime before December and the subsidiary sustained cold period is in March or early April. Occasionally the late summer minimum is bettered for a short period in January associated with a large offshore event. The spring minimum correlates with the observation of Andrews and Hutchings (1980) that the coldest water on the shelf occurs during September-October. Their limited data set which just exceeds two years shows a subsidiary minimum in February. The March-April minimum in the present data are associated with a favourable sequence of relatively long duration offshore events.

Although rather infrequent, a few significant decreases in temperature (to below -1 for residuals) occur during the winter period as seen in Figs. 4.5 and 4.2a&b; viz, none in 1975; three in 1976 winter, 3 in 1977 winter and one in the short 1978 winter record. When correlated with the CET data of Fig. 4.6 all these events occur as a response to remarkably small offshore CET events (less than 2 x 10^{9}g.cm^{-1}). There are in addition other offshore CET events during winter for which there are no significant decreases in temperature. Contrasting the "successful" offshore CET events that produce cold water and those that fail to do so, it is seen that the latter events always occur after a strong onshore CET event which tends to suppress subsequent full upwelling. The former events generally occur after either an extended calm period or after at most, a small onshore CET event and generally have a duration exceeding 5 days. The first offshore event in August 1977 has an associated significant temperature drop which is terminated by (see wind vectors in Fig. 4.1c) an easterly offshore contribution which, after checking with the daily synoptic pressure maps of the period, is confirmed to be due to "berg winds". See §1.4.2. This collaborates with the observations of Nelson and Hutchings (1983) that "berg winds" and subsequent coastal lows suppress upwelling in the Benguela region. On a larger scale much further north at Luderitz, Stockton and Lutjeharms (1988) suggest a contrary roll for berg winds from remote sensing data but do not confirm it with ships data. These temperature drops associated with small offshore events and the example of the event in May 1976 when very light offshore winds maintained a lower temperature are possibly indicative of processes occurring in the larger scale that enhance movement of cold water to the study site, e.g. the winds at Cape Point (Andrews and

Hutchings, 1980) have a larger southerly contribution during winter than those at Ou Skip.

Further aspects of the magnitude of events that bring cold water into the region will be discussed when the transition between winter and spring is considered later (4.2.6) The transition events are very variable in magnitude and seem to depend on the previous event history.

Inspection of the vector constituents (Fig. 4.1 and 4.3) of the offshore events reveal that in general those with a strong SSE vector are more efficient than SSW vectors in bringing cold water to the surface. Similarly temperature rises are more extreme with NW vectors than N vectors e.g. the relatively sharp temperature rise in June 1977 included one day of very strong NW, and the anomaly of November-December 1976 had associated with it many westerlies and North westerlies. (Remember the component axis has been rotated 20° west of north in the figures.)

The across-shore wind component

The LF across-shore wind component is shown in Fig. 4.1a&b for the years 1977&78. It is seen to be a lot smaller than the alongshore component. The vector representation shows frequent anticlockwise backing from northerlies to southerlies as cyclones move to the east, south of the continent. The across-shore component reflects these rotary changes in the predominant alongshore gradient winds.

This wind component is expected to show up any other E-W wind events such as land/sea breeze effects and berg winds. The former with their diurnal nature are attenuated by the filtering process at this time scale and are masked by the much larger contribution from the strong southerlies and northerlies. However as pointed out in the seasonal section (3.2) the offshore tendency for the across-shore winds in winter and onshore direction for the remainder of the year does also correlate with enhanced land breeze and sea breeze respectively.

The offshore oriented berg winds (1.4.2) occur most often in spring and autumn but intense events are not very common. At the Ou Skip site berg winds are often more northerly i.e. NE or NNE than across-shore and at times difficult to separate visually from other northerly events in the wind stick diagrams. Reference was made earlier to the suppression of upwelling by berg winds, which often preceed coastal lows, with the attendant limited temperature response. Other across-shore wind events are also transient having a small net across-coastal flow effect on the sea (Nelson and Walker

(1984)) and hence the sea temperature response is small compared with the alongshore winds. Further comment on across-shore winds are made in the section on wind temperature correlation (4.2.3) and at the diurnal time scale in Chapter 5 they are discussed at length.

4.2.2 Simple Statistics of Low Frequency Data

Simple statistics of the daily low frequency (LF) data are given in Table 4.1. The mean values are similar to those in Table 3.2 but the standard deviations are much larger which reflect the increased variability at this time scale. Compared with the wind the standard deviation for temperatures show the greatest difference between regimes; the standard deviation in the winter period is generally 2 to 3 times smaller than in the other periods. The small variability is due to lack of marked upwelling associated with onshore winds of winter. The variability of both temperature and wind data in spring is greater than summer for adjoining spring-summer regimes which lends some support to the subdivision of the southerly wind regime. The standard deviation for the winds are always greater than their mean value and are up to several times larger in the case of the winter period. The means of the winter period winds on an inter-annual basis are the most variable of any season, as is also apparent in the CET (Fig. 4.6) variability. There is a trend that the standard deviation for the 2 m depth temperature data is marginally smaller than for the other depths. This lower variability close to the surface is probably due to the wind and wave mixing effects.

Statistics for the ILF data are not tabulated. They have similar standard deviations to that in Table 4.1 but have zero means.

4.2.3 Correlations and Lags

Linear correlation coefficients for linearly detrended wind and sea temperature data with zero means and normalized by their variances are given in Table 4.2 and Table 4.3 for the ILF data set and the LF data set respectively. See Section 3.2.3 which comments on the confidence levels. Correlation analysis for the LF data is done using both daily and hourly time steps in contrast to the ILF data where only daily steps are available. The resulting correlation coefficients are however similar to that of the ILF data for the various winds and regimes. In Table 4.3 only the hourly analysis results of the LF data are therefore presented to illustrate aspects of lagged response.

In Table 4.2 it is seen that the annual across-shore wind and temperature is significantly negatively correlated at zero lag for

1976 and 1977 but with one day's lag in temperature the correlation coefficient falls to a near zero value and then gradually increases to a non-significant maximum after several days. The negative correlation is expected from the relative signs of the across-shore winds i.e. an offshore positive wind should cause a negative temperature change. The very rapid drop to zero correlation indicates that some process is operating at the diurnal time scale for the across-shore wind but not at any larger time scale.

The annual alongshore wind and temperature data sets are correlated at zero lag with a confidence level better than 99 % for both 1976 and 1977. With a one day lag in temperature the correlation increases to above the 99,9 % confidence level. In contrast to the across-shore falloff to zero correlation in one day the alongshore wind needs a lag of 3 to 4 days to drop below the 95 % confidence level. This is indicative of a temperature response to a synoptic event scale process operating on the alongshore winds. The alongshore winds for the winter period are not significantly correlated with temperature at zero lag but the correlation coefficient rises to a maximum after a two day lag and fluctuates about the 95 % confidence level. The alongshore winds for both spring and summer regimes have an initial correlation (zero lag) better than 95 % which rises to greater than 99,9 % after a one day lag in temperature.

Table 4.3 for the low pass frequency data hourly steps yields similar correlation coefficients. A lag for maximum correlation is of the order of 24 hours except for the winter regime. In winter the correlation coefficient rises to a value of 0.22 (less than the 95 % confidence level) after 36 hour lag then decreases and later increases again to reach a maximum correlation of 0,27 after 192 hours. The relatively long lag of 30 hours for the spring period (1976) is probably influenced by the anomaly for that period.

The highly significant correlation coefficients for the alongshore winds indicate how prominent a role they play at this time scale in forcing the temperature response. The longer lag in winter is probably evidence for the thermocline lying deeper and further offshore then.

There is no appreciable difference at this time scale in correlation between the wind and the temperature for the 2 m and 8 m depth temperature sets. In the one case given in Table 4.3 the lag for maximum correlation for 8 m is greater (21 hours) than for the 2 m data (18 hours).

Correlations between temperatures at different depths are all significant to better than 99,9 %. They are not tabulated. There is a very sharp decrease in correlation with both positive and negative lag. With hourly lags the correlation is usually maximum at zero lag but occasionally the first lag is marginally enhanced and thereafter the correlation decreases. At this time scale for such shallow depths the water column is expected to behave synchronously.

4.2.4 Wind Wave Correlations for intermediate frequency data

A visual comparison of data at intermediate frequencies for alongshore winds (Fig. 4.3) and waves (Fig. 4.7) shows a very similar pattern. The multiday event nature of the wind is mirrored in the wave data. Linear correlation analysis of the wind and waves reveals a definite lag between the two for maximum correlation as seen in Table 4.4 in which is also tabulated the standard deviation for the zero mean wave heights. For the annual data sets the initial correlation coefficients are low but peak dramatically to exceed the 99.9 % confidence level after a lag of one day (Table 4.4). This level of confidence is maintained for one further day's lag and then the correlation falls to below the 95 % confidence level. The correlation coefficients for the seasonal regimes have a similar behaviour with lagging, the peak occurring after one day's lag. The winter regime has the highest set of correlation coefficients, confirming the importance of this period's synoptic systems for wave generation (see Section 3.6). The standard deviation of the wave height is also maximum for this period. Gravity wave generation through wind action has a time scale of hours to a few days (Phillips, 1980). The sharp peaking in correlation coefficient after a one day lag suggests that the local generation of waves is not as important as that of swell generation due to more distance winds. For locally measured wave parameters the lag of one to two days corresponds to a generation location about 300 to 1000 kilometers offshore, which agrees with proposals by Shillington and Harris (1978) for wave generation off this coast. The more distant winds are in general linked to the same synoptic event as the local winds thus giving a good correlation.

4.2.5 Spectral Analysis

For both wind and sea temperature the intermediate low frequency (ILF) filtered data are subject to spectral analysis. The years 1976 and 1977 were analysed but only the results for 1977 are shown in Figs. 4.8a, b and c which depict on log/log scales a) the autospectra for the two wind components, b) the wind rotary spectra and c) the temperature autospectra. The temperature spectra are for the 2 m and 8 m depth. The 95% confidence levels and bandwidth as described in

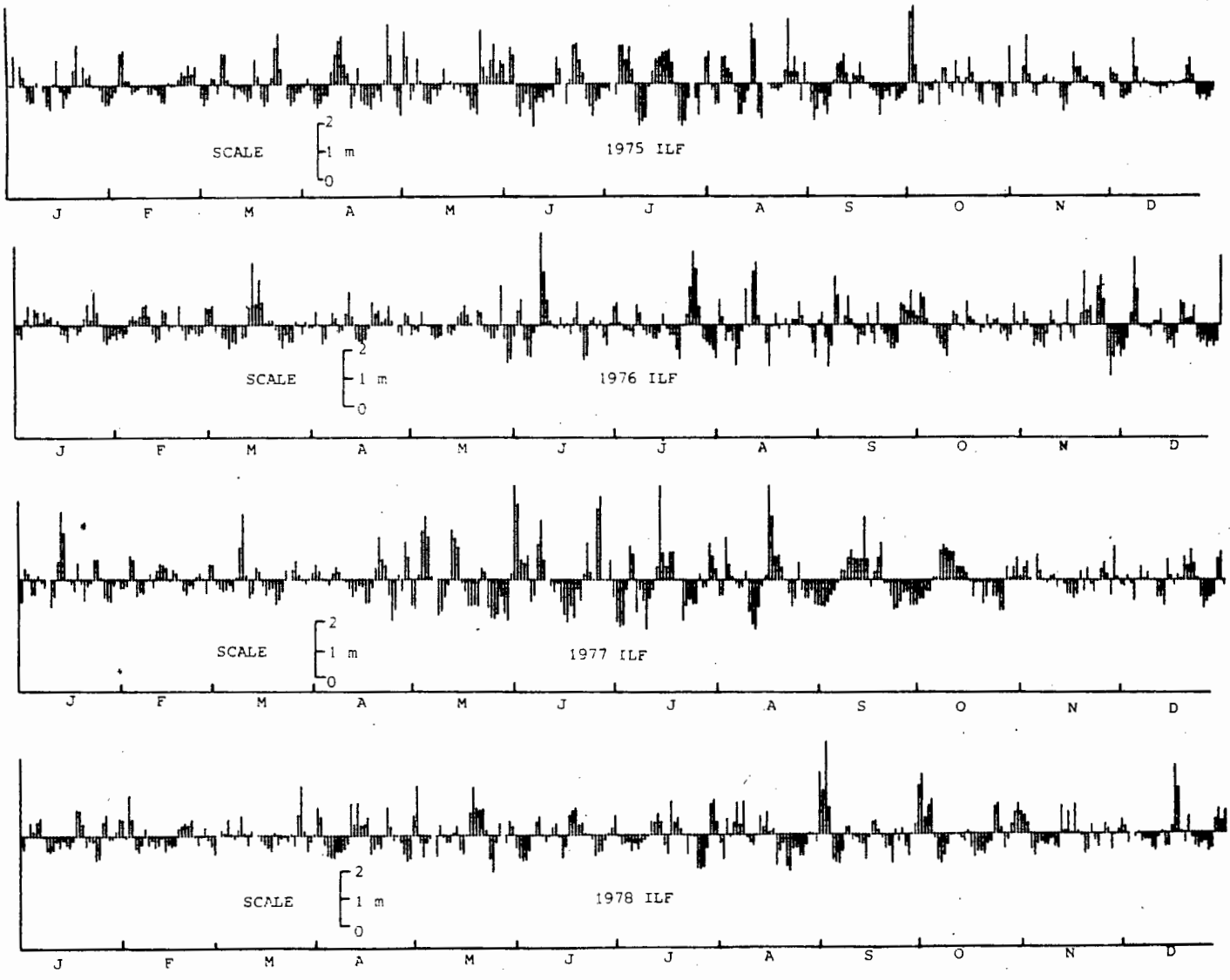

FIG. 4.7 TIME SERIES DIAGRAMME OF INTERMEDIATE LOW FREQUENCY WAVE HEIGHTS. FOUR ANNUAL SETS, 1975 TO 1978

Section 2.3.1 are given in each figure. Although calculated for 60 lags the spectra are plotted for only thirty lags where each 10th lag is indicated by a plotted symbol on the spectra.

A common feature of both the wind and temperature ILF spectra is the lack of any statistically significant peaks and the wide bandwidth, giving limited structural features. In order to improve the resolution relative to the year long cases mentioned above, a much longer portion of the time series data is also analysed. In the case of the wind data the hourly record from August 1974 to May 1978 is filtered and spectrally analysed. The 12 hourly 5 m depth temperature record from August 1974 to May 1978 is filtered to obtain an ILF data set and then spectrally processed. The spectra for the approximately 3,8 year long data set are plotted for 120 lags in Fig 4.9a, b and c in the same sequence respectively as given in the previous figures. Again each 10th lag is indicated by a plotted symbol on the spectra.

The latter wind and temperature spectra have greatly improved bandwidth characteristics and more structure is evident but still no prominent significant peaks are revealed. The spectra for firstly the wind then the temperature data will now be discussed for both the annual and the longer time series cases.

In all cases the alongshore (north) autospectra, series a) and the total rotary spectra, series b) in Fig. 4.8 and 4.9, have a trend in spectral power that follows a slope of less than $f^{-3/2}$ and is closer to f^{-1}. The across-shore (east) autospectra have an even flatter trend particularly for periods greater than about 4 days when there is no increasing trend in spectral power for increase in period. In the autospectra the alongshore component starts to dominate the across-shore component for periods greater than about 6 days. This is attributed to the fact that the alongshore winds are preferentially forced by the longer scale synoptic systems. The alongshore component ILF autospectra for the 3,8 y record (Fig. 4.9a) rise to a maxima at a period of 9 and 14 days, the latter period being somewhat shorter than the near 20 day period maxima for the annual cases.

The ILF rotary spectra in all cases (Fig. 4.8b, 4.9b) have the anti-clockwise component dominating at all the frequencies shown. At no frequency however does the rotary analysis give a significantly stable ellipse orientation. This means that no specific wind direction has a significant statistical dominance at any frequency, although as has been observed in the autospectra the alongshore winds

in general dominate at the lower frequencies. The anti-clockwise dominance is confirmed by inspection of the filtered wind stick vectors that show (Fig. 4.1) events of SW winds backing to SE; SE to ENE and NNE swinging to NW. The rotary coefficient varies from about 0,2 to 0,6 which indicates a variation from a more linear behaviour to a more circular anti-clockwise character respectively. In the annual case (Fig. 4.8b) the anti-clockwise component reaches a maximum at a period of about 20 days. For the 3,8 y case (Fig. 4.9b) the maximum occurs at about 9 and 14 days. Because of the superior resolution of this case, based over a few years' data the indications of maxima at the two shorter periods are preferred over the 20 day maximum in the annual cases.

The region of higher spectral power between about 8 and 15 days with a steeper increase in energy between periods of 6 and 9 days for the alongshore autospectra indicates the predominance of synoptic weather systems at this frequency range. Walker (1984) reports the annual mean frequency of coastal low occurrence for the Southern Benguela area to be 1 in 10 days. There is no evidence in the rotary wind spectra for a prominent 6 day cycle referred to by Nelson and Hutchings (1983) and reported by Preston-Whyte and Tyson (1973) for barometric pressure spectra. Kamstra (1987) presents annual pressure spectra for the 15 years 1970 to 1984 and notes on only 3 occassions a distinct peak at the 6 day period for Cape Town data; the 1976 and 1977 6 day peaks were very small. Since wind is a secondary phenomena with respect to the primary processes occurring in the pressure fluctuations any spectral peak in the pressure field is expected to be reduced or "whitened" in the spectrum of the corresponding wind data. Similarly as reported by Winant (1980) the spectra of coastal currents do not display as marked peaks as in the corresponding sea surface elevation (pressure) spectra that respond only to barotropic motions. The lack of a prominent 6 day peak in the wind spectra reported here is therefore not unexpected and is an indication of interannual variability. A spectral plateau between 5 and 20 days is reported by Kamstra (1987) which roughly corresponds with spectra reported here.

The autospectra for the temperatures (Fig. 4.8c, 4.9c) exhibit a f^{-2} power law trend for periods less than 15 to 10 days. This trend is discussed in Chapter 2.4.1. At longer periods a slightly gentler slope is observed which could be due to the maxima in that region. The 1976 spectral power tends to be still increasing beyond 20 days but the 1977 data have a maximum at about 20 days. The 3,8 year data spectrum (Fig. 4.9c) has a maximum at about 14 days with a generally enhanced power between periods of 8 and 15 days.

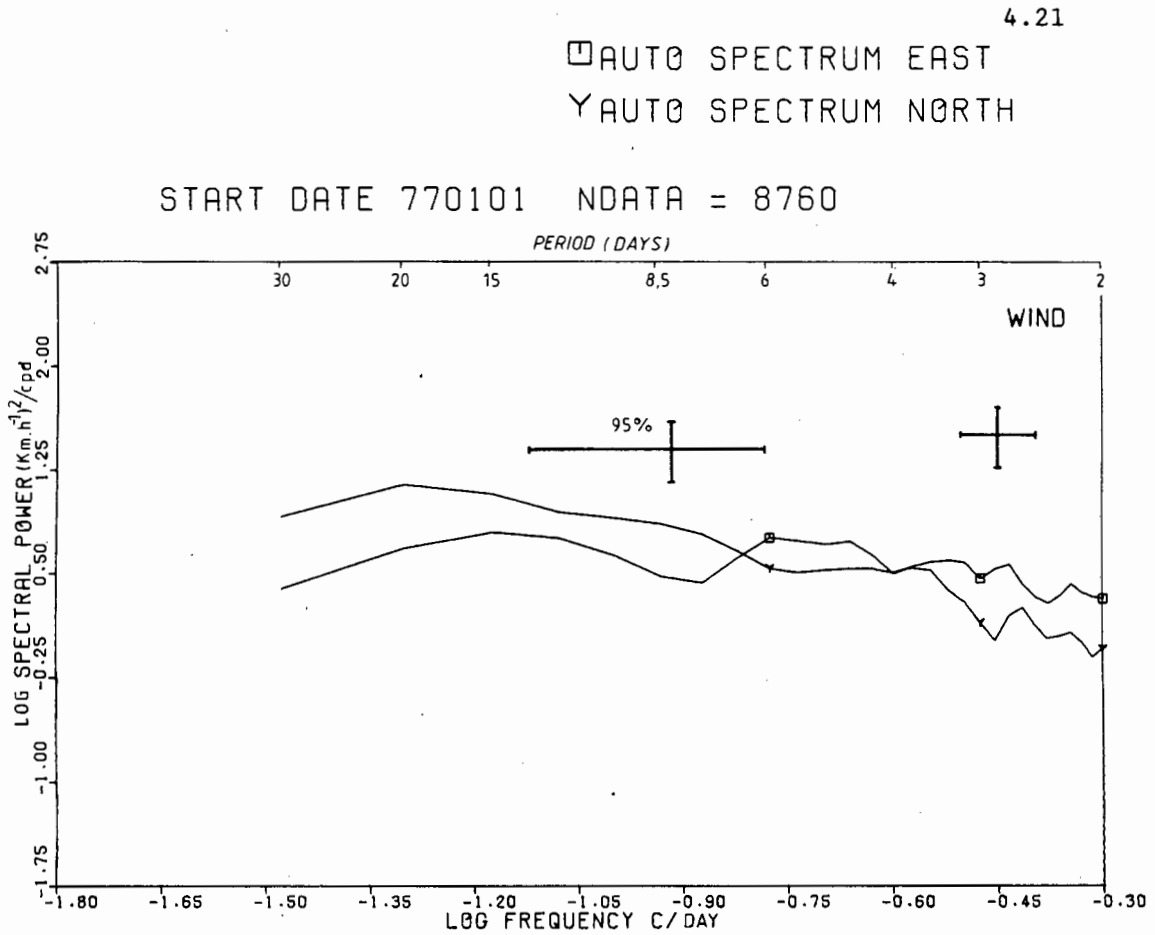

FIG. 4.8a LOG/LOG PLOT OF AUTO SPECTRA FOR INTERMEDIATE LOW FREQUENCY FILTERED OU SKIP WINDS FOR 1977. ALONGSHORE (NORTH) AND ACROSS-SHORE (EAST). MAXIMUM LAG NUMBER IN ANALYSIS IS 60 BUT ONLY PORTION CORRESPONDING TO LOWER FREQUENCIES SHOWN. PLOTTED SYMBOLS INDICATE EACH 10TH LAG NUMBER

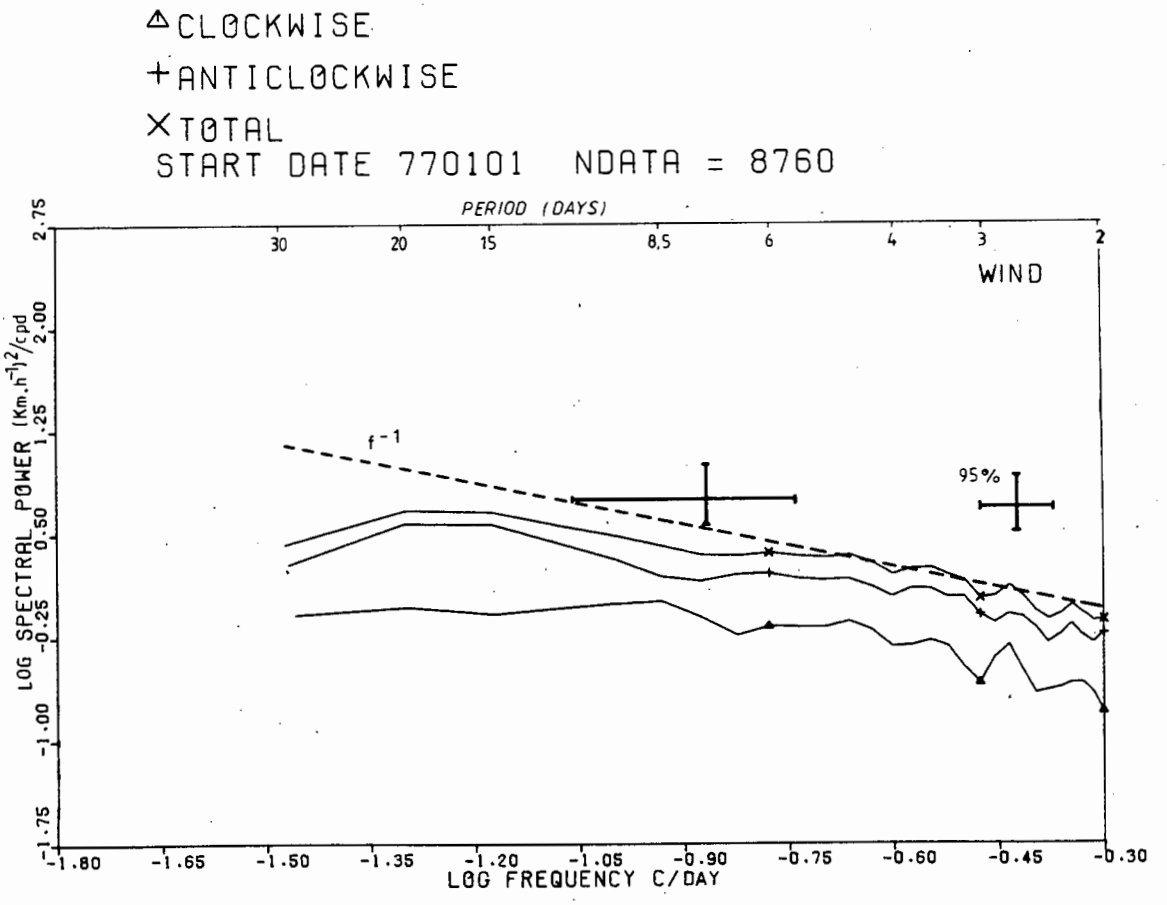

FIG. 4.8b ILF 1977 ROTARY WIND SPECTRA, OTHER DETAILS AS FIG. 4.8a

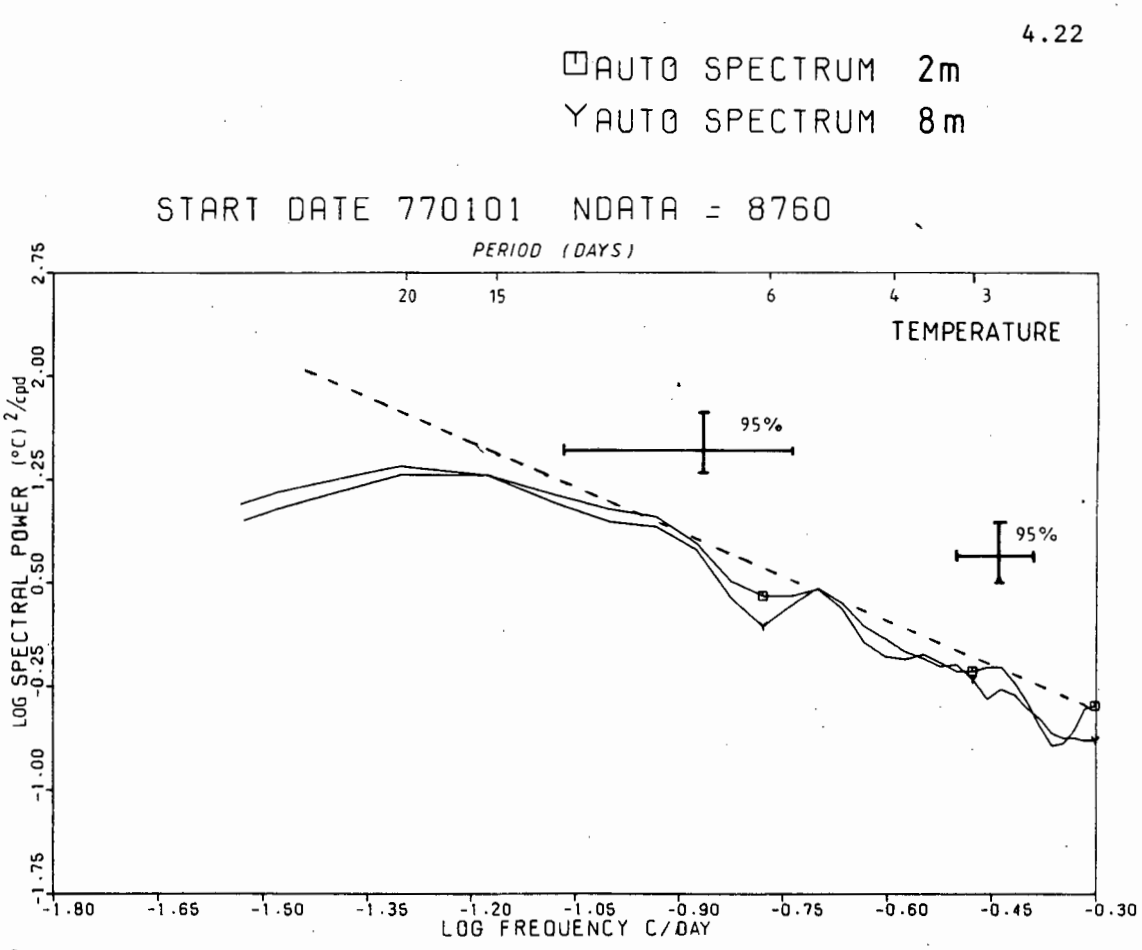

FIG. 4.8c ILF 1977 AUTO SPECTRA FOR 2 M and 8 M DEPTH TEMPERATURES, OTHER DETAILS AS FIG. 4.8a

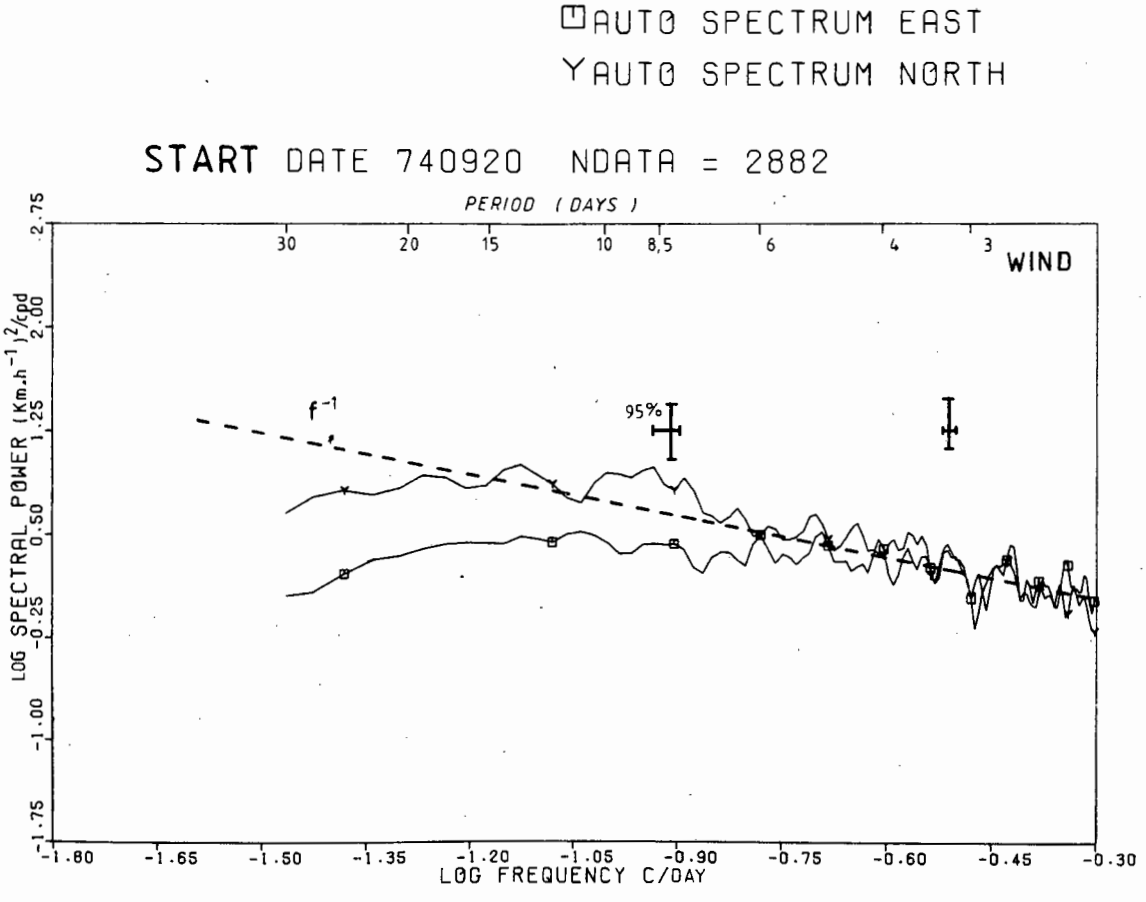

FIG. 4.9a ILF 3,8 YEAR WIND AUTO SPECTRA. MAXIMUM LAG NUMBER IN ANALYSIS IS 240 BUT ONLY FIRST FIRST 120 PLOTTED

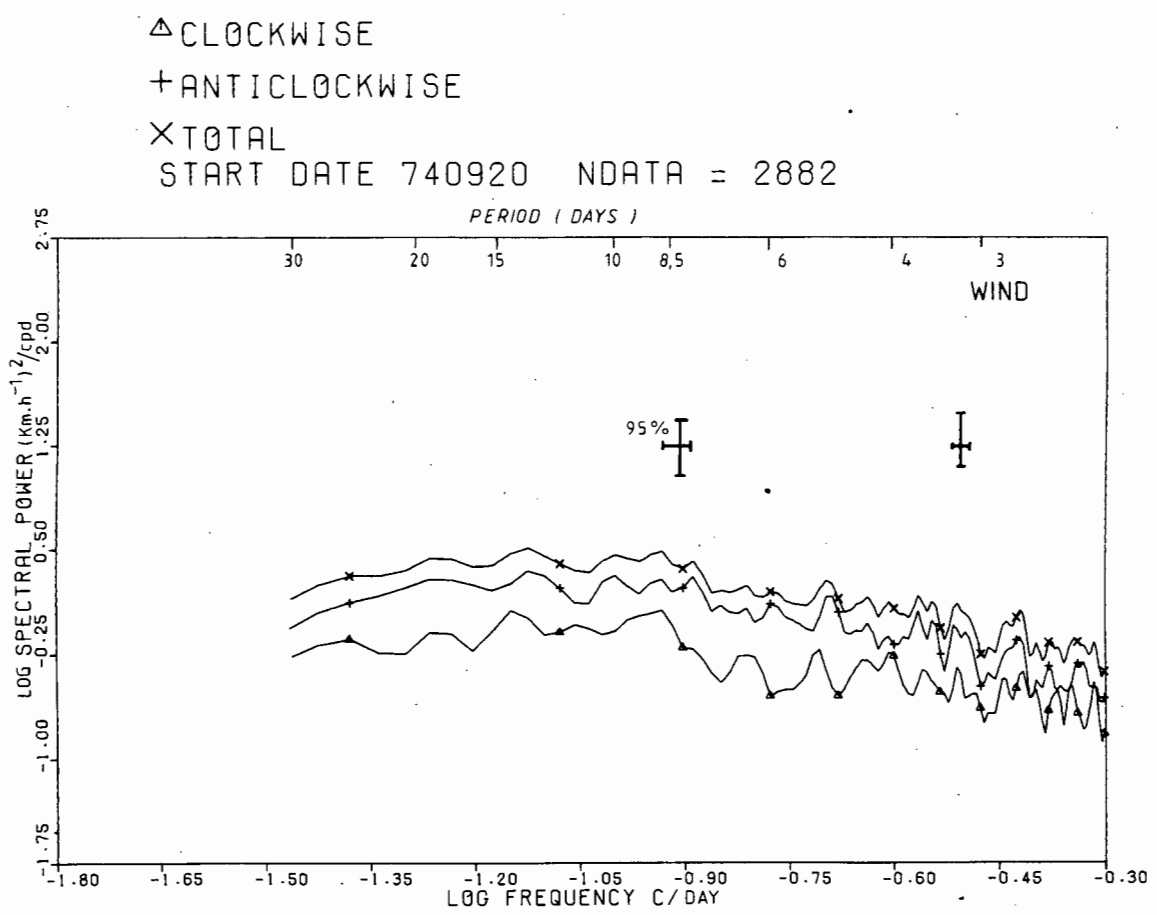

FIG. 4.9b ILF 3,8 YEAR ROTARY WIND SPECTRA

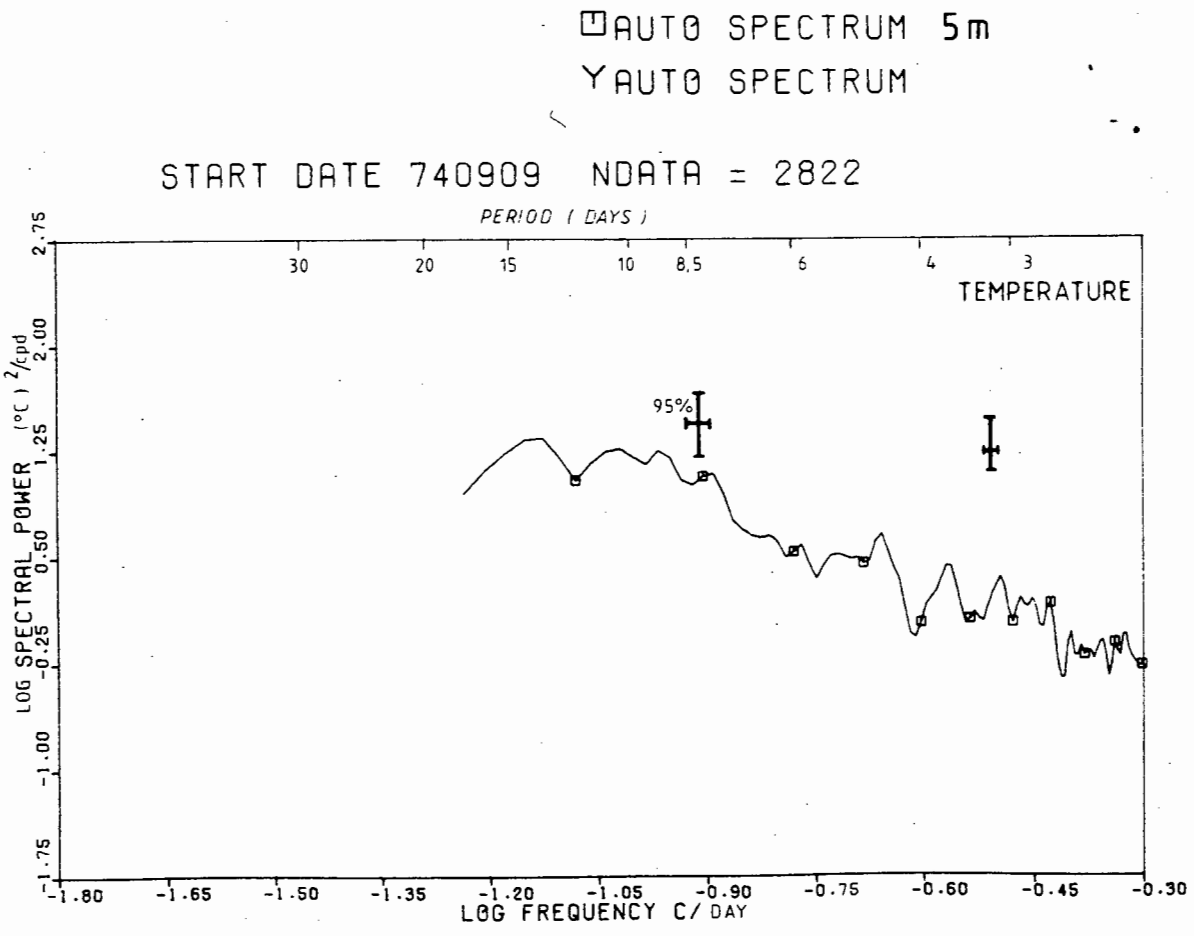

FIG. 4.9c ILF 3,8 YEAR AUTO SPECTRUM FOR 5 M DEPTH TEMPERATURE

The spectra for the 2 m and 8 m depths are very similar. At the lower frequencies a closer match in spectral energy is achieved between the depths; at higher frequencies more structure is noticed, with the 2 m depth spectra in 1977 showing a marginal tendency (within the confidence limits) of exceeding the 8 m spectral energy. Referal to that portion of the HF spectra (Fig. 5.6c, 5.7) with frequencies less than 1/24 cph reveals the 2 m data generally have more energy between 2 and 3 days period than the 8 m spectra. The slight enhancement of the 2 meter spectra at these frequencies could be ascribed to a stronger top-down effect at the relaxation stage of the upwelling cycle. For the longer period used in forming the simple statistics (4.2.2) the 2 m depth data has a marginally smaller standard deviation than the 8 m data, probably due to surface mixing.

A visual comparison between the temperature spectra and the wind spectra, particularly the alongshore autospectra shows some correlation. For the 3,8 year data spectra the minima at 3 days in the wind spectra (Fig. 4.9a) has a corresponding level trend in the temperature spectra (Fig. 4.9c); the steeper increase in spectral energy for periods from 6 to 9 days is shown in both the temperature and alongshore wind spectra; the maxima at 9 and 14 days also correspond. This supports the contention that at the frequencies of the ILF band the sea temperature responds to the alongshore wind stress that is driven by the synoptic scale processes.

4.2.6 Regime Transitions

In discussion of the seasonal time scale two major regimes were identified. Seasonal atmospheric changes indicated a more definite change between autumn and winter than the spring transition. The oceanographic regime however had indications for a more rapid change in spring. At the event time scale, this and other aspects of regime transitions are now considered.

The differences in the regimes are obvious in the wind related cumulative Ekman transport (CET) data (Fig. 4.6) and in the ILF temperature data (Fig. 4.5). The winter regime has a preponderance of northerly events and corresponding much smaller temperature fluctuations. The transition in the winds both in autumn and in spring is not as clear cut as that shown by the oceanographic temperature regimes where the ILF temperature data show large fluctuations ceasing in autumn and resuming at the end of the winter regime (Fig. 4.5 and Fig. 4.4a&b). The clearest evidence for a more rapid temperature transition at the end of winter than in autumn is given in the LF data, particularly for the 1975 and 1977 data (Fig. 4.2a).

The sudden appearance in spring of cold water at the site is initiated by a suitable equatorward wind event. The character of such a suitable transition event is a function of both the immediate history of the wind and of the wind stress, duration and direction. In discussing CET values here and later, more emphasis should be placed on the relative values than the absolute values. The CET data show that the actual transition events (marked with a T in Fig. 4.6) for 1975, 1976 and 1977 have offshore CET values of 4,8, 3,2 and 9,3 x 10^9 g.cm^{-1} respectively. All have durations longer than 6 days with peak daily mean wind speeds exceeding 6 m.s^{-1}. For the Oregon spring transition Huyer, et al. (1979) proposes a minimum offshore Ekman transport event of 1 x 10^9 g.cm^{-1}. In addition, although the coastal jet forms within hours, the establishment of a stable baroclinic coastal jet is only complete off Oregon after 5 days. This implies a minimum event duration of about 5 days is necessary to resist reversion to winter conditions. South of the Oregon site between 38° to 39°N Lentz (1987) shows that a minimum wind event is not required to establish the spring transition since at that site, unlike off Oregon, there is a dramatic transformation in the wind pattern at that time. The overall transition is linked to the sudden increase in the extent and strength of the high pressure system over the NE Pacific (Strub and James, 1988). The large scale nature of the transition is stressed by Strub et al. (1987b) particularly in that wind forcing over a scale exceeding 1 000 km is more effective in setting up the upwelling regime than a smaller scale (400-800 km) event of similar magnitude. The local expression of the single large scale event is different at 38°N and at 45°N (Oregon) where at the latter site the winds are more variable and it is appropriate to suggest a minimum event for the transition. Comparison of wind data presented for different latitudes by Strub et al. (1987b) and that of this study indicates a reasonable match with the Oregon winds. For this study then, with its limited data base the hypothesis of a minimum wind event initiating transition will be pursued.

Inspection of the local CET data show that several offshore events exceeding the minimum of 1 x 10^9 g.cm^{-1} occur before the successful transition events. In the case of 1975 the preceeding offshore event of 3,1 x 10^9 g.cm^{-1} is interrupted by a calm in the alongshore component that corresponds to an exactly orthogonal onshore flow for the across shore component. This is followed by an onshore event with a CET value of 1,7 x 10^9 g.cm^{-1} which also helps to counteract any regime change.

In both July 1976 and August 1977 there occur a triad of off-on-offshore events that in combination are not successful. In both cases although the initial offshore events of 2,2 and

3,0 x 10^9 $g.cm^{-1}$ respectively lower the sea temperature the following large onshore events of 7,6 and 9,2 x $10^9 g.cm^{-1}$ respectively cause complete reversion to winter regime conditions and nullify any effects of the immediately following offshore events of 1,3 and 2,8 x 10^9 $g.cm^{-1}$ respectively. In September 1976 two more offshore events of magnitude 2,4 and 1,8 x 10^9 $g.cm^{-1}$ are followed by a small onshore event of 1,6 x 10^9 $g.cm^{-1}$ that results in a reasonable rise in temperature. It is only the next offshore event of 3,2 x 10^9 $g.cm^{-1}$ that is the transition event. The two earlier offshore events although above Huyers minimum have reasonable wind strengths for only 3 days and this short duration probably renders them ineffective. In all the main transition events for the years 1975 to 1977, the time taken from the initial temperature dip to the minimum temperature is about 5 days.

It seems locally a minimum offshore transport of 3 x 10^9 $g.cm^{-1}$ and duration of 5 days or more is required to set up the spring sea temperature transition, but that a relatively small onshore transport of 2 x 10^9 $g.cm^{-1}$ can reverse the trend. The magnitude of these values relative to those reported by Huyer, et al. (1979) will be discussed later (Section 4.5). However, an obvious comment now is that whereas Huyer observed a large scale (~30 km) dynamic current transition this study just uses local inshore temperature values to indirectly indicate regime changes. On the larger local scale composite 3 year time series of currents near Cape Columbine (Holden, 1987) do not show any obvious seasonality or transition. Any deductions from this should be tempered by the fact that the current transition even for the US west coast is not always very obvious; it varies with latitude and position across the shelf, (Strub 1987b).

Another attribute of the transition events is the lag between the onset of the wind event and the initial temperature response. In the case of the 1975 transition the lag is about 24 hours and for 1977 it is 25 h for the 8,5 m depth and 28 h for the 2 m depth temperature probe. The time to reach minimum temperature is about 5 days. A non-transition event but one of interest occurs in early May 1977 where in Fig. 4.2a a sharp drop in temperature is noted. In this case the 8,5 m temperature had a 20 hour lag and the 2 m temperature had a 36 hour lag. These lags are the same order of magnitude as those reported by Huyer, et al. (1979) for sigma-t changes off Oregon. When the southerly regime is well established the lag time for temperature response to changing winds is much quicker and falls within the diurnal time scale. The deeper temperature probe responds earlier because the cold water enters the study area initially along the bottom then is upwelled.

The transition from the summer to the winter regime is not in general well defined and is less rapid than the spring transition. In 1975 an onshore transport of 4 x 10^9 $g.cm^{-1}$ seems to establish the more stable temperatures. In early 1977 the onshore transport of 3 x 10^9 $g.cm^{-1}$ is insufficient to inhibit the following small offshore event (1,5 x 10^9 $g.cm^{-1}$) from causing a sharp temperature drop. Only the next significant onshore event of value 5 x 10^9 $g.cm^{-1}$ in April re-establishes the winter regime. The autumn transition off the US west coast has not been investigated in detail but indications are that it is quite gradual and spread over several months (Strub and James, 1988).

4.3 EVENT CYCLES AND THERMOCLINE DISPLACEMENT

In the previous section (4.2) the close correlation between wind events in general and the sea temperature response was demonstrated through time series analysis and various statistics. Southerly wind events were seen to initiate transition to the spring temperature regime, but the actual nature of the event and its barometric forcing was not detailed. This section takes a closer look at individual events and their result on sea temperature structure. Comparison is made between observation and the theory of Csanady (1977a) for coastal upwelling to enable predictions of thermocline displacement due to wind forcing to be made.

4.3.1 Character of Individual Events

The meteorology of the area has complicated seasonal, synoptic and diurnal interactions. The synoptic mode appears most dominant (Jury, 1980). The character of individual events is thus controlled by synoptic barometric forcing factors and how they evolve with time. This is illustrated in Section 4.3.1.1 with a set of summertime daily surface pressure maps for southern Africa. The corresponding response of the sea's thermal structure due to the wind cycle is shown in Section 4.3.1.2, which is followed by comments on the winter event cycle.

4.3.1.1 A summer wind cycle

In Chapter 3, three wind regimes are identified with respect to seasonality and in Section 1.4.2 four summer synoptic conditions, (a-d) are classified according to a scheme by Jury (1987) each with a predominant wind direction.

The occurrence of wind events can be seen by inspection of the daily vector stick plots in Figs. 4.1a&b. During the spring and

summer periods the vectors can clearly be seen to change from NW to southerly, some times quite abruptly. Remember that in these vector stick plots the winds are rotated 20° to align with the coastal orientation. The duration and magnitude of alongshore events are well illustrated in the cumulative Ekman transport plots (Fig. 4.6).

The choice of a set of daily surface pressure maps of southern Africa to illustrate a 'typical' wind cycle is problematic since the real world is rather more complicated than Jury's (1987) a) to d) classifications given in Section 1.4.2. However the following choice is based partly on the fact that the period covered also includes field data for both sea surface temperature maps and for evolution of thermocline structure.

The period chosen is from 14 February 1978 to 21 February 1978 and is annotated on the daily wind vector plots (Fig. 4.1b). The daily pressure maps for 14h00 SAST from the Weather Bureau are shown in Figs. 4.10a-h. In this presentation the cycle starts on 14 February with the synoptic condition of a cyclonic low passing over the Cape corresponding to wind regime d) of Jury (1987). The corresponding winds at Ou Skip for the entire period using hourly wind data are depicted in a progressive vector diagramme (PVD) showing the distance blown in Fig. 4.11. The low-passed filtered wind components for this period are shown in Figs. 4.12a and b. On the 14th February moderate winds are shown to be from the NW and N sectors. On the 15th the condition of post cold front SW'erlies is shown in the synoptic pressure map, 4.10b. SW winds also occur in the PVD until 18h00 when the wind suddenly swings to SSE and strengthens signifying the rapid ridging in of the South Atlantic anticyclone which shows up in the pressure map 4.10c for 16 February. The synoptic pressure map 4.10d on the 17th shows the "budding" of the high to the south of the country (Hunter, 1987) but the strong southerly winds remains.

The offshore flow from the interior starts to generate a coastal low north of Luderitz. The bud off high is associated with the formation of such coastal lows on the west coast (Hunter, 1987). On both the 16th and 17th the PVD show a similar pattern of SSE winds at night and early morning and SSW during the middle of the day. This diurnal behaviour is due to land/sea breeze effects. When the average angle of the coastline at the site of about 20° to west of north is considered, the sea breeze during the day is seen to be more strongly onshore than the land breeze is offshore at night.

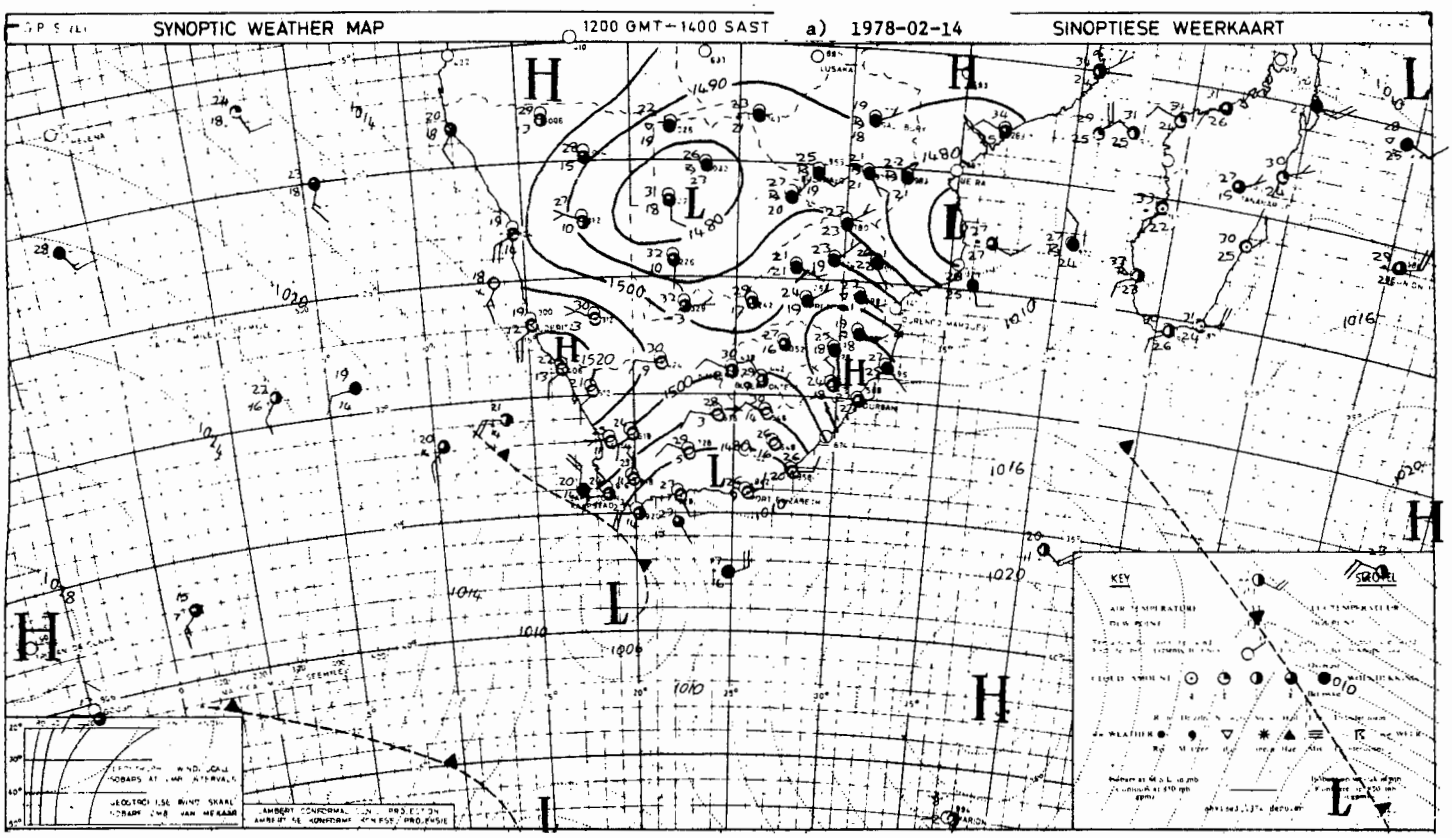

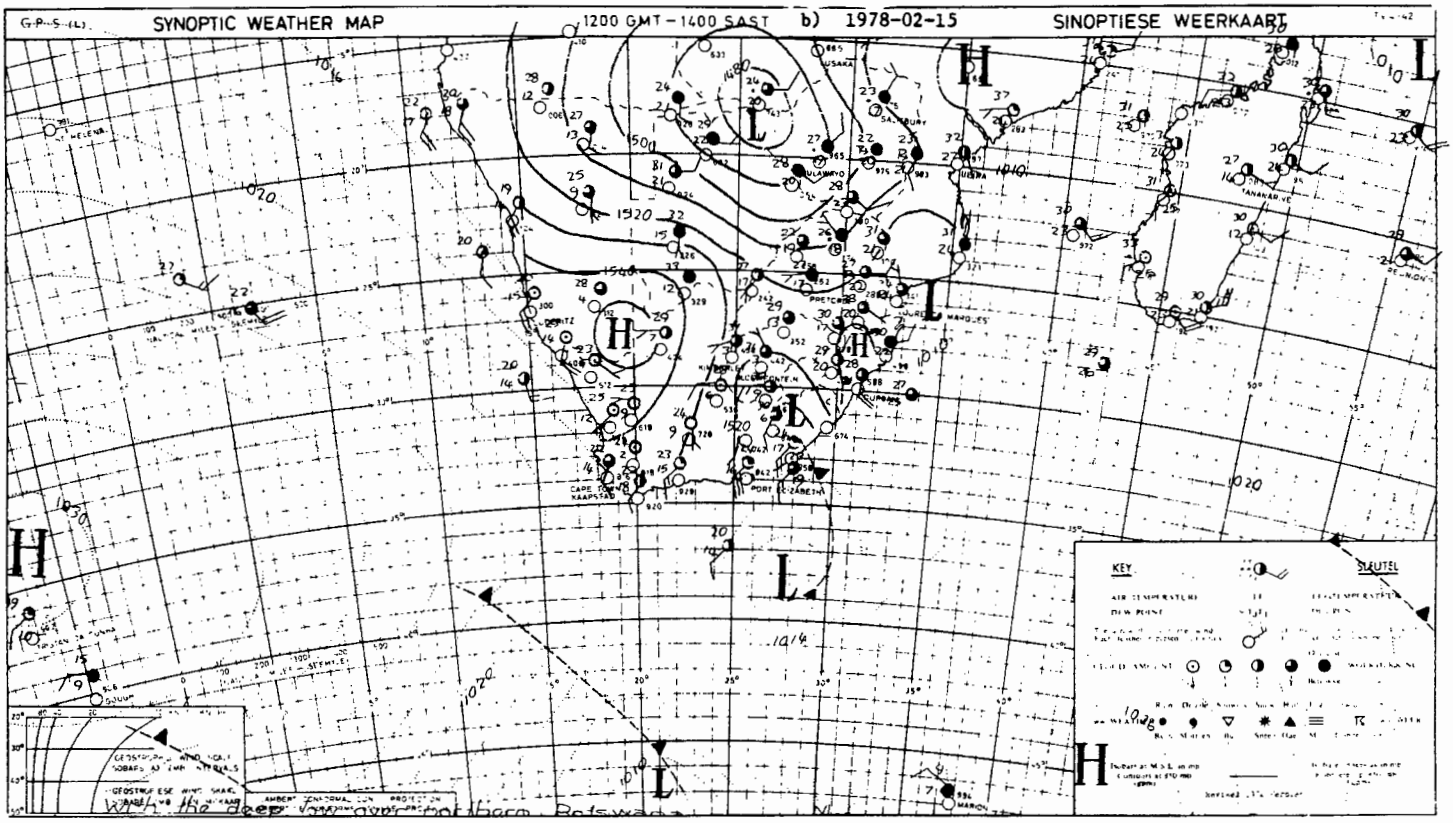

FIG. 4.10 DAILY SYNOPTIC WEATHER MAPS FOR 14h00 SAST.

a) 1978-02-14
b) 1978-02-15

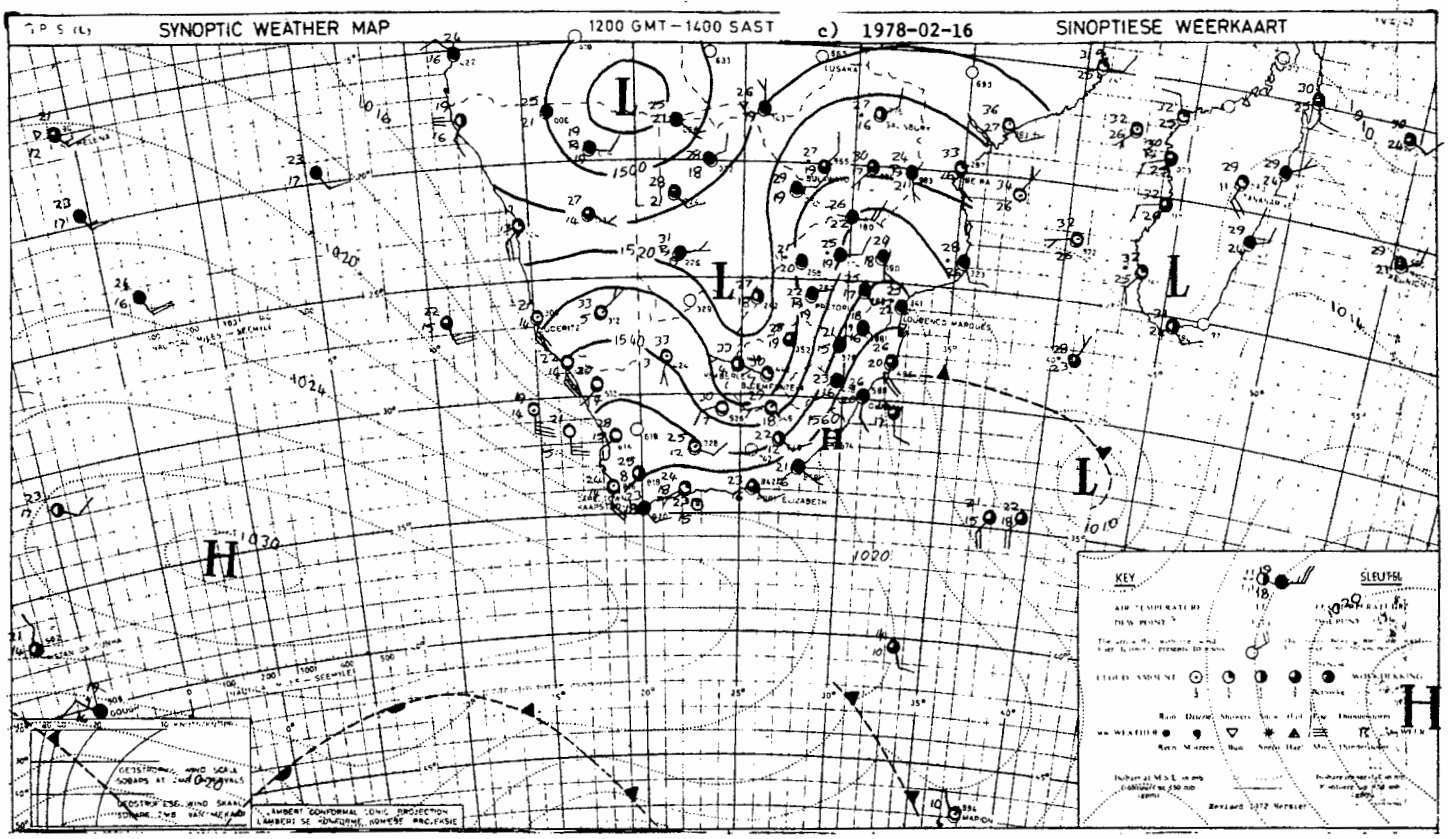

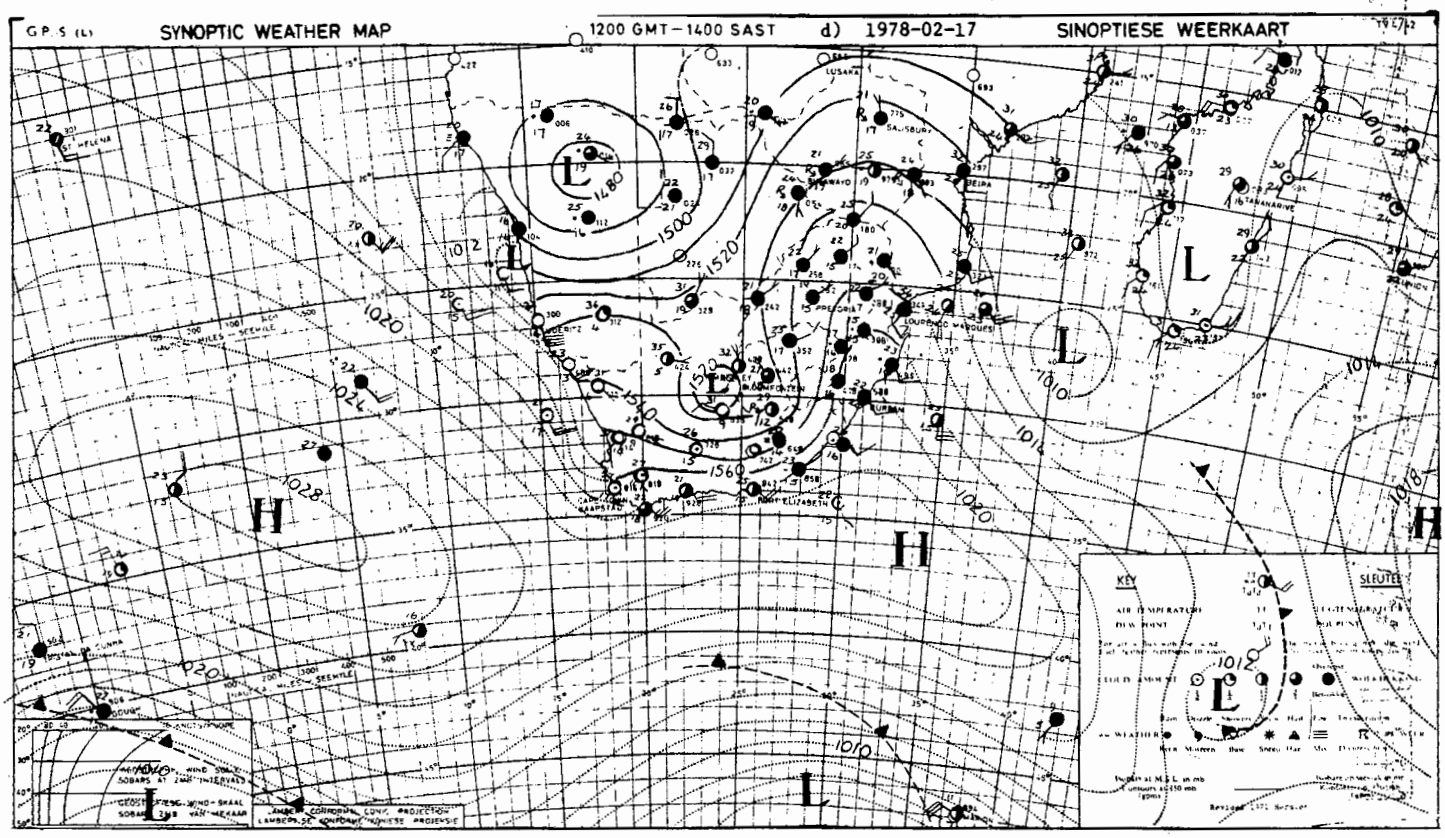

FIG. 4.10 DAILY SYNOPTIC WEATHER MAPS FOR 14h00 SAST.

c) 1978-02-16
d) 1978-02-17

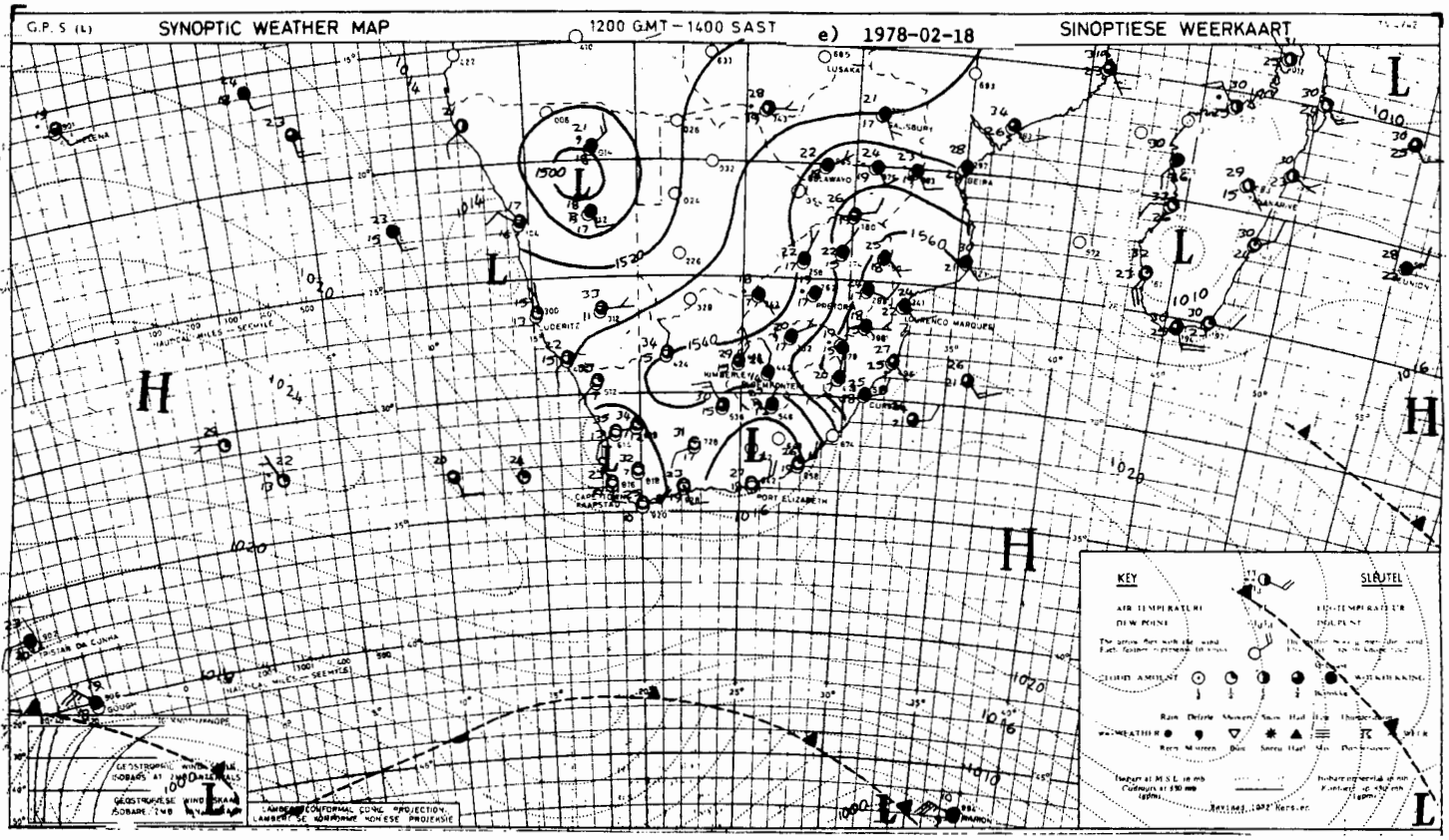

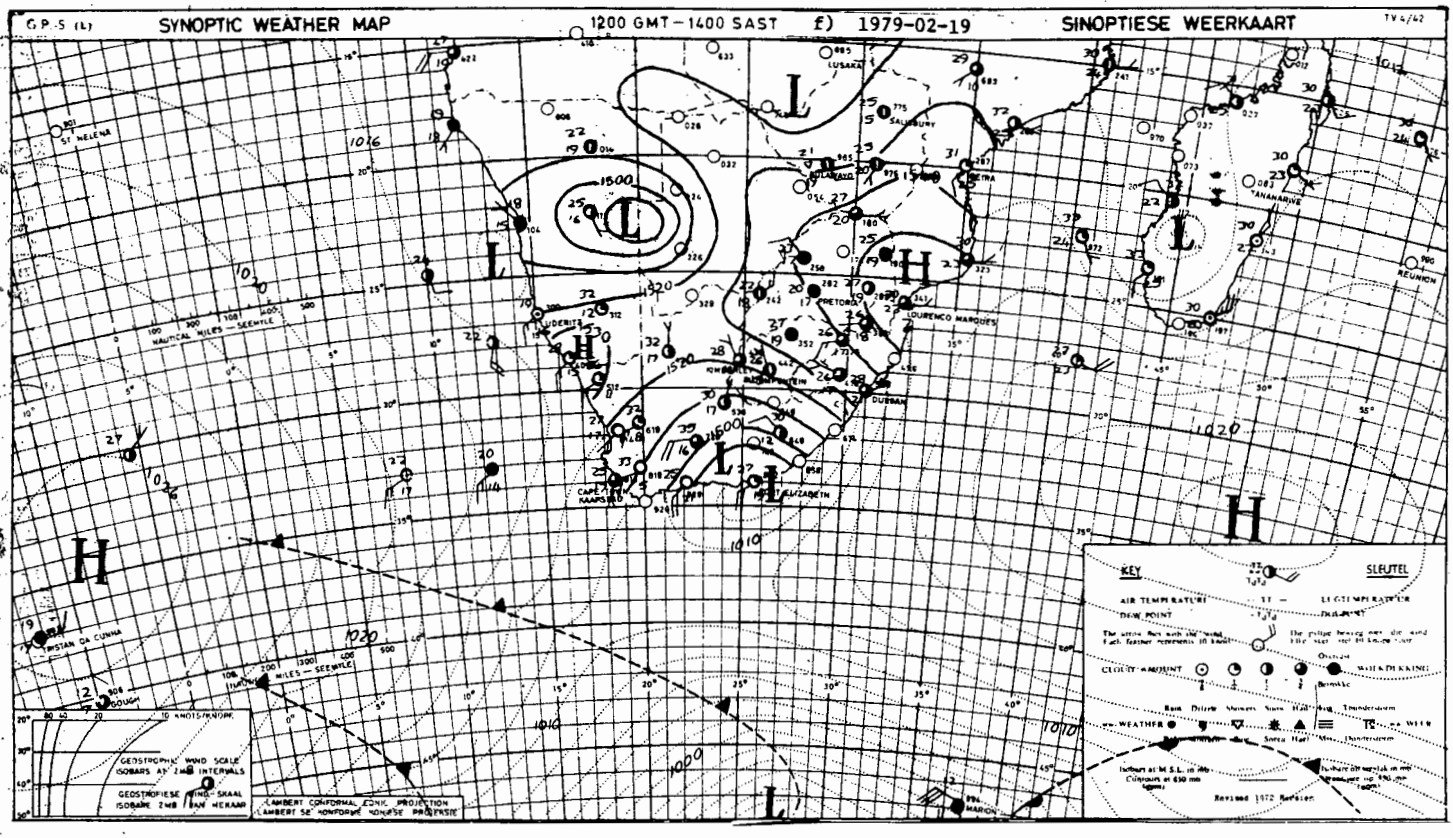

FIG. 4.10 DAILY SYNOPTIC WEATHER MAPS FOR 14h00 SAST.

e) 1978-02-18
f) 1979-02-19

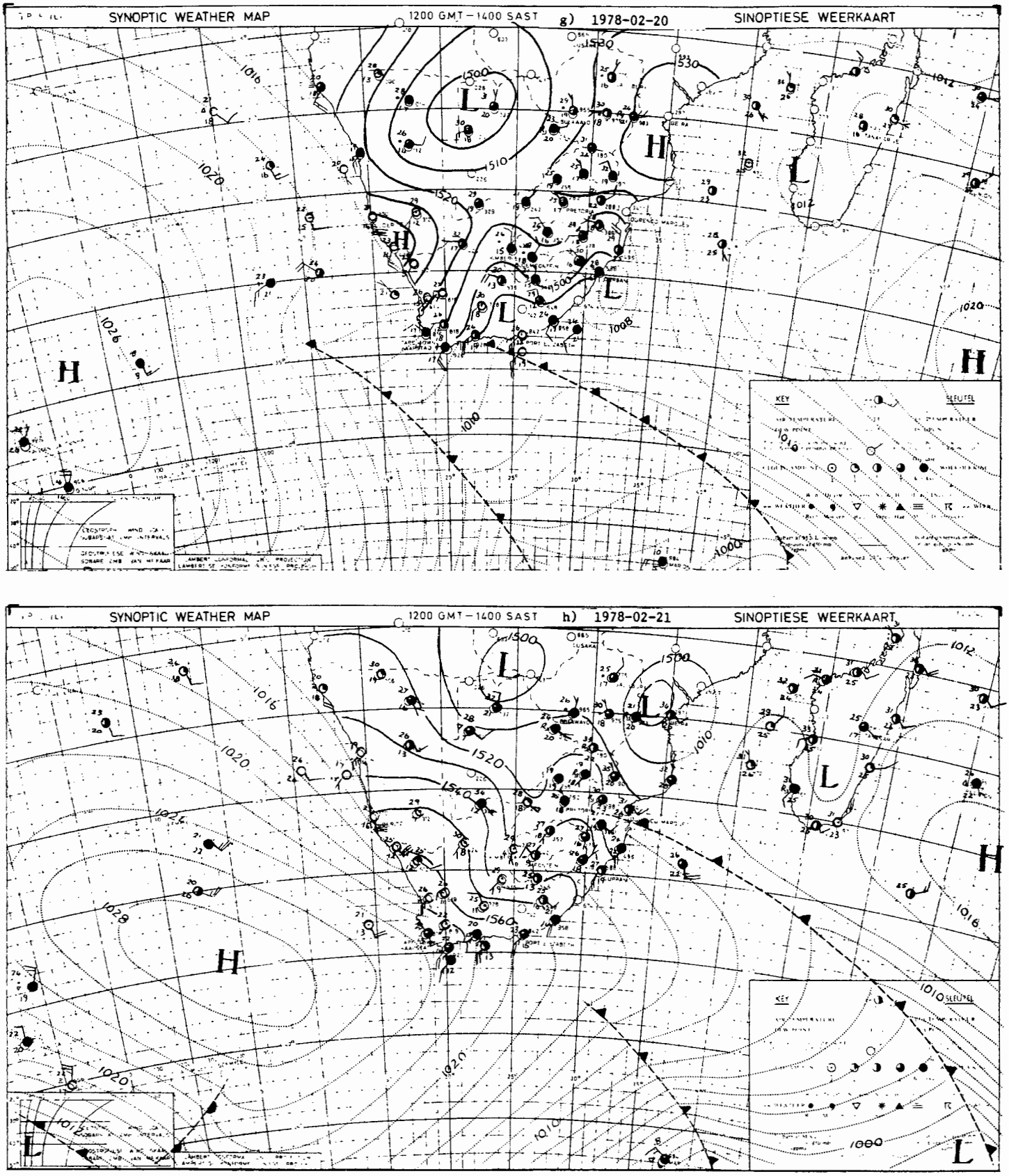

FIG. 4.10 DAILY SYNOPTIC WEATHER MAPS FOR 14h00 SAST.

g) 1978-02-20
h) 1978-02-21

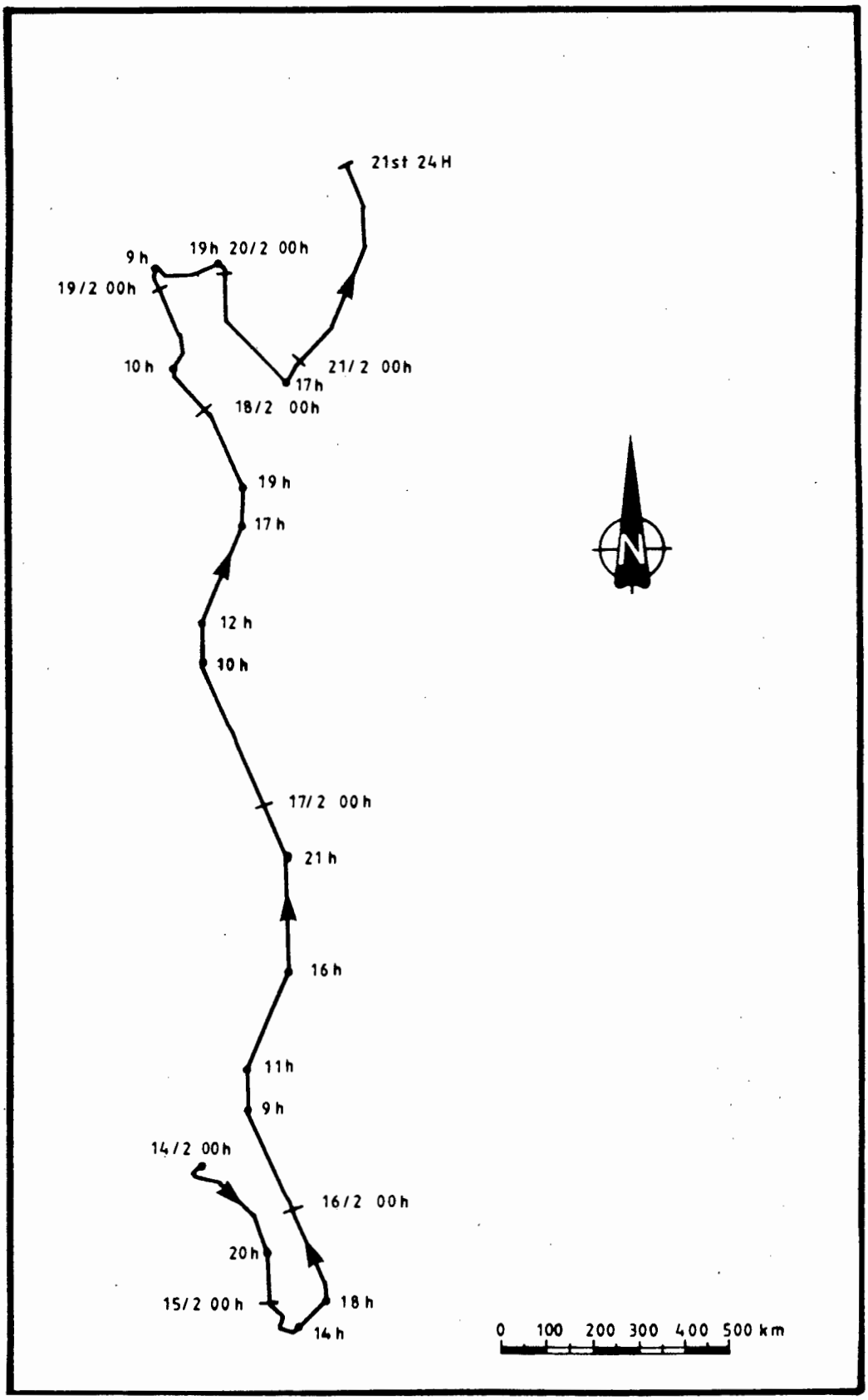

FIG. 4.11 PROGRESSIVE VECTOR DIAGRAMME FOR THE OU SKIP WINDS OF 14 TO 21 FEBRUARY 1978, SHOWING THE DISTANCE BLOWN

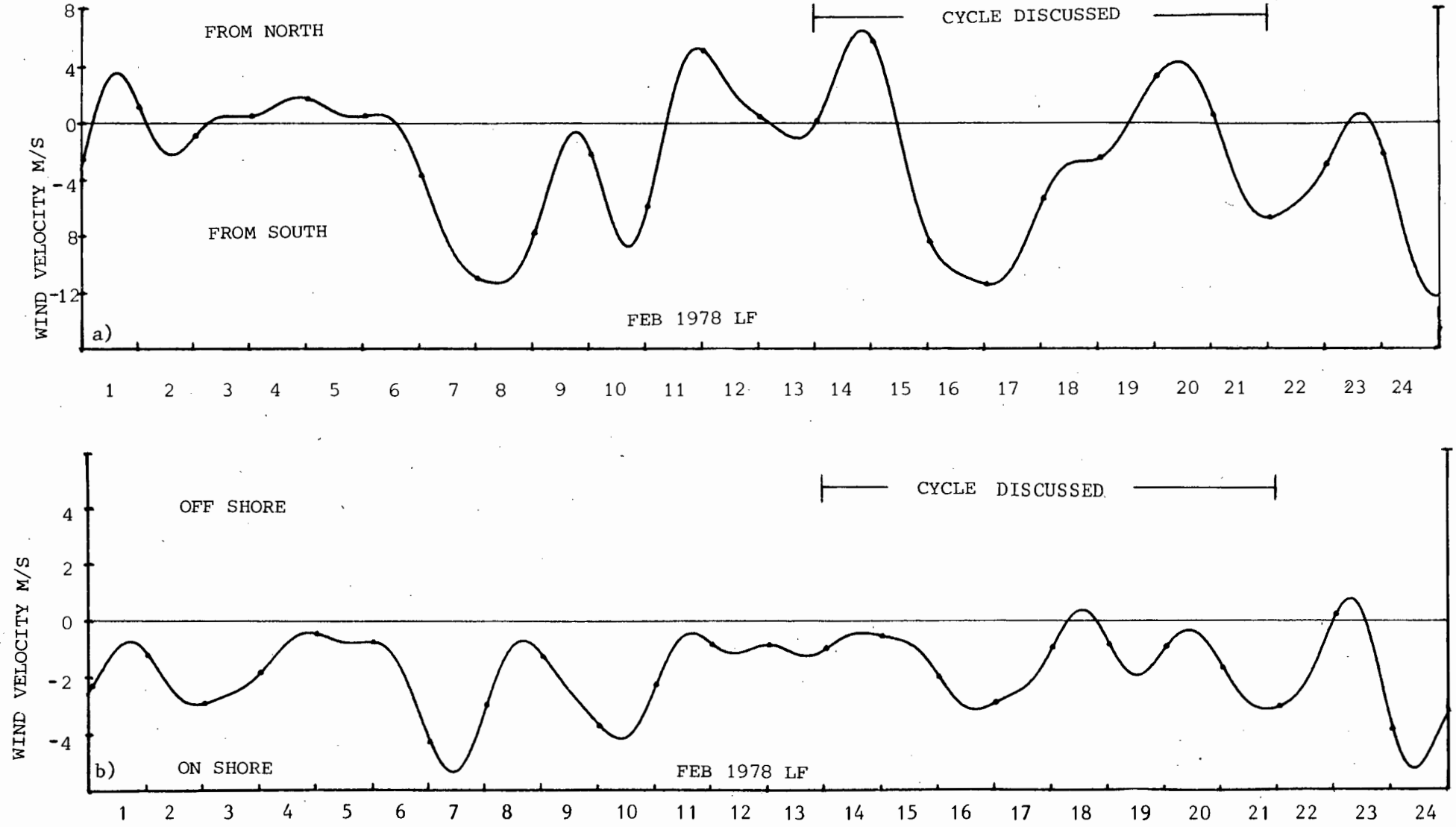

FIG. 4.12 TIME SERIES OF LOW FREQUENCY FILTERED OU SKIP WINDS FOR PERIOD 1 TO 24 FEBRUARY 1978 COMPONENT AXIS ROTATED 20° WEST OF NORTH. a) ALONGSHORE WINDS b) ACROSS-SHORE WINDS. NOTE THE DIFFERENT VELOCITY SCALES

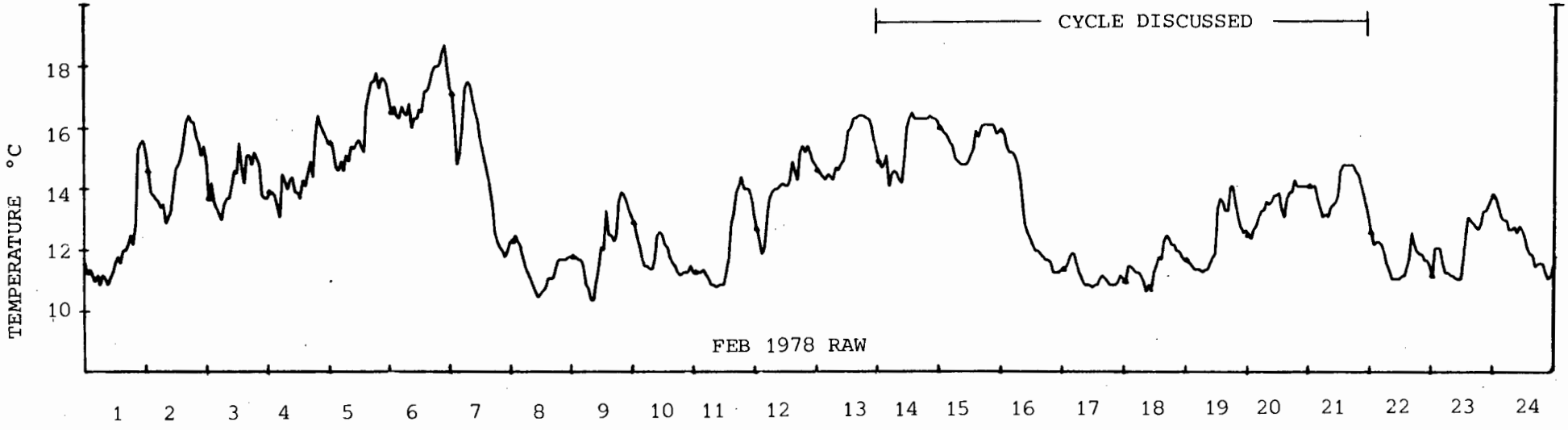

FIG. 4.13 TIME SERIES OF RAW HOURLY 2 M DEPTH TEMPERATURES FOR THE PERIOD 1 TO 24 FEBRUARY 1978

The next day the coastal low in the north has weakened and another has apparently formed near the Cape Peninsula. The PVD however shows for the 18th that winds are lighter and partially SE which could correspond with Jury's shallow ESE condition (c), but for exact categorisation needs cross checking with upper air data.

By the 19th the South Atlantic anticyclone moves further south and a weak cold front appears giving a light westerly flow seen in the PVD. The coastal low has "jumped" over the Peninsula or reformed on the south coast as a "leader cell", illustrating the difference in propagation on the west and south coast (Schumann, 1989). A second weak front arrives near the Cape on the 20th. The isobars do not indicate the NW winds seen in the PVD but the Cape Town and ships data on the synoptic map do confirm these winds. The cycle starts to repeat itself on the 21st as the anticyclone starts to ridge in south of the land and SW winds are again experienced. The overall pattern in the PVD (Fig. 4.11) well illustrates a wind event cycle. A similar pattern is reported for a site on the Cape Peninsula west coast in a paper by Nelson and Hutchings (Fig. 8a, 1983).

4.3.1.2 A Thermocline Structure Cycle

The response of the sea to the cyclic wind stress is an upwelling and downwelling episode, when first the surface waters are advected offshore and later back onshore again. The dynamic response of offshore displacement at the surface and onshore movement near the bottom of cooler water is revealed by a temperature change in the water column.

For the wind event 14 to 21 February 1978 described in the previous section the corresponding sea temperature cycle is illustrated in various figures. Thermocline structure evolution for part of the cycle is seen in Fig. 4.14a-d and sea surface temperature is shown in Fig. 4.20a-e and described in Section 4.4.2.1. Fig. 4.2b annotates the event as it occurs in the daily temperature stick plot for the 1978 2 m depth data. Numerous other temperature cycles are seen in this figure that correlate with the other wind cycles in Fig. 4.1b. The raw 2 m depth hourly temperature data for February 1978 is shown in Fig. 4.13 and is used in the following description. If the diurnal temperature pulsing is neglected at this stage (it is fully discussed in Chapter 5) the temperature cycle can be compared with the wind cycle. On the 14th February the sea temperatures are maintained high with the onshore flow. The initial SW'erly winds on the 15th cause onshore flow and temperatures are relatively stable but later as the anticyclone ridges south of the Cape and the southerly winds intensify the

temperature starts to drop. This drop is intensified on the 16th but flattens out at about 10.5 °C on the 17th, although the wind remains strong and southerly. This is because full upwelling has occurred and no colder water is in the near vicinity. The cool temperatures continue into the 18th but then start to rise as the wind weakens. The longshore wind impulse is expected to produce a baroclinic coastal jet with peak velocities offshore of the intersection of the thermocline with the surface, that should remain once the wind is switched off (Csanady, 1977a). Here on the 18th the wind remains in a favourable upwelling direction but has merely relaxed and yet the temperature rises, signalling some change in the dynamics. This indicates either that a baroclinic jet is formed, but is dissipated by bottom friction in less than an inertial period, or rather that it has probably formed further offshore and that at this shallow measuring position bottom friction is a dominant force that dampens the inshore effects of the jet.

In shallow water, wind generated currents can be in phase with the wind when the wind stress is balanced chiefly by bottom friction, Simons (1983) and Schwing, Oey and Blanton (1985) who report 10 m currents are almost in phase with the wind while currents at the 30 m contour lag by more than 12 hours. Consequently a relaxation in the wind stress can result in deaccelerating currents and lowering of the isolines. The temperature section for this date (Fig. 4.14d) at line 3 closest to the sea tower position, shows no firm evidence for a coastal jet within its 6 km extent but reveals a thin warm surface layer.

The weak coastal low observed on the 18th can actually play a more important role in the decay of the upwelling as proposed in recent papers by Jury (1986) and Jury and Brundrit (1987) for the larger scale in the Southern Benguela region. His scenario is that a decrease in longshore wind stress from south to north sets up a sea surface slope with higher sea levels to the north. The southward propagating coastal low accentuates the sea level differences as the winds moderate. The upwelling decays suddenly as reversed currents move southwards (Nelson, 1985) and cause onshore surface flow of warm water near the coast. The propagation of the coastal low southwards along the west coast and associated shelfwaves is discussed by Jury, MacArthur and Shillington (in press).

The light westerly winds on the 19th cause a sharper rise in temperature as the warm surface waters come inshore (Fig. 4.13). The moderate north and northwest winds on the 20th result in more stable elevated temperatures, while the initial SW flow on the following day increases the temperature again. By the end of the

21st the wind swings to the SSE as the high ridges in again south of the country and the temperature starts to drop steeply in consequence. Comparison of the temperatures in Fig. 4.13 and the alongshore wind (Fig. 4.12a) show a lag in the temperature response. The cross correlation between wind and temperature in Tables 4.2 and 4.3 for the low-pass filtered daily data shows a lag of about one day. This seems longer than the lag evidence in Fig. 4.13, but this figure is for unfiltered data. Further, however, in the diurnal time scale high frequency correlation in Chapter 5 shorter lags are tabulated in Table 5.1.

Bathythermograph data collected on various transect lines extending 6 km offshore between Melkbos Point and Ou Skip (see Research Methodology, Section 1.5, Fig. 1.7) are presented as temperature sections in Fig. 4.14a-d for 16 to 18 February 1978. The displacement of the thermocline illustrates the wind event of this period. Before midday of the 16th the offshore thermocline is still quite horizontal but inshore from about 2 km the topmost layer is sloping upwards and for line two the 13° and 14° isotherms intersect the surface. After midday the isolines are further lifted and driven offshore (Fig. 4.14b) and 10° water moves closer inshore along the bottom. This trend is continued on the 17th as the southerly winds remain strong and 10° water now appears as a bottom layer closer than 1 km from the coast for most transects. As the wind relaxes on the 18th warm waters return as a thin surface layer. The 10° bottom water is not yet downwelled and in fact 9° water is present in the section for line no 3. Unfortunately no further temperature section data are available for the remainder of the period. The sequence does reveal the bottom-up process during the upwelling phase on the 16th and 17th and the data on the 18th indicates the top-down process for the start of the downwelling phase. This is shown up in the different response times for the 2 m and 8 m depth sea tower temperature data for the high frequency data (Chapter 5).

These temperature section data also show the asymmetry of up and downwelling which is discussed by De Szoeke, et al. (1981) and Send, Beardsley and Winant (1987). During upwelling there is a tendency for homogenization of the water column, with the opposite occurring during downwelling. In the upwelling situation there is a well defined surface mixed layer (with considerable horizontal structure) but in the downwelling case especially near the coast as we see in Fig. 4.14d there is a thin and indistinct mixed layer. Even on the large scale on a transect extending from 20 to 100 km offshore, Hutchings et al. (1984) record a thin 5 m deep surface layer of warm water after vigorous upwelling followed by the onset of westerlies. On the Californian shelf the downwelling warming

has an important contribution from alongshore advection while onshore advection is of little importance (Send, Beardsley and Winant, 1987). De Szoeke, et al. (1981) consider that the asymmetries are a reflection of the adiabatic, irreversible and non-linear character of the dynamical process occurring in the real world. The effect of this wind event is further illustrated with sea surface temperature maps in Section 4.4.2.1.

4.3.1.3 Winter Events

The synoptic weather systems during winter are chiefly affected by the South Atlantic anticyclone being situated a few degrees further north and west than in summer (Taljaard, et al. 1972). The eastward moving depressions are also further north and often pass over the southwestern Cape interior producing strong northerly winds. Strong southerly winds are uncommon and the overall frequency of coastal low formation is lower than in summer (Walker, 1984), however the 'winter' south coast low is more frequent as it acts as a leader cell to the cold fronts (Brundrit, Diab and Jury, 1984). Hunter (1987) does not observe any seasonality for the coastal low in his year-long south coast data set. Offshore winds commonly preceed the passage of a coastal low in winter and the winds often back from southerly through easterly to northerly. This is seen in the daily wind vector sticks for the winter periods in Figs. 4.1a&b. The direction of northerly 'events' are more variable than the southerly 'events' in summer.

The response of the sea temperatures to winter events is observed to be markedly reduced to that in spring and summer. This is due to the large scale atmospheric changes and the resultant large scale thermal structure of the sea at that time. The cold, dense water is deeper and further offshore in winter (Hutchings et al., 1984) and usually stronger more persistent southerly winds are required before the effects of upwelling are noticed as temperature changes close to the coast in the study area. A few small upwelling events in winter are described in Section 4.2.1. Included in a dramatic set of colour plates of Nimbus-7 satellite imagery of the Southern Benguela region (Shannon, Walters, Mostert, 1985) are a few depicting winter sea surface temperature conditions. Although upwelling is observed at times it is generally not so intense as in summer and large patches of more uniform temperatures are seen.

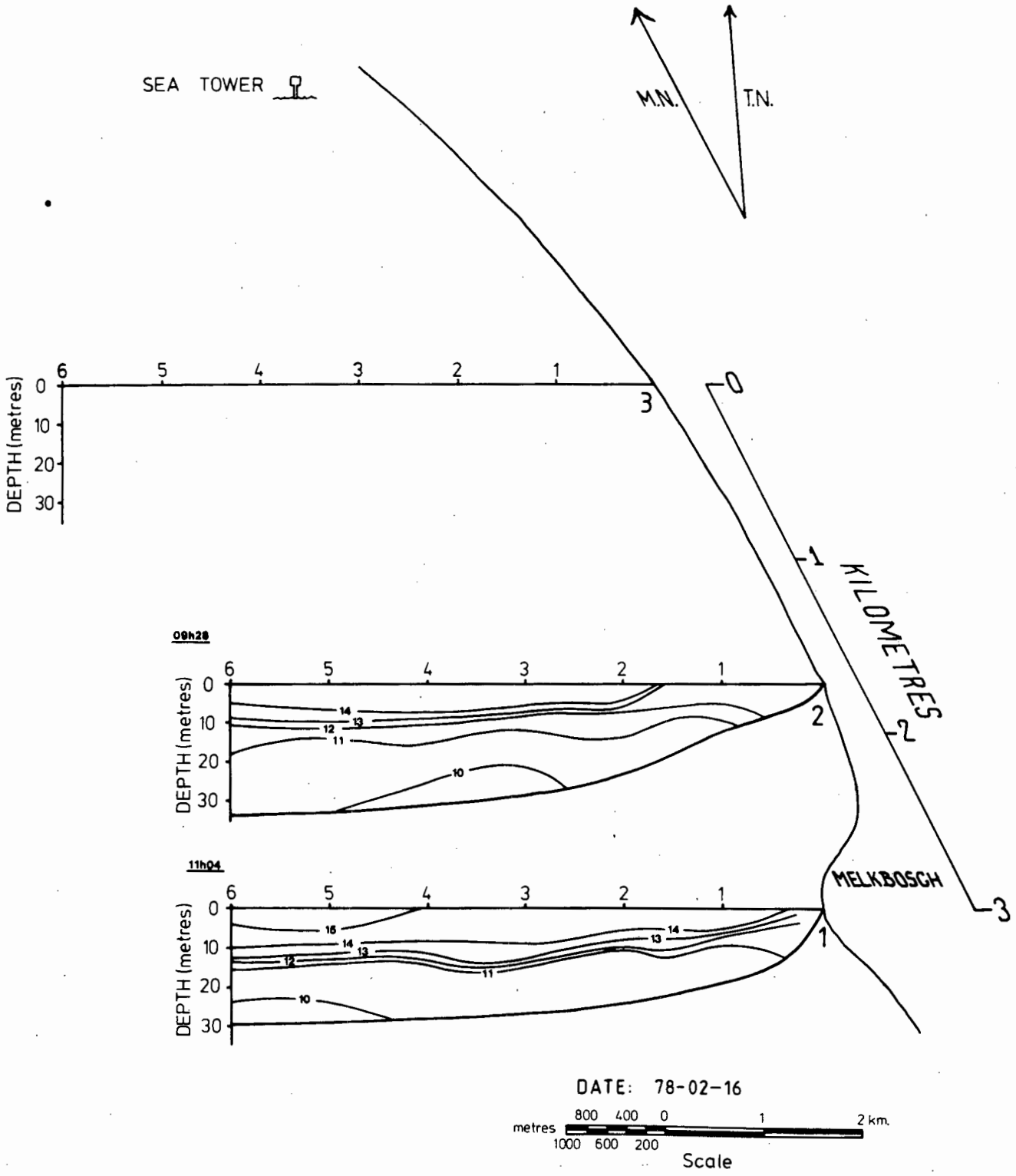

FIG. 4.14 TEMPERATURE TRANSECTS OFF MELKBOSSTRAND FOR THE PERIOD 16 TO 18 FEBRUARY 1978

a) 1978-02-16 MORNING

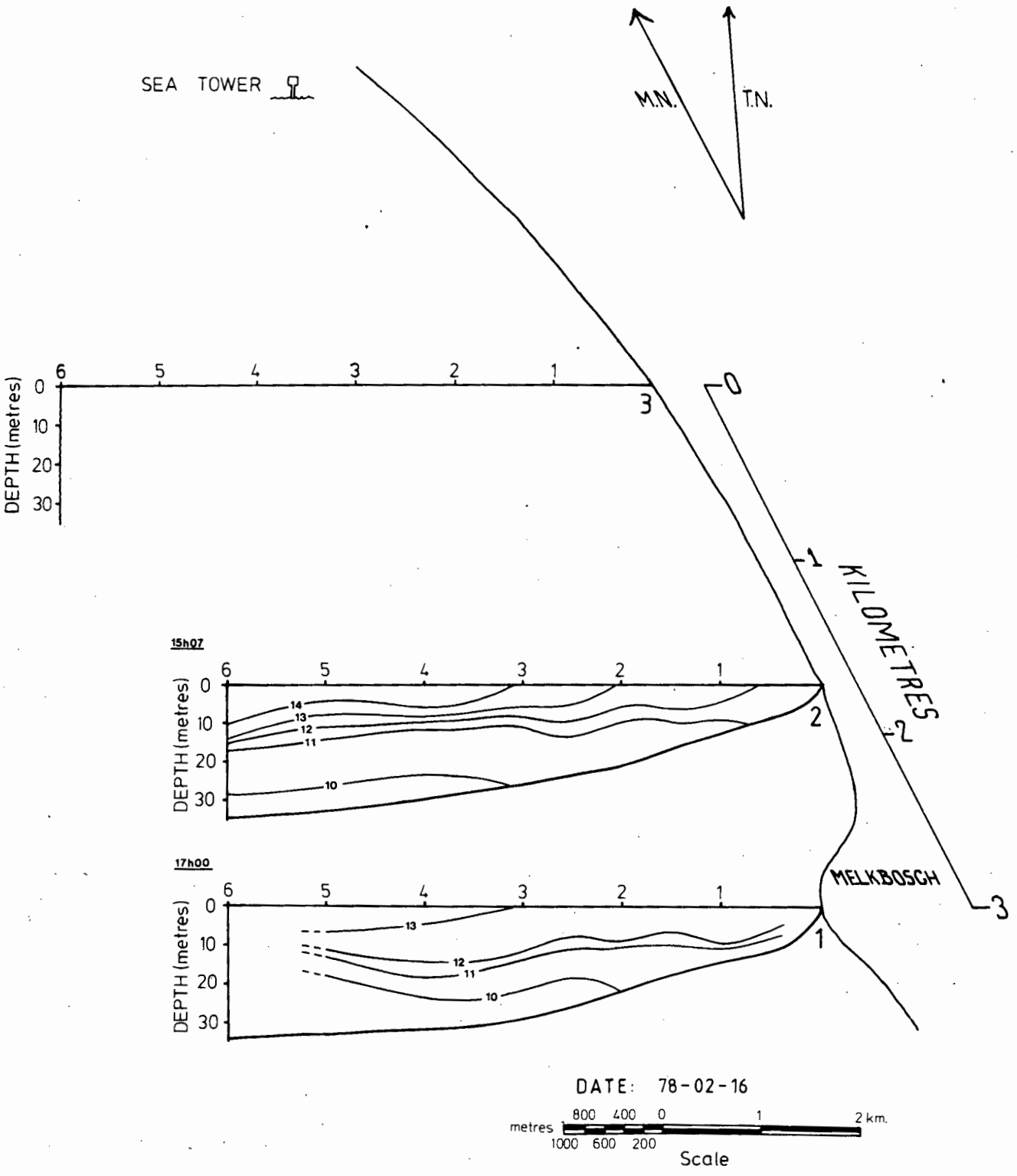

FIG. 4.14 TEMPERATURE TRANSECTS OFF MELKBOSSTRAND FOR THE PERIOD 16 TO 18 FEBRUARY 1978

b) 1978-02-16 AFTERNOON

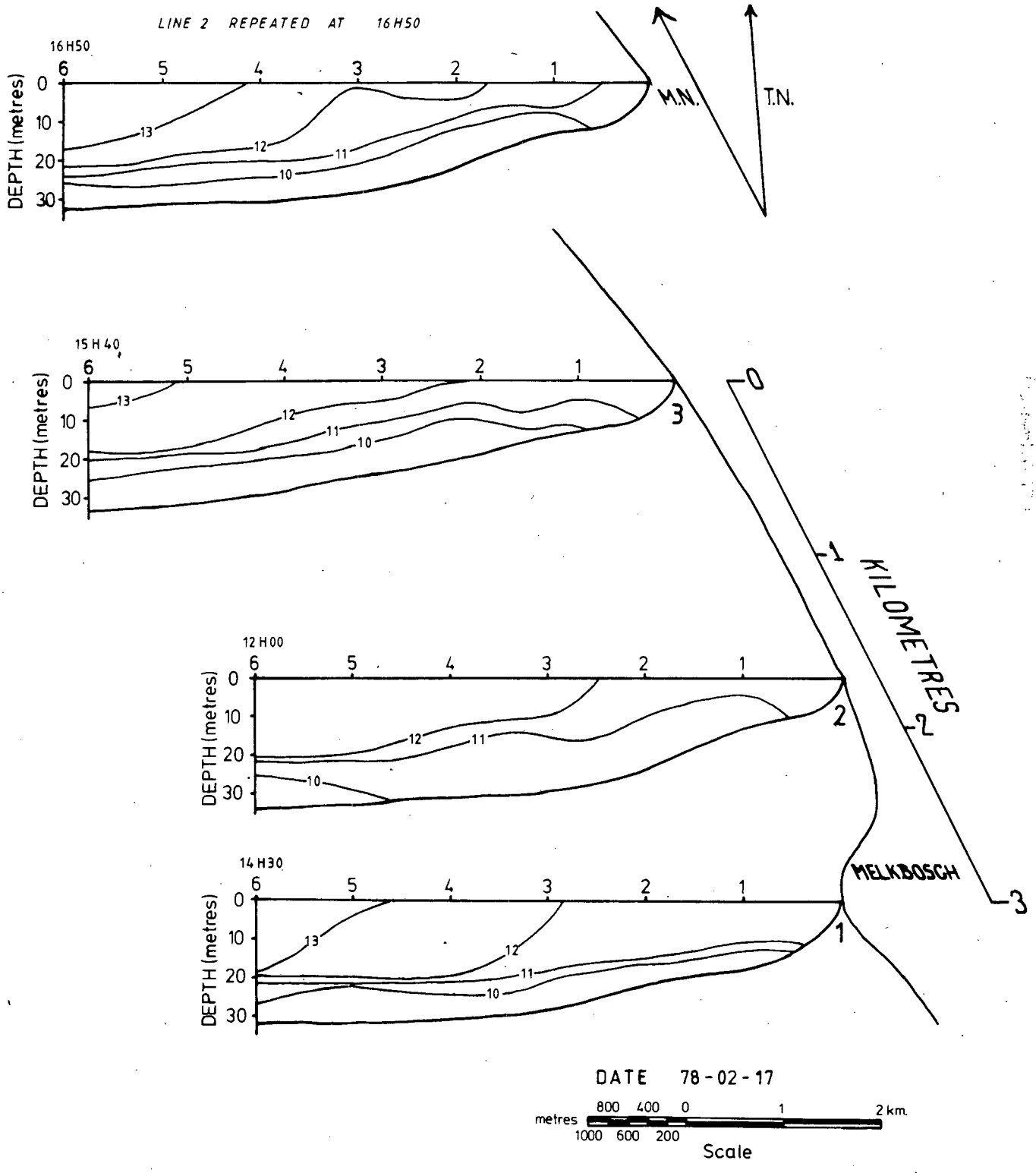

FIG. 4.14 TEMPERATURE TRANSECTS OFF MELKBOSSTRAND FOR THE PERIOD 16 TO 18 FEBRUARY 1978

c) 1978-02-17 AFTERNOON

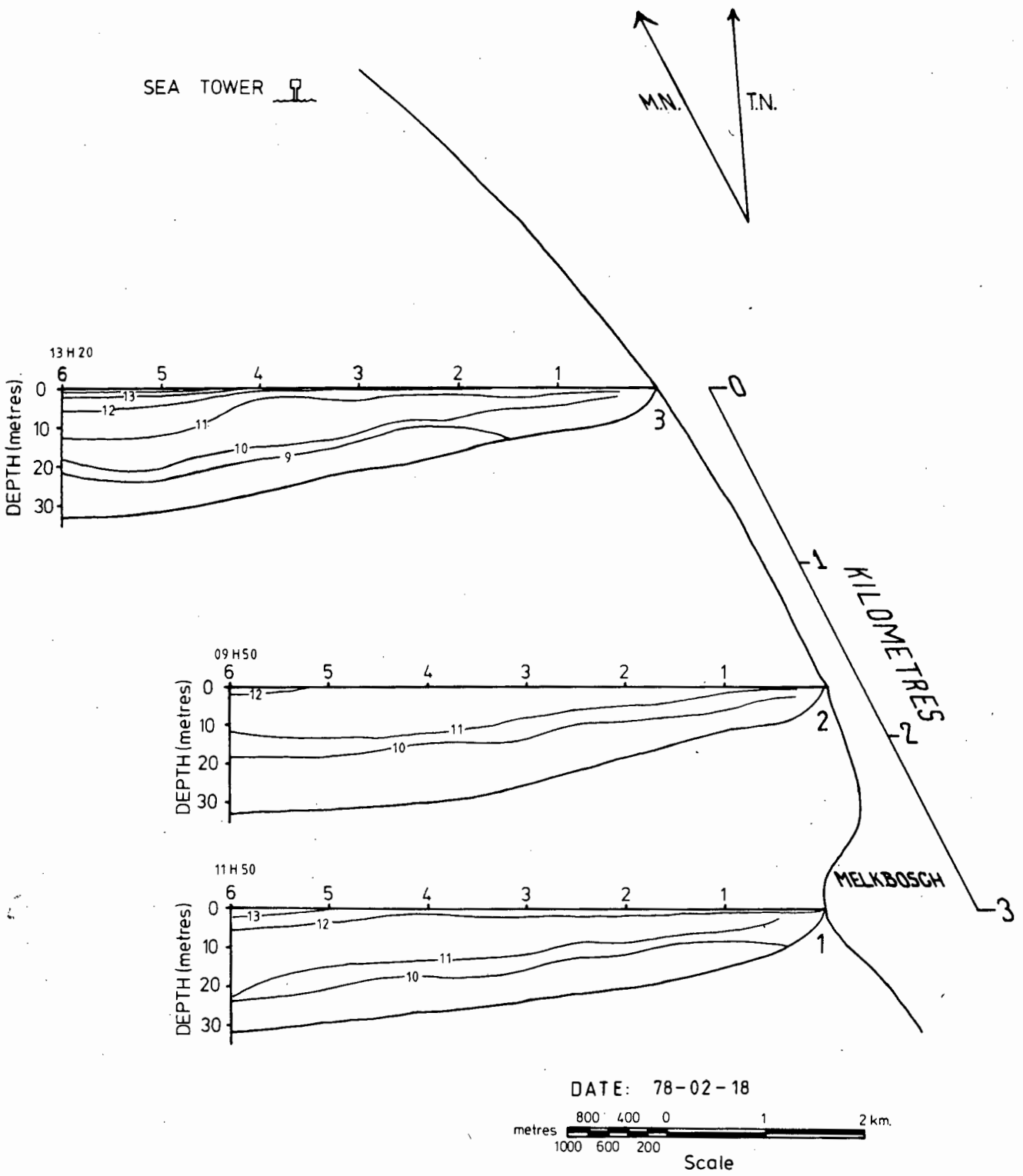

FIG. 4.14 TEMPERATURE TRANSECTS OFF MELKBOSSTRAND FOR THE PERIOD 16 TO 18 FEBRUARY 1978

d) 1978-02-18 MORNING

4.3.2 Prediction of Thermocline Displacement

In the preceeding Section 4.3.1, a qualitative description of the character of a wind event and the corresponding response of the sea is given. The description lacks the quantitative aspects and details of the forcing processes that result in temperature changes. A step towards gaining insight into the actual complex behaviour of the real ocean is to employ a conceptual model of the physics of the situation. Csanady (1977b) considers that a conceptual model aims to "reproduce the predominant characteristics of some distinctly identifiable observable phenomena". In the present case of coastal upwelling the characteristic observed is that, with a favourable alongshore wind stress at the coast, the thermocline is made to tilt upwards, break the surface and is displaced a certain distance offshore. A conceptual model on the dynamic behaviour of the thermocline subject to alongshore wind stress has in fact been formulated by Csanady (1977a) and is discussed in the following section.

Further insight into the behaviour of the system could be obtained by doing some form of sensitivity analysis to see which parameter variations have the greatest effect on the thermocline displacement. This is touched on briefly in Section 4.3.2.2. The prediction of the extent of thermocline movement and corresponding current velocities for different wind impulses can be of use to biologists who are concerned with the ecology of upwelling system and to engineers and environmentalists who wish to study the impact of pollutants and thermal wastes in the coastal region.

The following sections should help elucidate aspects of the processes that occur in a wind event and give a better quantitative idea of the upwelling response. They can be useful for other studies along the coast.

4.3.2.1 Csanady's Two Layer Inertial Adjustment Model

Csanady (1977a), working with data from the Great Lakes for comparison, has developed a model for successfully predicting "full" upwelling. "Full" upwelling describes the case where subject to an alongshore wind stress the thermocline is displaced upwards to intersect the free surface some distant offshore, compared with the case where the thermocline rises but does not meet the surface. The former case is usually revealed by the presence of a distinct 'front' on surface temperature maps of the coastal region. The model is a two layer inertial adjustment model that neglects interface and bottom friction. The chief case which is modelled, is that of alongshore wind that is impulsively exerted

on a two layer fluid over a time span short compared with the time taken for the top layer depth to change appreciably. Only the steady component of the flow is considered and the longshore flow is assumed to be in geostrophic equilibrium after the adjustment process.

The mathematical details of the model are given in Csanady (1977a) and are discussed in his book Csanady (1982a). Here the results are given with reference to Fig. 4.15 which defines the two layer sea and axes used in the model. For given initial values of the top and bottom layer depth h_t and h_b respectively and for the densities in the two layer ρ_t and ρ_b and for a given wind impulse I, the model predicts the distance offshore Y_o of the displaced thermocline front with the following equation:

$$Y_o = -R_i \frac{I}{f} \frac{h_b}{h_t(h_t+h_b)} \qquad \ldots\ldots\ldots \qquad A$$

where R_i is the Rossby internal radius of deformation

$$R_i = \frac{1}{f} \left(\frac{g \varepsilon h_t h_b}{h_t + h_b}\right)^{\frac{1}{2}}$$

$\varepsilon = \frac{\rho_b - \rho_t}{\rho_b}$ is the proportionate density defect

f = coriolis factor

g = acceleration of gravity

$I_{min} = h_t \frac{h_t + h_b}{h_b} . f . R_i$ is the minimum wind impulse required to just bring the thermocline to the surface at $Y_o = 0$

The model also estimates the alongshore velocity difference between the top and bottom layer U-U'.

$$U-U' = - \frac{h_t + h_b}{h_b} . f . R_i \exp - \left(\frac{Y-Y_o}{R_i}\right) \qquad \ldots\ldots \qquad B$$

Csanady (1977a) considers other wind stress combinations in developing his model further. He shows that an offshore wind impulse has no influence on the thermocline but that a steady offshore wind together with an impulsive alongshore wind does

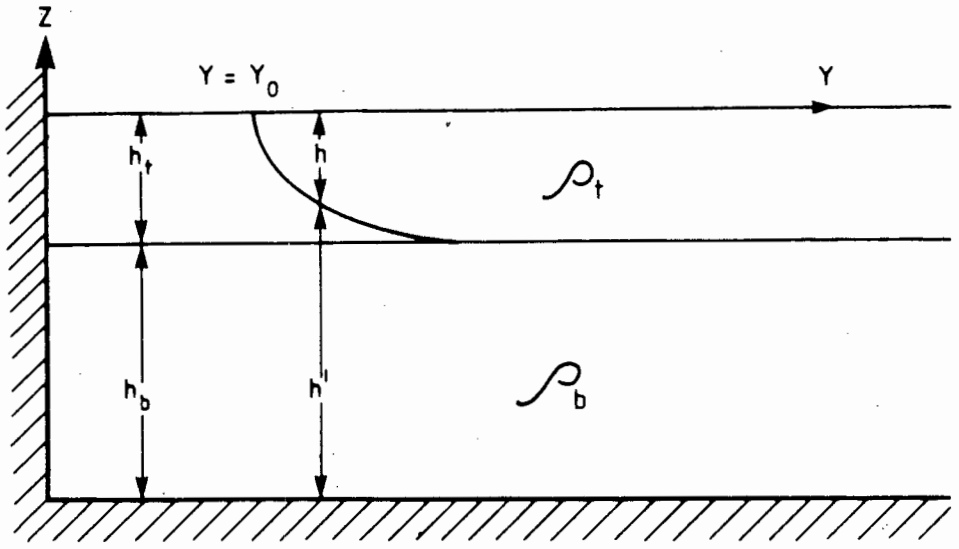

FIG. 4.15 REPRESENTATION OF A FULLY UPWELLED THERMOCLINE AFTER CSANADY'S (1977) TWO LAYER INERTIAL MODEL

change the thermocline shape by steepening the upwelling and increases the intercept distance Y_o offshore. His field data showed that unlike longshore winds, the strong across-shore winds did not have lasting upwelling effects. He investigates the effects of a second alongshore wind impulse on the developing upwelling by including the potential vorticity terms in the equations. The results of this include, that the second impulse has a somewhat greater influence in producing offshore displacement than the first; that the inclined portion of the front is squeezed together and that the equilibrium thermocline depth can overshoot to greater depths near the front.

The next section considers the applicability of Csanady's formulation to the present site and illustrates their use with local site data.

4.3.2.2 Case Studies of Thermocline Displacement Prediction

The Csanady (1977a) inertial model described above was developed in conjunction with upwelling studies in the Great Lakes where tidal motion is absent. Tidal motion in the coastal waters off Oregon on the North American west coast is not predominant neither is the associated bottom friction. The Great Lakes and Oregon sites therefore respond to wind impulses primarily in the inertial rather than the frictional mode (Csanady, 1982a). In contrast the east coast of North America is subject to strong tides that generate

large bottom stress that results in wind event response being controlled more by bottom friction than by inertial effects. The present study site is not subject to strong tidal flows and data from the site are considered applicable for testing Csanady's formulations. Furthermore the bottom profile at the site, out to a distance of 20 km is very similar to that at Oshawa, Lake Ontario, the site referenced by Csanady. A possible complication locally is that the wind can have a strong diurnal character that may affect the assumption of a wind impulse used in the model.

The field work undertaken included bathythermograph profiles on a number of transect lines to a distance of 6 km offshore where the depth was 30 to 40 metres. Section 1.5 gives further details. One or two sets of lines per day for a number of consecutive days were traversed in order to follow the upwelling response during a wind event. Temperature transects selected to illustrate the application of Csanady's model are shown in Fig. 4.14a-d for 16-18 February 1978, Fig. 4.16a-c for 26-28 January 1977 and Fig. 4.17a-c for 6-8 February 1978. The dates and times of the associated wind event and the properties of the assumed two layer sea are given in Table 4.5. These are then used to calculate (from the equations given in the previous section) the minimum impulse for full upwelling, the internal radius of deformation and the front displacement distance, which are tabulated in conjunction with the observed positions of selected isotherms in Table 4.6.

An obvious comment is that there is an arbitrary element in representing the real density distribution in a two layer model. The selection of top and bottom layer depths and their respective densities (temperatures) is somewhat subjective. In general the layer properties are based on the temperature profile data at the offshore extent of the transects. For model calculation an assumed depth of 40 m is used. Since temperature is considered the main contribution to density in the area (Gunn, 1977a, Bang, 1973), an arbitrary single value for salinity of 34.7, based on the findings of Gunn (1977a) for a similar site 15 km to the north, is chosen. This value also corresponds to the "upwelling water" classification of Andrews and Hutchings (1980). The salinity, together with the observed temperature is used to evaluate density from standard curves.

The cases tabulated in Table 4.5 are not all for separate events. Some sequential cases represent the evolution of the event from day to day and others for different transect lines in the same event.

Case 1 and 2 occur during the event discussed in Section 4.3.1.1 The temperature transects are in Fig. 4.14a-d and the wind is illustrated in Fig. 4.11 and 4.12. In case 1 for line 1, denoted as 1/1, the initial thermocline probably lies between 12° and 13 °C. After some 6 hours of strong southerly winds the warm surface water has been displaced beyond 6 km and the 13° isotherm intersects the surface at 3.1 km. The 12° isotherm is more undulating and reaches to near the surface at the coastline. The calculated front displacement is a small negative value (Table 4.6) which means the front does not surface but nearly does so. For the second line the predicted front position is 1,7 km which is in good agreement with the observed value between 0,7 km and 2,1 km. The width of the inclined portion of the thermocline is about 1 km compared with the somewhat larger radius of deformation of about 3 km.

Case 2/1 is the continuation of case 1/1 to the following day. The wind impulse is large, 203000 cm^2s^{-2} and the 12° and 13° isotherm are further displaced to 2,8 km and 4,6 km respectively but not to the extent predicted by the model i.e. 7,1 km. Inspection of the layer properties on the 17th February however show that the top layer is a lot deeper than the initial conditions on the 16th. The effect of this deepening in a two layer model is to reduce the offshore displacement which is demonstrated in versions a) and b) of the next case 2/2. In a) where the initial layer depth of 11 m is used a displacement of 13,9 km is calculated compared with the observation of between 2,5 km and >6 km (the outer limit of observations). If the initial top layer depth is modified to accommodate the evolving real thermocline structure and set to 16 m shown in 2/2 b) (Table 4.5) the calculated displacement is approximately halved to 6,3 km which is much closer to the observed value. This illustrates the sensitivity of the model to changes in layer depth.

A rough idea of currents in the water column is obtained from tracking of current drogues (see Section 1.5). The maximum predicted difference in current velocity across the thermocline is for case 1/2 33 cm s^{-1}, compared with an observed 17 $cm.s^{-1}$ at the 4 km position offshore. However the difference in velocity was measured between 1 m and 15 m, the latter not being adequately below the thermocline, which partly accounts for the smaller observed value for the difference. The predicted current difference for case 2/2 a and b is 33 cm s^{-1} and 44 cm s^{-1} respectively, whereas the measured value is only 12 cm s^{-1} between 1 m and 20 m depth. The low velocity difference is probably accounted for by frictional effects in the shallow water. Observations show that currents measured in the shallower inshore

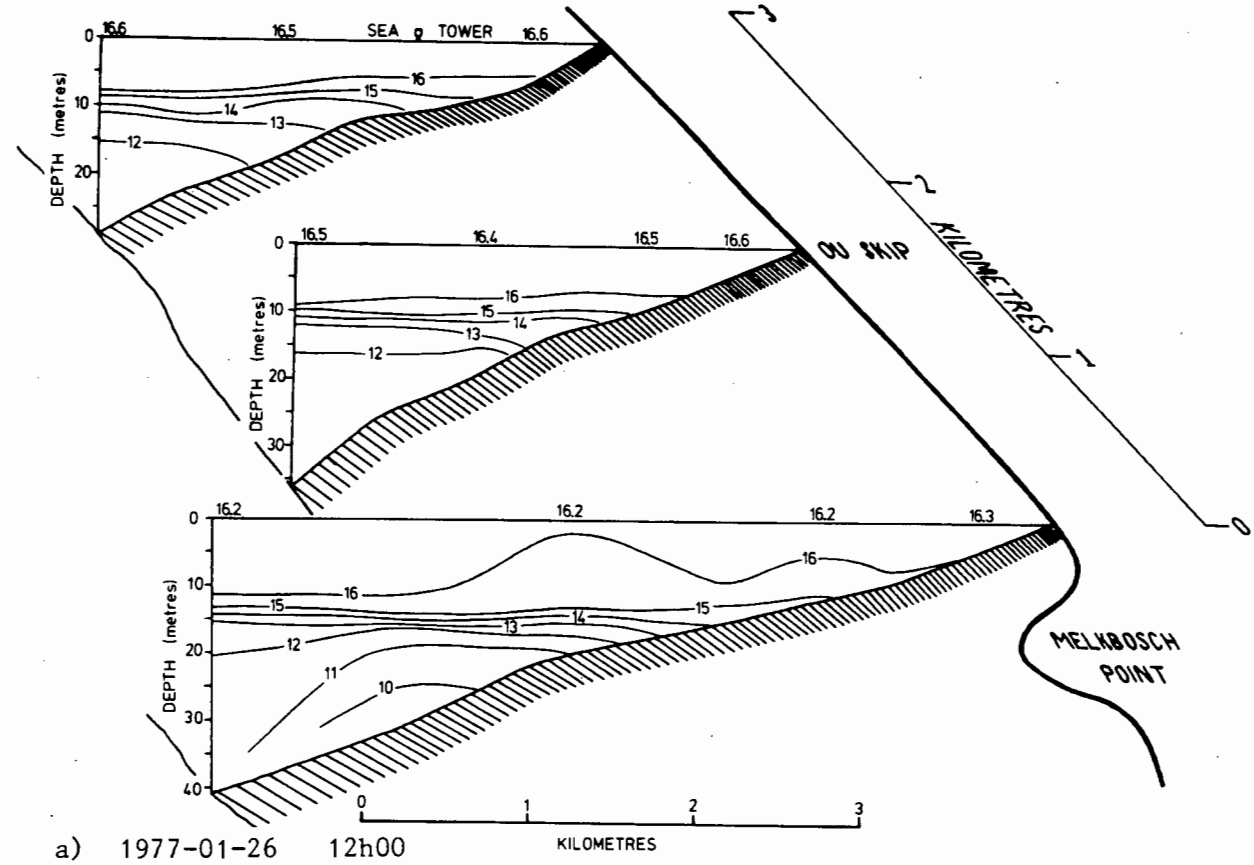

a) 1977-01-26 12h00

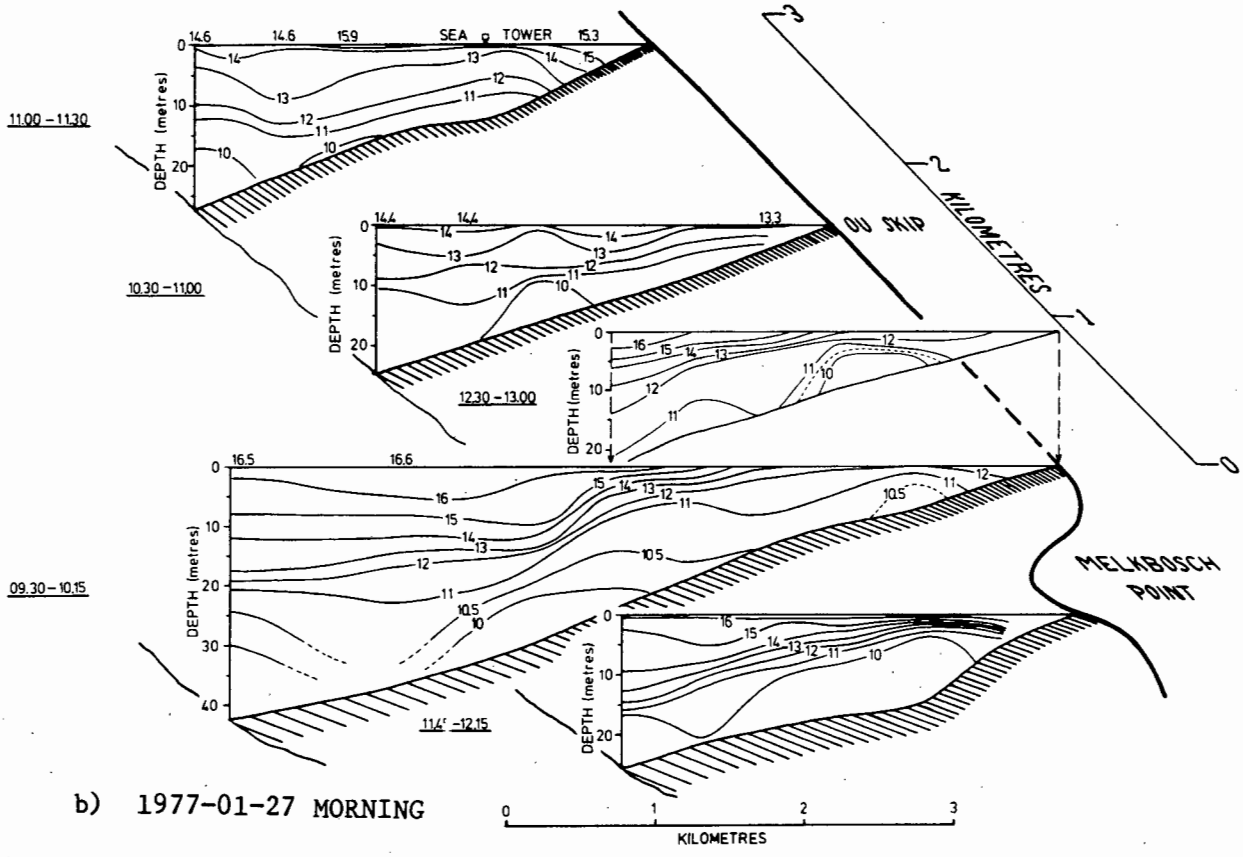

b) 1977-01-27 MORNING

FIG. 4.16 TEMPERATURE TRANSECTS OFF MELKBOSSTRAND FOR THE PERIOD 26 TO 28 JANUARY 1977. SOME INDIVIDUAL LINES ARE RESURVEYED LATER IN THE DAY

TEMPERATURE SECTIONS, 28 JAN., 1977.

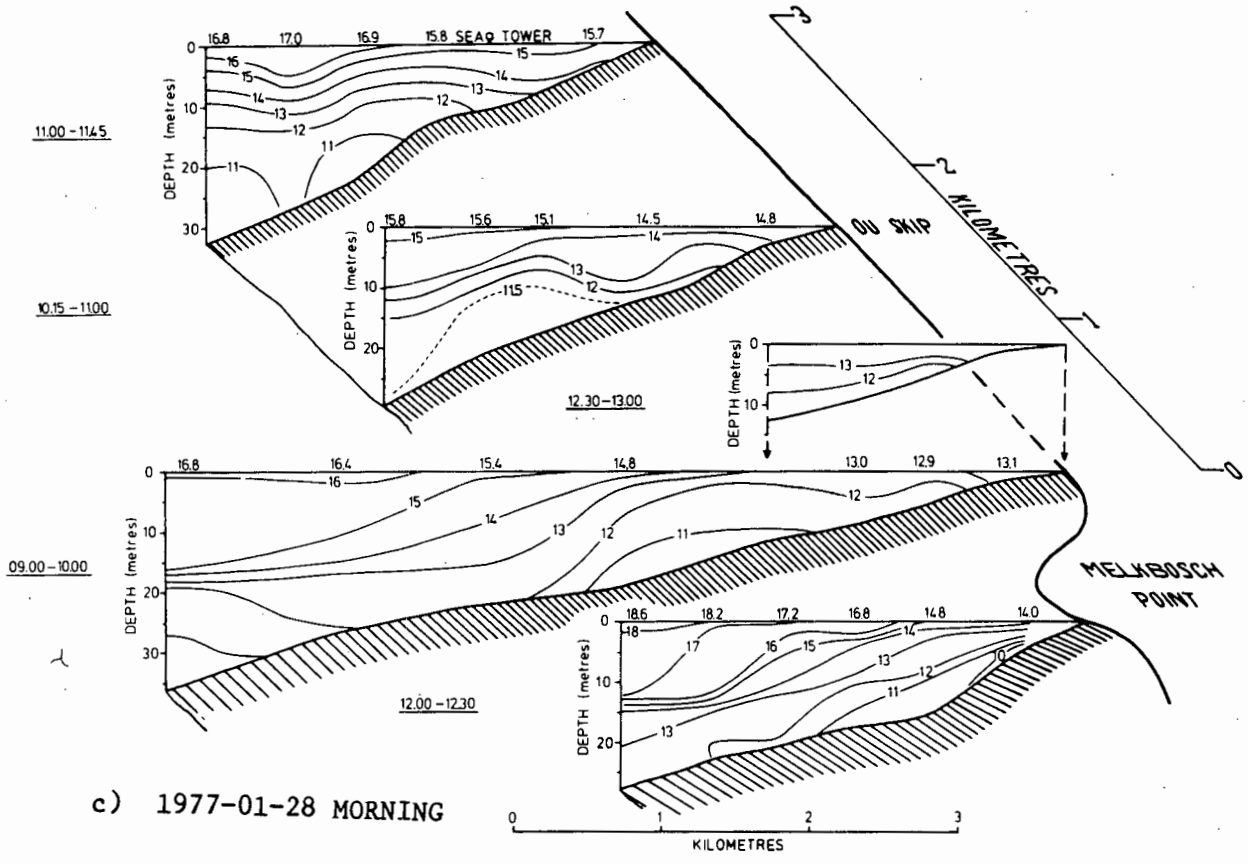

c) 1977-01-28 MORNING

FIG. 4.16 TEMPERATURE TRANSECTS OFF MELKBOSSTRAND FOR THE PERIOD 26 TO 28 JANUARY 1977. SOME INDIVIDUAL LINES ARE RESURVEYED LATER IN THE DAY

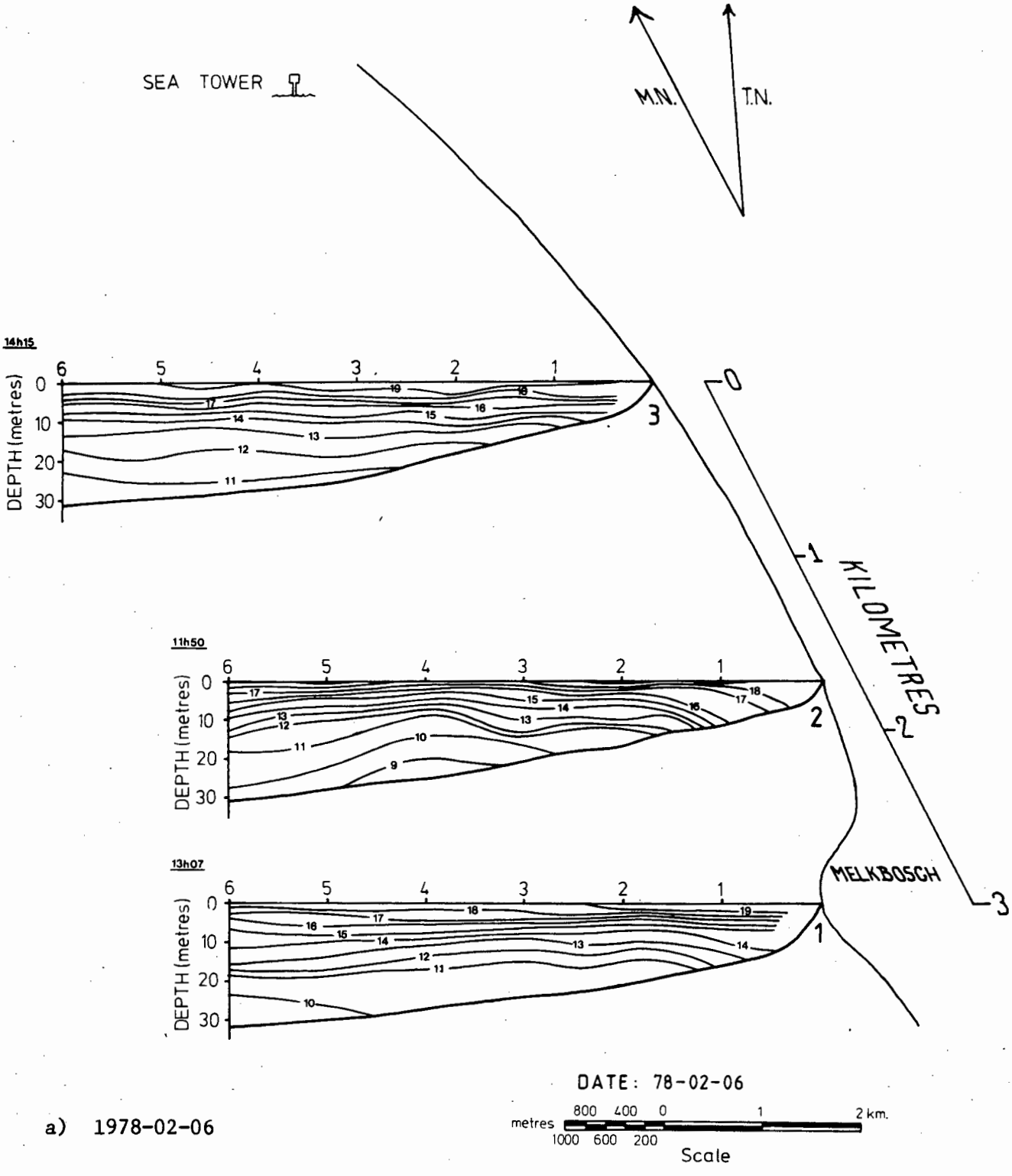

a) 1978-02-06

FIG. 4.17 TEMPERATURE TRANSECTS OFF MELKBOSSTRAND FOR THE PERIOD 6 TO 8 FEBRUARY 1978.

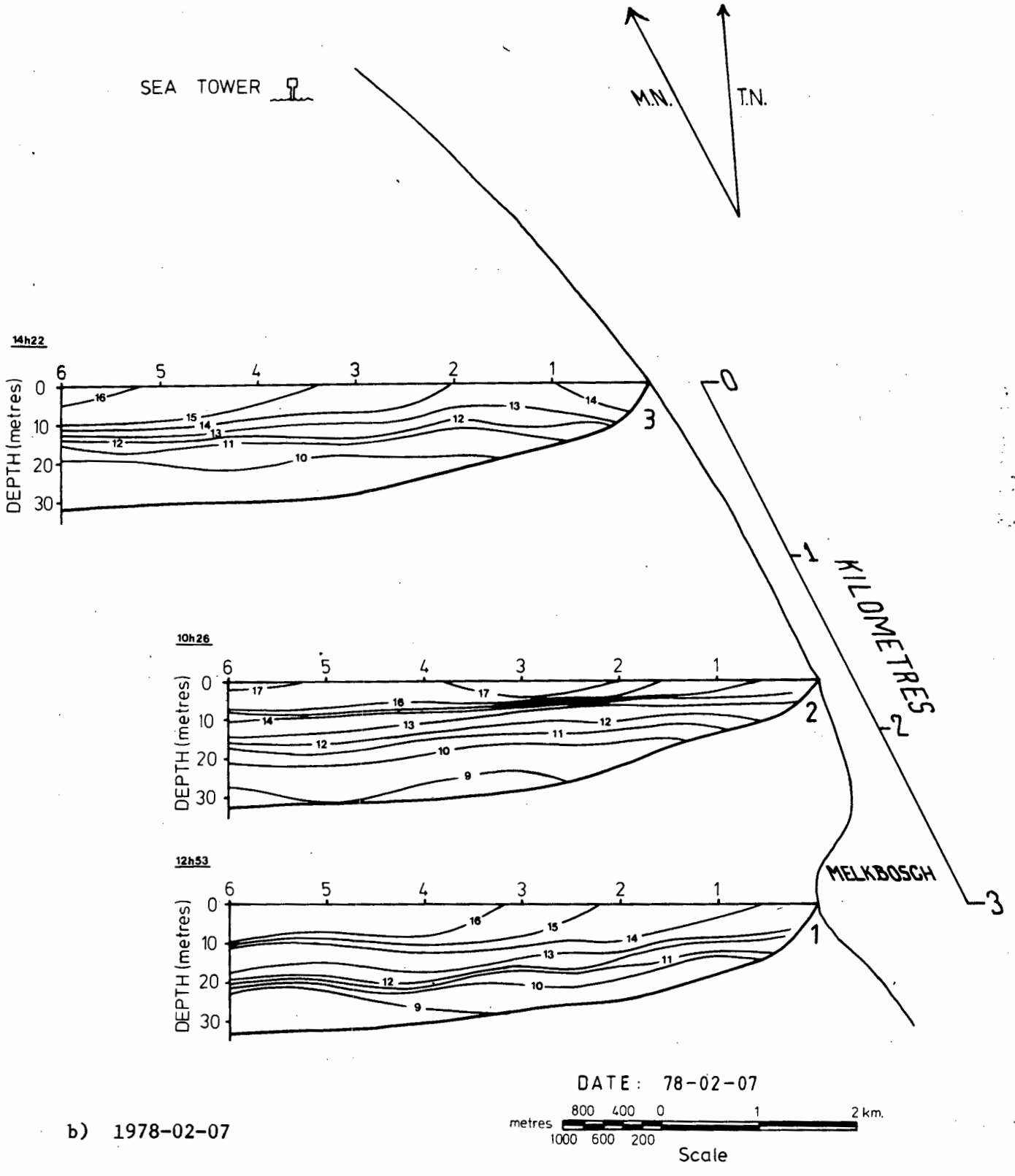

b) 1978-02-07

FIG. 4.17 TEMPERATURE TRANSECTS OFF MELKBOSSTRAND FOR THE PERIOD 6 TO 8 FEBRUARY 1978.

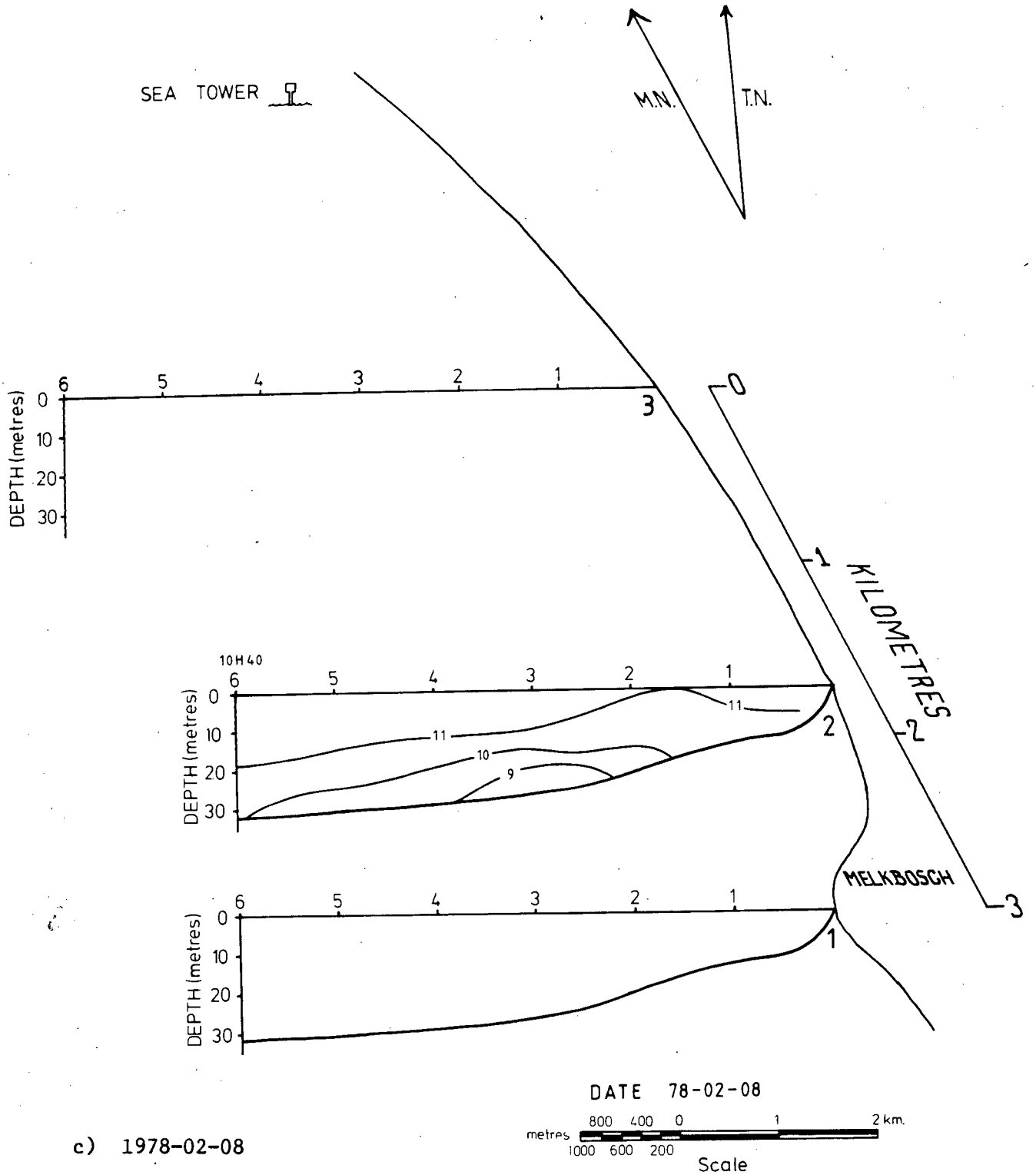

c) 1978-02-08

FIG. 4.17 TEMPERATURE TRANSECTS OFF MELKBOSSTRAND FOR THE PERIOD 6 TO 8 FEBRUARY 1978.

waters at the 1 km position are generally lower than those measured at the 4 km offshore position for the same measured wind conditions (Fig. 4.21).

The next two cases in Table 4.2, 3/2 and 4/2, are during a January 1977 event (Fig. 4.16a-c). The initial conditions have a fair approximation to a two layer system with a sharp horizontal thermocline of about 14 °C situated at a depth of 14 m. The wind event has a fairly strong impulse on the 26th and moderates on the 27th and 28th January. For case 3/2 the predicted displacement is 1,5 km which is slightly less than the observed value of between 1.8 and 2.2 km. The observed value could more reasonably be expected to have a value of about 2.8 km if the steeper slope of the thermocline is extrapolated to intersect the surface. A possible explanation of both the steep thermocline slope and the greater than predicted displacement is that this event of all those considered has, for a certain period, the largest offshore wind component. It is not large compared with the previous 24 hours alongshore stress but is comparable to the alongshore stress for the 12 hours just preceeding the measurements for line 2 on the 27th January. The steeper slope is explained by Csanady (1977a) who has shown that for a (steady) across-shore wind together with an impulsive alongshore wind the thermocline slope steepens and is displaced slightly further offshore than without the across-shore component. The relaxation of the thermocline slope a little distance before reaching the surface is probably due to the wind swinging onshore shortly before the measurements commenced. The continuation of the event to the next day, case 4/2 gives displacements in reasonable agreement with theory. The thermocline slope becomes more gentle and the width of the inclined portion increases to about 2 km which is still smaller than the internal radius of deformation which is 3.3 km. No current data for this period are available.

The two days prior to the starting of case 5/3 on 6 February 1978 had light westerly winds that resulted in closely packed isotherms in the top 10 m (Fig. 4.17a-c). The subsequent wind impulse "peeled" away the isotherms as progressive upwelling occurred. The centre of the thermocline is not well determined but probably occurs between 14 ° and 15 °C. The prediction for displacement of the front gives a value of 2.1 km which is in good agreement with the observation of between 2.0 and 3.4 km. Once more the width of the inclined isotherms is smaller than the internal radius of deformation.

The theoretically estimated current velocity difference across the thermocline is 38 cm s^{-1} but a low difference of 10 cm s^{-1} is observed.

Although the upwelling is initiated on the 6th February as described in case 5/3, the further upwelling from 7th to 8th February for line 2 is investigated in case 6/2. A deeper top layer is assumed and with the larger wind impulse a front displacement of 1 km is calculated. The observed values lie between 1.7 km and larger than 6 km (Fig. 4.17c). If the more realistic wind impulse is used that includes the stress in the previous 24 hours as well, the predicted value increases to 2.7 km. In this case with a large wind impulse, the limitation of the field data that only extends to 6 km offshore becomes apparent. The true extent and shape of the upwelled front is not adequately revealed and comparison with theory is hindered. No current velocities are available for the 8th February but are for the following day when the winds moderated and had a slight onshore flow. The currents then are much reduced in velocity compared with those on the 7th and are also equal across the water column, there being no obvious two layer structure.

The two layer model of Csanady (1977a) is patently idealistic yet at times there is fair agreement with observations presented here. Limitations of the model and other aspects will be discussed in Section 4.5.

The two dimensionality of Csanady's model is contrasted with the three dimensional character of the field data, where adjacent transect lines occassionally have notable differences in isotherm distribution. It is not always clear if such differences are due to unavoidable time differences between measurements along the transects in the quickly developing upwelling system or to spatial effects. This leads on to the discussion in the following section of spatial effects at the study site.

4.4 SPATIAL VARIABILITY

Up to this stage the true three dimensional complexity of the natural system has been neglected. If the characteristics of the local upwelling system are to be delineated then spatial factors such as variable wind field, coastline orientation and bottom topography have to be considered. In the introductory chapter (1.2) spatial aspects of centres of upwelling with fixed geographical bases are discussed. Similar upwelling positions at different sites have been explained with differing dominant factors. For example, the upwelling centres

at Cabo Nazca, Peru and at Gulf of Lions in the Mediterranean are similar in that they both occur on relatively straight segments of coastline and are generally not associated with sharp fronts. The Peruvian centering is attributed mainly to local bottom topography (Preller and O'Brien, 1980 referenced in Brink, 1983), while the Mediterranean case is explained chiefly by coastline orientation (Millot, 1979). The shape and size of the upwelling centres are also further affected particularly by the wind field and wind intensity. The Cape Peninsula upwelling is attributed to both wind stress curl induced by terrestrial topography and by relative vorticity changes in fluid flow around the marine topography of the Capes (Nelson, 1985). This section seeks to characterize spatial attributes of the site and its upwelling and relate it to other worldwide observations.

In this chapter the marked temporal variability of the wind field at the event time scale has already been highlighted. The importance of the concurrent spatial variability of the wind is given in the following Section 4.4.1. The upwelling patterns revealed by airborne radiation thermometry (ART) of sea surface temperatures and their evolution during an event are presented in Section 4.4.2. The study reveals a distinctive focus of upwelling just north of Melkbosstrand. The subsequent section gives a brief discussion of currents in the study area.

4.4.1 Spatial Variability of the Wind

The spatial variability of the wind over the larger scale of the Cape Peninsula is first mentioned together with its relevance for the smaller local study site. In an earlier section (1.4.2) Jury's (1987) selection of four wind regimes over the Cape Peninsula area is listed. In Jury's study each regime is seen to have a characteristic spatial distribution which is a function of the synoptic wind direction, the steep orography and the inversion layer depth.

Attributes of these distributions for the portion from Table Bay to further north past the study area include the following chief features. For southerly wind regimes a relatively calm area or wind shadow lies to the north of Table Mountain. The size and orientation of the calm patch is variable, being small for the deep SE winds and being more extensive for the shallow ESE regime. In the former case the calm area is flanked to the east with an essentially alongshore strong wind - the Cape Flats Jet; on the west strong winds descend from the high orography in the Bakhoven Downslope Jet. For the shallow regime the Cape Flats Jet can be greatly reduced in intensity and is modulated by a SW sea breeze system that is associated with a thermal low in the adjacent interior. An idea of the wind field variability for the area is also obtained from the wind roses (Fig.

3.12) presented in Section 3.7.1.

Jury (1984) demonstrates the importance of the inversion layer depth and wind shear in generating cyclonic wind stress curl that interacts with the coastal geometry to produce local variations in coastal upwelling on the scale of 10 to 40 km. The main sea surface temperature upwelling features that he observes for the area of interest are, for appropriate wind conditions:

a) a well developed cold water patch extending NW from the NW corner of the Peninsula
b) a shore-parallel band of cold upwelling water from the south end of Table Bay northwards and
c) a warmer region between a and b, centred just west of Robben Island, that may support a southward surface current.

The present study includes a much finer grid survey than Jury's of sea surface temperatures of the feature b) above, extending from the south of Table Bay to Bok Point in the north. In the following section these data and their relationship to the larger scale are highlighted.

4.4.2 Temperature Spatial Variability

4.4.2.1 Surface Temperature Patterns

Airborne radiation thermometry (ART) is a commonly used method for obtaining sea surface temperature (SST) data (Andrews and Cram (1969), Saunders, 1973). Its use here is described in Section 1.5. In the study area with its high percentage of cloud free days the technique is employed to good effect in following the surface temperature effects of upwelling. Firstly two SST maps extending from Table Bay to Bok Point are presented and discussed under the headings, Upwelling Phase, Upwelling Centre Position and Relaxation Phase. This is followed by a sequential set of SST maps of the Melkbosstrand area for the wind event cycle of 14 to 18 February 1978 described in Section 4.3.1.

Sea surface temperature maps for a coastal strip less than 10 km wide and extending 50 km north from Table Bay are shown for 11th and 12th November 1975 in Figs. 4.18a and b respectively. The prevailing wind conditions at Ou Skip are shown in the form of a progressive vector diagram as an insert in Fig. 4.18b. The wind regimes at the time are deduced from SA weather bureau synoptic maps to be as follows. Using Jury's (1980) terminology the 10th November experienced a post cold front southerly flow, followed on the 11th by a deep south easter which turned to a shallow

pre-coastal low south easter by the 12th which also experiences more noticeable diurnal see breeze forcing as seen on the progressive vector diagram (Fig. 4.18b).

Upwelling Phase

As a result of the strong southerly winds on the 10th and 11th November the SST map on the 11th, Fig. 4.18a shows a spatially complex temperature distribution with two distinctive cooler (upwelling) features. There is a "focus" of upwelling cold (9 to 10 °C) water just north of Melkbosstrand with a filament of 10+ °C water extending further northwards to Bok Point. The other region of upwelling is in the south and east side of Table Bay with a filament of 10+ °C water extending to the northwest. The orientation of this filament between Robben Island and the mainland is probably influenced by the bottom topography shown in Fig. 1.3. On the seaward boundary of the area surveyed a fairly sharp "front" occurs with a gradient of 2 to 3 °C in 2 km which is quantitatively similar to the gradient observed by Bang (1973) for fronts about 20 km offshore of the Peninsula. Numerous other ART surveys in this study have revealed similar features.

With one exception these features agree with Jury's findings and correlate with the winds spatial distributions. The more intense Cape Flats Jet in the south of Table Bay accounts for the upwelling filament starting there. The wind calm in the wake of Table Mountain limits the spread of the cool upwelled water to a band inshore of Robben Island. The exception is the intense localized "focus" of upwelling north of Melkbosstrand. One is tempted to use the term "fountain of upwelling" which Bang (1976) has used for even smaller patches of rapid upwelling off the coast. Jury puts more emphasis on orographic control and wind stress curl in producing differential upwelling on the scale of 10 to 40 km whereas, at this small focus of upwelling the probable cause is the change in average coastline orientation. Although anomalous mixed layer deepening resulting from strong winds could give a cold spot, this is not considered to be the case here because of the qualitative agreement of the observations with Csanady's (1977a) upwelling model. Nelson and Hutchings (1983) remark on small tongues of cold water formed off minor capes along the Cape Peninsula and Nelson (1985) mentions microsites at Yzerfontein and Bok Point on the west coast but this is the first small scale (10 km) site of upwelling to be studied in detail locally.

The Upwelling Centre Position

In comparing the positioning of this small centre of upwelling with

other world sites the first comment is that the space scale is smaller than most other investigations which therefore probably overlooked such features. Although Blanton (1975) reports discrete upwelling associated with cuspate features on the coastline of the order of a few kilometers, no details of other comparable upwelling feature has been found in the literature. In seeking an explanation for the observation of the intense upwelling just inside the embayment at Melkbosstrand the coastline shape, as a first approximation, can be considered as a straight line running north south with a 2 km wide offset to the east at Melkbos Point. The model of Hua and Thomasset (1983) considers wind blowing over right angled bays and capes and ignores bottom topography. Their minimum grid size is about one fifth of their local Rossby internal radius of deformation or about 2 km, which is the size of the total offset in our case. However there is some justification in trying to use their results when it is remembered that for certain local case studies the Rossby radius is smaller than their example i.e. about 3 km (see Table 4.5). If their results (neglecting vertical mixing) for a bay and a cape are combined and adapted for the southern hemisphere, Fig. 4.19 is obtained which shows for their grid size the two layer interface displacement map. Maximum upwelling is seen to occur in the corner of the southern bay, where the wind is offshore over the offset and minimum upwelling occurs in the northern bay where the wind is onshore over the offset.

Now as the offset distance is reduced to approach the prototype scale it is conceivable to get the situation which we observe in the field (Fig. 4.18a). (The warmer band inshore of the cold centre is discussed later in the section.)

Simply put, in our case, the generally alongshore winds because of the shallow water result in only slight Ekman offshore veering of the surface waters close to the coast, but at the offset the surface water flow has a much greater offshore component. This divergence is compensated by an upwelling process and cold water is manifest in the embayment. The case of minimum upwelling predicted by the model in the northern bay of Fig. 4.19 is in fact observed in another set of SST maps particularly (Fig. 4.20 (b, c and d), where just south of Bok Point and near the Quarry warmer water occurs.

The bathymetry of the region at the offset (Fig. 1.3) is uniform and the adjacent inland area is free of orographic effects which leads to the conclusion that the observed focus of upwelling can

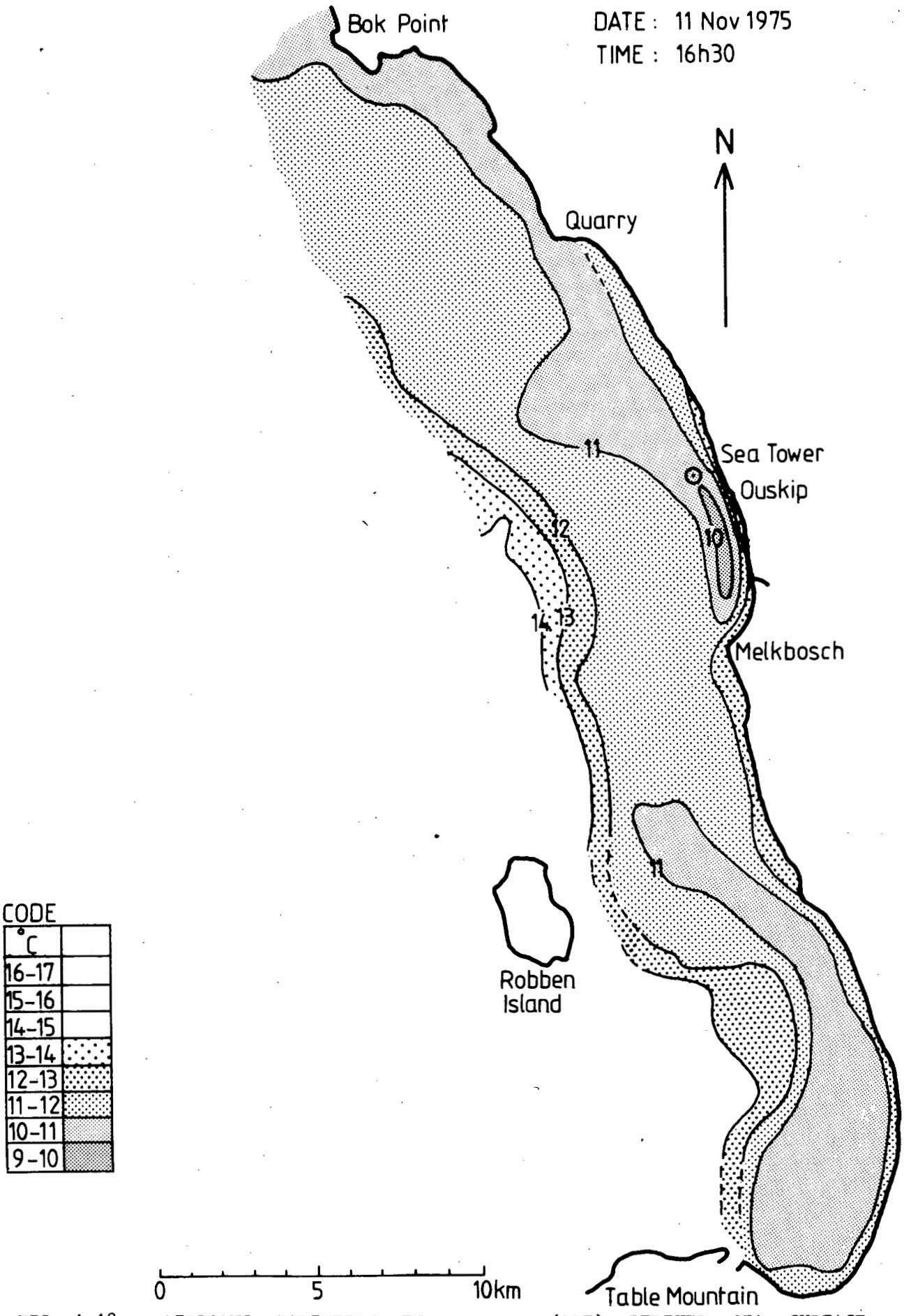

FIG. 4.18 AIRBORNE RADIATION THERMOMETRY (ART) DERIVED SEA SURFACE TEMPERATURE MAPS FOR THE AREA TABLE BAY TO BOK POINT
a) 11 NOVEMBER 1975

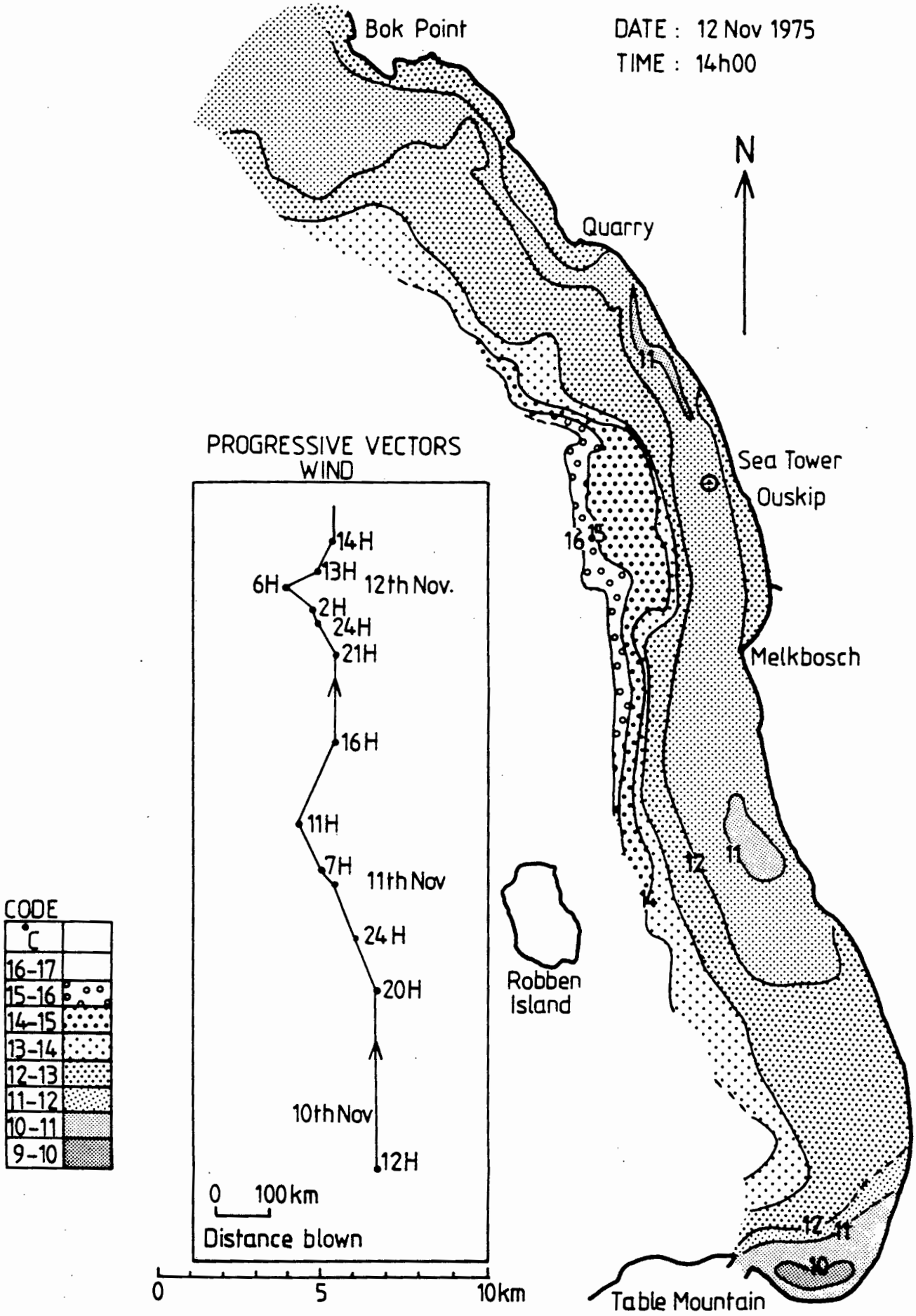

FIG. 4.18 b) 12 NOVEMBER 1975 WITH INSET PROGRESSIVE VECTOR DIAGRAMME OF THE WINDS FROM 10 TO 12 NOVEMBER

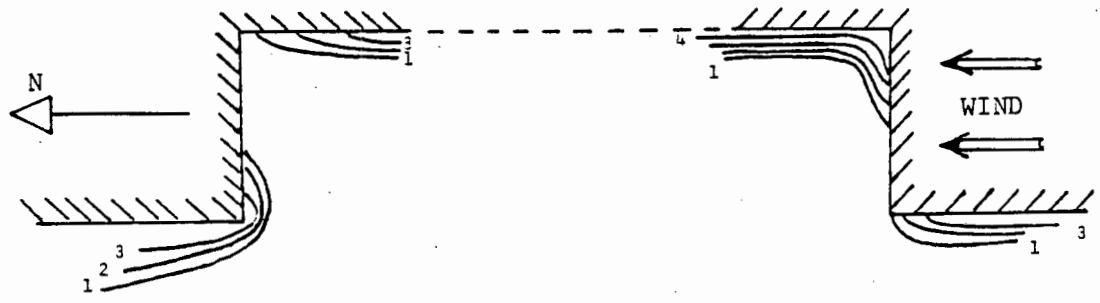

FIG. 4.19 RESULTS FROM MODEL OF HUA AND THOMASSET (1983) COMBINED FOR CAPE AND BAY AND ADAPTED FOR THE SOUTHERN HEMISPHERE. CONTOURS GIVE THE DISPLACEMENT IN METERS OF THE INTERFACE. THE SOUTH END SHOWS MOST ACTIVE UPWELLING IN THE CORNER OF THE BAY. OFFSET SCALE ORDER OF ROSSBY RADIUS VARYING FROM 3 KM TO 10 KM.
BATHYMETRY: MODEL FLAT BOTTOM BUT GULF OF LIONS SITE DEPTH 20 M WITHIN EMBAYMENT FALLING TO 50 M WITHOUT.

satisfactorily be explained by the action of the wind blowing over a coastline with changing orientation. The upwelling in the south of Table Bay on a slightly larger scale can also be partly ascribed to this process.

Relaxation Phase

We now turn to the conditions on 12 November when the wind moderates and a SW sea breeze causes some onshore flow. This relaxation phase causes considerable changes in the SST patterns and is shown in figure 4.18(b). Widespread downwelling is evident as the warm front moves in closer to the shore and the area enclosed by the 11 °C isotherm decreases considerably, breaking up into a few isolated patches. There is still evidence of upwelling in the extreme south of Table Bay. The focus of upwelling at Melkbosstrand has disappeared. The front in the region north of Robben Island is much sharper than observed during the upwelling phase. A steep gradient that in places exceeds 3 °C in one kilometer is observed. The 12 °C and warmer water moves in closest to the shore near the northern sector and touches the coast in the south east part of Table Bay. The warmest water observed lies north of Robben Island and bulges shoreward approximately opposite

where the centre of upwelling occurred. The existence of the wind calm area extending to the north of Robben Island during active upwelling and its associated warmer surface waters certainly plays an important part in the relaxation phase. The area seems to act as a ready source of warm water that can be advected shorewards with favourable winds such as the sea breeze and synoptic SW flows. The latter flow may be perturbed somewhat by Robben Island which may explain why the warmest water is not as close to the mainland near the island as it is slightly further north. Also in this area and slightly more offshore, the net southgoing current proposed by Nelson and Polito (1987) may enhance relaxation effects, as will the proposals by Jury (1986) for the sudden decay of upwelling (see Section 4.3.1.2). The surface temperature patterns for relaxation of upwelling on the northern California shelf is shown by Send Beardsley and Winant (1987) to be largely due to effects of poleward alongshelf advection and surface heat flux, while onshore advection of upwelled isopycnal field plays a lesser role.

Another feature of the relaxation phase is that the surface temperature pattern is much more patchy and the isotherms are more convoluted. This has been observed on the larger scale by Bang and Andrews (1974) who mention "disorganized" isotherms during light westerly winds. Brink (1983) contrasts an almost two dimensional front during upwelling and the complex three dimensional behaviour during relaxation when closed patches of warm and cold water occur. In our data of 12 November cold patches are seen and if the isotherms are contoured at a 0.5 °C interval some smaller patches are also revealed. The patchiness is probably a surface effect which is supported by the vertical temperature section data for a relaxation phase (Fig. 4.14d) where a very shallow layer of (<5 m) warm water occurs. Curtin (1979) makes a similar observation about the shallow nature of surface temperature patches. On the larger scale Hutchings et al., (1984) observe a thin 5 m deep surface warm layer in the relaxation phase. Similar comments are also made by Boyd (1987). The intrusion of warm water over a colder layer indicates the important role buoyancy effects play in modifying the SST distribution.

The scale of the meanders and patchiness observed locally of 1 to 10 km is similar to that in the coastal boundary layer (CBL) of Lake Ontario (Boyce, 1977) particularly in the aftermath of upwelling. The patchiness indicates active horizontal mixing processes and point to the instability of the baroclinic currents associated with the upwelling stage. In fact, Boyce (1977) using the results of Saltzman and Tang (1975) for oceanic currents, argues that baroclinic current instabilities must result in meanders and cutoff pools which are probably triggered by temporal and spatial variations in wind stress and variable bottom topography.

The reduction in the surface area of upwelling centres merely with a relaxation in wind strength and not a reversal of the wind

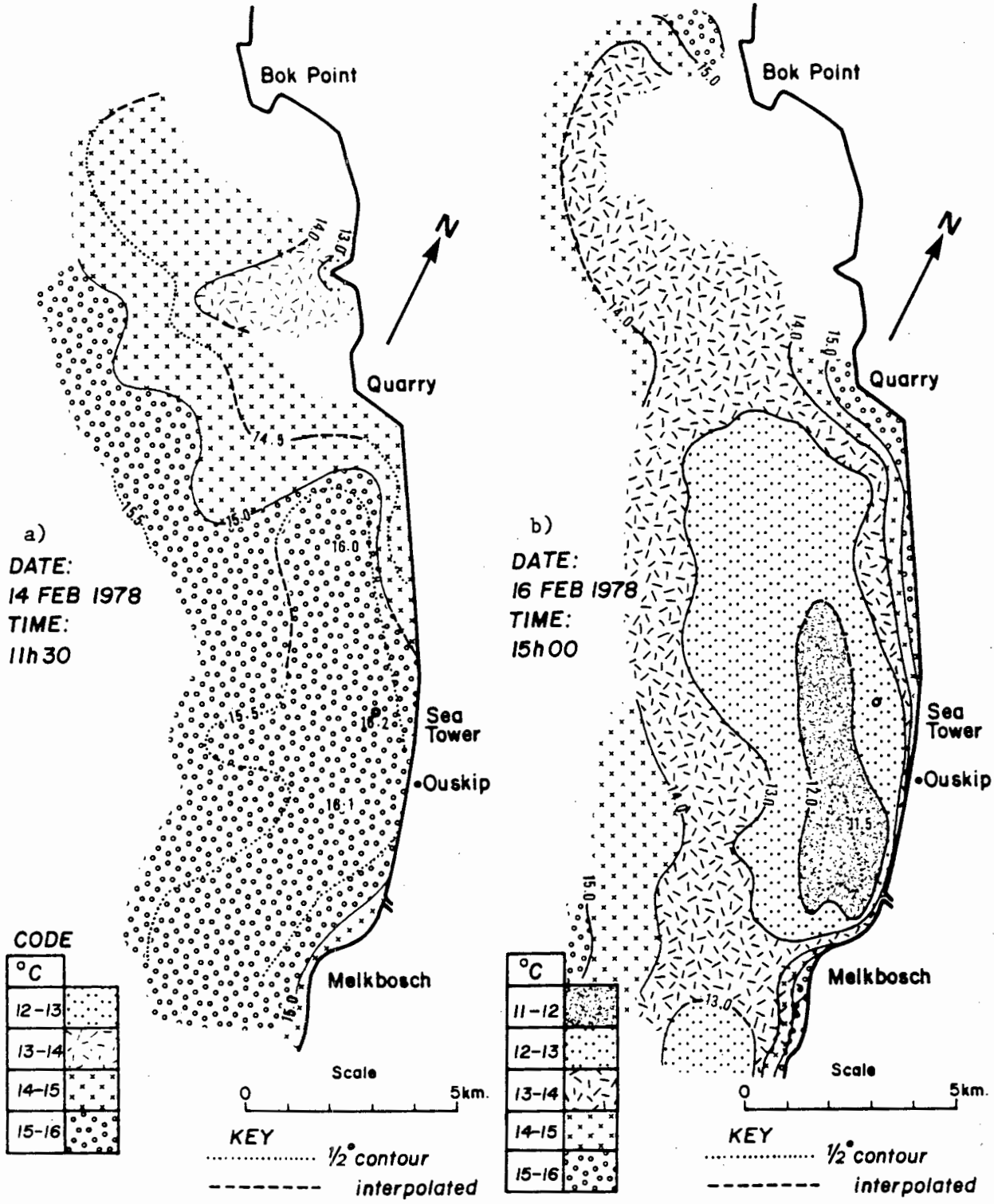

FIG. 4.20 AIRBORNE RADIATION THERMOMETRY (ART) DERIVED SEA SURFACE TEMPERATURE MAPS FOR THE AREA MELKBOSSTRAND TO BOK POINT FOR THE PERIOD 14 TO 18 FEBRUARY 1978

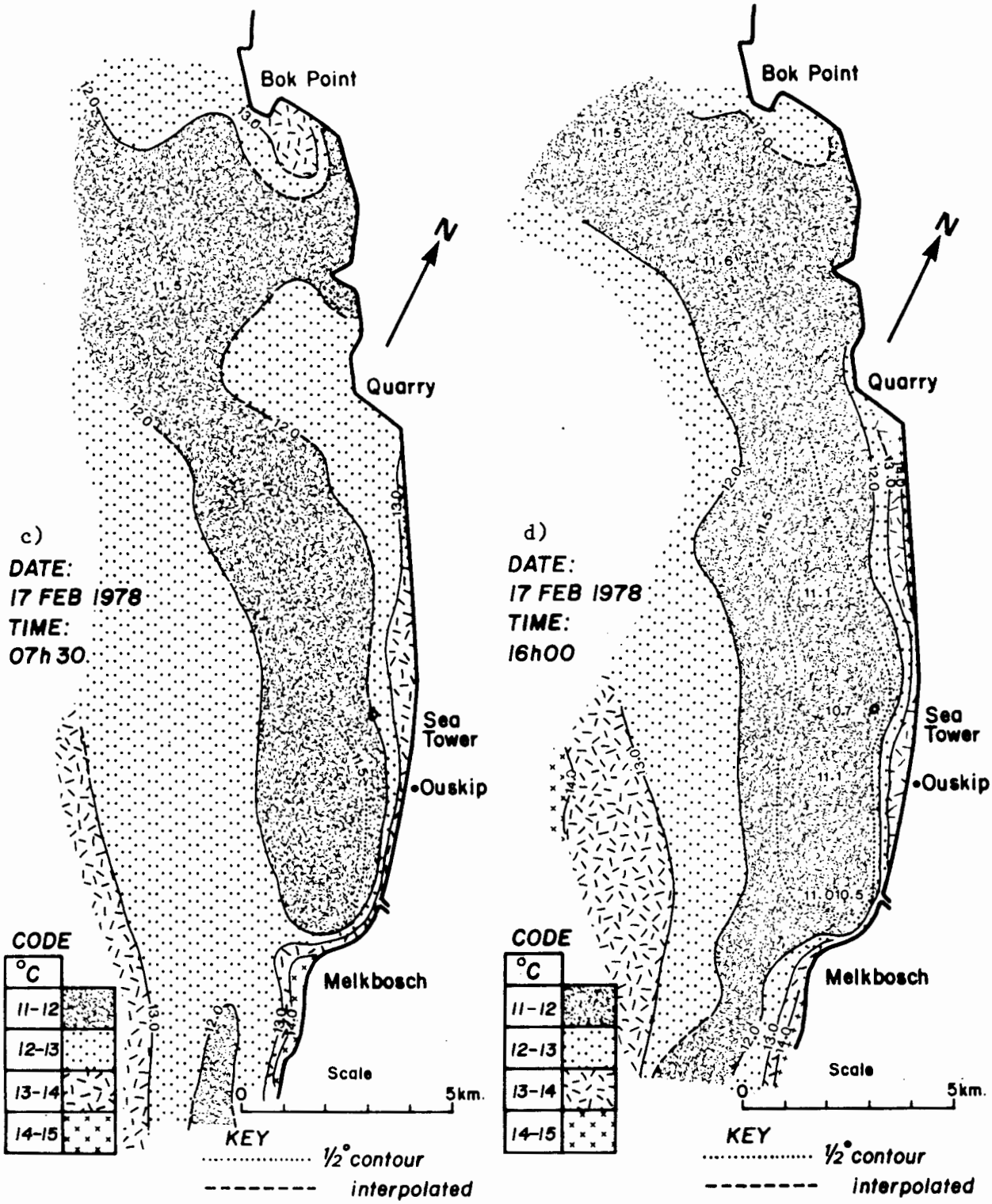

FIG. 4.20 AIRBORNE RADIATION THERMOMETRY (ART) DERIVED SEA SURFACE TEMPERATURE MAPS FOR THE AREA MELKBOSSTRAND TO BOK POINT FOR THE PERIOD 14 TO 18 FEBRUARY 1978

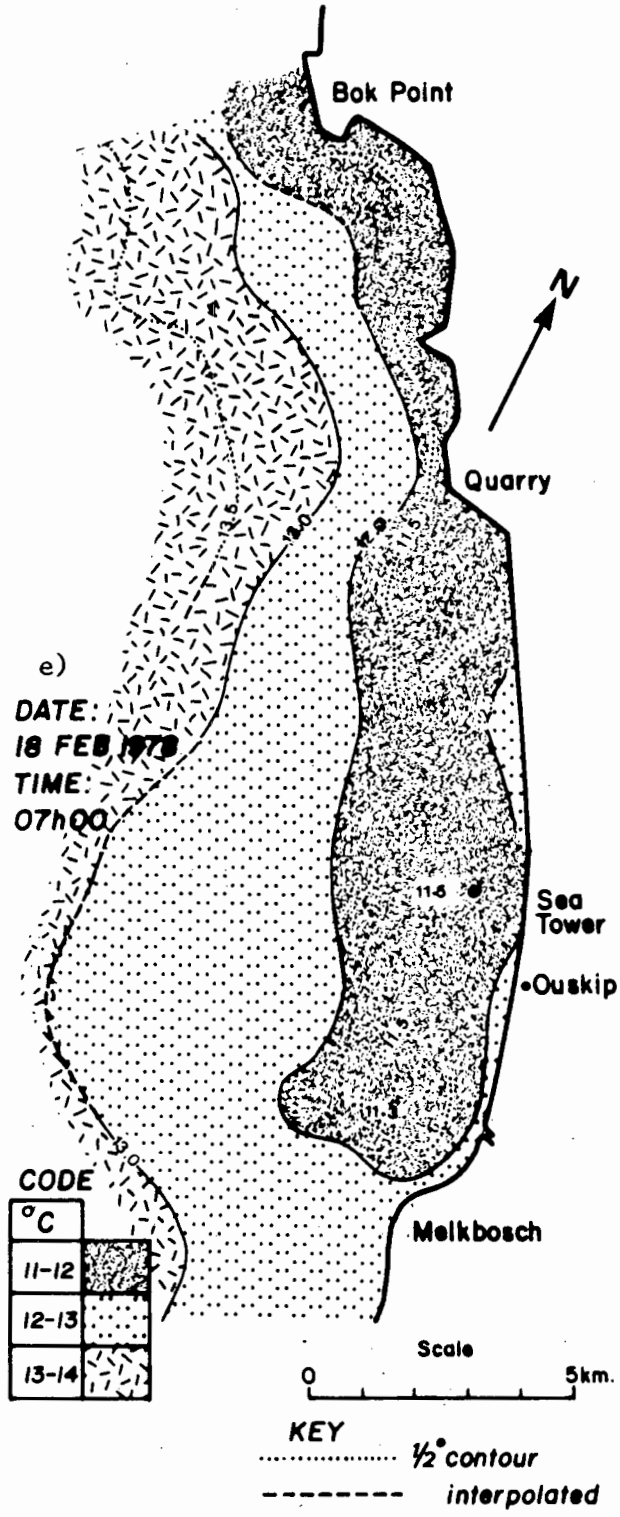

FIG. 4.2.0 AIRBORNE RADIATION THERMOMETRY (ART) DERIVED SEA SURFACE TEMPERATURE MAPS FOR THE AREA MELKBOSSTRAND TO BOK POINT FOR THE PERIOD 14 TO 18 FEBRUARY 1978

direction is also reported by Stuart (1981) for the Peruvian upwelling and by Kamstra and Nelson (1983) and Taunton-Clark (1985) for the Cape Peninsula system and by Send, Beardsley and Winant (1987) for the northern Californian shelf.

Sequential Set of Sea Surface Temperature Maps

In Section 4.3.1 a wind event cycle for 14 to 18 February 1978 is described which is now illustrated with a sequential set of SST maps in Fig. 4.20a-e. The data are derived from ART surveys described in Section 1.5.4.3.

This set of SST maps also serves to validate ART data for non calm conditions in that the timing of the survey coincides (not always simultaneously) with the temperature section data presented in Sections 4.2.2.1 and 4.2.2.2 and gives a reasonably good correlation between the two. The set starts on the 14th of February under northerly wind conditions and shows in Fig. 4.20a fairly homogenous distribution of warm water from Melkbosstrand in the south to Bok Point in the north. On the 16th the South

Atlantic high ridges in to the south of the continent and strong southerly winds result in a marked change in the SST map (Fig. 4.20b). The focus of cool upwelling water just north of Melkbosstrand is again prominent. The dotted contour line is for the 11.5 °C isotherm which encloses the coldest water. This feature grows considerably in size in the next two illustrations (Fig. 4.20c and d) but on the 18th as the wind slackens under shallow ESE conditions the area enclosed by the isotherm for 12 °C and cooler shrinks and the 12° isotherm moves closer inshore as warmer waters approach, initially near the northern sector.

Features of this sequence of up and downwelling include the following. During the upwelling phase (Fig. 4.20b, c and d) there occurs on the windward "capes" at the Quarry and Bok Point warmer waters than in the lee of Melkbos Point which supports the model of Hua and Thomasset (1983) (Fig. 4.19). As the upwelling event continues the upwelling centre grows larger than the initial "focus" area and extends seawards and alongshore to be joined from the south by similar upwelled water (Fig. 4.20d). Advection seems to play a significant role. An interesting feature is a narrow band of warmer water that occurs inshore of the cold upwelled water. ART survey flights were deliberately flown in the early morning (07h00) in addition to later in the day to check on insolation effects in the shallow nearshore waters. Comparison of the early morning flights (Fig. 4.20c and e) with the later flights (Fig. 4.20b and d) confirm that the warm band is most intense in the afternoon and is certainly

due to insolation effects. Hashimoto and Uda (1982) observe a nearshore thermal band of similar scale and gradient, 2 to 3 °C per 1 km, at a long sandy coastline and attribute it to the natural thermal diffusion from the heated beach to the sea. The present site also has a relatively wide sandy beach and insolation on this certainly contributes to the observations. The thermal band is widest near the quarry site and narrows towards Melkbosstrand. Opposite the sea tower site it is narrower and may not contribute as noticeably, to temperature measurements there. Such diurnal insolation effects are discussed further in the next chapter. The spatial character of the site is summarized in Section 4.5.

The offshore extent of the survey is not sufficient to reveal if there is any marked frontal feature during the upwelling phase. During the decay phase there is no obvious sharp front as observed on 12 Nov (Fig. 4.18b). This is probably because that occasion had fresher and longer duration onshore winds and even a wind reversal with 1 hour of NW whereas on the 16th Feb at the early time of the survey there had been only a few hours of light onshore winds.

4.4.2.2 Vertical Temperature Patterns

In the discussion on the thermocline structure cycle 4.3.1.2 and the case studies for the Csanady model (Section 4.3.2.2) vertical temperature sections for various lines from Melkbos Point to Ou Skip were presented in Fig. 4.14a-d, Fig. 4.16a-c and Fig. 4.17a-c. These figures are referred to here to illustrate the spatial variability of the temperature structures in three dimensions.

At the outset the lack of true synopticity (simultaneity) between the times for the surveys of a set of transect lines is stressed. Due to the rapid evolution of this upwelling system an hour or two's difference in the time of the survey which is indicated on each transect line in the figures can cause significant changes in the vertical structure of the temperature. This may result in errors of interpretation when lines are compared for spatial differences since on occasions temporal differences may be as great. Nevertheless some spatial trends are observed.

There are definite spatial differences in the temperature structure even with the 1 to 2 km lateral spacing between lines. During an upwelling phase line 2 which is about 1 km north of Melkbosch Point confirms the preferential upwelling observed there with ART surveys. A slight doming of colder water is seen on occasion near the inner stations (Figs. 4.14c and 4.16b).

Line 1 at Melkbos Point is characterized with more densely packed isotherms near the surface eg Figs. 4.14a and 4.16b than the lines to the north. Line 1 often has cold bottom water closer inshore than line 2 but at the same time the shallower isotherms are not inclined as steeply towards the surface as those at line 2. The colder inshore bottom waters at line 1 supports the more three dimensional aspect of the upwelling dynamics in that the compensation onshore bottom flow is expected to have a generally longshore component with a lesser onshore component. Lagrangian current data confirms this (Section 4.4.3). Thus the colder water appearing on the surface at the focus of upwelling on line 2 actually moves in obliquely round the corner from nearer the bottom to the south.

The relaxation phase shows the ingress of a warm water layer less than 5 m thick from the offshore area (Fig. 4.14d) for the 18th February. The corresponding SST map for this day but at an earlier time of 07h00 (Fig. 4.20e) indicates the warmer water is moving inshore first at the north. The surface temperature distribution in the vertical temperature data of Fig. 4.14d may support this contention but because of the relatively light winds on the day and the fact that the lines have a similar mid depth to bottom isotherm pattern the temporal differences between the lines (Line 2 09h50, Line 1 11h50 and Line 3 13h20) may be important and if taken in the sequence just bracketed indicates the consistent shoreward return of the warmer waters with a possible progressive insolation contribution.

The bathythermograph technique and the spacings used to collect the temperature section data is not suitable to reveal short wavelength (<1 km) internal waves. The waviness observed in some sections indicates some wave structure is possibly present. Boyce (1977) using a towed thermistor array has observed a rich field of internal waves present particularly near the upwelling front. He considers that below the scale of 10 km the evidence of meanders and patchiness support the importance of buoyancy and internal wave propagation effects in vertical mixing dynamics of an upwelling system.

The vertical thermal structure data unfortunately do not extend far enough offshore to link up with other larger scale data but they do confirm the essential three dimensional nature of the localized upwelling system and support the SST map findings.

4.4.3 Current Spatial Variability

Of all the variables involved in characterising the dynamic upwelling processes, currents are certainly of great importance, yet detailed current data are a shortcoming of this study. In fact even for the larger scale Benguela upwelling region it is only in recent years that time series data of currents are becoming available (Nelson and Hutchings, 1983, Nelson and Polito, 1987 and Holden, 1987). Spatial distribution of currents in the study area is obtained from Lagrangian techniques. Good synopticity is obtained by using dye floats dropped from an aircraft over a wide area. Details of this technique and that of boat deployed current drogues is given in Section 1.5.4.

A reasonable spatial coverage of surface (-1 m depth) currents is obtained with the air dropable drogues. Data on deeper currents is sparse. Not so many boat deployed drogues for deeper currents are used and such deployment lacks adequate synopticity. Measurements were obtained under various wind conditions. For light winds and calms additional measurements are reported using the radar tracked drogue technique (Section 1.5). The currents tend to form two or three distinct patterns.

Southerly alongshore winds

With moderate to strong southerly alongshore winds the surface currents are also alongshore but about 10° to the left of the wind giving a net offshore displacement. The surface currents reach just less than 3 % of the wind's speed except inshore of about 1 km where they are weaker. In the corner just north of Melkbos Point the surface currents are also reduced in speed but tend to remain parallel to those further offshore. The net offshore flow relative to the local coastline orientation in the corner are still actually higher than a few kilometers to the north or south. North of the sea tower and near the quarry there is a tendency for greater offshore surface flow beyond 1 km from the coast. A schematic representation of currents is given in Fig. 4.21a.

The deep currents in the bottom third of the water column associated with the southerly winds are generally about 20° to the right of the surface current giving a net onshore flow. The deep current's speed is always less than the surface speed and often less than 20 % of the surface speed. The difference in current speed above and below the thermocline were illustrated in several case studies in section 4.3.2.2. The differences varied from 10 to 20 $cm.s^{-1}$ and were significantly lower than predicted. As one approaches closer inshore than 3 km along the transect line north of Melkbos Point the bottom current vector progressively swings more to the right away from the

surface currents vector until it sometimes exceeds an angular separation of 50° and is almost normal to the local coastline. This behaviour of the bottom current in the Melkbosstrand corner and the surface divergence supports the dynamics of the focus of upwelling observed there.

Southwesterly winds

With southwesterly winds the surface flow is more onshore with the bottom currents now turning to the left of the surface vector to give a compensating offshore flow. Again the current in the Melkbosstrand corner are more sluggish. There is an overall downwelling tendency (see Fig. 4.21b).

Northerly winds

The current pattern with northerly winds is generally less uniform than with southerly winds. This is probably due to the fact that transition effects in the reversal of currents from north-going to south-going contaminate the latter. Currents during multiday northerlies are not surveyed so observation of uniformity is less common than with southerlies which are more persistent during the surveys. In particular there is confusion in the current patterns near Melkbos Point. On occasions a general south-going current develops over the whole area except where a sluggish counter clockwise circulation tends to occur just north of Melkbos Point with fresh north westerly winds (Fig. 4.21c). Data on deep currents are sparse with northerly conditions and firm trends cannot be deduced.

Light winds and calms

For light winds with a speed of less than 3 $m.s^{-1}$ and calm conditions the technique of radar tracked current drogues is used (Section 1.5). The main advantage of the radar is unattended tracking for extended periods that on one occasion exceeded three days. Under light air conditions the currents are generally weak and spatially varied. Drogues set at a 1 m depth only one or two kilometers apart often travel in opposite directions for several hours. Average current speeds over a 12 to 24 hour period at 1 m depth are sometimes lower than 0.05 $m.s^{-1}$ and at 6 m depth can be less than 0.01 $m.s^{-1}$. Directions are more commonly up or down the coast but onshore and offshore behaviour is also noted. Some evidence for rotary inertial currents is found (Bain and Harris, 1975ff), when surface speeds of 0.11 $m.s^{-1}$ are observed in circular anticlockwise current trajectories with a radius of about 1 200 m. On that occasion the net displacement over 3 days had an average of 1.5 km per day at the surface and 0.7 km per day at 6 m depth. On another occasion of

sluggish flow a slight onshore and offshore movement apparently correlating with the tides is observed.

Spatially the consept of a CBL includes a change in current structure as one moves offshore. Inshore, within the friction dominated region, linear currents predominate while further offshore rotary inertial currents become dominant (fig. 1.1). Evidence for this is deduced from surface current rose data of van Ieperen (1971) for a transect off Melkbosstrand Point. This shows that the inner most station at 1 km, depth 10 m has the most linear polarized current rose while as one moves offshore the linear dominance decreases and numerous other directions start appearing in the rose diagram until at 5 km offshore, depth 40 m six directions are more equally prevalent. Additional evidence for inertial currents and CBL structure is given in the next chapter. The limited data suggest that there may be a CBL flow in the study area.

There are no obvious steady north or south going alongshore currents inshore of 6 km which is probably inside of the proposed coastal boundary layer, the dynamics of which are controlled largely by local wind stress. Any net currents in this region over a period will be determined by the dominant wind direction. The net southgoing current proposed by Nelson (1983 and 1985) and Nelson and Polito (1987) for this coastal area is to be sought further offshore.

A final aspect of the spatial distribution of currents is that due to wave generated currents. Besides the longshore currents associated with wave forces in the surf zone and enhanced wave generated circulations near small headlands and embayments (Uda and Hashimoto, 1983 and Gunn, 1977b) large rip current systems are observed under appropriate conditions. When wave heights are greater than 7 m several rip currents spaced between Melkbosch and the quarry site have been observed to extend 3 km offshore. Such large waves generally occur in association with NW gales (Section 4.2.4) and the ensuing rip currents and 1 km wide surf zone play a dominant role in the dynamics on the space scale studied, but should better be included at the mesoscale temporal scale of the next chapter.

The temporal character of the currents during an event cycle has not been discussed partly because time series Eulerian data are not available and because Lagrangian data are too disjoint in time. The rate of change of direction and accelerations of the current at transition in the wind regime is unknown. A general outline of the change of the current system during a wind event cycle could be deduced from the description of the currents given for the wind categories above.

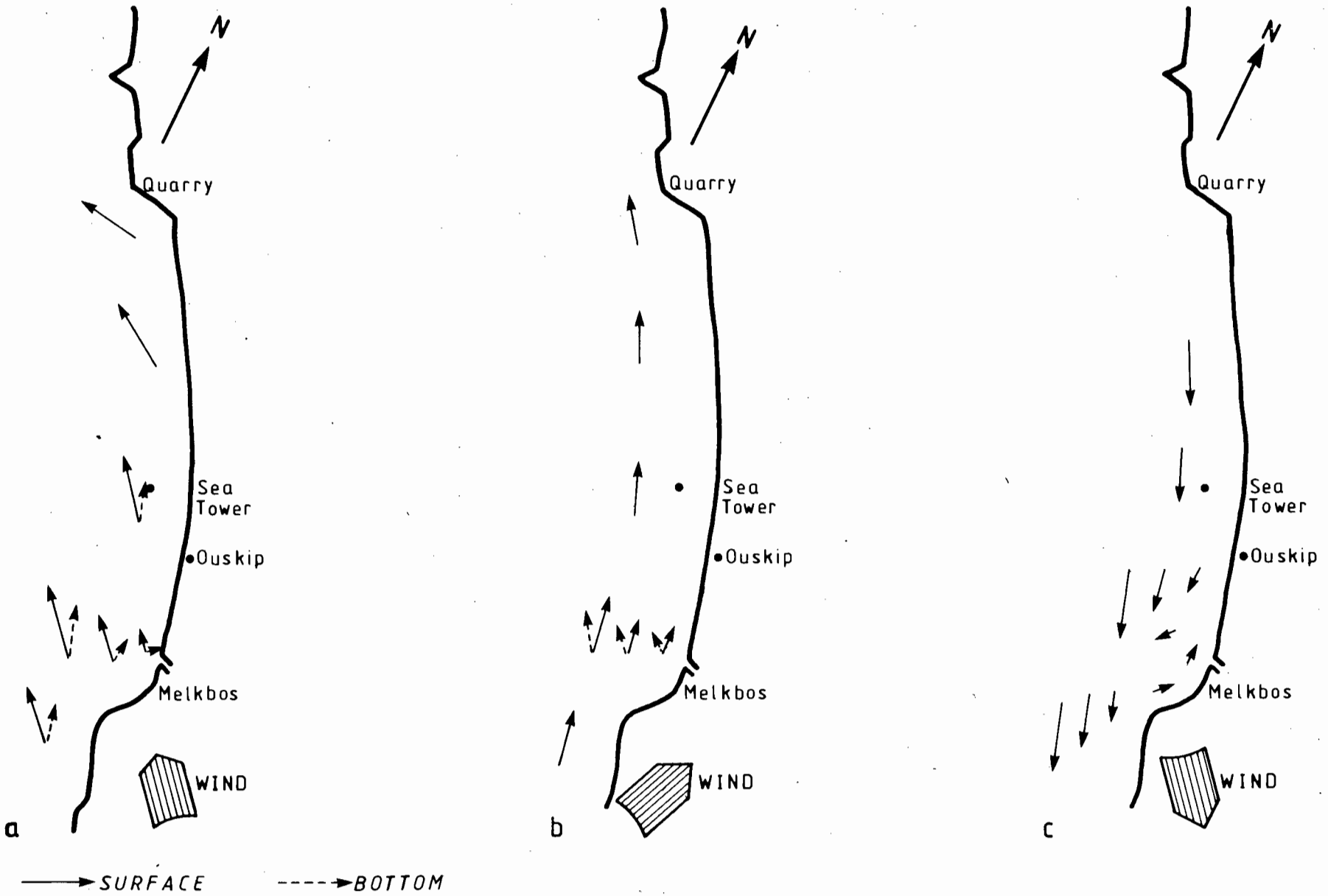

FIG. 4.21 REPRESENTATION OF LAGRANGIAN CURRENTS IN THE VICINITY OF MELKBOSSTRAND FOR DIFFERENT WIND CONDITIONS
a) SOUTH EAST WINDS b) SOUTH WEST WINDS c) NORTH WEST WINDS

Overall discussion on the spatial variability will be reserved for later in Section 4.5.

4.5 DISCUSSION OF THE EVENT TIME SCALE

The aim of characterizing the event time scale has been achieved through considering wind, temperature and wave time series data, the wind forced displacement of the thermocline and various spatial aspects. The importance of the event time scale alongshore wind in bringing about temperature changes as a response to upwelling dynamics has been established through the various approaches adopted in this chapter. A distinctive small scale focus of upwelling has been revealed at the coastal offset at Melkbosstrand.

The LF and ILF time series data reveal that the distinctive character of both the wind and sea temperature (and wave) data is that they occur in multiday groupings. The duration of these groupings varies from 2 to 10 days for the ILF data and extends to about 20 days for the LF data where the trends are still included. These groupings or events are associated with the synoptic scale barometric forcing factors but do not show any dominant periodicity in the spectral analysis. There is however a dominance for an anticlockwise sence of rotation for the atmospheric forcing. The across-shore autospectra have a flatter response at the lower frequencies which highlights the greater spectral energy of the alongshore winds at this time scale. For a series of annual pressure spectra for the Cape Town area Kamstra (1987) reports peaks between 15 and 30 days but no consistent peaking of energy occurs and he highlights the significant interannual variability between spectra; in particular the 6 day peak has considerable interannual variability. In the secondary process of the wind and by further association the sea temperature reported here, distinct energy peaks become lost in the event fluctuations as reported for currents by Lee & Mayer (1977).

Both the wind and temperature spectra do however show a broad maxima between about 8 to 15 or even 20 days. Some of the spectra of Preston-Whyte and Tyson (1973) also show a broad peak or shoulder at 20 days and Kamstra (1987) reports a tendency for a spectral plateau between 5 and 20 days. The dominance of the total kinetic energy variance of transient eddies, with periods less than about two weeks, in the wave structure of atmospheric processes at this latitude is noted by Trenberth (1981). Similarly, Holden (1987) observes on the larger scale near Cape Columbine a spectral peaking for wind and current data at 16 days (and shorter periods) and Nelson and Polito (1987) observe current periodicities of 8 to 10 days in the Yzerfontein area. These all point to synoptic scale processes with

periods between about 5 and 20 days being important for the study area. The filter used here does not allow for spectral investigation of longer periods which extend into the upper regions of Monin's (1977) classification of synoptic time scales, although Kamstra (1987) suggests an increase in pressure spectra energy for periods exceeding 30 days.

The event nature of the wind is well illustrated with the cumulative Ekman transport (CET) plots (Fig. 4.6). Such plots show for wind data that of all the seasons the winter regime is the most variable inter-annually, in that failures of significant northerly events do occur. This has an effect on the average seasonal winter sea temperature, see Chapter 3, but there is also a distinctive seasonal dependance for the sea temperature fluctuations. In winter with generally onshore winds prevailing the temperatures are fairly homogeneous with a small standard deviation of less than 1 °C whereas during the remainder of the year when southerly winds predominate the fluctuations are much larger with standard deviations of about 2 °C with the spring period being rather more variable. The distinctive seasonal temperature character, Fig. 4.2 and Fig. 4.5 prompt consideration of the transition between regimes.

Compared with other regime changes we observe a definite and rapid transition in sea temperature character from winter to spring. The change is brought about by a single southerly alongshore wind event that in order to be successful needs to have a cumulative Ekman transport exceeding about $3x10^9 g.cm^{-1}$ and a duration 5 days or longer. The temperature changes are indicative of dynamic changes but without time series current data the real nature of the transition cannot be defined although the observed character at the local scale is certainly linked to larger scale changes as proposed by Strub et. al. (1987b) for the spring transition off Western North America. The large scale spring transition there has features of a non-local nature that point to a coastal trapped wave contribution (Strub et. al., 1987b) that propagates polewards. Locally, Holden (1987) and Jury, MacArthur and Shillington (1989) gives evidence of poleward propagating barotropic shelf waves, but no seasonality is noted. The minimum CET magnitude for transition locally of $3x10^9 g.cm^{-1}$ agrees reasonably well with Huyer's value of $1,3x10^9 g.cm^{-1}$. The absolute value of the CET value is not of prime concern since inaccuracies are present due to uncertainties in the stress coefficient and in the winds spatial distribution offshore and of course in the inadequacies in the assumption to use the classical Ekman relation for such shallow waters locally. The ratio of CET values for establishment of the spring transition versus re-establishment of winterlike conditions show more disparity viz 1.3:4 for Huyer and 3:2 locally. The local study relies on a

temperature signature and not a direct larger scale current observation - the shallow nearshore waters respond quickly to relaxation in southerly wind stress and to onshore winds (see also Chapter 5) and what may be merely a near surface effect in larger scale offshore regions, affects the whole water column locally and the result of a relatively small downwelling event can mimic the winterlike temperature conditions. A larger event would be required to achieve dynamic reversal on the larger scale.

A generalization is that larger offshore CET events produce larger temperature drops although very large events reach a minimum temperture after a few days and then maintain the low temperature. The sequence and magnitude of off and onshore events also affects the temperature response and some offshore events have only slight temperature effects because of preceeding relatively large onshore events. Temperatures increase with merely a relaxation in southerly windstress but greatest increases occur with NW winds. This is particularly true during the warm anomaly of November/December 1976. SSE winds are most efficient in generating a temperature decrease.

The bimodal temperature response character of the seasonal data has its counterpart in individual minimum temperature events in spring and late summer. The former corresponds to Andrews and Hutchings (1980) observation of the ingress of the coldest water onto the shelf during September-October together with strong southerly winds. The March-April minima seen here do not correspond with particularly strong southerly winds but we propose, based on limited observational evidence from the CET plots that the duration of the events at that time are somewhat longer than average and are also effective in bringing cold water into the region. Other possible larger scale effects could also play a role; see Section 3.8.

The correlation analysis shows clearly (Table 4.2) the dominance of the alongshore wind - temperature response (correlation coefficient greater than 99,9%) after a one day lag in the temperature. Although not tabulated the correlation coefficient remains above 95% for several days indicating a synoptic time scale forcing process. In contrast the across-shore wind, although significantly correlated at zero lag quickly falls to near zero correlation with one day's lag indicating some process is operating at the diurnal time scale but not at the longer synoptic time scale. The correlation in the winter months is much poorer due to the lower incidence of southerly upwelling conditions and the greater seasonal depth of the thermocline. For the wave height data however, the winter regime winds have the best correlation which peaks with one day's lag, showing the importance of more distant swell generation.

The barometric forcing of an event is seen to follow the sequence - post cold front SSW wind - ridging anticyclone with deep SE winds - pre-coastal low - coastal low passage - wave cyclone with westerly winds. The thermocline structure alters in sympathy, with temperatures becoming cooler as upwelling progresses - "stable" cool temperatures obtained - then a collapse of upwelling with the ingress of a warm thin surface layer - and finally full downwelling of the thermocline. The initial upwelling phase reveals a bottom-up temperature response as cool bottom waters migrate inshore. The passage of a coastal low is implicated in the rapid decay of the upwelling when a marked top-down temperature signal is observed, which may have some diurnal insolation contribution (see 5.3).

The possibility exists that high wave action can erode the thermocline. Maximum wave heights of over 7 m have been observed at the site. However, three year average significant wave height data show that a 5 m significant wave height occurs about once per year while a significant wave height of 3 m or greater occurs 20 times per year for a duration of 12 hours or longer (CSIR, 1976).

Inspection of concurrent wave and temperature data indicates that generally for a significant wave height of 3 m full mixing of the thermocline does not occur. For significant wave height of 4 m and greater, isothermal conditions can be reached within 12 hours. On several occasions a temperature gradient is still observed even after a day of such large waves. Inspection of the temperatures at all three depths 2 m, 5 m and 8,5 m does not generally reveal a progressive erosion of the thermocline from the top down. Often the lower two temperatures are isothermal before the whole water column is mixed.

It is proposed that the time of arrival of the wave event relative to the upwell downwell cycle is a complicating factor. Further the large waves are associated with strong winds which also promote mixing and modify the thermocline response. Large rip currents occur that further modify the dynamics. The most frequent occurrence of large waves is in winter when the thermocline is either weak or absent. The lack of current data precludes further comment on winter time dynamics.

Without closer study the effects of wave versus wind mixing cannot be clearly separated. Bottom turbulenc also has its effects but a greater number of temperature probes over the water column would be required to start to investigate such effects.

Limitations of the Csanady Model

The quantitative response of the thermocline to an equatorward alongshore wind impulse is assessed with the help of the two layer inertial adjustment model of Csanady (1977a). This model is idealistic yet at times fair agreement with observations is obtained.

The chief limitations in the field data available for comparison with the theory are a) the relatively short transect lines of 6 km; 10 to 15 km would be preferable, particularly for the stronger wind events; and b) the inadequate data used to estimate the current velocity difference across the thermocline.

Other aspects of the field data such as: departure from an initial assumed two layer system; deepening of the top layer at the offshore boundary as the upwelling developes; and wind impulses that include onshore components and diurnal modulation, highlight the complexity of the real situation that cannot be adequately met with the model's assumptions.

Parts of Csanady's theory that are not tested include the cases for a second impulse and steady across-shore winds. For the former case the limited offshore extent of the data hinders the observation of change of thermocline shape with a second impulse. However, various transects were inspected to check for any thermocline overshoot to greater depths that is expected from a 2nd impulse, but no obvious candidate cases were revealed. A general waviness of the isotherms is noted in some cases and may be attributable to the influence of near-inertial oscillations that, if of a suitable wavelength, can modify the nearshore thermocline shape (Csanady, 1977a). The case of steady across-shore winds is not tested because at the time of the various transects synoptic conditions resulted in no strong across-shore winds. Any across-shore component tended to be modulated diurnally by the land/sea breeze effect and was not steady. Brief

mention is made of some possible across-shore effects in the discussion of cases 3/2 and 4/2. The limited offshore extent of the data precludes any worthwhile study of coastal jet characteristics discussed by Csanady (1977a).

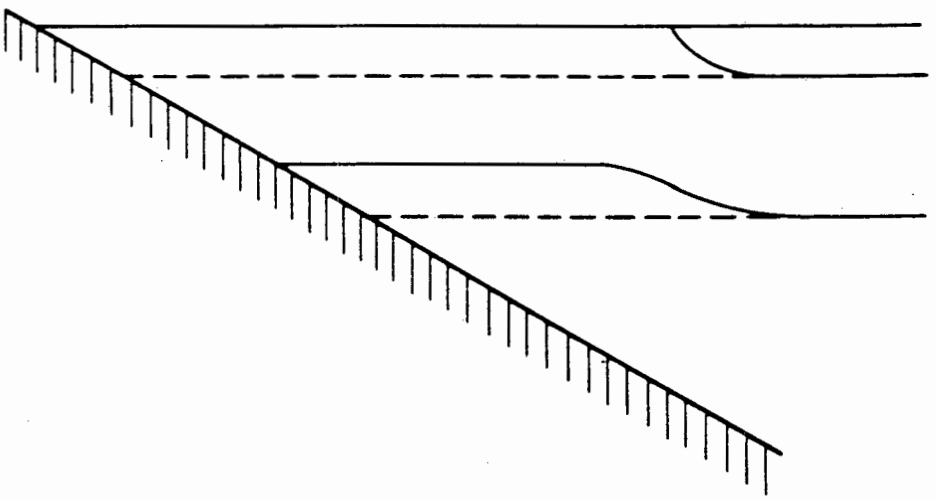

FIG. 4.22 REPRESENTATION OF A THREE LAYER FLUID ON AN INCLINED BEACH, AFTER FULL UPWELLING. FROM CSANADY (FIG. 11, 1982b)

In a subsequent more recent paper Csanady (1982b) developes the theory further to present a three layer model. He points to observational evidence that a wind stress event successively "peels" off layers of progressively denser water leaving the lower layers only slightly affected. The same behaviour is noted in the upwelling cases discussed earlier particularly that of Fig. 4.17b and c for 7th to 8th February 1978, when many warmer layers are peeled off but the 11 °C isotherm remains at a fairly constant depth of about 20 m. No calculations using Csanady's (1982b) three layer model are attempted but a visual comparison of field data with the idealized shape (Fig. 4.22) of the isotherms after full upwelling shows that there is some similarity. See line 1 on 7th February (Fig. 4.17b) and all the lines on 17th February 1978 (Fig. 4.14c). The three layer model can therefore probably give better results than the two layer model for certain cases.

The conclusion is that for suitable "two layer" situations the Csanady two layer inertial model is applicable to the site data when medium strength wind events are experienced and that it is probably also justified for large events that drive the front beyond the 6 km offshore data limit. The current data are less certain but the current velocity differences measured tend to support the model, although frictional dampening seems to be quite strong.

In an attempt to further characterize the dynamics of the study area, the criteria of Clarke and Brink (1985) for testing the shelf's dynamic response to synoptic wind forcing is applied using local data, even though the criteria is derived for much deeper waters. For a barotropic response $N^2\alpha^2f^{-2}<<1$ (page 1.11). The method described for determining the average N^2 and α values in the shelf-scale case on page 1.34 is applied to the local scale for the transect line off Melkbos Point in Fig 4.14a). The averaging positions are 1,5, 3, 4,5 and 6 km offshore, with the vertical step being 1 m. The density data, interpolated from Table 4.5, are used in estimating N^2 and the average slope, α, is derived from the four positions for each of the Melkbos Point transects in Fig 4.14 a to d. The average values determined are $N^2 = 3{,}36\times10^{-4}$ rad.s^{-1}, $\alpha = 3{,}5\times10^{-3}$ giving a criteria value of 0,61. Choosing other transects with different stratification for such calculations yields criteria with values varying from 0,1 to 2,0. Such values do not point to a universal dominant barotropic response. The attempt therefore to characterize the dynamic response by extending the criteria of Clarke & Brink (1985) to shallow local waters has suggested an ambivalent response, as was found for the larger scale. In any case the actual baroclinic or barotropic nature needs empirical confirmation from extensive current data which do not as yet exist.

Spatial Variability

Earlier sections have shown a remarkable degree of spatial variability in this region. The space scale for localized upwelling and structure on the front particularly during the relaxation phase has been demonstrated to be of the order of a few kilometers. The horizontal spatial variability in sea surface temperatures coupled with the vertical variability in the water column have indicated the complexity of a truly three dimensional system. Implicated in the variability is the wind field and the coastline orientation. The shadow in the lee of Table Mountain causes a relatively calm area on the western boundary of the study site and results in a positive wind stress curl. This and the associated Ekman drift at the adjacent coast results in a narrow band of coastal upwelling. The new finding is the localized focus of upwelling occurring at the change in coastline orientation at Melkbos Point. Because of the relatively smooth bottom

topography there and the lack of nearby orographic effects the change in coastline relative to the wind is considered the major cause of this localized site of upwelling. This cause finds some support from the theoretical model of Hua and Thomasset (1983). Bottom topography may play a part in steering the filament of cold upwelled water from Table Bay, between Robben Island and the mainland.

A particularly sharp front exceeding 3 °C in 1 km is observed during a relaxation phase, when meanders and patchiness of a scale 1 to 10 km is also prevalent. Boyce (1977) considers that at a scale greater than 10 km the geostrophic adjustment process dominates; (the two layer Csanady (1977a) model assumes a geostrophic adjustment process) and at the smaller scale of 1 to 10 km associated with meanders and cutoff pools, internal wave propagation and buoyancy effects are important. There is no direct measured evidence of short internal waves in this study and it may, in future studies be rewarding to search for such waves near the sharp front.

The earlier literature studies revealed (p 1.10) that there was a common depth of about 30 m for the boundary of the coastal boundary layer, the width of which was quite variable (Murthy and Dunbar, 1981; Csanady, 1980; Schwing et al., 1985; Mitchum and Clarke, 1986a). It is proposed from the limited evidence presented that some type of coastal boundary layer (CBL) exists in the study area with a seaward boundary at about the 30 m depth contour (~6 km offshore). Such a CBL has a dynamic identity different to that of further offshore waters which are possibly more affected by larger scale and remote processes. The delineation of such a boundary layer and its current structures awaits further field studies which could fit into Boyce's (1977) idea for regional coastal climatologies. Further comment on the CBL is found in Section 5.3.2.

These findings on spatial dynamics and event scale processes of the area do have relevance to coastal ecological studies and disposal of pollutants. The thermal nature of the natural sea conditions has particular relevance to the fate of cooling water discharges from the nuclear power station that has been built a few kilometers north of Melkbosstrand. Besides highlighting the focus of upwelling, the ART study has revealed the spatial feature of a diurnally modulated thermal band less than 2 km wide along the sandy coastline. This feature and other mesoscale phenomena with time scales between one day and a few hours are discussed in the following chapter.

TABLE 4.1

SIMPLE STATISTICS OF LOW FREQUENCY DATA FOR WINDS AND TEMPERATURES

DATE	PERIOD	TEMPERATURE VARIABLE	TEMPERATURE MEAN °C	TEMPERATURE STD DEV	WIND VARIABLE	WIND MEAN $m.s^{-1}$	WIND STD DEV
1975	Year	5 m	13,0	1,7	N/S	-1,3	4,8
1975	Jan-Apr	5 m	12,7	1,4	N/S	-2,6	4,5
1975	May-Aug	5 m	14,5	0,5	N/S	+1,1	3,6
1975	Sep-Dec	5 m	11,8	1,7	N/S	-2,5	4,6
1976	Year	2 m	13,0	1,8	N/S	-1,2	4,5
1976	Year	5 m	12,8	1,9	-		
1976	Year	8 m	12,5	2,0	-		
1976	Jan-Apr	2 m	12,1	1,3	N/S	-3,1	3,9
1976	May-Aug	2 m	13,6	0,9	N/S	+0,6	3,6
1976	Sep-Dec	2 m	13,2	2,5	N/S	-1,2	4,8
1977	Year	2 m	13,5	1,7	N/S	-0,8	5,1
1977	Year	5 m	13,2	1,8	-		
1977	Year	8 m	12,8	1,8	-		
1977	Jan-Apr	2 m	13,4	1,8	N/S	-2,2	4,0
1977	May-Aug	2 m	14,3	0,8	N/S	+2,0	4,3
1977	Sep-Dec	2 m	12,8	1,8	N/S	-2,1	4,1
1978	Year	-			N/S	-1,6	3,5
1978	Jan-Apr	2 m	12,8	1,6	N/S	-2,2	3,9
1978	May-Aug	-			N/S	+0,1	3,2
1978	Sep-Dec	-			N/S	-2,6	4,2

Winds have been rotated 20° to align with coastline

2 m = 2 meter depth

N/S - Alongshore Component. From north >0. From south <0.

TABLE 4.2
LINEAR CORRELATION COEFFICIENTS BETWEEN LINEARLY DETRENDED VARIABLES
INTERMEDIATE LOW FREQUENCY (DAILY VALUES)

Correlation Between Wind and Sea Temperature (2 m)

DATE	PERIOD	WIND COM	RECORD LENGTH DAYS	DEG OF FREEDOM	OBSERVED+ CORRELATIONS Co	Cm	LAG m DAYS	CRITICAL CORRELATION@ COEFFICIENT 95 %	99 %	99,9 %
1976	Year	E/W	340	134	-0,25	0,09	9	0,142	0,201	0,264
1976	Year	N/S	340	95	0,28	0,55	1	0,170	0,238	0,310
	Jan-Apr	N/S	94	25	0,42	0,74	1	0,323	0,445	0,568
	May-Aug	N/S	94	17	0,11	0,36	2	0,389	0,529	0,662
	Sep-Dec	N/S	94	27	0,32	0,61	1	0,312	0,430	0,550
1977	Year	E/W	340	-	-0,18	0,12	6			
	Year	N/S	340	83	0,31	0,55	1	0,180	0,251	0,330
	Jan-Apr	N/S		23	0,46	0,72	1	0,337	0,462	0,588
	May-Aug	N/S			0,16	0,42	2			
	Sep-Dec	N/S			0,38	0,67	1			
	Jan-Apr	N/S*			0,32	0,67	1			
	May-Aug	N/S*			0,21	0,50	2			
	Sep-Dec	N/S*			0,38	0,70	1			

* With 8 m depth temperature
@ From Underhill (1981) Table 5
N/S = Alongshore component
E/W = Across-shore component
+ Co = correlation coefficient at zero lag
Cm = maximum correlation coefficient at lag m

TABLE 4.3

LINEAR CORRELATION COEFFICIENTS BETWEEN LINEARLY DETRENDED VARIABLES

LOW FREQUENCY DATA (HOURLY VALUES)

Correlation Between Wind and Sea Temperature

DATE	PERIOD	WIND COM	RECORD LENGTH HOURS	DEG OF FREEDOM	OBSERVED CORRELATIONS Co	Cm	LAG m HOURS	CRITICAL CORRELATION COEFFICIENT 95 %	99 %	99,9 %
1976	Year	N/S	8784	95	0,37	0,52	23	0,170	0,238	0,310
	Jan-Apr	N/S	2880	70	0,43	0,68	18	0,195	0,274	0,358
	May-Aug	N/S	2880	49	0,11	0,27	192	0,23	0,32	0,42
	Sep-Dec	N/S	2880	-	0,40	0,59	30			
	Jan-Apr	N/S 8 m	2880	-	0,34	0,67	21			

TABLE 4.4
LINEAR CORRELATION COEFFICIENTS BETWEEN LINEARLY DETRENDED VARIABLES
INTERMEDIATE LOW FREQUENCY (DAILY VALUES)

Correlation Between Wind and Wave Height

DATE	PERIOD	WIND COMP	RECORD LENGTH DAYS	DEG OF FREEDOM	CORRELATION+ COEFFICIENT DAILY LAGS				CRITICAL CORRELATION COEFFICIENT			STD DEV WAVE HEIGHT*
					C_o	C_1	C_2	C_3	95 %	99 %	99,9 %	m
1975	Year	N/S	340	115	0,18	0,51	0,44	0,15	0,153	0,215	0,283	0,73
1975	Jan-Apr	N/S	94	34	0,29	0,48	0,42	0,24	0,279	0,385	0,498	0,66
	May-Aug	N/S	94	36	0,37	0,68	0,60	0,18	0,271	0,376	0,486	0,88
	Sep-Dec	N/S	94	41	0,19	0,60	0,41	0,06	0,254	0,354	0,458	0,65
1976	Year	N/S	340	-	0,06	0,38	0,41	0,21				0,69

* Wave height with zero mean for ILF data
+C_o = correlation coefficient, zero lag
C_1 = correlation coefficient, 1 day lag
C_2 = correlation coefficient, 2 day lag
C_3 = correlation coefficient, 3 day lag

TABLE 4.5
THERMOCLINE DISPLACEMENT CASE TIMES AND WATER LAYER PROPERTIES

Case/Line	Wind Event		Layer Properties				
			Top Layer			Bottom Layer	
	Start	End	Depth cm	Temp C°	Density σ_t	Temp C°	Density σ_t
1/1	78.02.16 11h00	78.02.16 17h00	1500	14	25,98	10	26,75
1/2	78.02.16 09h00	78.02.16 15h00	1100	14	25,98	10	26,75
2/1	78.02.16 11h00	78.02.17 14h00	1500	14	25,98	10	26,75
2/2 a)	78.02.16 09h00	78.02.17 12h00	1100	14	25,98	10	26,75
2/2 b)	78.02.16 09h00	78.02.17 12h00	1600	14	25,98	10	26,75
3/2	77.01.26 12h00	77.01.27 10h00	1400	16	25,54	12	26,38
4/2	77.01.26 12h00	77.01.28 10h00	1400	16	25,54	12	26,38
5/3	78.02.06 14h00	78.02.07 14h00	900	17	25,31	11	26,57
6/2	78.02.07 10h00	78.02.08 11h00	2000	16	25,54	10	26,75

TABLE 4.6
CALCULATED AND OBSERVED UPWELLING RESPONSE

Case/ line	Wind Stress Impulse	Minimum Impulse For Up= welling I_{min}	Internal Radius of Deforma= tion Ri	Predicted Displace= ment Y_o	Observed Front Position For Given Isotherm °C km				
	$cm^2.s^{-2}$	$cm^2.s^{-2}$	km	km	11°	12°	13°	14°	15°
1/1	48530	62990	3,2	-0,7		0	3,1		
1/2	57420	36730	2,9	1,7		0,7	2,1		
2/1	202920	62990	3,2	7,1		2,8	4,6		
2/2a)	209080	36730	2,9	13,9		2,5	>6		
2/2b)	209080	70830	3,2	6,3		2,5	>6		
3/2	84340	58190	3,3	1,5			1,8	2,2	
4/2	104830	58190	3,3	2,6			2,7	2,9	
5/3	53790	33770	3,6	2,1				2,0	3,4
6/2	169560	135930	4,1	1,0	1,7	>>6			

CHAPTER FIVE

MESOSCALE CHARACTER

C O N T E N T S

CHAPTER 5

MESOSCALE CHARACTER

5.1 INTRODUCTION

The high frequency (HF) data covering the range 0,5 cpd to 12 cpd are presented. They are obtained as residuals between the low-passed filtered and original hourly time series. The range coincides with Monin's (1977) classification of "mesoscale phenomena" for variability in the ocean. The phenomena which occur in this frequency range include diurnal winds, insolation, inertial effects due to the rotation of the earth, tidal effects and types of waves. The diurnally generated land/sea-breezes have a role to play in modulating coastal upwelling. Their effects have an interest for oceanographers and for meteorologists concerned with air pollution. For biologists the diurnal time scale is biologically significant in the economically important coastal waters (O'Brien, 1977). The diurnal coastal air circulation is also considered (Sonu et al, 1973) an important form of energy supply for nearshore and coastal processes such as wind-wave-current coupling and beach topography.

The significance of the different mesoscale frequencies and their corresponding forcing mechanisms will be established. Spatial and other aspects relevant to this scale will be addressed.

The literature on sea-breeze effects and insolation effects in shallow nearshore waters (<20 m depth, <10 km offshore) is limited. There is an apparent conflict in both observations and theory, particularly if comparisons are made with models and observations for deeper waters slightly further offshore. Bearing in mind that at this time scale, sea temperature oscillations can be produced by upwelling effects, inertial effects and/or insolation effects the observations from our local site will now be presented and an attempt at reconciling conflicting concepts will be made.

5.2 HIGH FREQUENCY WIND AND TEMPERATURE DATA

In the following sections we discuss the HF time series data of wind and temperature, their cross correlations and lags, and their spectral analyses.

5.2.1 Filtered Time Series Data

In this section a qualitative and semi-quantitative description is given of selected sections, representing summer and winter conditions, of the high frequency time series for the wind components and sea temperatures. As with the other frequency bands the wind data were resolved into components alongshore and across-shore. The data are shown for 3 week long hourly time series in the following figures:

5.1(a-d) high frequency data, January 1977; 5.2(a-d) raw data, January 1977; 5.3(a-d) high frequency data, May 1977; 5.4(a-d) raw data, May 1977, where in each case a) refers to alongshore winds, b) refers to across-shore winds, c) refers to temperatures at 2 m depth and d) refers to temperatures at 8 m depth. In each case 00h00 falls on the tick marks on the time axis, with equivalent tick marks on the curves.

The segments of data were selected after careful inspection of the full year long data sets. The January and May segments were considered to be fully representative of summer and winter conditions respectively.

The main feature of both the alongshore and across-shore winds and temperatures at this time scale is their diurnal nature. The strength and regularity however vary between the data and for different seasons and events. In general the across-shore winds have more regular diurnal character than the alongshore winds. This can be ascribed to land/sea-breeze effects (Jury, 1980 and Jury, Kamstra and Taunton-Clark, 1985).

5.2.1.1 Wind Characteristics

The high frequency residual plots for the two wind components e.g. Figs. 5.1a and b have positive and negative fluctuations about a detrended zero mean and as such the absolute sense is not preserved. The positive and negative (nominally from the north +, and south -; and nominally offshore + and onshore -) patterns are usually not symmetrical and vary with which wind, north or south in the absolute sense, is dominant at the time. For this reason the following discussion subdivides the characterisation into spring-summer and winter regimes, and into north or south dominant events. The north or south dominance or onshore offshore dominance is judged by reference to the raw (unfiltered) component data plots (Figs. 5.2a,b and 5.4a,b).

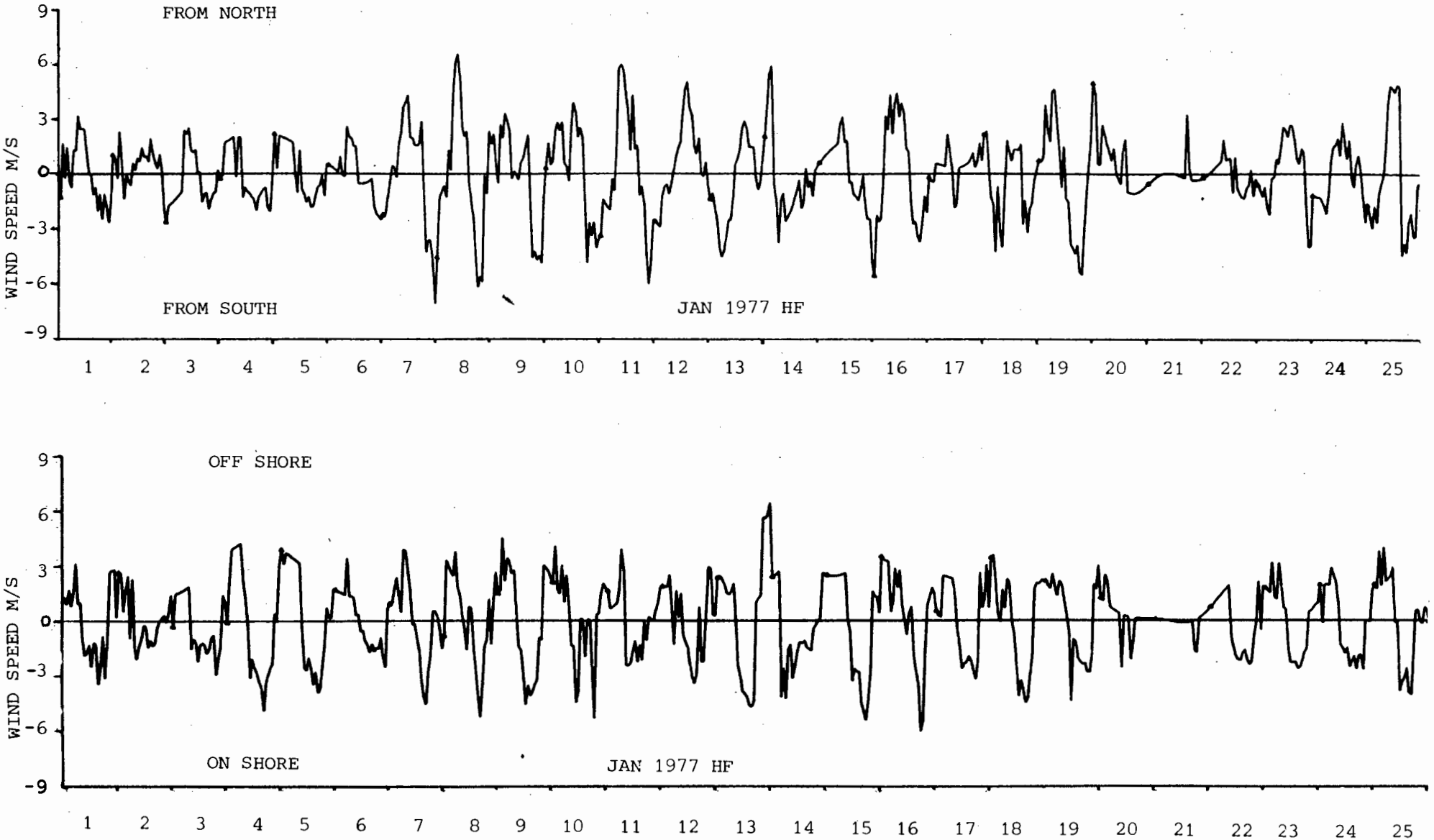

FIG. 5.1a,b TIME SERIES OF HIGH FREQUENCY FILTERED HOURLY DATA (ZERO MEAN) FOR OU SKIP WINDS FOR THE PERIOD 1 TO 25 JANUARY 1977. TICK MARKS EACH 24 HOURS. a) ALONGSHORE (NORTH) b) ACROSS-SHORE (EAST). THE WIND SENSE IS NOT ABSOLUTE

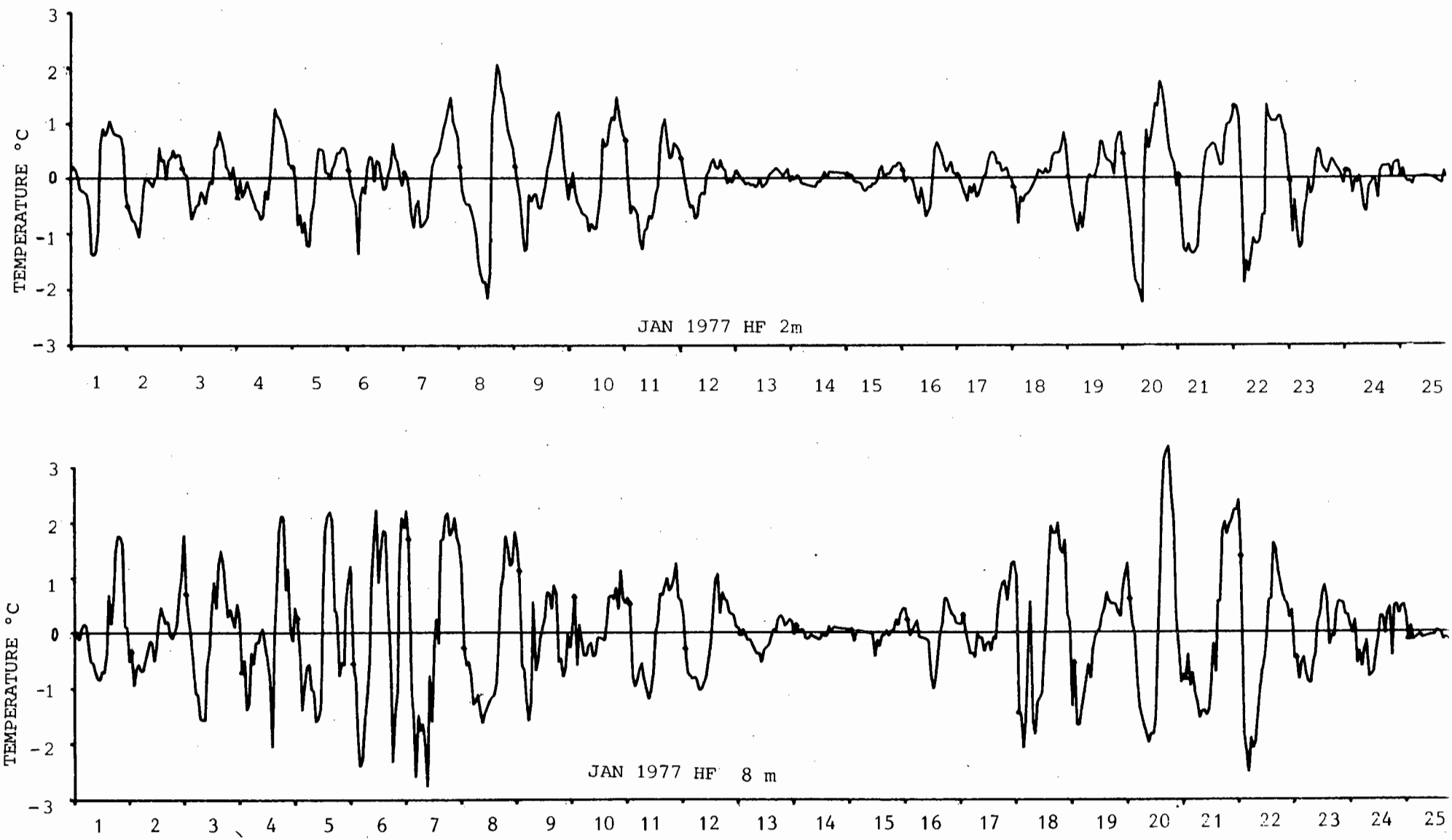

FIG. 5.1c,d TIME SERIES OF HIGH FREQUENCY FILTERED HOURLY DATA (ZERO MEAN) FOR SEA TEMPERATURES FOR THE PERIOD 1 TO 25 JANUARY 1977. TICK MARKS EACH 24 HOURS. c) 2 M DEPTH d) 8 M DEPTH

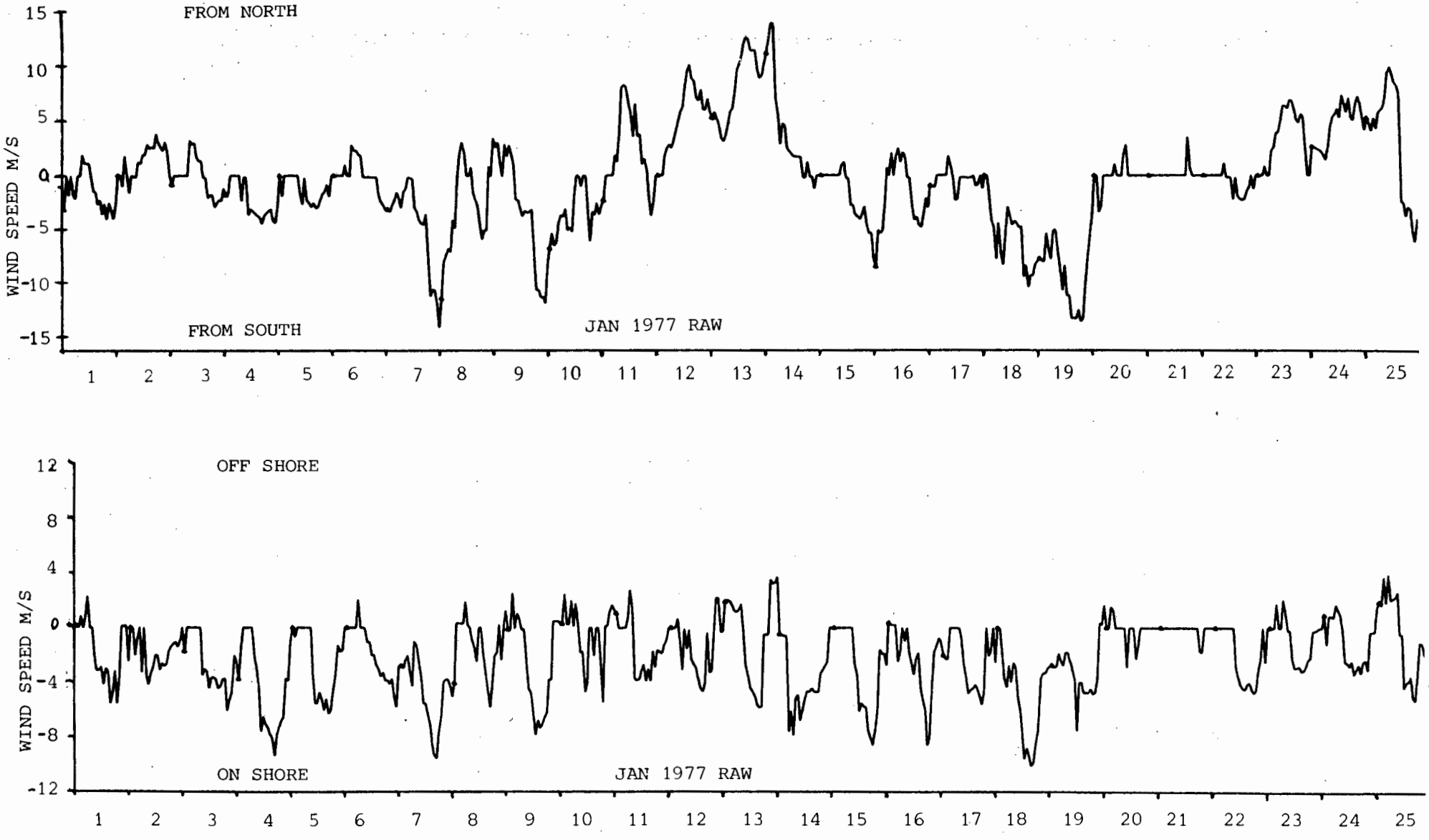

FIG. 5.2a,b TIME SERIES OF UNFILTERED (RAW) HOURLY DATA FOR OU SKIP WINDS FOR THE PERIOD 1 TO 25 JANUARY 1977 a) ALONGSHORE (NORTH) b) ACROSS-SHORE (EAST)

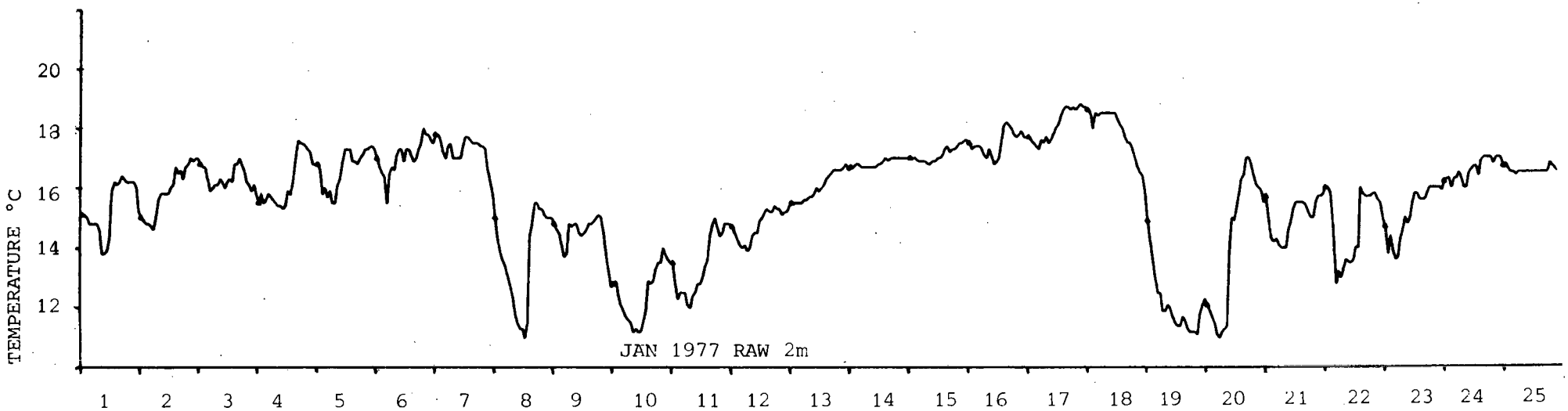

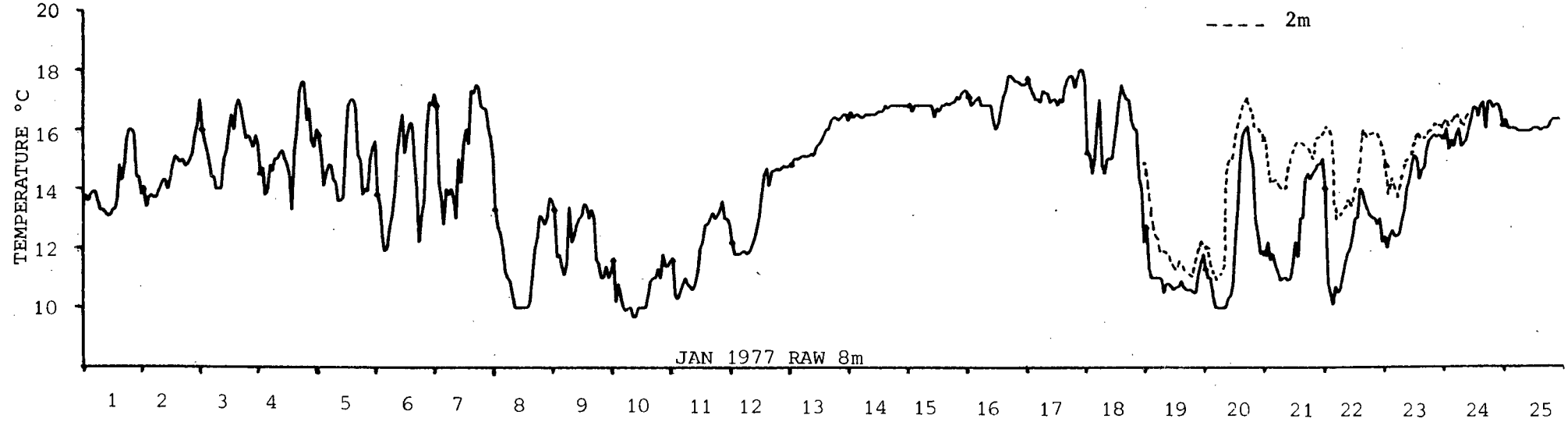

FIG. 5.2c,d TIME SERIES OF UNFILTERED (RAW) HOURLY DATA FOR SEA TEMPERATURES FOR THE PERIOD 1 TO 25 JANUARY 1977. c) 2 M DEPTH d) 8 M DEPTH

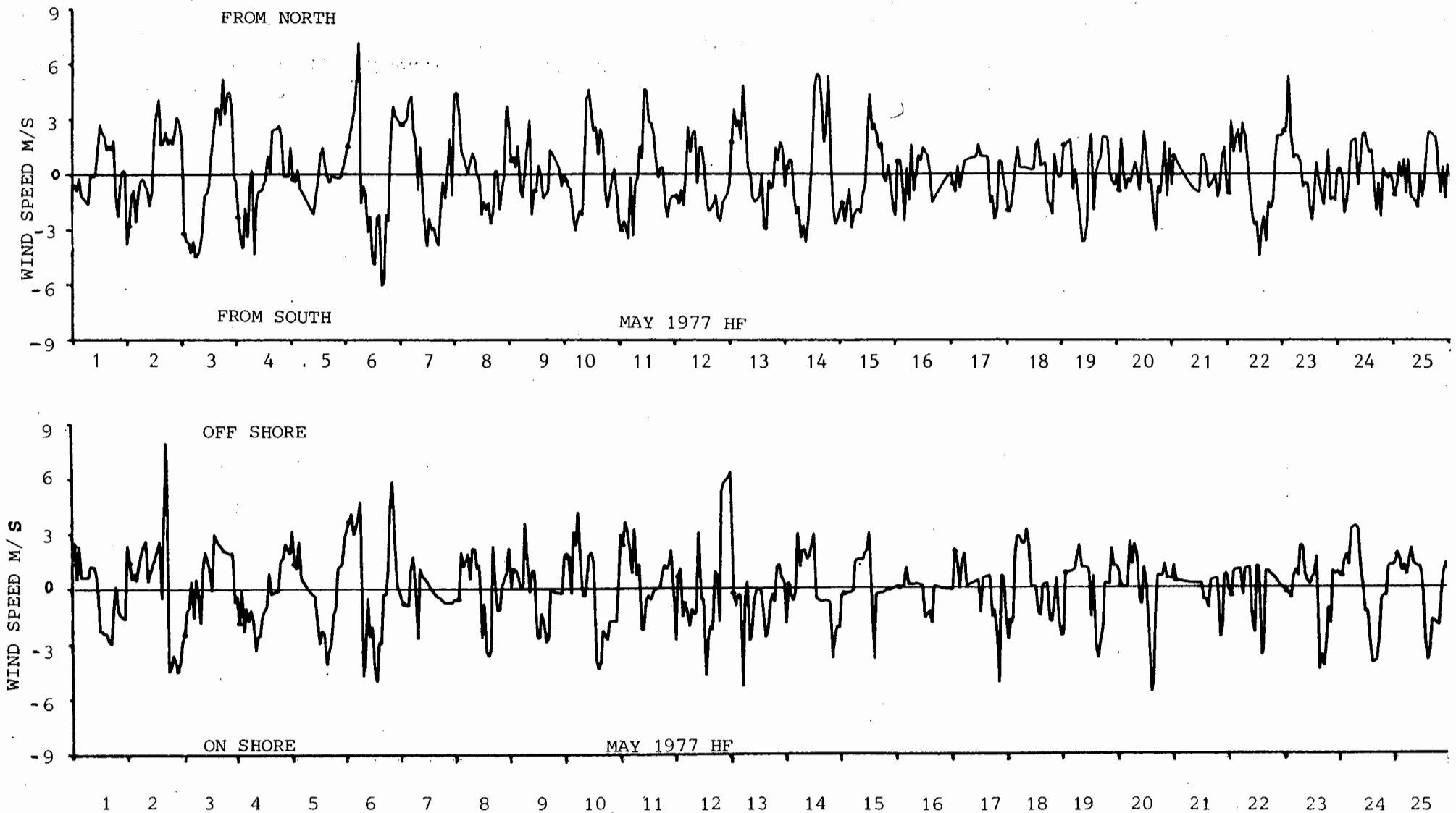

FIG. 5.3a,b TIME SERIES OF HIGH FREQUENCY FILTERED HOURLY DATA (ZERO MEAN) FOR OU SKIP WINDS FOR THE PERIOD 1 TO 25 MAY 1977. TICK MARKS EACH 24 HOURS. a) ALONGSHORE (NORTH) b) ACROSS-SHORE (EAST)

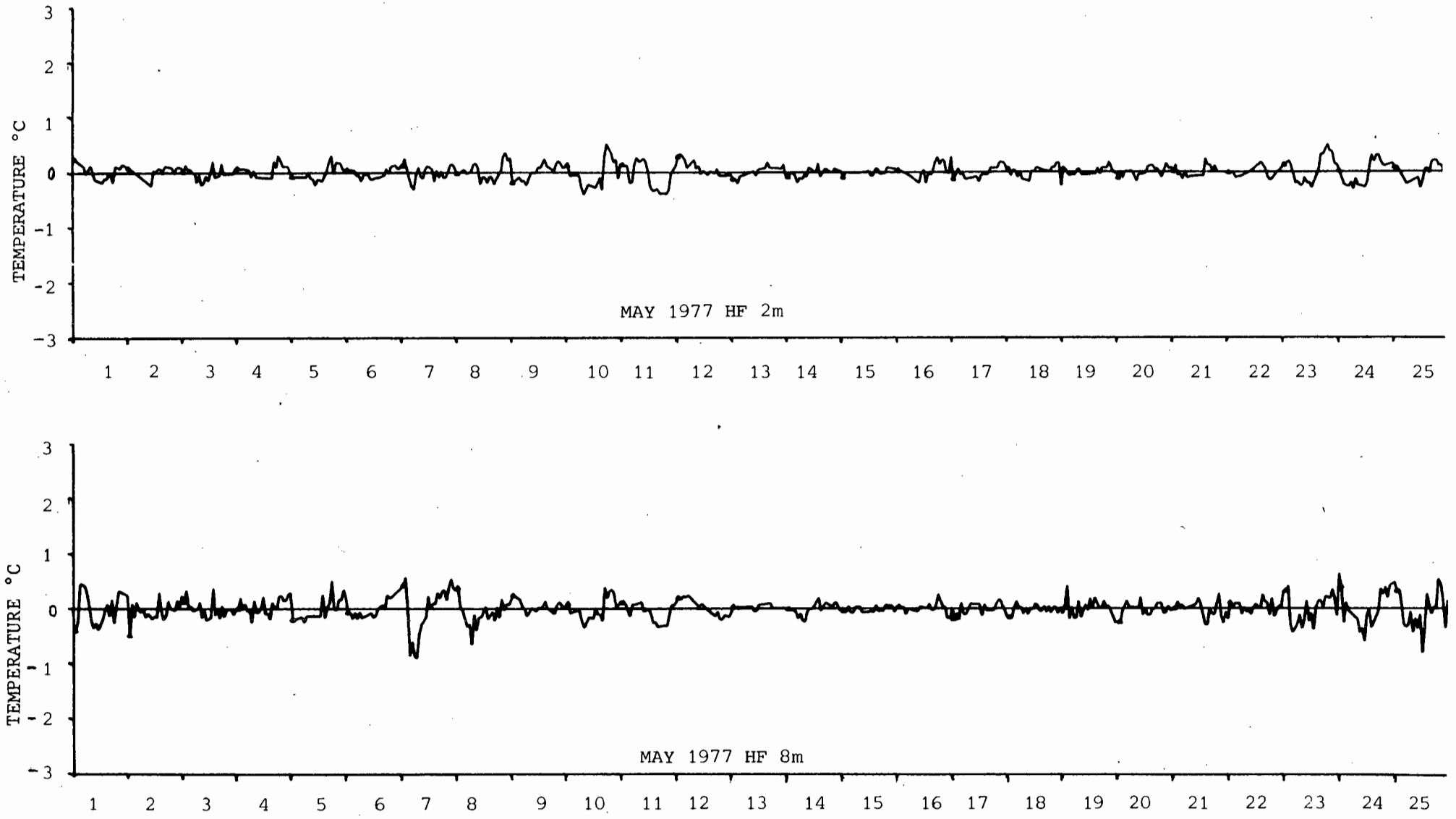

FIG. 5.3c,d TIME SERIES OF HIGH FREQUENCY FILTERED HOURLY DATA (ZERO MEAN) FOR SEA TEMPERATURES FOR THE PERIOD 1 TO 25 MAY 1977. TICK MARKS EACH 24 HOURS c) 2 M DEPTH d) 8 M DEPTH

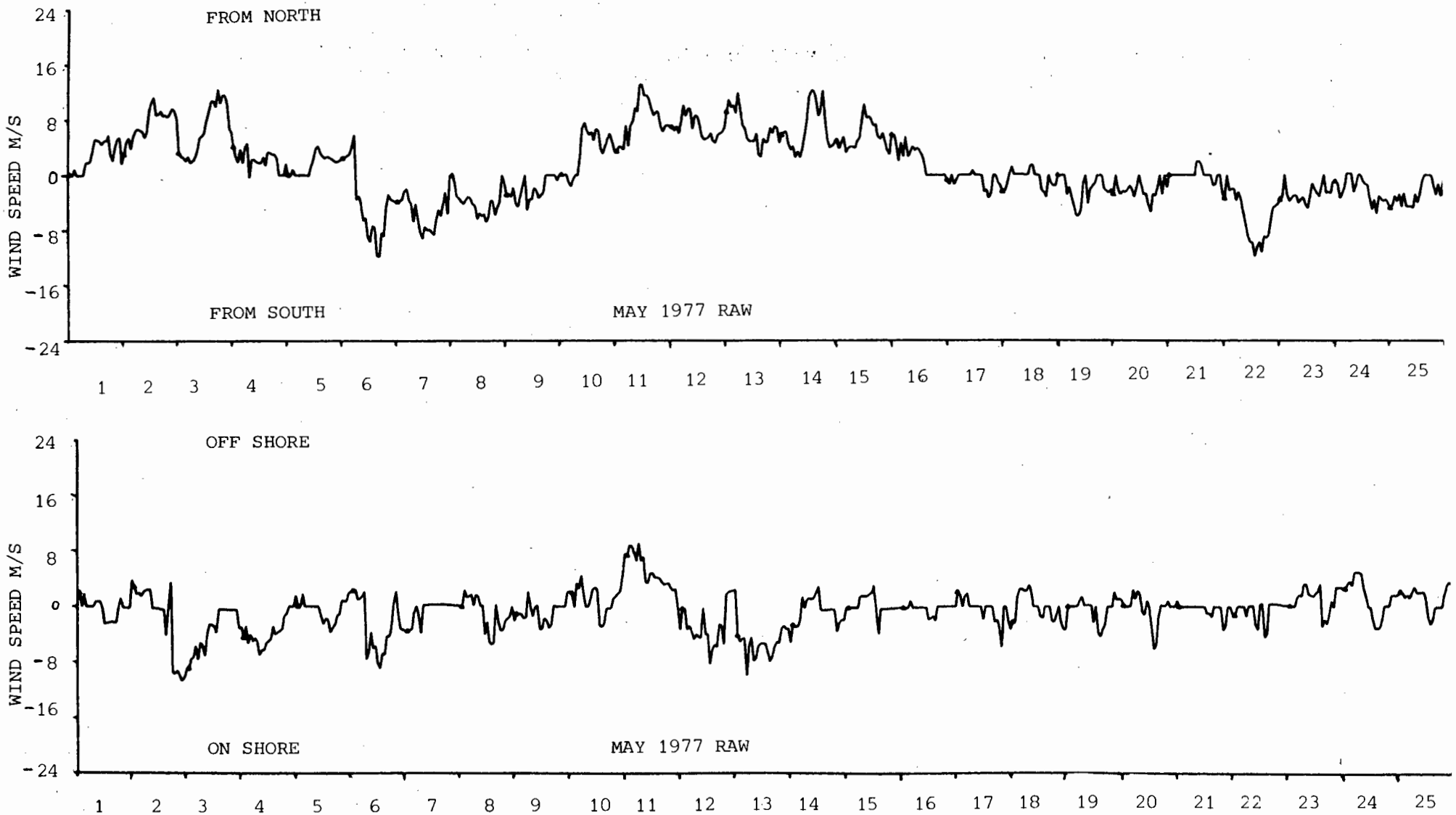

FIG. 5.4a,b TIME SERIES OF UNFILTERED (RAW) HOURLY DATA FOR OU SKIP WINDS FOR THE PERIOD 1 TO 25 MAY 1977. a) ALONGSHORE (NORTH) b) ACROSS-SHORE (EAST)

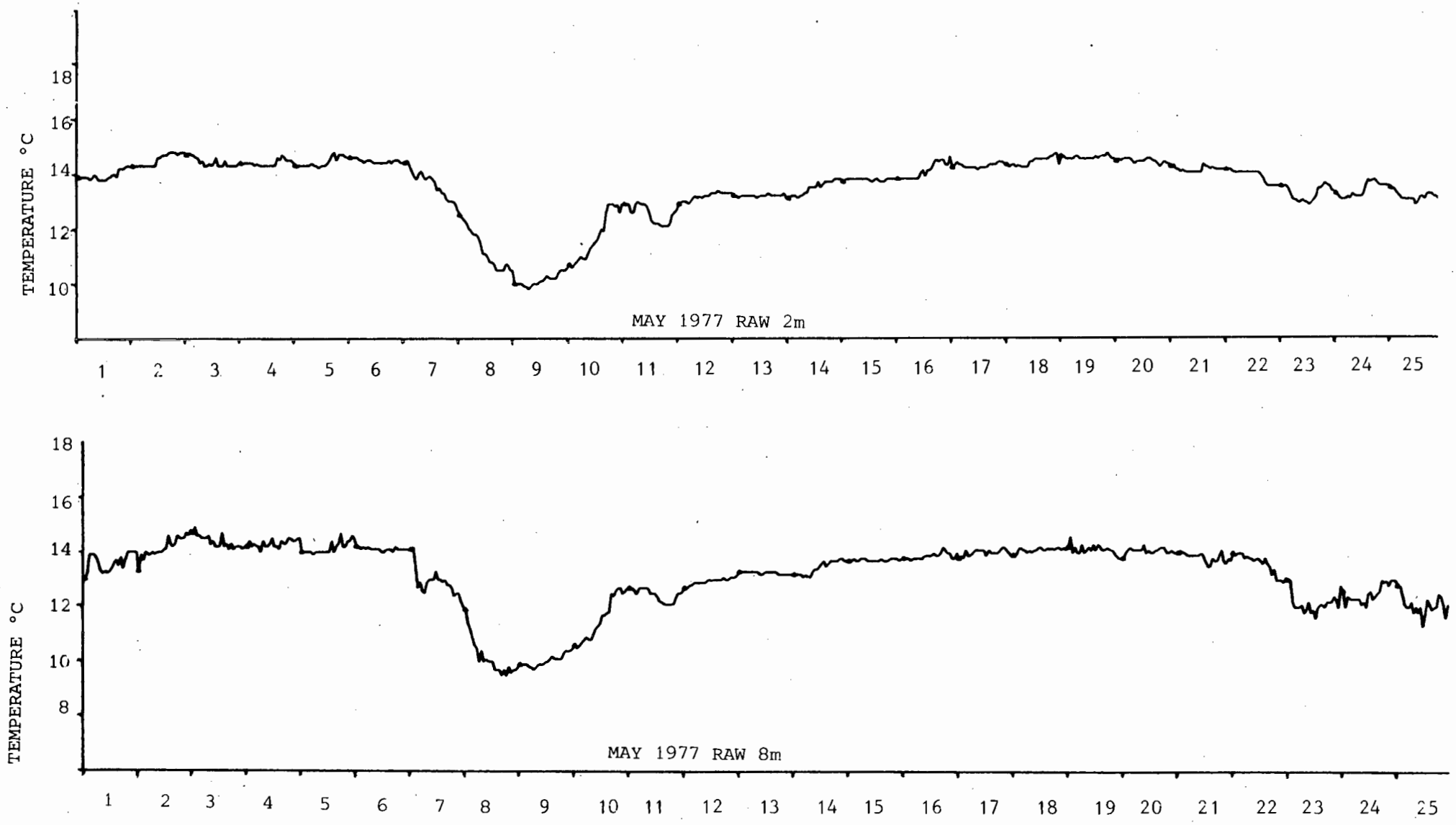

FIG. 5.4c,d TIME SERIES OF UNFILTERED (RAW) HOURLY DATA FOR SEA TEMPERATURES FOR THE PERIOD 1 TO 25 MAY 1977 c) 2 M DEPTH d) 8 M DEPTH

In **spring and summer**(Fig. 5.1a) with a southerly event the -ve alongshore residual is strong and diurnal, peaking in the late afternoon and has a typical duration of less than 8 hours. The +ve alongshore residual wind strength in contrast is lower with diurnal and higher frequencies; it peaks between about midnight and noon and has a duration of 16 hours or more. Under such conditions the positive residual maximum is in practice merely a minimum southerly wind. Under the same conditions the across-shore winds show (Fig. 5.1b) a more regular diurnal character with the -ve residual (onshore) being stronger than the +ve residual (offshore). The onshore peak occurs about midday or slightly later, before the southerly alongshore maximum and also has a duration of about 8 hours. The offshore tendency peaks after midnight (the oscillations tend to be cycloidal in shape rather than sinusoidal). The stronger sea-breeze (onshore) wind is expected in warmer months because of the development of a thermal low during the daytime in the immediate interior of the coastline (Jury, 1980, 1984). The observation of Jury (1980) that the coriolis deflection of the sea-breeze later in the afternoon causes the wind to become additive to the gradient wind from the south is confirmed in these data. Similarly a diurnal counter flow at mid morning tends to reduce the alongshore wind velocity.

This diurnal nature of the wind during a summer period with moderate to weak gradient southerly winds is revealed in a windstick diagramme (Fig. 5.5) of raw data from Posnik (Pers Com). The data are 15 minute average, wind vectors at 10 m above ground level covering a 5 day period for five anemometer stations on the Cape Flats and Robben Island. The positions are indicated on the map in Fig. 3.12. The winds at Melkbosstrand illustrate an afternoon sea-breeze maximum with calm to offshore winds in the morning. Winds at Robben Island exhibit a similar tendency but are weaker as are those at Table View. The tendency for the sea-breeze to be stronger to the north cannot be confirmed in this data since the northerly station at Atlantis is positioned somewhat inland. The coriolis produced anticlockwise tendency for the rotation of the diurnal wind vectors is clearly seen in Fig. 5.5. Another good illustration of the modulation of the alongshore wind is given in a progressive vector diagram (Fig. 4.11) - Chapter 4.

Still in spring or summer but with a northerly event being dominant the patterns for alongshore residual winds tends to a reversal from the previous case viz. the +ve (from north) peak occurs about midday and is narrower than under southerly dominance. The diurnal character of the +ve residuals is enhanced relative to the -ve residuals which in practice could be light northerlies. The across-shore residuals peak at about the same time of day as p

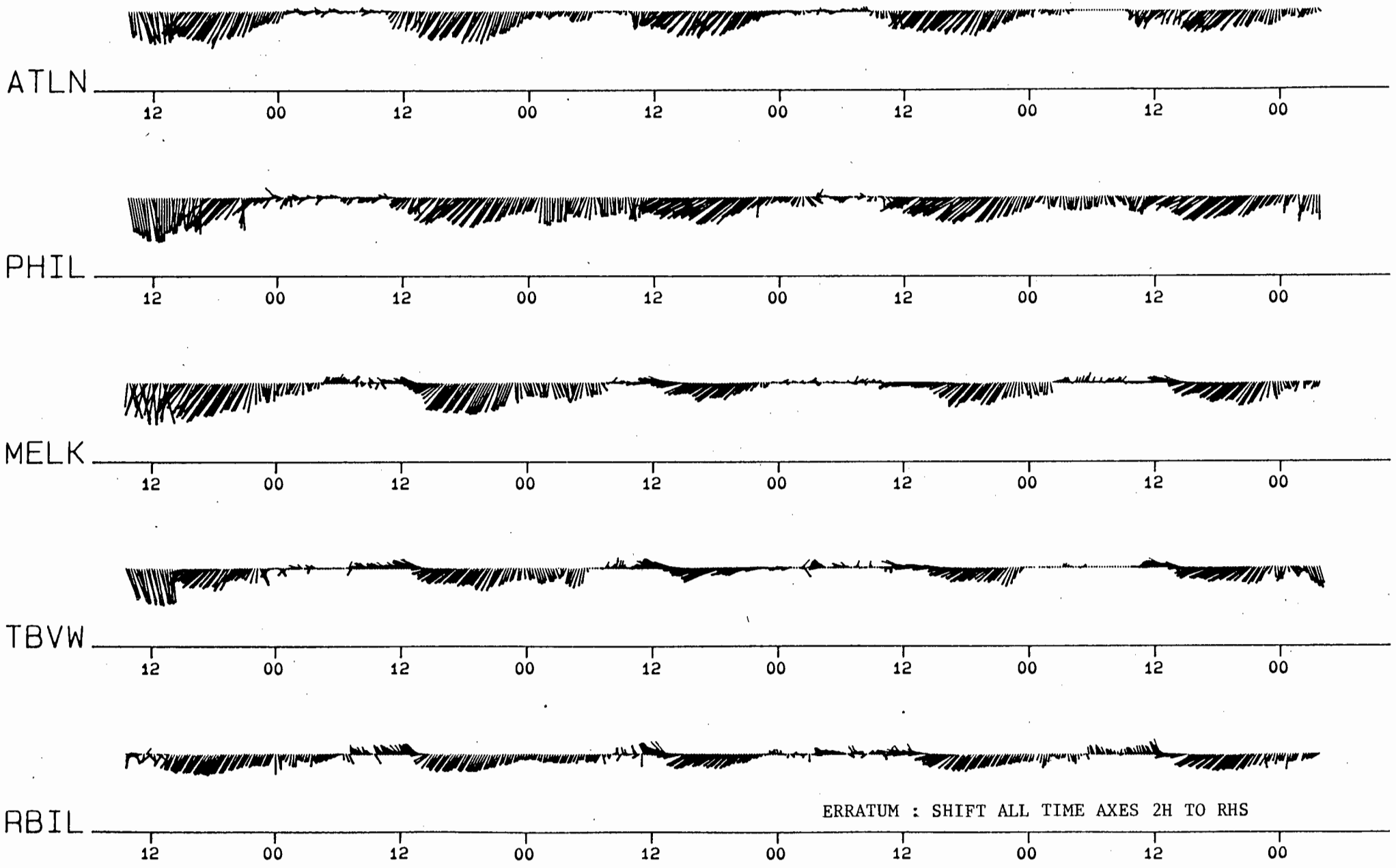

ERRATUM : SHIFT ALL TIME AXES 2H TO RHS

FIG. 5.5 TIME SERIES VECTOR STICK DIAGRAMME OF UNFILTERED 15 MIN AVERAGE WINDS FOR FIVE POSITIONS (SEE FIG. 3.12) FOR THE PERIOD 7h30 5 JAN 1982 TO 1h45 10 JAN 1982 (1 mm = 1 m/s) AFTER POSNIK (PER COM)

reviously (the diurnal heating process being similar) but the onshore sense is weakened.

In **winter** the diurnal signal in the alongshore winds is somewhat suppressed and higher frequencies occur (Fig. 5.3a). In comparison the across-shore winds however are at times more clearly diurnal, with the onshore peaks being reduced in strength and duration relative to the summer occurrence. This diurnal character is most evident when the gradient winds are light i.e. the cooler air temperatures over the land in winter have suppressed the onshore sea-breeze but have enhanced the offshore land breeze at night.

In general, despite large differences in the absolute wind strength for the two wind components, the fluctuations in the high frequency data are about equal for both components. However, particularly in winter the across-shore component is on occasion greater than the alongshore component and can influence the expected sea temperature response (compare the last few days of Fig. 5.3 a and b).

5.2.1.2 Temperature Characteristics

The high frequency temperature plots give the fluctuations about a detrended zero mean and indicate the increasing and decreasing phases of the temperature response. The high frequency temperature plots e.g. Fig. 5.1c and d also exhibit strong signals in the diurnal range which are modulated by the nature of the wind events. Between northerly periods that cause minimal temperature oscillations there appears almost a wave packet effect of high amplitude oscillations in the temperature at both the 2 m and 8 m depth (Fig. 5.1c + d) that correlate with southerly or calm periods. The delineation of the wave packet effect can be linked to coastal lows, because just prior to the passage of coastal lows the amplitude of both the direct insolation and the across-shore wind can be enhanced (Jury and Spencer-Smith, in press). More favourable wind/temperature correlation with across-shore winds is discussed later. In the **spring and summer** regimes the amplitude of the temperature fluctuations is $\pm$ 1 °C to $\pm$ 3 °C with southerly dominant winds, but can be suppressed to less than +0.5 °C when northerly alongshore winds occur. After full upwelling has occurred with strong consistent southerly winds the temperature response is also somewhat suppressed. The large temperature oscillation under relatively calm conditions on 20-22 Jan 1977 (Fig. 5.1c and d) is discussed in Sections 5.3.4 and 5.3.1.1 The temperature minima tend to occur most frequently between midnight and noon with a predominance after 06h00. The maxima occur chiefly between 14h00 and 24h00. North or south dominance in the winds does not make a major difference in the time of occurrence of the

maximum and minimum temperatures, however because the temperature fluctuations are generally of a higher frequency and much smaller under northerly conditions the times of occurrence are more variable then. The general trend of cooler waters before noon and warmer temperatures in the afternoon can be ascribed either to a direct insolation heating effect or indirectly through the diurnally forced across-shore winds which remain prevalent under both north and south conditions but weaker in the former case. An afternoon sea-breeze will tend to suppress upwelling then and cause an effective increase in temperature. The direct and indirect forcing is discussed at length in later sections.

Another feature of the HF temperature data is the larger amplitude oscillation for the deeper probe at 8 m than for the 2 m probe - compare Fig. 5.1c and d. This is particularly evident for the first few days in these figures, when the winds are light. The 8 m data also show some evidence for semi-diurnal or tidal frequencies then. The minima for the 8 m data tend to lead that of the 2 m data but the time of occurrence for the maxima exhibit both leads and lags.

During the **winter regime**(Fig. 5.3c and d) the temperature fluctuations are greatly reduced; they are generally less than $\pm$ 0.5 °C and often only $\pm$ 0.2 °C. The diurnal character is still present. During southerly wind episodes the temperature fluctuations are larger and more regular when the across-shore components are also generally larger, more regular and diurnal than with northerly events which are often accompanied by cloud and rain and consequent less insolation. The response at the 8 m depth is usually larger than at 2 m and has more high frequency "noise". At the onset of the southerly event e.g. 6-7 May 1977 (Fig. 5.4a), there is an obvious temperature response at 8 m depth (Fig. 5.3d) but no significant response at 2 m (Fig. 5.3c). At the relaxation phase of upwelling (10th May 1977, Fig. 5.4a) when temperatures are increasing, the near surface data show a higher amplitude oscillation than that at depth. (This could indicate an asymmetry between up and downwelling.) During winter with the generally small amplitude temperatures and high frequency "noise" it is not always clear to distinguish a difference between the 2 m and 8 m data for the time of occurrence of minima or maxima, but there is some bias towards the minima to occur earlier at depth.

Under relatively calm conditions, but with diurnal across-shore winds e.g. the last few days of Fig. 5.4a and Fig. 5.3b, the 8 m maxima, which are sharper, occur later than at 2 m which shows a more gentle diurnal trend with maxima before about 18h00. The smaller temperature response under northerly conditions (which also

occurs during summer northerlies) can be ascribed to a more homogeneous water column brought about either by advected offshore surface waters filling in the down-welled region or/and by enhanced mixing, due to the large waves that are generally associated with northerly conditions (Section 4.2.4). The low pressure cyclone accompanying the northerly condition often brings clouds and rain which will decrease insolation effects. In addition during winter the core of colder water is much deeper and further offshore (Andrews and Hutchings, 1980).

5.2.2 Correlations, Lags and Statistics

The linear correlation coefficients for linearly detrended high frequency wind and sea temperature data with zero means and normalized by their variances are now discussed. Direct visual inspection of the plots of the high frequency wind components and the temperature show interesting lags between them. Results of lagged cross correlation analysis between wind components and temperatures at two different depths and for different record lengths at different times of the year are shown in Table 5.1. Some of the cases given in Table 5.1 correspond to data in the set of Figs. 5.1a-d to 5.4a-d. Because of the sense of the wind components used in this study the wind temperature correlation coefficient is expected to be positive for alongshore winds that force upwelling processes (in the generic sense) and to be negative for across-shore winds that force upwelling processes; i.e. positive alongshore winds (northerly) will increase the temperature (downwelling) and negative alongshore winds (southerly) will decrease the temperature, (upwelling); positive across-shore winds (offshore) will decrease the temperature (upwelling) and negative across-shore winds (onshore) will increase the temperature, (downwelling). Of course the sign of the correlation coefficient will result from any other non-upwelling dynamics e.g. inertial advection that gives a similar wind/temperature response.

5.2.2.1 Alongshore cases

Throughout the year for the tabulated alongshore cases the zero lag correlation coefficient is either significantly negative or close to zero. In winter there is no significant zero lag correlation. When the temperature is lagged with respect to the alongshore wind, maximum positive correlation occurs with a lag of about 10 hours in spring and summer, and with a longer lag of about 15 hours in winter. In spring and summer the significance level of the lagged correlation coefficient exceeds 99.9 % for a long (2880 hour) record and is close to or greater than the 95 % level for the shorter records. In two cases the 8 m temperature is correlated at

a higher significance level than the 2 m. Visual inspection of the complete time series data generally supports this trend.

In winter the significance of the lagged correlation coefficients are generally smaller than in summer with a majority of cases having a level close to or less than 95 %. In one case (1-31 May 1977) the 2 m temperature data are poorly correlated with the alongshore wind although at 8 m the correlation is significant at the 95 % level. The proposed reason why the 8 m depth has a better correlation is that upwelling due to a favourable wind initiates a temperature change first at the bottom as cold water flows shorewards there and one has a bottom-up process occurring which for smaller southerly events does not always extend to the surface - e.g. compare Fig. 5.3c and d on the 7th May. The greater lags in the temperature response in winter compared to summer and spring is probably due to the cold water lying deeper and further offshore in winter (Andrews and Hutching, 1980).

The magnitude of the lags for maximum correlation are of the order of one half day which can explain the often significant negative correlation at zero lag (i.e. 180° out of phase). Generally the +ve lagged correlation coefficient is more significant than the -ve zero lag coefficient. There is no obvious trend in the tabulated (Table 5.1) lags between the 8 m and 2 m depth data. However visual comparison of alongshore wind plots and corresponding temperature plots reveals that for positive correlation the lag (8 to 14h) for decreasing temperature is generally longer than the lags (6 to 10h) for the increasing phase of the temperature response. The quicker response time for the temperature increase can be related to either a) insolation effects which are reported to be asymmetrical (Roll, 1965, Price et al., 1986 and Section 5.3.1) and/or b) sea-breeze effects which accelerate the relaxation of the upwelled thermocline (Sonu et al, 1973 and Section 5.3.2).

5.2.2.2 Across-shore Cases

In Table 5.1, for the across-shore cases the zero lag correlation coefficients with one exception are below the 95 % significance level. The exception is the case for the 8 m depth data in January when the negative correlation coefficient exceeds the 95 % level. When the temperature is lagged with respect to the wind a maximum negative (upwell favouring in the generic sense) correlation occurs with a lag of 2 to 4 hours in spring or summer and with a longer lag of up to 9 hours in winter. In spring and summer the lagged correlation coefficients comfortably exceed the 95 % confidence level and in the case of January 1977 exceeds the 99 % level. There is no clear trend in the behaviour of the correlation

coefficient or lag at the two different depths during spring or summer.

In winter the maximum negative correlation coefficient is close to or exceeds the 99 % significance level in the case of May 1977 but is less than the 95 % level in the July case. The lag for maximum negative correlation is larger for the 8 m data than the 2 m data (Table 5.1). This could indicate the operation of some top-down process; either surface heating or onshore advection of warmer waters. The winter correlation coefficients are generally smaller than in summer.

Temperature - Temperature correlation

For all cases the zero lag correlation between the temperature at the two depths exceeds the 99.9 % confidence levels. There is a rapid fall off in correlation coefficient with lagging - within 4 to 5 hours it falls to less than the 95 % level. Positive and negative lagging between the temperature data yield correlation coefficients (which are not completely tabulated in Table 5.1) that show that generally the fall off to the 95 % level is skewed to about one hour longer for the 8 m data lagging the 2 m data than for the 8 m data leading the 2 m data. The sharp drop in correlation from zero lag indicates that the temperature response across the water column mostly occurs within a few hours. Visual inspection of the raw temperature data indicates that the skewed distribution in leads and lags can be related to the 8 m depth response leading the 2 m response in the decreasing temperature phase and it lagging by a greater amount in the increasing phase. This asymmetry has also been mentioned in the Section 4.3.1.2.

5.2.2.3 Comparison of Alongshore and Across-shore Correlations

A comparison of maximum correlation coefficients obtained (Table 5.1) for alongshore and across-shore winds shows that overall the across-shore winds are significantly correlated and better correlated with the sea temperature than the alongshore winds, particularly at the 2 m level. However, the July 1977 case is contrary to the trend; the across-shore wind has a correlation coefficient with a significance level below 95 % and smaller than the alongshore component. In the January 1977 case they are equally highly correlated.

The contrary indication mitigates against an unequivocal explanation being given for the observed trend. Some insight is gained from correlation aspects of the 2 m and 8 m data. A better correlation between the across-shore and the 2 m data may indicate

some top-down process is operating. In Section 4.4.2.1 it is shown that in the relaxation phase with light onshore winds a thin warm surface layer appears. The generally significant correlation between the 8 m depth and alongshore winds indicates a bottom-up process which links with an upwelling process.

Another feature is the much shorter lag time for maximum correlation with across-shore winds than with alongshore winds. This can be simple due to the phase difference between the winds or in summer when the stronger sea-breeze is prevalent, downwelling is induced and gives a quicker temperature increase, compared with the slower upwelling response of the prevailing southerly alongshore wind. Both winds give longer lags in winter.

For both the alongshore and across-shore winds the temperature correlation is weaker in winter. This is linked to the fact that the overall temperature contrasts in the sea are suppressed in winter because, a) there is much less upwelling associated with the decrease in southerly winds b) daily radiation from the sun decreases by a factor 2,3 from mid summer to winter (Brown, 1984) and c) the the mixing of the larger waves in winter reduces stratification. Some of the aspects revealed in the correlation analysis are further reinforced in the later section on spectral analysis (5.2.3).

5.2.2.4 Standard Deviation Statistics

Standard deviations for the zero mean high frequency data are given in Tables 5.2 and 5.3 where the former table is for both wind and temperature data at various selected periods during the year and the latter table gives the monthly standard deviation for temperatures. The standard deviation for the wind components are fairly similar throughout the year. The alongshore and across-shore values are well matched in spring and summer but in winter the standard deviation increases for the across-shore and decreases for the alongshore wind. This indicates greater variability for the across-shore winter winds.

The standard deviation on the temperatures are markedly smaller during winter. The monthly tabulation in Table 5.3 shows the 8 m data are more variable. This may be due to bottom-up effects and possible internal wave activity, as well as wave and wind mixing that may cause a smoothing effect on near surface temperatures.

5.2.3 Spectral Analysis

The hourly high frequency time series data for wind and sea temperature are analysed spectrally and presented in various figures in this section. Firstly spectra for annual data sets of wind then sea temperatures are discussed. Secondly, spectra for seasonal or regime data sets are investigated. A summary of the individual years analysed is given in Table 5.4. Since the spectra for the different years are quite similar, only the spectra of 1977 are plotted here. Where appropriate reference is made to the non displayed spectra.

The spectra for 1977 are shown in Fig. 5.6a, b and c which depict a) the autospectra for the two wind components, b) the rotary wind spectra and c) the temperature autospectra for the 2 m and 8 m depths. For all the spectra, 720 lags are used in the analysis. All the above figures are plotted on a log/log scale, the horizontal scale covering the frequency range 1/63 cph to 1/2 cph. The figures include the 95% confidence limits and the bandwidth as described in Section 2.3.1. Every 10th lag is indicated by a plotted symbol on the spectra.

5.2.3.1 Annual cases

HF wind spectra

The most prominent features of all the HF wind spectra are the peaks at frequencies of 1/24 cph and 1/12 cph. The latter peak is probably a harmonic of the intense diurnal peak and has been discussed in 1.5.3 and 2.3.1 and is not further discussed here for the wind spectra. All the wind spectra also reveal a falloff in energy with increasing frequency that follows a $f^{-3/2}$ power law as indicated in Fig. 5.6b (see Section 2.3.2).

If the **autospectra** are considered for the years 1975, 1976 and 1977 (Fig. 5.6a), with numerical values for the peaks tabulated in Table 5.4, it is seen that at the diurnal frequency the across-shore (east) component dominates the alongshore (north) component by a factor of more than 3. The alongshore component tends to have greater energy than the across-shore component for frequencies less than 1/24 cph.

The diurnal dominance for the across-shore wind is indicative of a strong solar forcing at that frequency and is ascribed to a consistent land/sea-breeze system (Jury, 1980). The tendency for more energy at the lower frequencies for the alongshore component is linked to its dependence on the synoptic scale gradient winds.

In the **rotary spectra**(Fig. 5.6b) the anticlockwise component tends to dominate at all frequencies especially at the diurnal frequency where it is greater than the clockwise component by a factor of between about 4 and 8. See Table 5.4 which also lists the rotary coefficient - a measure of the rotary nature of the data. Inspections of wind vector data (Fig. 5.5) confirms the tendency for the winds to rotate preferentially anticlockwise. Owing to the Coriolis effect, diurnal sea-breeze winds are expected to rotate anticlockwise in the southern hemisphere.

The rotary analysis shows that the diurnal peak does have a statistically stable ellipse orientation. The major axis orientation is given in Table 5.4 When allowance is made for the orientation of the coastline, approximately 20° to W of N, the tabulation indicates that the favoured wind direction is within about 10° of being orthogonal to the coast which correlates with the across-shore dominance of the autospectra.

In one year, 1975 (not displayed) there is a small peak at the inertial frequency for the site (1/21,64 cph) with an anticlockwise dominance which supports an inertial mechanism. The peak is however below the 95 % confidence level. Although very shallow inversion heights of 5 m have been observed on site (Jury Per com) the uncoupling of the top layer from the boundary layer and subsequent inertial frequency winds at the 14 m height of the anemometer position is expected to be rare. At greater altitudes Gill (1982) and Thorpe et al (1977) report the occurrence of inertial winds associated with a nocturnal jet. Above the inertial frequency the clockwise and anticlockwise spectra tend to merge which confirms that at such higher frequencies the effect of the earth's rotation is unimportant.

HF Temperature Spectra

The two HF sea temperature spectra considered are for the years 1976 and 1977 with the latter illustrated in Fig. 5.6c. Numerical values are given in Table 5.4. As with the wind the most prominent feature in both years is the large peak at the diurnal frequency. This is ascribed to some solar influence either of a direct or indirect nature. The contribution of direct insolation and/or the diurnal wind effects to the temperature response at this frequency are discussed at length in 5.3. The 2 m spectra have slightly enhanced energy at the diurnal frequency relative to the 8 m spectra.

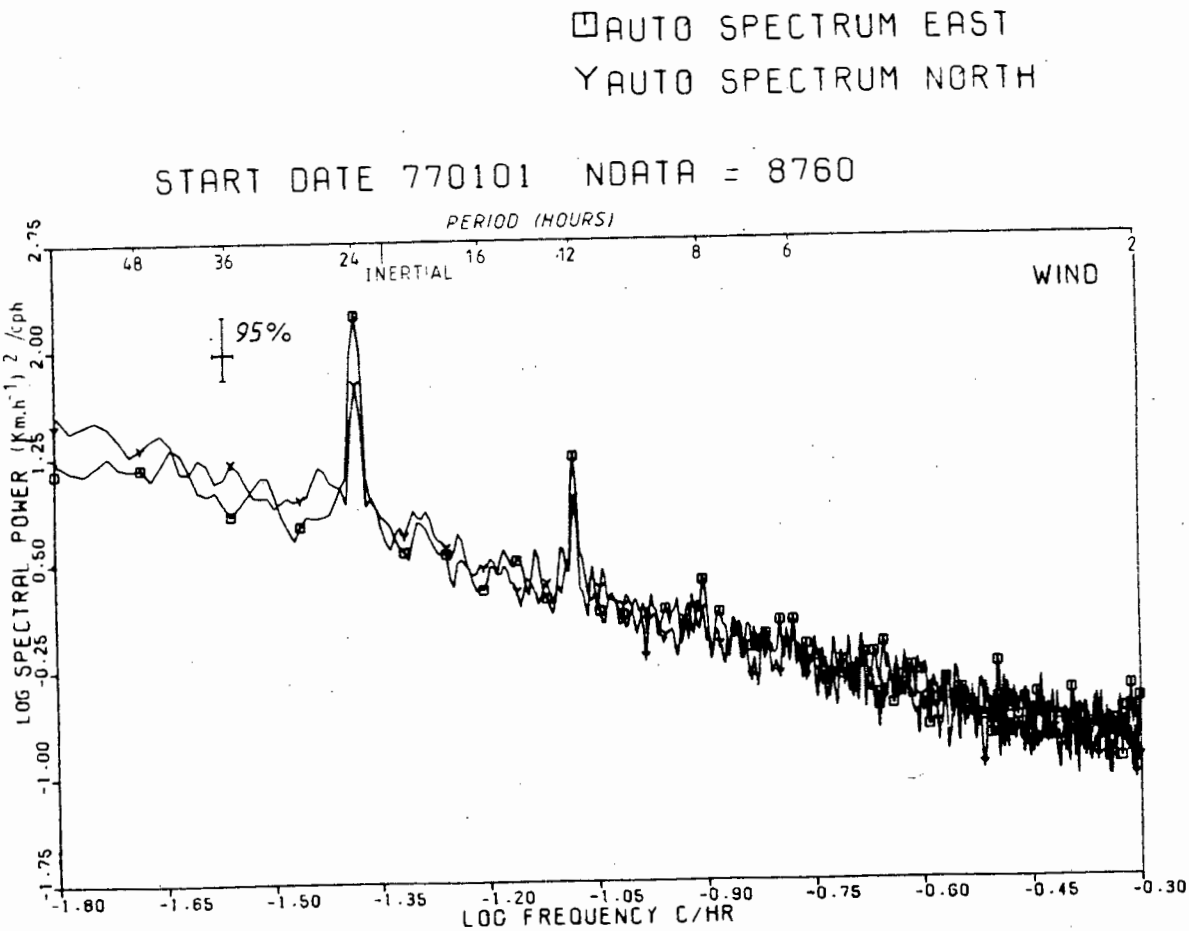

FIG. 5.6a LOG/LOG PLOT OF AUTO SPECTRA FOR HF FILTERED OU SKIP ALONGSHORE (NORTH) AND ACROSS-SHORE (EAST) WIND COMPONENTS FOR 1977. MAXIMUM LAG NUMBER 720. PLOTTED SYMBOLS INDICATE EACH 10TH LAG NUMBER.

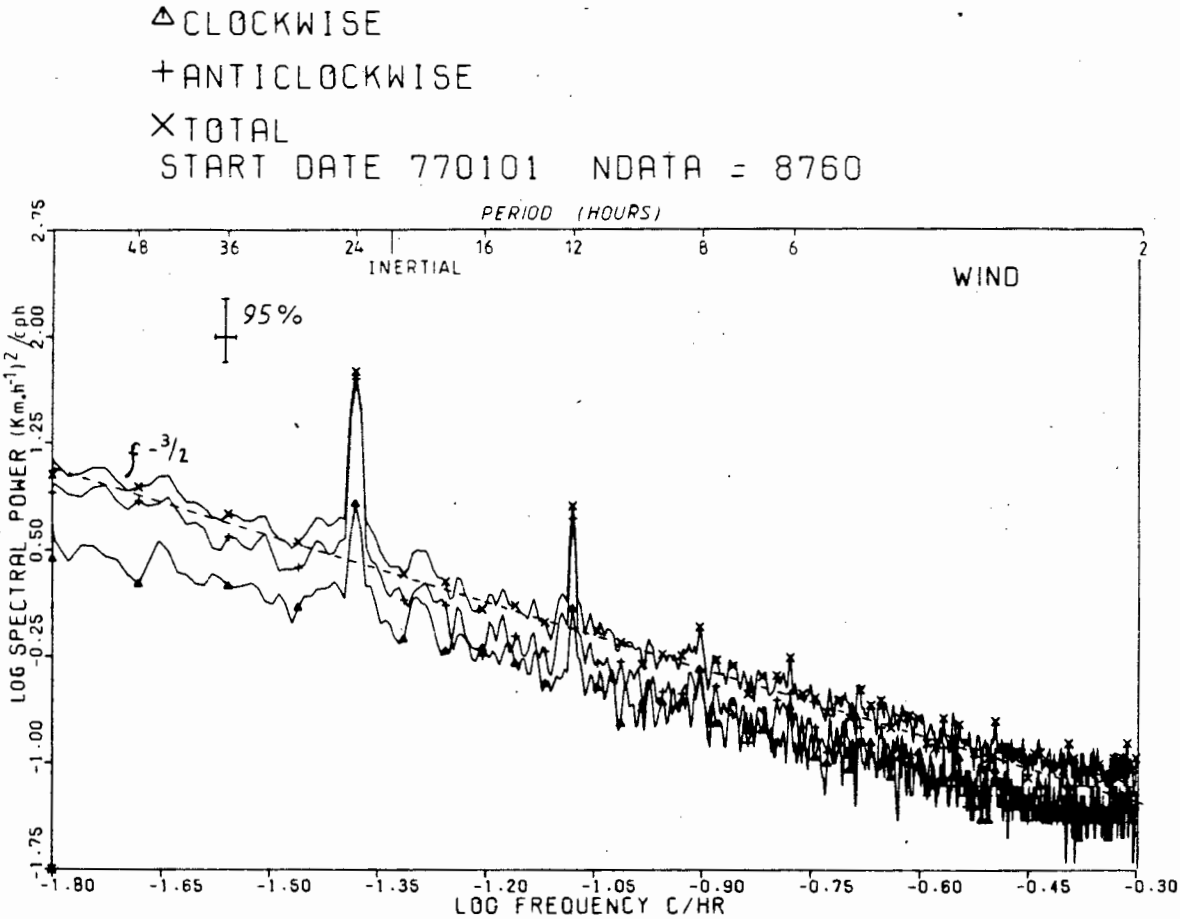

FIG. 5.6b LOG/LOG PLOT OF ROTARY SPECTRA FOR HF FILTERED OU SKIP WINDS FOR 1977

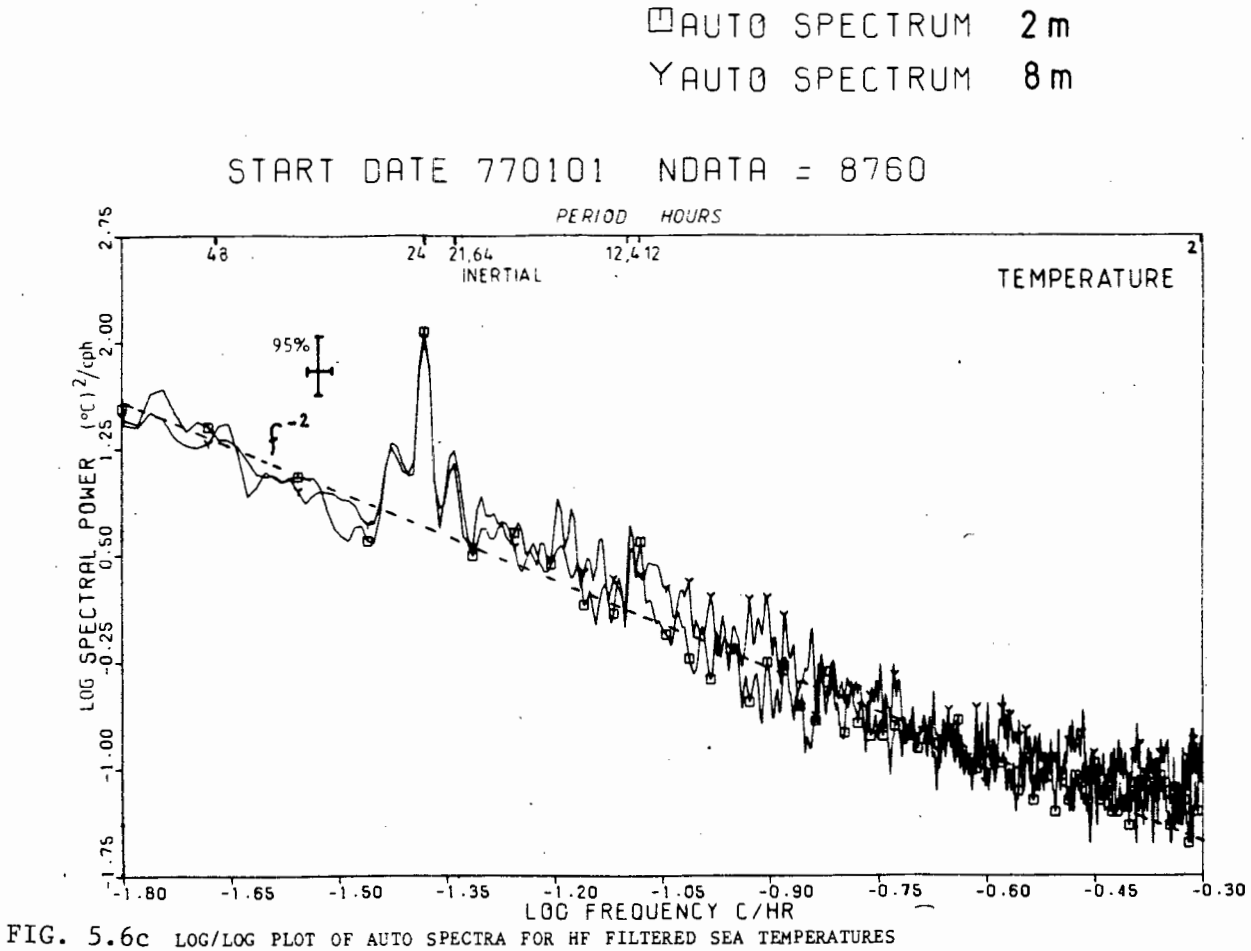

FIG. 5.6c LOG/LOG PLOT OF AUTO SPECTRA FOR HF FILTERED SEA TEMPERATURES AT 2 M AND 8 M DEPTHS FOR 1977

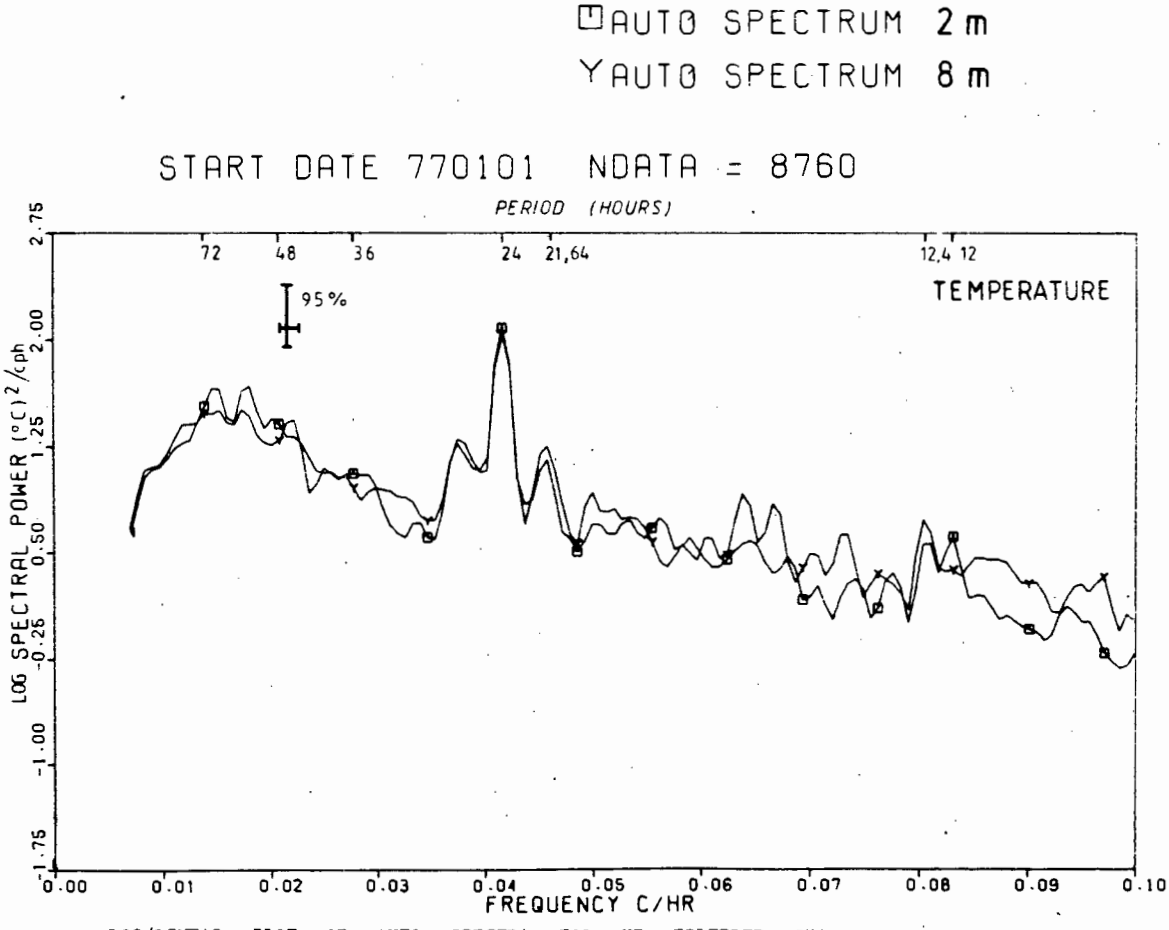

FIG. 5.7 LOG/LINEAR PLOT OF AUTO SPECTRA FOR HF FILTERED SEA TEMPERATURES AT 2 M AND 8 M DEPTHS FOR 1977 COVERING LOWER FREQUENCY PORTION OF FIG. 5.8c

Before other features of the spectra are mentioned a slight problem in interpreting the temperature spectra is discussed. Whereas the wind spectra have a significant breakthrough peak at 1/12 cph the temperature spectra do not. The semi-diurnal harmonic breakthrough in the wind spectra was ascribed to the asymmetrical diurnal periodicity of the wind (Section 1.5.3). The sea temperature too shows an asymmetrical diurnal behaviour as seen later in Fig. 5.12 and has a strong peak at 1/24 cph. Why then does it not have a prominent breakthrough at 1/12 cph? A possible explanation is that whereas the wind has a very "clean" well isolated peak at 1/24 cph the temperature spectra have large side lobes that tend to broaden the base of the 1/24 cph peak giving it a less clear cut nature. This idea is supported by the fact that in both 1976 and 1977 although the temperature spectra peak maxima at 1/24 cph are virtually the same for the 2 m and 8 m data the 1/12 cph peak is smallest for the 8 m depth data which has the broadest base to the 1/24 cph peak. Similarly in a following section on HF spectra for seasonal regimes it is generally observed that wind spectra with poorly defined peaks at periods of 24 hours also have ill-defined peaks at the semi-diurnal harmonic.

Other features of the temperature spectra include structure at the inertial and tidal frequencies. These are seen more clearly on plots with a linear frequency axis covering a portion of the frequency range; Fig. 5.9a and b for 1976 and 1977 respectively.

At these frequencies the significance of peaks are less than the 95% confidence levels. However, in the following paragraphs it is argued that the consistency in the spectra for the two years data presented indicate that although minor, tidal and inertial effects do exist.

On the west coast the chief tidal constituents in this HF region are the S2, main solar tide at a frequency of 1/12 cph and the M2, main lunar tide at a frequency of 1/12,42 cph. Relative to the M2 tide the S2 tide contributes 44% to the tidal range. (The other tidal frequencies and their relative percentage contribution to the range is given in Table 5.5 after E Shipley (per com). Therefore if tidal influences are present in the temperature spectra then the effects at the frequency of 1/12,42 cph should be more prominent that at 1/12 cph. (Due to resolution limitations the N2 tide of period 12,65 h will enhance the M2 spectral peak.) This is in fact the case for the 8 m depth data but not for the 2 m depth data. Tidal effects on the temperature data can be expected to be greater at the 8 m depth than at the 2 m depth since any density layering effects at the greater depth will be more well defined than near the surface where surface waves and wind mixing will tend to lessen

stratification. The 2 m data spectra have a lesser contribution than the 8 m data at the M2 frequency but has a greater contribution at the S2 frequency. The latter is probably partly due to harmonic breakthrough of the 1/24 peak since the 2 m data has a cleaner diurnal peak than the 8 m data. At frequencies greater than the tidal band there is a slight bias that the 8 m data have more energy than 2 m data (Fig. 5.6c). In summary there is evidence for a small tidal effect at the M2 frequency, more so at 8 m depth and probably an even smaller effect at the S2 tidal frequency which is marked by a variable small harmonic breakthrough. Any diurnal tidal effects such as from K1 will be totally masked by the large diurnal peak, but in any case K1 only makes up 10,2 % of the M2 contribution which is itself small in the temperature spectra. Any internal tides are of course limited to frequencies greater than the local inertial frequency (Gill, 1982) and internal diurnal contributions are thus excluded (see Section 5.3.4).

Observation of the temperature spectra (Fig. 5.6c and 5.7) reveal that close to the inertial frequency for the site (1/21,64 cph) a small peak does exist. (In the 1976 case it is less well defined than the 1977 case illustrated.) The 8 m depth data consistently have greater spectral energy at that frequency than the 2 m case. For coastal currents Hayes and Halpern (1976) find that at the surface, 3,4 m depth, there is more inertial kinetic energy than deeper down at 8 m or 10 m. For temperatures however as discussed for tidal effects the near surface response is reduced due to breakdown of shallow stratification and the temperature response is expected to be greatest near the thermocline position. This is observed by Millot and Crepon (1981) in the Gulf of Lions. They also observe that the temperature spectral peak is shifted to 10% above the inertial frequency. A slight shift to higher frequencies is expected theoretically, whereas in this work the small temperature peak occurs about 2% below the inertial frequency. This apparent shift is within the bandwidth limitations of the spectral analysis and the anomaly is assumed to be due to resolution problems. Inertial oscillations are a common feature in the first stages of transient upwelling (Hayes and Halpern, 1976, Pollard et al, 1970). For an inertial temperature response in the sea a corresponding inertial peak in the wind is not required since Pollard (1970) reports that the wind imparts most of the inertial response to the sea at impulse periods less than the inertial period. The smallness of the inertial peak observed here is probably due to the shallowness of the site and the attendent frictional dampening.

Another overall trend of the temperature spectra is that there is a falloff in energy with increasing frequency that follows a f^{-2} power law (Fig. 5.6c). The reasons for this behaviour have been discussed in 2.4.1 and is explained by Phillips (1971 and 1975). At the top of the frequency range there is a departure from this trend and a flatter response is seen which is ascribed to a slight aliasing effect.

5.2.3.2 Regime Cases

In order to assess any seasonal effects in the HF data the filtered time series data are subdivided into the three regimes, summer, winter and spring discussed and defined in Chapter 3. To simplify the analysis each regime is made 120 days long with the last few days of the year in each case being discarded. The relevant spectral numerical values for the regimes in 1976 and 1977 are given in Table 5.4 with only the spectra of 1977 being illustrated here. The spectral analysis is done with 240 lags for each regime. The spectra for the three regimes, summer, winter and spring of 1977 are respectively shown in Figs. 5.8, 5.9 and 5.10 where each figure has part a, b and c which depict a) the autospectra for the two wind components b) the rotary wind spectra and c) the temperature autospectra for the 2 m and 8 m depth data. On each figure the 95% confidence limits and bandwidths are indicated.

In all cases the $f^{-3/2}$ and f^{-2} power law trends are followed for the wind and temperature spectra respectively. Once more the most noteworthy spectral feature in all the regimes is the diurnal frequency peak. In both years the diurnal peak in the winter regime for both wind and temperature spectra are consistently greatly reduced compared to the other seasons. The numerical values of the spectral peaks are given in Table 5.4. The reduction in diurnal spectral energy in winter is linked either directly or indirectly to the decreased insolation effects then. There is no obvious trend in spectral differences between spring and summer regimes, although for the temperature spectra the summer regime has the greatest diurnal energy. Possibly the anomaly in the spring of 1976 has disturbed any more marked patterns.

The across-shore autospectra again dominate the alongshore winds at the diurnal frequency particularly in winter. Generally the wind spectra harmonic breakthrough peak at the semi-diurnal frequency is ill-defined for corresponding poor diurnal peak resolution.

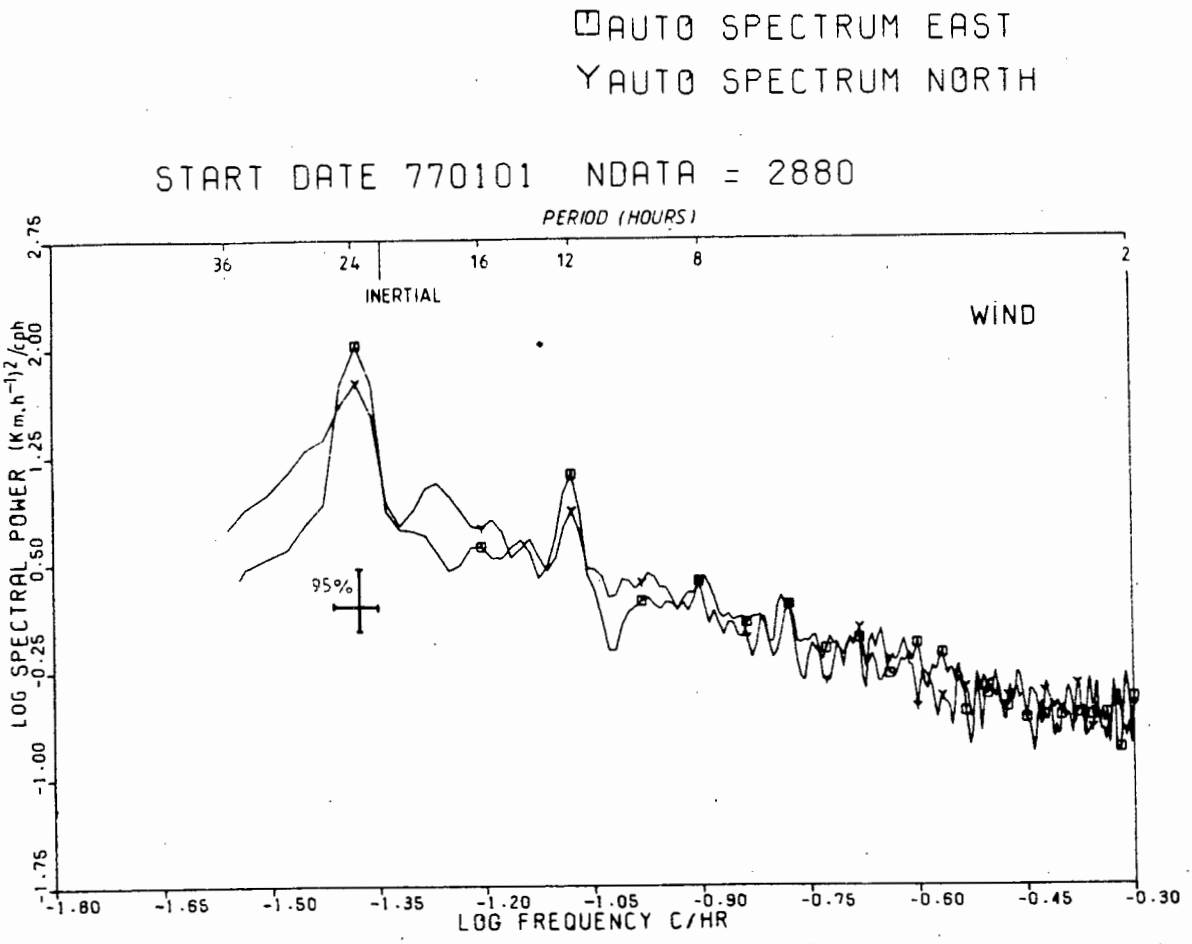

FIG. 5.8a SUMMER REGIME 1977 WIND AUTO SPECTRA FOR HF FILTERED OU SKIP DATA FOR A PERIOD OF 120 DAYS STARTING 1 JAN 1977. MAXIMUM LAG NUMBER 240. PLOTTED SYMBOLS INDICATE EACH 10TH LAG NUMBER

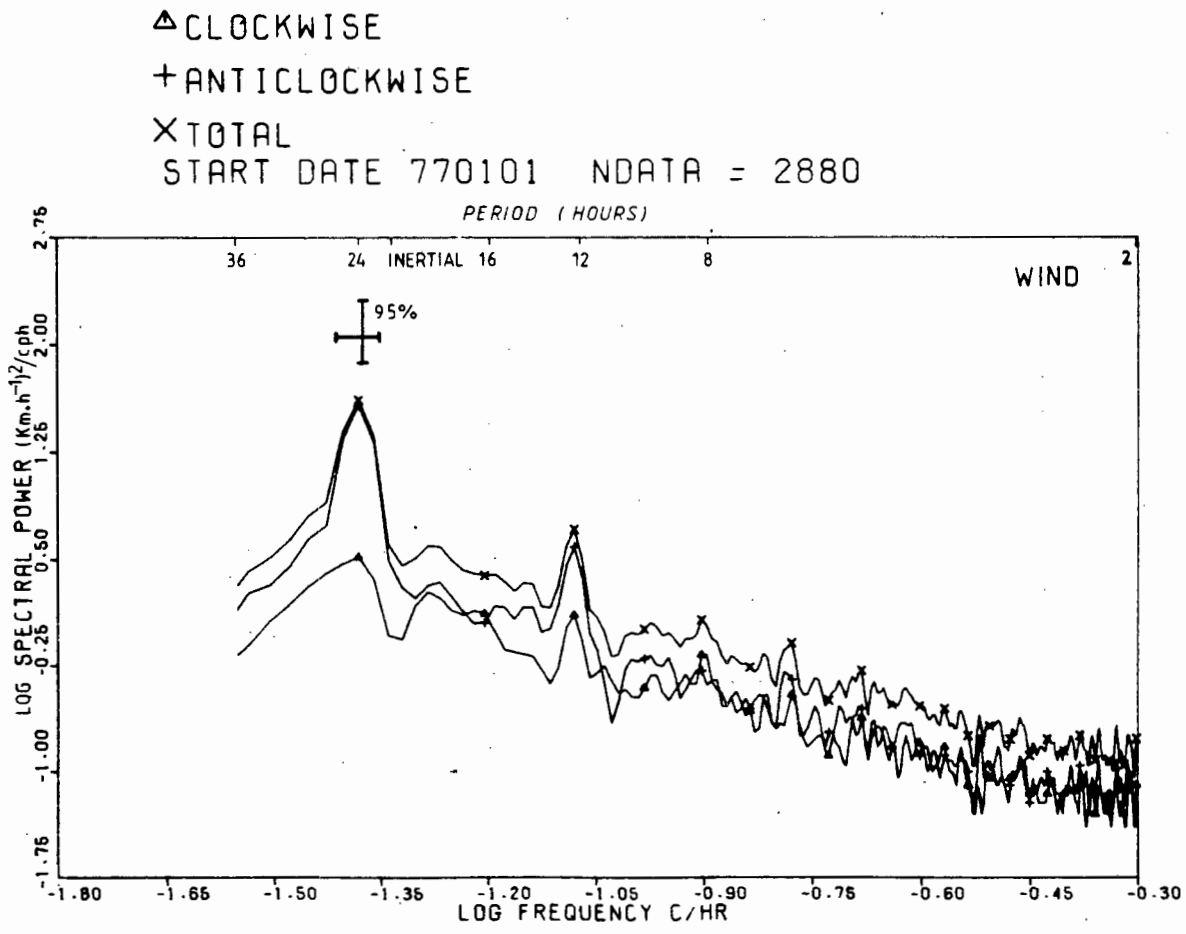

FIG. 5.8b SUMMER REGIME 1977 WIND ROTARY SPECTRA FOR HF FILTERED OU SKIP DATA FOR A PERIOD OF 120 DAYS STARTING 1 JAN 1977

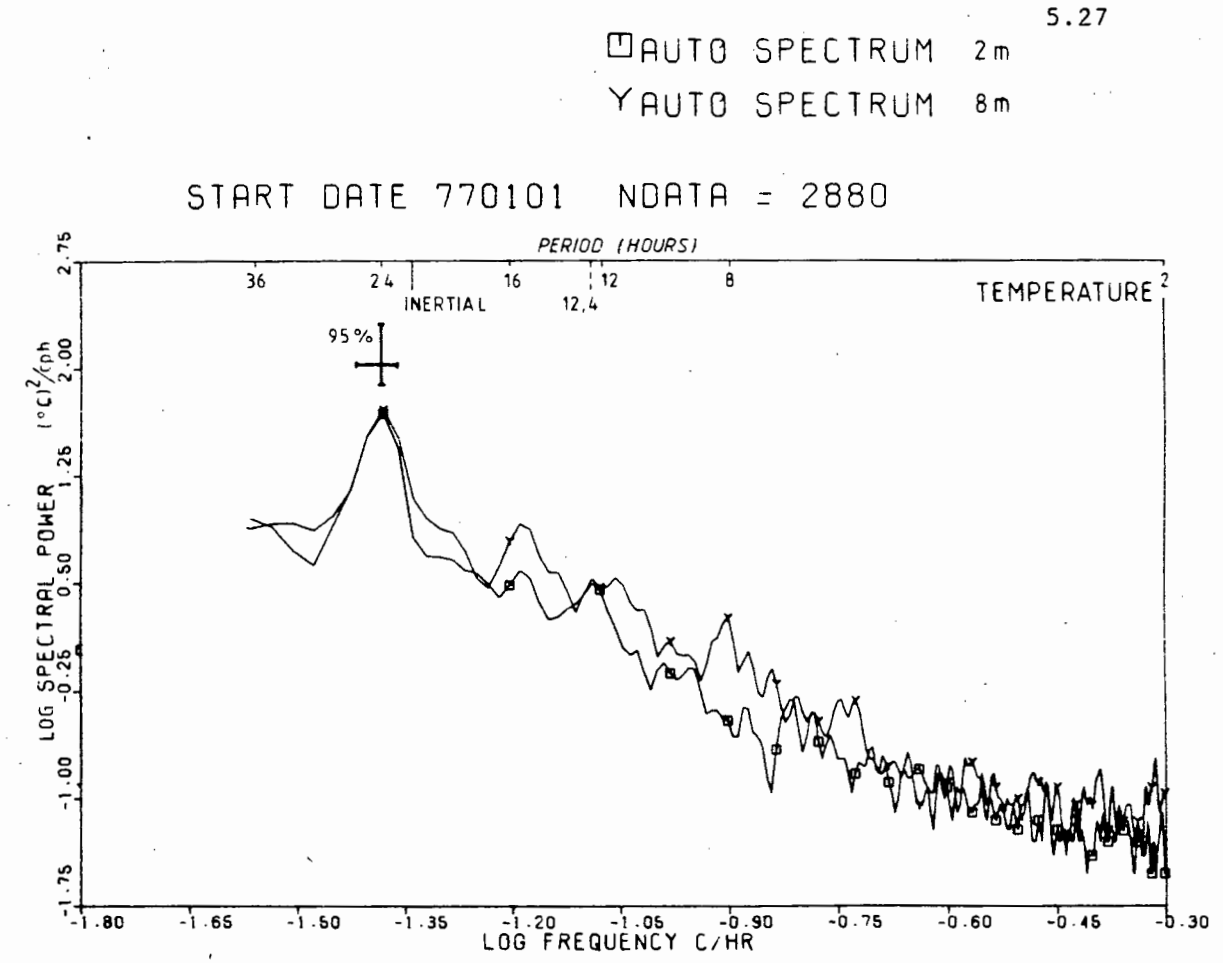

FIG. 5.8c SUMMER REGIME 1977 TEMPERATURE AUTO SPECTRA FOR HF FILTERED 2 M AND 8 M DEPTH TEMPERATURES FOR A PERIOD OF 120 DAYS STARTING 1 JAN 1977

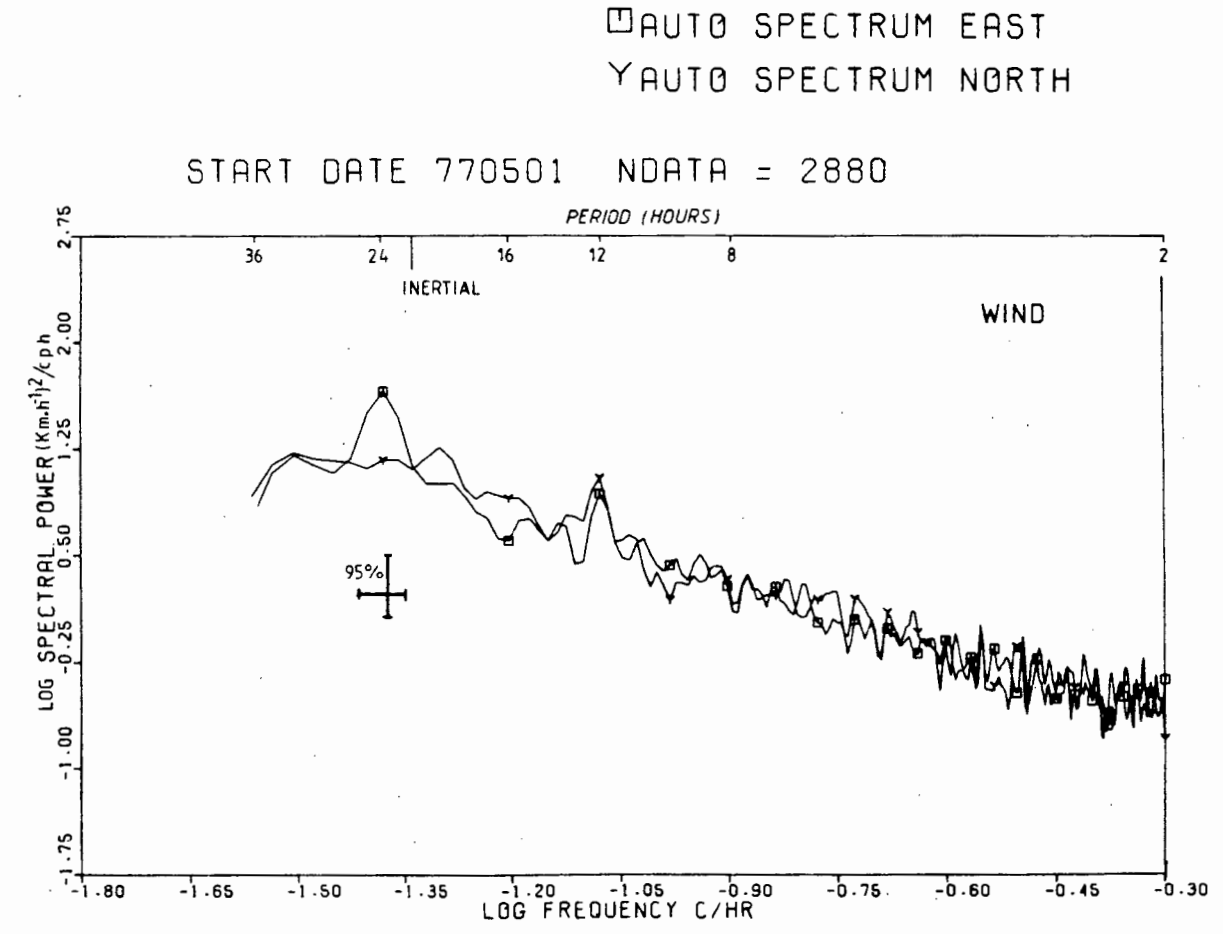

FIG. 5.9a WINTER REGIME 1977 WIND AUTO SPECTRA FOR HF FILTERED OU SKIP DATA FOR A PERIOD OF 120 DAYS STARTING 1 MAY 1977. MAXIMUM LAG NUMBER 240. PLOTTED SYMBOLS INDICATE EACH 10TH LAG NUMBER

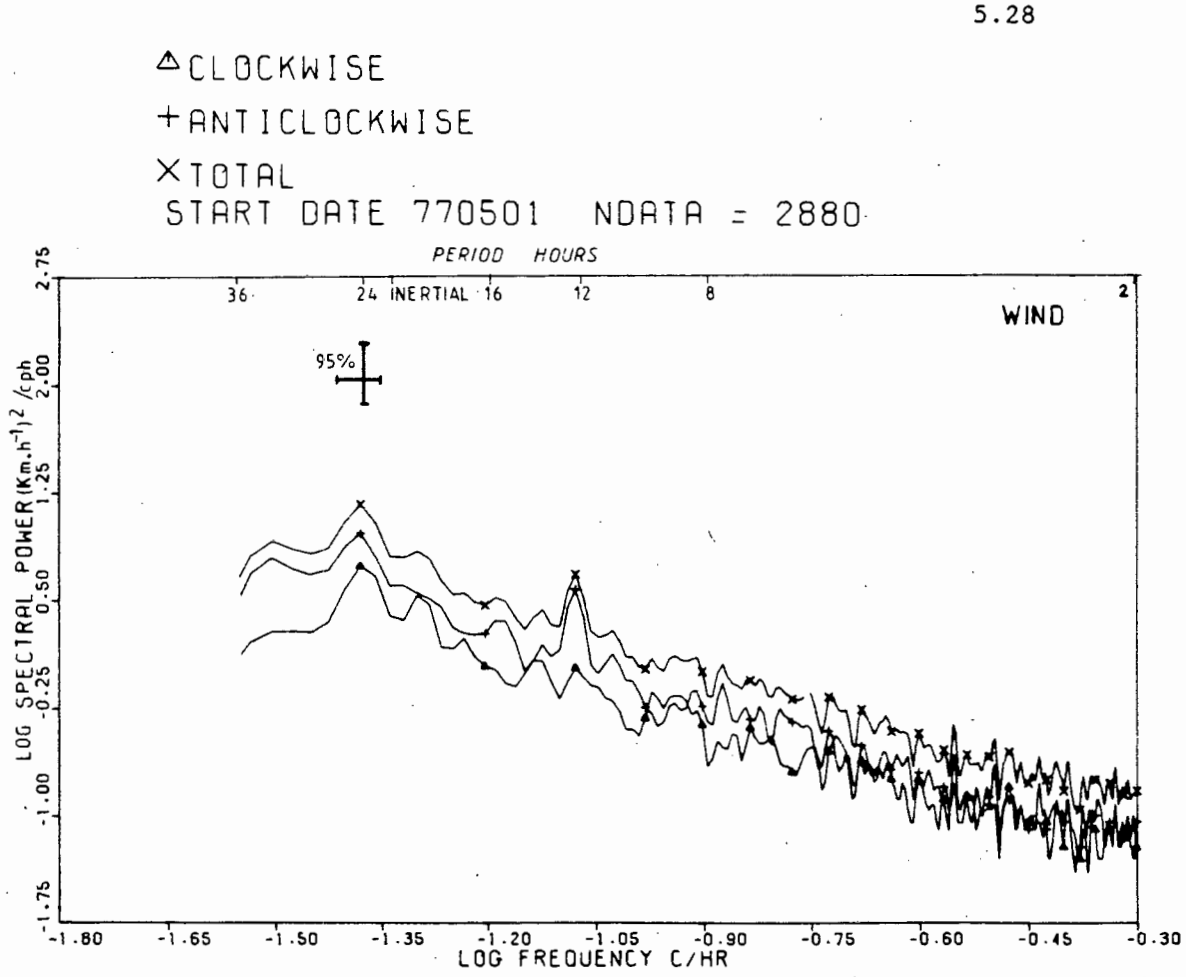

FIG. 5.9b WINTER REGIME 1977 WIND ROTARY SPECTRA FOR HF FILTERED OU SKIP DATA FOR A PERIOD OF 120 DAYS STARTING 1 MAY 1977

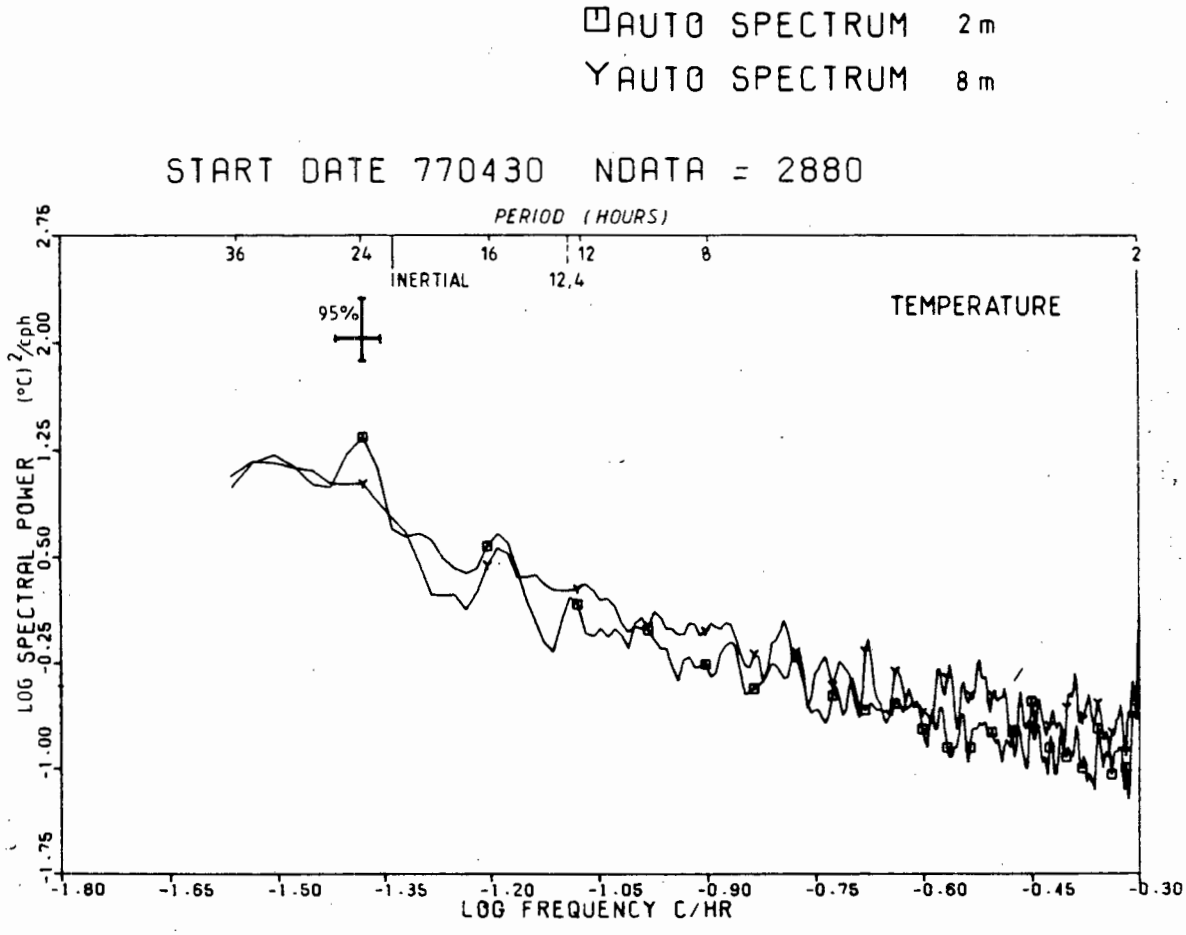

FIG. 5.9c WINTER REGIME 1977 TEMPERATURE AUTO SPECTRA FOR HF FILTERED 2 M AND 8 M DEPTH TEMPERATURES FOR A PERIOD OF 120 DAYS STARTING 1 MAY 1977

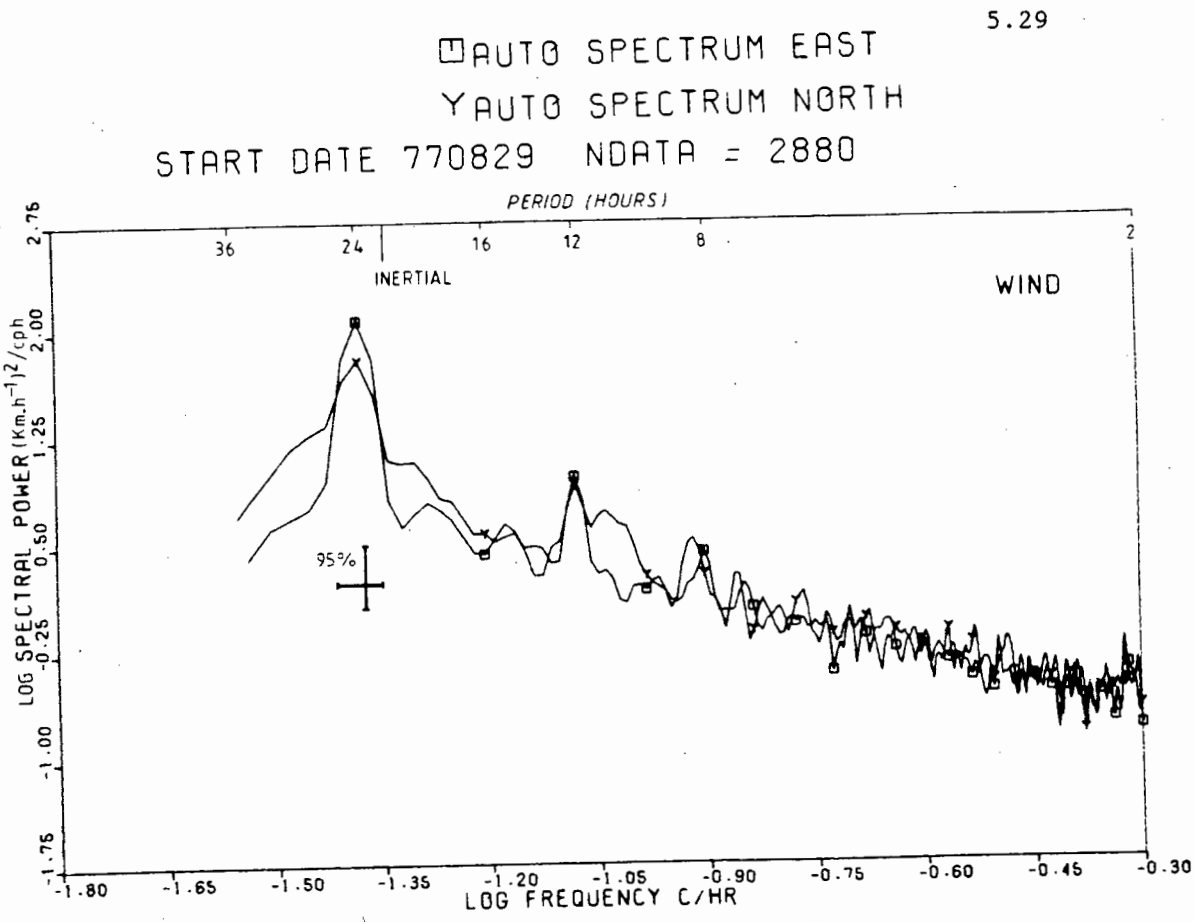

FIG. 5.10a SPRING REGIME 1977 WIND AUTO SPECTRA FOR HF FILTERED OU SKIP DATA FOR A PERIOD OF 120 DAYS STARTING 29 AUGUST 1977. MAXIMUM LAG NUMBER 240. PLOTTED SYMBOLS INDICATE EACH 10TH LAG NUMBER

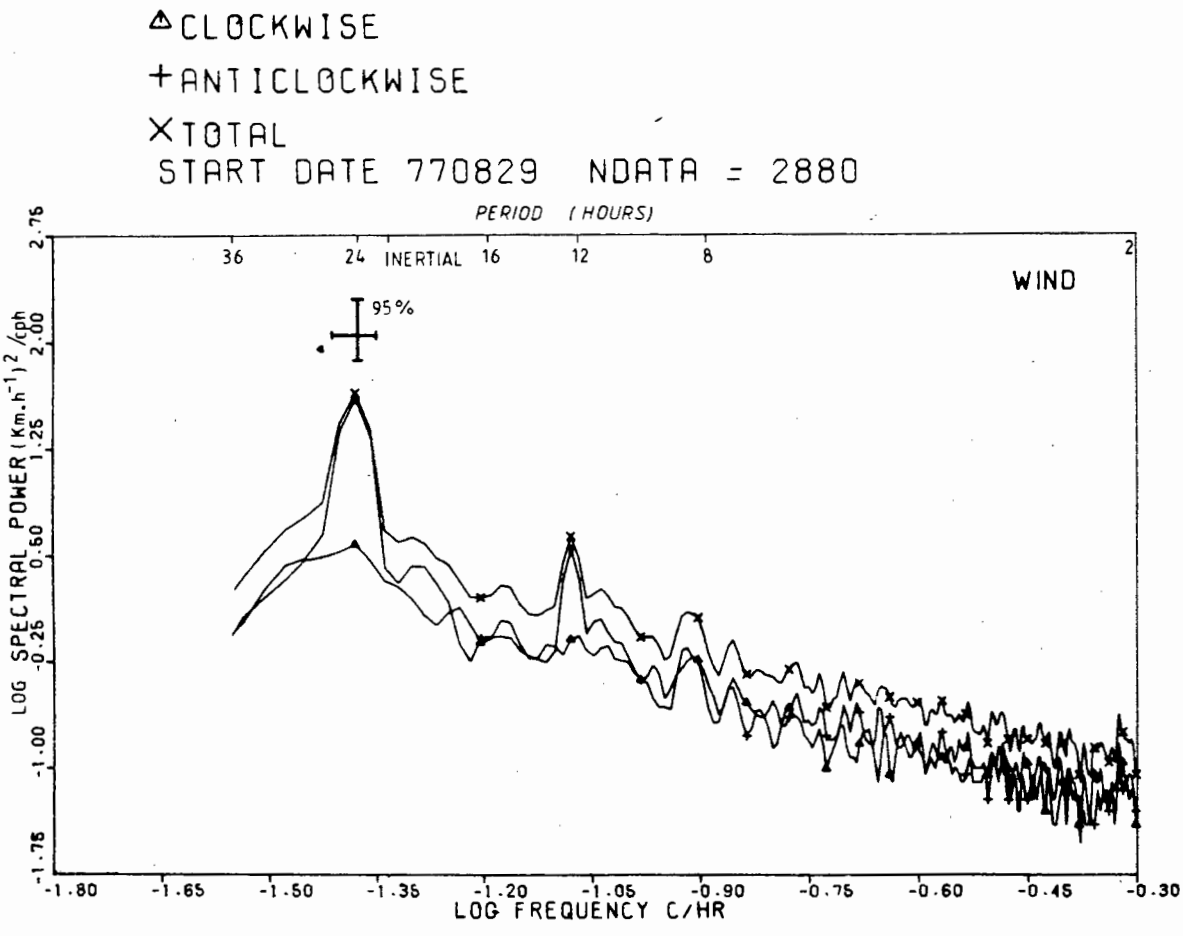

FIG. 5.10b SPRING REGIME 1977 WIND ROTARY SPECTRA FOR HF FILTERED OU SKIP DATA FOR A PERIOD OF 120 DAYS STARTING 29 AUGUST 1977

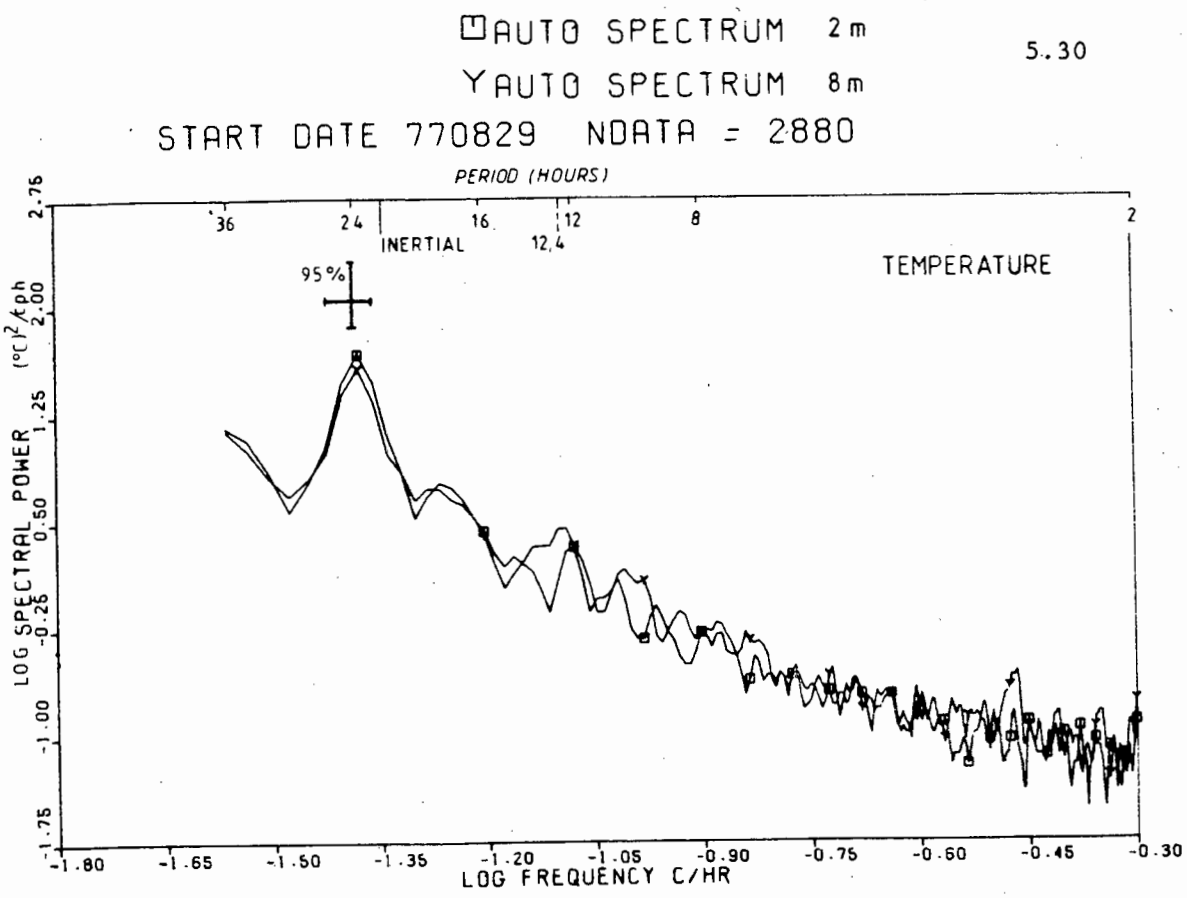

FIG. 5.10c SPRING REGIME 1977 TEMPERATURE AUTO SPECTRA FOR HF FILTERED 2 M AND 8 M DEPTH TEMPERATURES FOR A PERIOD OF 120 DAYS STARTING 29 AUGUST 1977

Surprisingly however in the winter regime of 1977, (Fig. 5.9a) the alongshore component which has no peak at 24 h period has a 12 h peak that is even larger than the across-shore peak. No satisfactory explanation can be found for this, except that it may lie within the range of statistical fluctuations.

In the rotary spectra the anticlockwise dominates at the diurnal frequency. At this frequency the ellipse orientation for all the regimes is significantly stable. From Table 5.4 it is seen that the preferred wind direction is closest to being orthogonal to the coast in the winter regimes when the axis orientations are 59° and 69° from true north for 1976 and 1977 respectively. The preferred diurnal wind orientation departs most from orthogonality in the summer regime when it is directed about the SW-NE axis. This is probably due to the effect of the stronger southerly gradient winds then. The rotary coefficient is smallest in winter indicating a tendency to more unidirectional (orthogonal) flow; the anticlockwise dominance is greatly reduced while the clockwise is somewhat increased (Table 5.4).

Because of bandwidth limitations any peak at the inertial frequency in wind and temperature seasonal regime spectra is not resolved. The 2 m depth data have consistently slightly greater diurnal energy than the 8 m data particularly in winter of 1977 when in fact the 8 m spectral data do not show any peak (Fig. 5.9c). This 2 m diurnal

dominance in the regime data is greater than the very slight enhancement in the annual cases. Although not statistically significant and of poor resolution there is structure in the temperature spectra near the M2 and S2 tidal frequencies, with a slight bias for more energy at the former frequency. No clear seasonal or depth dependent trend is observed at the tidal frequencies. At higher frequencies there is a bias for the 8 m data to be more energetic than the 2 m data.

In the temperature spectra of the summer and winter regime of 1977 (Fig. 5.8c and 5.9c) there is structure, close to a period of 15 hours, which approaches the 95% confidence limit. Since such features do not occur in other temperature spectra and do not have any counterpart in the wind spectra, any physical significance is doubtful.

In both the temperature spectra of 1976 and 1977 at frequencies above 1/12 cph the winter regime spectra have greater energy (by a factor of 2) than the other regimes. No such effect is seen in the wind spectra. Whether some high frequency processes contribute or a greater aliasing effect due to frequencies exceeding 1/2 cph is operating is not certain.

In summary one can say that the spectral analysis has very graphically proved the prime importance of diurnal forcing in both the wind and sea temperature data in the mesoscale range. The diurnal forcing is particularly noteworthy in the summer and spring regimes but is greatly reduced in winter. The good correspondence between the wind and temperature spectra except for the winds harmonic breakthrough peak at the semidiurnal frequency is corroborated by the section on correlation coefficients (5.2.2). The competing effects of direct insolation and diurnal wind forcing on the sea temperature response needs further consideration which is given in Section 5.3.

The analysis showed definite but small inertial and tidal effects in the temperature data. These were enhanced for the 8 m data whereas the 2 m data were enhanced at the diurnal frequency (across-shore predominant) particularly in winter. Discussion on this is reserved till later, however it seems the 8 m depth is responding to the upwelling dynamics and internal tides, with the 2 m surface response being linked to the relaxation phase of upwelling and possible insolation effects.

5.3 DIURNAL CYCLES AND FORCING PROCESSES

A feature of the sea temperature data at this time scale is its diurnal oscillations. The question arises, what is the chief cause of the diurnal behaviour? Is it due to direct effects of the daily insolation cycle or is it due to the wind field that is also modulated diurnally? In the discussion of the low frequency data (Chapter 4) the alongshore winds were significantly correlated with the sea temperature response and the across-shore winds had near zero correlation. In the high frequency analysis the across-shore winds are often better correlated with the sea temperature than the alongshore winds. Why is this so? The across-shore wind, together with the alongshore wind component and insolation evidently make up a complex inter-related system for potentially controlling the sea temperature. A review of firstly diurnal heating effects and secondly coastal water dynamics controlled by a land/sea-breeze system will now follow, and will be compared with the present data base in order to address the question posed above.

5.3.1 Diurnal Insolation Effects

Based on summaries and data from Roll (1965), Stommel et al (1969), Monin (1977), Price et al. (1986) and others the average characteristics of diurnal heating of **oceanic** waters is itemized below.

1. Time of occurrence of minimum temperature in surface waters <2 m depth is between 04h00 and 08h00 (local sun time). At 20 m depth the minimum can occur at 14h00. The maximum for surface to 5 m depth occurs between 14h00 and 17h00 in summer. The maximum deeper down lags the surface and can occur at 22h00 for 20 m depth. In winter the maximum can occur earlier at 13h00 (Koizumi, 1965).

2. Depth and temperature effects. The lag in temperature response with depth is noted above. There is also a definite decrease in the diurnal temperature range with depth, e.g. 0,3 °C range at 2 m and 0,05 °C at 30 m (Price, et al., 1986).

3. Range of temperature.
   1 °C in top 2 m at 30 N (Stommel, 1969).
   0.3 °C in top 6 m at 34 N (Howe and Tait, 1969).
   0.9° to 1.4 °C in top 5 m at 22 N (Halpern and Reed, 1976).
   0,05° to 0,4 °C in top 2 m at 30 N (Price, et al., 1986)
   Average annual diurnal range 0.28 °C at surface at 39 N.
   Minimum winter range 0.14 °C at surface at 39 N.
   Maximum summer range 0.54 °C at surface at 39 N (Roll, 1965).

4. Asymmetry in the diurnal cycle is noted. For subtropical waters the rate of temperature increase is greater than for the decrease and the temperature is above the daily average for 10 hours and below the average for 14 hours (Roll, 1965). Wind mixing causes further pronounced asymmetry in the surface temperature response by limiting the surface warming trend to about one quarter of the day (Price et. al., 1986).

The characteristics described above tend to be for multiday averages and are dependent on latitude and season and very much on the wind strength. Low winds with limited turbulence favour greater diurnal temperature ranges. References to shallow water observations will be made in the next section which deals with local findings.

5.3.1.1 Comparison with Local Observations

With a view to checking for insolation effects in the present study portions of the high frequency temperature record coinciding with light to calm winds are chosen. A 3 day section in January 1977 of the high frequency time series data for both 2 m and 8 m

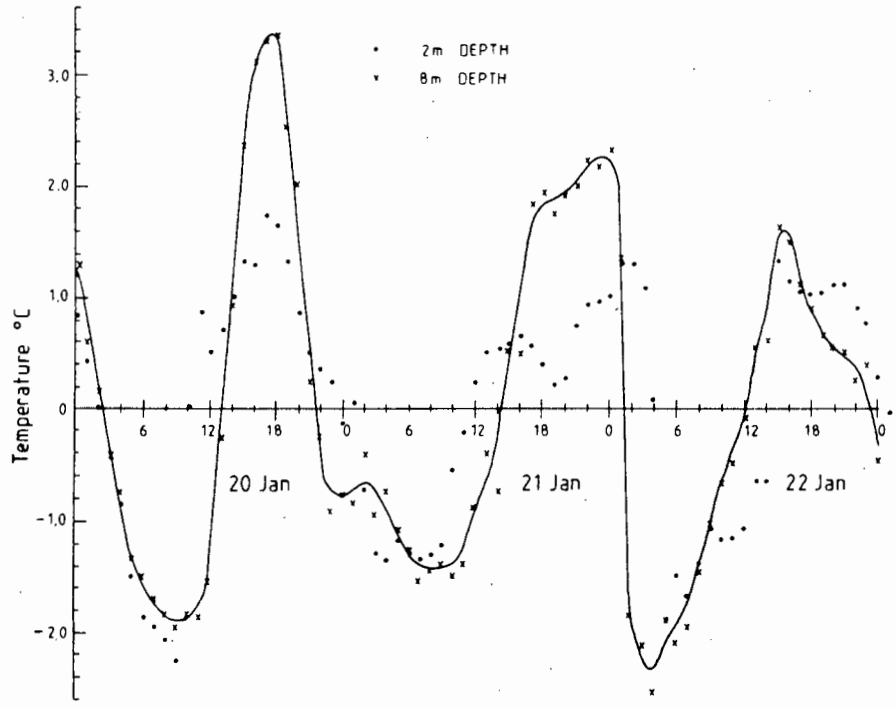

FIG. 5.11 TIME SERIES OF HIGH FREQUENCY FILTERED HOURLY DATA (ZERO MEAN) FOR 2 M and 8 M DEPTH TEMPERATURES FOR THE THREE DAY PERIOD 20 TO 22 JAN 1977. A VISUALLY FITTED CURVE IS PROVIDED FOR THE 8 M DATA

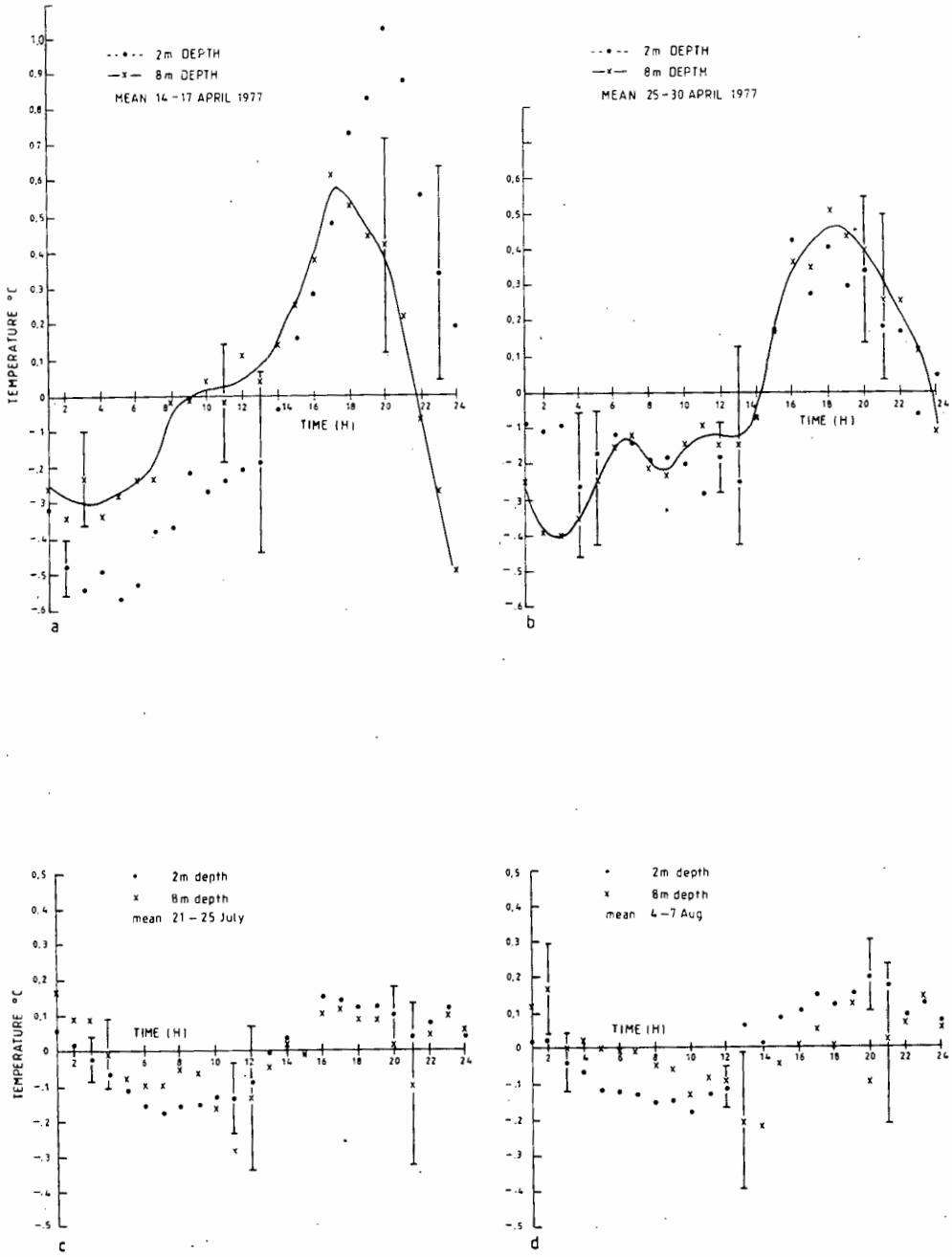

FIG. 5.12 MULTIPLE DAY HOURLY MEAN FOR THE DIURNAL CYCLE OF HIGH FREQUENCY FILTERED (ZERO MEAN) 2 M and 8 M DEPTH TEMPERATURES. STANDARD DEVIATIONS FOR SELECTED DATA POINTS ARE DISPLAYED. A VISUALLY FITTED CURVE IS PROVIDED FOR 8 M DATA IN CASE a AND b

depth temperatures is given in Fig. 5.11. The absolute temperatures are also depicted in Fig. 5.2c&d where the stratification can be gauged from an overlap of the 2 m and 8 m depth traces for the period 19 to 24 January 1977. In this case there are large temperature oscillations (which are also discussed in Section 5.3.4) with only light winds which are indicated on Fig. 5.1a and b and Fig. 5.2a and b. Multiple day averages for the diurnal cycle on an hourly basis are presented in Fig. 5.12a,b,c,d where data for two cases in April and one each in July and August are given for both 2 m and 8 m depth temperatures. The data are variable and average values of temperature at different hours of the day often have large standard deviations, so there is some spread in estimating maximum and minimum temperature values and their times of occurrence. Data from these cases are summarized in Table 5.6 which gives both the 2 m and 8 m data for 1) the times of occurrence of maximum and minimum temperature 2) the daily temperature range 3) the duration above the mean temperature; the mean wave height during each case is also listed.

In comparing these data with the four main characteristics of diurnal heating listed above the chief discrepancy relates to the first point i.e. the time of occurrence of maximum and minimum temperatures. The times quoted earlier are for local sun time. The time mentioned in this data is South African Standard time which is about 48 minutes ahead of the site's sun time. The times of occurrence (Table 5.6) for minimum temperatures for the 2 m case vary from 03h00 to 12h00 and are often past sunrise. The 8 m depth has minimum times even as late as 13h00, but also as early as 02h00. These minima are therefore often later than Rolls data. The time of occurrence of the maximum temperatures also tend to occur later than that expected from reported insolation effects, when for the 2 m depth a time of 20h00 is often observed. The deeper depth probe can be expected to have later times than the surface (point 2 above) but in this data the 8 m maxima occur both a few hours before and after the 2 m maxima and as late as around midnight.

Some shifts in the time of occurrence of maximum and minimum temperature are reported in the literature. In shallow water near the equator Morita (1978) reports that at a depth of 6 m the minimum occurs at 06h00 to 08h00 and the maximum between 16h00 and 19h00, which is later in each case than the reports for oceanic waters. Smith (1977a) finds in very shallow water (0.5 m) during winter that the maximum temperature occurs at 16h00 and that the minimum occurs at 08h00. Inspection of graphical data in Jacobs (1978) reveals some departures from the mean conditions he reports; the minima sometimes occur as late as 10h00. Pivovarov

et al (1976) notes that with an increase in vertical eddy exchange coefficient there is a shift of a few hours to a later time for the time of maximum and minimum diurnal temperatures. Larger shifts in time of the maximum at deeper levels is recorded by Jacobs (1978) for larger vertical density gradients. The vertical eddy exchange coefficient is expected to increase in nearshore waters (Simons, 1974) but these shifts to later times do not seem great enough to wholly account for the larger and more consistent shifts observed in this work and some wind forcing and advection may play a role.

In Table 5.6 the range of temperatures observed, 0,7 to 1,7 °C for April cases (Fig. 5.12a) and 0.4 °C for July and August (Fig. 5.12b and c) are consistent with insolation effects itemized in point 3 above. The January (Fig. 5.11) values of up to 4,0 and 5,4 °C for the 2 m and 8 m data respectively are much larger and more likely wind induced. This large range and the relationship between the 2 m and 8 m data is shown in the overlap section of Fig. 5.2d. Morita (1978) observes a range of only 0.9 °C at the 6 m depth near the equator, and Smith (1977a) reports a range of 2.4 °C in very shallow water (0.5 m) during winter at a latitude of 28°N. On the Agulhas Bank during February, Largier and Swart (1987) report a diurnal range near the surface of about 1 °C.

The 2 m depth data tends to be less variable from hour to hour than the 8 m data, and in cases 2, 3 and 5 in Table 5.6 have a smaller range than the 8 m data. The longer term averages over 10 to 30 days covering more representative wind conditions show that the 8 m data are more variable (Table 5.2). The smaller variability at the 2 m level is probably attributable to greater turbulence near the surface due to waves and wind which will smooth out temperature differences. The greater range at 2 m for case 1 could be ascribed to insolation effects that are enhanced near the surface under light air conditions and the fact that the average wave height of 1,3 m then was the least for the different cases. Jacobs (1978) who observes noisy temperature signals at lower depths (20 m) sites internal waves as being a possible cause, which may also be applicable to the 8 m depth behaviour reported here.

The fourth characteristic - asymmetry - in the diurnal heating cycle, has a counterpoint in the April cases when the temperature is above the average for 9 to 11 hours (Table 5.6). In very shallow water (0.5 m) Smith (1977a) finds a duration of 11 hours above the mean temperature. The winter July-August data have a less clear time balance because of the large standard deviation on the mean hourly readings but the duration above and below the average temperature appears fairly even, although the 2 m depth data have one contrary pattern of being warmer longer. Although

the individual cycles in the 3 day January set (Fig. 5.11) exhibit a fair amount of variability the mean for this summer case (Table 5.6) has an asymmetry favouring the 2 m temperature to have a period above the mean exceeding 12 hours while the 8 m data has a shorter period. The asymmetry in duration of insolation between summer and winter days should have some influence on the data; at the site daytime is an average 1,25 times longer in summer than in winter and the total daily radiation is 2,3 times greater (Brown, 1984).

Three papers, Arthur (1954), Cairns and Nelson (1970) and Winant and Olson (1976) deal with temperature (and current) characteristics in shallow (18 m or less) coastal waters near San Diego, California. They discuss observations of strong semidiurnal temperature oscillations due to internal tides but strangely they fail to make any mention of insolation effects.

Other local evidence for insolation effects is presented in Section 5.4 on spatial aspects; there is a direct diurnal temperature increase in January of 2,5 °C in 1,5 m water depth adjacent to a wide beach area and airborne radiation thermometry reveals an afternoon maximum in the thermal inshore band, flanking cold upwelled water. The width of the warmer band near the sea tower is typically less than 500 m and any temperature enhancement due to the band is probably well under 0,5 °C (see 5.4.1).

Some of the facts presented have pointed towards insolation being the process causing the temperature oscillation and others have detracted from a direct insolation effect. Before passing further comments on this mechanism the role of wind forcing will be discussed.

5.3.2 Diurnal Wind Effects

The classical explanation of coastal upwelling is for an alongshore wind to drive an Ekman surface flux offshore with cool water moving inshore along the bottom. This was demonstrated in Chapter 4 at the event time scale when the alongshore winds were positively correlated with the temperature response. At the diurnal time scale we have seen in contrast that at times the alongshore wind correlation with temperature is poor and that the across-shore correlation is good (Table 5.1). The across-shore dominance at the diurnal frequency is also demonstrated in the spectral analysis.

In a discussion of elementary Ekman currents Neumann and Pierson (1966) show that in shallow water, where the depth is one quarter of the Ekman depth of frictional influence D (see 1.2.1), there is

virtually no veering of current from the wind direction with winds either parallel or perpendicular to the coastline. The response to perpendicular winds is somewhat smaller than the alongshore response. The basic alongshore character of the flow is also given by Jeffreys (1923).

Under such conditions an offshore flux is only driven by a directly offshore wind. In Csanady's (1977a) full upwelling model the main effect is felt with a alongshore wind and none with an impulsive across-shore wind although a steady across-shore wind does cause some upwelling.

The models for wind driven currents by Thomas (1975) for shallow water and Madsen (1977) for deep and shallow water adopt a more realistic variable eddy viscosity coefficient than in the classical Ekman analysis. They are not extended to a coastal geometry but do show differences from the Ekman prediction of the angle between wind and current. Madsens model however predicts a much shorter response time ($\sim$3 pendulum hours or about 5 hours locally) to reach steady state after the application of a sudden wind stress. This rapid response may be relevant to the time scale of sea-breeze forcing.

In an oceanic study Price, Weller and Pinkel (1986) determine the trapping depth for surface currents in an insolation cycle. They observe a near surface diurnal jet that accelerates downwind during the morning and midday and turns into the wind by early evening due to the Coriolis force. Strongly surface trapped flow can occur over a depth of only 5 m (Price, Weller and Schudlich, 1987) that deepens into the evening with wind mixing; with the layer thickening the surface velocity decreases and a veering with depth occurs.

These theoretical or oceanic studies are limited in their application to this study by the complexity of the real situation occurring in shallow coastal waters. Advection causes contamination of the temperature signal (Price et. al., 1986) and the nearshore zone is excluded by McCormick and Meadows (1988) for serious study of mixed layer dynamics.

In a noteworthy field study of trajectories and speeds of wind driven currents within 800 m of the coast in depths of less than 14 m, Murray (1975) finds that the primary current generated by the local wind is directed within a few degrees of parallel to the coastline nearly independently of the wind direction. The current speed is more controlled by the wind angle than the wind speed, being maximum for alongshore winds and virtually zero for winds normal to the coast. His other important observation is the existence of a subtle vertical structure in the offshore-onshore components of the current

velocity. Unstratified water subjected to a generally onshore wind produces a two layer flow, onshore in the surface layer and offshore in the bottom layer. Moderately stratified waters produce a three layered flow; onshore in the surface and bottom layers and offshore at intermediate depths.

This onshore-offshore flow can induce upwelling or downwelling temperature effects on the local scale. Such effects are in fact shown for a land/sea-breeze system by Sonu and Murray et al. (1973) for a measuring site 500 m offshore at a depth contour of 9 m. They observe 3 m from the surface a diurnal cyclic behaviour for the water density with peak onshore winds of 5 $m.s^{-1}$. These near normal to the coast winds do succeed in diurnally reversing the prevailing alongshore current system. At Melkbosstrand HF filtered summer onshore winds vary from 3 to 6 $m.s^{-1}$ and in winter are up to 4 $m.s^{-1}$.

Unluata (1980) reports diurnally generated currents at a 20 m depth for a strong 15 $m.s^{-1}$ sea-breeze system at a site 2 km off the Turkish coast in a total depth of 30 m. His rotary spectral analysis shows that the current is approximately 90° to the wind at the 24 hour period. This behaviour he proposes is in agreement with time dependant Ekman boundary layer flow. His rotary analysis ellipse aspect ratio of 0.8 however, also implies that there is appreciable occurrence of current flow parallel to the wind. He also observes inertial period current oscillations. Millot (1979) reports transient upwelling with prominent inertial oscillations in temperature and current 2 km offshore (25 m depth) with strong winds normal to the coast.

In the earlier literature survey in section 1.2.1 the coastal boundary layer was discussed, where within the CBL linear alongshore currents predominate which agrees with Murray's (1975) observations for shallow water; beyond this region current are predominantly rotary or wavelike in motion and inertial frequencies are observed. Upwelling and downwelling effects are confirmed in the inner zone (Blanton, 1975, Csanady, 1977a).

Smith (1977b) also observes essentially alongshore currents in an inner zone (4.7 km offshore in 13.5 m depth water) but notes significant across-shelf currents that correlate with both alongshore and across-shore wind stress components on a 1 to 4 day time scale. He suggests that the across-shore motion may occur both as a simple return flow in response to across-shore wind stress, and as a result of an across-shore Ekman transport established by alongshore wind stress.

There are other models that consider the effects of diurnal time scale winds on the sea surface. The model of Pollard (1970) and Pollard et al (1970) shows that local winds that fluctuate with a time scale less than the inertial period are most efficient in generating inertial currents in the surface. His model is adapted by Boyd (1981) to include a diurnally varying wind force in a mid winter study of coastal currents in a land/sea-breeze regime off the coast of SWA/Namibia. Boyd favourably compares his results with those of the model of O'Brien et al (1977) for upwelling in a sea-breeze regime. Boyd's observations include: an anticlockwise rotating diurnal oscillation in a surface slab of 8 m depth; a diurnal fluctuation of about 3 m in the depth of the upper layer at a greater distance offshore (10 km) than that predicted by O'Brien, and a diurnal sea temperature fluctuation of about 1 °C. The predictions of the slab model of Pollard et al., (1970) is also used by Paduan et al., (1989) to compare with observation of mixed layer inertial currents in an oceanic study over a scale of 50 km. They show that small scale structure in the wind field has significant effects on the inertial current response.

In considering Murthy and Dunbar's (1981) concept of two coastal boundary layers, it seems fair to say that the models of Pollard, Boyd and O'Brien are more applicable to the Inertial Boundary Layer and the further offshore zone. In fact Begis and Crepon (1975) in a modification of Pollard's (1970) model find its validity depends on the distance offshore being much greater than the Rossby internal radius of deformation. Closer inshore the vertical diffusion coefficient increases (Simons, 1974) and inertial oscillations are damped out. However, Blanton (1975) still observes a 10 % inertial behaviour some 2 km (15 m depth) from the coast, and Murthy and Dunbar (1981) observe a 10 % contribution at a 4.5 km distance.

In what is probably the first integrated analysis of diurnal period wind stress and currents over the continental shelf, Rosenfeld (1988) shows that diurnal currents are strongly intensified at the surface and well correlated with the local diurnal wind stress. Strong upwell producing winds coincide with strong diurnal modulation of the wind stress which modulates the surface current. Rosenfeld (1988) uses a one dimensional mixed layer model forced by wind and surface heat flux to obtain reasonable agreement with the observed upper ocean diurnal currents.

5.3.2.1 Possible Local Wind Effects

In summary of all these findings on wind effects and in an attempt to relate them to the local data of the present study it appears that the classical Ekman solution cannot be directly used but that two

competing effects or their combination can be considered. Either a) the subtle onshore-offshore flow observed by Murray (1975) and/or b) the slab behaviour observed by Boyd (1981), can upwell or advect water masses into and out of the measurement area to give a diurnal temperature signal.

Which mechanism predominates will depend on the prevailing conditions but because of the shallowness of the measuring site probably a) will dominate. A discussion of the merits of a) and b) now follows.

a) This mechanism allows for across-shore diurnal wind forcing. A feature which is particularly relevant to the present data is timing of occurrence of on and off-shore flow of denser water. This relevance assumes the density changes are temperature related. Sonu et al. (1973) in his Fig. 7 for summer data, shows minimum densities occurring between 16h00 and 20h00 followed by a gentle rise which suddenly steepens at 10h00. These times lag by a few hours the maximum on and offshore winds. These lags correspond to our correlation data (Table 5.1) which show in summer time that the temperature response lags the across-shore wind by 2 to 4 hours. They note that the rebound of the density is accelerated by the offshore directed early morning land breeze. The times quoted, with their late occurrence of minima and maxima follow the present data fairly closely. This data with their often bottom-up response for ingress of cold water favours the two layer system of Murray (1975) rather than the three layer flow also reported by him. The diurnal across-shore wind component modulates the alongshore wind to give the on-off effect. Locally an example of regular diurnal across-shore winds coinciding with weaker alongshore winds occurs in the winter regime in Fig. 5.3a and b for 23-25 May 1977. This follows a strong southerly wind on the 22nd which causes some upwelling. Although the temperature response is small $\pm$0,5 °C a definite diurnal signature can be followed in Fig. 5.3c and d. This case forms part of the period 22-31 May 1977 used for correlation analysis in Table 5.1 and shows better correlation for the across-shore wind.

b) Despite its shallowness, inertial to diurnal frequency currents in an upper slab layer have been observed at the present site during an earlier phase of this study (Bain and Harris, 1975) when radar tracked drogues were tracked in near inertial circles for 2 to 3 days at a distance of 1 to 3 km offshore. Boyd (1981) shows in his model that near elliptical current trajectories with the major axis approximately normal to the coast are generated with diurnal winds. The greater the friction coefficient the greater the departure from a circular trajectory. Such diurnal trajectories superimposed on a

possible longshore drift will advect surface water on and offshore diurnally. Any horizontal temperature gradient can then be transported periodically across the measuring site. In the present study a horizontal gradient normal to the coast of +1 °C per 10 km and +0.5 °C per 1 km have been observed in winter (Bain and Harris, 1975) compared with the observed diurnal oscillation of about 0.3 °C. In summer and spring upwelled fronts with a gradient of several °C in less than 1 km are observed (Fig. 4.18b). A "slab" behaviour will favour a better correlation between the wind and the surface 2 m depth temperature data. Evidence for this is not definitive except that onshore winds have a tendency to favour a surface response. Boyd (1981) also observes a diurnal 3 m fluctuation in the depth of the upper layer which O'Brien et al (1977) ascribes to the periodic convergence and divergence associated with the oscillation and kinematic boundary condition at the coast. If a vertical temperature profile exists then such an oscillation in the upper layer depth will produce a temperature oscillation at the fixed measuring point.

One comes back to considering, why in this frequency range is the across-shore wind often better correlated with the temperature than the alongshore wind? Can either mechanism a) or b) provide an answer? For either case an existing temperature gradient has to be assumed. Consider an alongshore southerly wind initiating an upwelling event. From inspection of the raw wind and temperature plots a delay in the temperature response is seen. At the 8 m depth the initial response is within a few hours but the minimum temperature peaks after 8 to 12 hours. At the 2 m level, depending on the depth of the thermocline and strength of the wind there may be no response or the initial response is delayed, with minima lagging by more than 12 hours. When a diurnally rotating anticlockwise across-shore wind is superimposed, the southerly wind is modulated but does not necessarily reverse. With an onshore across-shore component a warm surface layer is advected inshore and downwelling can be initiated. This will correlate in a favourable way, for the across-shore wind (see Section 5.2.2), but is actually unfavourable correlationwise for the southerly alongshore wind. The across-shore wind is more likely to make an absolute change in the on or offshore sense and be well-correlated but if the alongshore wind stays southerly it will have a good initial lagged correlation at 8 to 12 hours but subsequently not so favourable. If the alongshore wind swings to the north, because of its rotary character it will have to pass through an across-shore phase which will then correlate sooner with the temperature change. The more probable mechanism for the shorter lag in across-shore correlations in the warmer months is that at that time the onshore winds are more prominent than the offshore component and the resulting across-shore correlation is essentially

at the downwell phase. This phase of temperature increase has been shown (5.2.2.1 and elsewhere) to be quicker than the decreasing response to southerly alongshore winds (even though the actual drop in temperature may be steep it is delayed) therefore the across-shore winds correlate with the shorter lag. This leads to the obvious question, why is the downwelling quicker? This will be discussed later in 5.5.

The process operating in b) can also favour across-shore winds since the horizontal temperature gradient is usually normal to the coast. Any elipticity in the current trajectories with the major axis having an offshore orientation which is the case for across-shore winds will enhance the diurnal temperature differences. The local diurnal winds have a dominant anticlockwise rotation which will support inertial currents.

Both processes therefore seem to favour across-shore winds to correlate better with sea temperature fluctuations at this frequency range. The primary upwelling feature with its associated temperature contrasts is still generated at the event time scale by the alongshore winds. At the diurnal time scale we conclude that it is chiefly the across-shore winds that modulate the sea temperature response through their modulation of the alongshore winds which will at times also correlate well with the sea temperatures. The on and offshore flow process a), of Murray (1975) should dominate compared to the slab flow of b) which may occur less than 10 % of the time (Blanton, 1975).

5.3.3 Appraisal of Wind versus Insolation Effects

Finally in considering the role of both wind forcing and insolation in the diurnal temperature oscillation we comment as follows:

The fact that the land/sea-breeze system is itself driven by an insolation process implies that there should be a correlation between these winds and any insolation heating effects in the sea. The minimum contribution of direct insolation can probably be gauged by the diurnal sea temperature oscillation after a multiday northerly storm when onshore advection, strong winds and large waves will produce a homogenous water mass. Under such conditions, which often include reduced insolation due to cloud and rain, diurnal temperature oscillation is still observed; about $\pm$ 0.1 °C in winter and about $\pm$ 0.3 °C in spring and summer. A maximum contribution in winter can be deduced from the data presented in Fig. 5.12c and d for July and August for very calm wind conditions, when $\pm$ 0.2 °C is observed. In winter therefore any fluctuation greater than about $\pm$ 0.2 °C can be attributed to advection processes which are usually wind generated.

Numerous occasions of the temperature oscillation exceeding 0.2 °C are observed in the winter data and are further illustrated by the size of the monthly standard deviations varying from 0.1 to 0.2 °C (Table 5.3). The biggest oscillations correlate with southerly wind events.

In the couple of months during spring/summer when there is maximum insolation, the maximum effect on sea temperature during wind calm periods cannot be deduced with any certainty. Firstly, there are few multiday calm periods during this period on which to base any conclusions and secondly the longest calm period selected (Fig. 5.11 and section of Fig. 5.2d) although it has very large fluctuations there are a few factors that mitigate against a significant direct insolation effect. The fluctuations are greater at 8 m viz $\pm$3 °C than at 2 m ($\pm$2 °C); the time of 8 m data-peaking both leads and lags the 2 m data; the time of peaking is sometimes late and close to midnight and over the three days there is a steady decrease in peak temperatures both at 2 m and 8 m depths. The fluctuations could rather be attributed to inertial effects supported by light across-shore winds (see Section 5.3.4).

For a given seasonal period the basic insolation input at the sea surface[e)] is very regular except when disturbed by atmospheric effects. In winter the across-shore wind component is observed to be generally more regular diurnally than the alongshore component (from spectral analysis) and tends to have a superior correlation with the sea temperature response. In summer the across-shore winds are still dominant at the diurnal frequency and their correlations with the temperature response are about equal to or greater than the alongshore correlations.

The skewed diurnal temperature distribution is most likely due to a diurnally forced wind advection process. In spring and summer, upwelling events can produce large horizontal temperature gradients (fronts) close to the coast (Fig. 4.18). When this occurs the comment by O'Brien et al (1977) "for a sea-breeze regime the diurnal sea temperature fluctuation with amplitude order (1 °C) is primarily because of horizontal advection" is probably true.

We conclude that in winter the maximum direct insolation effect on the sea temperature is about $\pm$ 0.2 °C and by deduction from the standard deviation of sea temperatures then, there is in addition a good contribution to temperature fluctuations by wind advection processes. During spring and summer the light air conditions that favour maximum direct insolation effects do not occur frequently. These maxima are difficult to separate from other effects but are about $\pm$ 1 °C and the minimum effect is about $\pm$ 0.3 °C. From the

observed diurnal temperature fluctuations in spring and summer the major cause of the oscillation is attributed to wind effects on a small scale local upwelled region.

5.3.4 Inertial and Tidal Effects

Prominent temperature oscillations due to semidiurnal internal tides are observed in shallow water (18 m depths) by Cairns and Nelson (1970) and by Winant and Olson (1976). In the present work visual comparison of the temperature and tidal record reveals no obvious evidence for any semidiurnal tidal influence on the temperature oscillations. However, apparent semidiurnal frequencies can be observed in a short section of 8 m temperature data from 4-7 January 1977 (Fig. 5.1d) and in Section 5.2.3, spectral analysis indicates a small peak at the M2 tidal frequency. At another site about 100 km further south in 100 m water depth significant temperature oscillations at the semidiurnal tidal frequency are observed (Largier, 1987). The lack of prominent semi-diurnal internal tides at the study site are probably due to the shelf slope not always being supercritical for the coastward propagation of interfacial tides. From a simple two layer theory of Largier (1987), propagation occurs if the topographic slope, δ, and the slope of tidal characteristics, γ, meets the criteria that the continental slope has a supercritical slope $\delta > \gamma$ and that the continental shelf has a subcritical slope $\delta < \gamma$.

$$\gamma = \left(\frac{\sigma^2 - f^2}{N^2}\right)^{1/2}$$

where σ = tidal frequency
f = inertial freq (local)
N = Brunt-Vaisala frequency (local).

Adjacent to the site the shelf slope is 0,004 and the continental slope is 0,044. For the semi-diurnal tide the tidal characteristic γ is calculated, with a range of N from 0,002 to 0,02 rad.s^{-1}, to be between $9{,}4 \times 10^{-3}$ and $9{,}4 \times 10^{-4}$. It is seen that the criteria for the continental slope is met but that the shelf slope is not always supercritical.

In the discussion on diurnal wind effects (5.3.2) reference was made to Pollard's (1970) model for generation of inertial currents by transient winds. He finds winds both generate and destroy inertial currents in the open sea, where the occurrence of such currents is ubiquitous (Webster, 1968). Inertial oscillations are often seen at the initiation of transient upwelling (Hayes and Halpern, 1976). In shallow water Albuisson et al. (1978) observe strong inertial temperature oscillations with a wind perpendicular to the coast in

the Gulf of Lions, but with shore parallel winds oscillations tend to be concealed by the large upwelling effect. In the Gulf of Lions where tidal influences can be neglected, Millot and Crepon (1981) show that inertial oscillations are associated with two different physical processes. The first describes the local response to the wind stress and the second is associated with the propagation of long internal waves generated at the shore in the transient phase of the geostrophic adjustment process. Reference has also been made earlier (5.3.2) to Murthy and Dunbar's (1981) inertial boundary layer region. One could therefore expect to find some evidence for inertial currents in the present data set. Earlier (5.3.2.1) reference is made to Bain and Harris (1975) who observed inertial like currents from drogue tracking studies - 1 km offshore at the site. The spectral analysis of temperature data (Section 5.2.3.1) has also shown a small peak close to the inertial frequency. On occassions, usually when a strong ($\sim$15 $m.s^{-1}$) southerly wind impulse is followed immediately by one or more days of light airs, relatively large temperature fluctuations are observed in the high frequency data without corresponding large wind fluctuations. Such large temperature oscillations are illustrated in Fig. 5.11 which shows over three days the skewed time distribution for late occurrence of the minimum and maximum diurnal temperatures. This fact, together with the observations that the 8 m depth has the greater oscillation and in the raw data there is actually a net decrease in maximum temperature over the three days of light winds, particularly for the 8 m depth (Fig. 5.2c and d), probably rules out a major direct insolation effect and favours an inertial process. The spacings of the temperature minima and maxima are at times less than 24 hours which suggests a possible inertial time scale. The local inertial period of 21.6 hours is very close to the 24h cycle and resonant excitation may occur between them as reported by Unluata (1980) for a 20.4h inertial period and the diurnal forcing period.

Hayes and Halpern (1976) report the generation of inertial-internal waves in the top 10 m layer at the start of an upwelling event and that they decay within a day or so; the diurnal band has a kinetic energy peak occurring slightly after the inertial band and the decay is slower. In our case the effects of the inertial and diurnal bands would tend to overlap and with just a short sharp upwelling wind impulse followed by a calm one may expect the decay to be less rapid. There is in fact a progressive decay in temperature amplitude over the three days shown in Fig. 5.11 and in Fig. 5.1c and d. The greater decrease in the absolute temperature for the 8 m data with respect to the 2 m data while the 8 m minima remain relatively constant (Fig. 5.2c and d) also indicates the decay in temperature can be associated with a mixing process that favours dilution with the upwelled colder water. Millot and Crepon (1981) who also observe

inertial temperature oscillations generated by a gust of wind calculate theoretically that the frictional spin-down time due to bottom friction is much larger than the inertial period.

Although the temperature fluctuations in Fig. 5.11 are for an essentially calm period there is in fact on each day a period of onshore winds. Short duration pulses of approximately NW winds (2 $m.s^{-1}$) occur on 20 and 21 Jan 1977 at about 13h00 and 17h00 respectively (see Fig. 5.2a and b). On the 22nd a stronger (4 $m.s^{-1}$) longer duration SW pulse starts about 9h00 and peaks in the afternoon. These light and short duration onshore winds will basically only reinforce the temperature increase phase. The continuing oscillation is probably linked to some inertial process.

The conclusion is therefore that we have reasonable evidence for inertial oscillations to occur at times in the study area. There is also a definite but minor tidal contribution to the temperature response.

5.4 SPATIAL ASPECTS

At the event time scale the spatial aspects of the upwelling plume are well illustrated (Section 4.4). The upwelling is forced chiefly at the event time scale but we have seen that it is modulated at the diurnal scale. The coverage of the diurnal spatial structure is not so comprehensive. Although the early morning ART flights usually intercept a near minimum diurnal temperature state, the afternoon flights do not necessarily measure the surface expression of the maxima. In future, in order to realistically characterize the diurnal sea surface temperature (SST) evolution, additional flights during the day and in the hours of darkness would be required.

5.4.1 Inshore Thermal Band

One feature of the diurnal SST distribution however is revealed graphically in the contour maps (Fig. 4.20a-e). A warmer thermal band is seen to develop close to the coast with the maximum contrast in the afternoon. The band is a narrow section of warmer inshore water flanked on the offshore side with cold upwelled water. In the SST maps (Fig. 4.18a, 4.20a-e) and in numerous others that are not presented, the band is non-existent or of small contrast near sunrise but is most conspicuous for midday to afternoon periods, particularly north of the sea tower where it is wider. In the afternoon the temperature difference between the shoreline and the colder mass offshore is typically a) 1 to 2 °C over a band less than 500 m wide adjacent to the focus region in the south; b) 1,5 to 3 °C over a

1 km width north of the sea tower. Generally, from observation of numerous SST maps the sea tower is positioned within the cold band several hundred meters from the edge of the thermal band. By checking the horizontal temperature gradient revealed in the SST contours, any enhancement of temperatures at the sea tower due to encroachment of the thermal band is suggested to be well below 0,5 °C.

The banding effect is most prominent during active upwelling. Under downwelling conditions the overall SST are warmer with no obvious warmer band - in fact the inverse can occur with cold water been sandwiched against the shore. The temperature transect data presented in Chapter 4 start at 0,5 km offshore and are thus unsuitable to reveal any banding effect inshore. On a slightly larger scale the transect data do show some evidence for warm thin layers of surface water in the afternoon with onshore winds.

The nature of the diurnal thermal band is also illustrated to a limited extent by a set of thermometer readings taken hourly between 06h00 and 18h00 in a shallow surf region. The measurement site is close to Little Salt River in the southern portion of the main study area (Fig. 1.7), where the sandy gently sloping beach is of the order of 100 m wide. The flow of the Little Salt River was virtually zero at the time and had no effects on the measurements. Effectively, bucket-type temperature measurements in total water column depths of 0,3 m and 1,5 m were taken hourly with a mercury thermometer. Readings covered five separate days distributed in the high insolation months of January/February. On three days the weather was virtually cloudless with light winds; one day overcast with some mist and one cloudless with moderate southerly winds. The set is biased towards periods with no strong winds and is expected to have above average insolation effects.

A clear diurnal behaviour is observed with maxima occurring at 15h00 or 16h00. The 5 day mean for the maximum increase in temperature from 06h00 to the afternoon, for the 0,3 m and 1,5 m positions is 2,8$\pm$0,7 °C and 2,5$\pm$0,7 °C respectively. The mean difference in temperature between the shallower and deeper position is 0,4$\pm$0,4 °C at 6h00 and 1,1$\pm$0,4 °C at 15h00. The shallower water column is seen to steadily gain more heat than the deeper position which is 30 to 50 m further offshore. The decrease in temperature from the maximum to 18h00 is about 0,4 °C.

These data corroborate the evidence for a thermal band revealed by the ART surveys. The warm band corresponds to a feature with similar temperature range and spatial scale reported by Hashimoto et al (1982) and Uda et al (1983) also on a long sandy beach. They

conclude that the main heat source is the insolation effect on the gently sloping beach. Thermal diffusion then occurs offshore giving the observed thermal band. Although the time of maximum temperature occurs earlier at 14h00, Hashimoto (1982) reports a similar diurnal temperature range at depths of 0,3 m and 2 m as observed in this work.

5.4.2 Other Spatial Effects

Another spatially related factor is that the sea-breeze effect gets stronger to the north of the site while the alongshore Cape Flats jet wind becomes weaker (Jury, 1984 and Kamstra, 1985). For certain southerly wind conditions the sea-breeze is favourably influenced to the north of the site, due to the wake effect behind Table Mountain (Jury, 1985 and Jury et al, 1985). Even over a 10 km length scale alongshore to the north therefore, there could be stronger diurnal onshore winds. This could advect surface waters inshore quicker in the north as is indicated in Fig. 4.20e. Such an effect could complement the proposals of Jury (1986) for a southward moving coastal low forcing the relaxation phase of upwelling (4.3.1.2).

The wave and current fields can be modulated by the diurnal wind forcing. The high frequency wave data has not been analysed in this study and such data do not exist for currents. Sonu et al. (1973) report a sea-breeze forced high frequency wave peak that dominates the background swell in the afternoon and evening; similarly, surface and wave generated currents have diurnally varying spatial characteristics. In this study inspection of aerial photographs shows a marked variation in surfwidth with wave height. Surfwidths vary from about 200 m with 1 m waves, 500 m with 3 m waves and 1000 to 1200 m with 6 m waves. During periods of large waves exceeding a height of 5 m, extensive rip current systems with plumes extending 2 to 3 km offshore have been observed from the air. Clearly, at times the wave field can completely dominate the dynamics of the study area.

Other features relevant to the sub-diurnal timescale that have been observed in this study but not further investigated include wind rows indicative of Langmuir circulation and surface slicks that hint at internal wave activity. Wind rows observed from the survey aircraft are particularly obvious during moderate to strong winds. Also observed from the air on a few occasions were groups of narrow bands of discoloured water or slicks several tens of meters apart and a few hundred meters in extent. These could relate to the infrequent occurrence in the raw temperature chart data of packets of short period cycles (10 min) of amplitude of about 0,5 °C. Such features are probably due to internal waves which Winant (1980) considers to

be ubiquitous for highly stratified water on continental shelves.

5.5 DISCUSSION

This chapter has aimed at establishing the mesoscale character of the study site. This it has done, chiefly through an analysis of wind and sea temperature data. The main attribute revealed in analysis of the high frequency data is the predominance of processes occurring at the diurnal frequency. Inertial and tidal processes play a lesser role. In the case of the wind the diurnal forcing is directly related to the formation to the interior of the study site of an insolation induced thermal low which sets up a land/sea-breeze system. These across-shore winds modulate the alongshore gradient winds. The sea temperature data manifest a similar strong diurnal periodicity. The investigation shows that the temperature response has a slight direct insolation contribution but that the main fluctuation is due to diurnal wind forced dynamics of a small scale upwelling system.

The temperature signature gives a good idea of the dynamic processes taking place. In the deep ocean Fofonoff (1969) shows a correspondence between temperature and kinetic energy spectra. Similarly in shallow coastal waters (30 m) temperature and current spectra are shown by Winant (1983) to have the same dominant diurnal and semi-diurnal peak structure. At Cape Columbine, spectra of winds and currents both show prominent diurnal peaks, Holden (1987). In this study although time series current data are lacking, we deduce from the high frequency temperature spectra that the chief dynamic process also occurs at the diurnal frequency and that the only other processes of any significance occurring in this mesoscale range are the small contributions from inertial and tidal effects.

The behaviour of the temperature at the 2 m and 8 m depths give important insights to the dynamics of the site. This is discussed in Chapter 6 - the 8 m temperature responds to a bottom-up process and the 2 m data response shows a top-down process that is primarily linked to the onshore winds and the attendant downwelling phase. The asymmetrical lagged response between the wind components is also discussed in Chapter 6 - the more rapid response to the across-shore winds is associated with the rapid relaxation phase of the upwelling process.

The study considered both direct insolation effects and wind effects in generating the diurnal sea temperature character and shows that the former effects are small in comparison with the wind forced onshore- offshore flow that modulates the upwelling dynamics. An

inertially driven surface slab effect occurs probably less than 10% of the time. Despite the shallow nature of the study site definite but infrequent inertial effects are noted in different ways - in the spectral analysis, in direct observation of Lagrangian current tracks and in temperature oscillations under light air conditions.

The interesting spatial characteristic of a diurnal thermal band lying adjacent to the shore with a temperature maximum in the afternoon can have some practical use. Using the measured temperature distribution in the inshore region for a similar thermal feature, Hashimoto et al (1982) have calculated the coastal thermal diffusion coefficient and compared it to the eddy viscosity values. The residence time and thermal diffusion coefficient of this band could be calculated using the model of Hashimoto et al (1982) but additional information is required such as the longshore current and vertical temperature profile in the band. However, using an estimate for the longshore current of 0,1 $m.s^{-1}$ and certain other assumptions an order of magnitude calculation gives a value of 0 ($1x10^4$ $cm^2.s^{-1}$) for the thermal diffusion coefficient, with a time scale of several hours. For Buffels Bay to the north of this site Gunn (1977b) calculates the residence time for the bay water to vary from 3 to 9 hours.

Such calculations are useful in estimating the fate of thermal effluents from coastal power stations. Although the further offshore portion of the thermal band, because of buoyancy effects may be a near surface phenomena, the offshore length scale of the band may be linked to coastal boundary layer dynamics, in particular the proposed frictional boundary layer (Murthy and Dunbar, 1981, 5.3.2). Also relevant to thermal dispersion conditions are the spatial scales of the diurnal surface currents. Under wind calm conditions when inertial currents are more prevalent Lagrangian current tracks several kilometers apart are observed to be quite variable. This corresponds to the observation of Winant (1983) that the near surface diurnal currents 3-5 km offshore are spatially coherent only over a 5 km scale.

The **transition** between seasonal regimes is discussed at length in the chapters on seasonal and event time scales. The high frequency data only covers two years; inspection of this limited record at times of transition show no distinctive initiating signature either for the HF winds or temperature. Later in the event a diurnal pattern evolves. The lack of a HF response confirms the essentially event time scale nature of the transition process that has a sea temperature response lagging the wind by more than 24 hours.

One of the most distinctive characteristics of the site data is the prominent diurnal wind and sea temperature signal and the role played by the across-shore wind in modulating the sea's response. Further discussion on the behaviour at the 2 m and 8 m depths and other aspects of mesoscale phenomena are reserved for the final chapter which brings perspective to the whole study.

TABLE 5.1 LINEAR CORRELATION COEFFICIENTS BETWEEN LINEARLY DETRENDED VARIABLES HIGH FREQUENCY DATA

Date	Period	VARIABLES				OBSERVED CORRELATIONS			LAGS		CRITICAL CORREL COEF[e]		
		Wind Comp	Temp Depth m	Record Length Hours	Deg of Freedom	C_o	Cm_1	Cm_2	m1	m2	95 %	99 %	99,9 %
									Hours				
1976	1 Jan-29 Apr	N/S	2	2880	187	-,301	+,316	-,348	10	23	,120	,169	,224
1976	1 Jan-30 Jan	N/S	2	720	39	-,389	+,459	-,51	10	23	,261	,362	,469
1976	1 Dec-30 Dec	N/S	2	720	64	-,229	+,228	-,17	11	22	,205	,286	,374
1976	1 Dec-30 Dec	N/S	8	720	50	-,333	+,301	-,25	10	23	,231	,322	,419
1976	1 Dec-30 Dec	2*	8	720	26	+,785	+,715	-,65	1	11	,317	,437	,559
1976	1 Dec-30 Dec	8*	2	720	26	+,785	+,761	-,62	1	11	,317	,437	,559
1977	1 - 31 Jan	E/W	8	744	38	-,361	-,465	+,459	2	15	,264	,367	,474
1977	1-13 Jan	E/W	8	312	23	-,361	-,474	+,477	2	15	,337	,462	,588
1977	1-13 Jan	E/W	2	312	16	-,314	-,583	+,547	4	15	,400	,543	,678
1977	1-13 Jan	N/S	2	312	19	-,497	+,583	-,538	9	21	,369	,503	,635
1977	1-13 Jan	N/S	8	312	26	-,234	+,452	-,453	9	20	,317	,437	,559
1977	1-31 May	E/W	8	744	124	-,075	-,22	+,258	9	21	,149	,210	,270
		E/W	2	744	109	-,088	-,20	+,216	4	16	,156	,220	,290
		N/S	2	744	106	-,014	oscillates 0,1		-	-	,159	,226	,294
		N/S	8	744	120	+ ,00	-,13	+,15	7	17	,150	,210	,280
		2*	8	744	83	+,547	+,428	-,311	1	13	,180	,250	,330
		8*	2	744	83	+,547	+,430	-,277	1	15	,180	,250	,330
1977	22-31 May	E/W	8	240	40	-,04	-,39	+,30	9	17	,257	,358	,463
		N/S	8	240	48	-,02	+,224	-,14	12	25	,235	,328	,427

Continued

Table 5.1 (continued)

Date	Period	VARIABLES: Wind Comp	Temp Depth m	Record Length Hours	Deg of Freedom	OBSERVED CORRELATIONS: C_o	Cm_1	Cm_2	LAGS: m1 Hours	m2 Hours	CRITICAL CORREL COEF@: 95 %	99 %	99,9 %
1977	24 Jul-17 Aug	E/W	2	600	64	-,09	-,16	+,21	3	15	,205	,286	,374
		E/W	8	600	79	-,07	-,14	+,19	2-7	19	,184	,257	,339
		N/S	2	600	120	+,01	-,11	+,18	8	15	,150	,210	,277
		N/S	8	600	120	-,09	-,13	+,16	6	16	,150	,210	,277
		2*	8	600	60	+,59	+,53	-,36	1	14	,211	,295	,385
		8*	2	600	60	+,59	+,52	-,52	1	14	,211	,295	,385
1977	14 Oct-7 Nov	E/W	2	600	29	-,21	-,35	+,39	3-4	16	,301	,416	,533
		E/W	8	600	28	-,16	-,39	+,41	4	17	,306	,423	,542
		N/S	2	600	42	-,11	+,23	-,17	6-8	19	,251	,350	,453
		N/S	8	600	41	-,20	+,25	-,19	9	22	,254	,354	,458
		2*	8	600	29	+,89	+,84	-,66	1	12	,301	,416	,533
		8*	2	600	29	+,89	+,77	-,61	1	11	,301	,416	,533

* Correlation between temperatures at different depths
@ from Underhill (1981) Table 5
C_o correlation coefficient at zero lag
Cm1 maximum correlation coefficient at lag m1
Cm2 maximum correlation coefficient at lag m2
N/S alongshore component
E/W across-shore component

TABLE 5.2
STANDARD DEVIATION FOR ZERO MEAN HIGH FREQUENCY DATA

DATE	RECORD LENGTH HOURS	WIND S ms^{-1}	WIND E ms^{-1}	TEMPERATURE 2 m °C	TEMPERATURE 8 m °C
1977 1-13 January	312	2.29	2.34	0.68	1.01
1977 1-31 May	744	2.00	2.12	0.14	0.19
1977 22-31 May	240	1.93	2.45	-	0.22
1977 24 July-17 August	600	1.91	2.64	0.18	0.22
1977 14 October-7 November	600	2.29	2.55	0.43	0.43

TABLE 5.3
STANDARD DEVIATION FOR MONTHLY ZERO MEAN HIGH FREQUENCY TEMPERATURES

1977	JAN	FEB	MAR	APR	MAY	JUN	JUL	AUG	SEP	OCT	NOV	DEC
2 m	.69	.51	.46	.34	.14	.10	.09	.18	.16	.35	.44	.50
8 m	.95	.60	.48	.34	.19	.15	.16	.22	.20	.37	.48	.55

TABLE 5.4

SPECTRAL ENERGY PEAK VALUES AT DIURNAL FREQUENCIES IN WIND AND TEMPERATURE SPECTRA

YEAR	PERIOD	MAX LAG	AUTO SPECTRA				ROTARY SPECTRA			
			TEMPERATURE $(°C)^2$/cph		WIND $(km.h^{-1})^2$/cph		WIND			
			2 m	8 m	E/W	N+/S	C	A*	θ°**	ROT*+
1975	Year	720	-	-	213	59	14,3	53,9	59	0,58
1976	Year	720	114	107	222	61	11,0	59,7	57	0,68
1977	Year	720	118	106	174	57	6,7	51,1	65	0,76
1976	Summer	240	52,4	43,1	115	69	4,7	41,3	41	0,79
1976	Winter	240	39,3	32,8	65,6	29,7	6,5	17,4	59	0,45
1976	Spring	240	39,5	38,8	112	44	6,3	32,6	57	0,67
1977	Summer	240	49,0	52,1	106	58	3,3	37,9	54	0,84
1977	Winter	240	22,1	10,2	44,8	14,7	5,5	9,4	69	0,25
1977	Spring	240	47,0	37,2	116	61,7	3,8	40,7	61	0,82

\+ E/W = Across-shore components N/S = Alongshore components

* C = Clockwise A = Anticlockwise

** θ^0 = Angle from true North of major ellipse axis at diurnal frequency

*+ ROT = ROTARY COEFFICIENT AT DIURNAL FREQ. = 1 for anticlockwise circle
= 0 for unidirectional
= -1 for clockwise circle

TABLE 5.5

TIDAL CONSTITUENTS ON THE SOUTH AFRICAN WEST COAST*

CONSTITUENT	PERIOD HOURS	HEIGHT M	% OF M2 TIDE
M2 Main Lunar	12,42	0,536	100,00
S2 Main Solar	12,00	0,236	44,0
N2 Lunar Distance Variation	12,65	0,127	23,7
K2 Solar-Lunar Declination	11,96	0,045	8,4
K1 Solar-Lunar	23,94	0,055	10,2

Each of the remaining diurnal and fortnightly tidal constituents contribute less than 5% of the M2 tide and are not considered further.

* Data from E Shipley (Pers Com) for Lamberts Bay.

TABLE 5.6 DIURNAL TEMPERATURE DATA FOR SELECTED CASES

CASE		TIME OF OCCURRENCE FOR MIN		TIME OF OCCURRENCE FOR MAX		RANGE °C		DURATION ABOVE MEAN HOURS		WAVE HEIGHT
		2 m	8 m	2 m	8 m	2 m	8 m	2 m	8 m	m
1. 14-17 Apr 1977 (4 day mean)		3h-6h	2h-4h	20h	17h	1,7	0,9	10	11	1,3
2. 25-30 Apr 1977 (6 day mean)		8h-12h	2h-4h	16h-18h	16h-19h	0,7	0,9	9	9	2,5
3. 21-25 Jul 1977 (5 day mean)		6h-9h	10h-12h	16h-18h	1h and 17h	0,3	0,4	11	12	2-3
4. 4-7 Aug 1977 (4 day mean)		8h-11h	12h-14h	19h-21h	19h and 23h-02h	0,4	0,4	14	12	2,5
5. 20-22 Jan 1977	20	8h-9h	8h-11h	17h-18h	17h-18h	4,0	5,4			1,4
	21	3h-9h	7h-11h	16h and 1h	22h-24h	2,6	3,8	14	11	1,3
	22	5h-7h	3h-6h	15h-16h	15h-16h	3,2	4,2			1,5

CHAPTER SIX

SUMMARY AND CONCLUSIONS

C O N T E N T S

CHAPTER SIX

SUMMARY AND CONCLUSIONS

6.1 INTRODUCTION

In the foregoing chapters aspects of the empirical dynamics of a small scale upwelling region have been expounded in the context of different time scales. These time scales were proposed in Chapter 2 as a means to distinguish between different processes and to aid in the characterization of the complex coastal environment. Naturally the time scales are not bound in rigid watertight compartments. Rather, there is a continual interaction between the different scales and processes. The change in the seasons is seen to be mediated in a transition at the event time scale. The events themselves are strongly modulated by a diurnal pulsing in the wind which is manifested in a similar diurnal sea temperature response. The succession of events over several months build up the seasonal trend and so the cycle is completed but for the longer term interannual changes. In this summary, where appropriate, the different time scales will be linked.

The significance of the study can be summarized under four generalities that were mentioned in the introductory literature review. The review indicated that internationally there was a paucity of small scale coastal upwelling studies of a scale less than the Rossby radius of deformation ($<$10 km) and that in addition in South African waters there was a lack of small scale coastal studies in general. Secondly the local oceanographic community lacks hourly time series data extending for more than about one year for coastal parameters - with the exception of tide and wave data. Thirdly, even including larger scale offshore studies there is inadequate coverage of processes occurring in the synoptic weather time scale. Lastly, little literature relates to diurnal effects in shallow inshore waters. In each of these aspects the present study has contributed, sometimes significantly. At this stage these four generalities will not be elaborated on but as the discussion proceeds the various topics will be seen to relate to these points. Besides the relevance to physical oceanography itself the findings will be shown to be relevant to, amongst others, fisheries biology, plankton dynamics, coastal ecology, marine pollution and the discharge of thermal wastes from coastal power stations.

The attributes of the site lent themselves well to the investigation. Uncomplicated bottom topography and minor local orography together with negligible tidal or coastal currents enabled

two major seasonal regimes; the northerly regime in winter (May to August) when these winds predominate and the southerly regime for the remainder of the year. In the case of the latter this regime is further subdidvided into a spring (September to December) and summer (January to April) regime. In this study therefore we have three equal duration regimes, each of which is characterized at the three time scales mentioned above. The long term DF Malan wind and Table Bay harbour temperature data confirm the choice of winter regime months and show the greater variability in spring (Fig. 3.9a and b). In broad outline the northerly or winter regime is characterized with sea temperatures being warmer than the annual mean and having a small variability; the other two regimes have colder sea temperatures indicating the importance of a process other than direct insolation. In addition, the temperature variability is much greater, with the spring regime showing more reversals to northerly conditions. The winter regime also delineates the occurrence of greater wave energy at the site.

6.2 SPECTRAL FEATURES

A link between the different time scales is provided by considering the power law trends displayed in the spectral analysis. For the winds, in the ILF range the trend has a dependance less than $f^{-3/2}$ for the lower frequencies but it steepens to $f^{-3/2}$ at the higher frequencies and continues with this trend right through the HF spectra. There are no obvious theoretical reasons for the numerical values of these power law trends but they are known to vary with latitude, topography and continental influence (Wunch, 1980). The slopes here tend to agree with the findings of Winant et al., (1987) of gentler slopes of $f^{-3/2}$ at the coast compared with f^{-2} offshore. There is in general more spectral energy at the event time scale than at the higher frequencies confirming the importance of synoptic processes. The power law trend in the temperature spectra is more consistent at f^{-2} from synoptic periods down to hourly periods. This behaviour of the temperature data indicates either a turbulent cascade of kinetic energy related to the 5/3 power law for wave number spectra (Brundit Pers Com) or an undulating temperature stratified water column (Phillips, 1975). Both processes can occur at the site. An f^{-2} dependance up to frequencies of 1 cph is also shown for kinetic energy spectra of currents in water depths of less than 20 m (Winant and Olson, 1976).

The most conspicuous spectral feature of all the time scales investigated is undoubtedly the strong diurnal peak for both winds and temperature. Such dominance in the mesoscale phenomena frequency band for this coastal environment was largely unappreciated prior to

this analysis. In a recent paper Holden (1987) also observes prominent diurnal peaks in spectra of wind and currents in the Cape Columbine area. Before expanding on details in this frequency range spectral attributes for the event time scale can be mentioned. There is no statistically significant structure but a broad maxima extends over periods from about 8 to 15 days for both winds and temperatures for the multiyear record used. For the individual years the maxima extends to about 20 days. These periods correspond to synoptic events.

Back with the mesoscale phenomena, the strong diurnal periodicity in the wind is forced by insolation forming an interior low that drives a land/sea breeze system (Jury, 1980). The preferred near orthogonal to the coast diurnal winds are confirmed by the greater across-shore component in the autospectra and by the ellipse orientation parameter derived from the rotary spectral analysis (Table 5.4). The sea temperature forcing is more complex, having both direct insolation and wind induced components. The skewed 24 hour sea temperature distribution and other evidence however points to a mainly wind forced process for the temperature oscillation where the diurnal land/sea breeze modulates the alongshore gradient wind that initiates the upwelling process and the attendant temperature contrast. The high frequency temperature data are modulated on a synoptic time scale to give a wave packet effect that is delineated by the passage of coastal lows or other onshore episodes. The wave packet effect can be most distinctive at times (Fig. 5.1 c,d). Contributions to the temperature oscillations are also at times received from the inertial behaviour of a layered slab (Boyd, 1981). The anticlockwise rotary nature of the sea breeze is favourable to supporting inertial oscillations and with the diurnal and inertial period (21,6 h) being so close some resonance coupling could occur (Unluata, 1980). The smaller, direct insolation contribution to the sea tower data is estimated to have, under favourable conditions a maximum of $\pm$0,2 °C in winter and $\pm$1 °C in summer compared to the total daily observed summer oscillation of $\pm$3 °C. The larger part being due to the upwelling signature. In the shallow, 0,3 m depth water on the gently sloping beach however the direct insolation effect in summer is quite marked resulting in a 2,8 °C rise between 06h00 and 15h00. The spatial extent of the diurnal thermal banding along the coast is estimated to contribute less than 0,5 °C increase at the sea tower position.

The spectra of the seasonal regime data sets show a marked drop in diurnal energy in winter relative to the other seasons. In particular the alongshore wind component and the 8 m depth temperature autospectra show the greatest reduction. The northerly predominance in winter that favours downwelling dynamics with uniform

temperatures and the reduction in insolation are the chief causes for this decrease in spectral energy.

Despite the shallow nature of the site (11 m at the sea tower) definite inertial effects of an infrequent nature are observed in different ways. a) The HF temperature spectra display small inertial peaks. b) During the calm after a strong southerly wind event, temperature oscillations are observed that relate to inertial processes. c) Near-circular Lagrangian current drogue tracks of inertial period occur. Favourable stratification allows uncoupling of layers which promotes inertial currents when suitable short impulse winds blow. The frictional boundary layer concept of Murthy and Dunbar (1981) within the coastal boundary layer limits the inertial behaviour to less than the order of 10% for such shallow waters. Tidal effects, as evidenced by small peaks at the M2 frequency in the temperature spectra, are of little influence in the region.

The main characteristic of the LF and ILF time series is the multiday grouping of the data into events but the corresponding spectra show no prominent peaks. The lack of a significant peak in the ILF wind spectra was initially found disconcerting in light of the widely quoted results of Preston-Whyte and Tyson (1973) who report a prominent 6 day cycle for barometric pressure spectra along the South African coast. Further consideration however resolves the matter. Since wind is a secondary phenomena with respect to the primary processes occurring in the pressure fluctuations any spectral peak in the pressure field is expected to be reduced in the corresponding wind spectra. Similarly as reported by Winant (1980) the spectra of coastal currents do not display as marked peaks as in the associated sea surface elevation (pressure) spectra that respond only to barotropic motions. Lee and Mayer (1977) observe that in this frequency band for coastal currents, "distinct energy peaks become lost in spectra ... due to the event nature of the fluctuations". Interannual variability also plays a role in increasing or decreasing the prominance of certain spectral peaks. Annual pressure spectra at Cape Town for the years 1970 to 1984 show only 3 years with a distinct 6 day peak (Kamstra, 1987). The varied time scales of the events as typified in the time series data of Fig. 4.1 and 4.3 support the lack of any significant 6 day spectral peak in these data. The ILF temperature spectra in sympathy with the wind spectra show no prominent structure although the autospectra for alongshore winds and temperature for the multiyear case, Fig. 4.9a and 4.9c, both have steeper increase in energy between 6 to 9 day periods and both have the same broad maximum region. In a regional context, recent current spectra near Cape Columbine have a prominent 16 day peak (Holden, 1987); current periodicities of 3 to 8 days and up to

10 days near Yzerfontein north of the site are reported by Nelson and Polito (1987).

Another aspect of the Preston-Whyte and Tyson (1973) pressure spectra is their unexplained 3 day spectral peak. A misinterpretation occurs when Nelson (1985), on insufficient statistical evidence ascribes this peak to the associated 3 day interval between low pressure cells passing the Cape. In Section 2.3.1 the harmonic breakthrough character of the 12 hour peak in the HF spectra is discussed. The 3 day pressure peak is probably also due to harmonic breakthrough, in this case of the prominent peak at 6 days. This is further supported by the fact that the only three spectra out of a total of 14 spectra depicted in Preston-Whyte and Tyson (1973) that do not reveal a 3 day peak, are those that either do not have a 6 day peak or have an unresolved peaking near 6 days. The lack of significance for a 3 day peak is collaborated in the spectra for the 3,8 year data set reported here, particularly for the autospectra (Fig. 4.9a) where there is in fact a minimum at 3 days. Similarly in a short time series (March to November) Schumann (1989) observes a spectral minimum for Cape Town at 3 days. Harmonic breakthrough peaks are often present in spectra but not always reported; this accentuates the need for careful interpretation of all peaks.

For the winds the spectral analysis confirms the dominance of alongshore winds and anticlockwise systems at these frequencies.

The multiyear ILF spectra (Fig. 4.9a and 4.9c) have a broad maximum spanning 8 to 15 days with a dip at longer periods. The study did not include spectral analysis into the seasonal time scale and it is not certain how sustained the falloff is for periods exceeding 20 days and to what extend the energy may rise at low frequencies. Kamstra (1987) observes a spectral plateau between 5 to 20 days and Kamstra and Taunton-Clark (1986) indicate for oceanic/climatic variability at Cape Town that seasonal spectra energy should dominate relative to the higher frequencies. However, in contrast to the open ocean where current spectra are energetic at periods exceeding 1 month, Düing, Mooers and Lee (1977) consider current spectra in coastal waters of the continental shelf to typically have a low frequency decrease. In studies off Florida, where winters are dominated by passing cold fronts and summers experience SE winds Düing et al. (1977) observe high spectral coherence between local atmospheric variables and currents in the 10 to 13 day band with a sharp falloff towards periods exceeding one month - lesser peaking occurs at 4 to 5 days and 2 to 3 days. Although here a good correlation exists between seasonal wind and temperature time series the characteristic of any falloff at periods longer than the event time scale needs further investigation for local waters. The ILF

spectra certainly confirm the importance of the event time scale.

The mean (seasonal) attributes of the study area have been established and can be used for elucidating general trends for pollutant transport or biological processes as suggested by Csanady (1976b). The seasonal time series data reveal periodicities of 30 to 60 days and longer. Periodicities exceeding 50 days dominate the anomalies in the Southern Hemisphere atmospheric circulation (Kidson, 1988). Various large scale oceanic features can influence the local response e.g. warm water from Agulhas current (Lutjeharms, 1981 and Lutjeharms and Van Ballegooyen, 1988) and cold water from Subantarctic water filaments that can persist for two months (Shannon, et al., 1989). Characteristic biological growth cycles also occur (phytoplankton, 0,5-10 d; zooplankton, 15-45 d; fish lavae, 20-125 d) and can be modulated by the physical cycles in marine parameters revealed by time series and spectral analysis. These growth cycles can be adversely affected by anomalies in the physical cycles (Shelton, 1986 and Olivieri and Hutchings, 1986) and thus quantifying such cycles and identifying conditions for survivorship is of benefit to marine biologists (Sharp, 1986).

Reviewing this section we see that various aims of the study (p 1.25) have been met, in that the time series data have been analysed spectrally and that dominant time scales and some of their characteristics have been identified.

Spectral Techniques

Spectral analysis is a powerful technique in investigating atmospheric/oceanographic phenomena as has been demonstrated in this work. Rotary spectral analysis (Gonella, 1972) revealed the essential anticlockwise dominance in local atmospheric systems and the ellipse orientation parameter demonstrated the orthogonal dominance of diurnal winds. Techniques such as those of Crew and Plutchak (1974) for time varying rotary spectra could be used to investigate the synoptic scale modulation of diurnal time scale processes. The short time series analysis techniques employed by Hayes and Halpern (1976) can help elucidate the time evolution of particular frequency bands during individual upwelling events.

An important practical aspect in the time series analysis is the choice of the orientation of the coordinate axes particularly for a site with uniform bathymetry and/or coastline orientation. Although the rotary spectral analysis is independant of axes choice the visual information conveyed by the plot of the filtered time series is dependent on the relative orientation of the components. In the case reported here the 20° tilt, which is similar to the principal ellipse

axis given by the rotary spectral analysis, helped to highlight the alongshore and across shore processes.

The choice of filter and its frequency reponse function is critical in obtaining sharp enough cut-off between frequency bands of interest. The advantage of the Lanczos-cosine filter used here is that by altering the number of weights the frequency response can be "tuned" for different cut-off properties relative to the frequency band being investigated. The penalty of a sharper cut-off is however greater truncation of the data set.

6.3 BIMODAL TEMPERATURE DISTRIBUTION

A feature of the seasonal time series data is the bimodal temperature structure seen in individual years (Fig. 3.4) and in the long term mean in Table Bay (Fig. 3.9 b). The associated wind data do not show as pronounced a bimodality particularly the long term data (Fig. 3.9 a). The temperature bimodality of the shallow inshore stations, based on good time series data confirms that the similar indication by a limited set of offshore monthly cruise data (Andrews and Hutchings, 1980) is also in fact a feature of the larger scale. This shows the smaller local scale measurements can contribute to characterizing the larger scale. Further north off Cape Columbine, Shannon (1985a) reports on an 8 year record showing an annual bimodal near surface structure with minima during Oct/Nov and Mar/Apr.

The warmer trend in winter is associated with the shift of the South Atlantic anticyclone which results in northerly and onshore winds that both suppress cool upwelling waters and enhance the onshore advection of the warmer offshore waters. The minima in spring, which are also reflected in sharp minima in the LF time series, are related to the strong southerly upwell favouring winds and the occurrence then, on the shelf, of cold oxygenated water. The latter spring priming of the system is thought to be mediated by a southward propagating Kelvin wave (Shannon, 1985a). This can be compared with interannual variability in the California current system which is shown in a numerical model (Pares-Sierra, O'Brien, 1989) to be due to disturbances of equatorial origin propagating into the region as trapped Kelvin waves. The slightly warmer temperatures in January are due to a combination of seasonal insolation increase, a slackening in wind strength and marginal onshore tendency for the wind. But reasons for the long term minimum in April are not that obvious and are not associated with stronger winds in the long term mean then. The limited Melkbosstrand record favours a March minimum (Fig. 3.4) with associated favourable winds. A conjecture here is that although these winds are not strong there is a tendency that the

event duration is longer, as seen by the CET traces (Fig. 4.6), at the end of summer and this results in some cooler upwelling. The larger scale wind field (Meeuwis and Lutjeharms, 1986) and also the upwelling favourable wind maxima reported for Cape Point in March (Andrews and Hutchings, 1980) may too affect the local data. Other factors that could result in lower temperatures are reduced insolation, the ingress of filaments of Subantartic water (Shannon, et al., 1989) and a Kelvin wave counterpart to that in spring that also brings cold water onto the shelf.

The large standard deviation in the long term temperature data (Fig. 3.9 b) is attributed chiefly to a phase shift in the seasonal pattern with additional contributions from interannual changes and strong to weak seasonal variations. A probable reason for the dominance of the phase shift in producing temperature variability is that the "normal" primary upwelling temperature (cool) signal, due to 'summer' winds, is out of phase with the insolation temperature (warm) signal where on the larger scale the offshore waters are definitely warmer in summer. Any failure or shift of the winds therefore results in a markedly different temperature signal.

Little has been published on the causes of interannual variability in the Southern Benguela (Shannon, 1985a) but more recently, the role of El Niño southern oscillation forcing is implicated (Shannon, 1987) and long time series of sea surface termperatures (ship collected) and wind stress have been published (Taunton-Clark and Shannon, 1988, Taunton-Clark and Kamstra, 1988). Future work on interannual variability would benefit from closer investigation of each year of the long data set of Table Bay Harbour temperatures and DF Malan winds.

6.4 REGIME TRANSITIONS

The regime related data indicates a very definite character for the winter period when northerly winds predominate and the sea temperature is slightly elevated and has a greatly reduced fluctuation compared with the spring and summer regimes. The transition to the winter regime and from the winter to the spring regime has been considered. Although in this study the temperature character is well defined the currents are ill defined and we cannot describe a regime class current nor say if there is a current transition. This contrasts with Huyer et al. (1979), Strub et al. (1987) who describe a rapid spring transition off Oregon and off Western North America based on an extensive shelf wide current data set. Within the context of this lack of current data and only indirect evidence available through a temperature data set from a

single close inshore measuring point this study does however give some insight to transition dynamics. No publications have been found that discuss the transition dynamics of the Benguela region.

Because of the link between wind stress and sea temperature the character of atmospheric transitions is first considered. At the seasonal time scale both local evidence and that of other authors (van Loon and Rogers, 1984 and Trenberth, 1979) shows a more definite autumn to winter atmospheric transition than that between winter and spring; the local sea temperature response at this time scale was not well defined. On the larger scale off the SW Cape coast however, quarterly averaged longterm sea surface temperature distributions reported by Kamstra (1985) in his Fig. 6 show a bigger change in temperature from autumn to winter than winter to spring. This is contrasted at the event time scale, when during spring, we show that a single southerly wind episode induces a definite transition in the local sea temperature character. This transition can be considered rapid as it is established in about five days. The high frequency filtered data do not show any characteristic signature at the time of transition and confirms the essentially event time scale nature of the alongshore wind initiated transition.

Similar to Huyer et al. (1979) this study assumes a minimum cumulative Ekman transport (CET) is required to establish the transition. Some regions such as the Northern California Shelf do not require the hypothesis of a minimum wind event to trigger the transition (Lentz, 1988).

Quantitatively it is estimated that a minimum offshore CET of $3x10^9$ $g.cm^{-1}$ with a duration of at least five days is required to set up the local sea temperature spring transition. Shorter duration events are not as effective and a relatively small onshore transport of $2x10^9$ $g.cm^{-1}$ can cause a reversion to winter-like characteristics. In contrast the less well defined transition from summer to winter apparently requires a larger onshore CET of greater than $3x10^9$ $g.cm^{-1}$. Although quantitative values of CET have been used these should be regarded with caution and in a relative sense because of limitations imposed by the shallow water and uncertainty of the larger scale wind field. However, at the order of magnitude level, the spring transition figures compare favourably with Huyer et al. (1979) CET values for Oregon of $1,3x10^9$ $g.cm^{-1}$ for establishment and $4x10^9$ $g.cm^{-1}$ for destruction of spring conditions but the ratio of establishment values to destruction values differ. The most probable explanation for this latter difference is that Huyer's values are based on a shelfwide current transition whereas the local study in shallow, 11 m deep water, reflects the behaviour of the inshore edge of the main thermocline

and flops back and forth with changes in the local wind. In particular in the relaxation phase of upwelling the shallow waters are very responsive to onshore winds and the approach of coastal lows (Jury, 1986) and a relatively small onshore CET value can cause reversion to a winterlike homogeneous water column, whereas for the larger scale a much larger event would be required.

This small scale study is nevertheless indicative of a wind event initiated spring transition in the larger scale but awaits confirmation through the study of suitable current data when they become available. This study is probably the first attempt to investigate the local spring transition and meets one of the aims stated earlier (p. 1.25). The role of the southward propagating Kelvin wave that may prime the system in spring also needs further investigation. In a review of upwelling in the California and Oregon current system Huyer (1983) highlights the lack of understanding of the interaction of processes with different time scales involved in the transition. Further insight to the large-scale spring transition off Western North America is given by Strub, et al. (1987) and Lentz (1987). Because of the asymmetry between up- and downwelling the first upwell event of the season i.e. at transition is very different from subsequent events and can be important for primary production (Send, et al., 1987). Much work remains to be done locally but even these results for minimum CET requirements for transition could be used in comparison with a few-week hindcast calculation of CET to indicate the probability of transition to a new upwelling season. This could show the magnitude of the seasonal phase-shift and whether an early or late start to conditions relevant to fisheries biology was occurring.

6.5 CORRELATIONS AND LAGS

The correlation and lags between the wind and temperature data reveal aspects of the forcing processes at the different time scales. The correlation analysis results from Tables 3.4, 4.2 and 5.1 can be summarized as follows:

Case of alongshore winds with zero lag:

- for spring and summer regimes at both the seasonal and event time scale the correlation coefficient is above the 95% confidence level. The HF data give negative correlation coefficient with a significance level varying from less than 95% to greater than 99%.

- for winter regime at all frequency ranges the correlation is generally poor.

Case of alongshore winds with lagged temperatures:

- for spring and summer regimes at both the seasonal and event time scales the correlation coefficient increases from the value at zero lag to exceed in some cases the 99,9% confidence level. The lags for maximum correlation vary from 1 to 8 days for the seasonal data and are 1 day for the event scale data. With lags of 6 to 11 hours the HF correlation coefficient swings to a positive significant correlation varying from near 95% to greater than 99% confidence level.

- for winter regime at both the seasonal and event time scale the correlation coefficient increases to near the 95% level and sometimes exceeds it. The lags for maximum correlation are significantly greater than for the other regimes i.e. 9 to 16 days for the seasonal time scale and 2 days for the event time scale. Because of the low number of degrees of freedom for the seasonal data the values of the coefficients and lag times are subject to uncertainty. Even with lagging the HF correlation coefficient generally stays negative and non-significant.

Case of across-shore winds:

- seasonal time scale

  (a) zero lag, for all regimes the correlation coefficient is variable from positive to negative and from being non-significant to 99% significant. Generally the coefficients are less than the corresponding alongshore case. A negative correlation coefficient is required for the positive sence offshore wind chosen if generic upwelling processes cause temperature changes. Only for the spring regime of 1976 (coinciding with the anomalous onshore winds) is the correlation coefficient both negative and greater than the 95% confidence level

  (b) with lagging there is an increase in the correlation coefficient but it remains variable. In the case of spring 1976 the lag for maximum correlation is 3 days.

- event time scale:

  The annual set gives a negative significant correlation of greater than 95% at zero lag, but within one day's lag in the temperature this falls to a near zero correlation.

- high frequency data:

  (a) zero lag. For spring and summer regimes the correlation coefficient is negative and varies from less than 95% to about 99% significance level and is generally equal to or better than the alongshore correlation coefficient. In winter there is poor correlation

  (b) with lagging there is a big improvement in the correlation coefficient and the confidence level generally exceeds 95% and even the 99% level. Generally the values exceed those for the alongshore case. Lags for maximum correlation are 2-4 hours for spring and summer and 3-9 hours in winter.

The deduction from the correlation coefficients is that at the seasonal and event time scales the gradient alongshore winds are the chief forcing mechanism for temperature change through an upwelling dynamic process, whereas at the diurnal time scale the across-shore land/sea breeze winds play an important role in modulating the sea's response. The several day lag for maximum correlation in the seasonal time scale data and the maintenance of the 95% confidence level for a similar period in the event data, points to the importance of wind events in causing temperature changes. In contrast the rapid falloff in significant correlation after one day for the across-shore winds at the event time scale points to a diurnally important mechanism for this wind. This is confirmed with the high frequency correlation coefficients, when the lagged across-shore winds are generally better correlated with the temperature than the alongshore winds and have shorter lags to maximum correlation. The negative correlation for HF alongshore winds at zero lag is produced by an approximately 180° out of phase response due to the near half day lag to maximum positive correlation. It is only through the filtering of the data sets into different frequency bands that the distinctive roles of the two wind components at the various time scales are revealed.

The behaviour of the temperature at the 2 m and 8 m depths give important insights to the dynamics of the site. The 2 m data have in general a better correlation than the 8 m data with the across-shore winds, whereas the 8 m data have a higher correlation with alongshore winds. The spectral analysis shows that the 2 m and across-shore data have greater energy at the diurnal frequency and in fact in winter the 8 m data has a much reduced diurnal contribution. The 8 m data often have greater oscillations than the 2 m temperature data but at the upwell relaxation phase the near surface oscillations can be greater. These facts point to a preferential bottom-up process occurring with alongshore southerly winds and confirms the primary nature of upwelling dynamics in initiating temperature changes.

In contrast the 2 m response shows a top-down effect which is linked to the across-shore winds and a slight insolation effect. The evidence favours that the better correlation for the near surface temperature is primarily due to the onshore winds and the attendant downwelling or advection process. Winant (1983) also reports that near surface currents in waters of 30 m depth have a higher diurnal energy than deeper down due to the influence of the sea breeze near the surface. At the 8 m depth where stratification is less influenced by mixing processes the temperature data show small contributions from inertial and tidal effects.

The lags associated with the correlation analysis show an asymmetry between the alongshore and across-shore forcing with the latter having the shorter lag at the diurnal time scale. Cushman-Roisin et al. (1983) report for Oregon waters that the coastal water response to across-shore winds is almost immediate but that for alongshore currents the response builds up over a period somewhat longer than the local inertial period, while Huyer et al. (1978) report maximum correlation between the first mode of vertical current structure and alongshore wind occurs at a lag of between 6 to 18 hours where the inertial period is 17 hours. For the midshelf region of the Northern California shelf Winant et al. (1987) observe a lag of order 10 hours between alongshore wind stress and curents, while the maximum correlation between the temperature and wind stress eigen functions occur when the temperature lags the wind by 42 hours. The large time lag is due to relaxation processes (Send, et al., 1987). On the larger scale locally, Bang (1973) notes a 12 to 16 hour time scale for wind forced changes in the superficial frontal gradients. With this study, the primarily upwelling southerly winds are modulated with the diurnal across-shore wind which has a quicker correlation with the temperature response (in the temperature increase phase) than the alongshore response. During summer the across-shore and alongshore lags are typically 2 to 4 hours and 8 to 10 hours respectively. With intense near-orthogonal offshore winds Jury et al (1985) observes a lag of 4 hours at Oudekraal. Why the temperature increase phase or downwelling process is quicker can be explained as follows. The upwelling process has to work against both gravity and bottom friction. More wind energy and time is required to reach a given state as indicated by a temperature change and the basic vertical displacement is relatively slow. In contrast, during the relaxation phase the outcroping pycnocline can flop back along the surface with minimal friction losses. The horizontal advection is relatively fast and can be further accelerated by an onshore wind particularly if in the afternoon the so-called "slippery sea" effect (Woods and Houghton, 1969 and Murray, 1975) occurs due to solar radiation differential heating of the surface layer which then uncouples from the lower layer and slides over it. The surface layer

is also subject to a diurnal jet effect (Price, Weller and Pinkel, 1986). The initial temperature increase phase which preceeds the full downwelling process therefore correlates sooner with the onshore wind than the temperature decrease does with the southerly alongshore wind.

For future work a modified temperature time series data set could be formed by taking first or second differences and be used to help quantify the relation between increasing or decreasing phase of temperature change and the different wind components.

In general at all time scales initial correlations during winter are poor. Lagging improves the correlation coefficient but not all cases reach the 95% significance level. The longer lags and poor correlation in winter relate to a more homogeneous water column at the shallow measuring site with the thermocline being deeper down further offshore and to the lower frequency of upwell favouring southerly winds.

The incidence of different wave heights at the study site is well correlated with the alongshore winds. At the seasonal time scale the correlation coefficient exceeds the 99% confidence level. For all the regimes at the event time scale one day's lag gives excellent correlation coefficients (generally above 99,9% level) with the highest being for the winter regime. The one day lag agrees with proposals by Shillington and Harris (1978) for swell generation off this coast.

Knowledge of the lags in temperature response relative to different wind time scales can be important in biological sampling strategies. Diurnal lags are relevant to night time Bongo net sampling of copepods and euphausids (Pillar, 1986), while both diurnal and event scale lags are relevant to studies of phytoplankton e.g. Pitcher (1986) and Brown (1986).

An important point regarding correlation analysis techniques is the proper consideration of degrees of freedom of the correlated variables and their associated critical correlation coefficients. Firstly, linearly detrended data sets with zero means and normalized by their variances should be used to enable meaningful comparison to be made between different variables. Secondly the act of filtering the data changes the degrees of freedom which must be known to set the critical correlation coefficients. The degrees of freedom can be estimated by the method of Davis (1976). For low degrees of freedom the cautionary note in Section 3.2.3 and Sciremammano (1979) should be referred to.

6.6 THERMOCLINE DISPLACEMENT

The thermocline is an ubiquitous feature of the ocean at all time scales. It has a seasonal depth dependence; it is modified by synoptic events when for example wind mixing can erode the thermocline or uplift it; diurnally, insolation can form a near surface thermocline that can migrate to greater depths. The processes at these time scales can dynamically interrelate. Reasons have already been given in section 1.3 why the available diurnal data was not used for even a limited mixed layer study.

At the shallow study site the main seasonal thermocline is not observed in winter but it lies at about 40 m then and rises to less than 20 m in summer (Shannon, 1985a). The outcropping of the seasonal thermocline occurs 18 to 28 km offshore at the so-called inshore frontal zone (Bang, 1973). In the present study a shallow thermocline is often observed during spring and summer between the 5 m and 20 m depth. The synoptic scale field work has amply demonstrated the rapid fluctuations of the nearshore thermocline under upwelling and downwelling conditions. Although aspects of diurnal sea temperature have been revealed by the sea tower data, e.g. minima between 3h00 to 11h00 and maxima between 16h00 and 24h00, the thermocline structure from 0,5 to 6 km offshore has only been charted irregularly between 9h00 and 16h00. Details of changes in the diurnal thermocline structure over the full 24 hour cycle await future studies. The greatest observed upwelling rate over a 24 hour period was 25 m but more typical values are 10 m per day. This compares with values of 20 to 30 m per day for parts of the larger scale Benguela system (Andrews and Hutchings, 1980).

Quantitatively the response of the thermocline to different wind stress impulses has been estimated using the two layer inertial adjustment model of Csanady (1977a). This model includes the prediction of the offshore displacement of the outcropped thermocline and although it is patently idealistic it gives at times good agreement with field observations. For example, from Table 4.6 case 3/2 with a wind impulse of 84 000 $cm^2.s^{-2}$ which represents a mean wind speed of 7,5 $m.s^{-1}$ over 23 hours, gives an offshore displacement of 1,8 km for an initial thermocline depth of 14 m. The observed displacement is 1,5 km. Limitations in the present observations that restrict a comprehensive comparison with the theoretical predictions include the relatively short transect lines of 6 km and the inadequate current data for determining the current difference across the thermocline. Field data indicate frictional damping of the current occurs. Future work could include - extending transect lines to 10 or 15 km to determine the effects of large wind events; - better current measurements; - measurements along the

transect lines at other times during the 24 hour period particularly at minima and maxima of the diurnal cycle. Computationally, comparisons should be made with the three layer model of Csanady (1982b) which initial investigations show has promise for better predictions as it reflects the "peeling off" behaviour for thermocline displacement observed in the field.

The present work nevertheless shows that with appropriate field conditions the two layer model gives reasonable predictions which could inter alia be used in estimating water mass exhange rates which are of use to biologists investigating nutrient exchange rates in kelp beds, Wulff and Field (1983), Field et al. (1981) and engineers studying ocean outfalls for pollutants and thermal effluents.

Mitchell et al. (1985) propose that low turbulence within the thermocline where life times of Kolmogoroff eddies can exceed 100 seconds allows sheet-like microzones for bacterial enhancement to occur. Bacterial clustering around phytoplankton and macroscopic aggregates (marine snow) is an important pelagic food source (Trent et al., 1978). The observation here and elsewhere of the progressive peeling off of layers of the thermocline in an upwelling event implies a longer duration of sheet-like structures which are favourable for motile bacteria and biological productivity. The diurnal behaviour of the thermocline and how the process of mixing and restructuring of layers affect the development and evolution of plankton communities is considered by Owen (1980) to be of considerable interest to marine biologists.

The importance of water column stratification at both the event time scale and the seasonal time scale on copepod biology through control of their phytoplankton food resource is discussed by Peterson (1986).

The thermocline behaviour that has been described is closely linked to cycles in the barometric forcing process. The seasonal change in depth is related - to the shift in the South Atlantic anticyclone and its associated change in predominant winds in the area - and also possibly to the southward propagating Kelvin wave that is proposed by Shannon (1985a) to bring cold water onto the shelf in spring. The event time scale oscillation observed here in the thermocline correlates well with the synoptic wind sequence of a post cold front SSW wind - a ridging anti-cyclone with deep SE winds - a pre-coastal low condition with shallow SE winds - the passage of a coastal low - and a wave cyclone with WNW winds. Findings in this study support the importance of the coastal low in terminating the upwelling phase of the cycle. As proposed by Jury (1986) the southward propagating coastal low accentuates a higher sea level to the north and with this southwards sea slope, moderating winds cause a reversed current and

onshore surface flow. The thin warm surface layer observed at this relaxation stage emphasizes the asymmetry between up and downwelling which indicates the presence of non linear dynamic processes (de Szoeke et al, 1981). This asymmetry is also highlighted for the California shelf by Send et al. (1987). Also implicated in relaxation phenomena, but on the diurnal time scale are sea breezes that modulate the upwelling response. The amplitude of the across-shore winds can be enhanced just prior to the passage of a coastal low, thus displaying a distinctive temperature pattern. The aims (p. 1.25) of predicting the upwelling response and identifying the barometric forcing process are seen to be met in this study.

6.7 SPATIAL ATTRIBUTES

The spatial attributes of both the wind field and the sea surface temperature have been investigated at various time scales. The following summary shows that the aim (p 1.25) to identify the spatial characteristics of the small upwelling region has been well met. The spatial variability of the wind field that most affects the small scale study site occurs at the synoptic time scale with the wind shadow effect in the lee of Table Mountain and Robben Island. The lateral extent of upwelling is affected and the differential surface current structure allows the easier onshore movement of a warm surface layer during the relaxation phase of an upwelling event. The sea surface temperature (SST) distribution varies with the different time scales.

One of the more important findings in the investigation is the localized focus of upwelling just north of Melkbosstrand Point which occurs at the synoptic time scale. Another notable spatial feature but at the diurnal time scale is the warmer thermal band adjacent to the coastline which has not been reported before for South African waters. In general there is a lack of contrasting SST distribution in winter and in this study a few ART surveys showed mild gradients off Melkbosstrand of 0,5 °C per 15 km. However, larger scale satellite imagery besides showing spectacular plumes in summer also reveals some plume activity in winter (Shannon, Walters and Mostert 1985).

Although localized sites of upwelling are mentioned by Nelson (1985) for Duiker Point, Bok Point and Yzerfontein on the west coast and observed by Schumann, Perrins and Hunter (1982) and Schumann, Ross and Goschen (1988) along the Cape south coast this is the first detailed study of such a site. Similar detailed small scale upwelling studies have not been encounted in the international literature. This site is positioned at a coastal offset feature at

Melkbosstrand that is even smaller than those features at Duiker Point, Bok Point and Yzerfontein where Nelson's "micro-sites" of upwelling occur. The upwelling focus at Melkbosstrand revealed by a fine grid ART survey as an area of cold water, has minimum dimensions of about 1x2 km and a temperature contrast with the surrounding water of typically 2 to 5 °C. Dependent on the magnitude of the wind stress and the duration of the southerly wind event the focus grows to 4 km wide by 12 km alongshore and can eventually merge into a larger scale ribbon of upwelling extending from Table Bay in the south to Bok Point in the north. Besides the temperature signature of the upwelling focus, aerial observations showed clear water in the centre, a feature of freshly upwelled water. The three dimensional complexity of the upwelling dynamics is also indicated by the sets of temperature transects through the area. Doming of the isotherms is observed at times and evidence points to bottom water moving obliquely inshore from around the Melkbosstrand Point. The consistent positioning of this centre of upwelling is ascribed to the change in coastline orientation at Melkbosstrand Point over which an essentially alongshore wind blows. The enhanced upwelling at that position and the warmer water in the northern embayment are accounted for to a certain extent by the theoretical upwelling model of Hua and Thomasset (1983). Because of the relatively uniform bottom topography and limited orographic features, such factors are not considered to play a role in this local focus of upwelling, although topographic steering may affect the Table Bay plume between Robben Island and the mainland.

The spatial attributes of the sea surface temperature distribution at the event time scale show relatively steep temperature gradients offshore of the upwelling plume and even steeper gradients, exceeding 3 °C in one kilometer, at the start of a relaxation phase. The initial relaxation phase also reveals meanders and patches of scale 1 to 10 km indicative of horizontal mixing and dynamic instabilities (Boyce, 1977). However the onset of active downwelling with NW winds restore more order to the surface temperature distribution. In the Californian coastal region within a few kilometers of the shore Winant (1983) observes that the near surface spatial coherence at the diurnal time scale extends over 5 km for currents and less than 2,5 km for temperatures which seems to be qualitatively matched by the local data. Winant (1983) warns against deducing circulations from ART imagery since temperature length scales are generally less than current length scales.

These length scales are important in determining dispersion rates in the sea (Okubo, 1976) and point to an application of the information in estimating the fate of thermal effluents released by coastal nuclear power stations. The observed cold water plume for upwelling

conditions has a tendency to veer offshore to the north and will assist in removing thermal releases away from the coast. The localized focus of upwelling has the advantage of supplying cold water for the cooling water intake system of the Koeberg power station. The knowledge gained in investigating this localized site of upwelling can be applied to any similar coastal offset which is subject to upwell favouring winds. The decreased residence time of the water mass under such conditions will enhance the dispersion of any introduced pollutant. In contrast under certain downwelling conditions current data shows a tendency for some stagnation in the southern embayment.

Aspects of the data can also be applied to biological studies. Based on work at a nearby site at Robben Island, Brown (1984) reports that optimum phytoplankton growth occurs at sites adjacent to those that experience active upwelling and benefit from horizontal advection of nutrients. In a mathematical model of water transport effects on trophic relations in a kelp bed Wulff and Field (1983) show that water exchange rates have greater effect on the animal community than the duration of summer and winter pulses of up and downwelling.

The diurnal time scale spatial feature of a warm band in the afternoon adjacent to the coast is attributable to direct insolation effects where the sun heats both the shallow inshore waters and the gently sloping beach. Adjacent to the upwell focus region the band is typically 0,5 km wide with a temperature contrast of 1 to 2 °C. Similar observations have been utilized by Hashimoto and Uda (1982) to calculate the thermal diffusion coefficient near the surf zone. Such coefficients are in turn useful in estimating the fate of thermal effluents from coastal nuclear power stations. The width of the thermal band which varies from 0,5 to about 1 km is, from the shore side, a function of diffusion processes in the nearshore zone that are influenced by waves and rip currents but its seaward extent is also subject to the wind induced upwelling dynamics which may be influenced by a frictional boundary layer.

The concept of a coastal boundary layer has been discussed in the introduction. Its offshore boundary can be set by modellers at 3x the Ekman scale depth (Mitchum and Clarke, 1986a) and empirically by either a kinetic energy criteria (Murthy and Dunbar, 1981) or by a phase difference between current and sea level (Schwing et al., 1985). For this study a nominal offshore boundary depth of 30 m was adopted based on various empirical findings of other studies. However, no direct evidence has been presented here nor in any other study in South African waters for such boundary layers. Here, some indirect evidence at the study site can be construed to point to

boundary flow behaviour.

Locally, inspection of numerous ART surveys shows that during the initial upwelling phase the plume centre line is usually positioned 1,5 to 2 km offshore and sometimes extends to 3 km. (For established upwelling events there is sometimes no obvious centre line and cold water extends many kilometers offshore.) These distances have corresponding depths of about 15 to 20 m and 30 m respectively. These parameters are qualitatively similar to those of Lake Huron (Murthy and Dunbar, 1981) for a frictional boundary layer that extends 2 km offshore where the kinetic energy is a maximum and where the depth is about 30 m. Although Winant (1980) considers depths less than 25 m to be frictionally limiting, Churchill (1985) observes intrusions of outer shelf water within the nearshore zone off Long Island - depth 15 m.

The other aspect of CBL's is the change in predominance of linear currents (long period) close to the shore to rotary inertial currents further offshore (see Fig. 1.1). Some evidence for such a behaviour can be deduced from inspection of the surface current rose data of van Ieperen (1971) for a transect off Melkbosstrand Point. The inner most station at about 1 km has the most linear polarized current rose and as one moves offshore linear dominance decreases while other directions start appearing i.e. randomness increases until at 5 km (depth 40 m) six directions are essentially equally prevalent.

Although inadequate this indirect evidence does point to the possibility of CBL flow in the area. CBL dynamics are important for the dispersion of shore trapped pollutants particularly at times of reversal of the coastal flow (Csanady, 1982a).

6.8 PERSPECTIVE

In establishing perspective for the study we return to the four generalities mentioned earlier and the aims outlined in section 1.3. A wealth of detail has been revealed in this small scale coastal study. Most of the aims have been achieved. An unsuspected intense localized focus of upwelling was discovered at the coastal offset near Melkbosstrand. The dynamics of the upwelling thermocline are to a certain extent predicted with a simple two-layer model i.e. for a given alongshore wind impulse the displacement offshore of the thermocline intersection with the surface can be determined. The crucial role of wind forcing at all time scales at the study site has been demonstrated. However the small scale study has revealed an insolation forced thermal band of width 0,5 km adjacent to the coastline. Characteristics of both this thermal band and the

displacement of the thermocline can in part be used to deduce the capacity of the area for dispersing thermal and other effluents.

Of the aims itemized (p 1.25) the two that are least adequately met are - evidence for a coastal boundary layer - links between shelf scale dynamics and processes within the CBL.
Although no direct evidence is presented the study gives some indirect evidence and has highlighted the concept of a coastal boundary layer which deserves future investigation with current meters placed on a transect out to 10 or 15 km. Such studies could be of relevance to coastal studies on a broad front. At the theoretical and modelling level very little has been published that deals with processes in water shallower than 3 times the Ekman scale depth. In order to link shelf scale dynamics and processes within the CBL, some knowledge of common oceanographic parameters is needed. The literature review revealed for the southern Benguela shelf a lack of reliable values and even estimates, in some cases, of such parameters. Nevertheless the criteria for shelf waters of Clarke and Brink (1985) for a wind driven response being barotropic if the condition $N^2.\alpha^2.f^{-2} << 1$ is met, was explored. The analysis suggested an ambivalent response for the shallow study area. The response classification awaits more extensive current data both inshore and on the shelf. However, the scale of the study provides a link between the nearshore and intertidal studies of engineers and biologists (Russell and Toms, 1983, Toms, 1987, Wulff and Field, 1983) and the large scale shelf studies of physical oceanographers and fisheries biologists (Nelson and Polito, 1987, Hutchings, 1981, Hutchings et al., 1987). The annual bimodal temperature structure and the seasonal transition have links to the large scale. The study area is of relevance to fisheries biology in that Hampton (1986) reports a corridor for fish recruits exists between Cape Columbine and Cape Town with highest densities occurring in a narrow coastal strip within several kilometers of the coast. Similarly, Pillar (1986) finds a trend for highest zooplankton biomass nearest the coast.

The locally observed small scale temperature fronts with steep horizontal temperature gradients of 3 °C per kilometer could provide the opportunity to study frontal dynamics on a modest affordable scale, yet yield insight to their larger scale counterparts further offshore.

The unique multiyear hourly time series of sea temperatures has enabled processes at various time scales to be identified and quantified through spectral analysis. The most distinct process is the diurnal forcing of the wind. The event time scale is more energetic but reveals no dominant frequency; periods up to about 20

days are observed. The alongshore wind dominates in the correlation with temperature at the seasonal and event time scale. This contrasts with the role of the across-shore winds at the diurnal frequency. The bimodal annual temperature pattern confirms the tendency seen on the larger scale with sparser data.

Additional statistical analysis of the time series data could provide frequency distributions of say different sizes of CET events, magntidues of temperature changes or of persistence thus providing further "climatological" data for the coastal sea. The time series data could be input to mathematical models of pelagic resource projections that utilize environmental time series covering several years (Butterworth, Bergh and Sparks, 1986).

The synoptic time scale field work demonstrated the very variable nature of the thermocline structure and reinforced the remark of Hutchings et al. (1984) how inadequate the traditional monthly cruises are in obtaining representative field data. The physical processes operating over the several day time scale dominate the biological processes for growth of phytoplankton (Brown, 1986). The cyclical upwelling and downwelling is linked to typical synoptic weather cycles of the area. The synoptic cycle, bracketed by coastal lows often results in a wave packet effect in the high frequency temperature response. In particular the role of the coastal low in the rapid decay of the upwelling cycle was seen. This data provided the basis for confirming, under suitable conditions, the simple upwelling model of Csanady (1977a). The distinctive transition in temperature regime between winter and spring is mediated by a single 5 day plus southerly event having a cumulative Ekman transport exceeding 3×10^9 $g.cm^{-1}$. The local temperature transition is probably indicative of a larger scale spring transition and the nature of the causative CET event could be used to delineate the start of a new upwell season.

The study has shown a very strong diurnal periodicity in the time series data. The wind is clearly forced by an insolation driven thermal low in the adjacent interior that results in a land/sea breeze. The sea temperature has a more complex response and although insolation contributes to the diurnal signal the chief contribution is from a modulation of the upwell response by the diurnal across-shore wind system. The diurnal behaviour needs further investigation and future studies need to correlate the radiation balance with sea temperature and thermocline structure changes throughout the diurnal cycle. However, meaningful mixed layer studies are probably precluded from within the coastal boundary layer (McCormick and Meadows, 1988).

A small inertial peak is seen in the temperature spectra; this is expected to become more prominent further offshore when the inertial boundary layer of the proposed CBL is entered.

Another process that suffers from neglected importance in this small scale study is Langmuir circulations associated with wind rows. In fact Thorpe (1985) considers it a profound embarrassment to physical oceanographers that the importance of Langmuir circulation for distributing heat and momentum in the upper ocean has yet to be established.

As man's knowledge grows so new questions are posed to gain yet more understanding. Particularly in South Africa the growth in population in the years ahead will see increased pressures from man on our fragile and limited coastline and its adjacent waters. More coastal nuclear power stations will be erected, more outfalls will be established. More demands will arise for offshore extraction of oil and sea bed minerals. Greater needs for sea harvested proteins will arise. All require careful planning to limit deleterious impact to man's marine environment. This study provides insight and a framework to better understand our coastal oceanography.

REFERENCES

ALBUISSON, M. (1978). Museum Nat. D'Historie Naturelle (Paris). Lab D'Ocean Phys. 15, 17-18.

ALLEN, J.S. (1980). Ann. Rev. Fluid Mech. 12, 389-433.

ANDERSON, R.J., HAY, C.H. (1986). Bontanica Marina 24, 523-531.

ANDREWS, W.R.H., CRAM, D.L. (1969). Nature 224, 902-904.

ANDREWS, W.R.H., HUTCHINGS, L. (1980). Prog. in Oceanog. 9, 1-81.

ANH, N.N., GILL, A.E. (1981) Quat. J. Roy. Met. Soc. (London), 107, 521-530

ARTHUR, R.S. (1954). Deep-Sea Res. 2(2), 107-121.

ARTHUR, R.S. (1965). J Geophys. Res. 70: 2799-2803.

BAIN, C.A.R. (1979). Trans. Roy. Soc. S. Afr. 44 Part 1, 130-131.

BAIN, C.A.R. (1982). Proceedings 18th International Coastal Engineering Conf. ASCE Cape Town Vol 3, 2390-2402.

BAIN, C.A.R., HARRIS, T.W.F. (1975 ff). Coastal Waters Movement Project, report series no 1 to 6 - 1975 to 1977. University of Cape Town.

BAKUN, A., PARRISH, R.H. (1980). Proc. of Workshop on Effects of Environmental Variation on the survival of Larval Pelagic Fishes. Lima, IOC Workshop rept no 28, 67-104.

BANG, N.D. (1973). Tellus 25, 256-265.

BANG, N.D. (1976). National Oceanog Congress - Port Elizabeth.

BANG, N.D., ANDREWS, W.R.H. (1974). J. Marine Res. 32 405-417.

BECKLEY, L.E. (1983). S. Afr. J. Sci. 79, 436-438.

BECKLEY, L.E. (1988). S. Afr. J. Sci. 84, 67-69.

BEGIS, D., CREPON, M. (1975). Museum Nat. D'Historie Naturelle (Paris) Lab. D'Ocean Phys 12, 25-57.

BENDAT, J.S., PIERSOL, A.G., RANDOM DATA (1971). Wiley-Interscience. N.Y. 407 pp.

BENNETT, J.R., MAGNELL, B.A. (1979). J. Geophys. Res. 84, 1165-1175.

BLACKMAN, R.B., TUKEY, J.W. (1958). "The Measurement of Power Spectra from the Point of View of Communications Engineering" Dover Press. New York.

BLANTON, J.O. (1974). J. Phys. Oceanog. 4, 415-424.

BLANTON, J.O. (1975). in "Proc. Conf. Combined Effects of Radioactive, Chemical and Thermal Releases to the Environment" 255-268, IAEA, Vienna.

BOYCE, F.M. (1977). J. Phys. Oceanog. 7, 719-732.

BOYD, A.J. (1979). Trans Roy Soc. S. Afr. 44, pt 3, 121.

BOYD, A.J. (1981). "An Intensive study of the Currents and General Hydrology of an Anomalous Upwelling Area off South West Africa". M.Sc. Thesis, University of Cape Town.

BOYD, A.J. (1983). 5th Nat. Oceanog. Sym. Grahamstown - in S. Afr. J. Science 79, 146.

BOYD, A.J. (1987). 6th Nat. Oceanog. Sym. Stellenbosch - paper C2

BOYD, A.J. (1987). "The Oceanography of the Namibian Shelf". PhD. Thesis, University of Cape Town.

BRINK, K.H. (1982). J. Phys. Oceanog. 12, 127-133.

BRINK, K.H. (1983). Prog. in Oceanog. 12, 223-258.

BRINK, K.H. (1986). Ibid, HUTCHINGS, 1986

BRINK, K.H., CHAPMAN, D.C., HALLIWELL, G.R. (1987). J. Geophys. Res. 92, 1783-1797.

BROWN, P.C. (1984). S. Afr. J. Mar. Sci. 2, 205-215.

BROWN, P.C. (1986). Ibid, HUTCHINGS, 1986.

BRUNDRIT, G.B (1981). Trans Royal Soc. of S. Afr. 44 pt. 3, 309-313.

BRUNDRIT, G.B., DIAB, R.D., JURY, M.R. (1984). Convenors summary - Proceedings "Coastal Low Workshop", Simonstown. 56-67

BRUNDRIT, G.B. (1984). Cabo Blanco y Benguella, Spain S. Afr. J. Marine Sci. 2, 195-203.

BRUNDRIT, G.B., DE CUEVAS, B., SHIPLEY, A.M. (1984). S. Afr. J. Sci. 80, 80-82.

BUTTERWORTH, D.S., BERGH, M.O., SPARKS, R. (1986). Ibid, HUTCHINGS, 1986.

BUYS, M.E.L. (1959). Investl. Rept. Div. Fish. S. Afr. No 37, 176 pp.

CAIRNS, J.L., NELSON, K.W. (1970). J. Geophys. Res. 75, 1127-1131.

CHAPMAN, D.C. (1987). J. Geophys. Res. 92, 1798-1816.

CHELTON, D.B., DAVIS, R.E. (1982). J. Phys. Oceanog. 12, 757-784.

CHERMACK, E.E. (1970). Proceedings 13th Conf. Great Lakes Research, 904-913.

CHRISTENSEN, M.S. (1980). S Afr. J. of Sci. 76, 541-545.

CHURCHILL, J.H. (1985). Limnology and Oceanog. 30, 972-986.

CLARKE, A.J. (1977). J. Phys. Oceanog. 7, 231-247.

CLARKE, A.J. (1988). J. Geophys. Res. 93, 15491-15501.

CLARKE, A.J., BRINK, K.H. (1985). J. Phys. Oceanog. 15, 439-453.

CLOETE, C.E. (1979). Proc. of Workshop "The Transfer of Pollutants in two Southern hemispheric oceanic systems" Plettenberg Bay, S.A. Nat. Sci. Prog. Rept. no 39.

CRAM, D.L. (1970). Trans Roy Soc. S.A. 39, 129-137.

CREW, H., PLUTCHAK, N. (1974). J. Oceanog. Soc. Japan 30, 61-66.

CSANADY, G.T. (1972a). J. Phys. Oceanog. 2, 168-176.

CSANADY, G.T. (1972b). J. Phys. Oceanog. 2, 41-53.

CSANADY, G.T. (1975). J. Phys. Oceanog. 5, 705-717.

CSANADY, G.T. (1976a). J. Phys. Oceanog. 6, 93-103.

CSANADY, G.T. (1976b). J. Geophys. Res. 81, 5389-5399.

CSANADY, G.T. (1977a). J. Geophys. Res. 82, 397-419.

CSANADY, G.T. (1977b). in "The Sea" 6, 117-144, editors Goldberg, E.D. et al, John Wiley, New York.

CSANADY, G.T. (1978). J. Phys. Oceanog. 8, 47-62.

CSANADY, G.T. (1980). J. Geophys. Res., 85, 1076-1084.

CSANADY, G.T. (1982a). "Circulation in the Coastal Ocean", D. Reidel Pub. Co Dordrecht, Holland.

CSANADY, G.T. (1982b). J. Phys. Oceanog. 12, 84-96.

CSANADY, G.T., SCOTT, J.T. (1980). J. Geophys. Res. 85, 2797-2812.

CSIR (1976). Oceanographic Investigation for Waste Disposal of Greater Saldanha - Rept no C/SEA 7611.

CSIR (1976). Field Data Analysis for proposed ESCOM NPS. Prog Rept 1 C/SEA 7608

CURTIN, T.B. (1979). "Physical dynamics of coastal upwelling frontal zone off Oregon" PhD Thesis, Univ. Miami, Florida.

CUSHING, D.H. (1969). FAO Fishing Tech Paper 84, 40 p.

CUSHMAN-ROISIN, B., O'BRIEN, J., SMITH, R.L. (1983). J. Phys. Oceanog. 13, 547-550.

DAVIS, R. (1976). J. Phys. Oceanog. 6, 249-266.

DAVIS, R.E., BOGDEN, P.S. (1989). J. Geophys. Res. 94, 4763-4783.

DE CUEVAS, B.A., BRUNDIT, G.B., SHIPLEY, A.M. (1986). Geophys. J. Royal. Astron. Soc. 87, 33-42.

DE SZOEKE, R.A., RICHMAN, J.G. (1981). J. Phys. Oceanog. 11, 1534-1547.

DE WET, L.W. (1984). Proceedings "Coastal Low Workshop", Simonstown, 6-7.

DESCHAMPS, P.Y., FROUIN, R. (1984). J. Phys. Oceanog. 14, 177-184.

DORAN, J.C., GRYNING, S-E. (1987). J. Climate app. Met. 26, 973-979.

DüING, W.O., MOOERS, C.N.K., LEE, T.N. (1977). J. Marine Res. 35, 129-161.

DUNCAN, C.P. (1964). Investl. Rep. Div. Sea Fish. S. Afr. no 50, 15 pp.

DUNCAN, C.P., NELL, J.H. (1969). S.A. Div. Sea Fish, Invest. Rept. no 76.

EKMAN, V.W. (1905). Arkiv för Matematik, Astronomi och Fysik, Stockholm 2:11, 52 pp.

FIELD, J.G., GRIFFITHS, C.L., LINLEY, E.A.S. (1981). in "Coastal Upwelling" editor F.A. Richards. American Geophysical Union - Washington, 507-513.

FOFONOFF, N.P. (1969). Deep Sea Res. 16 suppl. 59-71.

FRICKE, A.H., THUM, A.B. (1975). Trans Roy. Soc. S. Afr. 41 Pt 4, 351-357.

GILL, A.E. (1977). Quat. J. Roy. Met. Soc. (London), 103, 431-440

GILL, A.E. (1982). "Atmosphere - Ocean Dynamics". Internat. Geophys. Series Vol 30, Academic Press. 662 p.

GILL, A.E., CLARKE, A.J. (1974). Deep Sea Res. 21, 325-345.

GILL, A.E., SCHUMANN, E.H. (1974). J. Phys. Oceanog. 4, 83-90.

GILLOOLY, J.F., WALKER, N.D. (1984). S. Afr. J. Sci. 80, 97-100.

GONELLA, J. (1971). Deep Sea Res. 18, 775-788.

GONELLA, J. (1972). Deep Sea Res. 19, 833-846.

GOSCHEN, W.S., SCHUMANN, E.H. (1988). S. Afr. J. Mar. Sci. 7, 101-116.

GRANT, W.D., MADSEN, O.S. (1979). J. Geophys. Res. 84, 1797-1808.

GRANT, W.D., MADSEN, O.S. (1986). Ann. Rev. Fluid Mech. 18, 265-305.

GRASSL, H. (1976). Boundary Layer Met. 10, 465-474.

GRAY, B.M. (1988). J. Climatology (Roy. Met. Soc.) 8, 511-519.

GUNN, B.W. (1977a). "The Nearshore Dynamics of Matroos Bay - Field and Theoretical Investigations" M.Sc. Thesis, University of Cape Town.

GUNN, B.W. (1977b). "The Dynamics of Two Cape Coastal Embayments" in two volumes - unpublished report University of Cape Town.

HALPERN, D. (1974). J. Geophys. Res. 79, 2223-2230.

HALPERN, D., REED, R.K. (1976). J. of Physical Oceanog. 6, 972-975.

HAMPTON, I. (1986). Ibid, HUTCHINGS, 1986.

HANSEN, A.R., SUTERA, A. (1988). J. Atmos. Sci. 45, 3771-3783.

HARRIS, T.W.F. (1964). in "Some Techniques in Physical Oceanog" CSIR pub.

HARRIS, T.W.F., SHANNON, L.V. (1979). S. Afr. J. Sci. 75, 316-317.

HASHIMOTO, H., UDA, T. (1982). Coastal Engineering Japan 25, 239-250.

HAYES, S.P., HALPERN, D. (1976). J. Marine Res. 34, 247-267.

HOLDEN, C.J. (1985). Ibid., SHANNON 1985b, p. 97-110.

HOLDEN, C.J. (1987). S. Afr. J. Mar. Sci. 5, 197-208.

HOWE, M.R., TAIT, R.I. (1969). Limnology and Oceanography 14, 16-22.

HUA, B., THOMASSET, F. (1983). J. Phys. Oceanog. 13, 678-694.

HUNTER, I.T. (1987). "The weather of the Agulhas Bank and the Cape South Coast." MSc Thesis, University of Cape Town. CSIR Research Report 634.

HURLBURT, H.E. (1974). The Influence of Coastline Geometry and Bottom Topography on Eastern ocean Circulation. Ph.D. Thesis, Florida State University.

HUTCHINGS, L. (1981). in "Coastal Upwelling" editor F.A. Richards. American Geophys. Union - Washington, 496.

HUTCHINGS, L. (1986). Abstract in International Symposium on Population and Community Ecology in the Benguela Upwelling Region and Comparable Frontal Systems, 8-12 Sept 1986, University of Cape Town.

HUTCHINGS, L., BROWN, P. et al. (1987). 6th Nat. Oceanographic Sym. Stellenbosch, paper C-4.

HUTCHINGS, L., HOLDEN, C., MITCHELL-INNES, B. (1984). S. Afr. J. Sci. 80, 83-89.

HUYER, A. (1983). Prog. in Oceanog. 12, 259-306.

HUYER, A., SMITH, R.L., SOBEY, E.J.C. (1978). J. Geophys. Res. 83 no C10, 5077-5089.

HUYER, A., SOBEY, E.J.C., SMITH, R.L. (1979). J. Geophys. Res. 84 6995-7011.

IKEDA, M., EMERY, W.J. (1984). J. Marine Res. 42, 303-317.

JACOBS, C.A. (1978). J. of Phys. Oceanog. 8, 103-118.

JEFFREYS, H. (1923). Philosophical Mag. 46, 114-125.

JENKINS, G.M., WATTS, D.G. (1968). Spectral Analysis and its Application. Holden-Day publishers, San Fransisco.

Julian, P.R. (1975). J. Atmos. Sciencies. 32, 836-837.

JURY, M.R. (1980). "Characteristics of Summer Wind Field and Air-Sea Interactions over the Cape Peninsula Upwelling region" M.Sc. Thesis University of Cape Town.

JURY, M.R. (1981). Trans. Roy. S. Afr. 44 pt 3, 299-302.

JURY, M.R. (1984). "Wind Shear and Differential Upwelling along the S.W. Tip of Africa". Ph.D. Thesis University of Cape Town.

JURY, M.R. (1985). Ibid., SHANNON 1985b. p. 29-46.

JURY, M.R. (1986). S. Afr. J. Mar. Sci. 4, 111-118.

JURY, M.R. (1987). J Climate and App. Met. 26, 1540-1552.

JURY, M.R. (1988). Continental Shelf Res. 8, 1257-1271.

JURY, M.R., BRUNDRIT, G.B. (1987). 6th Nat. Oceanog. Sym. Stellenbosch, paper C8.

JURY, M.R., KAMSTRA, F., TAUNTON-CLARK, J. (1985). S. Afr. J. Mar. Sci. 3, 1-10.

JURY, M.R., MACARTHUR, C, SHILLINGTON, F.A. (1989). In press. S. Afr. Geographer.

JURY, M.R., SHILLINGTON, F.A., PRESTIDGE, G., MAXWELL, C.D. (1986). S. Afr. J. Sci. 82, 315-319.

JURY, M.R., SPENCER-SMITH, G. (In press). Doppler Sounder Observations of Trade Winds and Sea Breezes along the African West Coast near 34°S, 19°E. Bound. Layer Met.

KAIMAL, J.C., WYNGAARD, J.C., IZUMI, Y. COTE, O.R. (1972). Quat. J. Roy. Met. Soc. 98, 563-589.

KAMSTRA, F. (1985). Ibid, SHANNON (1985b), p 13-27.

KAMSTRA, F. (1987). Tellus. 39A, 509-514.

KAMSTRA, F., NELSON, B. (1983). 5th National Oceanog. Symposium - Grahamstown. Abstract in S. Afr. J. Sci. 79, 147.

KAMSTRA, F., TAUNTON-CLARK, J. (1986). Ibid HUTCHINGS (1986).

KEEN, C.S. (1979). "Meterological Aspects of Pollution Transfer in the Cape Town Area", INVEST. REP. Dept of Geography, Univ. of Cape Town.

KEEN, C.S. (1980). "The Future Management of False Bay" 34-41.

KIDSON, J.W. (1988). J. of Climate 1, 1177-1198.

KILLWORTH, P.D. (1978). J. Phys. Oceanog. 8, 188-205.

KOIZUMI, M. (1956). Papers Met and Geophys (Tokyo) 7, 144-154.

KUNDU, P.K., CHAO, S., MCCREARY, J.P. (1983). Deep-Sea Res. 30, 1059-1082.

LARGE, W.G., POND, S. (1981). J. Phys. Oceanog. 11, 324-336.

LARGIER, J.L. (1987). "Internal Shelf Tides and Wind-Driven Motions in deepening the Surface Mixed Layer". PhD Thesis, Univ. Cape Town.

LARGIER, J.L., SWART, V.P. (1987). S. Afr. J. Mar. Sci. 5, 263-272.

LE BLOND, P.H., MYSAK, L.A. (1978). "Waves in the Ocean", Elsevier Pub., Amsterdam, p 317.

LEE, T.N., MAYER, D.A. (1977). J. Marine Res., 35, 193-220.

LENTZ, S.J. (1987). J. Geophys. Res. 92, 1545-1567.

LUTJEHARMS, J.R.E. (1977). Tellus 29, 375-381.

LUTJEHARMS, J.R.E (1981). in Oceanography from space (ed Gower, J.) Marine Science 13, 195-199. Plenum Press, New York.

LUTJEHARMS, J.R.E. (1988). S. Afr. J. Sci. 84, 584-586.

LUTJEHARMS, J.R.E., GORDON, A.L. (1987). Nature 325, 138-140.

LUTJEHARMS, J.R.E., GRUNDLING, M.L., CARTER, R.A. (1989). S. Afr. J. Sci. 85, 310-316.

LUTJEHARMS, J.R.E., VAN BALLEGOOYEN, R.C. (1988). J. Phys. Oceanog. 18, 1570-1583.

LIVINGSTONE, D. and ROYER, T.C. (1980). Deep Sea Res., 27A, 823-835.

LOEWY, E., WITTHAUS, K.G. SUMMERS, L., MADDRELL, R.J. (1976). in Proc. 15th Internat. Coastal Eng. Conf. Copenhagen p. 226-229.

MADDEN, R.A., JULIAN, P.R. (1972a). J. Atmos. Sci. 29, 1109-1123.

MADDEN, R.A., JULIAN, P.R. (1972b). J. Atmos. Sci. 29, 1464-1469.

MADSEN, O.S. (1977). J. Phys. Oceanog. 7, 248-255.

MALORY, J.K., MAXWELL, C.D. (1971 ff). Oceanographic Investigations for the proposed ESCOM nuclear power station Duynefontein. Progress Reports no 1 to 16. Dept Oceanography, Univ. of Cape Town.

MARMORINO, G.O. (1983). J. Geophys. Res. 88, 4439-4457.

MAXWELL, C.D., RATTEY, D. (1977 ff). Oceanographic Investigations for the Koeberg nuclear power station. Progress Reports no 1 to 10, Electricity Supply Commission.

McCORMICK, M.J., MEADOWS, G.A. (1988). J. Geophys. Res. 93, 6774-6788.

McCREARY, J.P., LEE, H.S., ENFIELD, D.B. (1989). J. Mar. Res. 47, 81-109.

MEEUWIS, J.M., LUTJEHARMS, J.R.E. (1986). ibid HUTCHINGS (1986)

MIDDLETON, J.H. (1982). Deep Sea Res. 29, 10A, 1267-1269.

MIITA, T., TAWARA, S. (1984). J. Oceanog. Soc. Japan 40, 91-97.

MILLOT, C. (1979). Oceanol. Acta. 2, 261-274.

MILLOT, C., CREPON, M. (1981). J. Phys. Oceanog. 11, 639-657.

MILLOT, C., WALD, L. (1981). in "Coastal Upwelling", editor, F.A. Richards. American Geophysical Union, Washington, p 160.

MITCHELL, J.G., OKUBO, A., FUHRMAN, J.A. (1985). Nature 316, 58-59.

MITCHUM, G.T., CLARKE, A.J. (1986a). J. Phys. Oceanog. 16, 934-946.

MITCHUM, G.T., CLARKE, A.J. (1986b). J. Phys. Oceanog. 16, 1029-1037.

MITTELSTAEDT, E. (1983). Prog. in Oceanog. 12, 307-332.

MONIN, A.S. (1977). Variability of the Oceans, Wiley-Interscience Publication.

MOOERS, C.N.K. (1968). Dept of Oceanog. Oregon State Univ - Oregon Continental Shelf Vol. II Report no 30, Ref 65-5.

MOOERS, C.N.K. (1973). Deep Sea Res. 20, 1129-1141.

MORITA, J. (1978). Japan Far Seas Fisheries Res. Bull. 16 51-57 (Abstract)

MURRAY, S.P. (1975). J. Phys. Oceanog. 5, 347-360.

MURTHY, C.R., DUNBAR, D.S. (1981). J. Phys. Oceanog. 11, 1567-1577.

MYSAK, L.A. (1980). Ann. Rev. Fluid Mech. 12, 45-76.

NELSON, G. (1983). 5th National Oceanog Symposium - Grahamstown. Abstracts in S.A. J. of Sci. 79, 147.

NELSON, G. (1985). Ibid SHANNON (1985b) p. 63-95.

NELSON, G., HUTCHINGS, L. (1983). Progress in Oceanog. 12, 333-356.

NELSON, G., POLITO, A. (1987). (In) The Benguela and Comparable Ecosystems; eds. A.I.L. Payne, J.A. Gulland and K.H. Brink. S. Afr. J. Mar. Sci. 5, 287-304.

NELSON, G., WALKER, N. (1984). S. Afr. J. Sci. 80, 90-93.

NEUMANN, G., PIERSON, W.J. (1966). "Principles of Physical Oceanography" Prentice-Hall, Inc., New Jersey. 203, 545 pp.

NEWTON, C.W. (1972). Editor, Meteorology of the Southern Hemisphere. Meteorological Monograph 13 no 35, American Met. Soc. Boston, 263 pp.

NORDEN, C., VAN AS, D., REDDING, S.J. (1982). "Atmospheric Dispersion Characteristics of the Duynefontein Environment", Atomic Energy Board, PIN-636-(C/V).

O'BRIEN, J.J. (1983). Prog. in Oceanog. 12, 221-222.

O'BRIEN, J.J., et al. (1977). "Upwelling in the Ocean" in "Modelling the Upper Layers of the Ocean", E.B. Krauss, editor, Advanced Study Inst. Urbino, NATO, 325 pp.

OKUBO, A. (1976). Deep Sea Res. 23, 1213-1214.

OLIVIERI, E.T., HUTCHINGS, L., (1986). Ibid HUTCHINGS (1986).

OWEN, R.W. (1980). Proc. of Workshop on Effects of Environmental Variation on the Survival of Larval Pelagic Fishes, LIMA, IOC Workshop REPT no. 28, 167-200.

PADUAN, J.D., DE SZOEKE, R.A., WELLER, R.A. (1989). J. Geophys. Res. 94, 4835-4842.

PARES-SIERRA, A., O'BRIEN, J.J. (1989). J. Geophys. Res. 94, 3159-3180.

PEARCE, A.F. (1973). Tech. Dept. - Special current study at Richards Bay, CSIR Contr. Rept. CFIS 37.

PEARCE, A.F. (1977). M.Sc. Thesis "The Shelf Circulation off the East Coast of South Africa" Univ. of Natal. Professional Res. series no 1 NRIO, Stellenbosch.

PEDLOSKY, J. (1978a). J. Phys. Oceanog. 8, 171-177.

PEDLOSKY, J. (1978b). J. Phys. Oceanog. 8, 178-185.

PEFFLEY, M.B., O'BRIEN, J.J. (1976). J. Phys. Oceanog. 6, 164-180.

PERRINS, L. (1980). "Time Series Analysis of Vector Current Measurements" B.Sc. (Hons) Project - Oceanography Dept. University of Cape Town.

PETERSON, W.T. (1986). Ibid, HUTCHINGS, 1986.

PHILANDER, S.G.H. (1983). Nature 302, 295-301.

PHILLIPS, O.M. (1971). J. Physical Oceanog. 1, 1-6.

PHILLIPS, O.M. (1977). Dynamics of Upper Ocean 2nd Ed Cambridge Univ. Press. London, 336 pp.

PILLAR, S.C. (1986). Ibid, HUTCHINGS, 1986.

PITCHER, G.C. (1986). Ibid, HUTCHINGS, 1986.

PIVOVAROV, A.A., PROTASOV, S.N. (1976). Oceanology (Acadamy of Sciences USSR) 15, 291-294.

POLLARD, R.T. (1970). Deep Sea Res. 17, 795-812.

POLLARD, R.T., MILLARD, R.C. (1970). Deep Sea Res. 17. 813-821.

POPLE, W. (1971). Nature-Physical Science 234, no 44, 18-20.

POPLE, A. (1979). 4th Nat. Oceanog. Symp.

PRELLER, R., O'BRIEN, J.J. (1980). J. Phys. Oceanog. 10, 1377-1398.

PRESTON-WHYTE, R.A., TYSON, P.D. (1973). Monthly Weather Review. 101, 650-653.

PRICE, J.F., WELLER, R.A., SCHUDLICH, R.R. (1987). Science 238, 1534-1538.

PRICE, J.F., WELLER, R.A., PINKEL, R. (1986). J. Geophys. Res. 91, 8411-8427.

REDDING, S.J., NORDEN, C., VAN AS, D. (1982). "The Relationship Between Synoptic-scale Airflow and Local Windfields Over Duynefontein", Atomic Energy Board, PIN-629(C/V).

REID, F.M.H., STEWART, E., EPPLEY, R.W. and GOODMAN, D. (1978). Limnol and Oceanogr. 23(2), 219-226.

RETIEF, G. DE F. (1982). Proc 18th Intern. Conf. on Coastal Eng. Cape Town, paper 74.

ROLL, H.U. (1955). Q.J. Roy. Met. Soc. 81, 631-632.

ROLL, H.U. (1965). Physics of the Marine Atmosphere, Academic Press, New York, 426 pp, 227 ff.

ROSENFELD, L.K. (1988). J. Geophys. Res. 93, 2257-2276.

RUSSELL, K.S., TOMS, G. (1983). S. Afr. J. Sci. 79, 165.

RUSSOUW, J. (1982). Proceedings 18th International Conf. on Coastal Engineering. Cape Town, paper 41.

SALTZMAN, B., TANG, C. (1975). J. Phys. Oceanog. 5, 86-92.

SAUNDERS, P.M. (1973). Woods Hole Oceanographic Inst. Contribution no 3118, 99-108.

SCARPACE, F.L., GREEN, T. (1979). J. Phys. Oceanog. 9, 638-643.

SCHUMANN, E.H. (1979). 4th National Oceanographic Symposium.

SCHUMANN, E.H. (1981). J. Geophys. Res. 86, 6499-6508.

SCHUMANN, E.H. (1987). Trans. Roy. Soc. S. Afr. 46, Part 3, 215-229.

SCHUMANN, E.H. (1989). S. Afr. J. Sci. 85, 382-385.

SCHUMANN, E.H., PERRINS, L.A., HUNTER, I.T. (1982). S. Afr. J. Sci. 78, 238-242.

SCHUMANN, E.H. AND PERRINS, L.A. (1982). Proceedings of the 18th Coastal Engineering Conference ASCE/Cape Town, Nov. 14-19, 1982, p. 2562-2580.

SCHUMANN, E.H., ROSS, G.B.J., GOSCHEN, W.S. (1988). Cold water events in Algoa Bay. S. Afr. J. Sci. 84, 579-584.

SCHWING, F.B., OEY, L.Y., BLANTON, J.O. (1985). J. Phys. Oceanog. 15, 1733-1746.

SCHWING, F.B., OEY, L.Y., BLANTON, J.O. (1988). J. Geophys. Res. 93, 8221-8228.

SCIREMAMMANO, F. (1979). J. Phys. Oceanog. 9, 1273-1276.

SCOTT, J.T., CSANADY, G.T. (1976). J. Geophys. Res. 81, 5401-5409.

SEND, U., BEARDSLEY, R.C., WINANT, C.D. (1987). J. Geophys. Res. 92, 1683-1698.

SHANNON, L.V. (1970). Fisheries Bull no 6, 27-33.

SHANNON, L.V. (1985a). Oceanogr. Mar. Biol. Ann. Rev. (Aberdeen University Press) 23, 105-182.

SHANNON, L.V. (1985b). Editor. South African Ocean Colour and Upwelling Experiment. Sea Fisheries Research Institute, Cape Town.

SHANNON, L.V. (1987). 6th Nat. Oceanographic Sym., Stellenbosch, paper A-12.

SHANNON, L.V., NELSON, G., JURY, M.R. (1981). , in "Coastal Upwelling" editor F.A. Richards, American Geophysical Union - Washington, 146.

SHANNON, L.V., CRAWFORD, R.J.M., DUFFY, D.C. (1984). S. Afr. J. Sci. 80, 51-60.

SHANNON, L.V., WALTERS, N.M., MOSTERT, S.A. (1985). Ibid SHANNON (1985b) p. 183-210.

SHANNON, L.V., LUTJEHARMS, J.R.E., AGENBAG, J.J. (1989). S. Afr. J. Sci. 85, 317-322.

SHARP, G. (1986). Ibid HUTCHINGS (1986).

SHELTON, P.A. (1986). Ibid HUTCHINGS (1986).

SHILLINGTON, F.A., HARRIS, T.F.W. (1978). Deut. Hydr. Z., 31, 67-81.

SHIPLEY, E. PER COMMUNICATION - UCT Oceanography Dept.

SIMONS, T.J. (1974). J. Phys. Oceanog. 4, 507-523.

SIMONS, T.J. (1983). J. Phys. Oceanog. 13, 512-523.

SMITH, R.L. (1978). J. Geophys. Res. 83, 6083-6092.

SMITH, N.P. (1977a). Limnology and Oceanog. 22. 1079-1082.

SMITH, N.P. (1977b). J. Phys. Oceanog. 7, 615-620.

SONU, C.J., MURRAY, S.P. HSU, S.A. (1973). Transactions Am Geophys. Union 54 no 9, 820-833.

SPIGEL, R.H., IMBERGER, J., RAYNER, K.N. (1986). Limnology and Oceanog. 31, 533-556.

STACEY, M.W., POND, S., LE BLOND, P.H. (1986). Science 233, 470-472.

STANDER, G.H. (1963). Investl Rep. Mar. Res. Lab. S.W. Afr. No 9, 57 pp.

STOCKTON, P.L., LUTJEHARMS, J.R.E. (1988). Abstract in SA Society for Atmospheric Sciences Fifth annual conference, p.27, October.

STOCKTON, P.L., LUTJEHARMS, J.R.E. (1988b). S. Afr. Geographer 15(1/2), 27-35.

STOMMEL, H. (1963). in "Proceedings of Symposium on the Kuroshio", Tokyo, 22-23.

STOMMEL, H. et al (1969). Deep Sea Res. 16, suppl. 269-284.

STRUB, P.T., ALLEN, J.S., HUYER, A., SMITH, R.L., BEARDSLEY, R.C. (1987a). J. Geophys. Res. 92, 1507-1526.

STRUB, P.T., ALLEN, J.S., HUYER, A., SMITH, R.L. (1987b). J. Geophys. Res. 92, 1527-1544.

STRUB, P.T., JAMES, C. (1988). J. Geophys. Res. 93, 15561-15584.

STUART, D.W. (1981). in "Coastal Upwelling", Editor F.A. Richards, American Geophysical Union, Washington, 32-38.

SVERDRUP, H.U. (1942). in "The Oceans", Prentice Hall, New York, 1087 pp.

SZOEKE - see DE SZOEKE.

TALJAARD, J.J. (1972). Ibid NEWTON (1972) p. 139-211.

TAUNTON-CLARK, J. (1983). 5th Nat. Oceanographic Sympsoium, Grahamstown, B46.

TAUNTON-CLARK, J. (1985). Ibid SHANNON (1985b), p47-61.

TAUNTON-CLARK, J., KAMSTRA, F. (1988). S. Afr. J. Mar. Sci. 6, 273-283.

TAUNTON-CLARK, J., SHANNON, L. V. (1988). S. Afr. J. Mar. Sci. 6, 97-106.

TAYLOR, D.I., ALLANSON, B.R. (1987). Paper B-69. Sixth National Oceanographic Symposium (6NOS) Stellenbosch.

THOMAS, J.H. (1975). J. Physical Oceanog. 5, 136-142.

THOMSPON, R.O.R.Y. (1979). J. Atmos. Sciences. 36, 202-2021.

THOMPSON, R.O.R.Y. (1983). J. Phys. Oceanog. 13, 1077-1083.

THOMSON, K.P.B. (1972). 1st Canadian Symposium on Remote Sencing Vol I, 173-181.

THORPE, S.A. (1985). Nature 318 519-522.

THORPE, A.J., GUYMER, T.H. (1977). Quart. J. Roy. Met. Soc. 103, 633-653.

TOMS, G. (1987). 6th Nat. Oceanographic Sym., Stellenbosch, paper B.33.

TRENBERTH, K.E. (1979). Monthly Weather Review (USA) 107, 1515-1524.

TRENBERTH, K.E. (1981). J. Atmos. Sci. 38, 2585-2605.

TRENT, J.D., SHANKS, A.L. and SILVER, M.W. (1978). Limnology and Oceanogr. 23(4), 626-635

TYSON, P.D. (1986). "Climatic Change and Variability in Southern Africa", Oxford University Press, Cape Town, 220 p.

UDA, T., HASHIMOTO, H. (1983). Coastal Engineering Japan 26, 209-218.

UNDERHILL, L.G. (1981). "Introstat" 3rd Edition, Juta and Co., Cape Town, Table 5.

UNLUATA, U., OZSOY, E. (1980). Ves Journees Etud. Pollution, 929-936 C.I.E.S.M. Mediterranean.

VAN FOREEST, D. (1981). Trans S. Afr. Roy. Soc. 44 pt 3, 315.

VAN FOREEST, D. SHILLINGTON, F.A. and LEGECKIS, R. (1984). Cont. Shelf Res. 3, 465-474

VAN IEPEREN, M.P. (1971). "Hydrology of Table Bay" - Final Report to SANCOR. University of Cape Town.

VAN LOON, H. (1972). Ibid NEWTON (1972), p. 59-86.

VAN LOON, H. ROGERS, J.C. (1984). Tellus 36A, 76-86.

WALKER, N.D. (1984). Proc. "Coastal Low Workshop", Simonstown, 8-11.

WALKER, N.D., TAUNTON-CLARK, J., PUGH, J. (1984). S. Afr. J. Sci. 80, 72-77.

WALKER, N.D. (1987). S. Afr. Mar. Sci. 5, 121-132.

WEBSTER, F. (1968). Rev Geophys. 6, 473-490.

WEBSTER, F. (1969). Deep Sea Res. 16, suppl. 357-368.

WELLER, R.A. (1981). J. Geophys. Res., 86, 1969-1977.

WELLS, J.T., SHANKS, A.L. (1987). J. Geophys. Res., 92, 13185-13190.

WELSH, J.G. (1967). J. Marine Res. 25, 190-197.

WINANT, C.D. (1974). J. Geophys. Res., 79, 4523-4526.

WINANT, C.D. (1980). Ann. Rev. Fluid Mech. 12, 271-301.

WINANT, C.D. (1983). J. Phys. Oceanog. 13, 54-64.

WINANT, C.D., BEARDSLEY, R.C., (1979). J. Phys. Oceanog. 9, 218-220.

WINANT, C.D., BEARDSLEY, R.C., DAVIS, R.E. (1987). J. Geophys. Res. 92, 1569-1604.

WINANT, C.D., BRATKOVICH, A.W., (1981). J. Phys. Oceanog. 11, 71-86.

WINANT, C.D., OLSON, J.R. (1976). Deep Sea Res., 23, 925-936.

WOLANSKI, E. (1986). J. Phys. Oceanog. 16, 1694-1702.

WOLANSKI, E., HAMNER, W.M. (1988). Science, 241, 177-181.

WOODS, J.D., BARKMAN, W. (1986). Quart. J. Roy. Met. Soc. 112, (471), 1-27.

WOODS, J.D., HOUGHTON, D. (1969). New Scientist, 134-136.

WOODS, J.D., STRASS, V. (1986). Quart. J. Roy. Met. Soc. 112 (471), 29-42.

WULFF, F.V., FIELD, J.G. (1983). Mar. Ecol. Prog. Ser. 12, 217-228.

WUNSCH, C. (1980). in Evolution of Physical Oceanography edited by Warren, B.A. and Wunsch, C. M.I.T. Press. p 346-365.

WUNSCH, C., WIMBUSH, M. (1977). J. Marine Res. 35, 75-104.

YAO, N. et al. (1975). J. Phys. Oceanog. 5, 164-172.

YAO, N. et al. (1977). J. Phys. Oceanog. 7, 892-903.

YOSHIDA, K., MAO, H.L. (1957). J. Marine Res. 16, 40-54.